

Final Reports of GeoNickel project

J. Aarnisalo*, K. Mäkelä, B. Bourgeois, C. Spyropoulos, S. Varoufakis, E. Morten, K. Ma-glaras, H. Soininen, A. Angelopoulos, D. Eliopoulos, P. Lamberg, H. Papunen, A. Hattula, R. Pietilä, S. Elo, C. Ripis, E. Dimou, A. Apostolikas, M. Melakis, M. Economou-Eliopoulos, N. Vassilas, S. Perantonis, N. Ampazis, E. Charou, N. Gustavsson, M. Tiainen, M. Stefouli, D. Delfini, P. Venturini, G. Vouros, Y. Stavrakas and D. Katsoulas

**Author for correspondence. Outokumpu Mining Oy ,
P.O.Box 143, FIN-02201 Espoo, Finland .*



PROJECT FUNDED BY THE EUROPEAN COMMISSION
UNDER THE BRIT/ EURAM PROGRAMME

This report is a compilation of the following final GeoNickel reports and documents:

- Partners of the GeoNickel project
- Scientific and technical personnel of the GeoNickel project
- Summary report
- Synthesis report
- Exploitation report
- Final Technical Report Volume 1
- Final Technical Report Volume 2

Compiled by Jussi Aarnisalo and Markku Tiainen
16.6.2020

**INTEGRATED TECHNOLOGIES FOR MINERALS
EXPLORATION:
PILOT PROJECT FOR NICKEL ORE DEPOSITS**

GeoNickel

CONTRACT NO: BRPR-CT95-0052 (DG12 – RSMT)
PROJECT NO: BE-1117

Starting date: 02.01.1996 Duration: 36 months

COORDINATOR

OUTOKUMPU Mining Oy

P.O Box 27
02201 Espoo
Finland

PROJECT COORDINATOR: Antero Hakapää

ADMINISTRATIVE SCIENTIFIC OFFICIAL: Jussi Aarnisalo

Contact Person: Jussi Aarnisalo

Tel.: +358 9 4214235

Fax: +358 9 4214444

E-mail: jussi.aarnisalo@outokumpu.com

PARTNERS

LARCO

General Mining and Metallurgical Co, SA
20 Amalias Ave.
105 57 Athens
Greece

Contact Person: I. Kontos

Tel.: +30 1 3225018

Fax: +30 1 3237146

E-mail: larco@hol.gr

SOFTECO SISMAT S.p.A

Software Development Company
Via San Barborino, 7/82
16149 Genova
Italy

Contact Person: Enrico Morten

Tel.: +39 010 6457000

Fax: +39 010 412555

E-mail: enrico.morten@softeco.it

IRIS INSTRUMENTS S.A

1 Avenue Buffon
45060 Orleans, Cedex 2
France

Contact Person: Pierre Valla

Tel.: +33 2 38 638100

Fax: +33 2 38 638182

E-mail: irisins@ibm.net

GSF

Geological Survey of Finland
02150 Espoo
Finland

Contact Person: Heikki Soininen

Tel.: +358 40 544 9156

Fax: +358 20 55012

E-mail: heikki.soininen@gsf.fi

ASSOCIATED CONTRACTORS

BRGM

Bureau de Recherches Geologiques et Miniere
Avenue Claude Guillemin, B.P 6009
45060 Orleans, Cedex 2
France

Contact Person: Thierry Auge

Tel.: +33 2 38643526

Fax: +33 2 38643652

E-mail: b.bourgeois@brgm.fr

IGME

Institute of Geology and Mineral Exploration
70 Messoghion Str.
115 27 Athens
Greece

Contact Person: Dimitrios Eliopoulos

Tel.: +30 1 7798412

Fax: +30 1 7752211

E-mail: dkigme@compulink.gr

NCSR “Demokritos”

Institute of Informatics & Telecommunication

Aghia Paraskevi

153 10 Athens

Greece

Contact Person: Stavros Varoufakis

Tel.: +30 1 6503000

Fax: +30 1 6532175

E-mail: varou@iit.nrcps.ariadne-t.gr

SUBCONTRACTORS

University of Turku

Department of Geology

20500 Turku

Finland

Contact Person: Heikki Papunen

Tel.: +358 2 3335480

Fax: +358 2 3336580

E-mail: papunen@utu.fi

Athens University

Department of Geology

154 87, Athens,

Greece

Contact Person: Maria Ekonomou

Tel.: +30 1 7284214

Fax: +30 1 7284214

E-mail: meconom@atlas.uoa.gr

SCIENTIFIC AND TECHNICAL PERSONNEL OF THE *GeoNickel* PROJECT

NAME	ORGANISATION	WORKPACKAGES AND TASKS PARTICIPATED IN
Mäkelä, Kaarlo	Outokumpu Mining Oy	Administrative Scientific Official of the <i>GeoNickel</i> project in 1996
Aarnisalo, Jussi	Outokumpu Mining Oy	Administrative Scientific Official of the <i>GeoNickel</i> project in 1996 - 1998
Economou-Eliopoulos, Maria	Athens University	WP1 Task 3
Augé, Thierry	BRGM	WP1 Task 1
Bailly, Laurent	BRGM	WP1 Task 1
Bourgeois, Bernard	BRGM	WP2 Tasks 2.1, 2.2.2 and 2.3
Cocherie, Alain	BRGM	WP1 Task 1
Guerrot, Catherine	BRGM	WP1 Task 1
Lebert, François	BRGM	WP2 Task 2.3
Lerouge, Catherine	BRGM	WP1 Task 1
Elo, Seppo	Geological Survey of Finland	WP2 Task 2.1
Gustavsson, Nils	Geological Survey of Finland	WP3 WP4
Hongisto, Hannu	Geological Survey of Finland	WP2 Task 2.3
Lehtimäki, Jukka	Geological Survey of Finland	WP2 Task 2.1
Lerssi, Jouni	Geological Survey of Finland	WP2 Task 2.2.1
Luukkonen, Erkki	Geological Survey of Finland	WP5
Makkonen, Hannu	Geological Survey of Finland	WP5
Mononen, Risto	Geological Survey of Finland	WP2 Task 2.3
Oksama, Matti	Geological Survey of Finland	WP2 Task 2.3
Poikonen, Ari	Geological Survey of Finland	WP2 Task 2.3
Soininen, Heikki	Geological Survey of Finland	WP2 Tasks 2.1, 2.2.1, 2.2.2 and 2.3
Suppala, Ilkka	Geological Survey of Finland	WP3
Tiainen, Markku	Geological Survey of Finland	WP3 WP4 WP5 WP6 Task 6.2
Vanhala, Heikki	Geological Survey of Finland	WP2 Task 2.2.1
Jääskeläinen, Petri	Helsinki University of Technology	WP2 Task 2.4
Peltoniemi, Markku	Helsinki University of Technology	WP2 Task 2.4
Angelopoulos, Antonis	IGME	WP2 Tasks 2.1, 2.2.3-2.2.6 and 2.4 WP3 WP5 WP6 Task 6.2
Babalukas, Sotiris	IGME	WP2 Task 2.2.3-2.2.6
Dimou, Eleftheria	IGME	WP1 Task 3
Economou George	IGME	WP1 Task 3
Eliopoulos, Demetrios	IGME	WP1 Task 3 WP5 WP6 Task 6.2
Evangelos, Kyritsis	IGME	WP1 Task 3
Ioannidis, Spiros	IGME	WP2 Task 2.2.3-2.2.6

Klentos, Vasilios	IGME		WP2 Task 2.2.3-2.2.6					WP5 WP6 Task 6.2
Liontos, George	IGME		WP2 Task 2.2.3-2.2.6					
Markogiannakis, Evangelos	IGME		WP2 Task 2.2.3-2.2.6					
Nicolaidis, Michalis	IGME		WP2 Task 2.2.3-2.2.6					
Nikolaou, Sotiris	IGME		WP2 Task 2.2.3-2.2.6					
Noytsis, Vasilios	IGME		WP2 Task 2.2.3-2.2.6					WP5 WP6 Task 6.2
Pantelis, Grigoris	IGME	WP1 Task 3						
Perdikatsis, Vasilios	IGME	WP1 Task 3						
Photiadis, Adonis,	IGME	WP1 Task 3						
Rassios, Anna	IGME	WP1 Task 3						
Ripis, Costas	IGME	WP1 Task 3						WP4 WP5 WP6 Task 6.2
Stefouli, Martha	IGME						WP3	
Theodoridis, Theodoros	IGME		WP2 Task 2.2.3-2.2.6					
Tsailas, Panagiotis	IGME		WP2 Task 2.2.3-2.2.6					
Tsoyiannis, Anastasios	IGME		WP2 Task 2.2.3-2.2.6					
Abdelhadi, Abderraman	IRIS Instruments		WP2 Task 2.3					
Alayrac, Christophe	IRIS Instruments		WP2 Task 2.3					
Bernard, Jean	IRIS Instruments		WP2 Task 2.3					
Valla, Pierre	IRIS Instruments		WP2 Task 2.3					
Apostolikas, Athanasios	LARCO G.M.M.C	WP1 Task 3	WP2 Task 2.2.3-2.2.6			WP3 WP4 WP5 WP6 Task 6.2		
Maglaras, Costas	LARCO G.M.M.C	WP1 Task 3				WP4 WP5 WP6 Task 6.2		
Melakis, Michael	LARCO G.M.M.C	WP1 Task 3				WP3 WP4 WP5 WP6 Task 6.2		
Nikas, Ioannis	LARCO G.M.M.C		WP2 Task 2.2.3-2.2.6					
Pavliotis, Ioannis	LARCO G.M.M.C		WP2 Task 2.2.3-2.2.6					
Sigalas, Antonis	LARCO G.M.M.C		WP2 Task 2.2.3-2.2.6					
Alexandridis, Pavlos	LARCO/IGME		WP2 Task 2.2.3-2.2.6					
Triantafillou, Dimitrios	LARCO/IGME		WP2 Task 2.2.3-2.2.6					
Ampazis, Nikolaos	NCSR DEMOKRITOS					WP3		
Charou, Eleni	NCSR DEMOKRITOS					WP3		
Katsoulas. D	NCSR DEMOKRITOS						WP5	
Katzouraki, Maria	NCSR DEMOKRITOS						WP5	
Kokkotos, Stavros	NCSR DEMOKRITOS						WP5	
Koutras, C.	NCSR DEMOKRITOS						WP5	
Perantonis, Stavros J.	NCSR DEMOKRITOS					WP3		
Seretis, Constantine	NCSR DEMOKRITOS					WP3		
Spyropoulos, Costas	NCSR DEMOKRITOS						WP5	
Stavrakas. Y	NCSR DEMOKRITOS						WP5	

Tsenoglou, Theoharis	NCSR DEMOKRITOS		WP3				
Varoufakis, Stavros J.	NCSR DEMOKRITOS		WP3				
Vassilas, Nikolaos	NCSR DEMOKRITOS		WP3				
Virvilis, Vassilis	NCSR DEMOKRITOS		WP3				
Vouros, George	NCSR DEMOKRITOS				WP5		
Aarnisalo, Jussi	Outokumpu Mining Oy		WP3	WP4	WP5	WP6	Task 6.2
Grundström, Leo	Outokumpu Mining Oy				WP5	WP6	Task 6.2
Hattula, Aimo	Outokumpu Mining Oy	WP2	Tasks 2.1, 2.2.1, 2.2.2, 2.3 and 2.4			WP5	
Ilvonen, Erkki	Outokumpu Mining Oy				WP5		
Jokela, Jukka	Outokumpu Mining Oy					WP6	Task 6.2
Kokkola, Martti	Outokumpu Mining Oy				WP5		
Lahtinen, Jarmo	Outokumpu Mining Oy				WP5	WP6	Task 6.2
Lehtonen, Tapio	Outokumpu Mining Oy	WP2	Tasks 2.1, 2.2.1 and 2.2.2				
Mäkelä, Kaarlo	Outokumpu Mining Oy	WP1	Task 1			WP5	
Ojalainen, Jukka	Outokumpu Mining Oy					WP6	Task 6.2
Pietilä, Risto	Outokumpu Mining Oy	WP2	Tasks 2.2.2, 2.3 and 2.4			WP5	WP6 Task 6.2
Sandgren, Eero	Outokumpu Mining Oy	WP2	Tasks 2.1, 2.2.1, 2.3 and 2.4				
Välimaa, Jukka	Outokumpu Mining Oy					WP6	Task 6.2
Lamberg, Pertti	Outokumpu Research	WP1	Task 1			WP4	WP5 WP6 Task 6.2
Liipo, Jussi	Outokumpu Research	WP1	Task 1				
Ylander, Iikka	Outokumpu Research	WP1	Task 1				
Boero, Marco	SOFTECO				WP4		
Defini, Davide	SOFTECO				WP4	WP5	
Morten, Enrico	SOFTECO				WP4	WP5	
Venturini, Paolo	SOFTECO				WP4	WP5	
Hjelt, Sven-Erik	University of Oulu	WP2	Task 2.2.2				
Pirttijärvi, Markku	University of Oulu	WP2	Task 2.2.2				
Halkoaho, Tapio	University of Turku	WP1	Task 2			WP5	
Liimatainen, Jyrki	University of Turku	WP1	Task 2			WP5	
Papunen, Heikki	University of Turku	WP1	Task 2			WP5	

SUMMARY REPORT
FOR PUBLICATION

SYNTHESIS REPORT
FOR PUBLICATION

EXPLOITATION REPORT
~~CONFIDENTIAL~~

CONTRACT NO: BRPR-CT95-0052 (DG12 - RSMT)

PROJECT NO: BE-1117

TITLE: Integrated Technologies for Minerals Exploration,
Pilot Project for Nickel Ore Deposits
GeoNickel

PROJECT
COORDINATOR: OUTOKUMPU Outokumpu Mining Oy
Finland

PARTNERS: LARCO General Mining and Metallurgical Company
SA, Greece
BRGM Bureau de Recherches Géologiques et Minières
France
GSFIN Geological Survey of Finland
Finland
SOFTECO Softeco Sismat Srl
Italy
IGME Geological Survey of Greece
Greece
IRIS Iris Instruments SA
France
NCSR National Center of Scientific Research
'Demokritos', Greece

STARTING DATE: 1st January 1996 DURATION: 36 MONTHS



PROJECT FUNDED BY THE EUROPEAN
COMMISSION UNDER THE BRITE/EURAM
PROGRAMME

Date: February 28, 1999

GeoNickel

SUMMARY REPORT

FOR PUBLICATION

SUMMARY REPORT

FOR PUBLICATION

CONTRACT NO: BRPR-CT95-0052 (DG12 - RSMT)

PROJECT NO: BE-1117

TITLE: Integrated Technologies for Minerals Exploration,
Pilot Project for Nickel Ore Deposits
GeoNickel

PROJECT

COORDINATOR: OUTOKUMPU Outokumpu Mining Oy
Finland

PARTNERS: LARCO General Mining and Metallurgical Company
SA, Greece
BRGM Bureau de Recherches Géologiques et Minières
France
GSFIN Geological Survey of Finland
Finland
SOFTECO Softeco Sismat Srl
Italy
IGME Geological Survey of Greece
Greece
IRIS Iris Instruments SA
France
NCSR National Center of Scientific Research
'Demokritos', Greece

STARTING DATE: 1st January 1996 DURATION: 36 MONTHS



PROJECT FUNDED BY THE EUROPEAN
COMMISSION UNDER THE BRITE/EURAM
PROGRAMME

Date: February 28, 1999

CONTENTS

1.	Partnership.....	3
2.	Objectives and the work content	4
3.	Technical description	5
4.	Results and conclusions	6
5.	Collaboration sought	8
6.	Exploitation plans and anticipated benefits	8
7.	Keywords	8
8.	Names and addresses of the coordinator and other partners, and project reference numbers	8

SUMMARY REPORT

INTEGRATED TECHNOLOGIES FOR MINERALS EXPLORATION; PILOT PROJECT FOR NICKEL ORE DEPOSITS

GeoNickel

1. PARTNERSHIP

The availability of nickel, a strategic metal for the European industry, is a key factor for the industrial competitiveness and economic growth as well as for future development of high technology and advanced process industry. Annual consumption of nickel in the European countries in 90's has been well over one third of the world total consumption, but the regional nickel resources of Western Europe are insignificant. All measures to correct this imbalance are of vital importance in order to secure the nickel raw material base for European industry on a long-term basis and even under unexpected circumstances which may necessitate a high degree of self-sufficiency in raw materials. This should justify intense exploration for new nickel ore deposits as well as research and re-evaluation of known but uneconomic ones.

A prerequisite for successful mineral exploration is the understanding of the geology, mineralogy, geochemistry and geophysics of the ore deposits and ore-forming processes. This facilitates the development of novel, innovative exploration tools – instruments and software – for enhancing the effectiveness and success rate of nickel exploration projects.

The need of more effective tools for nickel exploration caused Outokumpu Metals and Resources Oy (later, Outokumpu Mining Oy) of Finland and General Mining and Metallurgical Company S.A LARCO of Greece, the European nickel producers, to join forces. Consequently a consortium was established consisting the above mentioned and the following companies: Softeco Sismat S.p.A. of Italy, expert in computer sciences, Iris Instruments of France, an instrumentation company, and the following research institutes: Geological Survey of Finland, BRGM of France, IGME of Greece, and the Institute of Informatics and Telecommunications of the National Center for Scientific Research (NCSR, Demokritos), Greece.

From the beginning of 1996 this consortium launched a three-year project named Integrated Technologies for Minerals Exploration, Pilot Project for Nickel Ore Deposits (acronym GeoNickel), supported by the European Commission under the Brite/EuRam Programme. The project was completed on December 31, 1998.

2. OBJECTIVES AND THE WORK CONTENT

The overall objectives of GeoNickel were to enhance geological and geophysical knowledge on nickel ore deposits, and to develop novel, integrated exploration methods and tools. Generally, such exploration methods are of generic nature and can be applied to a variety of base metals deposits other than the “nickel family” (Ni, Co, Cu and PGE).

To meet the objectives, three key areas of methodology in nickel ore exploration were selected for research and development:

- *Modelling the nickel deposits:* Development of models of ore-forming processes in mafic and ultramafic rocks to enhance the exploration of associated nickel ore deposits in various geotectonic environments. The work covered sulphide and laterite deposits.
- *Development of geophysical technology:* Improvement of the efficiency of regional and detailed geophysical exploration methods by developing prototype instrumentation (GPS-gravity system and 3D-Borehole hole EM system) and software. Emphasis was laid on measurement and interpretation tools in electric and electromagnetic exploration - especially a wide-band drill-hole and ground EM system, and spectral IP.
- *Geoscientific Information System (GEOSIS):* An integrated software system including innovative classification methods, GIS and novel Knowledge Based System based on the modelling of nickel deposits as well as on geological, geophysical, remote sensing and other data stored in geographic information system (GIS) database.

Due to the complexity of the geological, geophysical and information technology tools to be developed, the project was divided into six WorkPackages (WP) shown in the following table.

WP1 Mineralogy and modelling of Ni ore deposits Intrusion-related Ni sulphide deposits Extrusion-related Ni sulphide deposits Lateritic Ni deposits	WP2 Development of geophysical technology GPS-gravity system On-site ground surveys 3-component borehole EM methods Petrophysical database
WP3 Image processing/pattern recognition Data acquisition, quality evaluation Image processing Classification of lithology and alterations Delineation of lineaments using ANN Comparison of techniques	WP4 GEOSIS design and GIS tools development Requirements analysis GEOSIS application design Implementation of prototype GIS Development of tools Integration, validation, testing
WP5 Knowledge Based System Knowledge elicitation Design of Knowledge Based System Validation, testing, refinements	WP6 Final integration and testing Integration of GEOSIS and Knowledge Based System Validation, testing Refinements Field testing

3. TECHNICAL DESCRIPTION

WP1 developed geological, lithogeochemical, mineralogical and petrological models and tools for nickel exploration in three geological environments: sulphidic nickel related to mafic and ultramafic intrusions, sulphidic nickel related to komatiitic and picritic volcanics, and lateritic nickel. A data processing tool, Advanced Petrological Explorer (APE), was developed for intrusion-related deposits, and lithogeochemical, mineralogical, and isotope and REE chemistry tools were developed for discriminating barren and fertile intrusions. An extensive literature study was applied to define the features positive for nickel sulphide exploration in komatiitic lavas and cumulates. Potential indicators for sulphides were identified and descriptive models were created for nickel sulphide ore formation in different field target areas where the ore potential of preferred lava pathways were indicated. The Lokris and Vermion areas were selected for laterite deposit case studies. Six targets represented three different cases: in situ Ni-laterite deposits, transported Ni-laterite deposits, and bauxitic laterite deposits. Process models for ore formation were established based on existing and new geological data as well as mineralogical and lithogeochemical studies. The laterite models were combined with geophysical and image processing data from the studied nickel deposits and their host environment. Integrated data processing methods were developed for exploration and target selection.

WP2 developed and improved geophysical methods for nickel exploration. On regional scale, GPS elevation measurements and digital gravity measurements were combined to obtain accurate and cost-effective regional gravity surveying. On site scale, Spectral IP was applied; in particular specific measurement procedures were developed. Software was developed for fast interpretation of ground EM methods. For lateritic Ni, field-tests were done with existing geophysical methods to detect, map and outline lateritic Ni-Fe deposits. On deposit scale, cross-hole (tomography) and single-hole (borehole Slingram) EM methods with 3-component borehole probes were developed for locating off-hole targets and outlining intersected orebodies. Prototype equipment was designed for slim exploration boreholes, completed with processing and interpretation software, methodology and field tests. With the objective of serving the above applications, a petrophysical database for Ni deposits and host-rocks was compiled including statistical analysis for the correlation of mineralogical and petrological parameters.

WP3 developed advanced image processing, classification and pattern recognition techniques that can be used to locate geological features related to nickel ore deposits. Two software prototypes, ANNGIE (Artificial Neural Networks for Geological Information Extraction) and ASM (Advanced Statistical Methods), were developed. ANNGIE comprises algorithms and methods originating from neural networks and fuzzy processing to carry out classification. A selection of supervised and unsupervised methods is provided as well as a module that can combine results from different classifiers. A module was incorporated to locate linear structures (lineaments). ASM is also used for classification and employs advanced methods of statistical nature. A wide selection of supervised classification methods is provided. Algorithms for efficiently performing Discriminant Analysis (DA) are incorporated in this module, including Empirical DA, Linear DA, Quadratic DA, Flexible DA and Penalised DA. The GeoNickel partners, using satellite, geological and geophysical data from selected areas in

Finland and Greece, evaluated ANNGIE and ASM.

WP4 focused on the development of a geo-scientific information system, GEOSIS, which supports the management and analysis of the complex datasets used in nickel exploration. It integrates the advanced analysis tools developed in the other WorkPackages. GEOSIS is based on software environments available on market at low cost: the operating system is Windows, database ORACLE and GIS MapInfo. All of the GIS and data management functions available in the software environments used, as well as the other software analysis modules developed in the project (the expert system, neural network classification methods, and advanced statistical methods) were included in GEOSIS. Final tests were performed on real data from Finland and Greece.

WP5 developed GEOES, a knowledge-based expert system, to facilitate and promote the process of identifying nickel ore deposits. The advantage of GEOES is its ability to process quantities of geo-data in batch mode, and to produce results that embody expert opinions, in a fraction of time compared with computations performed with hand. At the heart of GEOES, there is the knowledge base and inference engine. The former keeps estimations and facts that reflect the knowledge and experience of geo-experts in a formal, organised fashion. The latter is a software module able to apply the knowledge base to input data and draw conclusions. GEOES handles geological models for komatiite, intrusive and laterite deposits. For each model, there are stages, namely «explore area», «identify potential zones» and «select target», that cover the entire exploration process. For each stage, there is a set of factors and sub-factors that can be assigned values. GEOES, through GEOSIS tools, provides graphic presentations for the overall results.

WP6 combined GEOSIS, GEOES, ANNGIE and ASM software prototypes into an integrated geoscientific software system using GEOSIS as user interface. Further, GEOES was tested and validated in Finland for intrusive and komatiitic nickel deposit environments, and for lateritic environment in Greece. APE software, developed in WP1, was also tested and used extensively in the study of mafic and ultramafic rocks in the Finnish test areas. Software problems encountered in GEOES and GEOSIS during the tests were solved and corrected by the software developers, and new versions of prototype GEOSIS and GEOES were delivered to the end user partners.

4. RESULTS AND CONCLUSIONS

The models and software prototypes developed in GeoNickel WorkPackages were tested by the end user partners with actual exploration data, and the novel geophysical instrument prototypes were tested in the field in France, Greece and in Finland. All of the WorkPackages met their goals in time, and the overall objectives of the project were achieved. A Final Report was prepared.

Models were developed for nickel ore-forming processes in intrusive, komatiitic/picritic and lateritic environments. Automated Petrological Explorer (APE) software is an innovative result developed for rapid and comprehensive analysis and modelling of litho-geochemical and mineralogical data for mafic-ultramafic intrusions but is also applicable to extrusions.

The development of geophysical technology resulted in a novel instrumentation prototype: versatile equipment for 3-component downhole electromagnetic measurements. An integrated GPS-gravity system was created for regional and local gravity surveys. Models and interpretation software were compiled for the spectral IP method, the frequency domain ground EM systems and 3-component borehole FEM data. A database for the petrophysical parameters of nickeliferous lithologies and deposits in magmatic and lateritic environments was established to support geophysical exploration.

Two software packages were developed to enhance the processing of multisource (geophysical, geochemical, satellite, etc.) data for locating geological features related to nickel ore deposits. One is focused on advanced statistical methods (ASM), the other on new pattern classification and image processing techniques involving neural network analysis approach (ANNGIE).

A Geoscientific Information System (GEOSIS) was developed for the management and processing of the vast variety of explorational data as well as maps and images (geological, geophysical, geochemical and other scientific data) which are currently used in mineral exploration. GEOSIS comprises two commercially available database and GIS applications, Oracle and MapInfo Professional, linked together with data management, interface and advanced GIS-function modules developed in GeoNickel. GEOSIS also serves as user interface for the integrated use of the ANNGIE and ASM modules, and the Knowledge Based System (GEOES).

GEOES embodies the knowledge of geoscientists specialized in nickel ore exploration and aims to facilitate the processes performed in its different phases. It is an expert system with a user-friendly interface, integrated within GEOSIS, emphasizing the combination of different approaches in nickel exploration and covering geological models for intrusive, komatiitic and lateritic deposits. It provides assistance during area selection, identification of potential zones, and target selection and can be run either in interactive, spatial, or hybrid mode, each one having a different role. GEOES was successfully validation-tested.

Tests on the Intrusive and Komatiitic, and on the Lateritic exploration models in Finland and in Greece, respectively, showed good results, corresponding well to those obtained using conventional exploration methodologies. In general GEOES is an interesting exploration tool for the area selection, identification of potential zones, and target selection exploration phases, covering and compiling explorational data from diverse origin (geology, geophysics, mineralogy and geochemistry). One of the powers of the GEOES Expert System is the systematic approach needed from the data acquisition to the output of results. It gives the exploration staff a good opportunity to systematically examine all of the available data, estimate its homogeneity and validity, showing where more information is required for well-balanced reasoning results. Ultimately, the most important feature in using such an expert system may be the fact that it forces different specialists in an exploration team to work more closely and coherently, enhancing the strengths of teamwork in mineral exploration.

Nickel exploration was the primary target of the project; however, most of the developed instruments and software are of generic nature. Consequently they can be applied to the explo-

ration of a variety of base metals deposits related to magmatic or even sedimentary rocks in various geotectonic environments.

5. COLLABORATION SOUGHT

Generally, the partners plan to use the products developed in GeoNickel inhouse; however, SOFTECO is seeking collaboration for the further development and eventual marketing of GEOSIS and the integrated GEOES, ANNGIE and ASM software.

6. EXPLOITATION PLANS AND ANTICIPATED BENEFITS

SOFTECO is planning to develop and commercialise a set of software packages: GEOSIS and the integrated GEOES, ANNGIE and ASM software. Further action includes investment estimate and risk analysis, market analysis and definition of the market policy, definition of patent and licensing policy, and, within two years, further development of the products. The benefits include financial income in a new market sector as well as the enlargement of SOFTECO's market opportunities and presence in the international market.

The objective of IRIS Instruments is to market worldwide the borehole EM system developed in GeoNickel. The action planned for 1999 includes further field testing in Finland and a field demonstration in Canada and/or Australia. The benefits include the enlargement of products offering, the further development of a high technology and innovative corporate image, and an increase in turnover and margins.

7. KEYWORDS

Nickel, exploration, modelling, geophysics, software, expert system

8. NAMES AND ADDRESSES OF THE COORDINATOR AND OTHER PARTNERS, AND PROJECT REFERENCE NUMBERS

Coordinator	Outokumpu Mining Oy P.O.Box 143, FIN-02201 Espoo, Finland Tel.: +358-9-4212647, fax: +358-9-4212403 E-mail: antero.hakapaa@outokumpu.fi
Partner 2	General Mining and Metallurgical Company S.A. 20 Amalias Ave., GR-105 57 Athens, Greece Tel.: +30-1-3225018, fax: +30-1-3237146 E-mail: larco@mai.hol.gr

Partner 3	Softeco Sismat Srl Via San Barborino 7/82, 16149 Genova, Italy Tel.: +39-10-6457000, fax: +39-10-412555 E-mail: enrico.morten@softeco.it
Partner 4	Iris Instruments S.A. 1, Avenue Buffon, 45060 Orleans, Cedex 2, France Tel.: +33-2-38 638100, fax: +33-2-38 638182 E-mail: irisins@ibm.net
Partner 5	Geological Survey of Finland FIN-02150 Espoo, Finland Tel.: +358-40-544 9156, fax: +358-2055012 E-mail: heikki.soininen@gsf.fi
Associate Contractor	Bureau de Recherches Geologiques et Minieres Avenue Claude Guillemin, B.P 6009 45060 Orleans, Cedex 2, France Tel.: +33-2-38643526, fax: +33-2-38643361 E-mail: b.bourgeois@brgm.fr
Associate Contractor	Institute of Geology and Mineral Exploration 70 Messoghion Str., GR-115 27 Athens, Greece Tel.: +30-1-7798412, fax: +30-1-7752211 E-mail: dkigme@compulink.gr
Associate Contractor	National Center for Scientific Research Aghia Paraskevi, GR-153 10557 Athens, Greece Tel.: +30-1-6503000, fax: +30-1-6532175 E-mail: varou@iit.nraps.ariadne-t.gr
Subcontractor	University of Turku, Department of Geology FIN-020500 Turku, Finland Tel.: +358-2-3335480, fax: +358-2-3336580 E-mail: papunen@utu.fi
Subcontractor	Athens University, Department of Geology GR-154 87 Athens, Greece Tel.: +30-1-7284214, fax: +30-1-7284214 E-mail: meconom@atlas.uoa.gr
Contract number	BRPR-CT95-0052 (DG12-RSMT)
Project number	BE-1117

GeoNickel

SYNTHESIS REPORT

FOR PUBLICATION

SYNTHESIS REPORT

INTEGRATED TECHNOLOGIES FOR MINERALS EXPLORATION; PILOT PROJECT FOR NICKEL ORE DEPOSITS

FOR PUBLICATION

CONTRACT NO: BRPR-CT95-0052 (DG12 - RSMT)
PROJECT NO: BE-1117

TITLE: Integrated Technologies for Minerals Exploration,
Pilot Project for Nickel Ore Deposits
GeoNickel

PROJECT

COORDINATOR: OUTOKUMPU Outokumpu Mining OY Finland
PARTNERS: LARCO General Mining and Metallurgical Company
SA, Greece
BRGM Bureau de Recherches Géologiques et
Minières, France
GSFIN Geological Survey of Finland, Finland
SOFTECO Softeco Sismat Srl, Italy
IGME Geological Survey of Greece, Greece
IRIS Iris Instruments SA, France
NCSR National Center of Scientific
Research 'Demokritos', Greece

STARTING DATE: 1st January 1996 DURATION: 36 MONTHS



PROJECT FUNDED BY THE EUROPEAN
COMMISSION UNDER THE BRITE/EURAM
PROGRAMME

Date: February 28, 1999

INTEGRATED TECHNOLOGIES FOR MINERALS EXPLORATION; PILOT PROJECT FOR NICKEL ORE DEPOSITS

CONTENTS:

Abstract.....	3
1. Introduction and Objectives.....	3
2. Summary of the Work Content.....	4
3. Description and Results of the Research Work Conducted	6
3.1. WorkPackage 1, Mineralogy and modelling of Ni Ore deposits.....	6
3.2. WorkPackage 2, Development of geophysical technology.....	12
3.3. WorkPackage 3, Image processing/pattern recognition.....	18
3.4. WorkPackage 4, The Geoscientific Information System (GEOSIS).....	22
3.5. Workpackage 5, The GEOES Knowledge-Based System.....	24
Discussion.....	28
References.....	30
Addresses.....	30

INTEGRATED TECHNOLOGIES FOR MINERALS EXPLORATION; PILOT PROJECT FOR NICKEL ORE DEPOSITS

J. Aarnisalo^{*}, K. Mäkelä, B. Bourgeois, C. Spyropoulos, S. Varoufakis, E. Morten, K. Maglaras, H. Soininen, A. Angelopoulos, D. Eliopoulos, P. Lamberg, H. Papunen, A. Hattula, R. Pietilä, S. Elo, C. Ripis, E. Dimou, A. Apostolikas, M. Melakis, M. Economou-Eliopoulos, N. Vassilas, S. Perantonis, N. Ampazis, E. Charou, N. Gustavsson, M. Tiainen, M. Stefouli, D. Delfini, P. Venturini, G. Vouros, Y. Stavrakas and D. Katsoulas

**Author for correspondence. Outokumpu Mining Oy,
P.O.Box 143, FIN-02201 Espoo, Finland.*

ABSTRACT

The overall objectives of the GeoNickel project were to enhance geological and geophysical knowledge on nickel ore deposits, and to develop novel, integrated exploration methods and tools for the European base metals industry. The developed technologies aim at enhancing the success potential in the exploration of sulphide and laterite nickel ore deposits. The research and development work concentrated on three main areas: 1) modelling of nickel ore deposits in intrusive, komatiitic/picritic and lateritic environments, 2) development of geophysical prototype instrumentation and software, and 3) development of Geoscientific Information System (GEOSIS) including database and GIS functionality, integrated with an expert system for nickel exploration, and with software packages for advanced statistical methods and ANN based pattern classification/image processing techniques. GeoNickel started in the beginning of 1996 and was completed at the end of 1998. Final tests on the developed geological models, instrumentation and software were encouraging, and the overall objectives of the project were achieved. Most of the developed instruments and software can be applied to a great variety of base metals deposits other than the "nickel family" (Ni, Co, Cu and PGE) and used to aid the exploration of ore deposits genetically related to magmatic or sedimentary rocks in various geotectonic environments.

1. INTRODUCTION AND OBJECTIVES

The availability of nickel, a strategic metal for the European industry, is a key factor for the industrial competitiveness and economic growth as well as for the future development of high technology and advanced process industry. Annual consumption of nickel in the European countries in 90's has been well over one third of the world total consumption, but the regional nickel resources of Western Europe are insignificant. All measures to correct this unbalance are of vital importance in order to secure the nickel raw material base for European industry

on a long-term basis and even under unexpected circumstances which may necessitate a high degree of self-sufficiency in raw materials. This should justify intense exploration for new nickel ore deposits as well as research and re-evaluation of known but uneconomic ones.

Despite decades of exploration, Archaean and Proterozoic areas of northern Europe can still be considered potential for discoveries of new sulphide nickel ore deposits and subsequent mining. However, the existing exploration methods are not effective enough to unearth the resources; the ore potential of deep levels, in particular, has remained unresolved. On the other hand, in Greece the geological formations potential for laterite nickel deposits have not yet been adequately explored. Existing information points to a strong possibility that some of these formations host large nickel ore deposits.

The first prerequisite for successful mineral exploration is adequate understanding of the geology, mineralogy, geochemistry and geophysics of the ore deposits and of the ore-forming processes. This facilitates the possibilities for developing novel, innovative exploration tools – both instruments and software – for enhancing the effectiveness and success rates of the exploration projects.

The need for more effective exploration tools in nickel exploration caused Outokumpu Metals and Resources Oy and General Mining and Metallurgical Company S.A LARCO, the two European nickel producers, to join forces in a consortium with a computer science expert (SOFTECO SISMAT S.p.A., Italy), an instrumentation company (IRIS INSTRUMENTS, France), and with research organisations (National Geological Surveys of Finland (GSF), France (BRGM) and Greece (IGME), and the Institute of Informatics and Telecommunications of the National Center for Scientific Research (NCSR , “DEMOKRITOS”), Greece).

At the beginning of 1996 this consortium launched a three-year project called Integrated technologies for minerals exploration; pilot project for nickel ore deposits (acronym GeoNickel), supported by the European Commission (Brite-EuRam III No BE-1117). The project ended successfully in December 31, 1998. The general description of the project, its objectives and planned research work as well as exploitation plans were discussed in the proceedings of the first annual Eurothen workshop (Eliopoulos et al. 1998) and hence will not be repeated here in detail.

The overall objectives of GeoNickel were to enhance the geological and geophysical knowledge on nickel ore deposits, and to develop novel, integrated exploration methods and tools for the European base metal industry. Exploration methods of generic nature, that have been the focus of this project, apply also to a great variety of base metals deposits other than the "nickel family" (i.e. Ni, Co, Cu and PGE), and can be more generally applied to any ore concentration genetically related to magmatic rocks.

2. SUMMARY OF THE WORK CONTENT

To meet the overall objectives of the project, three key areas of methodology in nickel ore exploration were selected for research and development work:

- *Modelling the nickel deposits*: development of models of ore-forming processes in mafic and ultramafic rocks for to enhance exploration of associated Ni(-Cu-Co-PGE) ores in

various geotectonic environments. The work covered both sulphide and laterite nickel deposits. Special emphasis was laid on mineralogy because it is an important factor in ore beneficiation and the key indicator of ore-forming processes

- *Development of geophysical technology*: improvement of the efficiency of several geophysical methods, for both regional and detailed exploration, by developing prototype instrumentation and software. Emphasis was laid on designing an integrated GPS-gravity system, and on various measurement and interpretation tools in electric and electromagnetic exploration methods - especially a wide-band drill-hole and ground EM system, and spectral IP
- *Geoscientific Information System (GEOSIS)*: development of a Knowledge Based System based on the modelling of nickel deposits, as well as on geological, geophysical and other data stored in geographic information system (GIS) database and on remote sensing data processed with innovative image processing/pattern recognition techniques. This integrated software system could act as a focal point for the active co-operation between experts of different backgrounds in effective nickel ore exploration.

Due to the complexity of the geological, geophysical and information technology tools to be developed for nickel exploration, the project was divided into six WorkPackages. These are shown in the following list that also states the main areas of research and development, i.e. Tasks, for each WorkPackage (WP).

WP1 Mineralogy and modelling of Ni ore deposits Intrusion related Ni sulphide deposits Extrusion related Ni sulphide deposits Lateritic Ni deposits	WP2 Development of geophysical technology GPS-gravity system On-site ground surveys 3-component borehole EM methods Petrophysical database
WP3 Image processing/pattern recognition Data acquisition, quality evaluation Image processing Classification of lithology and alterations Delineation of lineaments using ANN Comparison of techniques	WP4 GEOSIS design and GIS tools development Requirements analysis GEOSIS application design Implementation of prototype GIS Development of tools Integration, validation, testing
WP5 Knowledge Based System Knowledge elicitation Design of Knowledge Based System Validation, testing, refinements	WP6 Final integration and testing Integration of GEOSIS and Knowledge Based System Validation, testing Refinements Field testing

Each WorkPackage and different Tasks were led by one of the participating organisations and most of them were conducted jointly by several of the consortium partners, Outokumpu Metals and Resources Oy being the overall co-ordinator of the GeoNickel project.

3. DESCRIPTION AND RESULTS OF THE RESEARCH WORK CONDUCTED

Due to the structure of the Geonickel project, derived from the complexity of the geological, geophysical and information technology tools to be developed for Ni exploration, the results of each WorkPackage are presented separately. In the following the work conducted and results obtained in testing the developed prototype instrumentation, software and models are briefly described.

3.1. WorkPackage 1, Mineralogy and modelling of Ni ore deposits

3.1.1. Task 1.1: Mineralogy and modelling of nickel sulphide deposits related to mafic and ultramafic intrusions

The objective of WP1.1 was to develop geological, litho-geochemical, mineralogical and petrological models and tools for the purpose of discriminating nickel sulphide ore-bearing intrusions from barren ones and to locate Ni sulphide deposits within intrusions or their surroundings. For that purpose, nine selected case intrusions were studied, a data processing flowsheet was analysed and a computer program was built to automatize most of the routines. Therefore, WP1.1 possesses two levels of results. First involves a theoretical-empirical approach comprising the knowledge of Ni sulphide ore-forming processes and their identification methods. Second is a practical one, i.e., a 32-bit Windows program “Automated Petrological Explorer” (APE) which includes techniques and tools needed in applying litho-geochemistry and mineralogy to Ni sulphide ore exploration.

The case studies and literature reviews indicated that the following processes and requirements must be met in the formation of Ni sulphide ore:

1. A primitive magma (i.e., a magma rich in Ni and MgO).
2. A sulphide undersaturated magma.
3. A mechanism leading to sulphide saturation.
4. Depression structures which trap and enrich the sulphides.
5. A continued magma flow.

The magma primitivity may not be of great importance; Ni sulphide ore was formed within the Laukunkangas case study intrusion where the MgO content of magma was c. 10% (78% forsterite component in olivine). However, the primitivity of magma (more specifically, the Ni content) determines the quality of the ore (i.e. the Ni content of the sulphide phase).

The magma should be sulphide undersaturated but close to saturation when intruding. Sulphide saturation prior to intrusion is demonstrated in two case intrusions, Posionlahti and Porrasniemi (Finland), which are depleted in Ni, and the sulphide enrichments related to these intrusions are small and of poor quality (low Ni tenor). All of the three intrusions that host Ni ore deposits (Bruvann (Norway), Laukunkangas, and Stormi (Finland)), are depleted in PGE referring to magmas which were close to, and even reached, sulphide saturation in the deeper levels of the crust. Moreover, the whole cumulus sequence of Ni ore-hosting intrusions is relatively rich in sulphides (the non-ore samples average >2% total sulphides) which feature indicates that the systems remained in sulphide saturation through the whole crystallisation sequence.

A key process in Ni sulphide ore formation is the mechanism leading to sulphide saturation. In all of the Ni ore cases studied it appeared to be a favourable crustal contamination. Graphite- and sulphide-bearing black schists were favourable contaminants in at least two of the cases studied (Bruvann and Laukunkangas). This is evidenced by the following observations. Massive and disseminated ores (also within the intrusion and relatively far from contact) contain graphite; black schist inclusions exist in or close to the ore; ore (like black schist) is relatively rich in vanadium; black schists exist in direct contact with intrusions and ore. A feature common to all of the ore-hosting intrusion is also that orthopyroxene predominates over clinopyroxene, due to contamination of magma by country rocks rich in SiO₂.

A barren case study intrusion, Alter do Chao (Portugal), showed that contamination alone is not sufficient to form Ni sulphide ore, and that the quality of the contaminant is an important matter. There, a relatively primitive sulphide undersaturated magma (14.5% MgO), which formed an olivine and orthopyroxene rich core, was contaminated by limestones producing hornfels at the contact zone, and an outer zone rich in clinopyroxene and plagioclase. However, significant sulphide segregation did not take place, consequently the intrusion is exceptionally poor in sulphides due to an unfavourable contaminant (rich in CaO without reducing sulphide dissolution capacity) and the magma did not reach sulphide saturation.

The requirement for a depression structure and continued magma flow is fulfilled in all the Ni ore hosting case study intrusions. At Bruvann, Laukunkangas and Stormi the ore is hosted (at least partly) by the most primitive olivine mesocumulates lying in contact with country rocks. In a subeconomic intrusion, Rörmyrberget (Sweden), the trap is missing, consequently sulphide enrichment took place in the central parts of the intrusion within more evolved orthopyroxene(-olivine) cumulates.

The lithochemical and mineralogical data processing in sulphide Ni ore exploration is divided into four stages: 1) the processing of sample data, 2) the processing of target (intrusion) data, 3) the modelling and refining of the target data, and 4) the determination of target key figures. The key figures include: a) the chemical composition of parental magma, b) crystallisation series, c) the internal structure of the intrusion, d) contamination features, e) sulphide segregation features, and f) open vs. closed system. The magmatic history of the target (i.e. recharge-assimilation-eruption-crystallisation-accumulation events vs. time) is summarised in the figures and tells whether a particular target is fertile or barren of Ni sulphides.

The APE program (Figure 1) was designed and built for the purpose of fast data processing and reliable interpretation. APE concentrates on the thorough use of whole rock analyse data. Since the need diminishes for costly thin section microscope work as well as trace element and mineral analyses, significant reductions in cost and time are achieved. APE is GEOSIS compatible (cf. WP4) and it works upon a database, which makes the program capable of handling fast large amount of data. APE also includes quick-access reference databases that can be upgraded by user. In addition to common calculation methods (such as CIPW norms) APE includes some novel routines for single sample calculations from whole rock analyses:

- The cumulus naming procedure gives a reliable cumulus name for the rock.
- The mineral calculation routine estimates the Mg/(Mg+Fe) ratio and Ni content of mafic silicates (olivine and pyroxenes) within required precision.
- The volatile and sulphide free calculation routine reveals essential features in Ni sulphide ore host rocks.

3.1.2. Task 1.2: Mineralogy and modelling of Ni sulphide deposits in komatiitic/picritic extrusives

The programme conducted at the Department of Geology, University of Turku, Finland, was aimed to study the geological and geochemical features of extrusive komatiites and picrites which indicate potential for sulphide nickel ore formation. The extrusive Ni deposits are directly related to volcanic processes and are related to the high-Mg Archaean ultramafic komatiites and komatiitic basalts or moderately Mg-rich Proterozoic komatiites, (ferro)picrites and basalts. Due to extrusive environment the volcanic-hosted Ni sulphide deposits differ from those associated with intrusive rocks, and the main differences arise from the more open igneous system of extrusives, their extremely high temperatures, dynamics of the magma flow and low surface pressures. Physico-chemical rules and formulas applied for sulphide-silicate melt systems are common for extrusive and intrusive deposits and certain mathematical treatments can be applied for both types, but the coefficients vary and the final results are different.

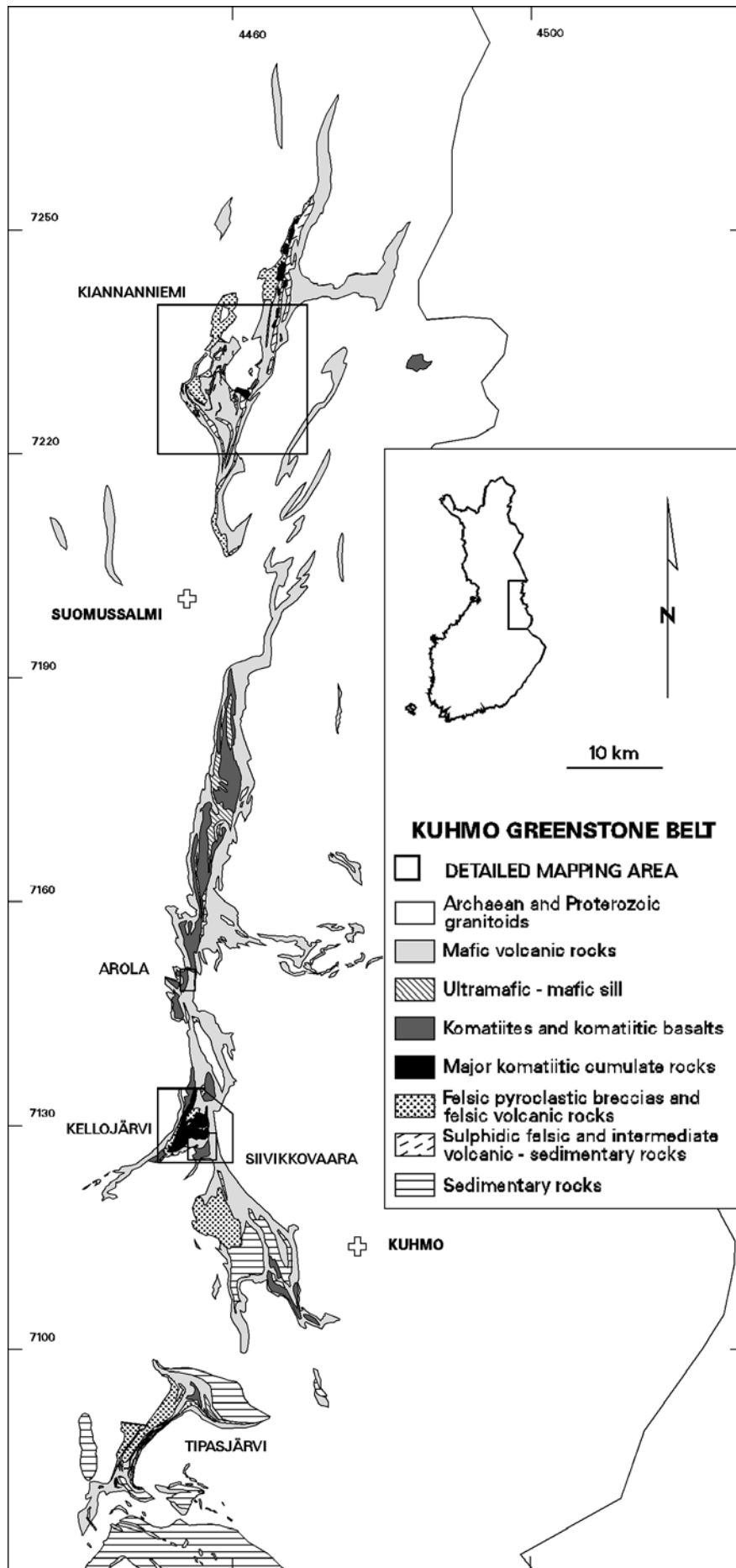
The work programme constituted a compilation of literature data and a comprehensive geological field work in eastern and northern Finland (Figure 2) to collect material relevant for volcanological, geochemical and mineralogical studies, laboratory analyses for petrography, geochemistry and mineralogy and compilation of a database suitable for GEOSIS applications. Exploration criteria were developed to characterise geological and geochemical features indicative of ore-forming processes.

The following factors have been observed indicative of komatiite-related Ni sulphides

- 1) Volcanic factors: large volcanic province with (thick units of) ultramafic volcanics; channelling lavas; elongated shape of the lava channel; thick poorly differentiated cumulate bodies of olivine meso- and adcumulates; MgO-rich volcanic units that are thermally eroded the (sulphidic) substrate; ultramafic volcanics that contain xenoliths or xenomelts
- 2) Geochemical and mineralogical factors: MgO-rich units; a province where some of the ultramafic lavas are depleted in Ni and PGE; ultramafics that are depleted or enriched in chalcophile elements; ultramafics that are contaminated relative to the associated units (e.g. LREE); Zn-rich chromites; olivines depleted in Ni
- 3) Structural factors: structural culmination areas and areas with subvertical layering are favourable for the study of the stratigraphic sequences, not necessarily critical for the existence of Ni-sulphides; tectonic setting indicates environment of rifting during volcanism
- 4) Stratigraphic factors: full series in stratigraphy of tholeiites-komatiites-high-Mg basalts indicate long-term evolution of volcanism and high heat flow necessary for sulphides and abundant komatiites; felsic volcanics, sulphidic sediments and massive sulphides are favourable as the substrate of komatiites; deep water environment in the komatiite-related strata, coeval felsic/ultramafic volcanism (not critical, probably favourable).

The factors can be tested for exploration using GEOSIS applications and the database collected of the studied areas.

Figure 2 (On the next page): Research and test areas for the development of komatiitic/picritic models in the Kuhmo greenstone belt, eastern Finland.



3.1.3. Task 1.3: Mineralogy and modelling of laterite Ni deposits

The Ni-laterite deposits and occurrences of Greece are mainly transported laterites with some in situ profiles and they are related to ophiolites of Upper Jurassic to Lower Cretaceous age. They are mainly found in the Sub-pelagonian and Pelagonian geotectonic zones of Greece, which continue into Albania and Yugoslavia, hosting also very significant laterite deposits.

These deposits have the form of lenses or beds and lie either on highly serpentinized peridotites (harzburgites) or on talc-schists or on sediments (limestones, cherts, sandstones). They are conformably overlain by Cretaceous to Palaeocene transgressive sediments (sandstones, conglomeratic limestone and flysch). The Ni-laterite deposits of Greece have been affected by intense tectonism which has created overthrusting, foliation, folding and faults, which in turn resulted to the transportation of the mineralised bodies to greater or short distance, disruption of their continuation and in some cases their mixing with the underlain rocks or the transgression lateritic cover.

For the implementation of the objectives of the present project two areas have been selected representing two different geological environments. The Lokris area in Central Greece including the deposits of Tsouka, Kopais and Nissi, and the West Vermion area including the deposits of Profitis Ilias and Metallion. Detailed geological, mineralogical and geochemical studies, including PGE and REE, resulted in the following data for both areas.

The Ni-laterite ores of Lokris (pisolitic and bauxitic types) are mainly composed of hematite, goethite, quartz, Cr-spinel, chlorite and the Ni-bearing minerals nepouite $(\text{Ni,Mg})_3\text{Si}_2\text{O}_5(\text{OH})_4$, and animate $(\text{Ni, Mg, Al})_6(\text{SiAl})_4\text{O}_{10}(\text{H})_8$ and takovite $\text{Ni}_6\text{Al}_2(\text{OH})_{16}(\text{CO}_3\text{OH})\cdot 4\text{H}_2\text{O}$. In the Vermion ores - both compact and pisolitic types - magnetite is the major mineral in the former type, while additional minerals such as stilpnomelane, riebeckite, garnet, and vesuvianite are common in the latter. Nickel is mainly located in serpentinites (garnierite) and to a lesser degree in micas (sericite).

The variation of major and minor (Ni, Co, Mn and Cr) elements is consistent with the mineralogical composition of the samples in both areas. More specifically:

- Major and trace element geochemical data from the Fe-Ni deposits in Lokris and Vermion areas show Ni, Co, Fe, and Cr contents which are indicating origin from ultrabasic rocks and to an extended degree from laterites. The presence of significant aluminum content in some karst type ores in Lokris is most probable to be attributed to the basic rocks of the ophiolite complex. The mineralogical relationship of the sedimentary ores with the laterites, which is especially supported by the presence of phyllopyritic minerals containing significant amounts of nickel, is also a strong supportive argument for their origin from ultrabasic rocks.
- The very low Al_2O_3 , TiO_2 , REE, Pd, Pt and Au content are common features of the Fe-Ni ores of Tsouka (Lokris), and Profitis Ilias (W. Vermion).
- A preference of Pt over Pd and an increase in the Pt/Pd ratio upwards, through the lateritic profile, may indicate that during a subsequent stage of the diagenesis, and downward leaching of metals Pt is less mobile than Pd.
- Assuming that Cr and Al content of chromite grain-fragments, within laterites represents primary compositions, the comparison between the composition of chromite in the saprolite zone and the overlain Fe-Ni ore may provide evidence for the discrimination between

ore linked with the in situ weathering and those derived by transportation to some extent of clastic and chemical material.

- The compositional variation of chromite in Ni-laterites and bauxitic laterites from Nissi (Lokris) suggests that a major factor controlling their composition are both the parental rocks and the conditions during their transportation and precipitation of their components.

Based on the above, it is concluded that the geological environment of the Fe-Ni deposits in both studied areas, their mineralogical and geochemical data indicate a sedimentary formation, either in situ or transported. It is considered that the formation of these deposits is mainly a seawater process that is affected directly or indirectly by the continent.

In the Lokris area, the Kopais and Tsouka deposits are typical Ni-laterites whereas the Nissi deposit is bauxitic laterite. The Kopais and Nissi deposits are of chemical and/or clastic sediments type, transported either short or greater distance from parent rock. The Tsouka deposit at its lower parts is comprised of in situ weathered material whereas its upper parts comprise transported material.

In the Vermion area, the Profitis Ilias and the Metallion deposits are typical Ni-laterites. More specifically the Profitis Ilias deposit comprises in situ weathered material whereas the Metallion deposit comprises transported material of clastic sediments type.

3.2. WorkPackage 2, Development of geophysical technology

The objective of WorkPackage 2 was to develop and improve several Geophysical methods intervening at the three basic stages of nickel exploration:

Regional scale exploration: Combine GPS elevation measurements and digital Gravity measurements to obtain accurate and cost-effective regional gravity surveying.

Site scale exploration: a) Apply spectral IP method to Ni exploration, in particular develop specific measurement procedures. b) Develop software for fast (approximate) interpretation of ground EM methods. c) For the lateritic Ni, field-test existing geophysical methods to detect, map and outline the lateritic FeNi bodies.

Deposit investigations: Develop the cross-hole (tomography) and single-hole (borehole Slingram) EM methods (with 3-component receiver) for locating missed targets and possibly outlining intersected orebodies. The task involves development of prototype equipment suited to slim exploration boreholes, processing and interpretation software, methodology and field tests.

With the objective of serving all the above applications, a petrophysical database of Ni deposits and host-rock was also compiled.

3.2.1. Task 2.1: Regional surveys

3.2.1.1. Sub-tasks 2.1.1 and 2.1.2: Testing and designing of an integrated GPS-gravity system

After extensive testing in varied configurations in Finland, Greece and France by GSF, OMR, IGME and BRGM, the conditions in which the GPS yields the expected vertical accuracy of a few centimetres have been determined. When there is an open view to the GPS satellites, measurements with a vertical accuracy of better than 5 cm can be effectively made in real time with station intervals from some meters to a few hundred meters and baseline lengths up to 3 - 10 km, and by post-processing with station intervals from a few hundred me-

ters to a few kilometres and baseline lengths less than 20 km. In full-grown forests, or other similar areas with obstructed view to the sky, the GPS is effective only in clearings, which are randomly distributed. Moreover, detecting errors caused by multipath and obstructed view to satellites requires prolonged observation times. For a tight and/or regular grid under such conditions, the GPS must be augmented by e.g. a hydrostatic chain level or a laser ranging/inclinometer device. On the other hand, GPS makes the use of other devices much more effective than previously. The range of radio link for real-time corrections depends on national radio traffic regulations. Directional antennas and refined tuning systems should be used to obtain maximum range under given regulations.

Differential GPS provide, in addition to an improved precision on the levelling (Z), an accurate horizontal positioning (XY), and thus a much better cost-effectiveness than optical levelling in regional gravity surveys. The GPS accuracy is such that the technique can also be applied in semi-detailed gravity surveys (e.g. strategic stage of mineral exploration) or even in detailed surveys (e.g. geotechnical studies).

As for processing, the tests have shown that the task of integrating GPS measurements into local geodetic systems is not trivial. Moreover, in order to transform the heights above the reference ellipsoid (the standard GPS output) into accurate heights above sea level, the effects of local geoid undulations have to be modelled and removed.

In conclusion, the project has assembled and tested a practical real-time gps-gravity system and gained relevant know-how to effectively apply such a system in various conditions and configurations.

3.2.2. Task 2.2: On-site ground surveys

Development of spectral IP method for Ni exploration

Laboratory determinations of resistivity spectra from sulphidic nickel deposits and their environments were carried out. More than 500 samples were measured. Relationships between the measured spectra and textural features of the samples were studied using image processing techniques.

Based on the laboratory spectral measurements the mathematical model to describe the behaviour of the spectra was constructed. The problem of the phase-spectra asymmetry can be solved by using a generalised Cole-Cole spectrum or by fitting the sum of several Cole-Cole spectra.

The problem of electromagnetic coupling was addressed by developing a non-collinear electrode array that minimises the primary coupling of the layered host. By using such optimal array, the highest available frequency can be increased at least one decade over the maximum frequency given by standard collinear dipoles (up to several kHz). Field-tests were carried out at Kuhmo and Ylivieska (Finland).

Development of interpretation software for ground EM methods

An interactive interpretation program (*EMPLATES*) has been developed for the ground electromagnetic (EM) dipole-dipole measurement systems operated in frequency domain (*Slingram*, *Sampo* and *Melis*). The *EMPLATES* program combines an approximate forward computation, based on thin plate models in layered conductive space, with an automatic optimisation and a user-friendly interface under Windows 95. Forward computation usually takes only a few minutes, inversion takes less than one hour.

The final report describes the basic theory and equations that form the approximate computational method and the inversion procedure used in the software. The results from EMPLATES were compared to those from a 3D integral equation software used by GSF (MARCO). When a MARCO forward model is inverted with EMPLATES, the XY location and 3D attitude of the initial plate are well retrieved, but its depth and conductivity are always over-estimated (strongly for the conductivity).

The EMPLATES software, though presenting some limitations, is useful for quickly deriving location and attitude of a target. It can be used for siting a borehole, but the user must remember that the depth is about 50% over-estimated. Its best use is probably to give first guess for other more sophisticated, but slower, interpretation software.

Geophysical methodology for lateritic Nickel ores

Gravity (with and without GPS), magnetics, induced polarisation (IP), transient EM, and high resolution seismics were all successfully tested in carbonated and ophiolitic environments. The most effective methods to detect the ore at a few tens of meters below the surface revealed to be gravity and IP, as well as high-resolution seismics for accurate determination of the geometry at depth.

Development of 3-component borehole EM methods

Versatile equipment for 3-component downhole electromagnetic (EM) measurements has been developed at IRIS Instruments. The 'SlimBoris' system covers the three configurations that can be envisioned in boreholes: a) the classical surface-to-hole¹ configuration, where the transmitter (Tx) is a large loop at the surface and the receiver (Rx) is a 3-component probe moving in a borehole, b) the less-developed cross-hole (or tomographic) configuration, where Tx is a magnetic dipole in a borehole and the 3-component Rx probe is in another hole, and c) the innovative single-hole (or borehole 'Slingram') configuration, where both the Tx and Rx probes move in a same borehole at a constant separation (the borehole equivalent of the 'Slingram' surface profiling method).

The Tx and Rx probes are 42 mm in external diameter for use in slim exploration holes (half of which are drilled in 46 mm). The challenge was to respect this requirement while keeping adequate sensor sensitivities at Rx and sufficient transmitting moment at Tx. Final sensitivities are 30 mV/nT for the axial coil and 50 mV/nT for the radial coil, and final magnetic moments are about 250 A.m² at low frequency down to only 50 A.m² at the highest frequency. Nine frequencies are available in the range 35 Hz - 8960 Hz, in geometric progression ratio of 2.

Probe envelopes are pressure-tested to 200 bars for use down to 2000 m. The equipment is devised to work with standard 4-conductor logging cables. Receiver power supply and communication scheme can operate through up to 2000 m of 4-conductor cable, whereas transmitter power supply is limited to only 1000 m of such a cable².

After fixing several problems found during the first field tests, especially on the single-hole configuration, the instrumentation and driving software are now operational.

¹ Needing of course a surface transmitter in addition to the borehole system.

² The Tx probe could however be operated down to 2000 m using a 7-conductor cable.

GSF and BRGM have carried out extensive 3D numerical modelling. The objective was a) to optimise the instrument design and field configuration as well as to define practical limitations for the new methods, b) to study the 3-component EM response from a conductive target in different geometrical configurations and resistivity settings, and c) to give interpretation guidelines for certain simple geometries.

A practical conclusion regarding the instrument design and field configuration is that, given the usual noise levels, the transmitter power obtained by IRIS should enable an investigation radius of about 50 m around a borehole. In the 'single-hole' configuration, a Tx-Rx spacing of about 100 m should be best suited in order to obtain this investigation range.

Another conclusion of these modellings is that both the single- and cross-hole arrays should give better resolution than the surface-to-hole array (at the expense of reduced investigation range). Elementary rules for deriving target's location and dip with respect to the borehole, have been elaborated for simple targets in the single-borehole configuration.

Inversion software (using Marquardt-Levenberg algorithm) was developed for rapid interpretation of borehole EM data. It is based on very simple models such as EM dipoles or current filaments, the calculation of which takes only a fraction of second on a standard PC (e.g. 486). Thanks to the speed of the forward calculation, the whole inversion process (needing tens to hundreds of iterations) is performed in only a few seconds. The validity and interest of such simple models have been assessed on synthetic data calculated with 'exact' 3D modelling software. The results are very satisfying: the 3D attitude of the target is always well retrieved and its 3D location is as accurate as a few percents of the target-to-borehole distance.

An example of interpretation of a surface-to-hole log recorded in Finland with the new equipment is presented on figures 3 and 4. The different variants of inversion all agree to locate a conductor in between the two barren boreholes JM9 and JM15.

The single-borehole configuration was tested during the second field test in Finland, i.e. after IRIS fixed the problems found in the earlier tests. This last experiment in single-borehole configuration proved that the system is operational. The responses obtained were consistent in magnitude with the modelling results, and consistent in depth with the known geology. The benefit of the modelling study was also demonstrated, considering for example the simple interpretation rules or the question of high response percentages. Further tests will take place in April 1999 in Finland in order to resolve some details found during the tests so far.

3.2.3. Task 2.6: Compilation of a petrophysical database

The petrophysical database concerning the density, magnetic and electrical properties of the Ni bearing lithology has been established and documented. The database includes petrophysical parameters of both magmatic and lateritic deposits. Laboratory measurements and statistical analysis of the samples related to WP1 deposits have been performed as well.

Statistical analysis has been applied to get correlation between different rock types, petrophysical parameters and chemical assays. Factor analysis appeared to be a very useful tool to analyse the inner variance of nickel ore.

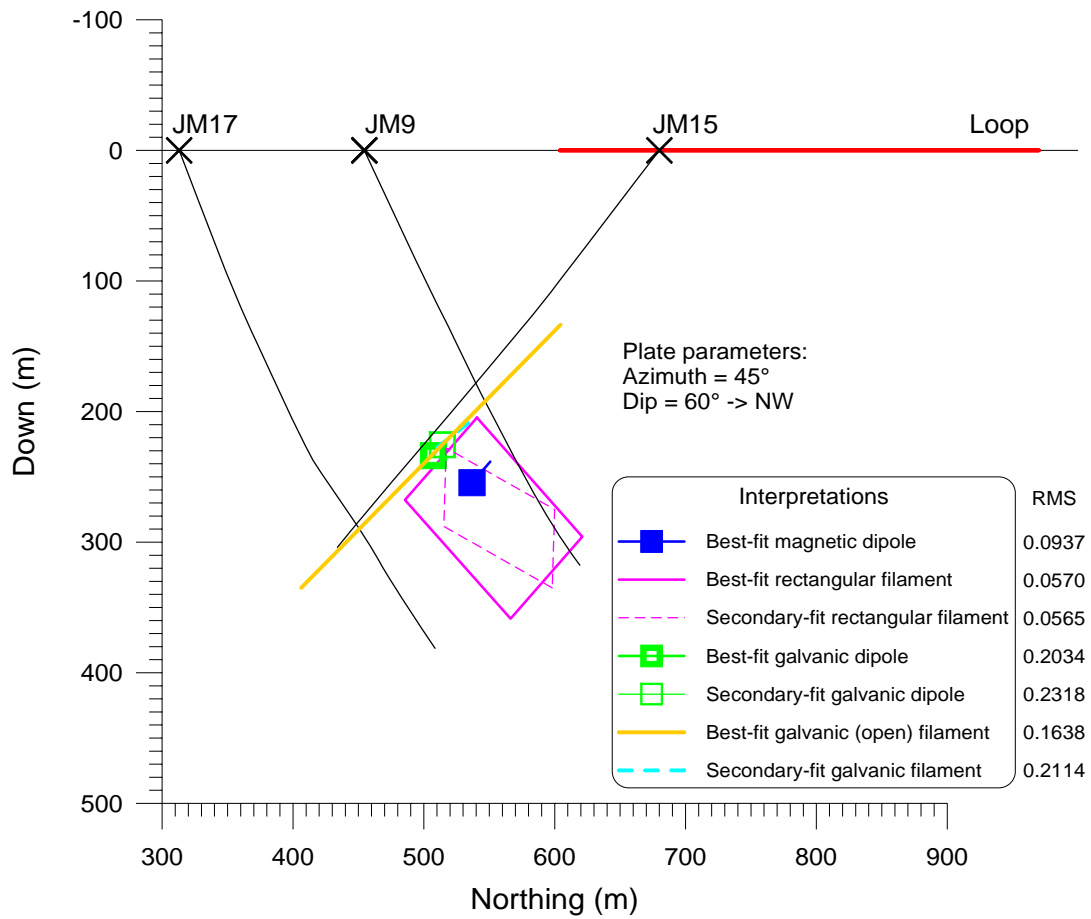


Figure 3: Borehole JM15 with surface loop. Interpretation of the 1120 Hz in-phase field reduced by low frequency with different models of dipoles and filaments in free space.

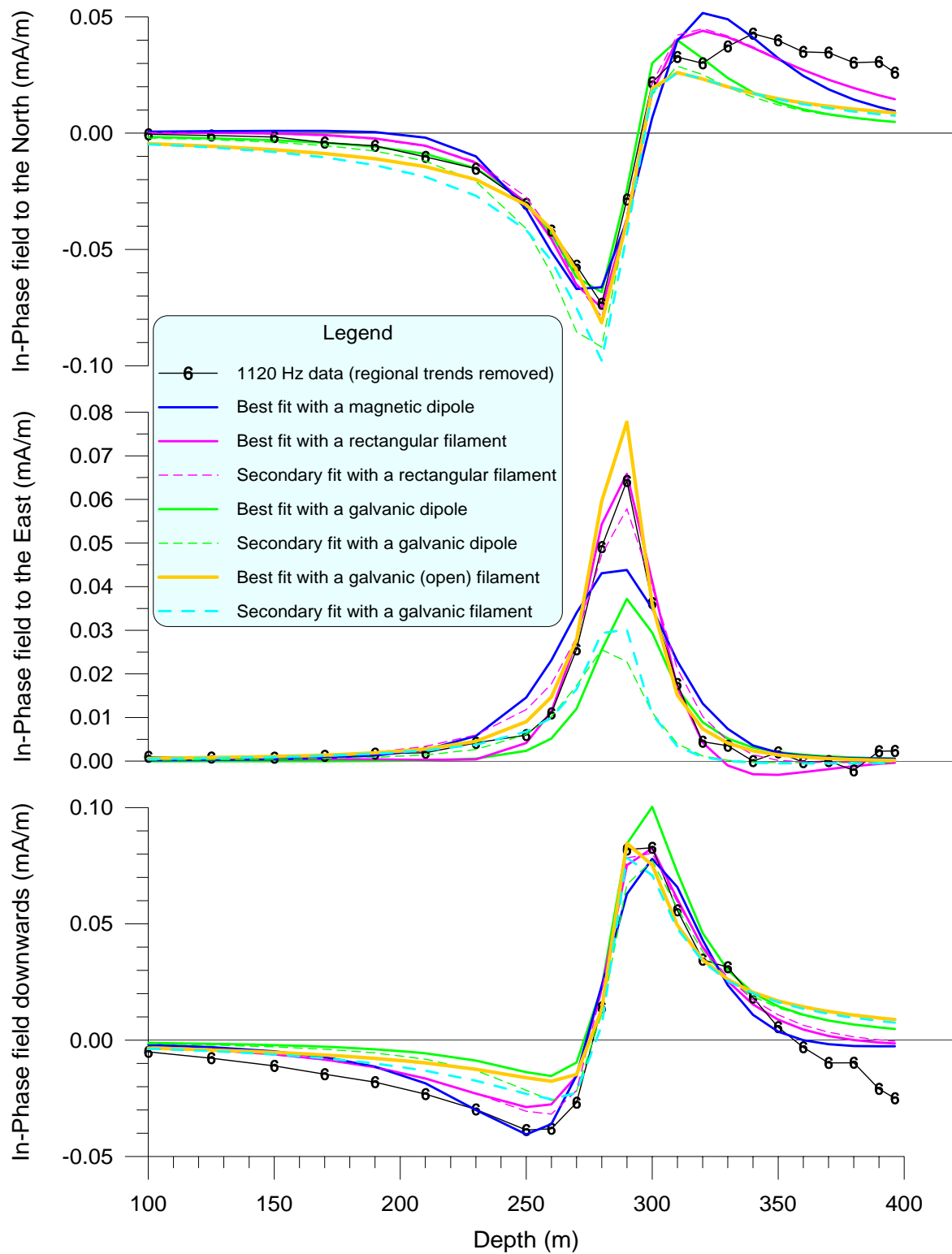


Figure 4: Borehole JM15 with surface loop. Fits obtained when interpreting the reduced in-phase field at 1120 Hz with different models of dipoles and filaments in free space.

3.3. WorkPackage 3, Image processing/pattern recognition

WorkPackage 3 has concentrated on development and testing of several conventional and new pattern classification and image processing techniques. These techniques are to be used for processing of multisource (satellite, geophysical etc) data and applied for extracting and locating significant geological features related to nickel deposit detection. In particular, of interest are the identification of lithological regions and possible ore potential targets, as well as the delineation of lineaments. The following activities have been performed in WP3:

1. Collection of multisource information (remotely sensed, geophysical etc) from the selected test areas and processing of the collected information. In particular, in this phase we have performed:
 - Interpolation and co-registration of satellite images (Landsat TM, SPOT, and ERS) along with the produced DEM and the digitised 1:50,000 geologic map
 - Reduction of high inter-band correlation due to the reflected part of the spectrum
 - Application of filtering and edge detection techniques
 - Speckle reduction and multi-linear regression techniques for noise suppression and enhancement of geological information content for the SAR images of ERS
 - Integration of different resolution images along with the 3-D representations
 - Image interpretation in terms of geologic features depicted on them
2. Development of an Advanced Statistical Methods (ASM) user friendly software package with the aim to provide alternative statistical classification techniques including flexible, quadratic, penalised and empirical discriminant analysis. These methods are supervised and based on training data. Each method is suitable for certain circumstances in the classification problems depending on the number of variables in the patterns and the number of training patterns. Options of various data input/output formats and graphics tools were implemented and the ASM package has been integrated to GEOSIS by a hot-link button.

The performance of the methods was tested with data sets available from the ELENA project. The achieved innovative component of this software is that it provides an integrated package of methods and tools applicable to various data types in various classification problems in image processing and geosciences in general and in exploration in particular.

3. Development of the Artificial Neural Networks Graphical Integrated Environment (ANNGIE) software package. ANNGIE includes various neural, fuzzy, multimodular, pattern recognition and image processing and classification algorithms within a user friendly GUI environment, written in Tcl/Tk. ANNGIE is integrated with GEOSIS but can also be used as a stand-alone module. The aim is to provide modern information processing technologies to assist geologists in the classification of remotely sensed, geophysical and geological data in lithological units and possible ore potential targets. ANNGIE also provides techniques for automatic lineament identification, capability of training set selection through polygonal region definition and labelling by the user and supports TIFF, PGM, GRD, ASCII and MapInfo-GEOTIFF formats. In particular, this package contains the following groups of algorithms for supervised classification methods, unsupervised classification methods and pattern recognition and image processing methods.

Supervised classification methods

In supervised classification tasks, data are forced into categories defined by the user. In the context of a GEOSIS application, the objects to be classified are sampling units such as samples, grid points or pixels coming from multisource data (geological, geophysical, remotely sensed). The desired classes are lithological units and ore potential targets. The algorithms included in this group are:

- the multi-layered feedforward neural network classifiers *BackPropagation*, *ALECO-1* and *ALECO-2* with the pre-processing option of forming high order correlation of the input data
- the reputedly fast single-layered neural network classifiers *LVQ* and *k-LVQ*
- the fuzzy *Pal-Majumder* classifier
- the *multimodular* classifier, whereby decisions made from other supervised algorithms are combined using voting schemes based on absolute or relative majority rules

Unsupervised classification methods

In unsupervised classification, such as automatic classification tasks, data are forced into categories defined by a clustering or by a self-organising algorithm rather than by the user. The algorithms included in this group are:

- Kohonen's *Self-Organising Feature Maps* neural network algorithm
- the *hierarchical min-max* statistical clustering algorithm
- the *ISODATA* statistical clustering algorithm
- the *Fuzzy ISODATA* clustering algorithm
- the *Batch-Map* neuro-statistical clustering algorithm

Pattern recognition and image processing methods

This group of pattern recognition and image processing algorithms is provided in order to perform automatic lineament extraction. It is assumed that a supervised or unsupervised classification result, obtained from gridded magnetic and electromagnetic (real and imaginary) data, is available by applying one of the above classification techniques. This group includes:

- An algorithm for thresholding the grey-level classification result produced by any supervised or unsupervised algorithm in order to obtain a binary image; four different thresholding options are provided to the user
- An algorithm for determining connected regions in the binary image, using 4- or 8-neighbor connectivity, followed by extraction of appropriate region shape descriptors (characteristics)
- A novel weighted Hough transform algorithm to locate the most prominent lines (lineaments) based on the above characteristics

4. Application of the software to the collected data.

The above software has been applied with success to satellite data from the Vermion area in Greece (lateritic deposits) and to geophysical data (airborne magnetic and electromagnetic) from the Vammala area in Finland. The resulting maps and lineaments are shown in figures 5, 6 and 7.

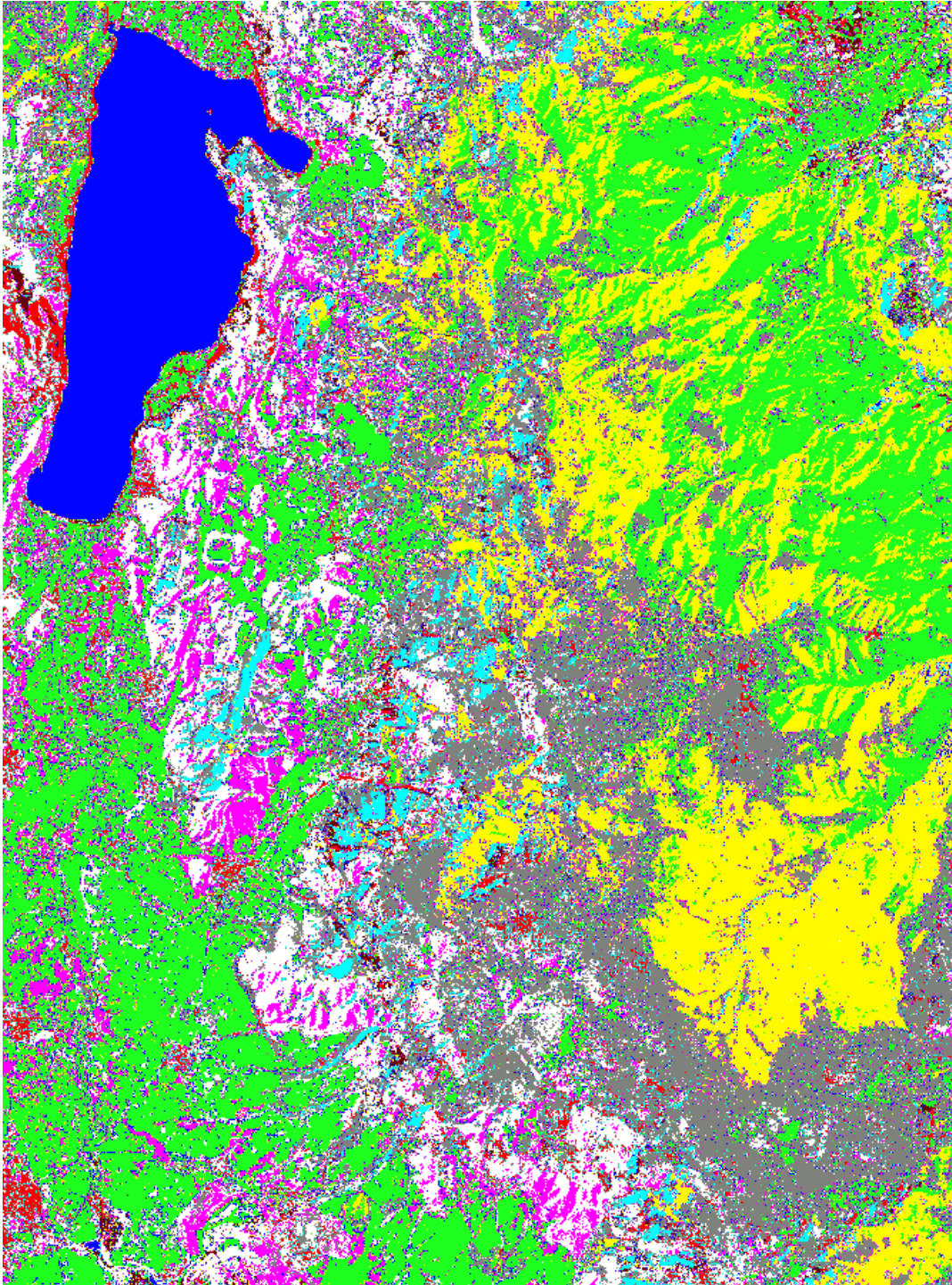


Figure 5: Classification in lithological units and mineral alteration zones (9 categories) using bands 7, 4, 1 of a Landsat TM image over the Vermion area in Greece. Method used: multi-layered neural network using the ALECO-2 algorithm.

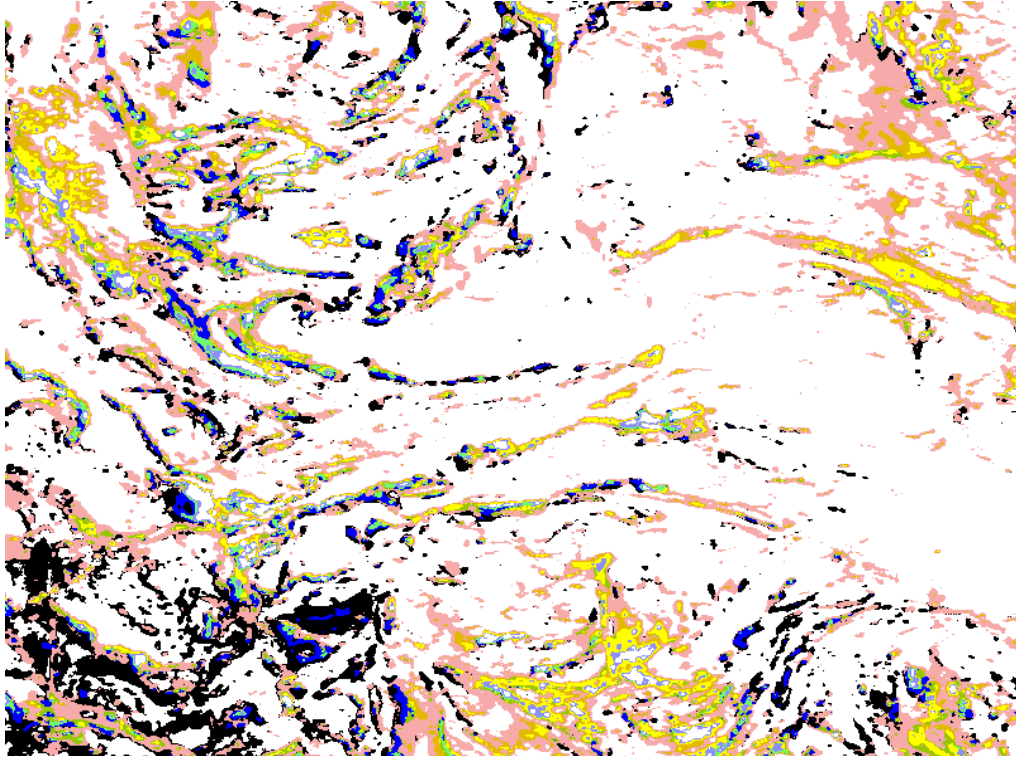


Figure 6: Classification in lithological units and possible ore potential targets (9 categories) using geophysical data from the Vammala area in Finland. Method used: unsupervised classification using self-organising maps and hierarchical min-max clustering.

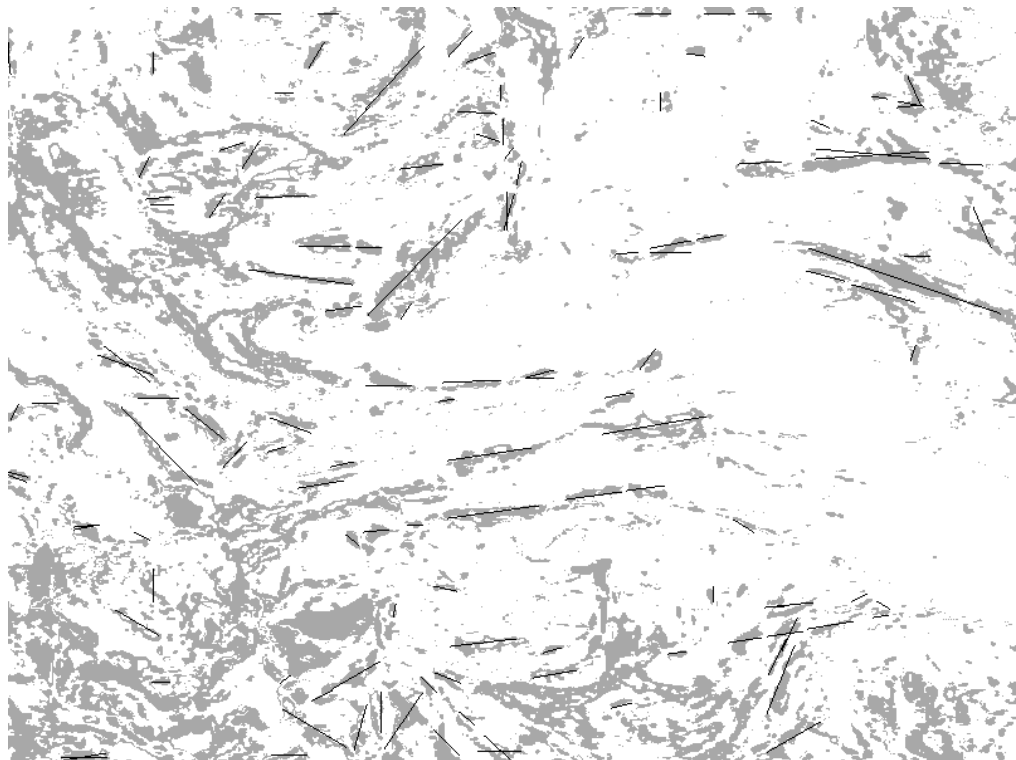


Figure 7: Lineament extraction and superposition to a binary version of figure 6.

3.4. WorkPackage 4, the Geoscientific Information System (GEOSIS)

One of the main tasks of the project was the design and the development of a “Geoscientific Information System” (GEOSIS). It allows the management of the huge variety of data, maps and images (geological, geophysical, geochemical and other scientific data) which are currently used in the mineral explorations. GEOSIS gives also access to the analysis tools that have been developed in the project: the expert system (GEOES), the neural network analysis module (ANNGIE), and the advanced statistical methods (ASM).

The development of GEOSIS required the co-operation of several experts from the different scientific disciplines with the software engineers. The work of analysis performed by this team allowed the design of a software system that is able to manage most of the complex data set and methodologies, required by a mineral exploration. The software architecture is based on powerful software environments available on the market, and allows flexibility and easy integration with external software tools. The easy-to-use Windows like interface hides the complexity of the system to the user, but allows complete control to the administrator.

GEOSIS has a Windows style user friendly interface, which is built around a commercially available GIS system: MapInfo (Therefore GEOSIS allows all the functions available in MapInfo). Through the interface the user can access to:

- The geo-database with all the geological, geophysical and geochemical data
- Specific internal GIS functions developed, which allows the association and analysis of tabular data, vector maps, and images
- The advanced external analysis modules developed in GeoNickel

Perhaps the more complex and innovative part of the software developed refers to the data management, which is based on a relational database (Oracle), and includes data coming from different disciplines and methodologies. The database has a complex architecture, but the user is supported and guided by the interface through the data entry, update and query. GEOSIS interface guides the user in the data entry to the database with appropriate windows and masks, and allows the updating of the data stored, assuring the safety of the original data.

GEOSIS is able to import and export the most common tabular raster and vector data files. A specific ASCII user defined format has also been developed to manage an easy input of tabular data. The user is able to define its own data format with an easy-to-use interface that allows the format definitions. The structure of the database is also flexible enough to accept new data definition and elaboration of the stored data, and all the data stored in the database are georeferenced.

Through a reporting module the user can access to all the data, performing complex queries and organising the output in the format he needs. The expert user is able to perform any kind of queries with a guided query editor, less experienced users can select among the standard reports which are prepared by the administrator.

After the geo-expert has completed his search for the data he needs in the Oracle database, he can download the data selected in his workspace, and perform a first analysis associating,

comparing and selecting tabular data, maps and images in a extended MapInfo environment. He can use the standard MapInfo mapping tools, like geocoding, mapping points, and create thematic maps, or he can use the tools which have been developed for handling GEOSIS maps, and link tabular data to vectors and areas in the maps. He can then start one of the advanced analysis tools developed in the GeoNickel project, review the results and eventually update the database.

3.4.1. GEOSIS architecture

The following figure 8 shows the global architecture of GEOSIS.

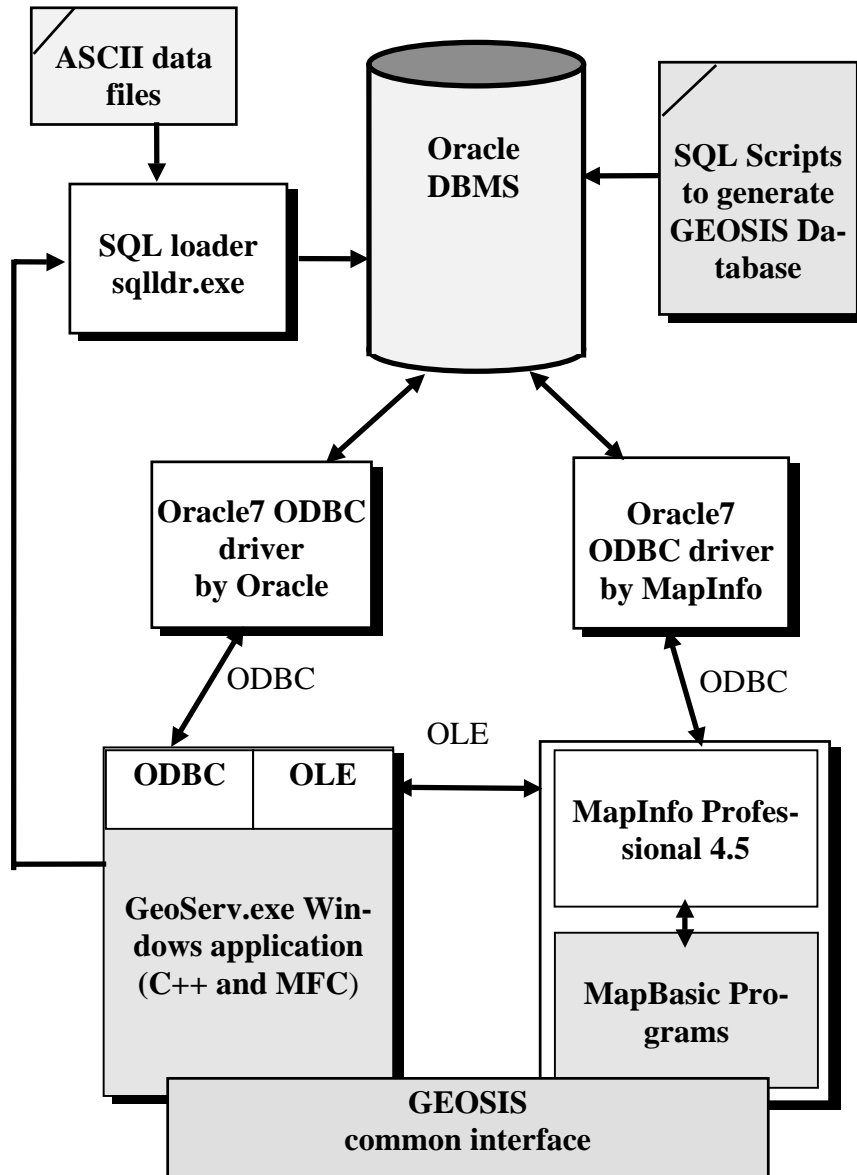


Figure 8. The architecture of GEOSIS

The shaded boxes in figure 8 refer to modules that have been specifically developed, while the white boxes refer to external modules that are available on the market. As figure 8 indicates, GEOSIS is based on a client-server and object-oriented architecture. Two external applications, Oracle and MapInfo Professional, will act as GEOSIS server:

- Oracle allows the management of the Database, through the use of ODBC drivers
- MapInfo Professional allows the management of the GIS functions, through the use of OLE services

The Oracle Database contains all the tables with the geological, geophysical, geochemical and other data sets that will be used for the mineral exploration. The Database is generated with a script written in SQL, which builds up the tabular structure of the Database.

A seamless interface allows access to all the GEOSIS services (which include all the MapInfo Professional functions). This interface was developed with the Microsoft C++ environment and MapBasic, and complies with the Microsoft Windows standards. One of the most important functions implemented with the C++ module manages the communications with Oracle through the ODBC driver and with MapInfo, through the OLE services, and allows an easy integration of the external software modules.

The advanced GIS functions available in GEOSIS have been implemented using MapBasic, the software development language of MapInfo, and are based on the standard functions of MapInfo.

The data entry function of GEOSIS manages the generation of the appropriate script for the Oracle SQL loader that will import the ASCII file containing the new data, which need to be entered into the Database.

GEOSIS has been implemented using object-oriented technologies and updated development tools, in order to optimise the maintenance, the portability and the easy integration of the software.

3.5. WorkPackage 5, The GEOES Knowledge-Based System

3.5.1. Introduction

The GEOES system embodies the knowledge of geo-experts and aims to facilitate the exploration process performed by geo-scientists. It is an expert system with a user-friendly interface that runs under the Windows 95 and the Windows NT operating systems. GEOES is integrated within GEOSIS, the software toolbox of the GeoNickel project. The system gives emphasis on the integration of a variety of different approaches for the nickel exploration tasks, combining a wide range of data and knowledge from all the geo-domains involved. It covers geological models for lateritic, komatiitic and intrusive nickel ore deposits and provides assistance to users during different phases of their exploration work, including:

- *Area selection*, where wide areas are examined for the existence of nickel ore deposit
- *Identification of potential zones*, where zones within a given area are examined
- *Target selection*, where a restricted small area is examined

For each combination of the above models and phases, there is a number of *observation entities*, grouped in specific geo-domains such as geology, geochemistry, geophysics, pedogeochemistry, lithogeochemistry and mineralogy. The observation entities correspond to factors and subfactors, which are associated with the favourability of existence of nickel ore deposits. The user provides qualitative data measurements for the observation entities that feed the expert system. Based on those data, GEOES is able to assess the favourability of existence of

Ni-ore deposit, provide a consultation that presents arguments to that assessment, even graphs that depict the contribution of each scientific geo-domain to the final result.

Within GEOSIS there are three versions of GEOES, each one having a different role. They all share the same knowledge engine, but they differ in the way they use this engine and in the functionality they offer to the user.

3.5.2. The Interactive GEOES

The interactive version of GEOES (Figure 9) was developed in the early stages of the project in order to help the knowledge acquisition process and test the knowledge engine against real geo-data. The tests were vital for the development of GEOES, which followed an iterative evolutionary approach with the end users playing a significant role in testing and improving the system.

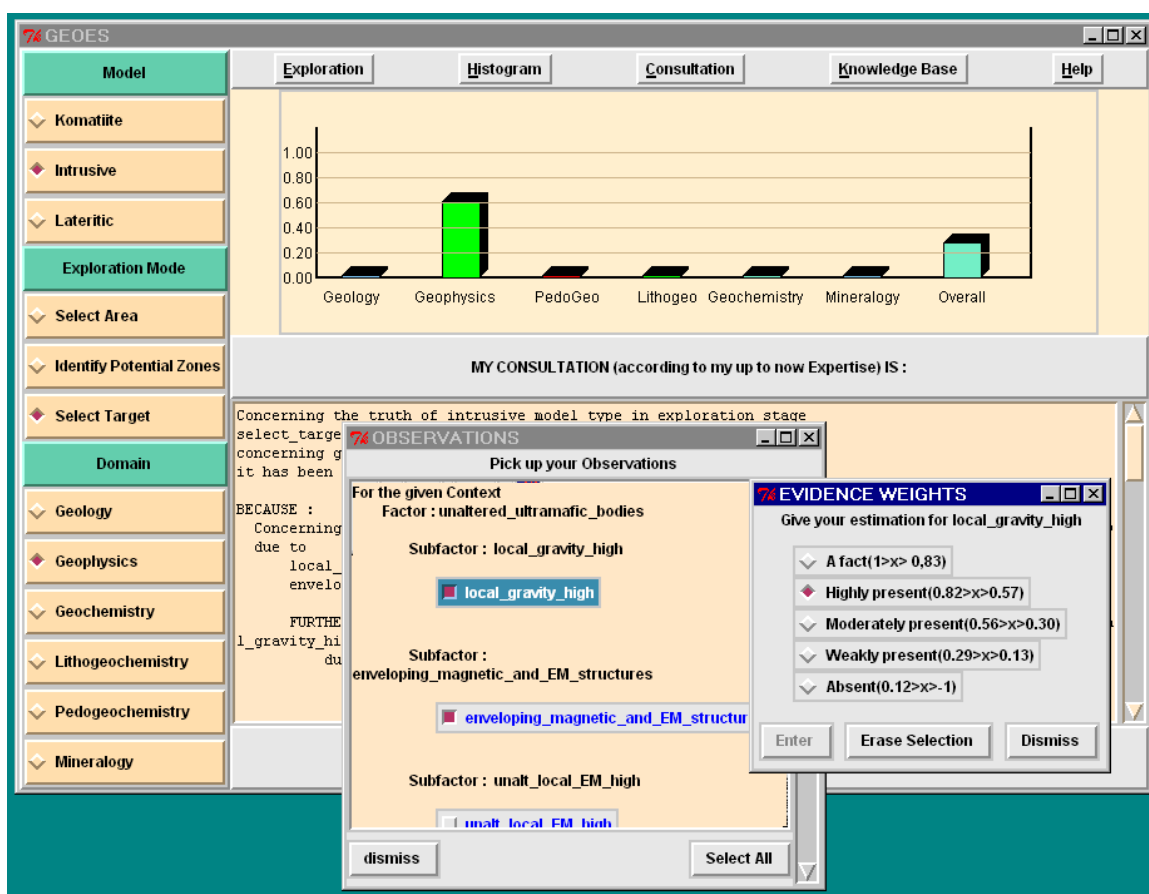


Figure 9: The user interface window of the Interactive GEOES.

The user interface gives access to all the functionality of the underlying system: it is possible to select various combinations of geological models and exploration phases, fill in values to the corresponding *observations*, and get the result of the expert system in the form of a verbal *consultation*, and in the form of a graph. Based on the results the user can experiment and engage in what-if scenarios by changing the values of a few observations and then check on the difference at the final results. Experimentations are supported at an even deeper level, as the user can set some of the internal parameters of the knowledge engine, namely the *necessity*

and *sufficiency* values for each observation.

Although interactive GEOES gives unrestricted access to all the functionality of the knowledge engine, it requires that each set of input values must be given to the system by the end user. This is very flexible when someone wants to experiment, but it clearly becomes impractical when one is going to use it in real situations, covering larger areas.

3.5.3. The Spatial GEOES

The spatial version of GEOES was developed to remedy this drawback. Furthermore, with spatial GEOES, the integration with GEOSIS becomes tighter. The goal was threefold:

- First, to make it possible for GEOES to exploit the GEOSIS database and avoid manual data entry
- Second, to run the knowledge engine in a batch mode for many sets of data at once (each data set corresponds to a cell of a map)
- Third, to present the results in a way that makes more sense to the users

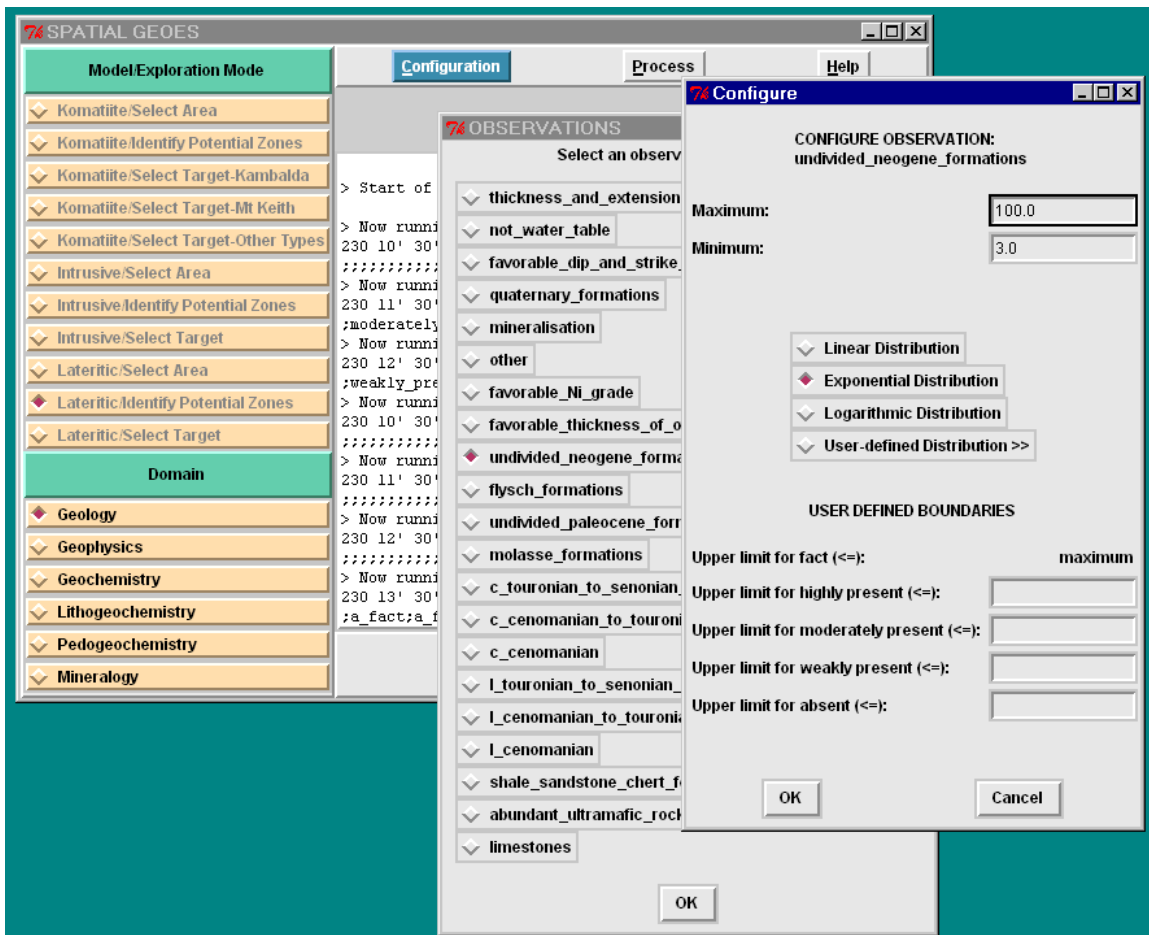


Figure 10: The user interface window of the Spatial GEOES

The intermediate tables provided by GEOSIS, are used as input for spatial GEOES (Figure 10), which runs the knowledge engine until all data have been processed. Each line in the in-

intermediate tables contains measurements that correspond to one cell of an area to be studied. The output is recorded in again another intermediate table used by GEOSIS to present the results on a colored map.

In contrast to the interactive version, spatial GEOES has functionality that makes it easier to deal with a lot of data. The user has absolute control on the way the knowledge engine assesses the data. It is possible to see the lowest and highest values for each observation, to set the lowest and highest admissible value, to select a method for evaluating the measurements from linear, exponential, logarithmic, or user-defined.

With the spatial version, GEOES becomes a truly useful and powerful tool in the GEOSIS toolbox. However, because spatial GEOES runs the knowledge engine in a batch mode for many data sets, it is not possible to get a consultation as in the interactive version.

3.5.4. The Hybrid Version

This problem is solved with the introduction of the hybrid GEOES version. The hybrid version completes the spatial GEOES, by elaborating on the results of the spatial version and combining the flexibility of the interactive version. Once the user has used the spatial version to produce a map colored according to the results, he/she may wish to select a map cell and get more information on the specific cell, or even try some what-if scenarios on that cell.

The hybrid version runs when the user selects a cell, loads automatically the data concerning that cell, and offers the flexibility of the interactive version: it is possible to view consultation and histograms, change the values and compare as many times as needed. This last version covers the needs of every possible scenario in the exploration process. However, experimentation and fine-tuning of the GEOES expert system is continued in close co-operation with the end users.

The geo-scientists have now a tool to help their tasks, from *area exploration* to *potential zones* and further to *target exploration* stage, in order to identify the most favorable target area for Ni-ore deposits. Moreover, the interactive version of GEOES can also be used for training new scientists and professionals.

3.5.5 Testing

GEOES was tested and validated in Finland for intrusive and komatiitic nickel deposit environments, and for lateritic environment in Greece. APE software, developed in WP1, was also tested and used extensively in the study of mafic and ultramafic rocks in the Finnish test areas. Tests both in Finland and in Greece showed good results, corresponding well to those obtained using conventional exploration methodologies.

The tests of the three modes of GEOS were made on data collected from the selected test areas; sulphidic exploration models were tested in Finland and the lateritic model in Greece. In both countries, the first step involved the testing of the Area Selection models using data covering most parts of the countries; Intrusive mode was tested in Finland and Lateritic mode in Greece. Test results showed that, based on input data, GEOES was able to locate the major zones and areas that host the modelled types of Ni deposit. The "Identification of Potential Zones" and "Target Selection" modes for Intrusive and Komatiite models were tested in two test areas in Finland, the Northern Bothnia test area and Pulju Komatiite Belt, respectively. The corresponding lateritic tests were carried out in four different test areas: Lokris, Euboea Island, Vermion, and Kastoria.

The tests for “Identification of Potential Zones” for both Intrusive and Komatiite models resulted in detecting the known areas potential for hosting nickel deposits. Further, they revealed interesting targets not recognised earlier. The data preparation procedure indicated, however, that the quality and coverage of the data and the objectivity of the preprocessing measures used in extracting information for the observations needed in spatial GEOES analysis, are of utmost importance for reliable results. The identification of potential zones for lateritic Ni deposits was tested among others in the Lokris area, where the results in geochemistry, mineralogy and geophysics correlated well with the existing background information, but the results for geology were partly weaker.

The target selection mode of spatial GEOES for intrusives was tested in the Northern Bothnia area using a large data set (6043 grid cells) collected digitally from the existing data. Several tests with different input data and evidence weight configurations were conducted in order to see how these affect the results. This also gave the possibility to evaluate, how the user can control the system for different exploration scenarios and “what if?” simulations. The tests conducted generally revealed three to six of the seven Ni deposits and occurrences used as reference targets in the test area, and a reasonable amount of other anomalies in geologically sound locations were detected. The tests also showed that the system could be well controlled by changing the evidence weights and/or selecting input data. In Greece, the target selection mode for the lateritic Ni deposits was evaluated mainly in the Lokris area. The results corresponded with the existing data for the area.

In general GEOES is an interesting exploration tool for the area selection, identification of potential zones, and target selection exploration phases, covering and compiling explorational data from diverse origin (geology, geophysics, mineralogy and geochemistry). One of the powers of the GEOES Expert System is the systematic approach needed from the data acquisition to the output of results. It gives the exploration staff a good opportunity to systematically examine all of the available data, estimate its homogeneity and validity, showing where more information is required for well-balanced reasoning results.

4. DISCUSSION

The models and software prototypes developed in WorkPackages have been delivered to the end user partners for testing and use with actual exploration data, and the novel geophysical instrument prototypes have been tested, and are being used in the field in France, Greece and in Finland. Even though it is early to comment on the final results, the preliminary ones have been encouraging. All the WorkPackages have been able to meet their goals in time, and the overall objectives of the project were achieved.

Different models have been developed for nickel ore-forming processes in intrusive, komatiitic/picritic and lateritic environments. An innovative result of the project is the “Automated Petrological Explorer” (APE) software. It was developed for rapid and comprehensive analysis and modelling of lithogeochemical and mineralogical data from mafic – ultramafic intrusions. APE will be of great value for exploration geologists when studying the potentiality for nickel deposits.

The development of geophysical technology resulted in novel instrumentation prototypes (the integrated GPS-gravity system and the versatile equipment for 3-component downhole elec-

tromagnetic (EM) measurements), and in the compilation of new models and interpretation software for spectral IP method, for the ground electromagnetic (EM) dipole-dipole measurement systems operated in frequency domain (EMPLATES), and for the rapid interpretation of borehole EM data. Further, a database on the petrophysical parameters of nickel bearing lithologies and deposits in magmatic and lateritic environments has been established to support the geophysical exploration.

Two software packages were developed in order to enhance the processing of multisource (geophysical, geochemical, satellite, etc.) data for extracting and locating significant geological features related to nickel ore deposits. One is focused on advanced statistical methods (ASM), and the other on new pattern classification and image processing techniques involving ANN approach (ANNGIE).

A “Geoscientific Information System” (GEOSIS) was developed for the management and processing of the vast variety of explorational data as well as maps and images (geological, geophysical, geochemical and other scientific data) which are currently used in mineral exploration. It comprises two commercially available database and GIS applications, Oracle and MapInfo Professional, linked seamlessly together with data management, interface and advanced GIS function modules developed in the project. GEOSIS also serves as user interface for the integrated use of the neural network analysis module (ANNGIE), the advanced statistical methods module (ASM), and the knowledge based system (GEOES).

The GEOES system embodies the knowledge of geoscientists specialized in nickel ore exploration and aims to facilitate the processes performed in the different phases of nickel ore exploration. It is an expert system with a user-friendly interface, integrated within GEOSIS, giving emphasis on the combination of a variety of different approaches for nickel exploration tasks. It combines a wide range of data and knowledge from all of the geo-domains involved, covering geological models for intrusive, komatiitic and lateritic nickel ore deposits and providing assistance for users during the area selection, identification of potential zones, and the target selection. It can be run either in interactive, spatial, or hybrid mode, each one having a different role. All of them share the same knowledge engine but differ in the way they use this engine and in the functionality they offer to the user. Evidently the geologists involved in nickel exploration will have a useful tool to help in the difficult task of identifying favorable targets for nickel exploration. Ultimately, the most important feature in using such an expert system may be the fact that it forces different specialists in an exploration team to work more closely and coherently, enhancing the strengths of teamwork in mineral exploration.

Even though nickel exploration was the primary target of the project, it is evident that most of the developed instruments and software are of generic nature. Consequently, they can be applied to a great variety of base metals deposits other than the "nickel family" (i.e. Ni, Co, Cu and PGE). Most of them can be used to aid exploration of commodities genetically related to magmatic, or even to sedimentary rocks in various geotectonic environments.

5. REFERENCES

Chai, G. and Naldrett, A.J., 1992: The Jinchuan ultramafic intrusion: Cumulate of a high-Mg basaltic magma. *J. Petrology*, 33, 277-303.

Eliopoulos D., Aarnisalo J., Papunen H., Apostolikas A., Economou M., Bourgeois B., Angelopoulos A., Gustavsson N., Stefouli M., Varoufakis S., Morten E., Ripis C. and Spyropoulos C., 1998: Integrated Technologies For Minerals Exploration: Pilot Project For Nickel Ore Deposits. In: A. Kontopoulos, I. Paspaliaris, A. Adjemian and G. Katalagarianakis, eds, *Proceedings of the first annual workshop (Eurothen'98), Athens, Greece, 12-14 January 1998*. European Commission, Industrial and Materials Technologies Programme (BRITE-EURAM III). Lab. Metall., Nat. Tech. U Athens, pp. 24-32.

Irvine, T.N., 1970: Crystallization sequences in the Muskox intrusion and other related intrusions. 1. Olivine-pyroxene-plagioclase relations. *Geol. Soc. S. Afr. Spec. Publ.*, 1, 441-476.

6. ADDRESSES

Project Coordinator (1) OUTOKUMPU Mining Oy
P.O.Box 143, FIN-02201 Espoo, Finland
Tel.: +358-9-4212647, Fax: +358-9-4212403 ,

Partner (2) LARCO
General Mining and Metallurgical Co, SA
20 Amalias Ave., GR-105 57 Athens, Greece
Tel.: +30-1-3225018, Fax: +30-1-3237146
E-mail: larco@mai.hol.gr

Partner (3) SOFTECO SISMAT S.p.A
Software Development Company
Via San Barborino 7/82, 16149 Genova, Italy
Tel.: +39-10-6457000, Fax: +39-10-412555
E-mail: enrico.morten@softeco.it

Partner (4) IRIS INSTRUMENTS S.A.
1 Avenue Buffon, 45060 Orleans, Cedex 2, France
Tel.: +33-2-38 638100, Fax: +33-2-38 638182
E-mail: irisins@ibm.net

Partner (5) GSF
Geological Survey of Finland
FIN-02150 Espoo, Finland
Tel.: +358-40-544 9156, Fax: +358-2055012
E-mail: heikki.soininen@gsf.fi

- Associate Contractor (6) BRGM
Bureau de Recherches Geologiques et Miniere
Avenue Claude Guillemin, B.P 6009
45060 Orleans, Cedex 2, France
Tel.: +33-2-38643526, Fax: +33-2-38643361
E-mail: b.bourgeois@brgm.fr
- Associate Contractor (7) IGME
Institute of Geology and Mineral Exploration
70 Messoghion Str., GR-115 27 Athens, Greece
Tel.: +30-1-7798412, Fax: +30-1-7752211
E-mail: dkigme@compulink.gr
- Associate Contractor (8) NCSR “Demokritos”
Institute of Informatics & Telecommunication
Aghia Paraskevi, GR-153 10.... Athens, Greece
Tel.: +30-1-6503000, FAX: +30-1-6532175
E-mail: varou@iit.nrcps.ariadne-t.gr
- Subcontractor (9) University of Turku
Department of Geology
FIN-020500 Turku, Finland
Tel.: +358-2-3335480, FAX: +358-2-3336580
E-mail: papunen@utu.fi
- Subcontractor (10) Athens University
Department of Geology
GR-154 87 Athens, Greece
Tel.: +30-1-7284214, FAX: +30-1-7284214
E-mail: meconom@atlas.uoa.gr

GeoNickel

EXPLOITATION REPORT

~~CONFIDENTIAL~~

EXPLOITATION REPORT

~~CONFIDENTIAL~~

CONTRACT NO: BRPR-CT95-0052 (DG12 - RSMT)

PROJECT NO: BE – 1117

TITLE: Integrated Technologies for Minerals Exploration,
Pilot Project for Nickel Ore Deposits
GeoNickel

PROJECT

COORDINATOR: OUTOKUMPU Outokumpu Mining OY
Finland

PARTNERS: LARCO General Mining and Metallurgical Company
SA,
Greece
BRGM Bureau de Recherches Géologiques et Minières
France
GSFIN Geological Survey of Finland
Finland
SOFTECO Softeco Sismat Spa
Italy
IGME Geological Survey of Greece
Greece
IRIS Iris Instruments SA
France
NCSR 'D' National Center of Scientific Research
'Demokritos', Greece

STARTING DATE: 1st January 1996 DURATION: 36 MONTHS



PROJECT FUNDED BY THE EUROPEAN
COMMISSION UNDER THE BRITE/EURAM
PROGRAMME

Date: February 28, 1999

EXPLOITATION REPORT

CONTENTS

1	SOFTECO SISMAT EXPLOITATION REPORT	3
1.1	Description of the results	3
1.1.1	Results and innovative aspects	3
1.1.2	New items.....	3
1.1.3	Scientific fields.....	4
1.2	Industrial applications	4
1.3	Market analysis	6
1.4	Industrial and intellectual property rights	8
1.5	Exploitation and marketing plan	8
1.5.1	Objectives.....	8
1.5.2	Exploitation strategy	8
1.5.3	Time table for the exploitation.....	10
1.5.4	Supplementary investments.....	11
1.6	Communication strategy	11
2	IRIS EXPLOITATION REPORT	12
2.1	Description of results	12
2.2	Industrial applications	12
2.3	Market analysis	13
2.4	Industrial and intellectual property rights	13
2.5	Exploitation and marketing plan	13
2.6	Communication strategy	13

1 SOFTECO SISMAT EXPLOITATION REPORT

In the following chapters the exploitation plan concerning the partner SOFTECO SISMAT is described.

1.1 Description of the results

1.1.1 Results and innovative aspects

As described with more details in the technical report, the work of analysis and development performed in WP3, WP4, WP5, and the work of integration, validation, test and refinement performed in WP6, resulted in a set of prototype software modules. The partners deem feasible a market exploitation of these prototypes which address, and seem to manage successfully, specific needs in the mineral explorations. Up to now geoscientific databases able to manage such a complex set of data are not available in the market, and the potential capabilities of the analysis tools developed, such as the expert system, the neural network classification tool and the advanced statistical methods, seem to be high.

1.1.2 New items

In GeoNickel the following new main software modules have been designed and developed:

- The database with its management module, and the GIS tools which extend the capability of MapInfo (GEOSIS)
- The expert system (GEOES)
- The neural network classification tool (ANNGIE)
- The advanced statistical methods (ASM)

Although these modules may be considered separately, they are all integrated in a unique software environment. These modules constitute the component of the geoscientific software environment, which supports the work of analysis in the mineral explorations, and which was one of the goals of GeoNickel project.

The database and its management module are the basis of all the software developed. One of the most critical aspects in the mineral exploration is the variety and the complexity of the data which the geoexpert need to consider and analyse. The main goal we aimed at with the design and the development of this module, was the management of these data. The database developed takes into account the large variety of data and allows to store them in an efficient structure. Up to now similar geoscientific database management systems are not available in the market.

The GIS module is based on MapInfo and includes all the capabilities of this common GIS environment. One of the basic decisions taken by the partners was to focus the development of the software on an area where tools and packages are not available and to exploit as much

as possible products already available on the market. Therefore the GIS module developed in the project implements specific functions, which extend the capability of MapInfo and support the mapping of the data present in the database on maps and images.

The GIS module allows an easy use of external packages which performs specific analyses and also supports the following specific analysis methods developed in the project:

The expert system, which allows to perform in depth analyses in the geological contexts taken into account for the nickel ore bodies, with different scale (area, target, zone), and considering different domains (Geology, Geophysics, Geochemistry...). The expert system allows performing the screening of large areas, with huge amounts of data, pointing out the more promising zones, and saving a considerable amount of time in the analysis of the data. It also allows a what-if analysis in the selected zones.

The neural networks, which are one of the most promising methods for the classification of images. The module developed in GeoNickel allows the testing and the combination of different techniques. It is an easy to use and powerful platform for the assessment of the capabilities of these analysis methods in the mineral explorations.

The advanced statistical methods, which allow to perform more traditional statistical analysis and new techniques based on a statistical approach. These analyses are currently used in data elaboration performed in the mineral explorations. This module improves the traditional methods and allows testing new techniques.

In the final period of the project the end user partners have tested the various software modules developed. The software was modified in order to overcome the problems found in the initial tests, the last revision has been tested with some real exploration data and the results are very promising.

1.1.3 Scientific fields

The items described refer to the following scientific fields

- C26 - Terrestrial science
- D09 – Expert systems
- D24 - Neural Networks
- E25 – Metals, alloys
- E27 – Mining

1.2 Industrial applications

On the basis of the software prototype developed in the project, we are planning to develop the following products:

A MapInfo based GIS environment with a geo-scientific database will be the basic system. This environment will allow the management of large amounts of data coming from different scientific disciplines. This is one of the key points of the system, since up to now geo-scientific databases able to manage such complex sets of data are not available on the market, and the industrial

potential of the prototype developed is very high. Also the mapping capabilities of MapInfo have been extended and the integration with the data stored in the database is straightforward. The characteristics of this software product will not be different from those of the actual GEOSIS. The overall client-server architecture of GEOSIS, based on MapInfo and ORACLE, is typical for a product ready for the market. The major modifications required will be focused on the interface and the structure of the database which will have to be further tested and improved.

A second product line will be constituted by some optional analysis tools which will be sold separately:

The Expert System, the Neural Networks, and the Advanced Statistical Methods. These tools will be integrated with the basic system. The potential of these modules needs to be further tested, but the results obtained during the project are very promising. These tools are innovative and they may become unique products in the market with high sales potential. The Expert System has proved to be a useful tool to analyse large sets of data and to concentrate the work in a what-if interactive analysis in the most promising areas. Its performances seem very interesting, but some work needs to be done if we want to focus the system on different minerals. The Neural Networks and the Advanced Statistical Methods seem to be excellent environments for testing the capabilities of these methodologies in mineral explorations. The user of these modules can be laboratories and research institutes which want to test these methodologies and assess their performances.

All these analysis tools may need some software redesign to improve the stability of the software and its integration with GEOSIS.

The target market for the products is the mining and mineral extraction. GeoNickel was focused on mineral explorations and most of the partners are mining companies and geological surveys, the potential products of the project are addressed to this sector.

The products will be applied in the exploration phase of the mineral production. The cost of an exploration project leading through feasibility study to a mining decision is in the order of 10 MECU while the gross value of a medium size Nickel ore deposit is in the order of 300 MECU. The results of the GeoNickel project have demonstrated that the new software tools developed can be successfully applied to the nickel exploration. GEOSIS allows an efficient management of the data, an activity which requires a great deal of resources in a mineral exploration. The analysis tools allow to save time in the analysis of a large set of data, and they may improve the success ratio of the exploration giving new information and allowing more precise ore bodies modelling.

The reduction of cost is not easily predictable but the good results obtained suggest a reasonable estimate of a reduction of the exploration costs of about 1%, which would allow the saving of about 100.000 ECU in every exploration. A set of software tools which allows such a reduction in the exploration costs will have good commercial opportunities.

The software modules developed in GeoNickel are based on low cost hardware platforms (Pentium) with Windows operating system. The cost of a powerful Pentium computer with 64 Mb of Ram 4 Gb of Hard Disk is less than 3.000 ECU. The cost of the basic software packages which are needed for GEOSIS is about 500 ECU for the run time license of MAPINFO (GIS) and about 1.500 ECU for the license of ORACLE (Database). Therefore we are plan-

ning to develop some low cost products which require a small investment compared to the resources required for mineral explorations.

For the mining companies, the risks related to the use of such new software tools lay in the investment needed to buy the software, and for the training of the personnel. But the cost of the software will be comparatively small, and the training of personnel in the use of innovative software tools may anyway be considered a positive investment (even if the new software tools prove not to be successful and are not adopted).

For SOFTECO, the risk related to the development of the software products described will be analysed in detail, in order to have a more precise evaluation of the effort required for the development and of the sales potential of the product.

Another potential market sector, which SOFTECO is planning to analyse, is the environmental monitoring. GEOSIS can be applied in the management of a wide variety of data which all refer to the earth resources, and also the neural networks and the advanced statistical methods can be applied to the environment analysis.

The products described address the following sectors:

- C09 – Environmental monitoring
- C23 – Soil Conservation
- E07 – Mineral extraction

1.3 Market analysis

The target market for the software modules described in the previous chapter comprises

- mines departments and geological surveys
- mineral exploration and mining companies
- consultancy groups to mineral exploration companies

This market includes some of the largest multinational companies, local miners and individual prospectors. It is a traditional and large industrial sector which gives employment to several hundred thousand people and which stands at the basis of the industrial production in many countries. The mining companies operate in an international market with a large number of players, and competition is strong. The companies are facing frequent prices variation due to demand instabilities, discovery and opening of large mining sites, financial and economical crisis. The Asian crisis, for instance, caused a drop in the price of many metals and the companies are now dealing with a relevant profit reduction.

In order to remain competitive in this market the mining companies need to intensify the efforts to reduce operating costs. This may cause a decrease of the long-term investment in new technologies, but increases the need for new available methodologies which allow a cost reduction.

The number of active mining companies, institutes, government services, and service providers in the world is over 5.000. Only in North-America www.infomine.com lists 2267 min-

ing/exploration companies in. There are at least 2000 large companies in the world involved in large-scale mineral exploration. The investment for mineral explorations is high: in the Canadian market (Canada has one of the world's largest mineral markets) expenditures on non-fuel mineral exploration were about \$804 million in 1997 (see Mike McMullen general review of the Canadian mineral industry in 1997). Considering only copper, the number of new large mines in the world in the period 1995-1997 is 82. The number of copper explorations performed which can be estimated is larger considering that some explorations do not lead to a commercial exploitation of the ore bodies. The potential market for the planned products is quite large.

GEOSIS and the analysis tools developed constitute an innovative software and they should not have immediate competitors in the market. In fact some software producers have specialised, successful products, which are sold to the mining industries: MicroImages, DATAMINE, GEOSOFT, ENCOM, ERMMapper, Neural Mining, Rockware and others; but they have products with different features, quite often addressing a specific task of the mineral exploration, mostly concentrated in the image and data processing area. The available software tools are not direct competitors of GEOSIS but the mining market is large and strong enough to support the life cycle of a software product, if the product demonstrates to be useful and if it is well supported.

One of the key factors for the exploitation of the software developed will be the management of different minerals. We are planning to extend our products to other mineral explorations, such as Aluminium, Coal, Copper, Gold, Iron, Steel, Lead, Zinc and Titanium. GEOSIS will be able to support other metal explorations without major modifications, also the Neural Networks and the Advance Statistical Methods should support them. The knowledge base of the Expert System is specific for the Nickel exploration, and addressing other minerals will require a modification of the rules and a new process of knowledge elicitation. Enlarging the target minerals is clearly very important in order to enlarge the potential market of our products, which otherwise will address a very small (even if important) segment of the market.

Considering the number of mining companies, national surveys, universities and consultants which is about 5.000, and considering the relevance of our potential products, which should allow a significant improvement in the explorations, our target can be 5% of the global market. We estimate to sell at least two licences in the major companies (about 2000) which means globally about 350 licenses.

Other markets will be analysed. The most promising one seems to be the environmental market. GEOSIS can be used in the management of a wide variety of data which all refer to the earth resources. During the project almost all the aspects concerning geo-sciences have been taken into account and the database may be used also for the management of environmental data: pollution, agricultural resources, climate, seismic and geographic investigations can be carried out. Also the Neural Networks and the Advance Statistical Methods can be applied to different environmental analyses.

1.4 Industrial and intellectual property rights

The results of the project which SOFTECO is planning to exploit consist of software code, and we are planning to protect the results of the project against software copying. We will probably not protect it by patent: the protection of software by patents is still a moot question and the software patenting rather complex. The most widely followed doctrine governing the scope of patent protection for software-related inventions is the "technical effects" doctrine that has been promulgated by the European Patent Office. This doctrine generally holds that software is patentable if the application of the software has a "technical effect". But while the "technical effect" of the software can be defined for typical industrial applications (for instance the control software of an electronic engine driver), it is not a simple matter to define it in a more complex and wide application such as that of the GeoNickel project.

Moreover the complexity of the different scientific disciplines which are involved in the project makes the copying of the software without a deep understanding of the related sciences rather complex. Therefore we are planning to protect the software produced within the project with a copyright.

All the partners will comply with the confidentiality requirements and will not disclose any detailed architectural information or software code details to other parties outside the Consortium.

All the undertaking will be taken in accordance with the Contract signed by the Consortium and the EC, and the Consortium Agreement signed by the partners and according to the Steering Committee decisions.

1.5 Exploitation and marketing plan

1.5.1 Objectives

SOFTECO is planning to develop and commercialise a set of software products which will

- provide a financial income in a new market sector
- exploit a new technology and begin to work in the mining market, with the knowledge acquired within the GeoNickel project and with innovative products
- develop products with innovative software technologies, improving the company knowledge and skill
- enlarge its market opportunities, also to other sectors different from the mineral extraction
- enlarge the presence of the company in the international markets

1.5.2 Exploitation strategy

The exploitation strategy foreseen follows the following steps:

- Analysis of the investments required and risk analysis for the development of the products.

In this preliminary phase the investments required to improve, complete and redesign the prototype (in order to obtain a product ready for the market) and the relative risks will be analysed.

- Market analysis and Definition of the market policy.
In this phase the market will be further analysed with the cooperation of the end user partners. A market study will be performed. Mining associations and potential users will be contacted, and the real interest for the products will be assessed. Also new markets will be investigated.
- Definition of patent and licensing policy.
In this phase a proper patent and licensing policy will be discussed with the partners and all the actions required to protect the results of the project will be taken.
- Development of the products.
In this phase the following development cycle of the product will be carried out
 - Implementation of the requirements defined by the end users during the project (which have not been implemented because deemed unnecessary in the prototype version, but needed in the product).
 - New test phase on the prototype to assess the performances and the limitations of the system.
 - Software re-design and implementation of the alpha-release
 - Alpha-release test phase
 - Software improvements and bugs correction to the beta-release
 - Beta-release ready for commercial action

The following market actions are foreseen to assess the potential of the products and to commercialise them:

- Market analysis
- Agreement with software producers and distributors in the mining market. This agreement is needed considering the weak presence of SOFTECO in the mining market. Also an agreement with end users, or an association of mining companies will be taken into account.
- Definition of some alpha-beta-release test sites, with the cooperation of some end users
- Commercial dissemination and marketing of the first release of the products.

1.5.3 Time-table for the exploitation

It is foreseen to develop a first version of the products within two years. This is the time-table defined:

Months	1	2	3	4	5	6	7	8	9	10	11	12	1	2	3	4	5	6	7	8	9	10	11	12
Investment required and risk analysis	■	■	■																					
market analysis and patent policy		■	■	■																				
Implementation of the requirem. Defined by the end users					■	■	■																	
New test phase on the prototype							■	■	■	■														
Software redesign and implem. of the alpha-release										■	■	■	■	■	■	■	■	■	■					
Product alpha-release test phase																			■	■	■	■		
Softw. Improvem. and correction to the beta-release																						■	■	■
Commercial dissemination and Marketing																						■	■	■

1.5.4 Supplementary investments

As shown in the time table an investment is needed to develop the products previously defined. Two main lines of activities need to be carried out: the market analysis and commercial actions, which need to be carried out by commercial personnel, and the product design, development and test activities, which need to be carried out by technical personnel (software engineers and also geo-experts). Also a first commercial dissemination and marketing activity to support the product is foreseen.

In the following table the man/month effort estimated for the two lines of activities is shown

Activity	Man/month required
Investment required and risk analysis	3
market analysis and patent policy	3
Implementation of the requirements defined by the end users	5
New test phase on the prototype	6
Software re-design end implementation of the alpha-release	14
Product alpha-release test phase	6
Software improvements and bugs correction to the beta-release	4
Commercial dissemination and Marketing	3

A global investment of about 44 man/month is estimated

1.6 Communication strategy

The communication strategy that SOFTECO is planning to follow aims at the widest diffusion among the potential end users of the new features and capabilities of the software developed. The source code will be protected and not diffused, but the performances and the characteristics of the software will be diffused together with examples and test cases of its application to mineral exploration.

Traditional commercial activities will be carried out, but, because of the weak presence of SOFTECO in the mining market, adequate partnership with other software distributors or producers, or with end users will be defined.

A participation to mining and mineral conferences and official meetings is also planned, to present the results of the project and of the products under development.

2 IRIS EXPLOITATION REPORT

In the following chapters the exploitation plan concerning the partner IRIS is described.

2.1 Description of the results

The prototype, which has been developed, allows investigating the surrounding of a mining exploration borehole with a moving array of fixed geometry; compared to existing surface-to-hole methods this offers the benefit of easier and more intuitive analysis of the results. However the developed system is versatile enough to be also used in surface-to-hole and hole-to-hole modes. The slim diameter characteristic of the system makes it usable in the large majority of mining borehole. The tests performed as part of the research contract have pointed out some undesired artefacts and some design modifications have been made to circumvent those. Hence the system will need to be further tested to assess whether the prototype now fully fulfils expectations. If tests are satisfactorily passed, IRIS Instruments will market the system.

The item described refer to the following scientific field

E27 – Mining

2.2 Industrial applications

The main application of the borehole EM system is in the field of mining exploitation and mine development. It will allow to optimise the sitting of further boreholes aimed at intersecting targeted ore bodies. Not only nickel but most other base metals are found as electrically conducting ores : the applications thus encompass most mining activities. Other use of the underground, such as underground storage, may also be facilitated by information provided by the new system.

As for an equipment manufacturer such as IRIS Instruments, the risks related to the marketing of the new system lie mostly in the very specialised nature of the market and its cycles linked to those of raw materials prices ; the benefits are the enlargement of the products offering and the development of a high technology corporate image.

As for a geophysical services provider such as GSF, the risks related to the marketing of new services based on the new system lie mostly in the pay off duration of the investment necessary to acquire a system and train a team on its use ; the benefits are the competitive advantage of being the first to market a hopefully successful new exploration technique.

As for a mining company such as Outokumpu or Larco, the risks related to the use of such a new technique, either through services contractors or through their own teams, also lie in the pay off uncertainty of the investment necessary to properly use the system and the data it provides ; the benefits are an increased efficiency of their exploration methodology and the possible discovery of a ore body that may be found or better delineated through this new technique.

The product described address the following sector

E07 – Mineral extraction

2.3 Market analysis

In this section only the instrument sales market will be considered.

The evaluation of the potential market can be made through a comparison with the existing market of surface-to-hole EM system, the latter being in the range of fifty systems used world-wide. A similar market potentially exists for the new system. The level of sales aimed at is in the order of ten systems per year, a turn-over of some 1 million Euro.

2.4 Industrial and intellectual property rights

For the non-oil geophysical instruments business patents are only of a defensive benefit since the cost of a world-wide patent is too high compared to the potential market. It is IRIS Instruments experience that non disclosure of any detailed design is the most efficient protection.

2.5 Exploitation and marketing plan

The objective of IRIS Instruments is to market world-wide the new system. The expected gains are the enlargement of its products offering, the further development of a high technology and innovative corporate image, and an increase in turn-over and margins. The new system will be promoted through presentation at trade shows, field demos for a few influential potential clients and general information dissemination (leaflet mailing, web site, ...).

The planned time-table is the following :

- February 1999 : completion of the modified two prototype units
- March 1999 : announcement at the PDAC trade show in Toronto
- March-April 1999 : further field testing in Finland
- June 1999 : finalisation of marketing materials
- Autumn 1999 : field demo in Canada and/or Australia.

2.6 Communication strategy

The core of the communication effort will be based on the technical results that will have been obtained from the further field testing in known geological structures in Finland. The aim is to publish the results in selected technical journals.

GeoNickel

FINAL TECHNICAL REPORT

VOLUME 1

FINAL TECHNICAL REPORT VOLUME 1

INTEGRATED TECHNOLOGIES FOR MINERALS EXPLORATION, PILOT PROJECT FOR NICKEL ORE DEPOSITS

~~CONFIDENTIAL~~

CONTRACT NO: BRPR-CT95-0052 (DG12 - RSMT)

PROJECT NO: BE – 1117

TITLE: Integrated Technologies for Minerals Exploration,
Pilot Project for Nickel Ore Deposits
GeoNickel

PROJECT

COORDINATOR: OUTOKUMPU Outokumpu Mining OY
Finland

PARTNERS: LARCO General Mining and Metallurgical Company
SA
Greece
BRGM Bureau de Recherches Géologiques et Minières
France
GSFIN Geological Survey of Finland
Finland
SOFTECO Softeco Sismat Srl
Italy
IGME Geological Survey of Greece
Greece
IRIS Iris Instruments SA
France
NCSR 'D' National Center of Scientific
Research 'Demokritos', Greece

STARTING DATE: 1st January 1996 DURATION: 36 MONTHS



PROJECT FUNDED BY THE EUROPEAN
COMMISSION UNDER THE BRITE/EURAM
PROGRAMME

Date: February 28, 1999

FINAL TECHNICAL REPORT

INTEGRATED TECHNOLOGIES FOR MINERALS EXPLORATION, PILOT PROJECT FOR NICKEL ORE DEPOSITS *GeoNickel*

VOLUME 1:

CONTENTS

Executive Summary	3
1. Objectives.....	11
2. Means used to achieve the objectives	11
3. Scientific and technical description of the project	13
4. Comparison of initially planned activities and the work actually accomplished.....	14
5. Conclusions for WP1-5	16
6. Conclusions and suggestions for WP6.....	22
7. Acknowledgements	24
8. Annexes.....	25
8.1 Publications.....	25
8.2 Conference presentations	25
8.3 Patents	27
8.4 Summary of GeoNickel output.....	27
8.5 Final Technical Reports of the GeoNickel WorkPackages.....	28
Annex 1 WP1 MINERALOGY AND MODELLING OF NI ORE DEPOSITS	
Annex 3 WP3 IMAGE PROCESSING / PATTERN RECOGNITION	
Annex 4 WP4 GEOSIS DESIGN AND GIS TOOLS DEVELOPMENT	
Annex 5 WP5 KNOWLEDGE BASED SYSTEM (GEOES)	
Annex 6 WP6 FINAL INTEGRATION, Task 6.2 Validation and testing	

VOLUME 2:

Annex 2 WP2 DEVELOPMENT OF GEOPHYSICAL TECHNOLOGY	
--	--

EXECUTIVE SUMMARY

In the following, the GeoNickel project is summarised by WorkPackages.

WorkPackage 1:

WorkPackage 1 developed geological, lithochemical, mineralogical and petrological models and tools for nickel exploration in three different geological environments: sulphidic nickel related to mafic and ultramafic intrusions (Task 1), sulphidic nickel related to komatiitic and picritic volcanics (Task 2), and lateritic nickel (Task 3).

Task 1 included two branches. The “practical tools” branch concentrated on data processing and the application of whole rock chemistry in nickel sulphide exploration. The work resulted in a 32-bit Windows program, “Advanced Petrological Explorer“ (APE), which includes calculation routines, and graphical tools and modelling modules, to determine the nickel exploration key figures in intrusions. The key figures include composition of parental magma, cumulate and crystallisation series, internal structure of the intrusion, contamination and sulphide segregation features, and the openness of the magmatic system. The “novel tools” branch developed new nickel exploration methodologies and enhanced the application of existing ones by studying nine selected intrusions. Mineralogical investigations, isotope (C, S, Sm/Nd) and REE studies resulted, that contamination by black schist triggered the ore-forming processes in intrusions studied hosting ore. Contaminated intrusions can be identified by high orthopyroxene/clinopyroxene ratio. Intrusions, which have experienced sulphide saturation, can be identified, since they are PGE-depleted but Ni-undepleted, and relatively rich in sulphides even at layered series. Continued magma replenishment is required for an effective concentration process. Such intrusions do not contain cyclic units and repetitive olivine cumulate layers.

Task 2 applied an extensive literature study to define the features positive for nickel sulphide exploration in komatiitic lavas and cumulates. Potential indicators for sulphides include high nickel content and sulphide saturation of the primary melt, sulphidic substrates of lava flows, indicators of thermal erosion and wall rock assimilation of channelled lavas, and the pressure (water depth) during lava extrusion. Such features were traced in Archaean Kuhmo and Suomussalmi Greenstone Belts and on the Proterozoic Pulju Greenstone Belt. By applying the conceptual nickel ore model to the data collected, descriptive models for nickel sulphide ore formation in different areas were created. As a project result, ore potential of the preferred lava pathways were indicated and characterised.

The objectives of Task 3 were the development of models of ore forming processes in representative laterite deposits of Greece, in order to be used in the exploration of associated Ni ores in different geologic environments in Greece and elsewhere. For the implementation of the objectives, the Lokris and Vermion areas were selected, and six targets representing three different cases: (1) in situ Ni-laterite deposits, such as the Tsouka in Lokris, and Profitis Ilias in Vermion; (2) transported Ni-laterite deposits, such as the Nissi and Kopais in Lokris and

Metallio in Vermion, and (3) bauxitic laterite deposits, such as the Nissi in Lokris. Ore-forming process models were established based on existing and new geological data acquired during the course of this project, mineralogical and lithogeochemical studies. Finally models were combined with geophysical and image processing data from the studied nickel deposits and their host environment. Integrated data processing methods were developed for exploration and target selection

WorkPackage 2:

The development of geophysical technology was focused on topics in regional, site and deposit scales of sulphide nickel exploration. At regional scale, a ready-to-use prototype, real-time GPS-gravity system and associated software, were assembled for exploration-oriented regional, semi-regional and local gravity surveys. Field campaigns were carried out to test the conditions under which GPS yields the vertical accuracy of a few centimetres, to find out the advantages and disadvantages of the GPS-gravity surveys, and to set guidelines for future work.

At site scale, the applicability of spectral IP method in Ni exploration was studied and proper data acquisition techniques were developed. In the interpretation of spectral IP data, a crucial feature is to use a mathematical model that depicts the behaviour of the spectra. Based on the laboratory spectral measurements, mathematical models describing the behaviour of the spectra were constructed. The problem of phase-spectra asymmetry was solved by using a generalised Cole-Cole spectrum or by fitting the sum of several Cole-Cole spectra. An interactive modelling program (EMPLATES) was developed for ground EM dipole-dipole survey systems operated in frequency domain (Slingram, Sampo, and Melis).

At deposit scale, two new configurations of a 3-component downhole EM method were developed. In the 'cross-borehole' (or tomographic) configuration, a magnetic dipole transmitter is in one hole and the 3-component magnetic receiver is moved in another hole. In the 'single-borehole' configuration, the dipolar source and the 3-D receiver are moved together in the same hole at a fixed separation; this configuration is called 'Borehole Slingram' for its analogy with the well-known dipole-dipole surface EM profiling method. Versatile prototype equipment for 3-component downhole frequency EM measurements was developed. The 'Slim-Boris' system covers the three configurations that can be envisioned in boreholes, i.e. the two configurations developed in this project using downhole transmitter, plus the classical surface-to-hole configuration where the transmitter is a large loop on surface.

In lateritic nickel exploration, gravity (with and without GPS), magnetics, IP, transient EM, and high-resolution seismics were successfully tested in carbonated and ophiolitic environments. Gravity and IP appeared to be the most effective methods to detect ore at a few tens of meters below the surface. High-resolution seismics was accurate for the determination of geometry in depth.

A petrophysical database was compiled for nickel deposits and host-rocks to serve the geophysical modelling and to statistically analyse correlation between mineralogical and petrophysical parameters.

WorkPackage 3:

Effort was concentrated in developing advanced image processing, classification and pattern recognition techniques that can be used to assist geoscientists to locate important geological features related to Ni deposits.

As a result of this work, two software prototypes were developed. Both packages receive as input ancillary data (geophysical, geological, satellite images) in the form of gridded data or images and can produce maps that classify each picture element or grid point into classes (bedrock type, type of ore, etc). Innovative methods recently developed by the information science partners are included in the software.

The first prototype, Artificial Neural Networks for Geological Information Extraction (ANNGIE), comprises a number of different algorithms and methods originating from the field of neural networks and fuzzy processing in order to carry out the classification task. A wide selection of supervised and unsupervised methods is provided for the benefit of the end user, as well as a module that can combine results from different classifiers, in order to take advantage of their benefits and improve individual results. In addition, a module was incorporated into ANNGIE that can be used to locate important linear structures (lineaments). The lineament detection module utilises the results of classification methods and postprocesses them using new image processing techniques in order to identify the required lineaments.

The second prototype, Advanced Statistical Methods (ASM), is also used for classification purposes and achieves its goal by employing advanced methods of statistical nature. A wide selection of supervised classification methods is provided by this prototype. Algorithms for efficiently performing Discriminant Analysis (DA) are incorporated in this module, including Empirical DA, Linear DA, Quadratic DA, Flexible DA and Penalized DA.

Both systems were developed as a result of close collaboration between information scientists and geologists, and appropriate user interfaces were designed and implemented to help the users select methods and related parameters in their effort to identify features of geological importance. Several of the methods included in the software prototypes are applied for the first time to data of geological interest. The software modules were evaluated by the geo-expert partners, using appropriately preprocessed satellite, geological and geophysical data from selected areas of interest in Finland and Greece.

WorkPackage4:

The work performed in WP4 was focused on the development of a geo-scientific information system: GEOSIS. This system supports the management and the analysis of the complex data sets, which are used in the nickel exploration, and integrates the advanced analysis tools developed in the other WorkPackages of the project.

GEOSIS was developed after an extensive work of analysis performed with the co-operation of experts from different disciplines, and using up-to-date software analysis and development tools. It is based on reliable software environments, available on the market at low cost: the operating system is Windows, database ORACLE and GIS MapInfo.

The initial work was focused on the analysis and definition of the requirements. This analysis work proved to be one of the most complex activities because of the great complexity of data and analysis methodologies used in the nickel exploration, and was successfully carried out with the co-operation of geo-experts and software engineers.

The development of the software was carried out within the timing foreseen in the project programme, mostly by taking advantage of object oriented technology and by including in GEOSIS all the GIS and data management functions available in the software environments used. Also the other software analysis modules developed in the project, the expert system, neural network classification methods, and the advanced statistical methods, were integrated in GEOSIS.

The prototype developed was validated and tested by the end user partners. The software was improved on the basis of the results of the first tests, and a final test was performed with real data in Greece and Finland. In the final test, data from real explorations, and referring to different scientific disciplines (geology, geophysics, geochemistry etc.), were loaded into the database and analysed with the available methodologies. The results of the test confirmed the validity of the approach followed in the project. The software developed proved to be easy to use and stable enough to support the real work of the experts during the explorations. The data management allows dealing with the high complexity of the data. The new analysis techniques developed seem promising tools for the mineral explorations. The mapping capabilities of MapInfo can support a large amount of the analysis work which needs to be performed (some specific analysis, for instance three-dimensional modelling, needs to be done with separate tools, but the communication of data with these specific tools is straightforward).

After the positive results obtained in the validation and test phase, and taking into account the industrial criteria which were at the basis of the software development, the partners are planning to proceed into the exploitation phase of the prototypes developed in the project. An analysis of the market opportunities and of the investment required to develop a first release of software products is in progress.

WorkPackage 5:

GEOES is an expert system developed within GeoNickel to facilitate and promote the process of identifying Ni-ore deposits. It was designed and implemented in close co-operation with geo-experts, whose knowledge of the domain has been encoded and transferred into the system. That knowledge is now available in a structured form for every geo-scientist to use, through an interactive and friendly Windows 95 / NT interface. A key advantage in GEOES is its ability to process in a batch mode large quantities of geo-data, and produce results that embody expert opinions, in a small fraction of the time that would be required if the computations were performed by hand.

At the heart of GEOES lie the knowledge base and the inference engine. The knowledge base keeps estimations and facts that reflect the knowledge and experience of geo-experts in a formal, organised fashion. The inference engine is a software module able to apply the knowledge base to input data and draw conclusions. Input data are mostly measurements concerning a certain number of specific factors / subfactors / observations that relate to the exis-

tence of Ni deposits. The conclusions reveal to the user the degree that input data are supportive of Ni deposit existence.

GEOES can handle three different geological models for komatiite, intrusive, and lateritic deposits. For every model there are three exploration stages, namely «explore area», «identify potential zones», and «select target». Those stages cover the whole process of exploration, starting from a wide geographical area, going through the identification of zones of interest, and ending at specific small target areas. For each model / stage combination, there is a distinct set of factors and sub-factors that can be assigned a value either directly by the user or by input data. Factors are grouped by geo-science to facilitate scientists. After the system has run for a data set, it gives in pictorial way an overall result and how much each geo-science has contributed to the overall result, plus a consultation that provides an answer as to how the system has reached those conclusions.

To better support the needs of geo-scientists in their work to identify favourable nickel ore deposits, GEOES is released in three modes of operation:

- Interactive GEOES: is a flexible version of the expert system, perfect for training and familiarising the end user with GEOES, but not suitable for large quantities of real data.
- Spatial GEOES: produces results from large data sets in a form that can be drawn on a map, making it easy to observe interesting spots and geological anomalies.
- Hybrid GEOES: gives the opportunity to further explore a specific spot on the Spatial GEOES results map, and allows the user to engage in what-if scenarios.

All modes of GEOES are fully integrated within GEOSIS, which automatically provides GEOES with input data and shows the results on maps.

WorkPackage 6:

The objective was to test the systems developed in GeoNickel against real known cases. In the earlier phases of the project GEOSIS and GEOES programs were first tested with virtual data. Malfunctions were encountered but once corrected, the programs functioned properly in virtual testing and the real case testing was initiated.

Real case testing for the exploration of sulphidic Ni deposits related to intrusives was done in the Northern Bothnia test area, Central Finland, where nickel mines and prospects occur in mafic-ultramafic intrusives. Existing data were collected from databases. Since the lithogeochemical data did not cover all of the prospective areas of mafic rocks, additional sampling was carried out, and lithogeochemical and mineralogical analyses were done on the 45 samples collected. Finally, a total of 1278 analyses from 61 targets were processed with APE.

Komatiites were tested on the Pulju greenstone belt (PGB), Finnish Lapland. PGB is composed of felsic metavolcanites and metasediments overlain by flow and cumulate (up to 50% MgO) komatiites, which in turn are topped by mafic metavolcanites. The succession underwent polyphase deformation. A total of 653 XRF-analysed samples were processed with APE with the purpose of identifying the nickel potentiality of PGB and classifying heavily altered rock types on the basis of the whole rock analyses. As a result, Ni-potential komatiites were

identified from less potential ones. Komatiite cumulus phases were classified and coherent naming was established.

APE was found to be a tool suitable for geologists dealing with lithochemical data.

In WorkPackage 6, the “Database and GIS” GEOSIS is integrated with advanced data analysis tools developed in the other WorkPackages of GeoNickel: the Expert System (GEOES), the Neural Network Analysis Module (ANNGIE) and the Advanced Statistical Methods (ASM). This leads to the expanded meaning for term GEOSIS: the whole software system developed during the project and integrated to operate through the common user interface.

The “Database and GIS” GEOSIS and GEOES modules were tested for sulphidic and lateritic Ni deposit exploration environments with virtual and real case data during the different phases of the software development. This facilitated an interactive, cyclic development process, where problems encountered were solved and corrected by the software developers, and new versions of both GEOSIS and GEOES were delivered for further testing. For instance, the interactive GEOES developed in the early phase of the project was tested extensively and systematically in order to locate errors and unbalanced parameters in the system. After a fine-tuning and correction phase, the next version of interactive GEOES was tested against known Ni deposits and real exploration targets in collaboration with Ni exploration geologists.

For the sulphidic Ni exploration, the database modules of GEOSIS were first tested in WP4 using the data collected in WP3 from the Vammala and Enonkoski areas, Finland. GeoNickel tools GEOSIS, GEOES and APE were used also in WP1. The final testing of the prototype, GEOSIS database modules, revealed technical features that should be developed further if commercialisation takes place. The most important area to be renewed in the software is the input and output tools. These processes should be developed from the simple prototypes to versatile and user-friendly software modules that would facilitate easy data entry to database and easy and fast access to all the data stored, with flexible reporting tools for data querying and output.

GEOES is an Expert System aimed to facilitate exploration performed by geoscientists. It is integrated within the GEOSIS system and can be used in three different modes (Interactive, Spatial and Hybrid), sharing the knowledge base but each one having a different role. The system gives emphasis on the integration of a variety of different approaches for the nickel exploration tasks, combining a wide range of data and knowledge from all geo-domains involved. It covers geological models for lateritic, komatiitic and intrusive types of nickel deposits and provides assistance to users during the different phases of their exploration work. These include “Area Selection”, where wide areas are examined for the existence of nickel ore deposits, “Identification of Potential Zones”, whereas zones within a given area are examined, and “Target Selection”, where restricted areas are examined.

The tests of the three modes of GEOS were made on data collected from the selected test areas; sulphidic exploration models were tested in Finland and the lateritic model in Greece. In both countries, the first step involved the testing of the Area Selection models using data covering most parts of the countries; Intrusive mode was tested in Finland and Lateritic mode in

Greece. Test results showed that, based on input data, GEOES was able to locate the major zones and areas that host the modelled type of Ni deposits. In Greece the “Laterite Area Selection” mode was also tested in the areas of Lokris, Euboea Island, Vermion and Kastoria. In three cases the results were well related to the real assessment and encouraging, but in the other two, they were not in agreement with the known geology of the areas. In both cases, the discrepancy may be attributed to limitations in geophysical data.

The “Identification of Potential Zones” and “Target Selection” modes for Intrusive and Komatiite models were tested in two test areas in Finland, the Northern Bothnia test area and Pulju Komatiite Belt, respectively. The corresponding lateritic tests were carried out in four different test areas: Lokris, Euboea Island, Vermion, and Kastoria.

The tests for “Identification of Potential Zones” for both Intrusive and Komatiite models resulted in detecting the known areas potential for hosting nickel deposits. Further, they revealed interesting targets not recognised earlier. The data preparation procedure indicated, however, that the quality and coverage of the data and the objectivity of the preprocessing measures used in extracting information for the observations needed in spatial GEOES analysis, are of utmost importance for reliable results.

The identification of potential zones for lateritic Ni deposits was tested in the Lokris area and Pyrgoi in Vermion. In the Lokris area, three nickel ore potential zones were defined. Results in geochemistry, mineralogy and geophysics correlated well with the existing background information, but the results for geology were weak in one of the studied map sheets. In the Vermion area, GEOES suggested a zone where the mineralised horizon is hosted, and geochemical, mineralogical and geophysical data corresponded with the background information.

The target selection mode of spatial GEOES for intrusives was tested in the Northern Bothnia area using a large data set (6043 grid cells) collected digitally from the existing data. Several tests with different input data and evidence weight configurations were conducted in order to see how these affect the results. This also gave the possibility to evaluate, how the user can control the system for different exploration scenarios and “what if?” simulations. The tests conducted generally revealed three to six of the seven Ni deposits and occurrences used as reference targets in the test area, and a reasonable amount of other anomalies in geologically sound locations were detected. The tests also showed that the system might be controlled by changing the evidence weights and/or selecting input data. In Greece, the target selection mode for the lateritic Ni deposits was evaluated mainly in the Lokris area. The results corresponded with the existing data for the area.

In general it is apparent that GEOES is a complete and powerful exploration tool for the Area Selection, Identification of Potential Zones, and Target Selection, covering and compiling geological data from diverse origin (geology, geophysics, mineralogy and geochemistry). It corresponds well to results obtained using conventional exploration methodologies. However, the developed prototypes in the GEOSIS system (GEOSIS database and GIS modules, GEOES, ANNGIE and ASM) at present form a conglomerate of complex software that has been developed in different environments and need different third party programs to be run. If commercialisation of the GEOSIS system takes place, the integration of these programs should be carried further than is the case in the prototypes.

Though nickel exploration was the primary target for GeoNickel, it is evident that most of the developed instruments and software are of generic nature. Consequently, they can be applied to a great variety of base metals deposits other than the "nickel family" (Ni, Co, Cu and PGE). Most of them can be used to aid mineral exploration genetically related to magmatic, or even sedimentary rocks in various geotectonic environments.

One of the powers of the GEOES Expert System is the systematic approach needed from data acquisition to output of results. It gives the exploration staff a good opportunity to systematically examine all of the available data, estimate their homogeneity and validity showing where more information is required for well-balanced reasoning results. An important feature in using such an expert system may also be the fact that it forces different specialists in an exploration team to work more closely and coherently, enhancing the strengths of teamwork in mineral exploration.

FINAL TECHNICAL REPORT

INTEGRATED TECHNOLOGIES FOR MINERALS EXPLORATION, PILOT PROJECT FOR NICKEL ORE DEPOSITS *GeoNickel*

1. OBJECTIVES

The securing of nickel raw material base for industries in Europe necessitates intense exploration for new nickel ore deposits as well as research and re-evaluation of known but uneconomic ones. However, most of the known nickel potential areas in Western Europe have already been surveyed using various existing exploration methods, and the European base metals industry is a nickel net importer. Consequently new approaches are needed to enhance effectiveness and success rates in nickel exploration projects.

Responding to the challenge presented above, the overall objectives of GeoNickel were set to enhance the geological and geophysical knowledge on nickel ore deposits, and to develop novel, integrated nickel exploration methods and tools. GeoNickel met the objectives by reaching the overall results summarised below. For detailed information, the Annexes of Final Report are referred.

- Geological models in various geotectonic environments were developed for nickel ore-forming processes in mafic and ultramafic intrusive and extrusive (komatiitic) rocks, and in laterite environment.
- The efficiency of several geophysical methods was improved for regional and detailed exploration by developing prototype instrumentation and software.
- A Knowledge Based System (GEOES) was developed, tested and implemented based on the modelling of nickel deposits, as well as on geological, geophysical and other data stored in Geographic Information System (GIS) database and on remote sensing data processed with innovative image processing/pattern recognition techniques.

Exploration methods are of generic nature, consequently the products developed in GeoNickel apply also to a great variety of base metals deposits other than the "nickel family" (Ni, Co, Cu and PGE).

1. MEANS USED TO ACHIEVE THE OBJECTIVES

The objectives of GeoNickel, an integrated multilateral research program, were to develop new exploration methodology and technology specific for nickel deposits but generic enough to be applicable also to other types of ore deposits. The development of deposit modeling was based on geochemistry, detailed mineralogical studies of silicates, oxides and sulphides, on isotope

geochemistry, and on geochemical and metallogenic modelling. The deposit models were formulated into knowledge base needed in nickel exploration.

New automated software systems were developed to extract information from a large amount of data of diverse origin (geological, geophysical, geochemical and satellite images), organized as database. The interpretation of data was made using different nickel ore deposit models. The integrated software systems developed in GeoNickel will act as a focal point for the active cooperation between nickel explorationists of different backgrounds.

To meet the overall objectives of GeoNickel, three key areas of methodology in nickel ore exploration were selected for research and development work.

1. Modelling of nickel deposits: development of models of ore-forming processes in mafic and ultramafic rocks to enhance exploration of associated Ni(-Cu-Co-PGE) ores in various tectonic environments. The work covered sulphide and laterite nickel deposits. Emphasis was laid on mineralogy-related studies because mineralogy is an important factor in ore beneficiation and the key indicator of ore-forming processes.

2. Development of geophysical technology: improvement of the efficiency of several geophysical methods, for regional and detailed exploration, by developing prototype instrumentation and software. Emphasis was laid on designing an integrated GPS-gravity system, and on various measurement and interpretation tools in electric and electromagnetic exploration methods - especially a wide-band drill-hole and ground EM system, and spectral IP.

3. Geoscientific Information System (GEOSIS): development of a Knowledge Based System (GEOES) based on the modelling of nickel deposits, as well as on geological, geophysical and other data stored in geographic information system (GIS) database and on remote sensing data processed with innovative image processing/pattern recognition techniques. This integrated software system will act as a focal point for the active co-operation between nickel explorationists of different backgrounds.

Due to the complexity of the geological, geophysical and information technology tools to be developed, the project was divided into six WorkPackages (WP) shown in the following list. Each WP was subdivided to Tasks led by one of the participating organisations, however most of them were jointly conducted by several of the consortium partners. Outokumpu Mining Oy was the overall co-ordinator. The following list summarises the six WorkPackages of GeoNickel.

WP1 Mineralogy and modelling of Ni ore deposits
Intrusion related Ni sulphide deposits
Extrusion related Ni sulphide deposits
Lateritic Ni deposits

WP2 Development of geophysical technology
GPS-gravity system
On-site ground surveys
3-component borehole EM methods
Petrophysical database

WP3 Image processing/pattern recognition
Data acquisition, quality evaluation
Image processing
Classification of lithology and alterations
Delineation of lineaments using ANN

WP4 GEOSIS design and GIS tools development
Requirements analysis
GEOSIS application design
Implementation of prototype GIS
Development of tools

Comparison of techniques	Integration, validation, testing
WP5 Knowledge Based System	WP6 Final integration and testing
Knowledge elicitation	Integration of GEOSIS and Knowledge Based System
Design of Knowledge Based System	Validation, testing
Validation, testing, refinements	Refinements
	Field testing

2. SCIENTIFIC AND TECHNICAL DESCRIPTION OF THE PROJECT

Due to the complexity of the geological, geophysical and information technology developed for Ni exploration, the project was divided into six WorkPackages. According to the general project schedule, the development work proceeded in each WorkPackage in different steps, produced a multitude of different deliverables, software and hardware. First in the last WorkPackage (WP6) the software tools developed in WorkPackages 3, 4 and 5 were integrated in the “GeoNickel toolbox” - GEOSIS – and tested with real data from various test areas in Finland and Greece. The Mineralogical knowledge and models for the Ni ore deposits developed in WP 1 were applied both in the development of the Expert System (WP5) and in the testing phase. The development of geophysical technology produced both hardware and software for Ni exploration.

The complexity and multitude of results from the project was considered to justify the separate description of the scientific and technical achievements in each WorkPackage. Accordingly, each WorkPackage has prepared a separate Final Technical Report which are presented in Annexes 1-6:

Annex 1 (Volume 1)	WP1 MINERALOGY AND MODELLING OF NI ORE DEPOSITS
Annex 2 (Volume 2)	WP2 DEVELOPMENT OF GEOPHYSICAL TECHNOLOGY
Annex 3 (Volume 1)	WP3 IMAGE PROCESSING / PATTERN RECOGNITION
Annex 4 (Volume 1)	WP4 GEOSIS DESIGN AND GIS TOOLS DEVELOPMENT
Annex 5 (Volume 1)	WP5 KNOWLEDGE BASED SYSTEM (GEOES)
Annex 6 (Volume 1)	WP6 FINAL INTEGRATION, Task 6.2 Validation and testing

As the work content of WorkPackage 2, Development of Geophysical Technology, was large, the report required a volume of its own.

Following from the above, scientific and technical description of the project are referred in the Annexes.

4. COMPARISON OF INITIALLY PLANNED ACTIVITIES AND WORK ACTUALLY ACCOMPLISHED

WorkPackage 1:

Task 1: The work in Task 1 was realised mainly as originally planned. Since the market price of nickel halved during the project and studied fertile intrusions were relatively small and of low grade; effort was directed to develop generic tools applicable to world class nickel deposits, as well. As a result a computer program Advanced Petrological Explorer (APE) was developed and installable prototype was delivered to the GeoNickel partners, though this kind of work and product were not literally included in the original project plan.

Resulting from above, the effort put on case studies of fertile and barren intrusions was slightly less than originally planned. However, the objectives in this area were achieved. Sophisticated techniques (stable and radiogenic isotopes, rare earth elements and trace element contents of minerals) were applied to find out the petrological differences between barren and fertile intrusions. Finally, simple and easy-to-use discrimination criteria were established. Even though the tools created are not totally new, Task 1 succeeded in sharpening some of the old ones. As a result, the determination of the key figures (required for the discrimination of barren and fertile intrusions) on the basis of litho-geochemistry and mineralogy is currently more reliable, faster and cheaper than it was when project started.

Task 2: The work was realised mainly as was planned originally. During the course of the work the detailed field data was observed pronounced in understanding the volcanic evolution and possible crustal contamination of the ultramafic and mafic magmas and the quality of the field data was hence emphasised. Detailed studies of the target areas allowed area-specific interpretations of the ore deposit models. Novel methods in GPS- and computer-aided mapping improved, facilitated and speeded up the laborious phase of the field work and very detailed information was obtained to support the area-specific deposit modelling. Geochemical data became more numerous than planned because identification and classification of mafic and ultramafic volcanics were impossible without comprehensive geochemical information. Geochemical data revealed unexpected Cr-rich basaltic lavas in the stratigraphic succession of the Kuhmo greenstone belt. Their origin and relation to komatiitic volcanism is the target of further study at the University of Turku. The stratigraphic schemes allow the construction of volcano-sedimentary evolution in Archaean and Proterozoic greenstone belts, which forms a firm basis to predict the geological units potential for Ni sulphides. The database can be applied for the testing of GEOSIS systematics.

Task 3: The objectives of Task 3 were the development of models of ore forming processes in representative laterite deposits in Greece, in order to be used in the exploration of associated Ni ores in different geologic environments in Greece and elsewhere.

These models were established based on existing and new geological data acquired during the course of this project, as well as mineralogical and litho-geochemical studies. Further, the ore forming process models were combined with geophysical and image processing data from the

studied nickel deposits and their host environment, in order to develop integrated data processing methods for exploration target selection.

The achieved objectives correspond to the stated ones. More specifically the following works were completed for all areas according to the original plan.

WorkPackage 2:

WP2 was executed according to the original work programme; however, testing was accomplished also in real field conditions both for 3-component down hole EM and GPS Gravity instruments.

WorkPackage 3:

There were no substantial deviations from the original plan.

WorkPackage 4:

On the whole, all the activities initially planned were performed, even if some modification in the time scheduling have been done, and the results which where in the original scope of the project have been obtained.

The most relevant modifications were caused by the need to allocate more resources in the analysis of the data, their structure and the interface needed for their management.

The database management proved to be very complex and required more efforts both in the design and development phase (Task 4.2 and 4.3), in the test and debug phase (Task 4.5), and also in the WP6 for the final refinement and consolidation. The extra effort required was compensated by the exploitation of object-oriented software development tools and methodologies, which allows to speed up the development process, and by the reduction of cost of the hardware platforms.

The validation and testing activity performed by the end user partners in the final phase of the project allowed to assess the performance of the software and confirms its correspondence with the initial objectives of the project.

Also the future exploitation of the results seems feasible on the basis of the reports of the end users.

WorkPackage 5:

The activities initially planned for GEOES, although not so clear at the beginning, were clarified during the project and were well accomplished. The early release of GEOES prototypes helped in the evaluation and subsequent successful knowledge acquisition process.

WorkPackage 6:

Despite the collection of 45 additional samples from the Northern Bothnia test area for intrusives, WP6 generally advanced as initially planned.

5. CONCLUSIONS FOR WP 1-5

WorkPackage 1:

Task 1, intrusive case: Task 1 developed new tools for nickel sulphide exploration related to intrusions. A practical data processing and research tool called “Advanced Petrological Explorer” (APE) was created. APE is 32-bit windows program consisting of seven executables. Prototype released in the end of the project does not have competitors in the world market. Small markets, however, may hinder the program to become a commercial product.

Novel Ni exploration tools were developed by the case studies of nine selected intrusions. A major conclusion of the studies is, that contamination by black schist triggered the ore formation process in studied ore-hosting intrusions. Methods to identify favourable contamination were created. These include mineralogical investigations, isotope (C, S, Sm/Nd) studies and REE analyses. In studied geological environments orthopyroxene/clinopyroxene ratio may provide a direct measure on favourable (SiO₂-rich) contamination.

Positive identification of the sulphide saturation in magma can be done on the basis of sulphide content, olivine composition (calculated) and PGE level of intrusion. PGE depleted but Ni undepleted intrusions, which are relatively rich in sulphides - even in the layered series - are the most prospective ones. Effective concentration process of sulphides can take place in intrusions, which have been formed as a result of continued magma replenishment in an open system. These kinds of intrusions do not contain cyclic units and repetitive olivine cumulate layers.

The determination of the key figures required for discriminating barren and fertile intrusions is more reliable, faster and cheaper than it was when project started.

Task 2, extrusive case: Task 2 concludes that minable Ni deposits have not as yet been discovered in the Kuhmo Greenstone Belt (KGB). The Ni occurrences studied (Hietaharju, Peura-aho, and Arola) are associated with either cumulates of the preferred pathways of high-Mg basalts (Hietaharju and Peura-aho) or an intensely deformed zone characterized by the metamorphic and hydrothermal alteration of high Cr basalts (Arola); even there, however, the proximity of komatiitic volcanics is evident.

Stratigraphic sequences of komatiitic flows in KGB rarely include sulphidic and graphitic inter-layers. These seem to correlate with Ni deposits in fertile komatiite areas. Only the known Ni-Cu deposits of the Kiannanniemi area are related to graphitic and sulphidic sediments. A question not resolved as yet is the relationships of sulphidic/graphitic sedimentary interlayers with the great depth of the environment of volcanic eruptions that could be a positive indication of favourable area. Accordingly, the areas where komatiitic ultramafic and felsic volcanics are interlayered are rare in KGB. This succession seems to be crucial for the formation of high-Ni massive sulphide deposits of Western Australia.

The indications of sulphide Ni deposits discussed above provide a positive model for sulphide Ni ore formation. The ore potential of the preferred lava pathways is indicated.

Task 3, laterite case: Task 3 concludes that major and trace element geochemical data from the Fe-Ni deposits in Lokris and Vermion areas show Ni, Co, Fe, and Cr contents which are indicating origin from ultrabasic rocks. The presence of significant aluminum content in some karst type ores in Lokris is most probable to be attributed to the basic rocks of the ophiolite complex. The mineralogical relationship of the sedimentary ores with the laterites, which is especially supported by the presence of phyllopyritic minerals containing significant amounts of nickel, is also a strong supportive argument for their origin from ultrabasic rocks.

The very low Al_2O_3 , TiO_2 , and REE content are common features of the Fe-Ni ores of The Tsouka (Lokris) and Profitis Ilias (West-Vermion).

A preference of Pt over Pd and an increase in the Pt/Pd ratio upwards, through the lateritic profile, may indicate that during a subsequent stage of the diagenesis, and downward leaching of metals Pt is less mobile than Pd.

Assuming that the Cr and Al contents of chromite grain-fragments within laterites represent primary compositions, the comparison between the composition of chromite in the saprolite zone and the overlain Fe-Ni ore may provide evidence for discrimination between ore linked with the in situ weathering and those derived by the transportation of clastic and chemical material to some extent.

The compositional variation of chromite in Ni-laterites and bauxitic laterites from Nissi (Lokris) suggests that major factors controlling their composition are both the parental rocks and the conditions during their transportation and precipitation of their components.

The geological environment of the Fe-Ni deposits in both studied areas, their mineralogical and geochemical data indicate a sedimentary formation either in situ or transported. It is considered that the formation of these deposits is mainly a seawater process that is affected directly or indirectly by the continent.

In the Lokris area, the Kopais and Tsouka deposits are typical Ni-laterites whereas the Nissi deposit is bauxitic laterite. The Kopais and Nissi deposits are of chemical and/or clastic sediment type transported either short or greater distance from parent rock. The Tsouka deposit at its lower parts is comprised of in situ weathered material whereas its upper parts comprise transported material.

In the Vermion area, the Profitis Ilias and the Metallion deposits are typical Ni-laterites. More specifically the Profitis Ilias deposit comprises in situ weathered material whereas the Metallion deposit comprises transported material of clastic sediment type.

WorkPackage 2:

WP2 developed useful geophysical nickel exploration tools for regional, site and deposit scale investigations. The deliverables of WP2 are also applicable to the exploration of the VMS type of sulphide ore deposits.

GPS elevation measurements and digital Gravity measurements were combined to obtain accurate and cost-effective regional gravity surveying. Spectral IP method was successfully applied to Ni exploration, in particular specific measurement procedures were developed. Software was developed for fast (approximate) interpretation of ground EM methods. For the lateritic Ni, field-tests were carried out with existing geophysical methods to detect, map and outline the lateritic FeNi bodies. In conclusion, the project has assembled and tested a practical real-time GPS-gravity system and gained relevant know-how to effectively apply such a system in various conditions and configurations.

Cross-hole (tomography) and single-hole (borehole Slingram) EM methods (with 3-component receiver) were developed for locating off-hole targets and possibly outlining intersected orebodies. The task involved development of prototype equipment suited to slim exploration boreholes, processing and interpretation software, methodology and field tests.

With the objective of serving all the above applications, a petrophysical database of Ni deposits and host-rock was also compiled.

Spectral IP: Laboratory determinations of resistivity spectra from sulphidic nickel deposits and their environments were carried out. More than 500 samples were measured. Relationships between the measured spectra and textural features of the samples were studied using image processing techniques. Based on the laboratory spectral measurements the mathematical model to describe the behaviour of the spectra was constructed. The problem of the phase-spectra asymmetry can be solved by using a generalised Cole-Cole spectrum or by fitting the sum of several Cole-Cole spectra.

The problem of electromagnetic coupling was addressed by developing a non-collinear electrode array that minimises the primary coupling of the layered host. By using such optimal array, the highest available frequency can be increased at least one decade over the maximum frequency given by standard collinear dipoles (up to several kHz). Field-tests were carried out at Kuhmo and Ylivieska (Finland).

Ground EM: An interactive interpretation program (*EMPLATES*) was developed for the ground electromagnetic (EM) dipole-dipole measurement systems operated in frequency domain (Slingram, Sampo and Melis). The *EMPLATES* program combines an approximate forward computation, based on thin plate models in layered conductive space, with an automatic optimisation and a user-friendly interface under Windows 95. Forward computation usually takes only a few minutes, inversion takes less than one hour.

The final report describes the basic theory and equations that form the approximate computational method and the inversion procedure used in the software. The results from *EMPLATES* were compared to those from a 3D integral equation software used by GSF (*MARCO*). When a *MARCO* forward model is inverted with *EMPLATES*, the XY location and 3D attitude of the initial plate are well retrieved, but its depth and conductivity are always over-estimated

(strongly for the conductivity). The EMPLATES software, though presenting some limitations, is useful for quickly deriving location and attitude of a target. It can be used for siting a borehole, but the user must remember that the depth is about 50% over-estimated. Its best use is probably to give first guess for other more sophisticated, but slower, interpretation software.

Geophysics for laterite: Gravity (with and without GPS), magnetics, induced polarisation (IP), transient EM, and high-resolution seismics were all successfully tested in carbonated and ophiolitic environments. The most effective methods to detect the ore at a few tens of meters below the surface revealed to be gravity and IP, as well as high-resolution seismics for accurate determination of the geometry at depth.

Three-component borehole EM methods: Versatile equipment for 3-component downhole electromagnetic (EM) measurements has been developed at IRIS Instruments. The 'SlimBoris' system covers the three configurations that can be envisioned in boreholes: a) the classical surface-to-hole configuration, where the transmitter (Tx) is a large loop at the surface and the receiver (Rx) is a 3-component probe moving in a borehole, b) the less-developed cross-hole (or tomographic) configuration, where Tx is a magnetic dipole in a borehole and the 3-component Rx probe is in another hole, and c) the innovative single-hole (or borehole 'Slingram') configuration, where both the Tx and Rx probes move in a same borehole at a constant separation (the borehole equivalent of the 'Slingram' surface profiling method).

A practical conclusion regarding the instrument design and field configuration is that, given the usual noise levels, the transmitter power obtained by IRIS should enable an investigation radius of about 50 m around a borehole. In the 'single-hole' configuration, a Tx-Rx spacing of about 100 m should be best suited in order to obtain this investigation range. Another conclusion of these modellings is that both the single- and cross-hole arrays should give better resolution than the surface-to-hole array (at the expense of reduced investigation range). Elementary rules for deriving target's location and dip with respect to the borehole, have been elaborated for simple targets in the single-borehole configuration.

Inversion software (using Marquardt-Levenberg algorithm) was developed for rapid interpretation of borehole EM data. It is based on very simple models such as EM dipoles or current filaments, the calculation of which takes only a fraction of second on a standard PC (e.g. 486). Thanks to the speed of the forward calculation, the whole inversion process (needing tens to hundreds of iterations) is performed in only a few seconds. The validity and interest of such simple models have been assessed on synthetic data calculated with 'exact' 3D modelling software. The results are very satisfying: the 3D attitude of the target is always well retrieved and its 3D location is as accurate as a few percents of the target-to-borehole distance.

Compilation of a petrophysical database: The petrophysical database concerning the density, magnetic and electrical properties of the Ni bearing lithology has been established and documented. The database includes petrophysical parameters of both magmatic and lateritic deposits. Laboratory measurements and statistical analysis of the samples related to WP1 deposits have been performed as well.

Statistical analysis has been applied to get correlation between different rock types, petro-physical parameters and chemical assays. Factor analysis appeared to be a very useful tool to analyse the inner variance of nickel ore.

WorkPackage 3:

Two software prototypes were developed for assisting geologists to identify important geological features related to Ni deposits. These prototypes were integrated into GEOSIS and can be applied for rock type classification and geomorphological structure identification.

Regarding the methods used to achieve the objectives of the project, the first prototype (ANNGIE-Artificial Neural Networks for Geological Information Extraction) comprises a number of different algorithms and methods originating from the field of neural networks and fuzzy processing. Innovative algorithms recently developed by the information science partners are included in the software. In addition, a module was incorporated into ANNGIE that can be used to locate important linear structures (lineaments). The second prototype (ASM-Advanced Statistical Methods) is also used for classification purposes and achieves its goal by employing advanced methods of statistical nature. Collaboration between information scientists and geologists led to the design and implementation of the user interfaces for selecting methods and related parameters for each task.

The software modules were evaluated by the geo-expert partners, using appropriately pre-processed satellite, geological and geophysical data from selected areas of interest in Finland and Greece. Several methods included in the software were applied for the first time to the geoscientific field. It was found that the developed methods are interesting new tools for the exploration geologists and are able to extract information useful to the exploration of Ni deposits. Evidently, there is still room for the refinement of the prototype software. Significant improvements could be made by adding the true georeferencing of data, extending the allowed geodata formats to those normally used in GIS and image processing systems, and by adding also point data to the suite of data types allowed in the classification. Application of the novel methods to real exploration problems also calls for further familiarisation of the geologists with the newly developed tools. It is important, however, that ANNGIE and ASM are advanced new information science products, now available to the geoscientists and capable of processing the ever increasing amount of remotely sensed data in regional and local scale.

WorkPackage 4:

WP4 focused on the development of a geo-scientific information system, GEOSIS, which supports the management and analysis of the complex datasets used in nickel exploration. It integrates the advanced analysis tools developed in the other WorkPackages. GEOSIS is based on software environments available on market at low cost: the operating system is Windows, database ORACLE and GIS MapInfo. All of the GIS and data management functions available in the software environments used, as well as the other software analysis modules developed in the project (the expert system, neural network classification methods, and advanced statistical methods) were included in GEOSIS. Final tests were performed on real data from Finland and Greece.

The development of the software was carried out within the timing foreseen in the project programme, mostly by taking advantage of object oriented technology and by including in

GEOSIS all the GIS and data management functions available in the software environments used. Also the other software analysis modules developed in the project, the expert system, neural network classification methods, and the advanced statistical methods, were integrated in GEOSIS.

The prototype developed was validated and tested by the end user partners. The software was improved on the basis of the results of the first tests, and a final test was performed with real data in Greece and Finland. In the final test, data from real explorations, and referring to different scientific disciplines (geology, geophysics, geochemistry etc.), were loaded into the database and analysed with the available methodologies. The results of the test confirmed the validity of the approach followed in the project. The software developed proved to be easy to use and stable enough to support the real work of the experts during the explorations. The data management allows dealing with the high complexity of the data. The new analysis techniques developed seem promising tools for the mineral explorations. The mapping capabilities of MapInfo can support a large amount of the analysis work which needs to be performed (some specific analysis, for instance three-dimensional modelling, needs to be done with separate tools, but the communication of data with these specific tools is straightforward).

After the positive results obtained in the validation and test phase, and taking into account the industrial criteria which were at the basis of the software development, the partners are planning to proceed into the exploitation phase of the prototypes developed in the project. An analysis of the market opportunities and of the investment required to develop a first release of software products is in progress.

WorkPackage 5:

GEOES belongs to the class of integrated systems. It integrates information from many geodomains in order to assess the existence of Ni-ore deposits. The GEOES knowledge based system is the result of a multidisciplinary approach to the problem of mineral exploration. It utilises knowledge and information from diverse domains (geological, geophysical, geochemical, pedogeochemical, lithogeochemical, mineralogical) and combines them to provide an overall conclusion concerning the assessment of Ni-ore deposits in certain areas.

Knowledge is exploited by a very generic inference mechanism that calculates the favourability of hypothesis with pictorial and text consultation. The explicit representation of the different types of knowledge using specific structures contributes to the development of a knowledge base that can be expanded and maintained with efficiency, effectiveness and safety. A key feature in this dimension is the effectiveness with which knowledge can be enriched so as to include more detailed and subtle issues concerning the assessment of the existence of Ni-ore deposits.

Furthermore, the generic mechanism that exploits the represented knowledge can be transferred to the exploration of other types of ore-deposits (except Ni deposits). Knowledge concerning these types of ore-deposits has to be structured using the knowledge structures mentioned above.

GEOES offers a complete suite of expert tools to geo-scientists, since it is designed to support all the stages of Ni exploration, from wide area selection to potential zones and further to target selection. In addition it comes in three modes of operation, interactive, spatial, and hybrid, that are adapted to be used for different but complementary purposes.

A crucial feature of the system is its complete integration with the overall GEOSIS system. Integration of these systems helps geo-experts to manage their exploration data more effectively and contributes to the identification of further (geological, geophysical, geochemical etc.) features, as well as to refine knowledge concerning the importance of known features to the assessment of Ni-ore deposits.

6. CONCLUSIONS AND SUGGESTIONS FOR WP6

Real case testing for the exploration of sulphidic Ni deposits were performed in the Northern Bothnia test area for intrusives, and komatiite test were carried out on the Pulju greenstone belt, Finland. The corresponding testing for the lateritic Ni deposits was carried out in the areas of Lokris, Euboea Island, Vermion and Kastoria, Greece.

For the sulphidic cases, data were acquired from existing files and in the field. The whole rock and mineralogical analyse results were processed with APE. This facilitated fast and versatile analysis of the available lithogeochemical and petrological data for both the intrusive and the extrusive case studies. Lithogeochemical factors important in the exploration of Ni deposits related to intrusives are readily calculated and transformed into input data for GEOES. In komatiite case APE was also used for renaming and classifying rocks into coherent types by comparing the chemistry and (calculated) mineralogy to rock type names given to the rocks in the field.

APE made it possible to have all the tools a researcher needs under the same software. It was designed for researchers and exploration geologists, who wish to analyse lithogeochemical data in detail, but use large data sets. The advantage in APE is the combination of the database, spreadsheet and visualisation tools in the same software. All this and the geology-oriented special features (certain type of diagrams, calculations, normalisation etc.) make APE a special tool, which does not have real competitors in the market. In general terms, APE has enough features to become a suitable tool for geologists dealing with lithogeochemical data. When the mineralogical data are included, APE becomes even better.

The APE program is in use on Outokumpu Mining Oy's komatiite exploration projects in Finland. Experiences of applying APE in practical exploration are good. Advantages of APE include the following.

1. Flexible program digests XRF data in original or volatile-free form, in percent and ppm.
2. There are possibilities for filtering, queries and classification of material.
3. It is possible to make various trend lines and compositional areas in library for the comparison of targets.
4. APE is handy for displaying 2-axis or triangular diagrams.

Such properties make APE a practical tool to identify original rock types, to classify them as Ni-potential or less potential ones, and to compare the analytical data of current project with those of known areas or economic deposits. On the Pulju Greenstone Belt, it was possible to separate the Ni-potential komatiites from less potential ones.

Final testing of the prototype GEOSIS database modules revealed technical features that should be developed further if commercialisation takes place. The most important area to be developed is the input and output tools in the software. These processes should be developed from the simple prototypes to versatile and user friendly software modules that would facilitate easy data entry to database and easy and fast access to all the data stored, with flexible reporting tools for data querying and output.

The developed prototypes in the GEOSIS system (GEOSIS database and GIS modules, GEOES, ANNGIE and ASM) at the present form a conglomerate of complex software that has been developed in different environments and need different third party programs for to be run. If the commercialisation of the GEOSIS system takes place, the integration of these programs must be carried further than in the prototypes. The entire system should be written in the same development environment, using the same standard Windows tools. This would ensure easier installation and would obviously provide more stable system free of technical hardware related compatibility problems.

In general, it is apparent that GEOES is a complete and powerful exploration tool for Area Selection, Identification of Potential Zones and Target Selection, covering and compiling geological data from diverse origin (i.e. geology, geophysics, mineralogy and geochemistry) well corresponding to results obtained using conventional exploration methodologies. Consultation and suggestions given by the Hybrid mode of the system are indeed very constructive in all evaluation steps.

However, in case of commercialisation of the product, the following suggestions are given for improvements and refining:

- Data entry to the intermediate Tables from GEOSIS database is very difficult and cumbersome due to their different structures. It is suggested the development of a methodology to automate the process of fill out the intermediate Tables.
- In the testing of Interactive GEOES for the lateritic model, separate processing of the various data sets (i.e. geology, geophysics, mineralogy and geochemistry) gives results corresponding exactly with the background information. However, in Spatial GEOES if a data set is absent, i.e. geophysics, then the system instead of ignoring this data set, gives negative score for geophysics and thus the OVERALL rate is low, even in cases where geological factors are strongly present.
- After the completion of a data set processing in GEOSIS, there are two directories on the hard disk where some files have been created. These files if they will not be deleted or transferred from these directories namely C:\TEMP and C:\GEODATA, create problems to the GEOES performance, since the application *overwrite* of new data on the old one is not functioning properly. Therefore the number of the system routines is doubled and the results obtained are not correct. We solved the problem during the tests by transferring the files in new directories and keeping the initial ones empty.
- After the data import into the system some names do not appear in the expected order and

the user has to search again the relevant column for the proper linking of the corresponding fields. Also, the text spaces of the same window are very narrow. The left column, accommodating long names, does appear on the screen completely and thus proper selection for the next step is difficult.

- The addition of the Hybrid mode of GEOES in the final version of the expert system was very helpful. Its contribution for the evaluation of the data sets on the maps is commendable.
- Finally, it is suggested that the end users would be provided with a CD-ROM containing all the installation procedures automated. Installation of so many software packages necessary for the complete performance of the system and interference of so many files and directories create difficulties not only to the end users but also sometimes to the system itself.

Even though nickel exploration was the primary target of the GeoNickel project, it is evident that most of the developed instruments and software are of generic nature. Consequently, they can be applied to a great variety of base metals deposits other than the "nickel family" (Ni, Co, Cu and PGE). Most of them can be used to aid exploration of commodities genetically related to magmatic, or even to sedimentary rocks in various geotectonic environments.

One of the powers of GEOES system is the needed systematic approach from the data acquisition to the output of the results. It gives the exploration staff a good opportunity to examine systematically all the available data, estimate its homogeneity and validity, showing where more information is required for well-balanced reasoning results. Ultimately, the most important feature in using such an expert system may be the fact that it forces different specialists in an exploration team to work more closely and coherently, enhancing the strengths of teamwork in mineral exploration.

7. ACKNOWLEDGEMENTS

The Brite/Euram II Programme of the European Community is acknowledged for supporting the GeoNickel project (Contract Nr: BRPR-CT95-0052). GeoNickel also wishes to thank the partners – companies and research institutes – for financially supporting the project. Finally, gratitude is expressed to the GeoNickel activists and all other persons who participated in this challenging project.

8. ANNEXES

8.1 Publications

Economou-Eliopoulos, M., Eliopoulos, D., and Laskou, M., 1996. Mineralogical and Geochemical Characteristics of Ni-laterites from Greece and Yugoslavia: Plate tectonic aspects of the Alpine metallogeny in the Carpatho-Balkan region. *In: Proceedings of the Annual Meeting of IGCP Project 356. Sofia, 1996, 2: 113-120.*

Economou-Eliopoulos, M., Eliopoulos, D., Apostolikas, A. and Maglaras, K., 1997. Precious and rare earth element distribution in Ni-laterites from Lokris area, Central Greece. *In: H. Papunen (ed), Mineral Deposits, Research and Exploration. Where do they Meet. Balkema, Rotterdam, pp 411-414.*

T.Halkoaho, J.Liimatainen, H. Papunen & J. Välimaa 1997. Cr-rich basalts in komatiitic volcanic association of the Archaean Kuhmo greenstone belt, Finland: Evidence for reducing conditions during magma generation. *In: H.Papunen (editor) Mineral Deposits, Balkema, Rotterdam, p. 431-434.*

Liipo, J., Papunen, H., Kilpeläinen, T. and Lamberg, P. (1997) The Stormi ultramafic complex and associated Ni-Cu deposits. *Geological Survey of Finland, Guide 44, 12-15.*

Spyropoulos, C.D. (1998) Intelligent techniques for identifying Ni-ore deposits. Technical Workshop, Mantoudi, Evia, Greece.

8.2 Conference presentations:

Eliopoulos, D.G., and Economou-Eliopoulos, M., 1999. Geochemical and Mineralogical features from Ni-laterite deposits, Vermion ophiolite complex, N. Greece. *Submitted for presentation in the SGA Meeting to be held in London, UK in August 1999.*

Lamberg, P., 1997. Litogeokemian käyttö sulfidisten Ni-malmien etsinnässä. Presentation and abstract in Neljännet geokemian päivät, 12.-13.11. 1997 Kuopio. *In Lestinen, P. (ed.) Neljännet geokemian päivät, 12.-13.11. 1997 Kuopio. Laajat tiivistelmät, 35-39.*

Bourgeois B., Alayrac C. and Soininen H., 1998. Requirements for a Three-component Downhole Frequency Electromagnetic System for Mineral Exploration. EAGE conference 1998, Leiptzig.

Bourgeois B. and Alayrac C., 1999. The Borehole Slingram Method in Mineral Exploration Using the SlimBoris system. To be held at EAGE Helsinki'99 conference.

Hattula A. and Soininen H., 1997. GeoNickel-eurooppalainen tutkimushanke. Sovelletun geo-

fysiikan XI neuvottelupäivät. In Finnish.

Jääskeläinen P., Pietilä R., Hattula A. and Peltoniemi M., 1999. Multivariate Analysis of Petrophysics and Litho geochemistry of Nickel Deposits. To be held at EAGE Helsinki'99 conference.

Mononen R., 1997. Sähkömagneettisten poranreikämittausten mallintaminen 3-D kohteeseen. Sovelletun geofysiikan XI neuvottelupäivät. In Finnish.

Mononen R. and Soininen H., 1998. Modelling of Three-component EM Borehole Measurements to 3D Target. EAGE Conference 1998, Leiptzig.

Mononen R. and Soininen H., 1999. Physical Modelling for Three-component EM Borehole System. To be held at EAGE Helsinki'99 conference.

Pietilä R. and Bourgeois B., 1999. Surface-to-Hole FEM Measurements Compared with Time Domain EM Data in Central Finland. To be held at EAGE Helsinki'99 conference.

Pirttijärvi M., Hjelt S.E., Hattula A. and Pietilä R., 1999. Modeling and Inversion of Electromagnetic Data Using Approximate Plate Model. To be held at EAGE Helsinki'99 conference.

Soininen H., Hattula A., Mäkelä K. and Aarnisalo J., 1996. Malminetsinnän ja Kaivosteollisuuden tulevaisuus Fennoskandian kilvellä. Laivasymposio. Vuorimiesyhdistys-Bergmannaföreningen r.y., Sarja B, No 63, 23-26.

Soininen H., Mononen R. and Oksama M., 1998. Modelling of Three Component EM Borehole Response. The 8th National Electromagnetic Meeting, Helsinki.

Vassilas, N., Charou, E. and Varoufakis, S., 1997: Fast and Efficient Land-Cover Classification of Multispectral Remote Sensing Data Using Artificial Neural Network Techniques, in *Proc. 13th Int'l Conference on Digital Signal Processing (DSP97)*, Santorini, pp. 995-998.

WP3 presentation at INFOWORLD'98 Exhibition, Athens, May 1998

Spyropoulos, C.D., Stavrakas, Y., Katsoulas, D, Vouros, G. et al. (1998) Integrated technologies for mineral exploration: pilot project for Nickel ore deposits. Eurothen Conference.

Eliopoulos D., Aarnisalo J., Papunen H., Apostolikas A., Economou M., Bourgeois B., Angelopoulos A., Gustavsson N., Stefouli M., Varoufakis S., Morten E., Ripis C. and Spyropoulos C., 1998: Integrated Technologies For Minerals Exploration: Pilot Project For Nickel Ore Deposits. In: A. Kontopoulos, I. Paspaliaris, A. Adjemian and G. Katalagarianakis, eds, *Proceedings of the first annual workshop (Eurothen'98)*, Athens, Greece, 12-14 January 1998. European Commission, Industrial and Materials Technologies Programme (BRITE-EURAM III). Lab. Metall., Nat. Tech. U Athens, pp. 24-32.

Aarnisalo J., Lamberg P., Papunen H., Mäkelä K., Eliopoulos D., Ripis C., Dimou E.,

Maglaras K., Apostolikas A., Melakis M., Economou-Eliopoulos M., Bourgeois B., Elo S., Pietilä R., Varoufakis S., Vassilas N., Perantonis S., Ampazis N., Charou E., Gustavsson N., Stefouli M., Morten E., Spyropoulos C., Vouros G., Stavrakas Y. and Katsoulas D., 1999: Integrated Technologies For Minerals Exploration: Pilot Project For Nickel Ore Deposits. In: *Eurothen '99. Eurothen '99 workshop. Preprints of the second annual workshop (Eurothen '99), Cagliari, Sardinia, Italy, 18-20 January 1999*. European Commission, Industrial and Materials Technologies Programme (BRITE-EURAM III). Pp 3-27.

8.3 Patents

GeoNickel did not produce patents.

8.4 Summary of GeoNickel output

	WP1	WP2	WP3	WP4	WP5	WP6	Total
Reports	18	10	3	12	23	1	67
Publications	4	7	3		1		15
Doctoral thesis		1					1
Master thesis	1	2					3
Conference presentations	2	11			1	2	16
Demonstrations		3					3
Database	2	2	1	2			7
Software	2	4	2	2	1	1	12
Hardware		3					3
Prototypes		2			1	1	4
Patents							0
Total	29	45	9	16	27	5	131

8.5 Final Technical Reports of the GeoNickel WorkPackages

Annex 1 WP1 MINERALOGY AND MODELLING OF NI ORE DEPOSITS

Annex 2 WP2 DEVELOPMENT OF GEOPHYSICAL TECHNOLOGY

Annex 3 WP3 IMAGE PROCESSING / PATTERN RECOGNITION

Annex 4 WP4 GEOSIS DESIGN AND GIS TOOLS DEVELOPMENT

Annex 5 WP5 KNOWLEDGE BASED SYSTEM (GEOES)

Annex 6 WP6 FINAL INTEGRATION, Task 6.2 Validation and testing

GeoNickel

Annex 1

FINAL TECHNICAL REPORT ANNEX 1

WP1 MINERALOGY AND MODELLING OF NI ORE DEPOSITS

~~CONFIDENTIAL~~

CONTRACT NO: BRPR-CT95-0052 (DG12 - RSMT)

PROJECT NO: BE – 1117

TITLE: Integrated Technologies for Minerals Exploration,
Pilot Project for Nickel Ore Deposits
GeoNickel

PROJECT

COORDINATOR: OUTOKUMPU Outokumpu Mining Oy, Finland

PARTNERS:

LARCO	General Mining and Metallurgical Company SA, Greece
BRGM	Bureau de Recherches Géologiques et Minières, France
GSFIN	Geological Survey of Finland, Finland
SOFTECO	Softeco Sismat Srl, Italy
IGME	Geological Survey of Greece, Greece
IRIS	Iris Instruments SA, France
NCSR	National Center of Scientific Research 'Demokritos', Greece

STARTING DATE: 1st January 1996 DURATION: 36 MONTHS



PROJECT FUNDED BY THE EUROPEAN
COMMISSION UNDER THE BRITE/EURAM
PROGRAMME

Date: February 28, 1999

CONTENTS

1. OBJECTIVES.....	7
1.1 TASK 1.....	7
1.2 TASK 2.....	7
1.3 TASK 3.....	7
2. MEANS USED TO ACHIVE THE OBJECTIVES.....	8
2.1 TASK 1.....	8
2.2 TASK 2.....	8
2.3 TASK 3.....	9
3. SCIENTIFIC AND TECHNICAL DESCRIPTION OF THE PROJECT	10
3.1 TASK 1.....	10
3.1.1 Introduction.....	10
3.1.2 Development of practical tools - APE software	11
3.1.2.1 Single sample data processing	13
3.1.2.1.1 The composition of the sulfide fraction	13
3.1.2.1.2 Normalisation calculations.....	14
3.1.2.1.3 Calculations of mineral composition from whole rock analysis	15
3.1.2.1.4 Automated cumulus naming procedure.....	15
3.1.2.1.5 Calculating the chemical composition of minerals	18
3.1.2.2 Key figures of the Ni sulfide exploration.....	18
3.1.2.2.1 Composition of parental magma	20
3.1.2.2.2 Crystallization series and cumulate sequence	21
3.1.2.2.3 The internal structure of the intrusion	21
3.1.2.2.4 Contamination features	21
3.1.2.2.5 Sulfide segregation features	21
3.1.2.2.6 Openness of the system.....	22
3.1.3 Development of novel tools - case studies	22
3.1.3.1 Case study intrusions	22
3.1.3.1.1 Stormi	24
3.1.3.1.2 Laukunkangas	25
3.1.3.1.3 Bruvann	25
3.1.3.1.4 Rörmyrberget.....	26
3.1.3.1.5 Ekojoki.....	26
3.1.3.1.6 Alter do Chao.....	27
3.1.3.1.7 Posionlahti	27
3.1.3.1.8 Porrasiemi.....	27
3.1.3.2 Methods to trace sulfide segregation	28
3.1.3.2.1 Ni depletion	28
3.1.3.2.2 Platinum-group elements	30
3.1.3.2.3 Sulphide quantity	32
3.1.3.3 Methods to trace contamination processes.....	33
3.1.3.3.1 Ore mineralogy	33
3.1.3.3.2 Rare earth elements.....	36
3.1.3.3.2.1 Drill hole 235-160.....	36
3.1.3.3.2.2 Modelling.....	37
3.1.3.3.2.3 Characterisation of the protolite and the contamination effect.....	39
3.1.3.3.3 Stable isotopes	40
3.1.3.3.4 Radiogenic isotopes	42
3.1.3.3.5 Conclusions on contamination studies	44
3.1.3.3.6 Orthopyroxene abundance as a favourable contamination indicator.....	45

3.1.3.4	Indicators of sulphide concentration	46
3.1.4	<i>Summary of the developed tools for sulfide Ni exploration</i>	46
3.2	TASK 2	48
3.2.1	<i>Descriptive model for nickel-sulphide deposits related to komatiitic volcanics</i>	48
3.2.1.1	Introduction	48
3.2.1.2	Factors controlling the compositions of extrusive Ni-sulphide deposits, a literature review	48
3.2.1.2.1	Composition of source and magma type	49
3.2.1.2.1.1	Two-stage melting of the mantle	49
3.2.1.2.1.2	Al-depleted and undepleted komatiites	50
3.2.1.2.1.3	Association of sulphides with different magma types	50
3.2.1.2.2	Ascent and emplacement of magma	50
3.2.1.2.2.1	Characteristics of komatiites	50
3.2.1.2.2.2	Ni-sulphide ore potential of different komatiite types	51
3.2.1.2.3	Assimilation	51
3.2.1.2.3.1	Thermal erosion	51
3.2.1.2.3.2	Indicators of assimilation	51
3.2.1.2.4	Segregation of sulphides	52
3.2.1.2.4.1	Supersaturation of a magma in sulphides	52
3.2.1.2.4.2	Assimilation of massive sulphides	52
3.2.1.2.4.3	Numerical modelling	52
3.2.1.2.4.4	Effect of dynamic volcanology on indicators	53
3.2.1.2.5	Effects of pressure, submarine alteration and metamorphism	53
3.2.1.2.5.1	Water depth	53
3.2.1.2.5.2	Post-eruptive hydrothermal alteration	54
3.2.2	<i>Mineralogy of komatiites and related Ni sulphide deposits</i>	54
3.2.2.1	Mineralogy	54
3.2.2.2	Mineralogical indicators of sulphides	55
3.2.3	<i>Deposit model for komatiite-related Ni sulphides</i>	55
3.2.4	<i>Review on komatiite geology of the Fennoscandian Shield</i>	57
3.2.4.1	Komatiite areas of the Shield	57
3.2.4.2	Archaean komatiites of NW Russia	57
3.2.4.3	Archaean komatiites of Finland	57
3.2.4.4	Proterozoic komatiites of Finland	58
3.2.5	<i>Application of Ni-ore factors to the Kuhmo, Suomussalmi and Pulju Greenstone Belts</i>	58
3.2.5.1	Volcanic factors of the Kuhmo and Suomussalmi greenstone belts	58
3.2.5.1.1	Volume of the volcanic province	58
3.2.5.1.2	Types of komatiites	59
3.2.5.1.3	Form of cumulate bodies	59
3.2.5.1.4	Poorly differentiated cumulate bodies	59
3.2.5.1.5	Indications of thermal erosion	59
3.2.5.1.6	Xenoliths or xenomelts	59
3.2.5.2	Geochemical and mineralogical indicators of sulphide precipitation	60
3.2.5.2.1	MgO (and Ni) content of the lavas	60
3.2.5.2.2	Ni depletion	60
3.2.5.2.3	Depletion in PGE and chalcophile elements	60
3.2.5.2.4	Contamination	60
3.2.5.3	Mineralogical indicators of sulphide precipitation	60
3.2.5.3.1	Chromites in the Kellojärvi and Pulju komatiitic cumulates	60
3.2.5.3.2	Composition of olivines	61
3.2.5.4	Structural and tectonic setting	61
3.2.5.4.1	Structural culmination areas	61
3.2.5.4.2	Vertical or subvertical layering	61
3.2.5.4.3	Geotectonic setting	61
3.2.5.5	Stratigraphic factors	61
3.2.5.5.1	Stratigraphic evolution of volcanics	61
3.2.5.5.2	Felsic substrate	62
3.2.5.5.3	Indications of deep-water environment	62
3.2.5.5.4	Coeval felsic/ultramafic volcanism	62
3.2.5.6	Alteration factors	62
3.2.5.6.1	Serpentinization and related reactions	62
3.2.5.6.2	Syn- and postdepositional hydrothermal activity	63
3.2.5.6.3	Metamorphic hydrothermal fluids	63
3.3	TASK 3	63

3.3.1	<i>Introduction</i>	63
3.3.2	<i>Geology of the Pelagonian and Sub-Pelagonian geotectonic zones of Greece</i>	64
3.3.2.1	Pelagonian geotectonic zone.....	64
3.3.2.2	Sub-Pelagonian geotectonic zone.....	65
3.3.3	<i>In situ Ni-laterite deposits</i>	66
3.3.3.1	Tsouka (Lokris, Sub-Pelagonian Zone).....	66
3.3.3.2	Profitis Ilias (Vermion, Pelagonian Zone).....	66
3.3.4	<i>Transported Ni-laterite deposits</i>	67
3.3.4.1	Kopais deposit (Lokris, Sub-Pelagonian Zone).....	67
3.3.4.2	Metallio deposit (Vermion, Pelagonian Zone).....	67
3.3.5	<i>Bauxitic laterite deposits</i>	67
3.3.5.1	Nissi (Lokris, Sub-Pelagonian Zone).....	67
3.3.6	<i>Mineralogy</i>	67
3.3.7	<i>Chemical composition of laterite ores</i>	68
3.3.8	<i>Discussion</i>	70
4.	COMPARISON OF INITIALLY PLANNED ACTIVITIES AND WORK ACTUALLY ACCOMPLISHED	72
4.1	TASK 1.....	72
4.2	TASK 2.....	73
4.3	TASK 3.....	73
5.	CONCLUSIONS	74
5.1	TASK 1.....	74
5.2	TASK 2.....	74
5.3	TASK 3.....	75
6.	ACKNOWLEDGEMENTS	76
6.1	TASK 1.....	76
6.2	TASK 2.....	76
7.	ANNEXES	76
7.1	LIST OF PUBLICATIONS, CONFERENCE PRESENTATIONS AND REPORTS RESULTING FROM THE PROJECT... 76	76
7.1.1	<i>Publications and conference presentations</i>	76
7.1.2	<i>Reports</i>	77
7.2	OTHER PROJECT OUTPUTS.....	78
8.	REFERENCES	78
	PLATES	87

EXECUTIVE SUMMARY

WorkPackage 1 developed geological, lithogeochemical, mineralogical and petrological models and tools for nickel exploration in three different geological environments: sulphidic nickel related to mafic and ultramafic intrusions (Task 1), sulphidic nickel related to komatiitic and picritic volcanics (Task 2), and lateritic nickel (Task 3).

Task 1 included two branches. The “practical tools” branch concentrated on data processing and the application of whole rock chemistry in nickel sulphide exploration. The result - a 32-bit Windows program “Advanced Petrological Explorer” - includes calculation routines, graphical tools and modelling modules to determine the nickel exploration key figures in intrusions: composition of parental magma, cumulate and crystallisation series, internal structure of the intrusion, contamination and sulphide segregation features, and the openness of the magmatic system. The “novel tools” branch developed new nickel exploration methodologies and enhanced the application of existing ones by studying nine selected intrusions. Mineralogical investigations, isotope (C, S, Sm/Nd) and REE studies resulted, that contamination by black schist triggered the ore-forming processes in intrusions studied hosting ore. Contaminated intrusions can be identified by high orthopyroxene/clinopyroxene ratio. Intrusions, which have experienced sulphide saturation, can be identified, since they are PGE-depleted but Ni-undepleted, and relatively rich in sulphides even at layered series. Continued magma replenishment is required for an effective concentration process. Such intrusions do not contain cyclic units and repetitive olivine cumulate layers.

Task 2 applied an extensive literature study to define the features positive for nickel sulphide exploration in komatiitic lavas and cumulates. Potential indicators for sulphides include high nickel content and sulphide saturation of the primary melt, sulphidic substrates of lava flows, indicators of thermal erosion and wall rock assimilation of channelised lavas, and the pressure (water depth) during lava extrusion. Such features were traced in Archaean Kuhmo and Suomussalmi Greenstone Belts and on the Proterozoic Pulju Greenstone Belt. By applying the conceptual nickel ore model to the data collected, descriptive models for nickel sulphide ore formation in different areas were created. As a project result, ore potential of the preferred lava pathways were indicated and characterised.

The objectives of Task 3 were the development of models of ore forming processes in representative laterite deposits of Greece, in order to be used in the exploration of associated Ni ores in different geologic environments in Greece and elsewhere. For the implementation of the objectives two areas were selected, the Lokris and Vermion, and six targets representing three different cases: (a) in situ Ni-laterite deposits, such as the Tsouka in Lokris, and Profitis Ilias in Vermion; (b) transported Ni-laterite deposits, such as the Nissi and Kopais in Lokris and Metallio in Vermion, and (c) bauxitic laterite deposits, such as the Nissi in Lokris. Ore-forming process models were established based on existing and new geological data acquired during the course of this project, mineralogical and lithogeochemical studies. Finally models were combined with geophysical and image processing data from the studied nickel deposits and their host environment. Integrated data processing methods were developed for exploration and target selection

PROJECT STAFF

The main activists in WP1 were as follows:

Task 1

Lamberg Pertti	Outokumpu Research
Augé Thierry	BRGM
Ylander Iikka	Outokumpu Research
Mäkelä Kaarlo	Outokumpu Mining
Liipo Jussi	Outokumpu Research
Cocherie Alain	BRGM
Bailly Laurent	BRGM
Guerrot Catherine	BRGM
Lerouge Catherine	BRGM

Task 2

Papunen Heikki	University of Turku
Halkoaho Tapio	University of Turku
Liimatainen Jyrki	University of Turku

Task 3

Eliopoulos Demetrios	IGME
Grigoris Pantelis	IGME
Photiadis Adonis	IGME
Kyritsis Evangelos	IGME
Economou-Eliopoulos Maria	ATHENS UNIVERSITY
Dimou Eleftheria	IGME
Perdikatsis Vasilios	IGME
Economou George	IGME
Ripis Costas	IGME
Rassios Anna	IGME
Apostolikas Athanasios	LARCO G.M.S.A
Melakis Michael	LARCO G.M.M.S.A
Maglaras Costas	LARCO G.M.M.S.A

1. OBJECTIVES

1.1 Task 1

The objectives of WorkPackage 1, Task 1 were to develop geological, lithogeochemical, mineralogical and petrological models and tools to discriminate Ni sulphide-potential intrusions from barren ones for locating Ni sulphide deposits within the intrusions or their surroundings.

During the course of work, a need arose to detail the objectives. Consequently the study was branched to the development of practical tools and the development of novel methods. The practical tools would make fast and reliable petrological conclusions and thus facilitate nickel sulphide exploration. The other branch of the objectives aimed to increase knowledge on nickel sulphide ore-forming processes and enhance their identification methods.

1.2 Task 2

The objective of Work Package 1.2 was to develop generic and area-specific models for the geological, geochemical and mineralogical features of extrusive ultramafic volcanics that indicate separation and precipitation of nickel sulphides. The generic model based on existing literature data will be transformed into area-specific with the aid of comprehensive field data collected from type localities in Archean and Proterozoic greenstone belts of the Fennoscandian Shield.

1.3 Task 3

The objectives of WorkPackage 1, Task 3 were the development of models of ore forming processes in representative laterite deposits of Greece, in order to be used in the exploration of associated Ni ores in different geologic environments in Greece and elsewhere.

These models were established based on existing and new geological data acquired during the course of this project, mineralogical and lithogeochemical studies. Further, the ore forming process models were combined with geophysical and image processing data from the studied nickel deposits and their host environment, in order to develop integrated data processing methods for exploration of target selection.

2. MEANS USED TO ACHIVE THE OBJECTIVES

2.1 Task 1

In the "practical tools" branch, research and modelling software were created. A data processing flowsheet for nickel sulphide exploration was analysed, and a software program named Advanced Petrological Explorer (APE) was built to automate most of the routines. APE includes seven executable programs. The programming tools used were Visual Basic Version 5 with Olectra Chart Version 1.1 ActiveX control and Formula One ActiveX control. APE software uses Microsoft Access databases.

Research methods in the "novel tools" branch were based on case studies. They were divided into four parts: case studies, modelling, testing, and reporting. Nine intrusions from four different geological environments and four countries were selected as case study targets (Fig. 1). Three of the intrusions have been subject to nickel sulphide mining, three are subeconomic and three barren ones.

Data on case study intrusions, related ores and surrounding areas were collected and compiled. Lithogeochemical and mineralogical data were processed with APE. Geological maps were digitised and a MapInfo-based GIS program was utilised for visualisation. Supplementary geological mapping and sampling were carried out at seven intrusions.

The mineralogy and lithogeochemistry of the targets were studied. Samples were analysed for main, accessory and trace elements with X-ray fluorescence, AAS, and Leco. Minerals in selected samples were analysed with electron microprobe. The extent and nature of wall rock contamination, as well as the source of sulphur, were traced with isotope (Sm/Nd, C, S) and trace element (REE, LILE, S-Se) geochemistry. Such data were studied and processed with APE programs.

At the preliminary stage, fractional crystallisation and sulphide ore segregation processes in intrusion were modelled using existing commercial programs: COMAGMAT (Ariskin et al. 1988) and MELTS (Ghiorso 1993). Final modelling was done using the APModel program developed in this Task.

The models and nickel exploration tools developed were tested at selected targets in north-western Europe and the Iberian Peninsula.

2.2 Task 2

Extensive literature study was applied in order to define the features positive for nickel sulphide exploration in komatiitic lavas and cumulates. Potential indicators of sulphides, e.g.

high nickel content and sulphide saturation of the primary melt, sulphidic substrates of lava flows, indicators of thermal erosion and wall rock assimilation of channelized lavas and the pressure (water depth) during the lava extrusion were traced in several target areas by field mapping and analyzing of geology, structure, mineralogy and geochemistry of the extrusive sequences. Geological, geochemical and mineralogical data was transformed to a computerized database suitable for MapInfo and GEOSIS systematics. Novel GPS methods were applied for the collection of detailed field data. Several hundred rock samples were analyzed for the main and trace elements in order to understand the geological evolution, volcanology and contamination of the extrusive melts.

2.3 Task 3

For the implementation of the objectives described above the areas of Lokris and Vermion (Plate 1.14) were selected, representing two different geologic and tectonic environments. The following research methods were applied on the selected areas.

Additional geologic and tectonic mapping in regional and local scales in order to update and complete the existing geological information according to the latest concepts on the evolution of the geotectonic zones of Greece, hosting the studied nickel deposits.

Mineralogical studies to define: (i) the mineralogy of the host rock and the ore itself (ii) the various ore types and the alteration scheme around the mineralizations (iii) the distribution of Ni in the Fe-Ni laterite ore deposits and host-rocks and (iv) the deposition environment. Electron microprobe analyses were carried out on selected samples for the definition of their chemical compositions.

Geochemical studies including analyses of major oxides, trace elements and rare earths of the different ore types and host rocks for the establishment of the factors controlling the spatial nickel distribution within these ores, the interelement relationships, the alteration patterns and the physicochemical conditions dominant during their deposition.

Platinum group element analyses and interpretation on different ore types and bedrocks to define their content, distribution and association with various trace elements and establishment of the physicochemical conditions dominant during the formation of the weathering crusts and/or their deposition (one or more stages).

Geological maps produced and data obtained were digitized and used as input to the GEOSIS database created for the needs of the project. A MapInfo-based GIS program was used for visualization. Models developed were tested on selected targets within Greece.

3. SCIENTIFIC AND TECHNICAL DESCRIPTION OF THE PROJECT

3.1 Task 1

3.1.1 Introduction

The application of mineralogy, lithogeochemistry and petrology to nickel exploration is complicated as well as time-, equipment- and resource-demanding work. So far, petrologists have been unable to give fast feedback and guidance for nickel exploration, and often this part of work has been neglected, or it has come too late being a part of subsequent academic work. For that reason, Task 1 objectives were mainly focused on creating practical tools that would give fast yet reliable petrological feedback for nickel exploration.

Following questions may be presented to petrologists by nickel sulphide explorationists: What are the magmatic names of intrusive rocks in the study area? What are the mineralogical compositions of such rocks? What is their genesis? What type of an intrusion are they part of? Are the rock types genetically related? An explorationist may ask more specific questions: Where is the bottom of the intrusion? Can one expect to find primitive olivine cumulates in the rock series? Is the intrusion similar to ore-hosting ones? Was the magma contaminated by country rocks, and if positive, to what extent? Where do erratic mineralised boulder derive from, does same type of material exist in bedrock? What is the source of geochemical or geophysical anomalies? Is it possible to rank various areas and targets according to their sulphide nickel ore potential? Finally he may present crucial questions: Which of the intrusions in the study area may host sulphide nickel ore? What type of ore may be expected, or what are the expected Ni, PGE, Cu and Co contents in the ore, and what are those values in the sulphide phase (sulphides recalculated to 100%)? At what part of the intrusion is the ore deposit located?

Most of the questions - even the first one - are difficult to answer and require lots of work. Petrologist should be able to determine the primary mineralogy, modal quantities and their chemical compositions. Usually the best method is to study the rocks microscopically, and analyse minerals by electron microprobe. However, mineralogy of studied rocks often is of secondary origin (see Plate 1.2). Therefore WP1, Task 1 made progress in determining primary mineralogy from whole-rock analyses.

WP1, Task 1 made case studies of fertile and barren intrusions to develop methods for discrimination purposes. The economic Ni-Cu-sulphide ores studied were relatively small and of low grade (Fig. 1.1-1). The largest is Stormi, 7.6 Mt of ore, and the highest grade Laukunkangas, 0.78% Ni (see Table 1.1-4). Therefore, the aim was set to develop generic tools, which would be applicable to world class nickel deposits, as well. Consequently the first set of developed tools concentrate on data processing and application of whole rock chemistry in in-

interpreting the key figures of Ni sulphide exploration referring to the development of practical tools.

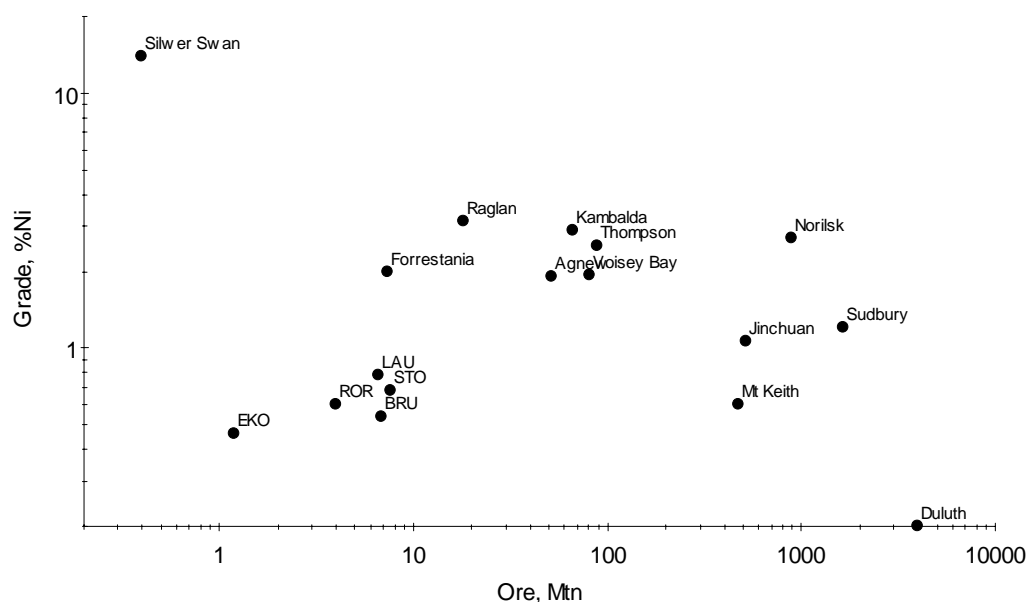


Figure 1.1-1 Ni grade and ore tonnages (=production+ore reserves+mineral resources) of some selected deposits and ore hosting – subeconomic case study intrusions. See intrusion codes in Table 1.1-3.

The other part of WP1, Task1 focused on case studies of fertile and barren intrusions. Petrological studies were carried out using the tools developed in the practical part. The differences between barren and fertile intrusions were revealed, and the reasons were critically studied and discussed. This part is called development of novel tools.

3.1.2 Development of practical tools - APE software

The first step in tool development work was to analyse the petrological data processing flow-sheet in Ni sulphide exploration. Such petrological data include all of the geological, litho-geochemical and mineralogical information collected.

The formation of major Ni(-Cu-PGE) deposits requires following factors (modified after Lightfoot & Keays 1994 and Naldrett et al. 1997).

1. Primitive (i.e. hot, olivine-bearing, rich in Ni and MgO) magma.
2. Major suture structure which allows primitive magma to ascend into the crust.
3. Sulphide undersaturated magma.
4. Mechanism leading to sulphide saturation.
5. Depressions structures that trap and enrich sulphides.
6. Continued magma flow.

In order to reveal whether the above requirements were fulfilled in intrusions studied, the petrological data processing - following the mapping and sampling period - was divided into the following four steps (see Fig. 1.1-2).

1. Single sample data processing.
2. Preliminary petrological analysis by processing the target (intrusion) data.
3. Refining the petrological analysis by modelling.
4. Determining the key figures of Ni sulphide exploration.

Once the processing steps were concluded, seven different Windows 32-bit executables were created to form the Advanced Petrological Explorer (APE) software. The programs were created to automate and facilitate most of the routines performed. The name given above describes the nature of the software: difficult and time-consuming calculations and data arrangements were made simple, fast and reliable.

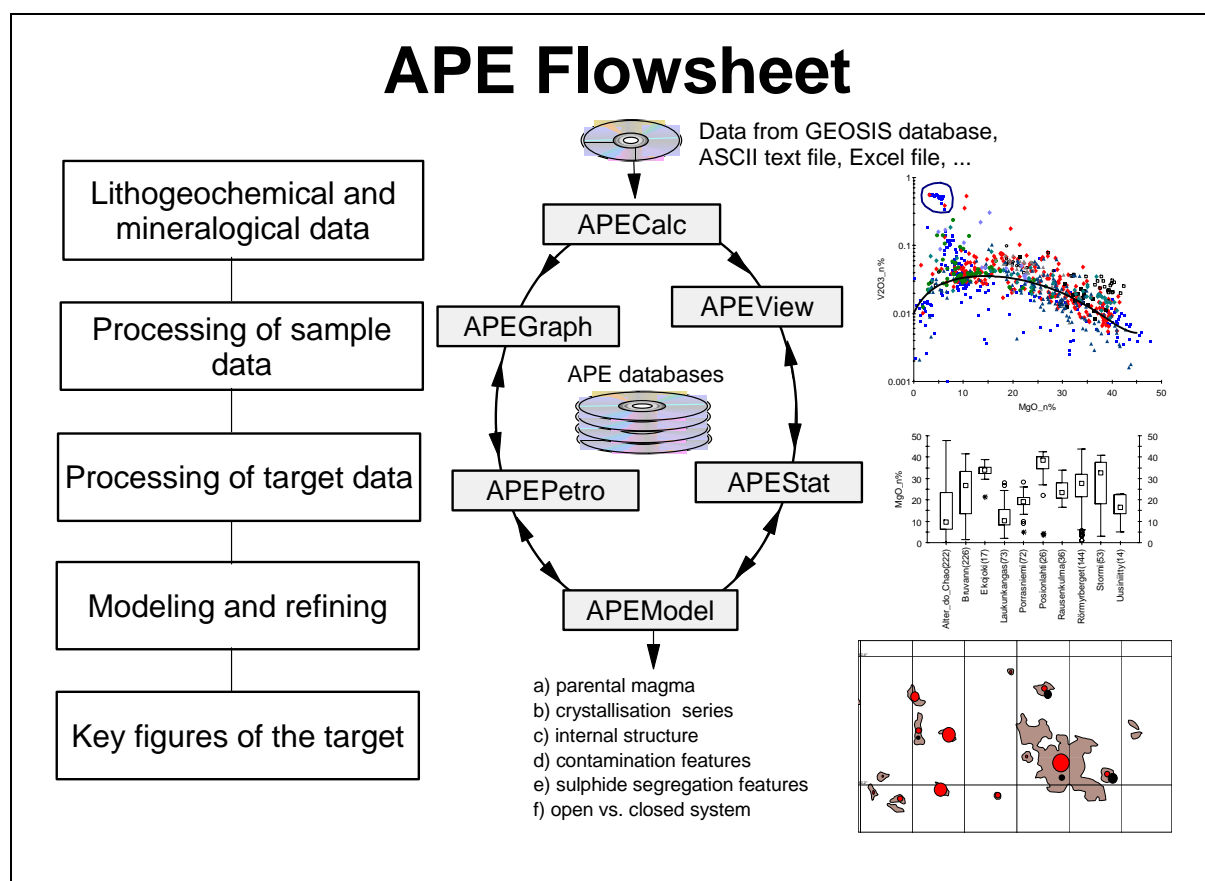


Fig. 1.1-2. Flowsheet of APE

APE software contains the following seven programs (see Fig. 1.1-2).

1. APECalc: petrological calculations of single samples.
2. APEPetro: petrological calculations of intrusions/extrusions.
3. APEModel: modelling fractional crystallisation and sulphide segregation in open magmatic systems.

4. APEGraph: a graphical tool for studying data in XY, ternary and spider diagrams.
5. APEView: viewing, editing and reporting data in tabular format.
6. APEStat: statistical analysis of data.
7. APECustom: for customising the program executables and database.

An installable version of the APE program with a Help module and manual was delivered to the GeoNickel partners. It is reminded that time for programming in Task 1 was limited and the amount of work was vast; consequently APE software is still at a prototype level. This report describes only the novelties program. For more detailed description of the program reader is referred to the APE manual.

3.1.2.1 Single sample data processing

The processing of single sample data includes a storage procedure for feed data, routine calculations for lithochemical and mineralogical data, calculations for specific problems, and the storage of calculated data for further processing.

Ordinary data processing tools (spreadsheet programs such as Excel and Lotus 1-2-3) are often inadequate to effectively handle large quantities of numerical data collected in exploration projects. Therefore APE data is stored in tailored database.

The single sample calculations aim to give rocks proper magmatic names, to estimate their mineral paragenesis, and to estimate the chemical compositions of minerals. Such calculations were divided into the following steps.

1. The calculation of sulphide fraction (i.e. sulphides recalculated to 100%).
2. The calculation of volatile-free composition.
3. The calculation of volatile- and sulphide-free compositions.
4. The calculation of CIPW normative mineral composition.
5. The calculation of true igneous mineral composition (called B-norm).
6. Calculation to give rocks proper cumulus names.
7. The calculations of chemical compositions of minerals.
8. The calculation of mineral formulas.

Steps 1 to 7 start from whole rock composition and step 8 from mineral analyses. APECalc takes care of the calculations for each sample. For a relatively large data set (several hundreds of samples), the execution in normal PC takes a few minutes.

Some of the procedures listed above are well known and computer programs exist to perform such calculations. APECalc, however, allows users to customise the calculations and save his or her own templates, and what is more important, it is the first program which binds all of the methods together in one program. Data transferring, which is often time-consuming, frustrating and sensitive to errors, is minimised.

Routines developed in the project are described in more details in the following chapters. The functionality of APECalc is described in the manual.

3.1.2.1.1 The composition of the sulfide fraction

The first step of the calculations is to determine the mineralogy and chemical composition of

the sulphide fraction and to remove that fraction from the whole rock composition for further calculations. Sulphide systems in mafic igneous rocks are Fe-Ni-Cu-Co-S systems. In addition to sulphides, significant amounts of iron, nickel and cobalt are bound to silicates and oxides; consequently the composition of sulphide phase is difficult to estimate reliably. Several simplifications are in use (e.g. Grundström 1980).

Bromine methanol leach (Penttinen et al 1977) attacks sulphides (except pyrite of which only 7% is dissolved in bromine methanol) leaving silicates and oxides untouched. When bromine methanol dissolution is used and the chemical composition of sulphides is known (as determined by electron microprobe), it is possible to calculate the composition of sulphide phase reliably as follows. First a set of linear algebraic equations is written for a "P" sulphide system (a=pyrrhotite, b=pentlandite, c=chalcopyrite, d=pyrite,...P=xx) and "C" components (e: 1=Fe, 2=Ni, 3=Cu, 4=Fe, ...,C=xx):

$$\begin{aligned}
 a1,axa + a1,bxb + a1,cxc + \dots + a1,PxP &= b1 \\
 a2,axa + a2,bxb + a2,cxc + \dots + a2,PxP &= b2 \\
 a3,axa + a3,bxb + a3,cxc + \dots + a3,PxP &= b3 \\
 \dots & \\
 aC,axa + aC,bxb + aC,cxc + \dots + aC,PxP &= bC
 \end{aligned}
 \tag{Equation 1.1-1}$$

The equations can be solved using, e.g., Singular Value Decomposition (SVD; for more detailed description in mineralogical problems see Lamberg et al. 1997).

When the weight fraction of minerals is solved, recalculation to 100% gives the mineral composition of the sulphide phase. Its substitution back to equation 1 gives the chemical composition of the sulphide phase on the right.

If chemical compositions of minerals are not known, simplification can be made on the basis of stoichiometric compositions. In most basic igneous rock studies it is enough to include in calculations the following phases: pyrrhotite (FeS), pyrite (FeS₂), pentlandite (Ni_{4.76}Fe_{4.24}S₈), chalcopyrite (CuFeS₂), Co-pentlandite (Co₉S₈), arsenopyrite (FeAsS), sphalerite (ZnS), molybdenite (MoS₂) and galena (PbS). The simplification allots all of Pb in galena, Mo in molybdenite, Zn in sphalerite, As in arsenopyrite, Co in Co-pentlandite, Cu in chalcopyrite and Ni in pentlandite. Remaining S and Fe are balanced between pyrrhotite and pyrite.

If only bulk assays are available (as is often the case), the chemical composition of a sulphide phase can still be estimated as described above. Only one should be cautious with samples containing less than 2% sulphides since significant amounts of Ni are bound also to silicates.

If pyrite is absent (as it often is), the amount of Fe bound to sulphides can be estimated reliably using the following equation:

$$\%Fe \text{ in sulphides} = 1.36363 * \%S \tag{Equation 1.1-2}$$

3.1.2.1.2 Normalisation calculations

The calculation of volatile-free (anhydrous) composition is a common usage in petrological studies. GeoNickel added precision to this routine, since reliable calculations of the sulphide

phase (see above) result in normalisation of better quality.

One of the novel approaches introduced by GeoNickel was the application of volatile- and sulphide-free compositions in studying Ni-Cu sulphide ores. Using volatile- and sulphide-free chemistries it is possible to compare the host rocks of sulphide-rich samples with ordinary cumulates and country rocks. In several cases (e.g. Bruvann and Laukunkangas) sulphide-rich samples display anomalous compositions. Such features may be used as direct evidence for contamination. Also, it may be possible to trace the contaminant that caused sulphide segregation and point out locations favourable for ore deposition.

The calculation proper is just a simple recalculation to 100%. If a sulphide phase was calculated from bromine methanol determinations, the recalculation is reliable even for ore rich in sulphur. However, the re-equilibrium of sulphides and non-sulphides in rocks during post-magmatic stages causes uncertainty in Fe distribution, and therefore one has to be cautious with samples rich in sulphides.

3.1.2.1.3 Calculations of mineral composition from whole rock analysis

CIPW normative mineral compositions provide reliable estimates on the mineral compositions of igneous rocks. However, there are defects: the method assumes that a magma is water-free, it uses an equal MgO/(MgO+FeO) ratio for all of mafic silicates (olivine, orthopyroxene and clinopyroxene) and the results are not in real weight percentage. All of the intrusions studied crystallised from hydrous magma; hence amphibole and phlogopite are frequently met with in intercumulus phases.

A novel calculation routine called B-norm was developed to make the estimations on mineral composition more reliable. B-norm differs from CIPW norm by containing phlogopite in the norm, by giving the result in weight percentage, and by estimating uniquely the Mg/(Mg+Fe) ratio of mafic silicates. The calculation routine is described in Table 1.1-1. Figure 1.1-3 illustrates the advantages of B-norm compared to CIPW norm.

3.1.2.1.4 Automated cumulus naming procedure

The proper naming of igneous rocks is often time- and effort-consuming work. Thin and polished sections of representative samples have to be studied. In Task 1 we found that CIPW and basaltic normative compositions are well in harmony with the actual primary igneous mineralogy. Therefore automated cumulus naming procedure was developed basing on B-norm (or optionally CIPW norm).

Comparing B-norm and microscopy-based cumulus names we were able to determine the boundaries above which minerals belong to cumulus phase. For orthopyroxene, clinopyroxene, and plagioclase it is roughly 25% and 10% for olivine. It was also realised that the cumulus minerals identified in such way tend to sum at less than 50% in non-cumulate rocks. From these observations, the automated cumulus naming procedure was developed. Table 1-1-2 describes the default rules, which can be customised in APECalc.

Table 1.1-1. B-Norm calculation.

Step	Phase	Formula	Calculated from	Note
1	Apatite	Ca ₅ (PO ₄) ₃ (OH)	P	
2	Zircon	ZrSiO ₄	Zr	
3	Albite	NaAlSi ₃ O ₈	Na	
4	Ilmenite	FeTiO ₃	Ti	
5	Magnetite	Fe ₃ O ₄	Fe ₃	Fe ₃ from eq. ilmenite/(ilmenite+magnetite)=0.311
6	Chromite	Mg _{0.5} Fe _{0.5} Cr _{1.5} Al _{0.5} O ₄	Cr	"average primary magmatic chromite" (from Roeder 1994).
7	Phlogopite	KMg ₃ Si ₃ AlO ₁₀ (OH) ₂	K, Mg	See below
8	Annite	KFe ₃ Si ₃ AlO ₁₀ (OH) ₂	K, Fe	See below
9	Anorthite	CaAl ₂ Si ₂ O ₈	Al	Residual Al
10	Diopside	CaMgSi ₂ O ₆	Ca, Mg	See below
11	Hedenbergite	CaFeSi ₂ O ₆	Ca, Fe	See below
12	Forsterite	MgSiO ₃	Mg, Si	See below
13	Fayalite	FeSiO ₃	Fe, Si	See below
14	Enstatite	Mg ₂ SiO ₄	Mg, Si	See below
15	Ferrosilite	Fe ₂ SiO ₄	Fe, Si	See below
16	Quartz	SiO ₂		

Steps 1-6 are straightforward. The following equations are used to overcome steps 7-16. Three last equations were derived empirically from large (n>20 000) database of mineral analyses by EPMA

w=weight fraction of element in mineral or (T=) bulk sample

x=weight fraction of mineral in sample

Mineral abbreviations: ol=olivine, opx=orthopyroxene, cpx=clinopyroxene, pl=plagioclase

$$W_{MgO,T} = X_{ol} * W_{MgO,ol} + X_{opx} * W_{MgO,opx} + X_{cpx} * W_{MgO,cpx} + X_{phl} * W_{MgO,phl}$$

$$W_{FeO,T} = X_{ol} * W_{FeO,ol} + X_{opx} * W_{FeO,opx} + X_{cpx} * W_{FeO,cpx} + X_{phl} * W_{FeO,phl}$$

$$W_{Al_2O_3,T} = X_{an} * W_{Al_2O_3,an} + X_{phl} * W_{Al_2O_3,phl}$$

$$W_{CaO,T} = X_{cpx} * W_{CaO,cpx} + X_{an} * W_{CaO,an}$$

$$W_{SiO_2,T} = X_{ol} * W_{SiO_2,ol} + X_{opx} * W_{SiO_2,opx} + X_{cpx} * W_{SiO_2,cpx} + X_{phl} * W_{SiO_2,phl} + X_{an} * W_{SiO_2,an} + X_{qtz} * W_{SiO_2,qtz}$$

$$W_{FeO,opx} = W_{FeO,ol} * 0.602598$$

$$W_{FeO,cpx} = W_{FeO,ol} * 0.196886$$

$$W_{FeO,phl} = W_{FeO,ol} * 0.254691$$

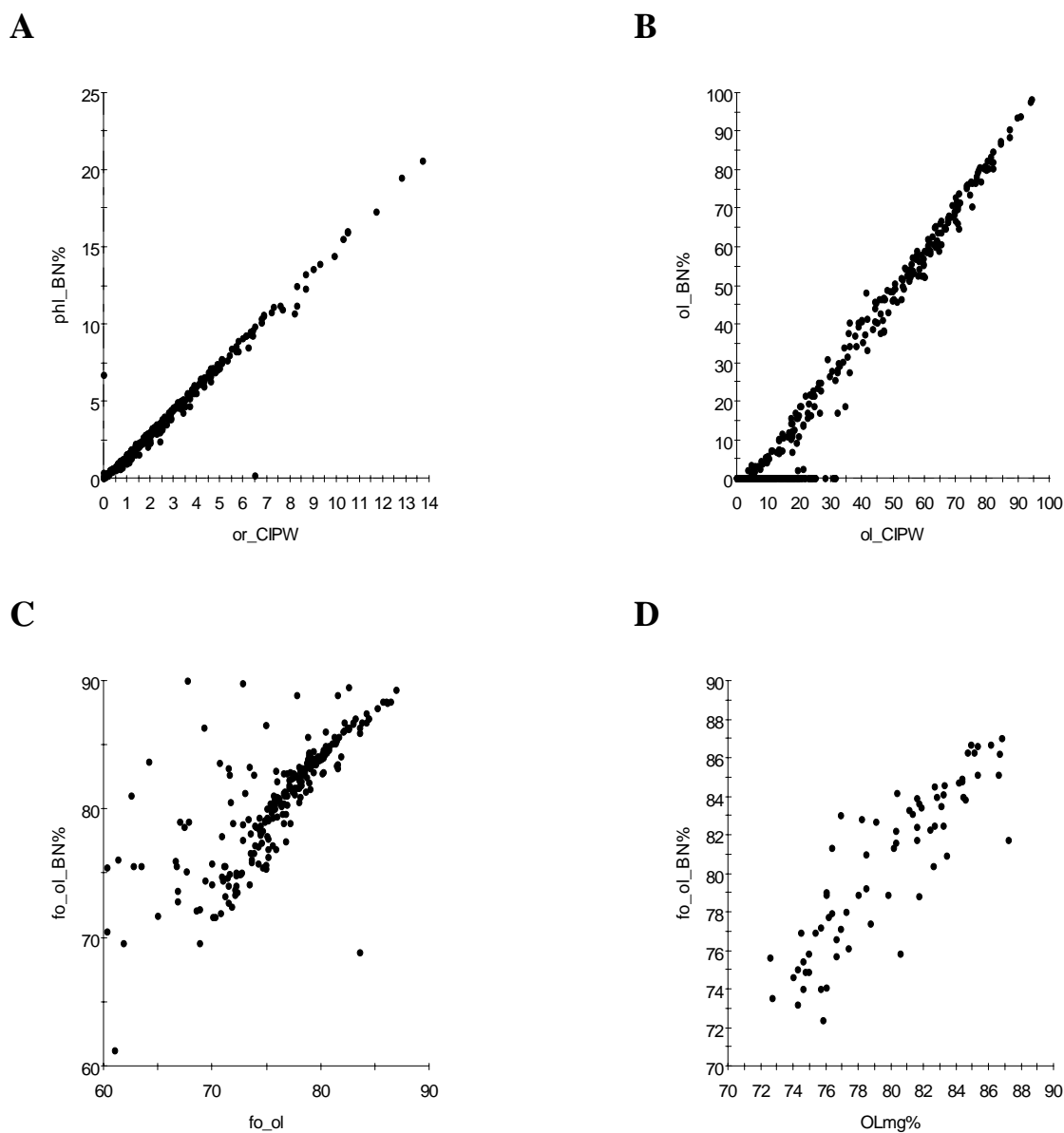


Fig. 1.1-3. Figures A-C illustrate the differences between B norm and CIPW norm. A) B-normative phlogopite vs. CIPW normative orthoclase. According to CIPW norm, cumulate samples are orthoclase normative even though they contain phlogopite. B) B-normative olivine vs. CIPW normative olivine content. The allocation of all K in orthoclase causes errors in the normative amount of olivine in CIPW norm. C) Forsterite content (mol-%) of olivine: B-norm vs. CIPW-norm. Mg/(Mg+Fe) ratio is equal for all mafic silicates in CIPW norm but is unique in B-norm. D) Correlation between analysed forsterite content (on abscissa) of olivine calculated value according to B-Norm (on ordinate).

Table 1.1-2. Automated cumulus naming procedure

Cumulus name consists of four parts; the naming rules in each part are as follows:

1 Cumulus minerals	2 Cumulus type	3 Cumulus/rock index	4 Intercumulus minerals
Listed in the order of abundance using the following abbreviations. The modal abundance must above the given boundary. o=olivine (>10%) b=orthopyroxene (>25%) a=clinopyroxene (>25%) p=plagioclase (>25%) m=magnetite (>10%) c=chromite (>1%) t=apatite(>1%)	If the rock is a cumulate, one of the following symbols is used to describe the amount of cumulus minerals. A=adcumulate (cumulus minerals>93%) M=mesocumulate (cumulus minerals 75-93%) O=orthocumulate (cumulus minerals 50-75%)	To distinguish if a rock is cumulate or non-cumulate: C=cumulate (cumulus minerals >50%) R=non-cumulate rock (cumulus minerals <50%)	Listed in the order of abundance using the following abbreviations. The modal abundance must be between the given boundary. b=orthopyroxene (10-25%) a=clinopyroxene (10-25%) p=plagioclase (10-25%)

e.g. oMCA=olivine mesocumulate with clinopyroxene as intercumulus mineral

bRpa=non-cumulate rock where the main phases, in the order of abundance, are orthopyroxene, plagioclase and clinopyroxene

3.1.2.1.5 Calculating the chemical composition of minerals

Minor and trace element compositions of minerals are widely used in petrogenetic discriminations but also as tools in mineral exploration. If whole rock analyses are of good quality, minor and in some cases even trace element content of some minerals can be estimated with required accuracy using the following technique.

Weight fraction of element E in sample is

$$W_{E,T} = \sum_{a=1}^n W_{E, Ma} * X_{Ma} \quad (\text{Equation 1.1-3})$$

where $W_{E, Ma}$ =weight fraction of element E in mineral Ma and X_{Ma} is weight fraction of mineral Ma in sample. When bulk composition ($W_{E,T}$) and weight fraction of minerals (X_{Ma}) are known, one can estimate weigh fraction of element in mineral $W_{E, Ma}$ by applying distribution coefficients of minerals from literature. Figure 1-1.4 shows the correlation between analysed Ni content of olivine (determined by electron microprobe using trace conditions: acceleration voltage 35 kV, beam current 350 nA, integration over the peaks) and calculated Ni content of olivine (estimated from whole rock composition).

3.1.2.2 Key figures of the Ni sulfide exploration

A literature review, the case studies and work done in WP4 proved that key figures of the Ni exploration target (intrusion), based on petrological analysis, are the following.

1. The composition of parental magma.
2. Crystallisation series and cumulate sequence.
3. The internal structure of intrusion.
4. Contamination features.
5. Sulphide segregation features.
6. The openness of a magmatic system.

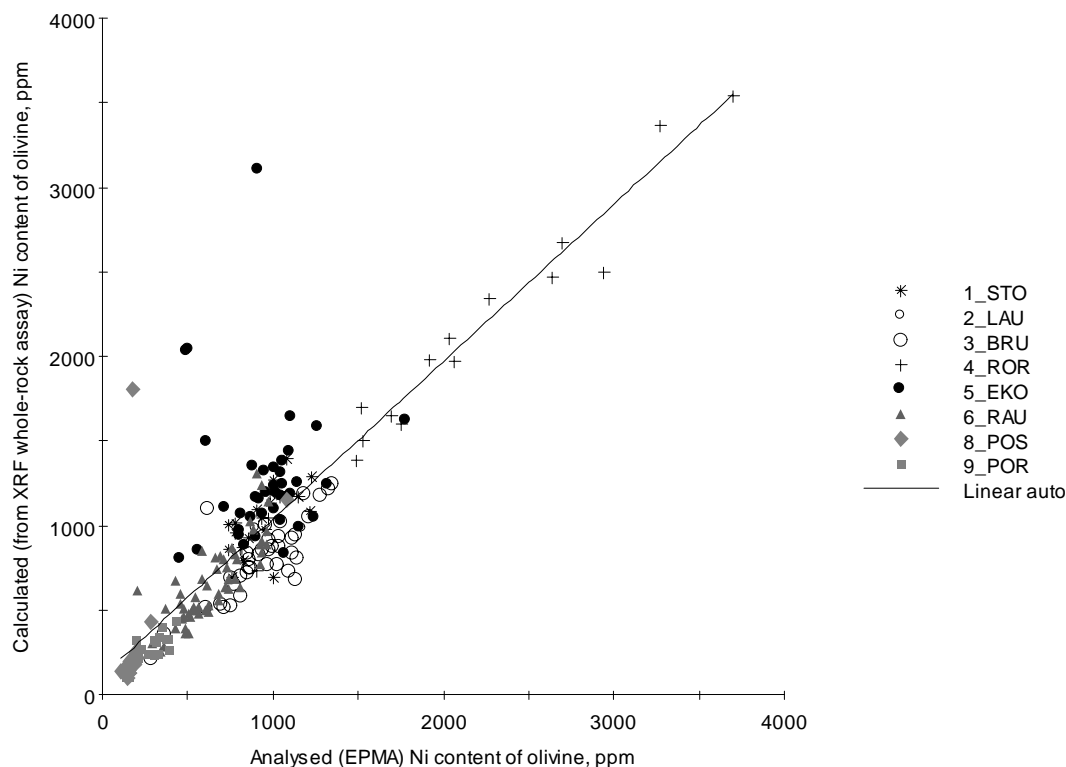


Figure 1.1-4 Correlation between analysed Ni content of olivine (analyses by electron microprobe using trace conditions) and calculated Ni content of olivine.

These figures are given by petrologists for Ni exploration projects and are used together with knowledge from general geology, geophysics, geochemistry and image processing (ref. WP2-6). An effective means of processing the data further is the expert system developed in WP4.

APE includes tools for such determinations. The approach is iterative: user makes the first estimations, models the magmatic system and compares the result in actual sample data. The estimation is refined, and modelling-comparison-refining loop continues until required accuracy is reached.

The modelling tool developed in Task 1 is basically similar to the one developed and used by Duke and Naldrett (1978) and Duke (1979), but it is capable to handle open systems subject to changes in recharge, assimilation, eruption, fractional crystallisation and sulphide segregation (see Fig. 1.1-5). APEModel has also database for distribution coefficients, and one can also use composition depended coefficients (Beattie et al. 1991). The functionality of APE is described in the manual.

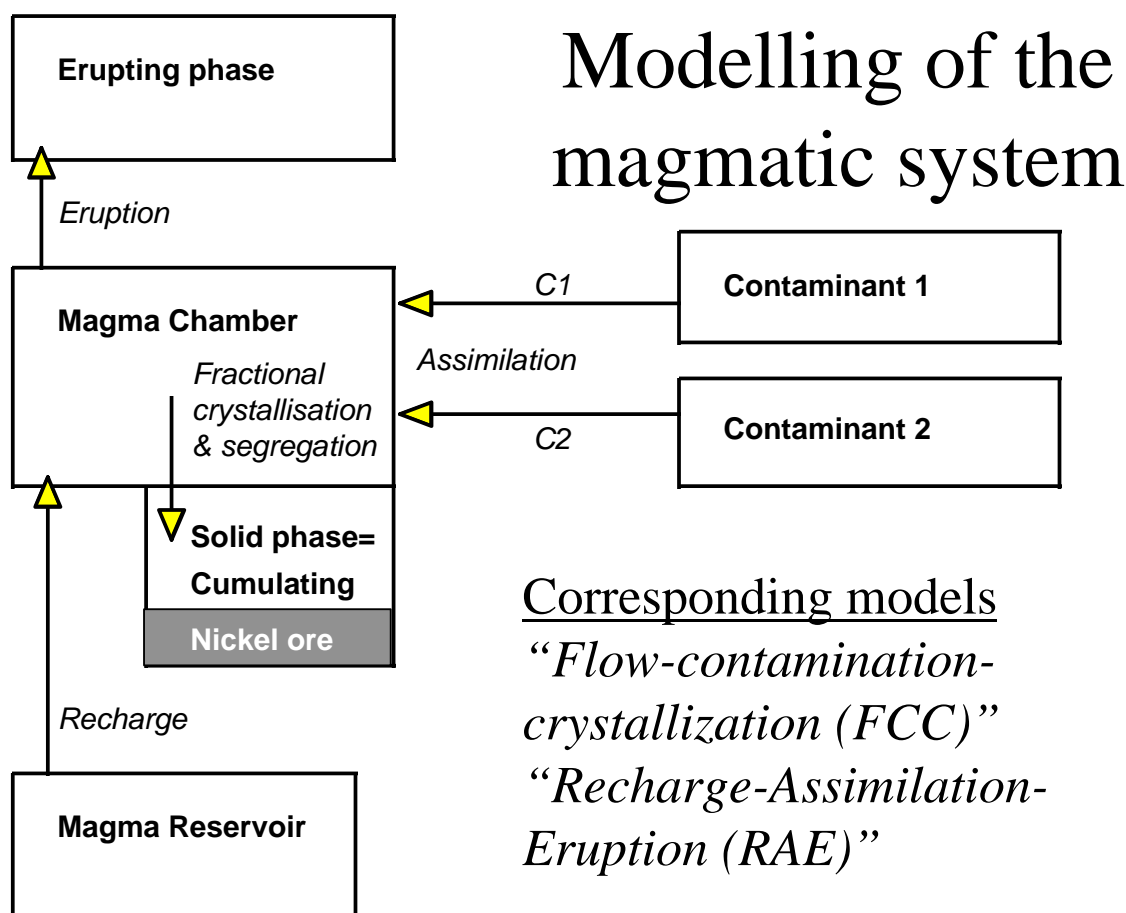


Fig. 1.1-5. Flowsheet of open magmatic system used in modelling.

3.1.2.2.1 Composition of parental magma

A magma as primitive as possible is liable of producing most nickel sulphide enrichment. This is caused by the following factors. 1) Ni-content of the magma is directly proportional to its primitivity. 2) A primitive magma is hot, hence capable of dissolving and assimilating country rock. 3) The more primitive the magma, the lower the viscosity and consequently the better are possibilities for efficient segregation and enrichment of sulphides in case sulphide oversaturation occurs. 4) The nickel content of sulphide phase (in the ore) is directly proportional to magma primitivity.

A method was created and computerised to determine the primitivity of parental magma from the whole rock composition of silicates. Basic approaches were adopted from Chai and Naldrett (1992). The determination starts from the most primitive olivine of the cumulus series. This is taken from mineral analyses, from B-norm (as described in chapter 3.1.2.1.3), or by studying the incompatible (Ti, Al, Zr) vs. MgO diagram of olivine cumulates and determining the intercept where incompatible=0 (method adopted from Barnes et al. 1988). The Mg-Fe distribution coefficient between olivine and liquid is as follows (Roeder and Emslie 1970).

$$K_D = (\text{FeO}/\text{MgO})^{\text{Olivine}} / (\text{FeO}/\text{MgO})^{\text{Liquid}} = 0.3 \pm 0.03 \quad (\text{Equation 1.1-4})$$

MgO and FeO contents of liquid is a crossing point in FeO vs. MgO diagram between regression line of olivine cumulates and the line for liquid in equilibrium with the most magnesian olivine (according to equation 1.1-4). This is possible only when olivine cumulates are present and they form a clear mixing line between olivine and parental magma. Abundance of other elements in the parental magma are estimated by studying the regression of olivine cumulates in XY diagram where the estimated element is placed on Y axis and MgO on X axis. Weight percentage of the element to be estimated is on the point where regression line intercepts MgO of parental magma.

3.1.2.2.2 Crystallization series and cumulate sequence

The studies revealed that there are clear differences in the crystallisation series of intrusions within the same geotectonic environment, and the crystallisation series can be used as a discrimination factor important in Ni exploration (see chapter 3.1.3.3.6). For that purpose, a technique developed and described by Irvine (1970) was computerised.

3.1.2.2.3 The internal structure of the intrusion

For nickel sulphide explorationists, is important to know the internal structure of the target intrusion, because ores are frequently located at or close to their primary bottoms. Best concentrations of ore often occur in depression structures. The determination of stratigraphic bottom may sound trivial, but in tectonised and poorly differentiated intrusions it is often a difficult task. The application of automated cumulus names (see chapter 3.1.2.1.4) and B-norm help in revealing cumulus layers, which otherwise could easily be neglected or incorrectly identified.

3.1.2.2.4 Contamination features

The qualification and quantification of contamination was almost solely done on isotopes. The case studies showed that intrusions might be totally contaminated – which possibly happened deeper in the feeder - so that in-situ contamination, important for the formation of Ni sulphide deposits, is masked by earlier contamination episode(s). As volatile- and sulphide-free compositions of ore samples were studied and compared with ordinary cumulates, many of the case study intrusions displayed features characteristically pointing to contamination. Favourable contaminants can be identified, and after such studies it is possible to identify mineralogical as well as main and trace element features related to contamination. Consequently they can be used as discriminating factors.

APE includes tools for creating trendlines and polygons, which can be used as discriminators. For later use they can be seven in library. Anomalous contents of incompatible elements are rapidly identified and quantified by using APEGraph. The modelling of contamination episodes by APEModel finally reveals whether a hypothetical process is feasible and if the products correspond to actual samples.

3.1.2.2.5 Sulfide segregation features

Sulphide segregation is one of the most important processes required for the formation of Ni sulphide ore. The correct identification and quantification of related features are key questions in Ni exploration. The composition of olivine, i.e. Ni vs. forsterite content, has been traditionally used as discriminator whether certain magma was subject to sulphide segregation. APE- Calc includes tools to estimate the composition of olivine from whole rock composition (see

chapter 3.1.2.1.5). APEModel can be used to model sulphide segregation processes by using different parental magmas, mass ratios of sulphide and magma, and adjusting several other parameters. Trendlines defined in APEModel can be stored in the APEGraph library, then the reference curves can be used in discriminating and quantifying Ni depletion features.

3.1.2.2.6 Openness of the system

The openness of a magmatic system is a factor important for nickel ore formation. In an open system, the original magma and sulphide volumes may have been much larger than the size of the intrusion proper. Consequently even small intrusion may host nickel sulphide deposits larger than size would justify. Such features are noted in most of the komatiite nickel deposits but also in several intrusion-related ones (e.g. at Stormi and Voisey's Bay).

Sulphides segregating in and settling from a turbulent magma may equilibrate with larger amounts of magma than those in laminar flows. In turbulent flows, sulphides only may settle on the bottom of the chamber over a long period during the evolution of the magma chamber. The presence of olivine ad- and mesocumulates are direct evidences of turbulent magma flow. It is possible to calculate the openness of a magmatic system provided that we know the composition of the parental magma, the mean composition of cumulates and the composition of the escaped phase.

The automated cumulus naming procedure of APE reveals monomineralic ad- and mesocumulates. The routines for determining the composition of primary magma, and the application of APEModel in simulating the formation of cumulus piles, finally reveal the mass ratios in the recharge–assimilation–eruption–cumulus settling chain.

3.1.3 Development of novel tools - case studies

3.1.3.1 Case study intrusions

Nine intrusions from four countries and geological systems were selected for target case studies. The following selection criteria were used.

- The intrusions should be well studied because GeoNickel aims to develop nickel exploration methods and tools rather than solve basic petrological problems.
- Samples and data should be freely available.
- Intrusions should cover various geological environments.
- Fertile and barren intrusions should be included.
- The targets should be located within EU.

The case study intrusions were divided into three groups mentioned below. Their code names, ages and ore resources are given in Tables 1.1-3 and 1.1-4, and their locations are shown in Fig. 1.1-6 and in Plate 1.1.

1. Economic Ni-Cu deposits: Bruvann, Laukunkangas and Stormi.
2. Subeconomic Ni-Cu deposits: Ekojoki, Rausenkulma and Rörmyrberget.
3. Barren intrusions: Posionlahti, Porrasiemi and Alter do Chao.



Fig. 1.1-6. Location of Workpackage 1, task 1 case study intrusions and Workpackage 6 test areas.

Most of the case study targets (Stormi, Posionlahti, Ekojoki, Rausenkulma, Porrasiemi, and Laukunkangas) belong to Svecokarelian ultramafic-mafic intrusions (e.g. Gaál 1985, Papunen et al. 1979, Mäkinen 1987). Naldrett (1989) classified them as orogenic intrusions: they intruded into active orogenic belts. The following is a brief description of the case study intrusions concentrating on new findings. References are provided for detailed information.

Table 1.1-3: WorkPackage 1.1 case study intrusions, their locations, ages and references.

Intrusion	Code	Area	Country	Intrusion type	Age Ma	Best Reference (Age ref)
Stormi/Vammala	1_STO	Vammala	Finland	SUMI		Peltonen 1995
Laukunkangas	2_LAU	Enonkoski	Finland	SUMI	1880±3 Ma	Grundström 1985, (Huhma 1986)
Bruvann/Råna	3_BRU	Ballangen	Norway	CAL	410 ±40	Boyd & Mathiesen 1979
Rörmyrberget	4_ROR	Vindeln	Sweden	SUMI		Ylander 1998
Ekojoki	5_EKO	Vammala	Finland	SUMI		Peltonen 1995
Rausenkulma	6_RAU	Kokemäki	Finland	SUMI		-
Alter do Chao	7_ALT	Badajoz	Portugal	HER		-
Posionlahti	8_POS	Vammala	Finland	SUMI		Peltonen 1995
Porrasiemi	9_POR	Lammi	Finland	SUMI	1879±3 Ma	Lamberg 1990

Intrusion type: SUMI=Svecokarelian ultramafic-mafic intrusions (1.8-1.9 Ga), CAL=Intrusions of Caledonian orogen (410 Ma), HER=Pre- to early hercynian intrusions in Spain and Portugal

Table 1.1-4: Ore resource information of the case study intrusions.

Intrusion	Code	Ore existence	Mtn	Ni%	Cu%
Stormi/Vammala	1_STO	Ore	7.6	0.68	0.42
Laukunkangas	2_LAU	Ore	6.7	0.78	0.22
Bruvann/Råna	3_BRU	Ore	6.8	0.54	0.10
Rörmyrberget	4_ROR	Subeconomic	4.0	0.60	0.06
Ekojoki	5_EKO	Subeconomic	1.2	0.46	0.41
Rausenkulma	6_RAU	Subeconomic	0.036	0.69	0.95
Alter do Chao (*)	7_ALT	Barren	0.00	0.32	0.016
Posionlahti (*)	8_POS	Barren	0.00	0.26	0.14
Porrasiemi (*)	9_POR	Barren	0.00	0.21	0.12

Data from Puustinen et al 1995, and Outokumpu internal reports. Rörmyrberget data from Nilsson (1985), cut-off 0.4% (raising cut-off to 0.8% gives 0.66 Mtn 1.1%Ni and 0.08%Cu).

(*) = No ore, resource estimation has not been done. For Ni and Cu values highest single sample values are given.

3.1.3.1.1 Stormi

Stormi represents a fertile intrusion and consists almost entirely of ultramafic rocks. It is located in southwestern Finland in the Vammala Nickel Belt. The Stormi intrusion was studied by Häkli et al. (1979), Häkli and Vormisto (1985), Mäkinen (1987), Marshall and Mancini (1994) and Peltonen (1995a and b). The comprehensive studies by Peltonen (1995a and b) concluded that there are two types of genetically unrelated ultramafic units juxtaposed on each other. The lower unit hosts Ni-Cu sulphide ore and is of igneous origin while the upper one is an older picritic volcanite.

Approximately 100-m thick olivine-chromite-(sulphide) cumulate (olivine > 75%) does not show differentiation at all. Only the upper and lower contacts are less magnesian and contain pyroxenes as main minerals, which is most probably due to (in situ) contamination. Composition of olivine varies a little from 79 to 82 mol-% forsterite, and Ni content between 700 and 1100 ppm. Following are the results of modelling the formation of Stormi ore hosting cumulate pile. 1) The system was open, only c. 5% of magma responsible for cumulates is currently visible in the Stormi intrusion. 2) Magmatic system was pumping (several increments), otherwise the forsterite content of olivine could not stay constant through the cumulus pile. 3) Variation in Ni vs. forsterite content of olivine can not be explained by fractional crystallisation of olivine alone; the olivine:sulphide ratio of 1:0.05 gives a reasonable fit. 4) Scattering in the composition of olivine (Ni vs. forsterite) requires not only pumping, but also a rather chaotic system, where the relationship between different parts and stratigraphic levels is difficult to establish.

3.1.3.1.2 Laukunkangas

The Laukunkangas intrusion with a related Ni-Cu ore deposit is located in Enonkoski town at the southeastern end of the Kotalahti nickel belt, southeastern Finland (Grundström 1980 and 1985). It represents a differentiated, mainly gabbroic ore-hosting intrusion. Compared with Stormi it is less mafic. The Laukunkangas intrusion is embedded in migmatized mica gneisses that contain intercalations rich in sulphide and graphite.

The stratigraphic thickness of the Laukunkangas cumulate series is c. 400 m. Two units can be distinguished. The lower unit consists of the following cumulate sequence: olivine-orthopyroxene cumulate, orthopyroxene-plagioclase cumulate and plagioclase-orthopyroxene cumulate. The second unit starts with slight reversal (e.g. in $MgO/(MgO+FeO)$), and orthopyroxene returns to be the most abundant cumulus mineral in orthopyroxene-plagioclase cumulate. This is followed by plagioclase-orthopyroxene cumulate, and finally quartz norites follow this.

The exceptionally high Ni content in olivine and sulphides recalculated to 100%, and high Ni/Cu ratio compared to relatively evolved nature of magma, indicate that olivine did not fractionate voluminously from the magma. Such features, as well as the abundance of orthopyroxene, were modelled, and the following model fitted well with observed cumulates: Relatively primitive magma (relevant to the parental magma of Stormi) was contaminated by country rock rich in SiO_2 . The melt moved from the olivine crystallisation field to orthopyroxene field, and magma oversaturated with respect to sulphides. The contaminant was most probably black schist, because ore is intimately associated with graphite schist and graphite is abundant everywhere in the ore and is frequently met also in the cumulate sequence.

3.1.3.1.3 Bruvann

The Bruvann deposit is located at the northwestern part of the Råna intrusion near Narvik, Nordland county, Norway (Fig. 1.1-6). Bruvann represents ore-hosting intrusions in a geological environment, which differs from that at Stormi and Laukunkangas. At Bruvann, ore was discovered in 1912-1914, and mining was started 1989.

Boyd & Mathiesen (1979) and Boyd (1980) described the geology of the Råna layered intrusion. Its idealised rock sequence is the following: an ultramafic zone with subordinate norite

at rims, a norite zone with subordinate ultramafics, and quartz norite in the core. Ore is located in the ultramafic zone partly in the contact with enclosing gneisses, but mostly 50-200 metres from the closest contact. The whole intrusion is depleted in PGE due to segregation of small quantities of sulphides prior to intruding (Barnes 1985, 1988; Boyd et al. 1987, 1988).

The features adjacent to Ni ores in Bruvann are as follows. Ores are located stratigraphically some 100-300 meters above the basal contact, in ca. 500 m thick cumulate sequence, which consists of cyclic units of following cumulates: olivine cumulate, olivine-orthopyroxene cumulate, orthopyroxene cumulate, orthopyroxene plagioclase cumulate, and plagioclase orthopyroxene cumulate. Two ore types can be distinguished: disseminated and semimassive ore. Disseminated ore is hosted by olivine cumulate, which is relatively thick, the most primitive one with forsterite content ca. 82%. Semimassive ore is hosted by orthopyroxene cumulate (pyroxenite), orthopyroxene-plagioclase cumulate (norite) or hybrid rock containing crustal fragments. Both ore types show clear contamination features: Gneiss and black schist inclusions and xenoliths are found adjacent or close to the ore. Graphite is abundant and associated with sulphides. Lithophile element contents are anomalously high adjacent to the ore. High V and the presence of graphite refer to black schist contamination. Following conclusions derive from the modelling of Bruvann: Black schist contamination especially increased the SiO₂ and S contents of magma, which drifted the crystallisation series to olivine-orthopyroxene-plagioclase route instead of olivine-clinopyroxene-orthopyroxene series, and sulphide oversaturation and segregation. Bruvann magma chamber was replenished episodically several times producing rhythmic layering and cyclicity.

3.1.3.1.4 Rörmyrberget

The Rörmyrberget mafic-ultramafic intrusion is located 14 km northeast of Vindeln, central Västerbotten, Sweden. Åkerman (1981), Ekström (1981), Nilsson (1980, 1985) and Ylander (1997) studied the intrusion. Rörmyrberget was selected for case studies to represent an ultramafic intrusion hosting subeconomic mineralisation.

The layered sequence at Rörmyrberget is up to 360 m thick. Up to seven cyclic units consisting (in ideal cases) of olivine cumulate, olivine orthopyroxene cumulate, orthopyroxene cumulate and orthopyroxene plagioclase cumulate were identified. There exist ten discontinuous ore horizons, which occur inside the intrusion in layered sequence, not in the basal contact. Ore samples display anomalously high contents in lithophile elements compared to common cumulates. Modelling resulted in the following conclusions. High-Mg basaltic magma was contaminated by country rocks rich in SiO₂ and, orthopyroxene became an abundant cumulus mineral. Open magma chamber was replenished several times and the residue erupted continuously from the chamber. Sulphide oversaturation was met several times and at several places through the magmatic evolution of the intrusion.

3.1.3.1.5 Ekojoki

The Ekojoki intrusion lies c. 3 km northeast of Stormi. It does not outcrop and is covered by lake and soil overburden. Three mineralisations (not mined) have been located above 150 m level and total 0.84 Mt grading 0.40% Ni and 0.30% Cu (Vesanto and Katajarinne 1984). Ekojoki represents subeconomic ultramafic intrusions, similar to that at Stormi.

Ekojoki displays higher Cu/Ni ratios and much higher PGE contents than Stormi; several

other features are similar. Modelling gave as result, that Ekokjoki magma did not experience sulphide saturation prior to intrusion event, even though some of the olivine had fractionated before.

3.1.3.1.6 Alter do Chao

The Alter do Chao intrusion is located in western Portugal (Fig. 1-1.6). It represents barren intrusions in a geological environment different from the other cases.

The parental magma of Alter do Chao was relatively primitive ($MgO > 15$) compared to other intrusion studied. Smooth and well defined Ni vs. forsterite -evolution trend of olivine could be explained by the fractional crystallisation of olivine in sulphide undersaturation. Zoned structure of the intrusion with olivine cumulates in the central part and less mafic gabbros on the rim were explained by the contamination of magma by limestone. This episode switched the crystallisation path of magma from orthopyroxene field to that of clinopyroxene-plagioclase.

3.1.3.1.7 Posionlahti

The Posionlahti intrusion is located north of Stormi in the Vammala nickel belt. It is totally ultramafic, relatively large in size and known as Ni-depleted type. Extreme low Ni contents (in sulphides recalculated to 100% and in olivine) can be explained by the segregation of relatively large amount of sulphides, prior to the crystallisation of olivine in the intrusion. The intrusion was an open system and olivine cumulates only represent c. 5% of the total magma volume. Ni content of magma varied through the magmatic history, which refers that R factor (silicate magma/sulphide melt) - though being low - was not constant.

3.1.3.1.8 Porrasniemi

The Porrasniemi intrusion is located 30 km north of Lammi, central Finland (Lamberg 1990). It has features similar to Laukunkangas but is barren of nickel sulphides.

The Porrasniemi intrusion is a layered gabbroic sill. Its structure is revealed by macroscopic layering (modal rhythmic layering), microscopic layering (grain size lamination) and megascopic layering (series and zones). The intrusion consists three blocks, namely Kytö, Kärki, and Terrinen. They occur conformably in migmatized garnet-biotite-mica gneisses (originally graywackes) and have been tilted to an almost vertical position. The blocks are divided into marginal and layered series. The marginal series is heterogeneous representing bottom parts of the original intrusion. It separates the layered series from bottom gneisses. Reversal differentiation, country rock fragments and angle discordance with layered series characterise the marginal series.

The layered series consists of peridotite zone (prdZ), pyroxenite zone (pxZ), and a gabbro zone (gbZ). The zones display gradual phase contacts. The peridotite zone comprises olivine augite±bronzite cumulates. The disappearance of olivine by peritectic reaction and its replacement by bronzite mark the boundary between peridotite (oa±bC) and pyroxenite (augite bronzite cumulate, abC) zones. Plagioclase appears as cumulus mineral in the gabbro zone (gbZ). Its lower parts consist augite-bronzite-plagioclase cumulate (abpC) and upper parts plagioclase bronzite cumulate (pbC). Formation of intrusion can be explained by one magma pulse, which fractionated in situ. Some part of magma, however, erupted from the chamber.

Ni depletion nature in the intrusion requires segregation of sulphides prior to intrusive event in the feeder channel.

3.1.3.2 Methods to trace sulfide segregation

3.1.3.2.1 Ni depletion

The intrusions studied are classified into three classes according to their nickel contents as indicated in figures 1.1-7 and 1.1-8: 1) depleted (Posionlahti and Porrasiemi), 2) undepleted and well defined (not scattered) (Alter do Chao, Laukunkangas), 3) undepleted but scattered (containing both undepleted and depleted samples; Stormi, Rausenkulma, Bruvann and Rörmyrberget).

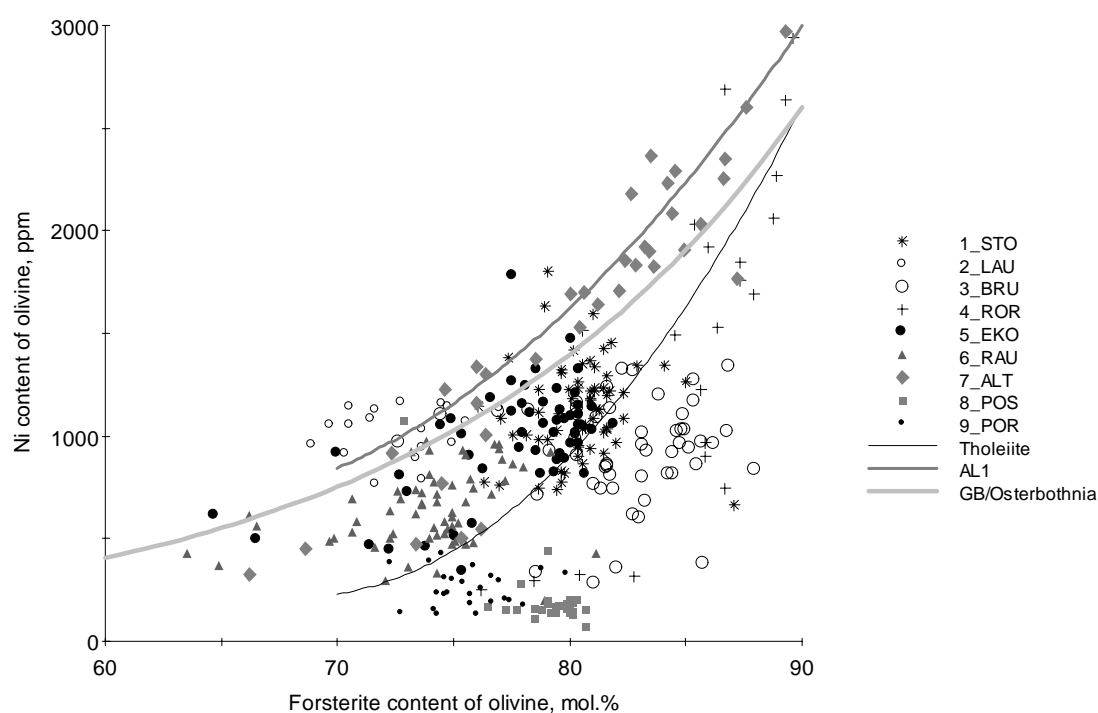


Figure 1.1-7. Ni vs. forsterite content of olivine in case study intrusions. Sulfide rich samples excluded. Model curves are as follows: Tholeiite=modelled fractional crystallization of olivine in sulfide undersaturation, AL1=polygonal fit of Alter do Chao olivines, GB/Osterbothnia=modelled fractional crystallisation of olivine followed by pyroxenes in tholeiitic magma (Osterbothnia WorkPackage 6 material used as empirical data).

When certain magma becomes - for some reason - oversaturated with respect to sulphur, immiscible sulphide melt segregates from the silicate melt. Denser sulphide melt tends to sink to the bottom of the magma chamber or lava flow or -lake. Group VIIIA metals have high tendency to bond in sulphide melt, and therefore remaining silicate liquid will be depleted in these metals. The depletion grade depends on distribution coefficient and silicate/sulphide

melt ratio (R factor). If a system remains closed cumulates stratigraphically above the ore should display Ni depletion, the magnitude of which depends on R factor.

Task 1 studies indicated that ore-bearing intrusions show extreme variability in Ni-contents of olivine even in non-ore samples. This refers to the fact that the nickel content of magma varied strongly during fractional crystallisation. On the other hand, such features refer to an open system (or several subsystems). Cumulates above the ore show Ni depletion only in very few cases, and as a conclusion it can be said, that in intrusions studied either the R factor was relatively large or the system was so open that cumulates above the ore crystallised from different magma than the ore itself. Therefore Ni depletion can be used in exploration to exclude Ni depleted cases, to focus on intrusions showing scattered nature, but (generally) not to directly locate ore.

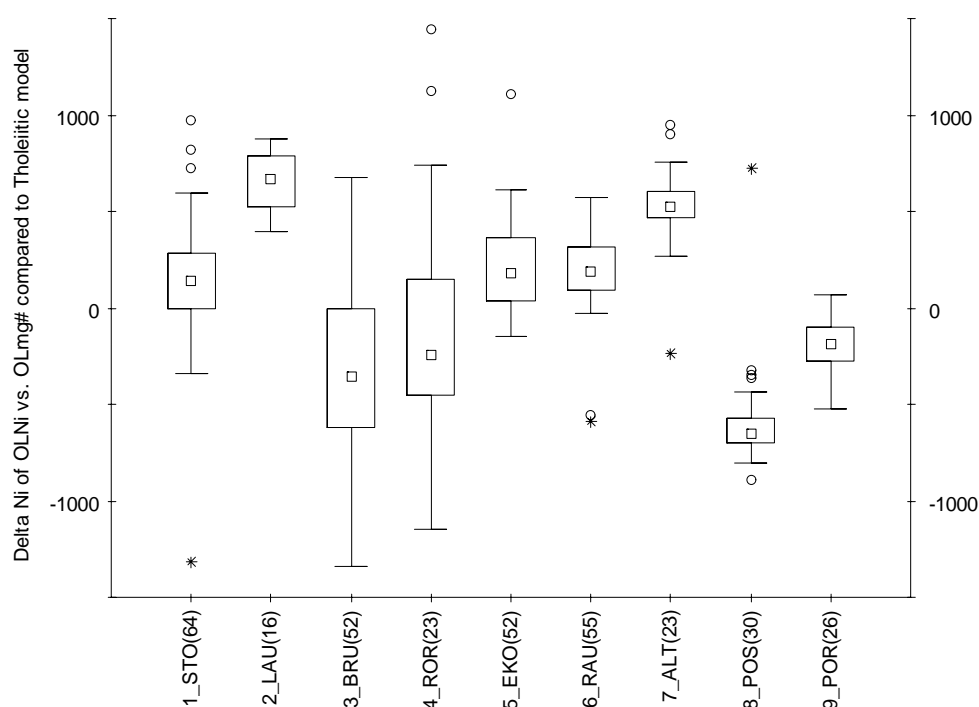


Figure 1.1-8. Box and whisker diagram of delta Ni values compared to tholeiite model shown in Fig. 1.1-7.

For the positive identification of Ni depletion, a known method is electron microprobe analyses of trace quantities of nickel in olivine. Olivine, however, is frequently altered to secondary hydrous phases (serpentine, talc, carbonate), consequently analyses are not always feasible. In such cases it is possible to use trace analyses of Ni in other minerals (orthopyroxene, Cr-spinel, clinopyroxene, amphibole, and even phlogopite). Orthopyroxene and the chromian spinel are regarded as the most reliable ones.

Nickel depletion can be identified also from whole rock analyses by examining calculated compositions of olivine or orthopyroxene (see chapter 3.1.2.1.5). Samples rich in sulphides should be omitted since such calculations may fail due to errors in Fe reallocation between sulphides and non-sulphides.

3.1.3.2.2 Platinum-group elements

Platinum-group elements (PGE) are strongly chalcophile. In presence of sulphide liquid, they will be partitioned into the sulphide phase and thus are useful for studying the sulphur saturation of the melt. The reason for studying the PGE content of some samples from this study was to trace the appearance of sulphide in the evolution of a specific complex assuming a similar PGE content for all the initial magma.

Previous studies have demonstrated that some samples of Ekojoki are significantly enriched in PGE. The presence of platinum-group minerals (PGM) has been reported by Peltonen (1995).

In a preliminary investigation, 7 samples containing disseminated ore from Bruvann (hole 235-159) were analysed for Ir, Ru, Rh, Pt and Pd by ICP/MS, plus one submassive ore from hole n° 260-125, and 4 samples from Ekojoki (hole EJ-17).

The PGE content of the Bruvann samples appears to be extremely low, in the range of less than 2 ppb PGE for a sample containing traces of sulphide, to a maximum of 46.6 ppb for a sample also poor in base-metal sulphide. Values vary between 9.5 and 43.3 for base-metal sulphide (BMS)-rich samples with Pt and Pd dominating strongly over the other PGE. Thus, the PGE content appears not to be related to the presence of BMS.

The results obtained for Ekojoki confirm a relative PGE enrichment in the sulphide-rich samples, with values ranging from 314.5 to 1654.5 ppb. Pd dominates over the other PGE, with a Pd/Pt ratio greater than 1 (varying between 1.5 and 2.6), and a relatively good linear correlation between the two elements. It should be noted that the PGE content in Ekojoki is not related to the amount of sulphide in the sample.

Plots of S versus PGE (Fig. 1.1-9) and Pd versus Pt (Fig. 1.1-10) underscoring the differences between the two complexes.

Table 1.1-5 gives major, minor and trace element compositions of representative samples from Bruvann and Ekojoki. Both have similar compositions in terms of major elements, and similar Ni and S contents, indicating a similar proportion of ore minerals. The Bruvann sample contains 15 ppb PGE and Ekojoki sample 1042 ppb. Other differences between the samples relate to their CaO and Cr₂O₃ contents. The Bruvann sample contains clinopyroxene, and no chromite, whereas the Ekojoki sample does not contain clinopyroxene but does contain disseminated chromite. This indicates that the Ekojoki sample, which is enriched in PGE, is more «ultramafic» than Bruvann sample, whereas both contain the same proportion of BMS mineralisation.

This difference in PGE content could reflect a difference in the degree of fractionation of the magma, with the most evolved magma being the most impoverished in PGE. However, such an interpretation is not supported either by petrological study of the intrusions, or by the consistently low PGE content of all samples.

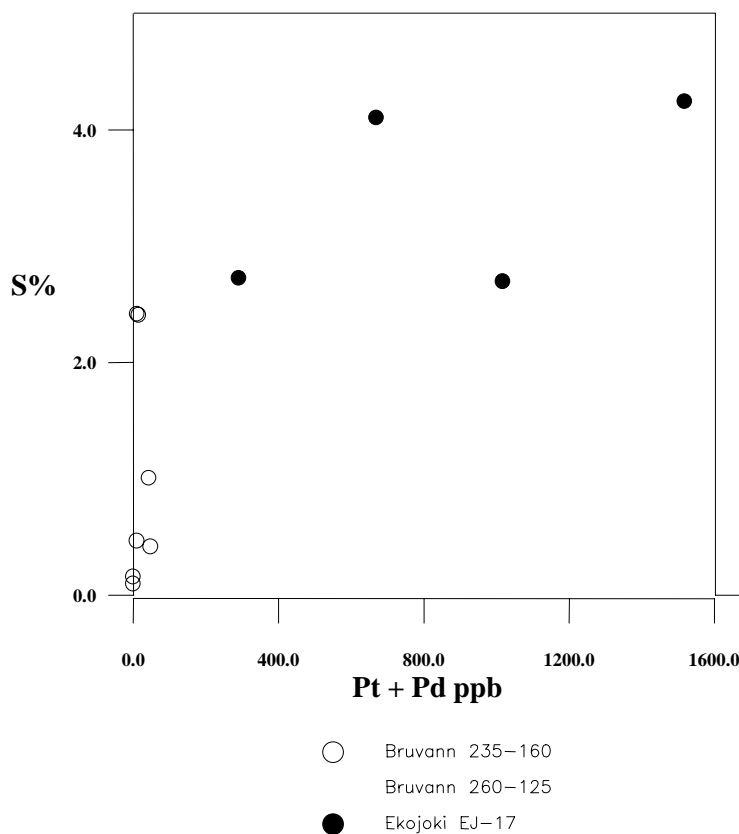


Figure 1.1-9: Correlation between the Pt+Pd and S content for samples from Bruvann and Ekojoki.

Table 1.1-5: Major, minor and trace element compositions of representative samples from Bruvann and Ekojoki.

	Bruvann	Ekojoki
Sample n°	9619315	9619548
SiO ₂ (%)	38.8	34.2
Al ₂ O ₃	4.5	3.8
FeO	15.5	16.5
MgO	34.2	34.9
CaO	3.1	0.9
Cr ₂ O ₃	0.15	1.44
S	2.4	1.7
Ni	0.55	0.4
Ir+Ru+Rh+Pt+Pd (ppb)	15	1042

An alternative explanation for the low PGE values of the Bruvann samples is to consider a first stage of depletion (since the Bruvann sample is the more 'evolved' in term of major elements) resulting from a first stage of sulphur immiscibility in a deeper magma chamber, or from a lower initial PGE content of the magma. The mineralogical study indicates the presence of disseminated BMS in most 'barren' samples. This is an evidence for an early over-saturation of the magma, with the appearance of immiscible sulphide droplets. The appearance of this early sulphide phase should have impoverished the magma in PGE, explaining the very low PGE content of the main ore zones.

Thus, PGE content appears to be a good tracer of the appearance of sulphide in the magma, with the low PGE values reflecting a high amount of sulphide in the system.

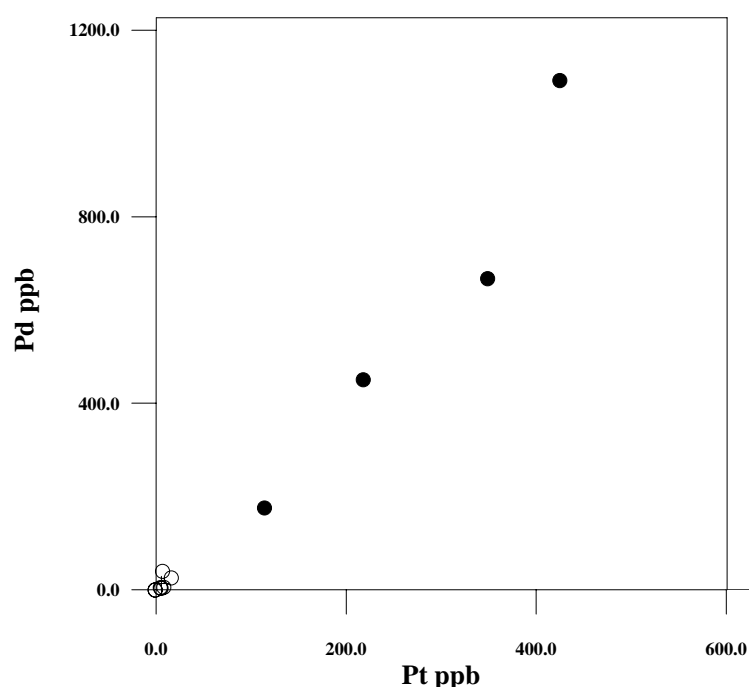


Figure 1.1-10: Correlation between the Pt and Pd content for samples from Bruvann and Ekojoki.

3.1.3.2.3 Sulphide quantity

The sulphide contents in ore-hosting intrusions generally average higher than in barren ones, even when ore samples are excluded and only cumulates examined (Fig. 1.1-11).

In order to produce significant sulphide enrichment the magma has to be close to sulphide saturation, i.e., at a stage before the actual saturation takes place. Unless a necessity, at least it is an advantage for making sulphide saturation easier. For a large-scale ore-forming process, a rapid and violent event where sulphide content of magma exceeds its sulphide-dissolving capacity is required. At the point of sulphide saturation, sulphides start to cumulate from the magma and finally reach equilibrium as the sulphide contents meet sulphide saturation. Frac-

tional crystallisation lowers ability of magma to dissolve sulphides causing the magma to stay at sulphide saturation; consequently sulphide may remain as cumulating phase throughout the layered sequence.

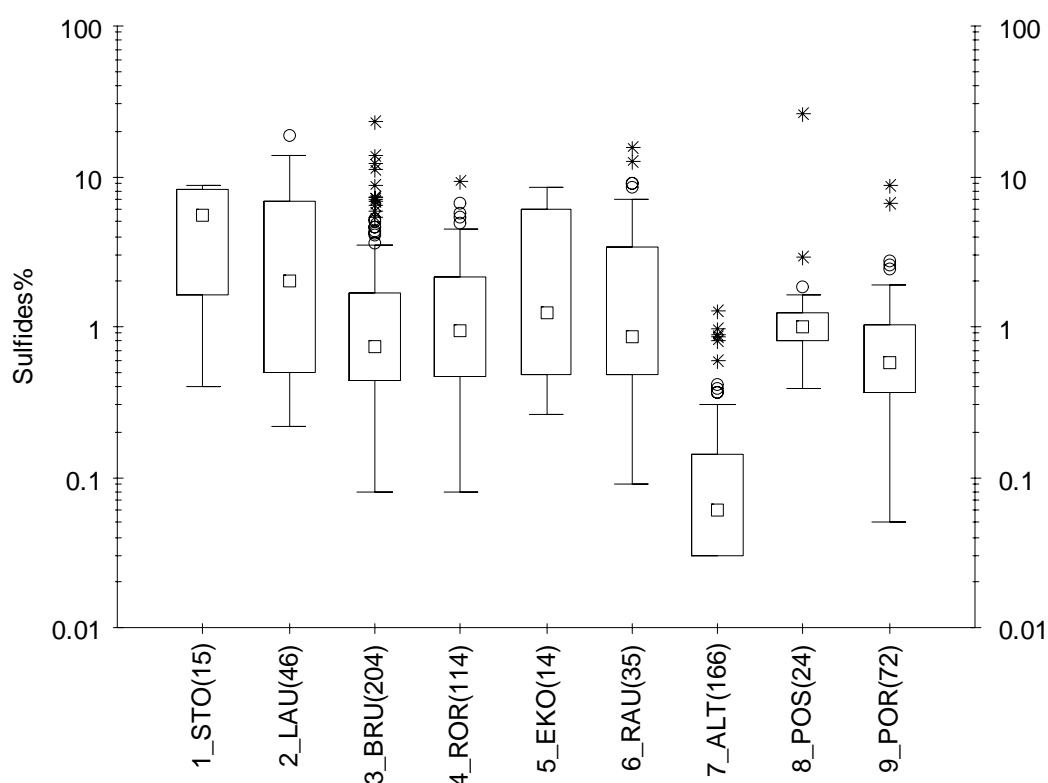


Figure 1.1-11 Box and whisker diagram of sulfide content in non-ore (Ni<0.5%) cumulate samples. Box represents 25th and 75th percentiles, centre box is median, ticks non-outlier min and max, circles outliers, stars extremes. Case study intrusions are arranged in the order of decreasing ore grade & tonnages

Relatively high sulphide contents in intrusive rocks indicate that magma reached sulphide saturation and ore-forming processes may have operated during the history of the intrusion. On the other hand, low overall sulphide contents indicate that magma did not reach sulphide saturation and, if the system remained closed, the intrusion cannot contain significant sulphide enrichments.

3.1.3.3 Methods to trace contamination processes

3.1.3.3.1 Ore mineralogy

To better understand the sulfide segregation process and to characterise the different intrusions, a mineralogical study of sulfides in mineralised and barren samples was undertaken. The Råna intrusion was studied in detail, while the Stormi, Ekojoki and Laukunkangas intru-

sions where also subject to investigation. The mineralogy of all samples was established by optical observation (see images A to L in plate 1.3), complemented by a scanning electron microscope study (SEM) and electron microprobe (EPMA) analyses.

The mineralisation occurs as disseminated sulphides, submassive to massive sulphide ore, or locally as veinlets. Pyrrhotite, pentlandite and chalcopyrite are the most common sulphides (images A, B, C in plate 1.3), present in all samples from the 4 intrusions. Ni-As-Co-S minerals (nickeline, maucherite, cobaltite-gersdorffite), molybdenite and Bi-tellurides occur as rare and small disseminated crystals in all intrusions (images D, G, J in plate 1.3) whereas cubanite and mackinavite are only observed in the Stormi and Ekojoki intrusions (Table 1.1-6). The presence of a rare Re-mineral in one Bruvann sample was also noted, as discussed below. There are no significant differences in terms of composition between the different ore forming minerals from the different intrusions.

One of the most striking features of the sulphide-rich samples is the systematic presence of graphite in various amounts, frequently in close association with pyrrhotite, chalcopyrite and pentlandite. In many cases, graphite laths, or flakes, are intimately associated with sulphide (images B, E, F, H, I, K, L in plate 1.3). In some cases, the graphite-sulphide association suggests that graphite was attached to the sulphide droplets before their crystallisation. This observation implies that graphite was present before sulphide formation.

In order to establish a possible relationship between presence of graphite and the formation of immiscible sulphides, 9 'barren' samples from Bruvann were studied. All the samples contain trace amount of sulphides (of the same nature as the sulphides forming the ore), and a trace amount of graphite. Thus a rough positive correlation can be demonstrated between sulphide and graphite abundance.

Re-sulphides have been rarely reported in the literature. They are described in association with chalcopyrite and Re-bearing molybdenite (see Barkov and Lednev, 1993). In almost all cases they are closely associated with platinum-group minerals in the pegmatoid facies (Ekström and Halenius, 1982, Volborth and Housley, 1984, Mitchell et al., 1989) in a late episode where PGE and Re are scavenged by a sulphide melt along with other chalcophile elements. Platinum group minerals (PGM) were not detected in the sample from this study, but the platinum group element (PGE) values are extremely low in Bruvann samples. Note that Peltonen et al. (1995) described a Re-Mo-Cu-Os sulphide in one sample from Ekojoki. Peltonen (1995) considers that this mineral, together with presence of molybdenite, are indicative of contamination from the host rock.

Differences in the ore mineral assemblages and compositions between samples from the four intrusions are very limited. A mineralogical difference appears between samples containing cubanite (as exsolution in chalcopyrite in the Stormi and Ekojoki massifs) from those where this mineral is absent (Bruvann and Laukunkangas massifs). Nickeline and maucherite occurrences seem to be limited to the Bruvann massif. No significant difference appears in the composition of the mineral species between the different massifs.

Obviously a link between presence of graphite and base-metal sulphide exists and must be understood. The origin of graphite in the orebody is still uncertain. Two origins can be pro-

posed: (1) graphite is inherited from the surrounding host graphite schists and therefore provides evidence of contamination from the host, (2) graphite has crystallised early from the melt. It is well known that graphite can be derived from magmatic fluids (reduced and saturated in graphite, Ballhaus, 1988). The abundance of graphite in some samples (see images K, L) does not seem to be compatible with a magmatic origin. However textural relationships between graphite and sulphide suggest that graphite could have been trapped and concentrated together with the sulphides and would therefore be classed as secondary accumulations.

Table 1.1-6: Sulfide occurrences in various drill holes of the 4 intrusions

		Pyrrhotite (Fe _{1-x})S	Chalcopyrite FeCuS ₂	Pentlandite (Fe,Ni) ₉ S ₈	Cobaltite-Gers. (Co,Ni)AsS	Nickeline NiAs	Maucherite Ni ₁₁ As ₈	Pyrite FeS ₂	Cubanite CuFe ₂ S ₃	Bi-tellurides Bi-Te	Molybdenite MoS ₂	Undetermined Re-mineral
Bruvann												
325	235-160											
420	260-125											
Stormi												
521	OK/VA 280											
527	OK/VA 280											
530	OK/VA 280											
538	OK/VA 762											
Ekajoki												
542	EJ 17											
545	EJ 17											
Laukunkangas												
618	EK/LA 25											
636	EK/LA 25											

The systematic presence of graphite in most samples (including barren samples) together with its enrichment close to host rock xenoliths suggests a residual origin for the graphite. Graphite was probably present in the magma before the formation of the sulphide liquid, and could have been locally concentrated by the sulphide. It is thus hypothesised that the graphite provides evidence of an early contamination of the magma.

3.1.3.3.2 Rare earth elements

The rare earth elements (REE) have important applications in igneous petrology, as a result of their chemical and physical properties. A large number of parameters control the distribution of REE in rocks, including partial melting in the source region, crystal fractionation, crystal accumulation and contamination processes.

To understand the magmatic processes affecting the Bruvann intrusion, 13 samples were studied. Nine were taken from a single bore-hole (235-160) including barren and weakly mineralised samples, one from the host rocks, one from an ore-rich zone (bore-hole 260-125), one from a mafic dyke cutting the intrusion and one from the middle of the intrusion.

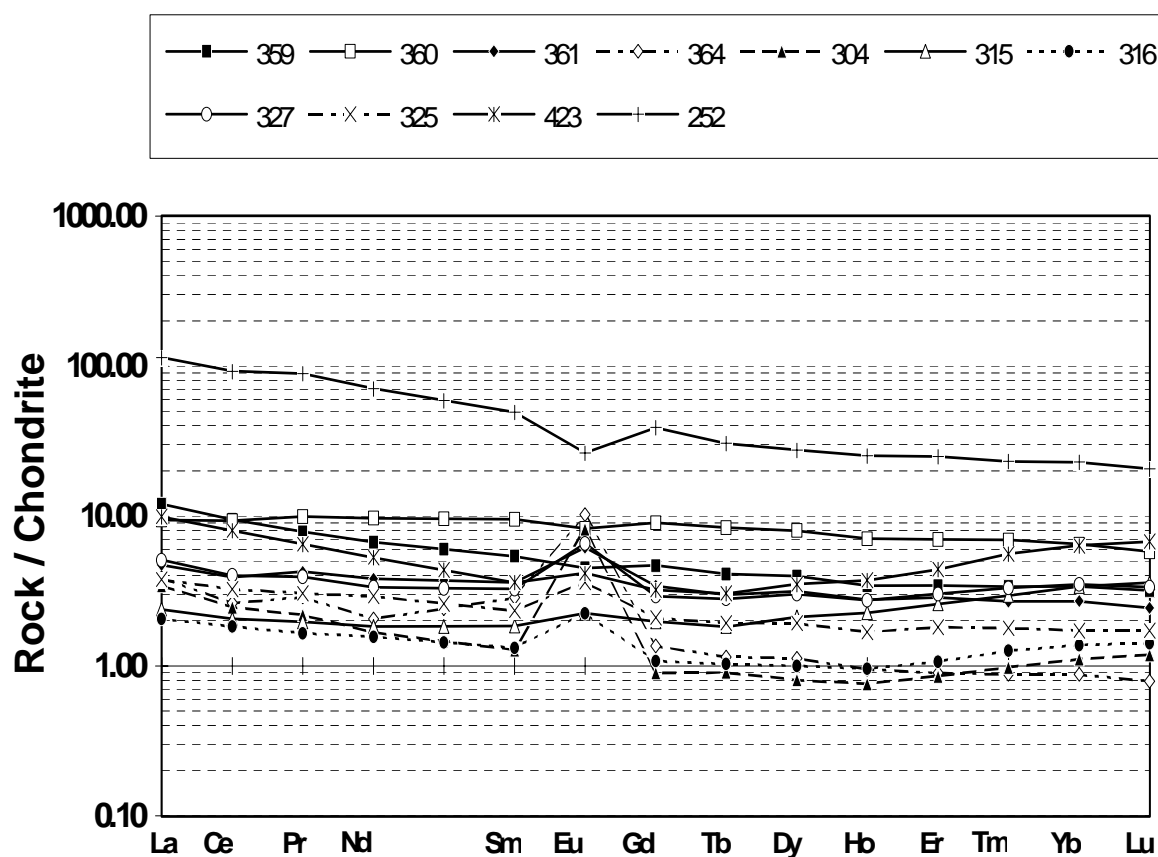


Figure 1.1-12: Chondrite-normalized rare earth element abundances in samples from Bruvann (drill-hole 235-160).

3.1.3.3.2.1 Drill hole 235-160

The REE content of all samples varies in a narrow range, between 1 and 10 times the corresponding chondrite values (Nakamura and Masuda, 1973, Masuda, 1975). Chondrite normalised patterns (Fig. 1.1-12) show a positive Eu anomaly for 7 samples, while 2 have a slight

negative Eu anomaly. The latter (359, 360) are the richest in REE (22.4 and 29.1 ppm respectively) and have the characteristics similar to magmas, whereas the former (304, 315, 316, 325, 327, 361, 364) have the characteristics of cumulate rocks. The host graphite schist has a pattern typical of "continental crust", i.e., the sample is enriched in REE (210 ppm) and in light REE (La/Yb 7.6), and also has a negative Eu anomaly.

One sample (423) shows a different pattern, with a U shape. This pattern corresponds to a mafic rock that cannot be genetically related to the cumulate series.

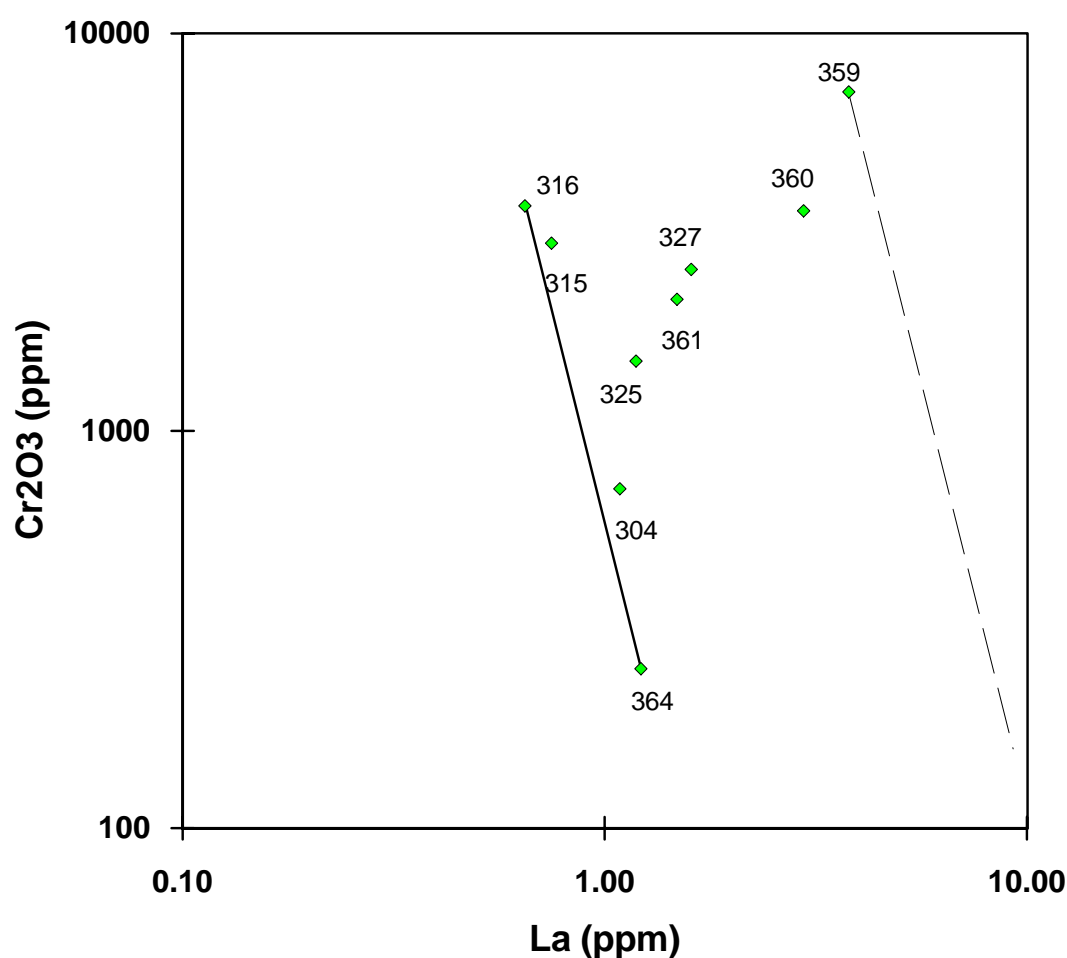


Figure 1.1-13: Plot of Cr₂O₃ vs. La for 9 samples from the Bruvann intrusion. The dashed line corresponds to the liquid trend, the solid line to the cumulate trend

3.1.3.3.2.2 Modelling

If fractional crystallization is considered to be the main differentiation process, then the relationships between the different rock types (cumulates or liquids) can be established. The graphical method (Cochevie, 1986) involves compatible element, against an incompatible

element on a binary diagram. The composition representing the liquid phase will plot on a straight line while cumulate phases crystallising from these liquids will plot on a second line, parallel to the first.

Figure 1.1-13 shows the Cr_2O_3 vs. La diagram. The diagram suggests that sample 359 has the most primitive liquid composition, and that the line from sample 316 to 364 corresponds to cumulate compositions without trapped interstitial liquid. Compositions which plot between the two lines correspond to cumulates containing varying amounts of trapped liquid. This corresponds to another type of liquid composition.

Having characterised the different samples, the global distribution coefficient for the compatible and incompatible elements can be calculated, as well as the degree of crystallization rate calculated using the composition of the extreme samples and the distribution coefficients. An average F value (proportion of residual liquid) of 0.49 is obtained. Thus a degree of crystallization of 51% could explain the observed evolution from the most primitive cumulate (316) to the most evolved (364).

On the other hand cumulate 316 appears not to be in equilibrium with liquid 359. Composition 348, with too high compatible element concentration, represents a more primitive liquid than the one from which sample 316 has been derived.

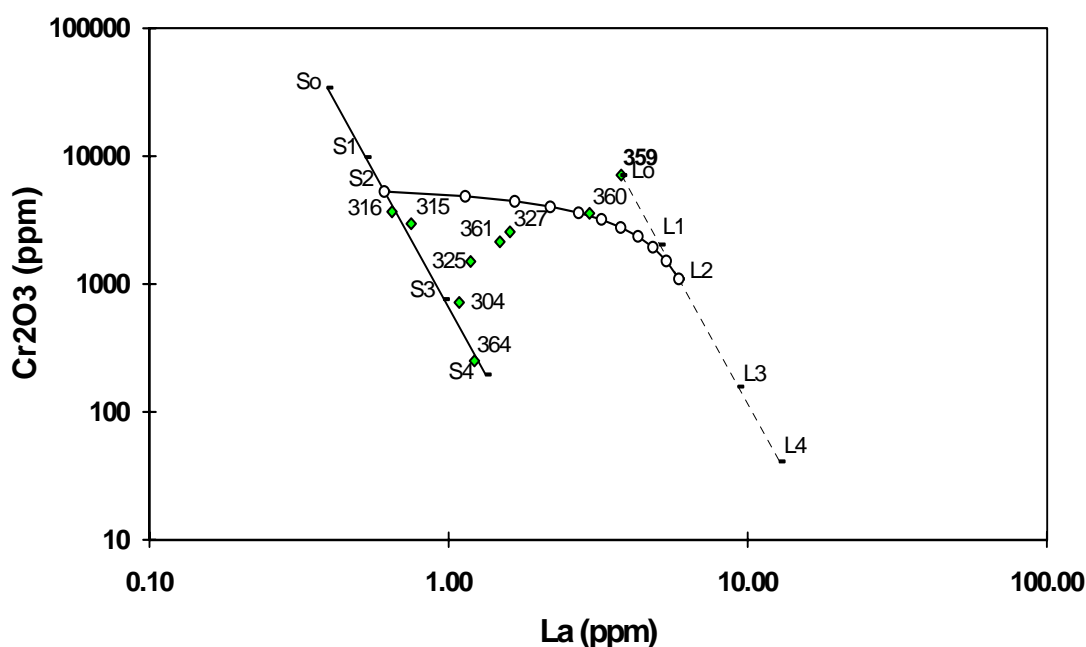


Figure 1.1-14: Plot of Cr_2O_3 vs. La showing the calculated evolution of liquid and cumulate compositions.

Using the calculated distribution coefficient for Mg, Cr and La in conjunction with the com-

position of sample 359 (which is assumed to correspond to the most primitive liquid - L0), the composition of the most primitive cumulates (S0) can be calculated. Figure 1.1-14 illustrates the calculation for Cr_2O_3 . The most evolved cumulate (364 or S4) corresponds to a degree of crystallisation of 74 %.

3.1.3.3.2.3 Characterisation of the protolite and the contamination effect

A study of the REE distributions also provides information regarding the nature of the rocks from which the initial magma has been derived. Using the partial melting model of Shaw (1970), three types of mantle have been tested (spinel lherzolite, amphibole lherzolite and garnet lherzolites). The REE content of the source (average primitive mantle) is taken from Sun and McDonough (1989). Models based on spinel and amphibole lherzolites give calculated REE patterns similar to the observed patterns but cannot account for the composition of sample 359. The model based on garnet lherzolite give results not compatible with the observed composition and must be rejected.

The only model which can account for the observed composition is a spinel or amphibole lherzolite source having a chondritic value, with a degree of melting close to 10 % (Fig. 1.1-15).

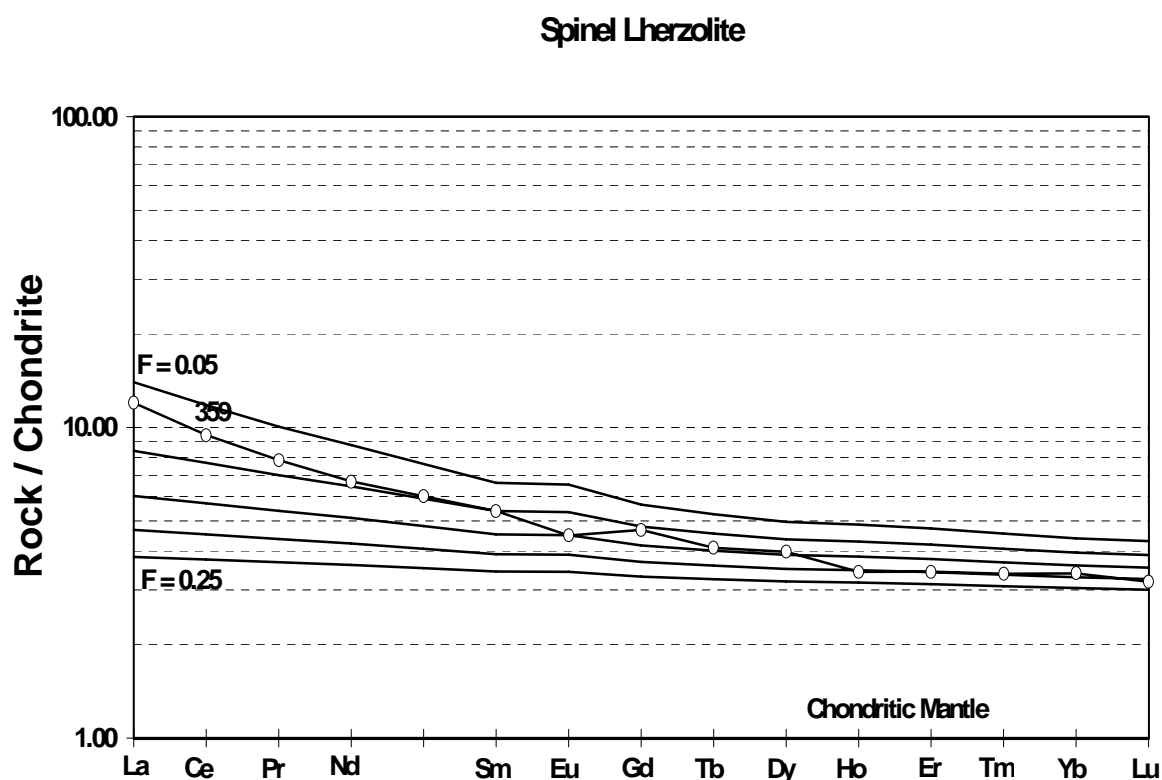


Figure 1.1-15: Calculated REE pattern ($F = 0.05, 0.10, 0.15, 0.20, 0.25$) for partial melting of a chondritic spinel lherzolite source. The composition of liquid 359 is indicated.

However, this diagram shows that the liquid (359) has an REE pattern that is not entirely coincident with the calculated patterns for a liquid derived from partial melting of a spinel lherzolite source. The heavy REE pattern corresponds to a degree of melting of about 20 % whereas the light REE indicate a much lower degree of melting, of about 10 %. This apparent enrichment in light rare earth elements can be explained by an early contamination of the liquid by the host schist, which is enriched in light REE. In this hypothesis, the true degree of melting of the source would be about 15 to 20 %. A contamination rate of only 5 % of the crustal material (similar to sample 252) could account for the observed light REE enrichment of the liquid, giving an apparent degree of melting of about 10 %.

3.1.3.3.3 Stable isotopes

From the ore mineral study, it appears that C (occurring as graphite) and S (occurring as sulphides) are the two major components involved in the ore forming system. Both elements, are intimately associated in some instances, but are not systematically related throughout the ore-body. These minerals are also found in the host graphite schists. It is thus possible that C and S have been incorporated (at least in part) from the host rock into the magma, invoking changes in the physical conditions within the magma body. Such changes might include local oversaturation in S leading to the immiscibility of some sulphide phases. One of the ways to test if the mineralisation resulted from such a contamination process is to study the C and S isotopes.

A range of sample types were selected from Bruvann, representing different graphite and sulphide contents (Table 1.1-7). The sulphur and carbon-isotope compositions of sulphides and graphite were determined for ore-types containing more than 10 wt% sulphides, for cumulates containing graphite and disseminated sulphides, and for the host schists.

Table 1.1-7: S and C isotopic data for the Bruvann samples

Sample N°	DH N°	Nature	$\delta^{34}\text{S}$ ‰	$\delta^{34}\text{C}$ ‰	S %	MgO %	CO ₂ %
9619252	235-120	graphite schist	-10.4	-21.5	7.3	6.10	39.6
9619285	235/120	BMS pyroxenite	-1.6	-19.8	11.7	9.53	6.7
9619315	235/160	Pyroxenite	-0.7		2.9	28.68	0.5
9619325	235/160	Pyroxenite	-0.1		2.7	34.42	1.9
9619385	235/160	graphite pyroxenite	-4.7	-14.0	0.62	9.58	2.6
9619387	235-160	graphite-bearing gabbro	-6.0	-14.8	5.0	12.20	8.8
9619395	260/125	Peridotite	1.0		0.20	33.92	1.4
9619419	260/125	Massive ore	0.6		33.8	14.46	0.5
9619421	260-125	bC\$ next to massive ore	-0.3	-20.4	14.6	10.70	5.7
9619423	260-125	graphite-bearing gabbro	-2.8	-20.3	10.1	19.50	17.
9619464	270/135	BMS peridotite	1.8		7.1	40.90	0.40

Sulphides from the host schists (Fig. 1.1-16, Table 1.1-7) have a low $\delta^{34}\text{S}$ value of -10.4‰, within the range commonly reported for sedimentary sulphides (Coleman, 1977; Ohmoto, 1986). The $\delta^{34}\text{S}$ values of sulphides from graphite-bearing cumulates and from ores with less than 50 wt% sulphides are heterogeneous and range from -6.0 to +1.8‰, whereas the $\delta^{34}\text{S}$

value of sulphide from the massive ore is +0.6‰. Most of these values are close to those of mantle-derived sulphur (from -3 to +2‰; Ohmoto, 1986), however, the lowest $\delta^{34}\text{S}$ values (-4.7 and -6.0‰) and the heterogeneity of $\delta^{34}\text{S}$ values are suggestive of local contamination by sulphur originating from the host schists.

Graphite from the host schists exhibits a low $\delta^{13}\text{C}$ value of -21.5‰, similar to the isotopic composition of matured organic matter (Ohmoto, 1986). The $\delta^{13}\text{C}$ of graphite from graphite-bearing cumulates and from the ore show two ranges of values (Fig. 1.1-16, Table 1.1-7): (1) high values between -14 and -15‰ for sulphide-poor cumulate, and in one ore sample with low sulphide content; and (2) low values, around -20‰, for ore samples with a sulphide content higher than 20 wt%.

The $\delta^{13}\text{C}$ values of graphite from all barren cumulates are similar to values previously reported for pyroxenites, eclogites and kimberlites (Pineau et al., 1987; Deines et al., 1987; Pearson et al., 1991; 1994). If the highest values of around -14‰, are relatively close to the $\delta^{13}\text{C}$ values of graphite derived from mantle carbon in mafic rocks (Pearson et al., 1994), then the lowest values of around -20‰, may be interpreted in two ways: (1) a contamination of the magma from the host schists or, (2) a possible impoverishment in the ^{13}C content of the dissolved magmatic carbon resulting from Rayleigh distillation during CO_2 degassing (Pineau and Javoy, 1994). Two important observations argue in favour of hypothesis 1:

- (1) the $\delta^{13}\text{C}$ value of graphite in the cumulates is inversely related to its abundance, which is the opposite of the trend expected from CO_2 degassing with accompanying Rayleigh distillation (Pineau and Javoy, 1994);
- (2) the cumulate which has the highest graphite content (4.8 wt %), exhibits a $\delta^{13}\text{C}$ value that is relatively close to the $\delta^{13}\text{C}$ value of graphite in host schist.

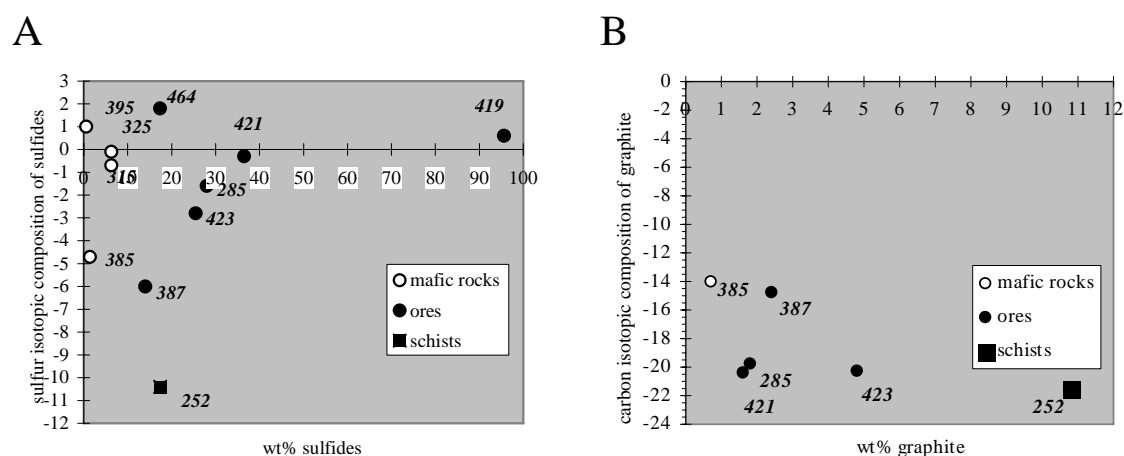


Figure 1.1-16: Correlation between $\delta^{34}\text{S}$ and the weight per cent of sulfide (A) and $\delta^{13}\text{C}$ versus the weight per cent graphite (B) for the Bruvann samples.

The C and S isotope data in combination suggests that the sulphur from which the mineralization has been derived is of magmatic origin, from a magma originally rich in S. However, some samples (with low S contents) reflect local contamination, with the sulphur in these

samples derived from the host schists. Graphite associated with the ore has been inherited from the host, and provides further evidence of contamination from the host schists.

Thus, a model can be proposed where sulphur oversaturation of the magma is induced by changes in the physical and chemical condition of the magma resulting from assimilation of the host schists, with the contribution of S from the host schists to the ore-forming system being minor. In contrast, graphite in the sulphide-bearing samples has been incorporated from the host into the magma and provides further evidence of contamination.

The combination of both carbon- and sulphur-isotope composition appears to be a very suitable tool for tracing contamination in this orebody.

3.1.3.3.4 Radiogenic isotopes

One of the major reasons for studying a radiogenic isotope system such as Sm/Nd is that such studies can facilitate an understanding of how the magmatic reservoir interacts with its surroundings and can enable an estimation of the stage at which contamination of a melt occurs.

Table 1.1-8: Sm-Nd analytical data for the Brevann samples.

Sample N°	DH N°		Sm ppm	Nd ppm	$^{147}\text{Sm}/^{144}\text{Nd}$ d	$^{143}\text{Nd}/^{144}\text{Nd}$ $\pm 2\sigma(m)$	$\epsilon_{\text{Nd}}(0)$ [1]	$\epsilon_{\text{Nd}}(T)$ [2]	T_{DM} Ga [3]
9619359	235/160	trace BMS	1.03	4.00	0.15567	0.512514 ± 3	-2.46	-0.2	1.66
9619360	235/160	trace BMS	1.83	5.76	0.19207	0.512645 ± 4	+0.10	+0.4	-
9619364	235/160	barren	0.55	1.23	0.27033	0.512719 ± 9	+1.54	-2.6	-
9619304	235/160	trace BMS	0.25	1.00	0.15114	0.512425 ± 20	-4.19	-1.7	1.76
9619315	235/160	diss BMS	0.35	1.09	0.19412	0.512640 ± 7	+0.00	+0.1	-
9619325	235/160	diss BMS	0.45	1.74	0.15635	0.512555 ± 13	-1.66	+0.6	1.57
9619421	260/125	BMS	1.23	6.01	0.12373	0.512112 ± 4	-10.30	-6.2	1.75
9835543	Surface	barren norite	2.96	13.50	0.13256	0.512404 ± 5	-4.60	-1.0	1.39
9619595		peridotite	84.2	1631.00	0.03121	0.510716 ± 4	-37.53	-28.3	2.02
9619252	235/120	Host	9.47	42.3	0.13535	0.512135 ± 9	-9.85	-6.4	1.96

Notes :

[1] : $\epsilon_{\text{Nd}}(0) = \left[\frac{(^{143}\text{Nd}/^{144}\text{Nd})_{\text{sample}}}{(^{143}\text{Nd}/^{144}\text{Nd})_{\text{CHUR}}} - 1 \right] 10^4$ where $(^{143}\text{Nd}/^{144}\text{Nd})_{\text{CHUR}} = 0.51264$ and

CHUR = Chondritic Uniform Reservoir

[2] : calculated at emplacement time = 437 Ma

[3] : $T_{\text{DM}}^{\text{Nd}} = \frac{1}{\lambda} \ln \left[1 + \frac{(^{143}\text{Nd}/^{144}\text{Nd})_{\text{sample}} - (^{143}\text{Nd}/^{144}\text{Nd})_{\text{DM}}}{(^{147}\text{Sm}/^{144}\text{Nd})_{\text{sample}} - (^{147}\text{Sm}/^{144}\text{Nd})_{\text{DM}}} \right]$ where $(^{147}\text{Sm}/^{144}\text{Nd})_{\text{DM}} = 0.2137$;

$(^{143}\text{Nd}/^{144}\text{Nd})_{\text{DM}} = 0.51315$ (or $\epsilon_{\text{Nd}} = +10$); $\lambda^{147}\text{Sm} = 6.5410 \times 10^{-12} \text{ yr}^{-1}$; DM = depleted mantle.

Nine samples from Brevann were measured for Nd isotopic composition, 6 from drill-hole 235-160 (either barren or containing disseminated base-metal sulphides – BMS), one ore-rich sample from drill hole 260-125 (421), one norite taken from the centre of the intrusion (543) and one host graphite schist (252). Samples 359, 360 and 364 belong to the same cyclic unit.

The REE data suggests that 359 has a composition with characteristics of the liquid, whereas 360 and 364 are cumulates, the latter being the most evolved. Samples 304, 315 and 325 are cumulates of intermediate composition.

One sample from Rausenkulma (595), which is very enriched in REE ($Nd > 1600$ ppm) has also been analysed. Analytical results are reported in the Table 1.1-8.

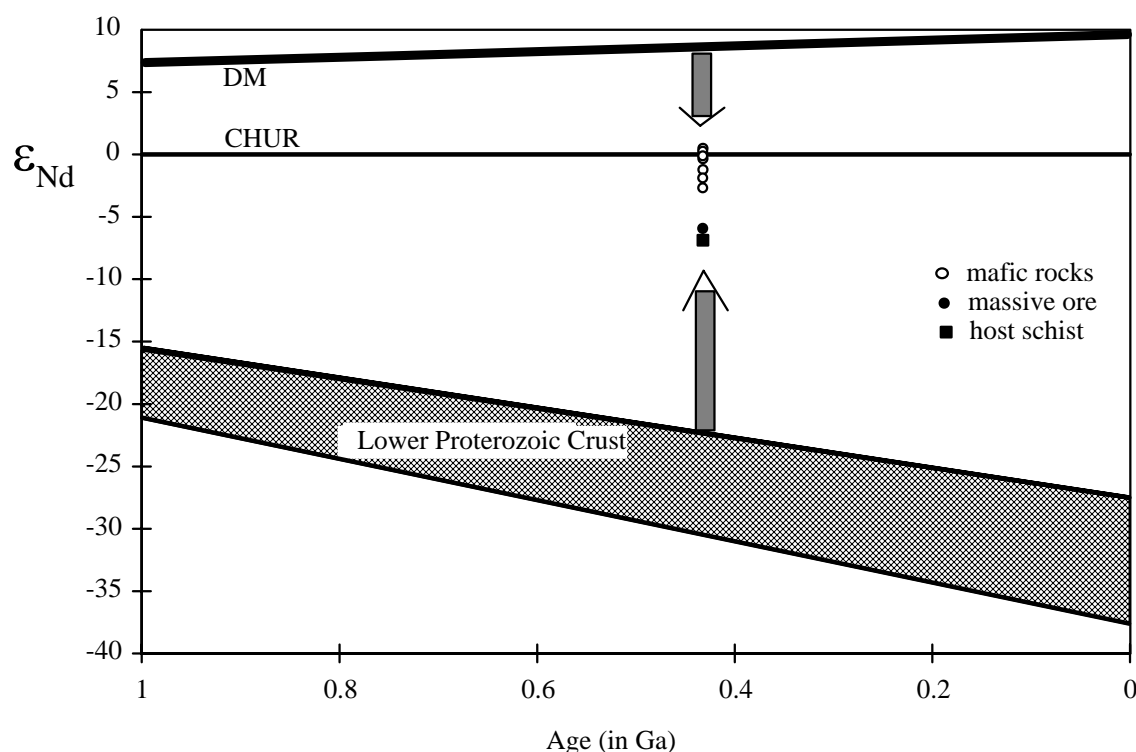


Figure 1.1-17: Plot of ϵ_{Nd} vs. Age for the Bruvann sample.

The $\epsilon_{Nd}(T)$ calculated at the emplacement age of the complex (437 Ma, in Barnes, 1989) are very close to zero for the barren and weakly mineralised samples (-2.6 to +0.6) (Table 1.1-8, Fig. 1.1-17) and correspond to chondritic values. For the massive ore (421), the value is lower (-6.2), very close to the value obtained for the host schist. Values around zero could either reflect a chondritic mantle source for the complex, or contamination of a depleted mantle source with Lower Proterozoic (or Archaean) crust. Most of the upper mantle is depleted in light REE, similar to MORB. A considerable body of data indicates that this depletion occurred subsequent to the Archaean as a consequence of continental crust formation. Thus, a chondritic source for the Bruvann complex is uncertain; a depleted mantle origin, combined with crustal contamination is more probable. An approximate measure of the amount of contamination can be determined using the classical two component mixing equation (Pushkar et al., 1972). For this calculation, the parameters are as follows:

Depleted mantle: $Nd = 10$ ppm (MORB), $\epsilon_{Nd}(437Ma) = +9$

Crustal component: $Nd = 33$ ppm, $\epsilon_{Nd}(437Ma) = -26$ (estimated from data on Lower Proterozoic granitoids from Northern Finland (Huhma, 1986).

Calculations indicate a level of crustal contamination of around 10% for the barren to weakly mineralised rocks, and around 19% for the mineralised sample. Assuming a Nd content of about 2.4 ppm for the mantle source (as suggested from the REE study), the level of contamination appears much lower, around 3% for the unmineralized samples and 5% for the ore sample. Whatever the actual percentage, the ore sample seems to have been subject to a higher degree of crustal contamination.

3.1.3.3.5 Conclusions on contamination studies

Studies of mineralisation and ore mineral assemblages show that there are no major differences in either mineral assemblage or mineral composition from one intrusion to another. Detailed study of the Bruvann intrusion has demonstrated the existence of graphite in most barren and mineralised samples. Graphite is interpreted as mineralogical evidence of contamination from the host graphite schist which has been partly mechanically collected by the sulphide phase. The presence of minor phases, such as molybdenite, also argues in favour of contamination.

Bruvann is characterised by a very low platinum-group-element (PGE) content, in contrast to Ekojoki, where platinum-group minerals have been described. This low PGE content reflects the early appearance of an immiscible sulphide liquid phase which has scavenged PGE, leaving the residual magma impoverished in PGE. The mineralogical expression of this sulphide phase is disseminated sulphide which is present in most 'barren' samples. This could be an expression of the first contamination stage described below, but there is no evidence that it corresponds to a massive concentration of sulphides.

The study of carbon-isotopes in graphite samples from Bruvann clearly confirms a contamination process, which does not appear to have affected the sulphur-isotope composition of the deposit. We conclude then, that the effect of contamination was to change the physical and chemical evolution of the magma, leading to sulphide immiscibility. Sulphide in the ore originated from the magma, whereas most of the graphite is interpreted as residual and derived from the host schist.

A study of the rare earth element (REE) patterns has enabled us to better understand the relationships between the different rock types, and to conclude that the magma from which cumulates were derived, originated from partial melting of a spinel lherzolite having a chondritic REE content. The degree of melting has been estimated at 15 to 20 %. The REE study also indicates early contamination of the magma.

Nd isotope systematics confirm the hypothesis of an early contamination of all the series, estimated at 3 %, whereas the massive ore seems to have been subject to a stronger contamination episode.

All the above data suggest the existence of a contamination process. The contamination appears to have occurred in at least at two stages. The first is very early in the evolution of the magma. This phase may have resulted in the early appearance of a disseminated sulphide phase in the Bruvann complex, causing an impoverishment of the residual magma in PGE. The second contamination stage is associated with the major mineralising events.

3.1.3.3.6 Orthopyroxene abundance as a favourable contamination indicator

When the crystallisation series, chemical compositions of parental magma, and cumulate series are compared, clear differences are found in the relative abundance of orthopyroxene, or more specifically in the orthopyroxene/(orthopyroxene+clinopyroxene) ratios. Figure 1.1-18 depicts the variations in orthopyroxene/pyroxenes ratio in cumulates of each intrusion. All of the ore-hosting intrusions, as well as the subeconomic Rörmyrberget, are clearly dominated by orthopyroxene. Bruvann has two main (megacyclic) units of which the lower one is dominated by orthopyroxene and upper by clinopyroxene. The lower unit hosts ore. At Alter do Chao, crystallisation started with olivine cumulates which feature would point to orthopyroxene crystallisation; however, orthopyroxene cumulates are scarce and there is a sudden jump to clinopyroxene field producing olivine-clinopyroxene cumulates followed by gabbros (clinopyroxene-plagioclase cumulates).

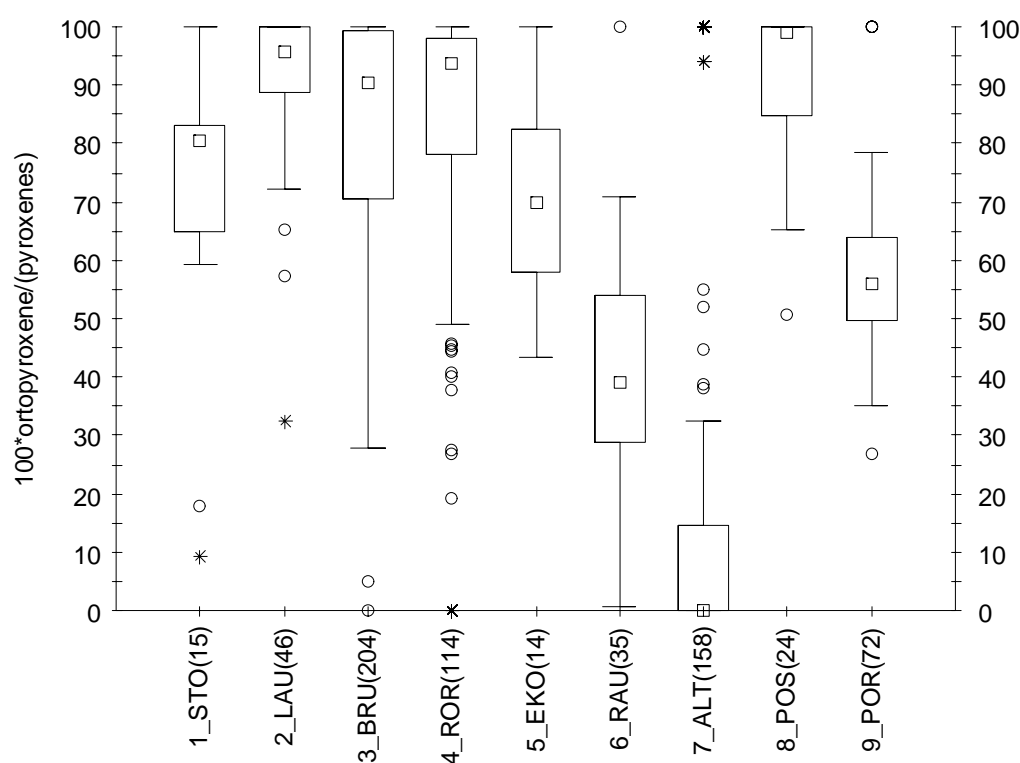


Figure 1.1-18: Box and whisker diagram describing the ratio of orthopyroxene/(pyroxenes) % in non-ore cumulates of the case study intrusions.

This study revealed that Ni-sulphide ore-hosting intrusions frequently represent a series where olivine is the first mineral to crystallise followed by orthopyroxene and plagioclase, clinopyroxene being the last one. In several of ore-hosting intrusions (e.g. Sudbury, Montcalm) orthopyroxene cumulates are voluminous. This is at least partly due to contamination by materi-

als rich in SiO₂ which factor, on the other hand, shifts the melt towards orthopyroxene crystallisation but also lowers its capacity to dissolve sulphides. This study brought to light also an observation that the ore-hosting intrusions lack magnetite-plagioclase cumulates. The last phases of crystallisation series are rich rather in Si and Zr than Fe, P and Ti.

3.1.3.4 Indicators of sulphide concentration

Contamination, sulphide saturation and sulphide segregation alone in a primitive magma are not enough to produce economic Ni-Cu sulphide ore, yet another kind of concentration process is required. In the case studies, this factor was clearly demonstrated at Rörmyrberget, Ekojoki and Rausenkulma, where sulphide segregation has taken place but effective concentration was lacking; consequently economic ore was not formed.

If sulphide segregation were significant, one would expect to find depletion in chalcophile elements above the ore. However, none of the case study intrusions showed such features. Bruvann may be an exception since Ni depletion was observed on one of the profiles. This indicates that the magmatic systems were open and the amount of magma was large, consequently sulphides were able to equilibrate with fresh magma undepleted in Ni. Therefore, sulphide segregation was not able to deplete magma in Ni and Cu. Possibly depletion in PGE could be seen, but generally all of the ore-hosting intrusions are depleted in PGE due to the segregation of sulphides at deeper levels (or small amounts of sulphides retained in mantle residue during melting). Therefore, PGE are not useful for monitoring sulphide segregation in Ni-Cu exploration.

It appears that the study of lithochemical and mineralogical data alone cannot tell whether the process produced economic nickel ore. The answer must be sought using other data such as geological observations. Deposits containing classical text-book sulphide enrichment at the bottom of the intrusion (Stormi and Laukunkangas) do not show several olivine cumulate layers and rhythmic layering, as is the case at Bruvann and Rörmyrberget. Almost without exception, world class nickel sulphide ores are hosted by the most primitive cumulates, i.e. olivine cumulates located on the bottom of the intrusion.

Geological, lithochemical and mineralogical data demonstrate whether sulphide segregation has taken place and at which part of the intrusion one can expect to find the best sulphide concentrations. Geophysical surveys usually are the final tools in locating nickel sulphide deposits within intrusion.

3.1.4 Summary of the developed tools for sulfide Ni exploration

Two kinds of tools were developed in Task 1 for nickel sulphide exploration. The first one is a computer program "Advanced Petrological Explorer" (APE), which enhances the application of lithochemical and mineralogical data in nickel exploration. APE helps in carrying out basic petrological calculations for single samples. For that purpose, it includes traditional normalisation and norm calculation routines. It also contains novel routines for the estimation of mineral compositions in samples, for naming cumulate rocks and estimating chemical compositions of minerals on the basis of whole rock data. To determine the key figures in nickel exploration, APE includes graphical and modelling tools for the determination of the

chemical composition of parental magma, and to identify cumulate and crystallisation series, to solve internal structures of intrusions, to qualify and quantify contamination features, to qualify and quantify sulphide segregation features, and to estimate the openness of the magmatic system. The comparison of various nickel exploration targets is made fast and easy with APE.

Task 1 developed novel nickel exploration tools and enhanced the application of existing methods by studying nine selected intrusions. The studies resulted in several important features, such as the identification of sulphide segregation and favourable contamination; they also can be quantified from whole rock chemistry.

Sulphide saturation in a magma can be positively identified by sulphide content, olivine composition (trace-Ni by EPMA), and PGE level in the intrusion. PGE-depleted but Ni-undepleted intrusions that contain sulphides in the layered series are the most prospective ones. Intrusions barren of sulphides or depleted in Ni can be excluded.

Several means were tested and developed to identify favourable contamination. The mineralogical investigations, isotope (C, S, Sm/Nd) and REE studies resulted, that contamination by black schist triggered the ore-forming processes at Bruvann. The close association of ore with black schist, presence of graphite and molybdenite in ore samples, and anomalously high V- and Mo-contents in the cumulates of other ore-hosting intrusions studied (Stormi and Laukunkangas) indicate that similar processes were significant in those cases, as well. The dominance of orthopyroxene (over clinopyroxene) may provide a direct measure on favourable (SiO₂ -rich) contamination, and it is proposed that intrusions displaying crystallisation series olivine-orthopyroxene-plagioclase-clinopyroxene, and having high orthopyroxene/clino-pyroxene ratio, are more prospective than clinopyroxene-dominated ones.

Table 1.1-9. Summary of the target intrusions. The nickel exploration tools developed in Task 1 were used. The summary is based on whole rock chemistry and PGE analyses. Ore samples were excluded. X = requirement fulfilled, 0 = requirement not fulfilled, - = no data.

Intrusion	Ni undepleted	Sulfides abundant	PGE depleted	High opx/cpx	Repetitive olivine cumulate layers missing	All requirements fulfilled
1_STO	X	X	X	X	X	X
2_LAU	X	X	X	X	X	X
3_BRU	X	X	X	X	0	
4_ROR	X	X	-	X	0	
5_EKO	X	X	0	X	X	
6_RAU	X	X	X	0	X	
7_ALT	X	0	-	0	X	
8_POS	0	X	X	X	X	
9_POR	0	X	X	0	X	

Even though an intrusion may have experienced favourable contamination and sulphide segregation, it may not necessarily result in the formation of economic Ni-Cu ore. Yet another kind of concentration process is required. The case studies indicated, that such a process was

absent in intrusions that formed as a result of episodic replenishment, separated by peaceful periods of fractional crystallization, as is the case at Bruvann and Rörmyrberget. Such systems can be identified from repetitive olivine cumulate layers.

Table 1.1-9 provides an estimate on the nickel exploration potential of the case study intrusions. Ore samples were excluded from the data. The requirements were fulfilled in the Stormi and Laukunkangas intrusions. Stormi is more favourable because of more primitive parental magma.

3.2 Task 2

3.2.1 Descriptive model for nickel-sulphide deposits related to komatiitic volcanics

3.2.1.1 Introduction

Magmatic Ni-Cu sulphides are hosted by cumulate rocks, dunites, peridotites and gabbros, but the characteristics of the deposits vary widely, depending on the type, composition and process of emplacement of the host magma. The main subdivision of mafic and ultramafic igneous rocks is based on the environment of the rock-forming processes (endogenic or exogenic, intrusive or extrusive), and this subdivision can be applied to the classification of sulphide Ni-Cu deposits, too. The extrusive deposits are directly related to volcanic processes whereas all the other refer to an intrusive environment. Extrusive Ni deposits are associated with the high-Mg Archaean ultramafic komatiites and komatiitic basalts or moderately Mg-rich Proterozoic komatiites, (ferro)picrites and basalts. Due to the extrusive environment, volcanic-hosted Ni-sulphide deposits differ from those associated with intrusive rocks, the main differences arising from the more open igneous system of extrusives, their extremely high temperatures, the dynamics of the magma flow and the low surface pressures. All these features result in characteristics that require extrusive-related Ni sulphides to be treated as a specific ore type in ore deposit modelling. The physico-chemical rules and formulas applied to sulphide-silicate melt systems are the same for extrusive and intrusive deposits, and certain mathematical treatments can be applied to both types, but the coefficients vary and the final results differ. The modelling of extrusive Ni deposits developed by this project in parallel with that of intrusive ore deposits will apply genetic interpretations to the observed differences. The extensive literature is reviewed in an effort to establish the factors controlling the compositions of extrusive Ni-sulphide deposits. These factors are then inductively compared with the field data to model the Ni deposits of the Archaean komatiites of eastern Finland.

3.2.1.2 Factors controlling the compositions of extrusive Ni-sulphide deposits, a literature review

Old textbooks, such as those by Lindgren (1933) and Schneiderhöhn (1941), regarded Ni-Cu deposits as type examples of intrusive-related ore deposits. It was only with the discovery of the Kambalda deposits in Western Australia in the 1960s that the existence of ultramafic extrusive-related Ni deposits became known (Ross and Travis 1981). The literature on ultramafic volcanics accumulated since the first description of komatiites (Viljoen and Viljoen 1969) is considerable, and the reader is referred to reviews of the characteristics of komatiites and komatiitic basalts by, among others, Nesbitt et al. (1979), Arndt and Nisbet (1982), Hill et al. (1990) and Leshner and Stone (1996), and of picrites and ferropicrites by Hanski (1992) and

Francis (1995).

As komatiites are formed from melts derived from the mantle, their chemical composition is mainly influenced by the mineralogical and chemical compositions of the mantle source, the characteristics of partial melting, the nature of the assimilation and fractional crystallization of the melt during its ascent and emplacement, and the characteristics of post-magmatic alteration processes (Fig. 1.2-1). The processes are treated here in detail only if they are essential for the formation and composition of magmatic sulphides.

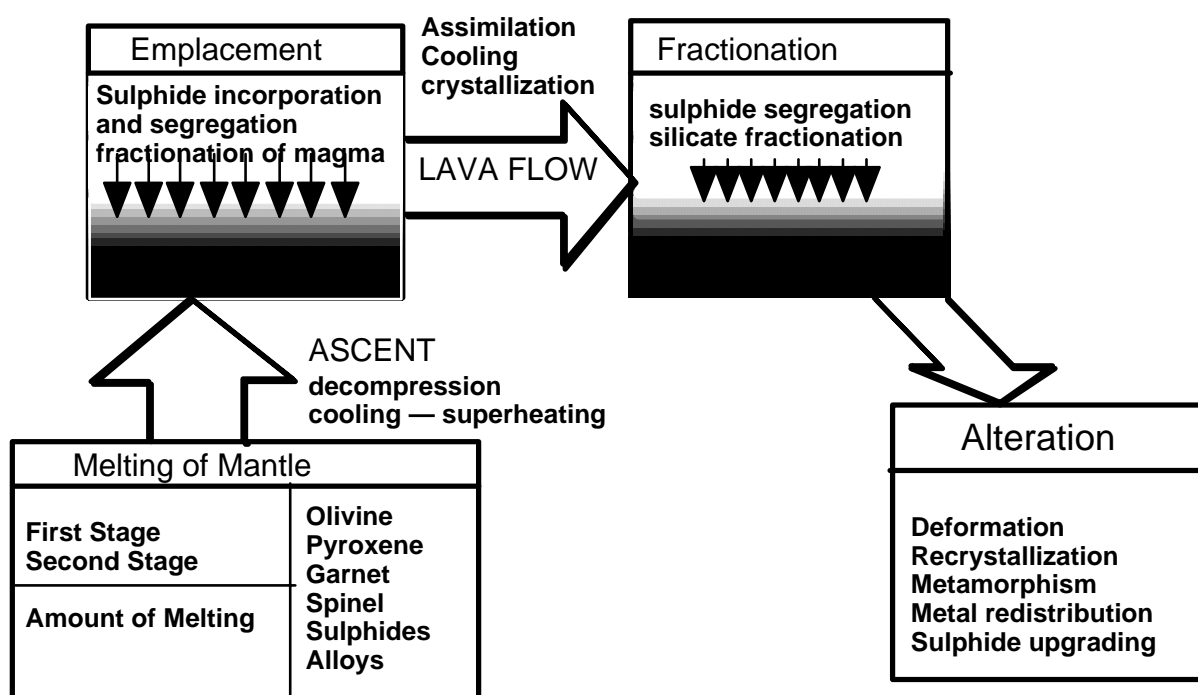


Fig. 1.2-1 Processes influencing the compositions of komatiites and associated Ni sulphides (modified from Naldrett 1969 and Lesher and Stone 1996)

3.2.1.2.1 Composition of source and magma type

The differences between major ultramafic and mafic extrusive magma types (Al-depleted and undepleted komatiites, picrites, ferropicrites and komatiitic basalts) can be attributed to differences in melting depths (e.g. Ohtani et al. 1989, Herzberg 1992) or the composition of the source (Barnes and Often 1990, Hanski 1992), or to the multiple melting and extraction processes of magma (Rigati and Wilson 1995, Lesher and Stone 1996).

3.2.1.2.1.1 Two-stage melting of the mantle

The formation of komatiitic melt requires two-stage melting of the mantle. In the first stage, the mantle is depleted in incompatible elements such as LREE, HFSE and LILE. As indicated, however, by the high PGE and Os of the second stage (Barnes et al. 1988, Walker et al. 1988), the degree of melting in the first stage was not high enough to consume all the sulphur available in the source area. The chalcophile elements (Ni, Co, Cu and PGE) were therefore partitioned in the source area and accumulated in the komatiite melt during the high-

grade melting of the second stage. In regional stratigraphy, these two stages of melting are reflected in the existence of tholeiitic basalts, e.g. the Lunnon basalt in the Kambalda area, at the substrate of komatiites.

3.2.1.2.1.2 Al-depleted and undepleted komatiites

The difference between Al-depleted and undepleted komatiites is attributed to the mineralogy of the mantle and, basically, to the depth of partial melting. The near-chondritic ratios of the refractory lithophile elements (Al, Ti, Ca, Zr, Y, Hf) of the Al-undepleted komatiites indicate that all phases of the source except olivine have been consumed. The high-pressure source area produces a melt depleted in aluminium. The Al-related elements incorporated in the residual majorite garnet and the melt are then typical of an Al-depleted komatiite melt.

3.2.1.2.1.3 Association of sulphides with different magma types

Despite the differences in ultramafic magma types, Leshner (1989), Leshner and Stone (1996) and Barnes and Often (1990) emphasize that the magmatic processes responsible for the variations in magma types are not crucial in the metallogenesis of magmatic sulphides because it is known empirically that Ni sulphides can be associated with magma types representing a wide range of source compositions, depths and degrees of partial melting. What is important in terms of Ni sulphides is that the first-stage of melting was small enough in volume to retain sulphides in the source area and that the second stage consumed all the sulphides in the source and became sulphide-unsaturated when erupting on the surface (Leshner and Stone 1996). Basalts heavily depleted in PGE (MORB as an example) indicate that they were sulphide saturated in the source area or that sulphides segregated during the ascent of the magma.

3.2.1.2.2 Ascent and emplacement of magma

3.2.1.2.2.1 Characteristics of komatiites

Komatiite eruptions were voluminous. The melt was formed by a high degree of partial melting at great depth and erupted at high temperature (up to 1650 °C). There was a long interval between the liquidus and solidus, and the magma had low viscosity (3-4 Pa's), thus forming large lava fields with channel flow, sheet flow and lava lobe facies (Leshner and Stone 1996, Hill et al. 1990). Lava channels and conduits continuously process the magma and collect the crystallizing liquidus phases. These are then marked by olivine ad- and mesocumulates, and locally by olivine-chromite cumulates, too. The cumulate type depends on the type of magma flow: crystallizing turbulent flows form ad- and mesocumulates, and laminar flows orthocumulates. Turbulent flows commonly mark the early stage of the flow facies, laminar flows the declining, late stage. The lava channels often form lava tubes separated from the overlying ocean by a thin roof. The magma may flow long distances in the lava tube without a marked decrease in temperature. Thin flows cool and crystallize more rapidly due to the large surface against the overlying seawater. Different textures develop, depending on the undercooling and nucleation ratios of the magma (Hill et al. 1990), resulting in typical fractionated flows with A and B layers of different olivine crystal textures in the ponded flows. Thick, large units are considered to represent proximal facies and small, thin ones distal facies (Hill et al. 1990). For the schematic distribution of different komatiite types in the lava field, see Fig 1.2.2.1.

3.2.1.2.2.2 Ni-sulphide ore potential of different komatiite types

The Ni-sulphide ore potential cannot be evaluated without an understanding of the physical volcanology and volcanic facies of komatiites. Ad- and mesocumulates of channelized sheet flows (Kambalda), lava channels (Mt Keith, Perseverance) and magma conduits (Thompson) are the host units for komatiite-associated Ni-sulphide deposits whereas thin sheet flows, lava lobes and sheet sill facies are barren (Lesher and Stone 1996).

3.2.1.2.3 Assimilation

3.2.1.2.3.1 Thermal erosion

Hot lava flows can erode the substrate thermally. Such erosion is well documented in the modern basaltic flows of Hawaii even if the composition of the substrate is about the same as that of the overflowing lava. Ancient komatiitic flows, with temperatures up to 400 °C higher than those of modern basaltic flows, can thermally erode the substrate more readily than can the basaltic flows (Huppert and Sparks 1985). In thermal erosion, the substrate is melted and either assimilated by the komatiite flow to form a homogeneous melt differing in chemical composition from the original material, or the remelted material remains in the komatiite magma as an immiscible melt. For example, felsic remelted material is not easily homogenized with ultramafic melt, and the ocelli structures in komatiitic sequences have been interpreted as droplets of immiscible felsic melt (Frost and Groves 1989). Assimilation and homogenization of considerable amounts of a silica-rich substrate, e.g. banded iron formation (BIF), may increase the concentrations of Si and Fe but leave those of trace elements little changed. The pyroxenitic flows observed in the basal parts of the Forresteria komatiite sequences, W. Australia, for instance, have been attributed to high silica assimilation (Perring et al. 1995).

Felsic/intermediate lavas and volcanoclastic rocks, cherty sediments and banded iron formations with sulphidic interlayers are favourable substrates for fertile ultramafic flows capable of causing thermal and mechanical erosion and deposition of massive nickeliferous sulphides (Hill 1997)

3.2.1.2.3.2 Indicators of assimilation

Assimilation is well indicated by the trace element spectrum of the flows. If the assimilated substrate is continental crust material or weathered continental crust, it is depleted in Nb, Ta and Ti relative to other incompatible elements, and contamination is indicated by increased Si content and La/Sm, La/Yb, and Zr/Y ratios and by decreased Nb/La and Nb/Zr ratios (Lesher and Stone 1996). In crustal contamination the major element pattern does not necessarily change much but the chondrite-normalized REE pattern of Al-undepleted komatiites changes from LREE depleted to non-depleted and probably even to LREE enriched. According to Lesher and Stone (1996), La/Sm, La/Yb, Zr/Y, Nb/La and Nb/Th exhibit the greatest geochemical contrasts in assimilation. LREE and LILE (Cs, Rb, U, Ba) enrichment is an indication of sedimentary rock assimilation whereas LREE and U can be introduced by fluids from hydrated basalts.

The main factor controlling contamination is physical volcanology. High-temperature komatiitic flows have low viscosity, turbulent flow and a long interval between the liquidus and solidus. The turbulently flowing lava transfers heat to the substrate effectively, especially in

channellized flows, and hence there is considerable melting of the substrate. As the surface of the flow is against seawater, the flow soon obtains a solidified chilled roof, which insulates it from the seawater and causes the lava to flow in a tube. Insulated lava flows with a chilled roof lose their heat capacity mainly by melting the substrate and can flow for long distances. The contaminated lavas are not necessarily found at or near the locality of contamination. In places, the sheeted flows flanking the channels are contaminated but the channels have been flushed and filled with uncontaminated lava or vice versa (Leshner and Arndt 1995; Leshner and Stone 1996).

As the contamination of crustal material has been considered the main factor in the sulphide saturation of magma, signatures of contamination in derivative magmas are positive indications of regional sulphide ore potential, even though the contaminated lavas may be far from the precipitated sulphides. The abundances of chalcophile elements in derivative magmas are mainly related to the segregation of sulphides, but the composition of the contaminant can also modify these abundances. The keys to understanding the type of contamination are therefore the local geology and the variance in substrates.

3.2.1.2.4 Segregation of sulphides

3.2.1.2.4.1 Supersaturation of a magma in sulphides

Supersaturation of a magma in sulphides segregates the sulphide phase to be enriched in chalcophile elements. Hot komatiitic magma dissolves considerable amounts of sulphur, and the sulphide saturation is a function of T, P, fO₂, fS₂ and the composition of the magma. The characteristics of the sulphide deposits are defined by the stage of supersaturation in relation to crystallization.

In a closed system, as in komatiites, magmatic sulphides may be saturated in the interstitial melt relatively late during the crystallization of olivine, resulting in sparse nickeliferous disseminated sulphides in olivine cumulates. The process generates disseminated sulphides in olivine mesocumulates, thus forming type-2 komatiite-related sulphide deposits (Mt Keith, Perseverance etc.).

3.2.1.2.4.2 Assimilation of massive sulphides

On the other hand, a komatiite flow can assimilate sulphides from the substrate sediments before olivine starts to crystallize, and the assimilated sulphide melt is not necessarily dissolved in the silicate melt. In a turbulent lava flow, the sulphide melt can effectively intermix with the silicate melt, and the chalcophile elements will enter sulphides, which will eventually accumulate as massive sulphides in suitable traps at the base of the lava flow. Large amounts of pristine silicate melt can flow over the sulphides and transfer more and more chalcophile elements into it. The result is a type-1 massive sulphide deposit at the basal part of the preferred lava pathway.

3.2.1.2.4.3 Numerical modelling

The segregation of magmatic, dissolved sulphides can be modelled as batch equilibration between sulphides and the crystallizing silicate magma. According to Campbell and Naldrett (1979), the abundances of trace elements in silicate magma are defined by the equation $C_L = C_o(R+1) / (R+D)$, where C_o = the concentration of the element in the initial magma, C_L = the

concentration of the element in the derived magma, D = the sulphide/silicate-melt partition coefficient for the element and R = the magma:sulphide mass ratio. As the D values of chalcophile elements range in the order $\text{Co} < \text{Ni} < \text{Cu} \ll \text{PGE}$, the elements with a high D value (PGE) become depleted at higher R factors than do those with a relatively low D value (Co, Ni).

In disseminated sulphides (type-2 deposits), the R factor will be high if the sparse sulphides have an opportunity to equilibrate with a large amount of magma before olivine is crystallized, and consequently the abundances of chalcophile metals in sulphides are high. Basically, the dynamics of the magma and associated sulphides define the amount of silicate magma in equilibrium with the segregated sulphides and thus also the R factor mentioned above.

The sulphides of type-1 deposits (massive sulphides at the base of the lava flow) can also have a high value of the R factor if large amounts of magma flow over the trapped sulphides, and chalcophile metals enter them. The process, called zone refining (Leshner and Stone 1996) has an effect on sulphide composition if the magma is superheated, is not crystallizing and can react with the sulphides in a turbulent flow.

3.2.1.2.4.4 Effect of dynamic volcanology on indicators

The depletion of komatiitic lavas and derived rocks in nickel and other chalcophile elements has only regionally significant exploration potential. If the Ni-depleted parts of komatiitic volcanic systems can be detected (olivine compositions and Ni-MgO diagrams are useful tools), Ni sulphides probably exist in the system; however, the exact location of the sulphides is still not known.

The segregation and accumulation of massive sulphides need a trap in the flow, either a topographic low or a locality where the turbulent flow slowed down to become laminar, and the sulphides separated and settled.

Detailed field mapping, interpretations of dynamic volcanology and knowledge of the stratigraphy of komatiites are key factors in efforts to pinpoint targets with potential for Ni sulphides

3.2.1.2.5 Effects of pressure, submarine alteration and metamorphism

3.2.1.2.5.1 Water depth

Eruptions of Archaean komatiitic lavas were submarine, either deep or shallow marine. Archaean subaerial komatiites are rare, but pyroclastic explosive komatiitic lavas occur in the Proterozoic Central Lapland Volcanic Belt (Saverikko 1985, Barnes and Often 1990, Lehtonen et al. 1992).

A high confining pressure during eruption is important for the stability of sulphides because, at low pressure, sulphur — an essential component of sulphides — becomes volatile and disappears from the system. In a deep oceanic environment, hydrostatic pressure prevents volatility. We lack reliable indicators of water depth: one such could be the vesicular lavas common in subaerial and shallow water environments. The vesicles are often formed by low-pressure volatilization of H_2O , which is soluble at high pressures in the basic melt, but they

can also be formed by CO₂, which has very low solubility in basic melts and can already form vesicles at high pressures and a great depth of water. The most reliable basis on which to estimate water depth is the stratigraphic sequence. A lack of tidal and continental margin sediments in the sequence and the existence of pillow basalts with only a limited amount of pyroclastic material could be indicative of deep water basins. High-energy, coarse clastic sediments at the substrate of komatiites might indicate rapid deepening of the basin. A volcanic environment with coeval or underlying felsic volcanism might be a favourable feature because felsic volcanism is often accompanied by sulphidic precipitates, which are considered important for komatiite-related Ni deposits (Leshner and Stone 1996, Hill 1997).

3.2.1.2.5.2 Post-eruptive hydrothermal alteration

Submarine ultramafic volcanics undergo hydrothermal alteration shortly after their eruption. Serpentinization of olivine and progressive carbonization of serpentinites result in zoned bodies of dunites-serpentinites and talc-carbonate rocks. The progress of hydrothermal alteration is well documented by Barnes et al. (1988). Serpentinization of the dunite containing disseminated sulphides can upgrade sulphides partly because the nickel in olivine cannot enter serpentine and will be incorporated in the sulphides and partly because the iron of sulphides will be oxidized and the sulphide mineral composition will become-rich (pentlandite-millerite-heazlewoodite instead of primary pentlandite-pyrrhotite). Serpentinization is accompanied by deposition of secondary magnetite, and serpentinites are commonly highly magnetic rocks, whereas carbonization of magnetite-bearing serpentinite results in the disappearance of magnetite, and carbonated ultramafics display low values of magnetic susceptibility. The alteration can thus be followed with geophysical, mainly magnetic, parameters.

An interesting feature in terms of hydrothermal alteration is the existence of interlayer sediments between the komatiitic flows. These sediments are often chemosediments with precipitates of chert and iron oxides/sulphides or they are Na-rich quartz-albite rocks. In some areas, massive base metal sulphides have accumulated in the interlayer sediments, forming VMS-type deposits stratigraphically above the komatiitic flows. In that case, the thick komatiitic flow might act as the heat reservoir necessary for the formation of hydrothermal precipitates and ore deposits. It is also important to consider the post-depositional heat effect of ultramafic flows, the thick cumulate flows in particular, and to chart all the possible effects of hydrothermal alteration and deposits related to komatiite sequences.

3.2.2 Mineralogy of komatiites and related Ni sulphide deposits

3.2.2.1 Mineralogy

Olivine is the first mineral to crystallize from komatiitic magma and the solidified lavas are composed of glass formed from the melt and olivine ± chromite and pyroxene phenocrysts. The crystallized minerals settle or grow at the base of the flow to form a cumulus layer, and if the lava is ponded, the melt-rich part of the flow can crystallize rapidly in closed system to form the A-layer of a fractionated flow. Undercooling of the magma, nucleation of crystals and their growth rate are the factors to define the shape and form of the crystals in rapidly cooling magma. In typical A layer of fractionated flow the shapes of spinifex crystals vary regularly downwards from the flow top. During the rapid crystallization of the spinifex-layer the residual magma is developing and different minerals come to liquidus in the order of fractional crystallization and the final minerals to crystallize are plagioclase and biotite. Cumu-

lates constitute of olivine, chromite and pyroxene, that crystallized from the magma, and intercumulus minerals that crystallized from trapped intercumulus liquid. Poikilitic crystals are common in cumulates and their crystallization is related to growth rate and nucleation of the minerals. Poikilitic clinopyroxene is common in olivine cumulates where the nucleation of cpx has been low compared with the rate of crystal growth and also poikilitic chromite can crystallize in similar way in komatiitic cumulate.

Chemical compositions of ferromagnesian minerals reflect the composition of magma and because $K_{\text{MgOl/magma}} > 1$, the Fo-content of crystallizing olivine is an indicator of Mg content of magma. In crystallization of intercumulus melt the olivine reacts with the melt and become less forsteritic during the reaction. Nickel partitions in olivine and the Ni tenor of olivine reflects the composition of the primary magma.

Very seldom the primary igneous minerals are preserved in komatiites because they have been altered in serpentinization and talc-carbonate alteration. In the alteration process the elements redistribute between metamorphic minerals and the T, P and pH-Eh conditions of the fluid phase define the minerals that are stable in alteration.

3.2.2.2 Mineralogical indicators of sulphides

Olivine has been considered a good indicator of nickel depletion due to sulphides. The nickel depletion of olivine has, however, only regional significance for ore potential. For example, in the type-1 massive Ni sulphides, the magma in equilibrium with sulphides and depleted in nickel was flushed away and the cumulus olivine filling the preferred pathway was crystallized from a later, pristine magma, which probably did not "see" the sulphides at all. Only a thin cover of olivine crystals above the sulphide melt pool is in equilibrium with the sulphides and depleted in nickel whereas the olivines in the preferred lava pathway above the massive sulphides do not indicate sulphide saturation. The silicate magma in equilibrium with the sulphides crystallized far away from the trap retaining the sulphides.

Ni tenor of primary magmatic chromite can reflect the Ni content of magma. Groves et al. (1977, 1981) reported that Zn concentrations are high in chromites associated with sulphide-bearing komatiite flows, and hence high Zn chromites have been considered an indicator of sulphide saturation. In the crystallization of co-existing silicate and sulphide melts, Zn is partitioned into early crystallizing chromite more than in sulphides and hence high Zn in chromite indicates only a high tenor of Zn in the silicate magma, which might be a result of crustal (inter-flow sediment) contamination (Leshner and Groves 1984). A problem in the quantitative determination of Zn in chromite is the metamorphic exsolution zoning of chromite with Cr-rich cores and magnetite margins. As Zn favours normal spinel it becomes concentrated in chromite cores whereas the inverse spinel (magnetite) margins become depleted in Zn. The redistribution does not allow us to calculate the primary Zn content in magmatic chromite, and zoned chromites are not appropriate for the estimation of primary Zn tenors. Non-zoned chromites occur only in deposits of low-grade greenschist facies metamorphism and most of the amphibolite facies chromites are zoned.

3.2.3 Deposit model for komatiite-related Ni sulphides

The following Table (Table 1.2-1) lists the factors that are indicative of komatiite-related Ni-

sulphide deposits

Table 1.2-1: Factors indicative of komatiite-related Ni-sulphide deposits

1 Volcanic factors:

- 1.1 large volcanic province with (thick units of) ultramafic volcanics
- 1.2 channelling lavas
- 1.3 cumulate bodies that extend for long distances along the plunge but only moderately across the plunge (shape of lava channel)
- 1.4 thick poorly differentiated cumulate bodies: olivine meso- and adcumulates
- 1.5 MgO-rich volcanic units that have thermally eroded the (sulphidic) substrate
- 1.6 ultramafic volcanics containing xenoliths or xenomelts

2 Geochemical and mineralogical factors:

- 2.1 MgO-rich units
- 2.2 a province where some, but not all, ultramafic / mafic lavas/intrusions are depleted in Ni and PGE
- 2.3 ultramafics depleted or enriched in chalcophile elements
- 2.4 ultramafics contaminated relative to associated units (e.g. LREE)
- 2.5 Zn-rich chromites
- 2.6 olivines depleted in Ni

3 Structural factors:

- 3.1 structural culmination areas (favourable for the study of stratigraphic sequences, not necessarily potential for Ni sulphides)
- 3.2 vertical or subvertical layering (favourable for the study of stratigraphic sequences, not potential for Ni sulphides)
- 3.3 tectonic setting: environment of rifting during volcanism

4 Stratigraphic factors:

- 4.1 stratigraphic evolution of volcanics: full series of tholeiites-komatiites-high-Mg basalts indicate long-term evolution of volcanism and the high heat flow necessary for sulphides and abundant komatiites
- 4.2 substrate of komatiites: presence of felsic volcanics, sulphidic sediments and massive sulphides is favourable; interlayers of graphitic/sulphidic sediments
- 4.3 deep water environment of komatiite-related strata
- 4.4 coeval felsic/ultramafic volcanism (not potential, probably favourable)

5 Alteration factors

- 5.1 serpentinization and related reactions, which upgrade the sulphides by oxidizing iron in primary sulphides, resulting in high-Ni sulphide minerals in the assemblage
- 5.2 syn- and post-depositional hydrothermal activity, which can deposit chemosediment interlayers between komatiitic flows, but also the thermal effect of komatiitic flows, which can bring about VMS-type deposits upwards in the stratigraphic sequence
- 5.3 external hydrothermal fluids (granitic), which can alter the chemical and mineralogical compositions of the host rocks, affect the composition of sulphides and even form secondary (barren?) sulphides

3.2.4 Review on komatiite geology of the Fennoscandian Shield

3.2.4.1 Komatiite areas of the Shield

The deposit modelling of WP 1.2 was developed on the basis of literature and field data. Inductive deposit modelling required concentration of the work in the field study of komatiites. The collected data is presented in database and the geological observations, and interpretations relevant for Ni sulphide exploration were collected to regional review reports presented as appendices in this technical report (Appendices 6.1-6.6).

Komatiitic ultramafic volcanics are essential constituents of Archaean greenstone belts of the Fennoscandian Shield. Figure 4.1.1 (Plate 1.5) depicts the distribution of Archaean greenstone belts and also the belts where komatiites have been indicated. Unfortunately, only a few areas are described in relevant and available publications. Large areas of the Archaean bedrock of the Fennoscandian Shield were overprinted by Proterozoic deformation and alteration and the relatively high grade of Archaean metamorphism indicates that the present surface represents deep section of the Archaean crust. Hence the greenstones are only locally preserved well enough to allow detailed mapping in the scale suited to unravel the dynamic volcanology. The isotope datings of the Archaean greenstone belts mainly range from 2810 Ma to 2740 Ma, although somewhat older ages (up to 3000 Ma) have been reported for the Luoma Group of the Suomussalmi greenstone belt. In the Kuhmo greenstone belt the upper age limits derive from felsic volcanics and the younger from the mafic rocks. In the Kostamuksha greenstone belt Puchtel et al. (1997a) report older (Sm-Nd) age, 2843 ± 39 Ma, for Kostamuksha komatiites and basalts and somewhat younger age (U-Pb), 2795 ± 29 Ma for the rhyolites that intrude and overlie the mafic-ultramafic unit.

3.2.4.2 Archaean komatiites of NW Russia

The Archaean komatiites of NW Russia are described by Bogatikov (1988) and the relevant parts of the book were translated to English and included in the reports of this project (Appendix 6.1). Puchtel et al. (1997) list in their recent paper on the Karelian granitoid-greenstone terrain 16 greenstone belts that vary in size from small fragments in the granitoid area (Kostamuksha) to an areally extensive synform structure in the east (Shumozero-Kenozero belt). Kushev (1997) described briefly the Inari-Kola craton and Borisov et al. (1995) described the komatiites of the area. Because his article is not in common distribution, essential parts are referred in the report (Appendix 6.1). Exploitable mineral deposits of the Russian greenstone belts are Kostamuksha and Olenegorsk iron deposits and the Allarechen Ni deposit in the Kola peninsula.

3.2.4.3 Archaean komatiites of Finland

Detailed mapping has revealed komatiitic rocks in most of the archaean greenstone belts of Finland (Fig 4.1.1, Plate 1.5). Komatiites of Ilomantsi, Kovero-Mönni, Nunnanlahti, Tainiovaara, Tipasjärvi, Tuntsa and Ruossakero greenstone belts have been studied in other connections and this work includes example areas of the Kuhmo and Suomussalmi greenstone belts (Fig. 4.1.2, Plate 1.6; Appendices 6.2, 6.3 and 6.4) that have been mapped in detail with main emphasis in dynamic volcanology and geochemistry of komatiites.

3.2.4.4 *Proterozoic komatiites of Finland*

A major rift-related zone of supracrustal rocks extends through the Shield from Karasjok in Norway to north Lapland in Sweden, Central Lapland in Finland to Salla and further to the Vetreny Belt in southeast of the Shield. Igneous activity in the belt was long-lived starting about 2500 Ma ago with continental basalts in eastern Lapland (Lehtonen et al. 1998) and voluminous ultramafic volcanics of the Vindy Belt and continuing without major orogenic deformation together with the evolution of rift-related basin until the deposition of the volcanic formations of Kittilä Group dated to 2012 Ma (Lehtonen et al. 1998). In Central Lapland minor amounts of komatiites include in the Onkamo Group (Möykkelmä) low in the sequence but these komatiites are intensely contaminated thin layers of volcanic breccias. Komatiites appear again in the upward succession in the Savukoski Group, where Kummitsoiva, Sattasvaara, Peurasuvanto, Karasjok and Pulju are central areas of komatiite extrusions. Description of the komatiites of the Pulju area is included in the report (Appendix 6.5).

3.2.5 **Application of Ni-ore factors to the Kuhmo, Suomussalmi and Pulju Greenstone Belts**

The field study carried out in the Archaean Kuhmo and Suomussalmi Greenstone Belts (KGB and SGB) is presented in detailed geological descriptions and included in this report separately for the Siivikkovaara-Kellojärvi area (Appendix 6.2), the Arola area (Appendix 6.3), the Kiannanniemi area (Appendix 6.4) and the Proterozoic Pulju greenstone belt (Appendix 6.5). As the Siivikkovaara-Kellojärvi area was studied in the greatest detail (Fig. 5.1 and 5.2, Plates 1.7 and 1.8), the stratigraphy and rock descriptions of the other Archaean areas are compared with those of the Siivikko-Kellojärvi area. The Pulju area, as an intensely altered and deformed Proterozoic greenstone belt, is described and modelled separately.

By applying the conceptual Ni-ore model to the data presented in the descriptions, we can compile descriptive models for Ni-sulphide formation in different areas. A map of the komatiitic cumulate bodies in the southern part of the Archaean Tipasjärvi-Kuhmo-Suomussalmi greenstone belt is presented in Fig. 5.3.

3.2.5.1 *Volcanic factors of the Kuhmo and Suomussalmi greenstone belts*

3.2.5.1.1 *Volume of the volcanic province*

The greenstone belts of Tipasjärvi, Kuhmo and Suomussalmi together constitute the largest Archaean greenstone belt system in Finland. The different parts of the belt form a row, the breaks on the present surface indicating culminations of the initially continuous belt (Fig. 5.3). Stratigraphy and general evolution are similar along the belt (Figs 5.1.1.1 and 5.1.1.2-4). Ultramafic rocks are voluminous either as sheeted lava flows or as cumulate bodies. The Kellojärvi ultramafic complex is a layered komatiitic cumulate created by the outpouring of large volumes of komatiitic magma (Fig. 5.1.1.3); the Rytys and Kauniinvaara bodies of the Suomussalmi (Saarikylä) area are of similar origin (Fig. 5.1.1.5). The layered cumulates either formed at the surface as a large lava lake or they are sub-surface, subhorizontal magma conduits. High-Mg basalts, considered to be related to the komatiitic lavas, commonly overlie the komatiites. The proportion of komatiitic lavas and related high-Mg basalts varies from one part of the belt to another, in general being more abundant in the proximity of the large cumulate bodies.

3.2.5.1.2 *Types of komatiites*

The lavas are either fractionated flows with typical A and B layers or non-fractionated thin flows. The fractionated flows commonly occur in the basal parts of komatiitic lava sequences but are less abundant than the non-fractionated thin flows. Serpentinite bodies are hydrothermally altered and locally carbonated, poorly differentiated komatiitic meso- and orthocumulates. They represent the former preferred pathways of channellized komatiitic lavas (see the scheme in Fig. 5.1.1.5). The thin sheeted lava flows and lava lobes are not potential for sulphide Ni deposits, whereas the thick channellized flows (the serpentinite bodies) are.

3.2.5.1.3 *Form of cumulate bodies*

The dip of the layering in the KGB is in general subvertical, and thus often only cross-sections of the channellized flows are visible. The plunge of the primary channel may, however, deviate from the tectonic axial direction, causing the dimensions of the surface horizontal section of the body to vary. Drilling and careful interpretation of magnetic data can indicate the true direction of the primary channel. The local stratigraphy is indicative of the original way-up and the stratigraphic basal contact is the most potential site for massive sulphides.

3.2.5.1.4 *Poorly differentiated cumulate bodies*

The Kellojärvi cumulate body and the related cumulates at Suomussalmi are olivine ad- and mesocumulates. Only in the contact zones does the Kellojärvi cumulate body display compositional pyroxene/olivine layering, metapyroxenitic contact varieties and pyroxenitic xenoliths in the olivine mesocumulates, indicating an interaction of ultramafic melt with continental crustal material. The bulk of the ultramafic sequence is homogeneous metacumulate and we call it poorly differentiated because the fractionation sequence is not complete.

Early Proterozoic tholeiitic mafic fractionated dykes intersect the komatiitic cumulates, and only the geochemical signature can distinguish the pyroxenitic Proterozoic metacumulates from the komatiites.

Indications of the interaction of the poorly differentiated cumulates with the wall rocks (contamination, metapyroxenitic contact rocks crystallized from hybrid melts) have significant potential for disseminated Ni sulphides.

3.2.5.1.5 *Indications of thermal erosion*

The KGB is intensely deformed, and structural indications of thermal erosion cannot be discerned. The lowermost fractionated komatiitic lava flow of the Pahakangas sequence overlies a pyroxenitic unit, a few metres thick, interpreted as having been crystallized from a hybrid magma formed by thermal erosion of the underlying BIF. The overlying fractionated komatiitic flow is depleted in nickel and chromium and enriched in LREE. Another example of thermal erosion in the Pahakangas sequence is the granite-embedded "small serpentinite" with its strong crustal signature of (Nb/La)_N and (Nb/Th)_N ratios.

3.2.5.1.6 *Xenoliths or xenomelts*

The "small serpentinite" of Pahakangas includes a layer with granitic xenoliths. The xenoliths are embedded in a layer that roughly corresponds to the komatiitic lavas in composition and can be interpreted as the chilled roof of the underlying lower part of the channellized cumu-

late. The granitic fragments dropped from the wall of the channel onto the chilled lava. The upper part of the channel was filled with a lava flowing over the chilled basal part and it preserved the granitic xenoliths at the margin of the flows. The Kellojärvi cumulate complex contains numerous xenoliths of a pyroxenitic marginal rock variety, indicating erosion of the earlier cumulates; some of the xenoliths may be tholeiitic lava rock in composition. Rounded xenoliths of foliated tonalite have been met with in the Kelloperä serpentinite body (No. 7 in Fig. 5.3), southwest of Kellojärvi.

3.2.5.2 *Geochemical and mineralogical indicators of sulphide precipitation*

3.2.5.2.1 *MgO (and Ni) content of the lavas*

The chilled flow-top of massive, non-fractionated komatiitic lava at Siivikkovaara contains 25% MgO, 0.32% TiO₂, 7.18% Al₂O₃, 7.67% CaO, 0.38% Cr₂O₃ and 1100 ppm Ni (Ni/Cu > 20); accordingly, the thin, spinifex-textured "sills" of the lava complex contain 23% MgO, 0.32–0.49% TiO₂ 800–1000 ppm Ni and 0.25% Cr₂O₃. The calculated olivine composition was Fo_{86.9}. Compared with the calculated, most magnesian, olivine composition of the Kellojärvi complex (Fo_{92.2}, Ni 2800 ppm), the Siivikkovaara Ni tenors are too high for pure silicate melt, and more likely suggest the presence of cumulus olivine in the lavas analysed. The MgO and Ni of the pristine magmas were, however, high enough for the formation of high-quality Ni sulphides.

3.2.5.2.2 *Ni depletion*

The calculated DN_i values indicate Ni depletion in the lowermost fractionated lava flow of the Pahakangas sequence and, similarly, in the lower portion of the Pahakangas "small serpentinite". Ni tenors in the Kellojärvi cumulate vary slightly, but the variations are largest in the cumulates close to the margins. Ni values might be useful indicators of sulphide potential in the serpentinite bodies studied.

3.2.5.2.3 *Depletion in PGE and chalcophile elements*

The PGE determinations indicate the tenors of PGE typical for komatiites and related rocks and they do not show any depletion of the elements. The Cu and Co values may indicate chalcophile element depletion if the magma has been sulphide saturated. These are, however, low in the ultramafics, and metamorphic redistribution may have affected the results.

3.2.5.2.4 *Contamination*

Despite metamorphic mobility, the REE distribution pattern is a good indicator of contamination. Examples are numerous: the B layer of the lowermost fractionated komatiite flow and the pyroxenitic layer underlying the lowermost flow at Pahakangas both have a "mixed" REE pattern, as do also the "small serpentinite" of the Pahakangas sequence and the marginal pyroxenites of the Kellojärvi ultramafic complex. REE analyses can be applied to study the contamination of cumulate lenses of the channellized flows.

3.2.5.3 *Mineralogical indicators of sulphide precipitation*

3.2.5.3.1 *Chromites in the Kellojärvi and Pulju komatiitic cumulates*

Some chromites of the Kellojärvi complex display relatively high Zn, and low Ni and Co tenors, but all the chromites analysed are zoned due to metamorphic exsolution of chromite and

Cr magnetite and only their cores have high values. The original Zn tenors are thus difficult to establish, and Zn-rich chromite has only marginal significance as an indicator of contamination. A detailed study on Kellojärvi and Pulju chromites is presented in Appendix 6.6

3.2.5.3.2 Composition of olivines

All the olivines discovered in the Archaean ultramafics of the KGB are metamorphic, and none show the composition of the primary magma. Primary olivine compositions can be calculated from the total analyses of olivine cumulates; the depletion in Ni is reflected in the whole rock analyses. The calculated Ni values indicate the Ni depletion of olivine as mentioned above (2.2). Details of Ni depletion are discussed in Appendix 6.2.

3.2.5.4 Structural and tectonic setting

3.2.5.4.1 Structural culmination areas

Located between two convergent strike-slip fault zones, the area around Siivikkovaara and Kellojärvi is structurally a low-strain environment (Luukkonen 1991). The quartz diorite body south of Siivikkovaara is younger than the KGB and has risen up and pushed the overlying komatiitic layers into a subvertical position. The other parts of the KGB are intensely folded and faulted, and tectonic stress has imbricated the layers to such an extent that the stratigraphic and structural features are difficult to discern. Tipasjärvi, Kiannanniemi and Saarikylä are all relatively well-preserved areas and, in that respect, comparable to the Pahakangas-Siivikkovaara area.

3.2.5.4.2 Vertical or subvertical layering

In most areas, the layering is subvertical, only in some limited parts of the Kellojärvi cumulate complex and the Tipasjärvi komatiite sequence is it flat-lying. Knowledge of the orientation of the layering is important in geophysical interpretations.

3.2.5.4.3 Geotectonic setting

Several different interpretations of the geotectonic setting of the KGB have been presented. Our view supports Luukkonen's (1991) model of intracratonic rifting due to a mantle plume. The mafic-ultramafic sequence erupted in a (deep) sea environment, but the basin was a narrow rift valley. The basin topography limited the directions and distribution of volcanic flows. The interpretations are presented in the figures of Appendix 6.2.

3.2.5.5 Stratigraphic factors

3.2.5.5.1 Stratigraphic evolution of volcanics

The outcropping basal contacts of the komatiitic lavas are against tholeiitic basalts (Pahakangas tholeiite), which are submarine, pillow basalts interlayered with thin Algoma-type oxide and sulphide BIF. The BIF sequences are at their thickest in the Tipasjärvi area and at Siivikkovaara, where there are several in the tholeiitic sequence or at the contact of the felsic and mafic volcanic sequences. At Siivikkovaara, the komatiite basal contact is against sulphidic BIF. The overlying komatiites are depleted in Ni and show also other geochemical indications of wall-rock contamination.

The stratigraphic interpretation presented in Fig. 5.1.1.1 is based mainly on observations

made in the Siivikkovaara-Kellojärvi area, but it can well be applied to the entire KGB. The stratigraphic position of the coarse volcanoclastic sedimentary-volcanic rock (Ronkaperä member) was confirmed the uppermost unit of the sequence. The Siivikkovaara-Kellojärvi stratigraphy implies a full sequence of fertile volcanic evolution.

3.2.5.5.2 Felsic substrate

Local occurrences of felsic-intermediate-mafic calc-alkaline volcanics have been interpreted as the lowermost stratigraphic member of the KGB. The unit is well preserved in the Taivaljärvi area of the Tipasjärvi greenstone belt, at Ontojärvi and Vuosanka in the Kuhmo belt and in the Kiannanniemi-Saarikylä area of the SGB. At Tipasjärvi and Suomussalmi, the stratigraphy is well documented and the felsic units commonly show disseminated or even massive sulphides, locally also anomalously high values of Zn.

It is interesting to note that graphitic and felsic sedimentary interlayers of komatiites are rare in the Kuhmo greenstone belt. In fertile komatiite areas of the Kambalda field W. Australia and in Munro township, Canada, the komatiitic flows are interlayered with graphitic and sulphidic sediments. Assimilation of graphitic sedimentary material can reduce Eh of the ultramafic flows and, accordingly, increase the sulphur solubility of the melt (Boctor & Yoder 1983). This can be the case in the Ni deposits of the Kiannanniemi area, Suomussalmi, where Ni-Cu sulphides are related to sedimentary-volcanic association.

3.2.5.5.3 Indications of deep-water environment

Indications of a deep water environment in the type sequence of Siivikkovaara are the lack of textures of volcanic explosions, the small amount of amygdaloidal volcanics, the interlayering of pillow lavas of tholeiites with massive lavas suggestive of inflating major flows in which the pillows are indicators of the lava surfaces, and the abundance of BIF with local sulphide facies (the "Kiisumonttu" layer) types. The calc-alkaline felsic volcanics of the Tipasjärvi area imply a shallow water environment because the hydrothermal fluids related to volcanism were boiled off before they could reach the surface (Papunen et al. 1989) and the volcanics are of pyroclastic material, but the overlying sequence of mafic and ultramafic volcanics is probably of deep-water origin.

3.2.5.5.4 Coeval felsic/ultramafic volcanism

This criterion, although not crucial, is probably favourable with reference to the high-grade Silver Swan massive Ni sulphides of Western Australia. In the type section of the KGB, komatiites overlie tholeiitic Pahakangas-type basalts; direct indications of felsic-ultramafic contacts or coeval volcanism are rare. The felsic volcanics seldom crop out, however, even though they have been indicated by diamond drilling and geochemical sampling, and certain areas are potential for felsic volcanics / komatiite interaction.

3.2.5.6 Alteration factors

3.2.5.6.1 Serpentinization and related reactions

Serpentinization is a prominent feature of all the komatiitic cumulates of the KGB and SGB, but because there are no sulphides in the serpentinites, we cannot test the effect of serpentinization on the composition of the sulphides. Carbonation altered the ultramafics into talc-magnesite rocks in association with the disappearance of disseminated magnetite. Hence the

talca-magnesite rocks display low values of susceptibility.

3.2.5.6.2 Syn- and postdepositional hydrothermal activity

Interlayers of chemosediments are common only in tholeiitic basalts of the Pahakangas type. This feature must be taken into account if the lack of chemosediment interlayers in komatiites is a negative sign for sulphide deposition.

There are slight indications of VMS-type deposits in the felsic volcanic sequence underlying the mafic and ultramafic volcanics. Low-grade base-metal mineralization occurs in the Siivikkovaara area ("Piiraisen malmi") stratigraphically above the komatiitic lava sequence, but there is no direct correlation with a thick cumulate flow or komatiitic heat source.

The Arola Ni occurrence displays features that might be attributed to hydrothermal activity. If that is indeed the case, the heat source could be the large ultramafic cumulate body to the east and stratigraphically below the sulphide occurrence.

3.2.5.6.3 Metamorphic hydrothermal fluids

Metamorphic hydrothermal fluids circulated during deformation affected the geochemistry of the Pulju ultramafics and deposited barren iron sulphides in the serpentinites. The southern part of the KGB was a target of Proterozoic fluid activity, and chlorite-kyanite rocks deposited in the Proterozoic fracture zones (M. Pajunen, personal comm.). The effect of Proterozoic fluid activity on the chemical compositions or trace element spectrum of the ultramafic rocks of the KGB is not known in detail but Grauw et al. (1992) observed Proterozoic resetting of REE systematics of the Siivikkovaara ultramafic flows. Tuisku and Sivonen (1984) considered the youngest peak of recurrent metamorphism Proterozoic in age.

3.3 Task 3

3.3.1 Introduction

The Fe-Ni laterite deposits in Greece are mainly found in the Pelagonian and Sub-Pelagonian geotectonic zones (Plate 1.15), which extended into Albania and Yugoslavia, and are related to ophiolites of Upper Jurassic to Lower Cretaceous age.

These deposits have been affected by intense tectonism, which has created overthrusting, foliation, folding and faults. This has resulted in the transportation of the laterite bodies disrupting their continuity and in some cases mixing them with the underlying rocks. The multi-stage deposition of the Fe-Ni ores, the re-distribution of ore metals, the intense tectonism and the metamorphism, which have affected all the Ni-laterite deposits of Greece, have almost totally changed the initial mineralogical composition and textures of the ores. Any interpretation of the mechanism(s) and conditions of their genesis is very complicated. Apart from this typical laterite type in the Balkan peninsula, Ni-laterite deposits which exhibit some features of in situ laterites at their lowest part are found (Albantakis 1980; Valetton et al. 1987; Economou-Eliopoulos et al. 1996, 1997).

For the implementation of the objectives set in the workprogramme two areas have been se-

lected, the Lokris and Vermion (Plate 1.14), and six targets representing three different cases: (a) in situ Ni-laterite deposits, such as the Tsouka in Lokris (Plate 1.16.), and Profitis Ilias in Vermion (Plate 1.17); (b) transported Ni-laterite deposits, such as the Nissi and Kopais in Lokris (Plate 1.16) and Metallio in Vermion (Plate 1.17), and (c) bauxitic laterite deposits, such as the Nissi in Lokris (Plate 1.16).

3.3.2 Geology of the Pelagonian and Sub-Pelagonian geotectonic zones of Greece

3.3.2.1 Pelagonian geotectonic zone

The stratigraphic sequence of the Pelagonian Zone, exposed in the studied area (Profitis Ilias-Metallion) includes from bottom to top the following formations:

- Pelagonian marbles of Triassic to Jurassic age, overlain by meta-volcanosedimentary rocks, and schists
- Ophiolitic nappe, consisting of dismembered units of serpentized hartzburgites, dunites and opx-bearing dunites, hosting also the lateritic horizon
- Conglomerates and debris flows, containing mainly carbonate material
- Rudist-bearing limestones, and
- Flysch formation

The Pelagonian marbles comprise white to grey microcrystalline marbles with white silex nodules and cherty intercalations. Their lowest part consists of dolomitic marbles containing algae of Triassic age. During the Late Jurassic, an early tangential tectonic phase affected the marbles and created characteristic isoclinal and recumbent folds of long length, accompanied by flow schistosity. Towards the top, the carbonate sequence with silex phases passes gradually to calc-schists and brown meta-pelitic schists, containing quartz veins and passing in turn to chlorito-schists with lenses of metavolcanic rocks. These Middle Jurassic metasediments exhibit parallel bedding with the underlain marbles and actually are meta-volcanosedimentary material accumulated on the plunged Pelagonian continental margin.

The ophiolitic rocks of the area are tectonically emplaced during the Upper Jurassic. They are comprised of hartzburgites, dunites occasionally accompanied by chromite concentrations, and opx-bearing dunites carried along with serpentinitic masses, the base of which is mylonitized. They are partly superposed, laminated and dismembered units, the tectonic contact of which is traced by the presence of amphibolites and marbles in the form of lensoidal units. In the upper parts the ultramafic rocks develop intense lateritization phenomena, due to extensive uplift movements of the Pelagonian zone (simultaneous closing of the Pindos and Al-mopia oceans), during the whole Lower Cretaceous, leading to the formation of the Ni-laterite horizon having a maximum thickness of 10m. This horizon locally decreases and takes the form of lensoidal wedging out during the whole Lower Cretaceous due to erosional factors.

The conglomeratic limestones and the flow debris are genetically related to the endo- Turo-nian tectonic phases, which caused the uplift and weathering of extended parts of the Pelago-nian zone. The conglomeratic limestone formations are unconformably overlain the Ni-laterite horizon or the ultrabasic rocks through an argillaceous-pelitic formation. They are developed in massive horizons of varying thickness. The clastic series are flow debris, which are graded

in micro-coarse-sandstone flyschoid rhythmic alternations, locally rich in brownish horizons with reworked lateritic material, poor in Ni content, and containing multiple alternations and beds of microbrecciated limestones.

On the dark colored clastic limestones, dark grey rudist-bearing limestones of Senonian age are developed overlain subsequently by grey limestones rich in organogenic fragments. Their upper members are developed to thin laminated light colored pelagic limestones with *Globotruncana* of Maestrichtian age.

The flysch formation at its base, is comprised of light grey thin bedded marly limestones with *Globotruncana* of Upper Maestrichtian. From an intense marly and siltstone formation it changes in the upper levels to sandstone and conglomeratic alternations rich in quartz pebbles and from material derived from the weathering of metamorphosed rocks of the basement of the Pelagonian zone.

The present structure of the Vermion area is the result of successive deformation caused during the tectonic emplacement of the ophiolitic nappe during the Upper Jurassic, the compressive tectonic phase of the Eocene which resulted the overthrust of the Almopias on the Pelagonian Zone, and the formation of extensive nappes affecting the visible thickness of the Pelagonian formations. The Late Jurassic compressive tectonic phase caused overthrust of the ophiolites as well as folding and metamorphism of the underlying Pelagonian carbonate formations. The ophiolites formed successive folded nappes with a N-S axis of folding, with amphibolitic rocks coming from the subophiolitic sole. Marble lenses from the underlying, metamorphic carbonate continental margin of Triassic-Jurassic age, were detached and carried with the ophiolitic masses.

Another compressive tectonic phase, of probably Eocene age, succeeding the flysch deposition, provoked the final overthrust of the Internal Zones on the External Zones, connected with the wide detachments of the serpentinites and the Cretaceous formations of the Pelagonian Zone and the N-S micro-and macro-folding structures. During the same tectonic phase the less plastic deformation suffered dextral and strike-slip faulting with an N-S or E-W direction.

After the compressive tectonism the area of Vermion was affected by normal faults, usually perpendicular to the dinaric direction (N-S), whereas the faulting tectonism activated previous tectonic episodes which formulate the present morphology of the area.

3.3.2.2 *Sub-Pelagonian geotectonic zone*

The main characteristic of this zone is the presence of ultrabasic complexes related to Ni-laterite ores. The Sub-Pelagonian zone, which extends into Albania and Yugoslavia, continues to the south along the main Greek territory with NW-SE direction.

The stratigraphic sequence of the zone from basement to top consists of:

- Paleozoic crystalline basement
- Upper Paleozoic semi-metamorphosed mainly clastic formations
- Lower - Middle Triassic formations (clastic formations, igneous rocks and limestone)
- Non metamorphosed limestone formations of Middle Triassic - Upper Jurassic

- Overt thrust large masses of ophiolite complexes, on the Upper Jurassic limestone, accompanied by deep sea sediments
- Transgressive Upper Cretaceous limestone
- Flysch formations, Neogene and Quaternary sediments.

Limestones, ultrabasic rocks of Tertiary and clastic sediments of Quaternary age are predominant in the study area (Plate 1.18). The Upper Jurassic limestones are the oldest sequence present in the area consisting of medium to thick-bedded oolitic limestones. On the top of this sequence the Fe-Ni ore occurs in the form of lenses or beds which are developed unconformably on their paleokarst surface. At the Tsouka area (Plate 1.16) the ore overlies the ultrabasic rocks which are mainly comprised of serpentinites. After a dryness period the sedimentation continued in the Sub-Pelagonian zone with the transgression of the Upper Cretaceous limestones on the mineralization parallel to its bedding. Flysch sediments and molasse of the Sub-Pelagonian Zone overlay the Upper Cretaceous limestones unit. The Quaternary lacustrine sediments of the Kopais basin and the slope debris belong to the recent sediments of the area.

The Lokris area has undergone intense tectonism and it is characterized by the formation of the tectonic graben of the Kopais basin. Large-scale foliation and intense fault tectonism mark the area south and southeast of the basin. The foliation has affected the original succession of the lithological units, resulting thus to the re-appearance and deposition of older stratigraphic units on recent ones. The meta alpine intense fault tectonism is represented by elongated and oblique faults. The dominant direction of the main faults is E-W and N-S.

3.3.3 In situ Ni-laterite deposits

3.3.3.1 Tsouka (Lokris, Sub-Pelagonian Zone)

The Tsouka Ni-laterite deposit (Plate 1.19 & 1.20) is developed on highly altered peridotite and it is characterized by a saprolite zone followed by a pelitic-pisolitic horizon, the upper part of which is comprised of material transported short or greater distance. Lower Cretaceous limestone layers alternating with Ni-laterite ore are conformably overlying the mineralized horizon (Valeton et al., 1987; Alevizos, 1997; Economou-Eliopoulos et al., 1997).

3.3.3.2 Profitis Ilias (Vermion, Pelagonian Zone)

Unweathered peridotite overlain by a saprolite zone is exposed in the area of Profitis Ilias, Vermion (Plate 1.17 & 1.19). The weathering crust is overlain by a highly silicified zone, which is transected by calcitic veinlets, while intense hematitization and silicification characterize its upper part. The Fe-Ni ore is 5-7 m thick, overlies this zone and at its lowest part is of pelitic and upgrades to pisolitic character. The Fe-Ni ore is mainly comprised of goethite, hematite, chlorite, quartz, calcite and chromite. Talc is a common mineral at the lowest part of the ore, while illite is dominant at its upper part.

3.3.4 Transported Ni-laterite deposits

3.3.4.1 Kopais deposit (Lokris, Sub-Pelagonian Zone)

The Kopais deposit (Plate 1.20 & 1.21) is developed on karstified limestones of Jurassic age underneath the Quaternary lacustrine sediments of the Kopais basin. These meta-Cretaceous sediments are comprised of marls and clays. The ore is extended in a zone of 600 m length, 500 m of width and has an average thickness of 20 m.

3.3.4.2 Metallio deposit (Vermion, Pelagonian Zone)

The ore shows all the characteristics of an heterochthonous formation, although it is developed on ultramafic rocks (Plate 1.17 & 1.19). The Fe-Ni ore lies on the serpentinite, which derives from serpentization of a pyroxene peridotite, without any transition zone present. It is a poor sedimentary iron ore siliceous at the base and its top with a clastic polymict ore, cemented by a mixture of clay minerals and Fe-oxides in the intermediate part. The thickness of the formation is 10-15m and it is poor in nickel and iron as well.

3.3.5 Bauxitic laterite deposits

3.3.5.1 Nissi (Lokris, Sub-Pelagonian Zone)

The Nissi deposits (Plate 1.16 & 1.20) lie on karstified Jurassic limestone and are conformably overlain by Lower Cretaceous limestone. The peculiarity of the Nissi deposits is that they may occur either as isolated typical Ni-laterite or bauxitic laterite ores or as an association of Fe-Ni ore at the lowest part of the deposit, followed by bauxitic laterite towards its upper part (Valeton et al., 1987; Economou-Eliopoulos et al., 1997). The Ni-laterite ore is mainly composed of goethite, hematite, chlorite, illite, quartz, calcite and chromite. In the bauxitic laterite apart from goethite, hematite and chromite (usually as very small fragments), boehmite, gibbsite and kaolinite are common minerals, whereas smectite and takovite are more abundant towards the lowest part of the deposit. A small amount of sulfides is also present in the laterite ore.

3.3.6 Mineralogy

A common feature of all Ni-laterite samples studied from the Tsouka, Kopais and Nissi deposits is their pisolitic-oolitic character (Plate 1.22). Pisolites in a variable proportion are consisting of hematite, goethite and fine inclusions of quartz, chlorite, and sometimes fragments of chromite. Usually pelitomorphous iron ore gradually upgrades to a pisolitic-oolitic ore, although they exhibit a small variation in their chemical proportion.

The groundmass is fine grained and it is composed of pelitic matrix and clastic grains of quartz, chromite and fragments of carbonate and chert material. Moreover, the pelitic matrix consists of fine-grained hematite aggregates, illite and chlorite. Beds of ore with pisolites as the main component are alternating with pisolite poor beds.

Fragments and various-sized spherulitic concentrations consisting of transparent material are joined with opaque mass of Fe-oxides as cementing material. Based on microprobe analyses the above transparent aggregates, are minerals of the group "chlorite-serpentine" with a high Ni proportion, about 12%. Using X-ray diffraction techniques, these Ni-minerals are deter-

mined as Nepouite $(\text{Ni,Mg})_3\text{Si}_2\text{O}_5(\text{OH})_4$ and Nimite $(\text{Ni,Mg,Al})_6(\text{SiAl})_4\text{O}_{10}(\text{OH})_8$. Metallic grains such as chromite and hematite are located into the internal part of these aggregates.

The mineralization at Profitis Ilias, overlain the saprolite zone, is divided in three parts from base to top:

- reddish altered peridotite
- massive Fe-Ni ore with clearly oriented structure
- upper part massive Fe-Ni ore with pisolitic-oolitic texture.

In the reddish altered peridotite zone, the cellular texture of the initial serpentinized peridotite is preserved, although presenting a high almost total silification (Plate 1.22). The initial cellules are filled with chalcedony, while the presence of abundant fragmented veinlets, consisting mainly of chalcedony and quartz, suggest a strong tectonic strain. The silification is a result of the ultrabasic rock alteration and should be not considered as a sedimentary offer of quartz material. The metallic minerals of the rock are hematite, goethite, limonite and residual grains of chromite.

The following metallic minerals are dominant in the massive Fe-Ni ore: hematite in grains and oriented lenticular concentrations (start of pisolite formation), goethite, Fe-hydroxides and residual dispersed grains of chromite. The gangue material is very few, represented by oriented quartz monocrystals, bearing at their periphery a garnierite ring (Plate 1.23). They are initial residual olivine islets transformed to quartz, while remained the serpentine crust, representing a part of the cellular texture of the initial ultrabasic rock. As confirmed by the micro-probe analysis, these rings are garnierite with a NiO percentage around 8%.

The upper part constitutes a massive Fe-Ni ore with pisolitic character. Small pisolites and ooid concentrations of hematite-goethite- Fe-hydroxides and gangue material show a slight orientation. Residual chromite grains are dispersed or enclosed into pisolites (Plate 1.23). The gangue material consists of sericite, garnierite, chalcedony and calcite.

Ni minerals defined in the Profitis Ilias Fe-Ni ore are: Nepouite $(\text{Ni,Mg})_3\text{Si}_2\text{O}_5(\text{OH})_4$, Nimite $(\text{Ni,Mg,Al})_6(\text{SiAl})_4\text{O}_{10}(\text{OH})_8$ and Willemseite $(\text{Ni,Mg})_3\text{Si}_4\text{O}_{10}(\text{OH})_2$.

3.3.7 Chemical composition of laterite ores

The average Ni content in the ultrabasic rocks of the studied areas is 0.23 wt% and it is significantly increasing in the alteration zones. The presence of Ni is also characteristic in all the deposits studied with values up to 6.23 wt% Ni. However, the Ni content shows large variations vertically and horizontally and there is a preference for its concentration in the upper and lower parts of the mineralization. Based on mineral chemistry analyses Ni is mainly related to phyllopyritic and iron minerals in Lokris, whereas in Vermion is related to the serpentinites (garnierite) and in lesser amounts to the micas (sericite).

The variation of the cobalt concentrations is similar to that of Ni since their behavior is similar and the ratio of Ni/Co is around 15. The cobalt content exhibits a wide range from 0.04-0.69 wt% Co with an average value of 0.07.

In the sedimentary ores the SiO₂ values represent a differentiation not only among the various ore types but also within the same ore type. The high SiO₂ content in some ore types is related mainly to the presence of clastic chert fragments. To the contrary the low SiO₂ values are related with ores having high iron or aluminum contents.

Although the iron content is the most important component of the Fe-Ni ores it shows a wide range of its content in the different ore types reaching a value of 78.9 wt% Fe₂O₃ in the Tsouka deposit. It also shows a negative correlation with aluminum and especially with SiO₂.

The aluminum content in the lateritic ores shows a significant variation ranging from 1.0 to 44.0 wt% Al₂O₃ in the Lokris area. More specifically in the Nissi deposit a high variation in the aluminum content is observed within the same orebody. The specific ore type represents a peculiarity since it is coexisting with bauxite ore. Very often aluminum horizons show significant nickel enrichment. The aluminum content and its variations in the Ni-laterites of the Vermion area are relatively low, ranging from 4.0 to 9.8 wt% Al₂O₃ with an average value 5.5.

The average manganese content in the Fe-Ni ores from Lokris is 0.3 wt% MnO. Its range in these ore types seems to be attributed to the presence of oxide minerals. However, the presence of asvolane horizons locally in the karst type ores is indicating that epigenetic processes have also affected the MnO distribution. Manganese content in the Fe-Ni ores from the Vermion deposits is higher, ranging from 0.4 to 1.1 wt% MnO, with an average value of 0.6.

The chromium content ranging from 0.4 to 5.9 wt% Cr₂O₃ in the Fe-Ni ores from the Lokris area and between 0.9 to 2.7 wt% Cr₂O₃ in the ores from the Vermion area is predominantly associated with Cr-spinnels and also in silicates. The chrome spinel is generally inherited from the ophiolitic peridotites. Thus, the Cr₂O₃ content in the residual chromite grains exhibits a wide variation in the deposits of the Nissi, ranging from 23.7 to 63.0 wt%. Cr₂O₃ content is reasonable since it is coming from the laterite weathering of ultramafic rocks, representing members of ophiolite complexes and/or different portions of ophiolitic slices, during the evolution of marginal basins. However, the range of this compositional variation is limited in the samples along the profile in Tsouka, ranging from 42.0 to 50.0 wt% Cr₂O₃, which is consistent with an in situ lateritization with a limited vertical reworking.

The rare earth element (REE) content in the Tsouka and Profitis Ilias deposits is very low (less than 10 ppm). In contrast, much higher is the REE content, some hundreds ppm, in both bauxitic- and Ni-laterite karst type deposits of Nissi (Plate 1.24). Finally, REE content reaches thousands ppm in samples from the contact between the lowest part of the bauxitic laterite and the footwall limestone at the Nissi deposits. A limited fractionation of the REE is exemplified by the ratio of La/Lu (representative of light and heavy REE) which is 40 for the Ni-laterites of Profitis Ilias and 58 for the laterites of Nissi. Only in samples from the contact between the lowest part of the bauxitic laterite of Nissi and the footwall limestone the La/Lu ratio reaches values more than 560 (Economou-Eliopoulos et al., 1997).

Thorium and uranium contents are generally low in the Ni-laterite ores. In contrast, in the bauxitic laterite of Nissi Th ranges from 5 to 25 ppm, and U from 7 to 66 ppm. In general, an increase of the Al content is accompanied by an increase in Ti, REE, Th and U contents

throughout the Nissi laterite deposits (Plate 1.25).

The platinum-group element (PGE) concentrations in the laterites are generally low. The lowest values were recorded in the saprolite zone and are lower compared to the bedrock and ultramafic rocks values in a regional scale (Economou-Eliopoulos, 1996). An enrichment in Pt (up to 48 ppb), Pd (7 ppb) and Au (16 ppb) was recorded in the reddish altered peridotite overlying the saprolite zone at Profitis Ilias. The highest PGE concentrations are found in the overlying Fe-Ni ore ranging as follows: 14 ppb Os, 32 ppb Ir, 66 ppb Ru, 20 ppb Rh, 86 ppb Pt and 186 ppb Pd (Plate 1.26). Gold content is low, less than 36 ppb. Although the PGE content is very low, it is higher than in typical bauxites (Laskou and Economou, 1989). Finally, in certain laterite samples the PGE content is higher than that in the majority of chromite ores (Economou-Eliopoulos 1996). Also, a preference of Pt over Pd content and an increase in the Pt/Pd ratio vertically in the studied laterites is apparent, although samples from the uppermost parts exhibit lower Pt, Pd contents.

3.3.8 Discussion

Generally, it has been accepted that ultramafic masses have undergone strong weathering, producing laterite covers, to an extent depending upon the climatic conditions and the topographic situation. The primary source of nickel is the forsteritic olivine, which typically contains 0.3 to 0.4 wt% Ni, as well as serpentinite. Elements may be strongly leached (Mg, Si, Ca), supergene enriched (Ni, Mn, Co, Zn, Y) or residually concentrated (Fe, Cr, Al, Ti). Various rock types may be highly weathered and developments of a saprolite zone overlain by a ferruginous zone seem to be common feature in several laterite deposits in the area. However, due to the great instability of olivine and serpentine during weathering the majority of thick weathering profiles are developed on peridotites (Golightly, 1981; Schellmann, 1989).

The mafic-ultramafic rocks in the Balkan peninsula are ophiolite complexes, which are found in a variety of tectonic settings; the most typical for the Balkan peninsula being marginal basins. During the Jurassic-Cretaceous the Alpine orogeny and the Sub-Pelagonian emergence resulted in the weathering of the ophiolitic rocks. During the continental stage which followed the emergence of the Lower Cretaceous the laterite deposits which had been formed were eroded and their erosion products were transported and re-deposited in new sites forming secondary sedimentary Fe-Ni deposits, in one or more stages.

Several questions arise with respect to the source and the conditions during the formation of the weathered crusts, the transportation and re-deposition of Ni-laterites, their diagenesis and the subsequent stage of the diagenesis. However, due to the presence of high porosity and strong fracturing, a downward leaching of metals is common.

In a comparison of the studied Ni-laterites of northern and central Greece it seems likely that there are some common features between the Tsouka and Profitis Ilias deposits in Greece. These features are: (a) they have serpentinized peridotite as bedrock, overlain by a saprolite zone (affected by intense tectonism, which in turn is overlain by a ferruginous zone, (b) low Al₂O₃, TiO₂ and REE contents, (c) low Pt, Pd and Au contents, but higher Pt and/or Pd contents than in bauxites and often higher than that in chromite ores, (d) a preference of Pt over Pd content and an increase in the Pt/Pd ratio upwards, through the laterite profile, while sam-

ples from the uppermost part exhibit lower Pt and Pd content (Economou-Eliopoulos et al, 1996, 1997). Furthermore, the composition of residual chromite grains or fragments through vertical laterite profiles from the above deposits indicate some differences as far as the composition of chromite itself or the range of the compositional variation (Eliopoulos and Economou-Eliopoulos, 1999).

The difference in the composition of chromite within each deposit (high-Cr or -Al) is probably related to the type of weathered ultramafic rock type, such as harzburgite, dunite, and opx-bearing dunite in the case of Profitis Ilias. Moreover, the homogeneous composition of chromite through vertical laterite profiles may be related to either homogeneous composition of the ultramafic parent rocks in a large regional scale or to in situ weathering followed by re-deposition of components at the upper parts by transportation within limited distance. Nevertheless, the wide variation in the composition of chromite grain-fragments in Ni-laterites is consistent with contribution of clastic and chemical material from various ultramafic rock types. These rock types are members of ophiolite complexes, as it is well exemplified by laterites lying on karstified limestones of Jurassic age Nissi 2 and bauxitic laterites Nissi 1 and 3. Thus, the comparison between the composition of chromite in the saprolite zone and the overlying Fe-Ni ore may provide valuable insights for the discrimination between Fe-Ni ore linked with in situ weathering and ore derived by transportation of clastic and chemical material (Eliopoulos and Economou-Eliopoulos, 1999).

Among the main factors controlling the concentration of rare earth elements (REE) in laterites are the composition of the source rock, the duration of the lateritization process, the size of the ore bodies, the distance of transportation, the pH and Eh conditions (Maksimovic and Panto, 1991). The REE element content is very low in the Profitis Ilias and Tsouka deposits with in situ or small degree of reworking, in contrast to karst type Ni-laterites and bauxitic laterites of Nissi. This REE distribution coupled with the wide compositional variation of chromite and the very small size of chromite fragments in the bauxitic laterites of Nissi, may indicate that the distance of transportation is probably a major controlling factor rather than the composition of the source rock. In addition, the REE, Al, Ti, Th and U content in the studied laterites their interelement positive relationship, and associations mostly with bauxitic laterites suggest similar conditions for their leaching, transport and deposition/ re-deposition.

Furthermore, the available data on laterites revealed enrichment in Pt (up to 86 ppb) and Pd (up to 186 ppb), much higher than that of typical chromitites related to ophiolites (less than 10 ppb). Osmium, Ir, Ru and Rh concentrations are also significant. Primary PGE mineralization in ophiolite complexes is mostly associated with chromite mineralization at the base of the cumulate series and/or the uppermost part of the mantle sequence, near the Moho or the magmatic sequence of ophiolites (Auge and Maurizot 1995; Economou-Eliopoulos 1996). It is well known that lateritic weathering strongly affects primary PGE mineralization, and leads to the dissolution and transport of PGE, resulted in the formation of new minerals, in particular as Pt-Fe oxides (Bowles, 1986; Auge and Legendre 1994. Bowles et al., 1995) indicated that possible mechanisms of solution, transport and precipitation, and organic compounds could provide a potential means of transport in solution during weathering. Fuchs and Rose (1974) have shown that Pd occurs in natural environment as more soluble than Pt. Thus, Pt and Pd can be taken into solution, leached from rocks under oxidizing conditions, and subsequently precipitated in a reducing environment, such as in sedimentary rich in organic matter (Bowles

et al., 1995).

Thus, the recorded low PGE content in the saprolite zone, the PGE enrichment in the overlying Fe-Ni ore, the preference of Pt over Pd concentration and an increase in the Pt/Pd ratio upwards through the studied laterite profile, may be related to the conditions during the lateritization process, (formation of the weathered crusts) during remobilization and re-deposition of components and their diagenesis. The re-deposition may have taken place in very short distance (Profitis Ilias) or long distance, such as the karst type deposits (Nissi), although they are found lying on peridotites. In addition the lower Pt, Pd content in samples from the uppermost parts of the laterite bodies may be related to strongly oxidized conditions resulted to high mobility of Pt and Pd, and a very restricted field of stability for Pt and Pd in natural environment. The importance of controls by organic compounds has been emphasized for leaching, transport and deposition of rare earth elements and Th, U and several other metals as well (Wood, 1996). Moreover, the PGE distribution and PGE-patterns, coupled with the common presence of sulfides, even in small amounts, may be related with reduced to weakly oxidized conditions during and after the diagenesis stage of the ore.

4. COMPARISON OF INITIALLY PLANNED ACTIVITIES AND WORK ACTUALLY ACCOMPLISHED

4.1 Task 1

The work in Task 1 was realised mainly as originally planned. Since the market price of nickel halved during the project and studied fertile intrusions were relatively small and of low grade; more effort than planned was put to develop generic tools applicable to world class nickel deposits, as well. As a result a computer program "Advanced Petrological Explorer" was developed and installable prototype was delivered to the GeoNickel partners, thought this kind of work and product were not literally included in the original project plan.

Resulting from above, the effort put on case studies of fertile and barren intrusions was slightly less than originally planned. However, the objectives in this area were achieved. Sophisticated techniques (stable and radiogenic isotopes, rare earth elements and trace element contents of minerals) were applied to find out the petrological differences between barren and fertile intrusions. Finally, simple and easy-to-use discrimination criterias were established. If this way created tools are not totally new, at least task 1 succeeded in sharpening some old tools. As a result determination of key figures (required for discrimination of barren and fertile intrusions) on the basis of litho-geochemistry and mineralogy is currently more reliable, faster and cheaper than it was when project started.

4.2 Task 2

The work was realized mainly as was planned originally. During the course of the work the detailed field data was observed pronounced in understanding the volcanic evolution and possible crustal contamination of the ultramafic and mafic magmas and the quality of the field data was hence emphasized. Detailed studies of the target areas allowed area-specific interpretations of the ore deposit models. Novel methods in GPS- and computer-aided mapping improved, facilitated and speeded up the laborious phase of the field work and very detailed information was obtained to support the area-specific deposit modelling. Geochemical data became more numerous than planned because identification and classification of mafic and ultramafic volcanics were impossible without comprehensive geochemical information. Geochemical data revealed unexpected Cr-rich basaltic lavas in the stratigraphic succession of the Kuhmo greenstone belt. Their origin and relation to komatiitic volcanism is the target of further study. The stratigraphic schemes allow to construct the volcano-sedimentary evolution of the Archaean and Proterozoic greenstone belts and form a firm basis to predict the geological units potential for Ni sulphides. The database can be applied for the testing of GEOSIS systematics.

4.3 Task 3

The objectives of WorkPackage 1, Task 3 were the development of models of ore forming processes in representative laterite deposits of Greece, in order to be used in the exploration of associated Ni ores in different geologic environments in Greece and elsewhere.

These models were established based on existing and new geological data acquired during the course of this project, mineralogical and litho-geochemical studies. Further, the ore forming process models were combined with geophysical and image processing data from the studied nickel deposits and their host environment, in order to develop integrated data processing methods for exploration of target selection.

The achieved objectives correspond to the stated ones. More specifically the following works were completed for both areas according to the planned activities:

- Update and modifications of two geological maps in 1:50,000 scale, which subsequently were digitized
- Production of eleven (11) geological maps in 1:5,000 scale, including geological cross-sections and stratigraphic columns. The above maps were also digitized
- A total of 520 samples from the different ore types and host rocks were analyzed for major oxides, Ni, Cr, and Co, and 85 selected samples were analyzed for PGE, Au, REE and trace elements
- Mineralogical studies made on 175 thin and polished sections for rock and ore characterization. X-Ray diffraction and X-Ray spectrometry made on 68 selected powder samples from boreholes, from the Lokris area, for mineral characterization and trace element detection. Finally microprobe analyses to determine minerals chemical composition and definition of Ni-bearing minerals in selected samples
- Digitization of all data obtained from the works described above
- Testing, validation and evaluation of the GEOES system.

5. CONCLUSIONS

5.1 Task 1

Task 1 succeeded in developing new tools for nickel sulphide exploration related to intrusions. A practical data processing and research tool called "Advanced Petrological Explorer" (APE) was created. APE is 32-bit windows program consisting of seven executables. Prototype released in the end of the project does not have any competitors on markets. Small markets, however, may hinder the program to become a saleable product.

Some novel Ni exploration tools were developed by case studies of nine selected intrusions. A major conclusion of the studies is, that contamination of black schist has triggered the ore formation process in studied ore hosting intrusions. Methods to identify favourable contamination were created. These include mineralogical investigations, isotope (C, S, Sm/Nd) studies and REE analyses. In studied geological environments orthopyroxene/clinopyroxene ratio may provide a direct measure on favourable (SiO₂ rich) contamination.

Positive identification on the sulfide saturation of magma can be done on the basis of sulphide content, olivine composition (calculated) and PGE level of intrusion. PGE depleted but Ni undepleted intrusions, which are relatively rich in sulphides - even in the layered series - are the most prospective ones. Effective concentration process of sulfides can take place in intrusions, which have been formed as a result of continued magma replenishment in an open system. These kind of intrusions do not contain cyclic units and repetitive olivine cumulate layers.

Determination of the key figures required for discriminating barren and fertile intrusions is – as a result of task 1 - more reliable, faster and cheaper than it was when project started.

5.2 Task 2

Mineable Ni deposits have not as yet been discovered in the KGB. The Ni occurrences studied - Hietaharju, Peura-aho and Arola - are associated with either cumulates of the preferred pathways of high-Mg basalts (Hietaharju and Peura-aho) or an intensely deformed zone characterized by the metamorphic and hydrothermal alteration of high Cr basalts (Arola); even there, however, the proximity of komatiitic volcanics is evident.

Stratigraphic sequences of komatiitic flows of KGB rarely include sulphidic and graphitic inter-layers. These seem to correlate with type 1 Ni deposits in fertile komatiite areas. Only the known Ni-Cu deposits of the Kiannanniemi area are related to graphitic and sulphidic sediments. A question not resolved as yet is the relationships of sulphidic/graphitic sedimentary interlayers with the great depth of the environment of volcanic eruptions that could be a positive

indication of favourable area. Accordingly, the areas where komatiitic ultramafic and felsic volcanics are interlayered are rare in KGB. This succession seems to be crucial for the formation of high-Ni massive sulphide deposits of Western Australia.

The indications of sulphide Ni deposits discussed above provide us with a positive model for sulphide Ni. The ore potential of the preferred lava pathways is indicated in Fig. 8 and their characteristics are listed in Table 1. They can be improved with the data to be collected in the course of more detailed follow-up work.

5.3 Task 3

Major and trace element geochemical data from the Fe-Ni deposits in Lokris and Vermion areas show Ni, Co, Fe, and Cr contents which are indicating origin from ultrabasic rocks. The presence of significant aluminum content in some karst type ores in Lokris is most probable to be attributed to the basic rocks of the ophiolite complex. The mineralogical relationship of the sedimentary ores with the laterites, which is especially supported by the presence of phyllopyritic minerals containing significant amounts of nickel, is also a strong supportive argument for their origin from ultrabasic rocks.

The very low Al_2O_3 , TiO_2 , and REE content are common features of the Fe-Ni ores of The Tsouka (Lokris) and Profitis Ilias (W. Vermion).

A preference of Pt over Pd and an increase in the Pt/Pd ratio upwards, through the lateritic profile, may indicate that during a subsequent stage of the diagenesis, and downward leaching of metals Pt is less mobile than Pd.

Assuming that Cr and Al content of chromite grain-fragments, within laterites represents primary compositions, the comparison between the composition of chromite in the saprolite zone and the overlain Fe-Ni ore may provide evidence for the discrimination between ore linked with the in situ weathering and those derived by transportation to some extent of clastic and chemical material.

The compositional variation of chromite in Ni-laterites and bauxitic laterites from Nissi (Lokris) suggests that major factors controlling their composition are both the parental rocks and the conditions during their transportation and precipitation of their components.

The geological environment of the Fe-Ni deposits in both studied areas, their mineralogical and geochemical data indicate a sedimentary formation either in situ or transported. It is considered that the formation of these deposits is mainly a seawater process that is affected directly or indirectly by the continent.

In the Lokris area, the Kopais and Tsouka deposits are typical Ni-laterites whereas the Nissi deposit is bauxitic laterite. The Kopais and Nissi deposits are of chemical and/or clastic sediments type, transported either short or greater distance from parent rock. The Tsouka deposit at its lower parts is comprised of in situ weathered material whereas its upper parts comprise transported material.

In the Vermion area, the Profitis Ilias and the Metallion deposits are typical Ni-laterites. More specifically the Profitis Ilias deposit comprises in situ weathered material whereas the Metallion deposit comprises transported material of clastic sediment type.

6. ACKNOWLEDGEMENTS

6.1 Task 1

We thank nickel exploration geologists and geophysicists of Outokumpu Mining Oy, specifically Leo Grundström, Tapio Karppanen, Risto Pietilä, Harry Rosenqvist, Jukka Jokela, Jochen Beck, Maria Montes, Aimo Hattula and Heikki Saarnio, for their important role in providing background information on case study targets as well as constructive co-operation for GeoNickel. Professor Heikki Papunen, Jarmo Lahtinen and Dr. Tapio Halkoaho were always ready for discussions and gave valuable support in solving petrological problems. Antti Roine and Kai Anttila helped in several practical questions on programming in Visual Basic environment. We appreciate the work of APE beta testers; among them Jukka Konnunaho and Jyrki Liimatainen deserve special thanks.

6.2 Task 2

We thank Dr. R.E.T. Hill of CSIRO, W.Australia, and the geologists of the Geological Survey of Finland, Dr. Erkki Luukkonen in particular, for fruitful and inspiring discussions and co-operation in different stages of the field work in the Kuhmo greenstone belt.

7. ANNEXES

7.1 List of publications, conference presentations and reports resulting from the project

7.1.1 Publications and conference presentations

Economou-Eliopoulos, M., Eliopoulos, D., and Laskou, M., 1996. Mineralogical and Geochemical Characteristics of Ni-laterites from Greece and Yugoslavia: Plate tectonic aspects of the Alpine metallogeny in the Carpatho-Balkan region. *In: Proceedings of the Annual Meeting of IGCP Project 356. Sofia, 1996, 2: 113-120.*

- Economou-Eliopoulos, M., Eliopoulos, D., Apostolikas, A. and Maglaras, K., 1997. Precious and rare earth element distribution in Ni-laterites from Lokris area, Central Greece. *In: H. Papunen (ed), Mineral Deposits, Research and Exploration. Where do they Meet. Balkema, Rotterdam, pp 411-414.*
- Eliopoulos, D.G., and Economou-Eliopoulos, M., 1999. Geochemical and Mineralogical features from Ni-laterite deposits, Vermion ophiolite complex, N. Greece. *Submitted for presentation in the SGA Meeting to be held in London, UK in August 1999.*
- T.Halkoaho, J.Liimatainen, H. Papunen & J. Välimaa 1997. Cr-rich basalts in komatiitic volcanic association of the Archaean Kuhmo greenstone belt, Finland: Evidence for reducing conditions during magma generation. *In: H.Papunen (editor) Mineral Deposits, Balkema, Rotterdam, p. 431-434.*
- Lamberg, P., 1997. Litogeokemian käyttö sulfidisten Ni-malmien etsinnässä. Presentation and abstract in Neljännet geokemian päivät, 12.-13.11. 1997 Kuopio. *In Lestinen, P. (ed.) Neljännet geokemian päivät, 12.-13.11. 1997 Kuopio. Laajat tiivistelmät, 35-39.*
- Liipo, J., Papunen, H., Kilpeläinen, T. and Lamberg, P. (1997) The Stormi ultramafic complex and associated Ni-Cu deposits. *Geological Survey of Finland, Guide 44,12-15.*
- Ylander, I., 1997: Rörmyrbergetin mafinen-ultramafinen Svekofenninen intruusio, Västerbotten, Ruotsi: petrografia ja rakenteellinen kehitys. (Petrography and evolution of the Svecofennian Rörmyrberget intrusion in Västerbotten, Sweden). *M. Sc. Thesis, University of Turku, 117 p. (in Finnish with English abstract).*

7.1.2 Reports

- S. J. Barnes, T. Halkoaho & H. Papunen 1998. Chromites of the Kellojärvi and Pulju komatiites. *Brite-EuRam BE-1117, GeoNickel, Turku University, Department of Geology, Technical Report 6.6, 7 p. 2 figs*
- T. Halkoaho & H. Papunen 1998. Geology and mineral deposits of the Arola area, Kuhmo. *Brite-EuRam BE-1117, GeoNickel, Task 1.2. Turku University, Department of Geology, Technical Report 6.3, 9 p. 9 figs.*
- T. Halkoaho & H.Papunen 1998. Geology and mineral deposits of the Kiannanniemi area, Suomussalmi. *Brite-EuRam BE-1117, GeoNickel, Task 1.2. Turku University, Department of Geology, Technical Report 6.4, 15 p. 8 figs.*
- Lamberg, P. and Augé, T., 1996: GeoNickel Task 1.1 of WorkPackage 1 (WP1) "Mineralogy and modeling of Ni deposits related to mafic and mafic intrusions". Updated and corrected version January 1995. *Report 96003-GAL-M. Outokumpu Research.*
- Lamberg, P., 1996: GeoNickel Task 1.1 of WorkPackage 1 (WP1) "Mineralogy and modeling of Ni deposits related to mafic and ultramafic intrusions" Applied to Ni exploration in

Råna intrusion. *Report 96021-GAL-M, Outokumpu Research.*

Lamberg, P., 1996: Preliminary results from the Bruvann samples collected for GeoNickel - interpretations for the Ni exploration purposes. *Report 96034-GAL-M, Outokumpu Research, 27. November 1996.*

Lamberg, P., 1997: Flowsheet of the data processing in discriminating Ni sulphide-potential intrusions from barren ones and locating Ni sulphide deposits within the intrusions or their surroundings. *Report 98020-ORC-T, Outokumpu Research, 28. January 1996.*

Lamberg, P., 1999: APE – Advanced Petrological Explorer. Manual. *Report Outokumpu Research, March 1999.*

Lamberg, P & Augé, T., 1999: Data collected on case study intrusions. *Report Outokumpu Research, March 1999.*

H. Papunen 1998. Technical Report 6.5: Geology and ultramafic rocks of the Paleoproterozoic Pulju Greenstone Belt, Western Lapland. *Brite-EuRam BE-1117, GeoNickel, Turku University, Department of Geology, Technical Report 6.5, 41 p. 23 figs, 6 tables*

H. Papunen, editor 1998. A review on komatiites in NW Russia. *Brite-EuRam BE-1117, GeoNickel, Turku University, Department of Geology, Technical Report 6.1,*

H. Papunen, T. Halkoaho, J. Liimatainen & T. Tulenheimo 1998. Komatiite geology of the Siivikkovaara and Kellojärvi areas of the Kuhmo greenstone belt. *Brite-EuRam BE-1117, GeoNickel, Task 1.2. Turku University, Department of Geology, Technical Report 6.2, 33 p. 23 figs, 3 tables*

7.2 Other project outputs

Advanced Petrological Explorer (APE) Windows 32-bit computer program. © *Outokumpu Research.* (Additional financing from Outokumpu Mining Oy.)

WP1.1 and 1.2 digital database in ACCESS format including 475 whole rock analyses, 900 mineral analyses. Digitized geological maps were delivered in MapInfo format.

8. REFERENCES

Albandakis, N.D., 1980. The nickel-bearing iron-ores in Greece. UNESCO, IGCP 169 Inter.Symp. Metallogeny of mafic and ultramafic complexes. 1: 194-213.

Alevizos, G., 1997. Mineralogy, geochemistry and origin of the sedimentary Fe-Ni ores of Lokris. Ph.D. Thesis, Technical University, Crete, 245 pp.

- Ariskin, A.A., Frenkel, M.Ya., Barmina G.S., Nielsen R., 1992: COMAGMAT: A FORTRAN program to model magma differentiation process. *Computers & Geosci.* 19, 8, 1155-1170.
- Arndt, N.T. and Nisbet, E.G., 1982: Komatiites: London, George Allen & Unwin, p. 526.
- Auge, Th. and Legendre O. 1994. Platinum-Group Element Oxides from the Pirigue Ophiolite Mineralization, New Caledonia: Origin and Significance. *Econ. Geology*, 89: 1454-1468
- Auge, Th., and Maurizot, P., 1995. Stratiform and alluvial platinum mineralization in the New Caledonia ophiolite complex. *Can. Mineral.*, 33 : 1023-1045.
- Ballhaus, C.G., 1988: Potholes of the Merensky Reef at Brakspruit shaft, Rustenburg Platinum Mines: primary disturbances in the magmatic stratigraphy. *Economic Geology* vol. 83 pp. 1140-1158.
- Barkov, A.Y. and Lednev, A.I., 1993: A rhenium-molybdenum-copper sulfide from the Lukalaisvaara layered intrusion, northern Karelia, Russia. *European Journal of Mineralogy* vol. 5, pp. 1227-1233.
- Barnes, S.J. (1985) Investigation of the potential of the Tverrfjell portion of the Råna intrusion for platinum group element mineralization. *NGU report 86.201*.
- Barnes, S.-J., 1989: Sulphide segregation history of Tverrfjell portion of the Råna Layered Intrusion. In: *Magmatic Sulphide – the Zimbabwe Volume*. M.D. Prendergast and M.J. Jones, Ed., pp. 107-116
- Barnes, S.-J., and Often, M. , 1990: Ti-rich komatiites from northern Norway. *Contrib. Mineral. Petrol.* 105: 42-54.
- Barnes, S.-J., Boyd, R., Korneliussen, A., Nilsson, L.-P., Often, M., Pedersen, R.B. & Robins, B. , 1988: The use of mantle normalization and metal ratios in discriminating between the effects of partial melting, crystal fractionation, and sulphide segregation on platinum-group elements, gold, nickel and copper: Examples from Norway. In: Prichard, H.M., Potts, P.J., Bowles, J.F.W & Cribbs, S.J. (eds.) *Geo-Platinum 87*: London, Elsevier, 113—143.
- Barnes, S.J., Hill, R.E.T. and Cole, M.J. , 1988: The Perseverance ultramafic complex, Western Australia: the product of a komatiite lava river. *J.Petrol.* 29: 305-331.
- Barnes, S.J., Hill, R.E.T. et al., 1988: The Perseverance ultramafic complex, Western Australia: product of a komatiite lava river. *J. Petrol* 29, 305-331.
- Bates, R.L and Jackons, J.A., eds, 1987: *Glossary of Geology*. American Geological Institute, Alexandria, Virginia, Third Edition.
- Beattie, P., Ford, C. and Russel, D., 1991: Partition coefficients for olivine-melt and orthopyroxene-melt systems. *Contrib. Mineral. Petrol.* 109, 212-224.
- Boctor, N.Z. & Yoder, H.S.Jr , 1983: Partitioning of nickel between silicate and iron sulfide melts. *Carnegie Institution Washington, Year Book* v. 82, 275—277.
- Bogatikov, O.A. (editor) , 1988: Early Precambrian komatiites and high-MgO volcanics of the Baltic Shield. Russian version: Nauka Press, Leningrad; English translation by Galina G. Gonchar, Turku, 1997, 66 p

- Borisova, V., Borisov, A. & Smolkin, V., 1995: Komatiitic associations of the Uraguba-Kolmozero-Voronya Archaean greenstone belt (Kola Peninsula). Geology of the Kola Peninsula (Baltic Shield), 9th Meeting of the Associations of European Geological Societies, Post-meeting Field trip 10-15 September, 1995. Russian Academy of Sciences, Kola Science Centre, Geological Institute. 3—23.
- Bowles, J.F.W., Gize, A.P., Vaughan, D.J., and Norris, S.J., 1995. Organic controls on platinum-group (PGE) solubility in soils: initial data. *Chron. Rech. Min.*, 520 : 65-73.
- Bowles, J.F.W., 1986. The development of Platinum-Group Minerals in Laterites. *Econ. Geol.*, 81: 1278-1285.
- Boyd R. (1980): Excursion Guide to the Råna Norite and the Bruvann Nickel Deposit. - Nickel Sulfide Field Conference 1980, *IGCP Project No.161 Sulfide Deposits in Mafic and Ultramafic Rocks*.
- Boyd R. (1980): Geologisk oversiktsrapport, Bruvannfeltet, Ballangen kommune, Nordland. Rånaundersøkelsene 1970-1979. - *NGU-rapport, Oslo, no. 1582A*,
- Boyd R. and Mathiesen C.O. (1979): The Nickel Mineralization of the Råna Mafic Intrusion, Norland, Norway. - *Can. Mineral.*, v. 17, p. 287-298.
- Boyd R., McDade J., Millard H.T.Jr. and Page N.J. (1987): Platinum metal geochemistry of the Bruvann nickel-copper deposit, Råna, North Norway. - *Norsk Geologisk Tidsskrift, Oslo*, v. 67, p. 205-213.
- Boyd, S. Barnes S.-J. & Grønlie A. (1988): Noble Metal Geochemistry of some Ni-Cu Deposits in the Sveconorwegian and Caledonian Orogens in Norway. - In: Prichard, H.M, Potts, P.J., Boules, J.F.W. and Gribb, S.J.(Ed.), *Geo-Platinum 87*. Elsevier Applied Science, London.. - , p. 145-158.
- Campbell, I. H., and Naldrett, A. J. , 1979: The influence of silicate:sulfide ratios on the geochemistry of magmatic sulfides. *Econ. Geol.* 74: 1503-1506.
- Chai, G. and Naldrett, A.J., 1992: The Jinchuan ultramafic intrusion: Cumulate of a high-Mg basaltic magma. *J. Petrology*, 33, 277-303.
- Cocherie, A., 1986: Systematic use of trace element distribution patterns in log-log diagrams for plutonic suites. *Geochim. et Cosmochim. Acta*, vol. 50, pp. 2517-2522.
- Coleman, M.L., 1977: Sulphur isotopes in petrology. *Jl geol. Soc. Lond.*, vol. 133, pp. 593-608.
- Deines, P., Harris, J.W. and Gurney, J.J., 1987: Carbon isotopic composition, nitrogen content and inclusion composition of diamonds from the Roberts Victor kimberlite, South Africa. *Geochim. Cosmochim. Acta*, vol. 51, pp. 1227-1243.
- Duke, J.M., 1979: Computer simulation of the fractionation of olivine and sulfide from mafic and ultramafic magmas. *Can. Mineral.*, 17, 507-514.
- Duke, J.M., Naldrett, A.J., 1978: A numerical model of the fractionation of olivine and molten sulfide from komatiite magma. *Earth Planet. Sci. Lett.*, 39, 255-266.
- Economou-Eliopoulos, M., 1996. Platinum-group element distribution in chromite ores from ophiolite complexes: implications for their exploration. *Ore Geol. Reviews*, 11: 363-381.

- Economou-Eliopoulos, M., Eliopoulos, D., and Laskou, M., 1996. Mineralogical and Geochemical Characteristics of Ni-laterites from Greece and Yugoslavia: Plate tectonic aspects of the Alpine metallogeny in the Carpatho-Balkan region. In: Proceedings of the annual meeting of IGCP project 356. Sofia, 1996, 2: 113-120.
- Economou-Eliopoulos, M., Eliopoulos, D., Apostolikas, A. and Maglaras, K., 1997. Precious and rare earth element distribution in Ni-laterites from Lokris area, Central Greece. In: H. Papunen (ed), Mineral Deposits, Research and Exploration. Where do they Meet. Balkema, Rotterdam, pp 411-414.
- Ekström, M, 1981: Mineralogisk undersökning av två borrhåll från Rörmyrberget. *Sveriges Geologiska AB, BRAP 81012*.
- Ekström, M. and Halenius, U., 1982: A new rhenium-rich sulfide from two Swedish localities. *N. Jb. Mineral. Mh*, vol. 1, pp. 6-10.
- Eliopoulos, D.G., and Economou-Eliopoulos, M., 1998. Mineralogical and geo-chemical constraints from representative Fe-Ni laterite deposits of Greece. *Chemical geology* (in press).
- Fouillac, A.M. and Javoy, M., 1988: Oxygen and hydrogen isotopes in the volcano-sedimentary complex of Huelva (Iberian Pyrite Belt): example of water circulation through a volcano-sedimentary sequence. *Earth and Planetary Science letters*, vol. 87 pp. 473-484.
- Francis, D. M. , 1995: The implications of picritic lavas for the mantle sources of terrestrial volcanism. *Lithos* 34: 89-105.
- Frost, K.M. and Groves, D.I. , 1989: Ocellar units at Kambalda: evidence for sediment assimilation by komatiite lavas. In Prendergast, M.D. & Jones, M.J. (eds) *Magmatic Sulfides - the Zimbabwe Volume*. London, Inst. Min. Metall.: 207-214.
- Fuchs, W.A. and Rose, A.W., 1974. The geochemical behavior of Pt and Pd in the weathering cycle in the Stillwater Complex, Montana. *Econ. Geol.*, 69: 332-346.
- Gaál, G., 1985: Nickel metallogeny related to tectonics. *Geol. Surv. Finland Bull.* 333, 143-155.
- Ghiorso M.S., 1993: MELTS: Software for the thermodynamic analysis of phase equilibria in magmatic systems. *GSA Abstracts with Programs* 25(6), A-96.
- Golightly, J.P., 1981. Nickeliferous Laterite Deposits. *Econ. Geol.*, 75th Anniv. Vol., 710-735.
- Groves, D.I., Barret, F.M. & Brotherton, R.H. , 1981: Exploration significance of chrome-spinels in mineralized ultramafic rocks and Ni-Cu ores. In: deVielliers, J.P.R & Gawthorn, G.A. (eds.) *ICAM 81: Proceedings of the 1st International Conference on Applied Mineralogy*, 7. Special Publication: Johannesburg, Geological Society of South Africa 21—30.
- Groves, D.I., Barret, F.M., Binns, R.A. & McQueen, K.G. , 1977: Spinel phases associated with metamorphosed volcanic-type iron-nickel sulfide ores from Western Australia. *Econ. Geology* 72, 1224—1244.
- Grundström, L., 1980: The Laukunkangas nickel-copper occurrence in Southeastern Finland

Bull. Geol. Soc. Finland, 52, 23-53.

- Grundström, L., 1985 The Laukunkangas nickel-copper deposit. *Geol. Surv. Finland Bull. 333, 240-256.*
- Hanski, E.J. , 1992: Petrology of the Pechenga ferropicrites and cogenetic, Ni-bearing gabbro-wehrlite intrusions, Kola Peninsula, Russia. Geological Survey of Finland, Bulletin 367, 192 p.
- Herzberg, C. , 1992: Depth and degree of melting of komatiites. *Journal of Geophysical Research 97: 4521-4540.*
- Hill, R.E.T. , 1997: Komatiite volcanology and associated nickel sulphide deposits. In Papunen H. (editor) *Mineral Deposits: Research and exploration — where do they meet?*, Balkema, Rotterdam, 3—6.
- Hill, R.E.T., Barnes, S.J., Gole, M.J. and Dowling, S.E. , 1990: The physical volcanology of komatiites in the Norseman - Wiluna belt , Western Australia. *Geol. Soc. Australia, Western Australia Division, Excursion Guide 1. 100 p.*
- Huhma, H., 1986: Sm-Nd, U-Pb and Pb-Pb isotopic evidence for the origin of the Early Proterozoic Svecokarelian crust in Finland. *Geological Survey of Finland, Bull. 337, 48 p.*
- Huppert, H.E. and Sparks, R.S.J. , 1985: Cooling and contamination of mafic and ultramafic magmas during ascent through continental crust. *Earth and Planetary Science Letters 74: 371-386.*
- Häkli, T.A. and Vormisto, K. 1985 The Vammala nickel deposit. In Papunen, H. and Gorbunov, G.I. (editors) *Nickel-copper deposits of the Baltic Shield and Scandinavian Caledonides. Geol. Surv. Finland Bull. 333, 273-286.*
- Häkli, T.A., Vormisto, K. and Hänninen, E. 1979 Vammala, a nickel deposit in layered ultramafite, southwest Finland. *Economic Geology, 74, 1166-1182.*
- Irvine, T.N., 1970: Crystallization sequences in the Muskox intrusion and other related intrusions. 1. Olivine-pyroxene-plagioclase relations. *Geol. Soc. S. Afr. Spec. Publ., 1, 441-476.*
- Kushev, V.G. , 1997: The Inari-Kola craton. In: M.J. de Wit and L.D. Ashwal, editors: *Tectonic evolution of greenstone belts. Elsevier, Amsterdam 707—709*
- Lamberg, P, 1990: Porrassniemen intruusio, sen rakenne ja petrologia – 1.9 Ga magmatismi ja Ni-malmit. *M. Sc. Thesis, University of Oulu, Department of Geology, 151 p.*
- Lamberg, P., Hautala, P. and Saavalainen, S., 1997: Mineralogical balances by dissolution methodology. *COM/IMA Short course on ore and environmental mineralogy. Modern Approaches to ore and environmental mineralogy. 8-10 September, 1997, Laboratório do IGM, S. Mamede de Infesta, Portugal.*
- Laskou, M., and Economou, M., 1989. Platinum-group element and gold concentrations in Greek bauxites. *Geologica Balkanica, 21 (2) : 65-77.*
- Lehtonen, M., Airo, M.-L., Eilu, P., Hanski, E., Korteialinen, V., Lanne, E., Manninen, T., Rastas, P., Räsänen, J. & Virransalo, P. , 1998: Kittilän vihreäkivialueen geologia, Lapin vulkaniittiprojektin raportti. *Geological Survey of Finland, Report of investigation 140. 1—144.*

- Lehtonen, M.I. Manninen, T. Rastas P. & Räsänen J. , 1992: On the early Proterozoic metavolcanic rocks in Finnish central Lapland. In: Balagansky, V.V & Mitrofanov, F.P. (eds.) Correlation of Precambrian formations of the Kola-Karelia region and Finland. Apatity, Russian Academy of Sciences, 65—85.
- Leshner, C.M. & Groves, D.I. , 1984: Geochemical and mineralogical criteria for the identification of mineralized komatiites in Archaean greenstone belts of Australia. *Petrology: Igneous and Metamorphic rocks*: Utrecht, VNU Science Press, 283—382
- Leshner, C.M. , 1989: Komatiite-associated nickel sulfide deposits. In Whitney, J.A. & Naldrett, A.J. (eds) *Ore Deposition Associated with Magmas*, 4. *Reviews in Economic Geology*: El Paso, Society of Economic Geologist: 45-101.
- Leshner, C.M. and Arndt, N.T. , 1995: REE and Nd isotope geochemistry, petrogenesis and volcanic evolution of contaminated komatiites at Kambalda, Western Australia. *Lithos* 34: 127-157.
- Leshner, C.M. and Stone, W.E. , 1996: Exploration geochemistry of komatiites. In Wyman, D.A. (ed.) *Igneous Trace Element Geochemistry Applications for Massive Sulphide Exploration*. Geological Association of Canada, Short Course Notes 12: 153-204.
- Li, C. and Naldrett, A.J., 1997: The Voisey's Bay Ni-Cu-Co deposit, Labrador; Canada: Variations of olivine composition related to multiple magma injections and sulfide segregation. In *Papunen, H., (ed) Mineral Deposits: Research and Exploration. Where do They Meet? Proceedings of the 4th Biennial SGA meeting, Turku/Finland, 11-13 August 1997, 461-462.*
- Lightfoot, P.C. & Keays, R.R. (1994) New approaches in targeting giant magmatic Ni-Cu-PGE deposits in Ontario. Short Course Notes, Laurentian University.
- Lindgren, W. , 1933: *Mineral Deposits*. McGraw-Hill Book Company, Inc. New York. 930 p.
- Luukkonen, E.J. , 1991: Late Archaean and early Proterozoic structural evolution in the Kuumo-Suomussalmi terrain, eastern Finland. Turun Yliopiston julkaisu. Annales Universitatis Turkuensis. sarja-Ser. A. II. Biologica-Geographica-Geologica 78.
- Maksimovic, Z., and Panto, G., 1991. Contribution to the geochemistry of the rare earth elements in the karst-type bauxite deposits of Yugoslavia and Greece. *Geoderma*, 51: 93-109.
- Marshall, B., and Mancini, F. 1994 Major- and minor-element mobilization, with implications for Ni-Cu-Fe- sulphide remobilization, during retrograde metasomatism at the Vammala Mine, southwest Finland. *Chemical Geology*, 116, 203-227.
- Masuda, A., 1975; Abundances of monoisotopic REE, consistent with the Leedey chondrite values. *Geochemical Journal*, vol. 9, pp. 183-184.
- Mitchell, R.H., Laflamme, J.H.G. and Cabri, L.J., 1989: Rhenium sulfide from the Coldwell complex, Northwestern Ontario, Canada. *Mineralogical Magazine*, vol. 53, pp. 635-637.
- Mountrakis, D., 1994. Introduction to the geology of Macedonia and Thrace. Aspects of the geotectonic evolution of the Hellenic Hinterland and Internal Hellenides. *Bull. of Geol. Soc. of Greece*, V. XXX/1: 31-46.
- Mäkinen, J. 1987 Geochemical characteristics of Svecokarelidic mafic-ultramafic intrusions

- associated with Ni-Cu occurrences in Finland. *Geol. Surv. Finland. Bull.* 342, 1-109.
- Mäkinen, J., 1987: Geochemical characteristics of Svecofennian mafic-ultramafic intrusions associated with Ni-Cu occurrences in Finland. *Geol. Surv. Finland Bull.*, 342, 1-109.
- Nakamura, N. and Masuda, A., 1973: Chondrites with peculiar rare-earth patterns. *Earth and Planetary Science Letters*, vol. 19, pp. 429-437.
- Naldrett, A. J., 1989: Magmatic sulfide deposits. *Oxford monographs on geology and geophysics no. 14*.
- Naldrett, A.J., Li, C. and Krstic, S., 1997: The Voisey's Bay Ni-Cu-Co deposit, Labrador, Canada: Implications for exploration elsewhere. In *Papunen, H., (ed) Mineral Deposits: Research and Exploration. Where do They Meet? Proceedings of the 4th Biennial SGA meeting, Turku/Finland, 11-13 August 1997, 9-10*.
- Nesbitt, R.W., Sun, S.-S. and Purvis, A.C. , 1979: Komatiites: geochemistry and genesis. *Can. Miner.* 17: 165-186.
- Nilsson, G., 1985: Nickel-copper deposits in Sweden *Geol. Surv. Finland Bull.* 333, 313-362.
- Nilsson, G., Ekstöm, M., Lundberg, B., and Åkerman, C., 1980: IGCP-project no. 161. Sulfide deposits in mafic and ultramafic rocks. Nickel sulfide field conference 1980, excursion guide, Sweden.
- Ohmoto, H., 1986: Stable Isotopes in High Temperature Geological Processes. Mineralogical Society of America: Reviews in Mineralogy, vol. 16, pp. 491-555.
- Ohtani, E., Kawabe, E., Moriyama, J., and Nagata, Y. , 1989: Partitioning of elements between majorite garnet and melt and implications for petrogenesis of komatiite. *Contrib. Mineral. Petrol.* 103: 263-269.
- Papunen, H. 1980 The Kylmäkoski nickel-copper deposit in southwestern Finland. *Bull. Geol. Soc. Finland* 52, 129-145.
- Papunen, H. Häkli, T.A. Idman, H., 1979: Geological, geochemical and mineralogical features of sulfide-bearing ultramafic rocks in Finland. *Can. Mineral.*, 1, 217-232.
- Papunen, H., Kopperoinen, T. & Tuokko, I. , 1989: The Taivaljärvi Ag-Zn deposit in the Archaean greenstone belt, eastern Finland. *Econ. Geol.* 85, 1262—1276.
- Pearson, D.G., Boyd, F.R., Haggerty, S.E., Pasteris, J.D., Field, S.W., Nixon, P.H. and Pokhilenko, N.P., 1994: The characterisation and origin of graphite in cratonic lithospheric mantle : a petrological carbon isotope and Raman spectroscopic study. *Contrib. Mineral. Petrol.*, vol. 115, pp. 449-466.
- Pearson, D.G., Davies, G.R., Nixon, P.H. and Matthey, D.P., 1991: A carbon isotope study of diamond facies pyroxenites from the Beni Bousera peridotite massif, N. Morocco. In : Nicolas A. Dupuy C., Menzies MA (Eds) Orogenic lherzolites and mantle processes. *J. Petrol. Spec. Issue*, pp. 175-189.
- Peltonen, P. 1995a Magma-country rock interaction and the genesis of Ni-Cu deposits in the Vammala Nickel Belt, SW Finland, *Mineralogy and Petrology*, 52, 1-24.
- Peltonen, P. 1995b Petrogenesis of ultramafic rocks in the Vammala Nickel Belt: Implications for crustal evolution of the early Proterozoic Svecofennian arc terrane. *Lithos*, 34,

253-274.

- Peltonen, P., 1995: Magma-country interaction and the genesis of Ni-Cu deposits in the Vammala Nickel Belt, SW Finland. *Mineralogy and Petrology*, vol. 52, pp. 1-24.
- Peltonen, P., Pakkanen, L. and Johansen, B., 1995: Re-Mo-Cu-Os sulphide from the Ekojoki Ni-Cu deposit, SW Finland. *Mineralogy and Petrology*, vol. 52, pp. 257-264
- Penttinen, U., Palosaari, V. and Siura, T. (1977) Selective dissolution and determination of sulphides in nickel ores by the bromine- methanol method. *Bull. Geol. Soc. Finland* 49(2), 79-84.
- Perring, C.S., Barnes, S.J., and Hill, R.E.T. , 1995: The physical volcanology of Archaean komatiite sequences from Forrestania, Southern Cross Province, Western Australia. *Lithos* 34: 189-207.
- Pineau, F. and Javoy, M., 1994: Strong degassing at ridge crests : the behaviour of dissolved carbon and water at 143n, mid-Atlantic ridge. *Earth and Planetary Science Letters*, vol. 123, pp. 179-198.
- Pineau, F., Javoy, M. and Kornprobst, J. 1987: Primary igneous graphite in ultramafic xenoliths : II. isotopic composition of the carbonaceous phases present in xenoliths and hosts lava at Tissemt (Eggéré, Algerian Sahara). *J. of petrology*, vol. 28, pp. 313-322.
- Puchtel, I.S., Hofmann, A.W., Jochum, K.P., Mezger, K., Shchipansky, A.A. & Samsonov, A.V. , 1997b: The Kostamuksha greenstone belt, NW Baltic Shield: remnant of a late Archaean oceanic plateau? *Terra Nova* 9: 87—90.
- Puchtel, I.S., Shchipansky, A.A., Samsonov, A.V. & Zhuravlev, D.Z. , 1997a: Greenstone belts of the Karelian gneiss-greenstone terrain, Baltic Shield. In M.J. deWit and L.D. Ashwal, editors: *Tectonic evolution of greenstone belts*. Elsevier, Amsterdam 699—706.
- Pushkar, P., McBirney A.R. and Kudo A.M., 1972: The isotopic composition of strontium in Central America ignimbrites. *Bull. Volc.*, vol. 35, pp. 265-294.
- Puusinen, K., Saltikoff, B. and Tontti, M., 1995: Distribution of metallogeneis types of nickel deposits in Finland. *Geological Survey of Finland, Report of Investigation 132*.
- Riganti, A., and Wilson, A.H. , 1995: Geochemistry of the mafic/ultramafic volcanic associations of the Nondweni greenstone belt: constraints on their petrogenesis. *Lithos* 34: 235-252.
- Roeder, P. L. and Emslie, R.F., 1970: Olivine-liquid equilibrium. *Contrib. Mineral. Petrlo* 29, 275-289.
- Roeder, P.L, 1994: Chromite: from the fiery rain of chondrules to the Kilauea Iki lava lake. *Can. Mineral.* 32, 729-746.
- Rollinson, H., 1993: *Using Geochemical Data: Evaluation, Presentation, Interpretation. Longmans Harlow, 352 p.*
- Ross, J.R. & Travis, G.A. , 1981: The nickel sulphide deposits of Western Australia in global perspective. *Econ. Geology* 76, 1291—1329.
- Saverikko, M. , 1985: The pyroclastic komatiite complex at Sattasvaara in northern Finland. *Bull. Geol.Soc. Finland* 57, 55—87.

- Schellmann, W., 1989. Composition and origin of lateritic nickel ore at Tagaung Taung, Burma. *Mineral. Deposita*, 24: 161-168.
- Schneiderhöhn, H. , 1941: Lehrbuch der Erzlagerstättenkunde. Gustav Fischer, Jena. 858 p.
- Shaw, D.M., 1970: Trace element fractionation during anatexis. *Geochim. et Cosmochim. Acta*, vol. 34, pp. 237-243.
- Sun, S.S. and McDonough, W.F., 1989: Chemical and isotopic systematics of oceanic basalts: implications for mantle composition and processes. In: Sanders and Norry (Ed), *Magma-tism in the Ocean Basins*. Blackwell, Oxford, pp. 313-345.
- Valeton, I., Biermann, M., Reche, R., and Rosenberg, F., 1987. Genesis of Ni-laterites and bauxites in Greece during the Jurassic and Cretaceous, and their relation to ultrabasic parent rocks. *Ore Geol. Reviews*, 2 : 359-404.
- Walker, R.J., Shirey, S.B. & Srecher, O. , 1988: Comparative Re-Os, Sm-Nd and Rb-Sr isotope and trace element systematics for Archaean komatiitic flows from Munro Township, Abitibi Belt, Ontario. *Erath and Planetary Science Letters*. 87, 1—12.
- Vesanto, J. and Katajarinne, T. 1984: Tutkimusraportti. Vammala, Ekojoensuu 2121 07. *Research Report 001/212107/JJV, TVK/1984, 1985, Outokumpu Oy, Exploration*.
- Viljoen, M.J., and Viljoen, R.P. , 1969: The geology and geochemistry of the lower ultramafic unit of the Onverwacht Group and a proposed new class of igneous rock. *Special Publication of the Geological Society of South Africa* 2: 221-244.
- Volborth, A. and Housley, R.M., 1984: A preliminary description of complex graphite, sulphide, arsenide and platinum-group element mineralisation in a pegmatoid pyroxenite of the Stillwater complex, Montana, U.S.A. *Tschermaks Min. Petr. Mitt.*, vol. 33, pp. 213-230.
- Wood, S.A., 1996. The role of humic substances in the transport and fixation of metals of economic interest (Au, Pt, Pd, U, V). *Ore Geol. Reviews*, 11: 1-31.
- Ylander, I., 1997: Rörmyrbergetin mafinen-ultramafinen Svekofenninen intruusio, Västerbotten, Ruotsi: petrografia ja rakenteellinen kehitys. (Petrography and evolution of the Svecofennian Rörmyrberget intrusion in Västerbotten, Sweden). *M. Sc. Thesis, University of Turku*, 117 p. (in Finnish with English abstract).
- Åkerman, C., 1981: Nickelmineraliseringarna i Rörmyrberget. *Sveriges Geologiska AB, BRAP 81011*.

PLATES

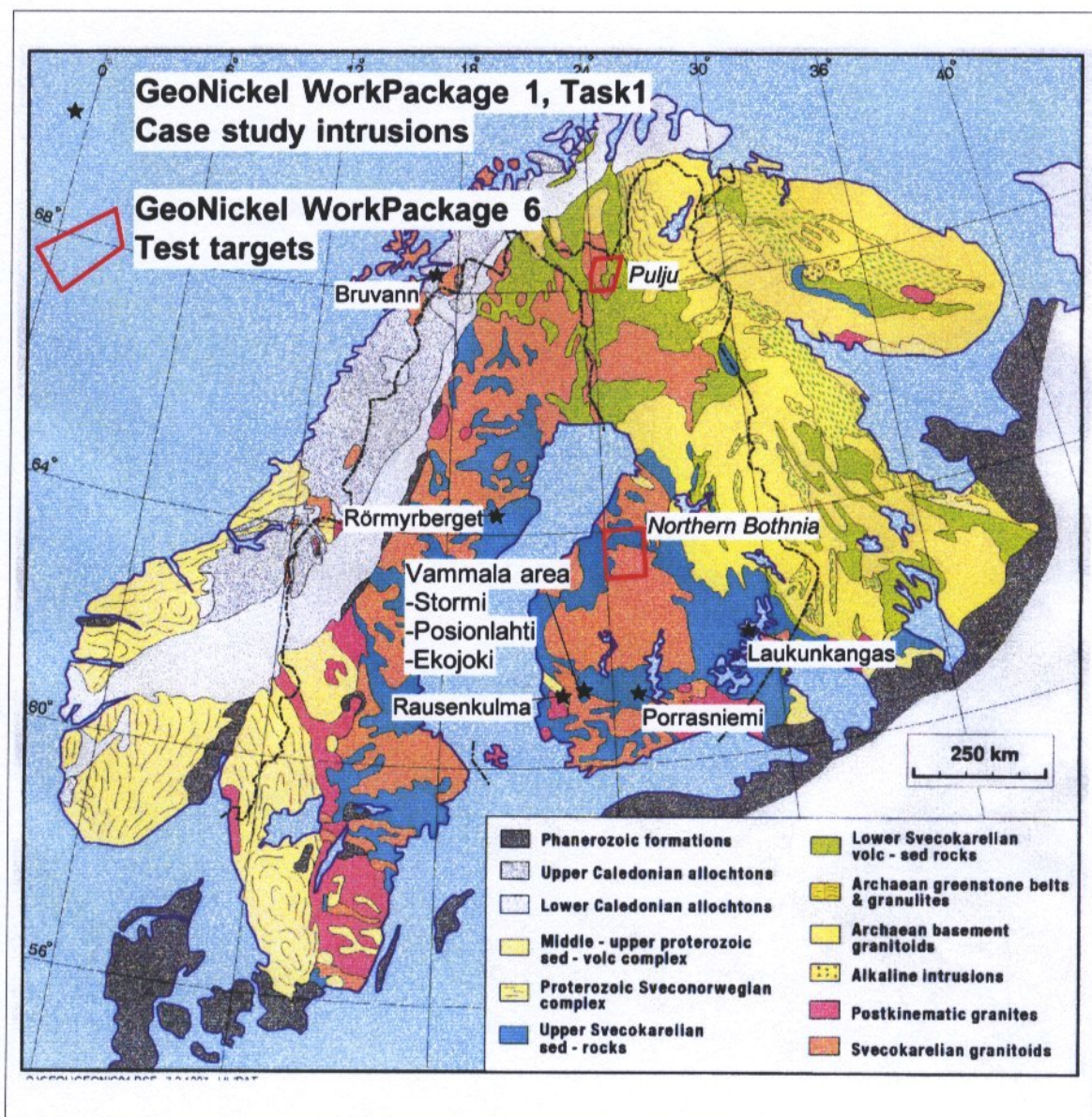


Plate 1.1. GeoNickel WorkPackage 1, Task 1 case study intrusions and WorkPackage 6 test targets on geological map of Baltic Shield.

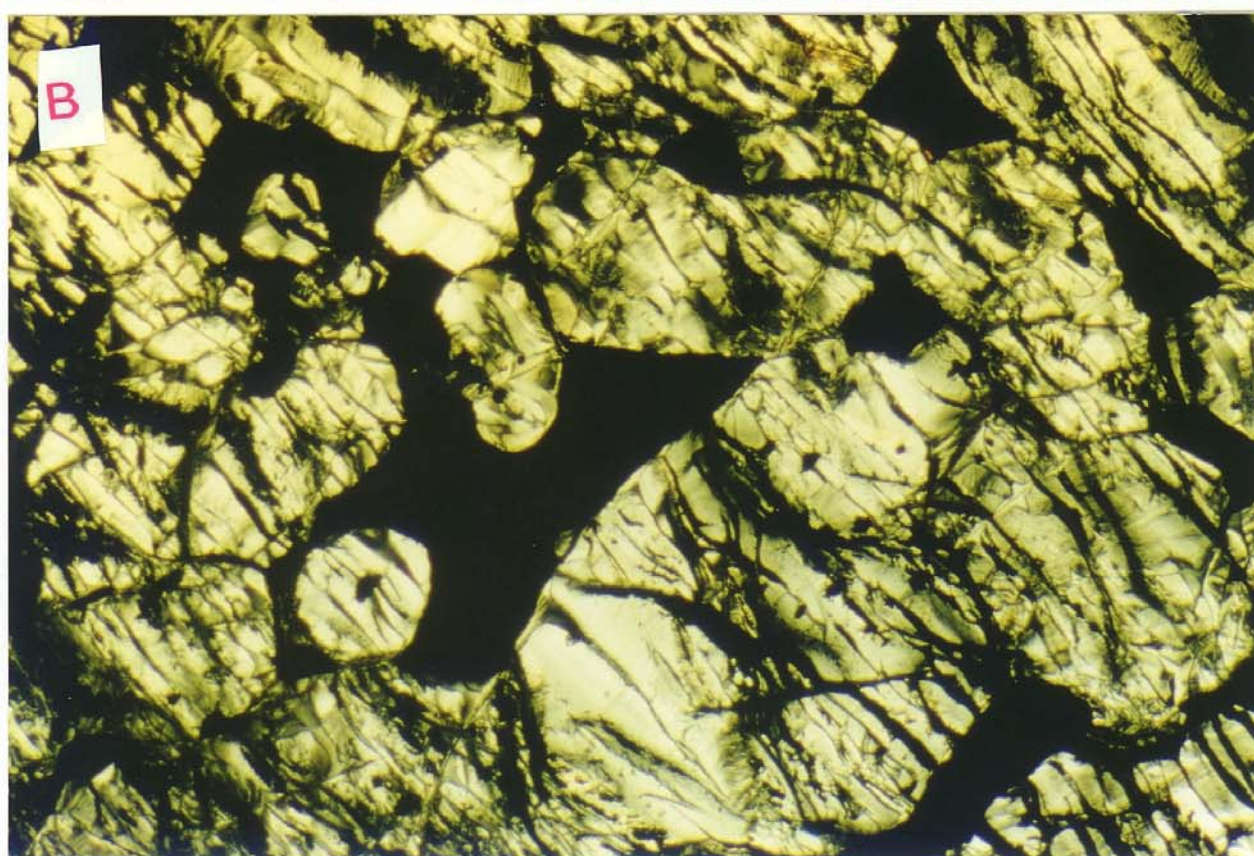
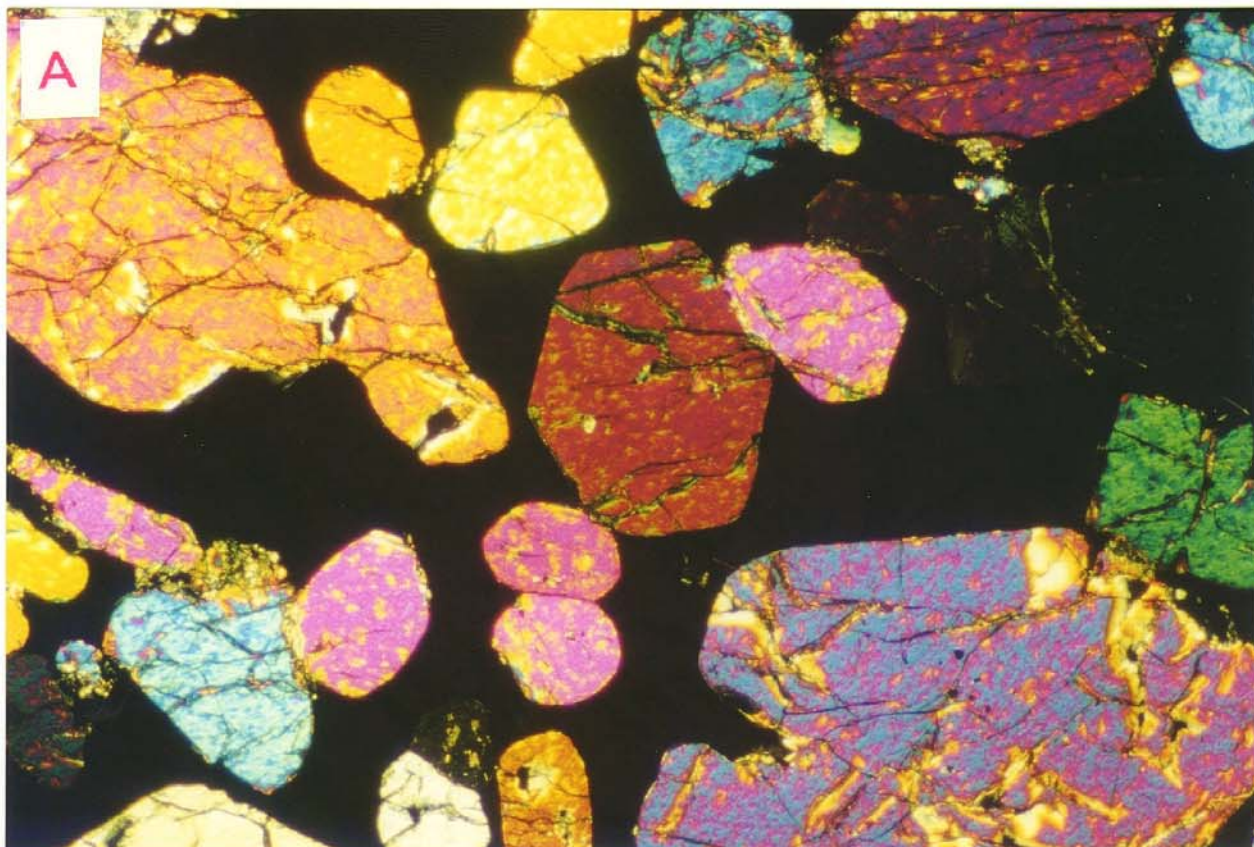
Plate 1.2 A-B. Microscope images illustrating alteration.

Plate 1.2. A and B. Two compositionally almost similar olivine cumulates. Sample above is practically fresh and sample below totally hydrated. A) Sample 9619465, Bruvann, drill hole 270-135/ 211.7-212.1 m. o\$MC, Ni=1.63%, Cu=0.285, \$=34.5% , MgO_n=39.27%. B) Sample 9619510, drill hole TY-183/226.05-226.55 m, o\$OC Ni=0.387%, Cu=0.094, \$=5.5%, MgO_n%=37.5%. Plane polarized light, crossed nicols, magnification 35x.

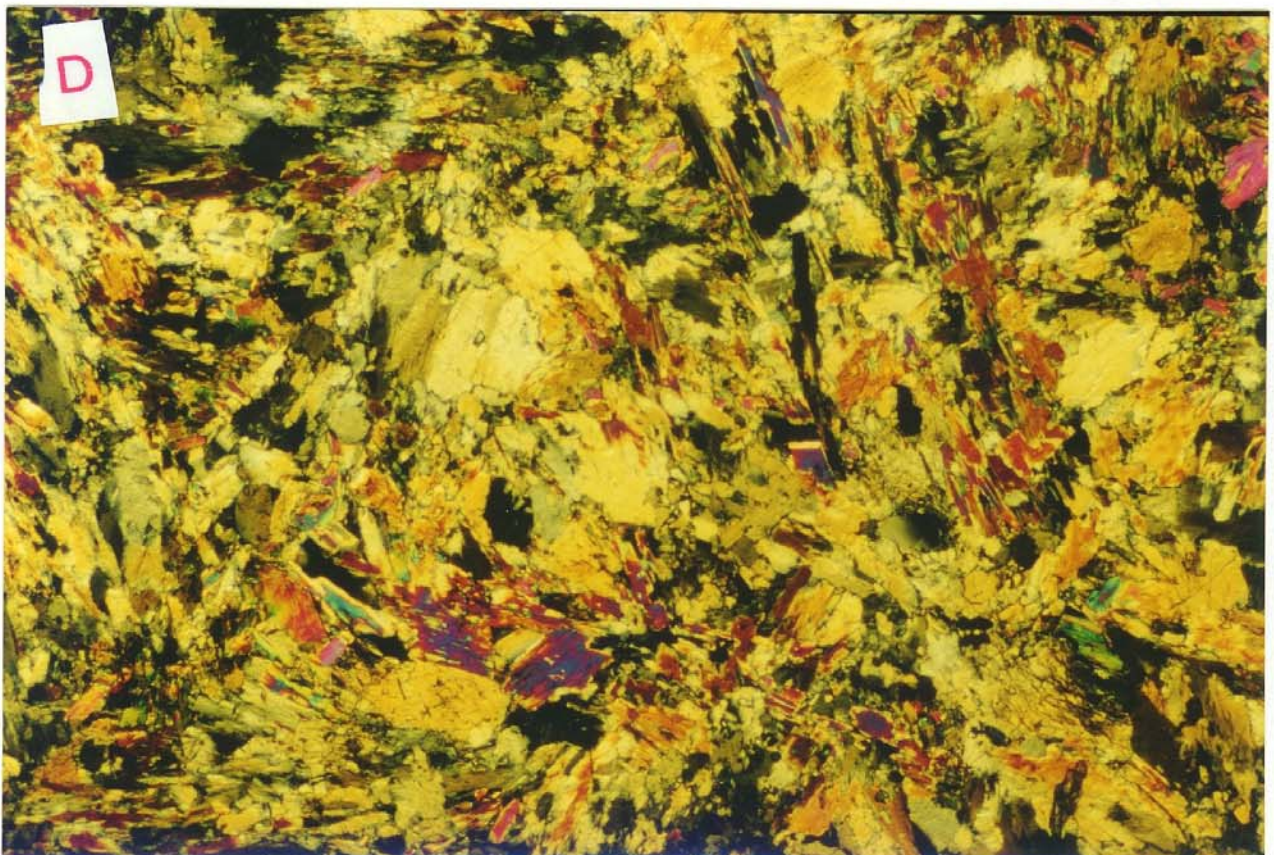
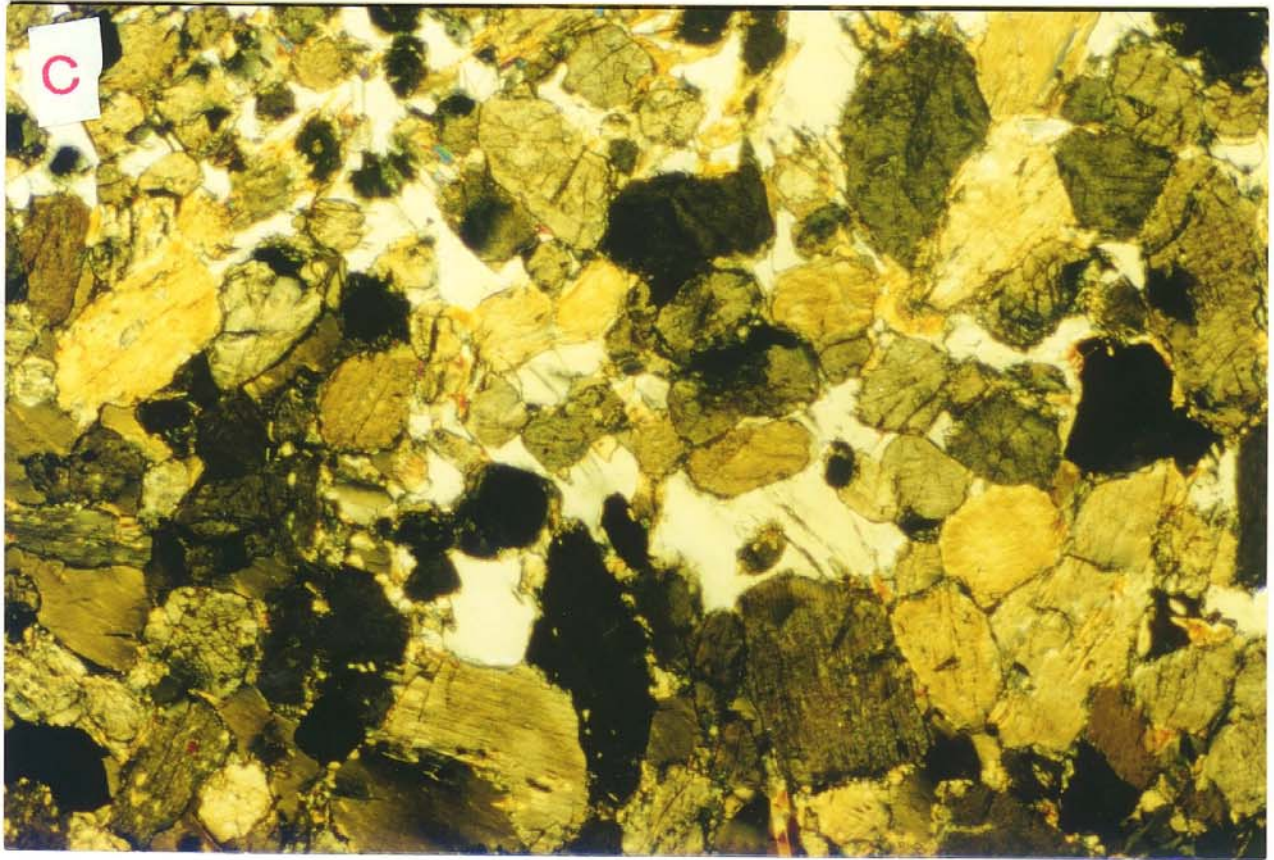
Plate 1.2 C-D. Microscope images illustrating alteration.

Plate 1.2. C and D. Two compositionally almost similar orthopyroxene cumulates. Sample above is practically fresh and sample below totally of hydrated. C) Sample 9619402, Buvann, drill hole 260-125/66-66.5, bOC MgO_n%=24.32, D) Sample 9619322, Buvann, drill hole 235-160/263.2-263.5 m, bMC, MgO_n%=25.96. Plane polarized light, crossed nicols, magnification 35x.

Plate 1.3 Microscope images of the ore minerals. All images are in reflected plane polarised light.

A - Typical ore mineral assemblage (pyrrhotite, chalcopyrite, pentlandite, molybdenite) in a silicate matrix (dark grey). Graphite laths (centre) are brown-grey. X5. Sample 9619387, Bruvann drill hole 235-160.

B - Detail of image A, showing laths of graphite trapped within chalcopyrite in pyrrhotite and pentlandite. Blue mineral: molybdenite. Dark grey: silicates. X20. Sample 9619387, Bruvann drill hole 235-160.

C - Base-metal sulphide association consisting of pentlandite (white), pyrrhotite (grey), chalcopyrite (yellow) and molybdenite laths (blue). X20. Sample 9619419, Bruvann drill hole 260-125.

D - Nickelinite crystal (pinkish) rimmed by cobaltite (blue) in pyrrhotite and pentlandite. X50. Sample 9619415, Bruvann drill hole 260-125.

E - Graphite (light grey laths) - chalcopyrite - pyrrhotite - association in silicates (dark grey). X20. Sample 9619421, Bruvann drill hole 260-125.

F - Graphite laths (brown grey) in pyrrhotite. X5. Sample 961387, Bruvann drill hole 235-160.

G - Complex association of pyrrhotite, chalcopyrite, graphite (laths, brown) and molybdenite (bluish tinge). X20. Sample 9619421, Bruvann drill hole 260-125.

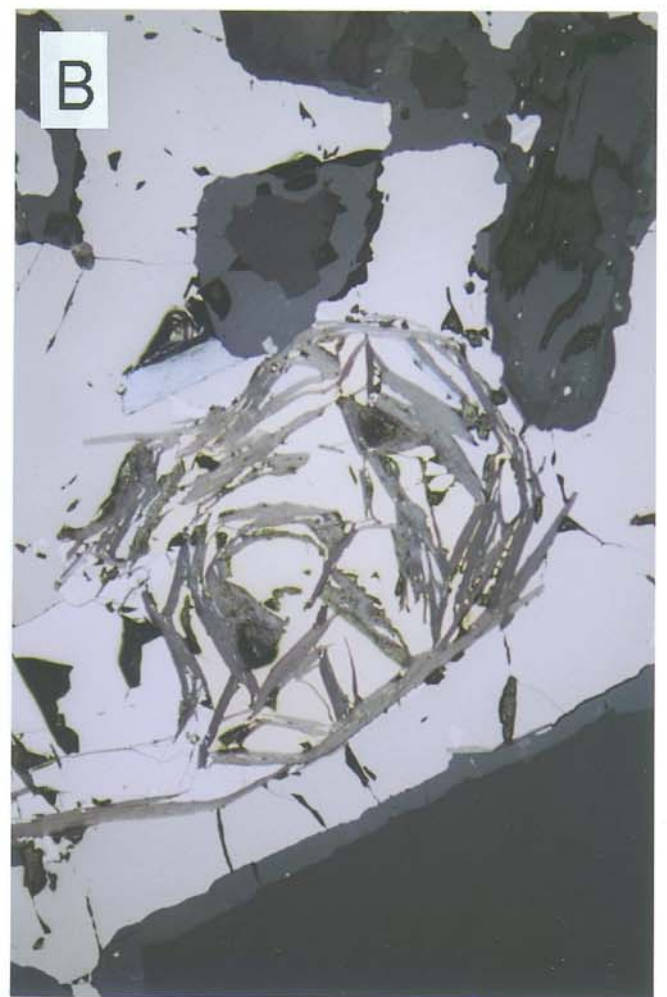
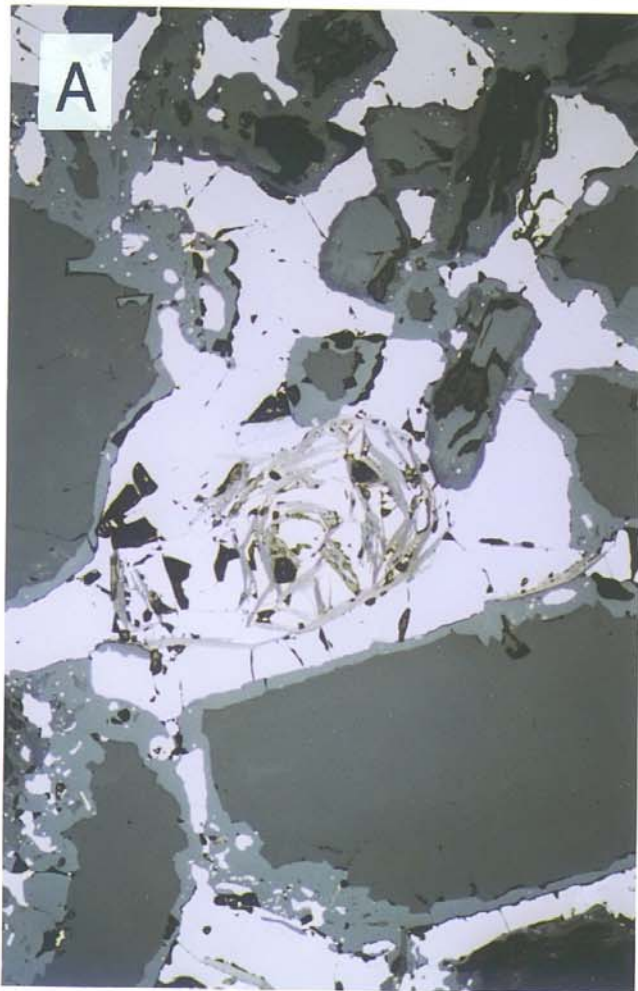
H - Graphite lath associated with pentlandite in a silicate matrix. X10. Sample 9619545, Ekojoki drill hole EJ17.

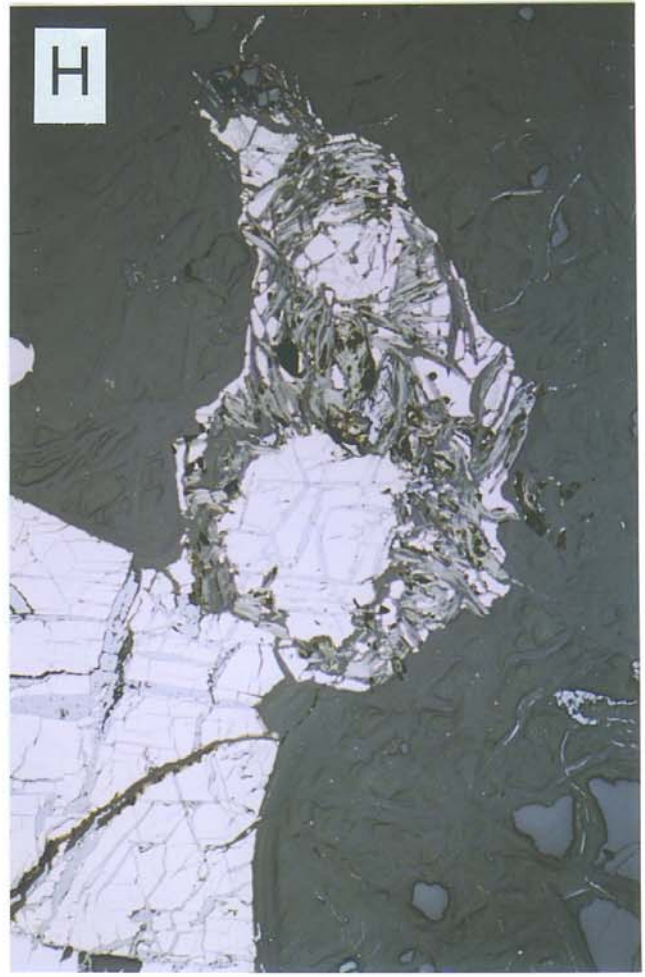
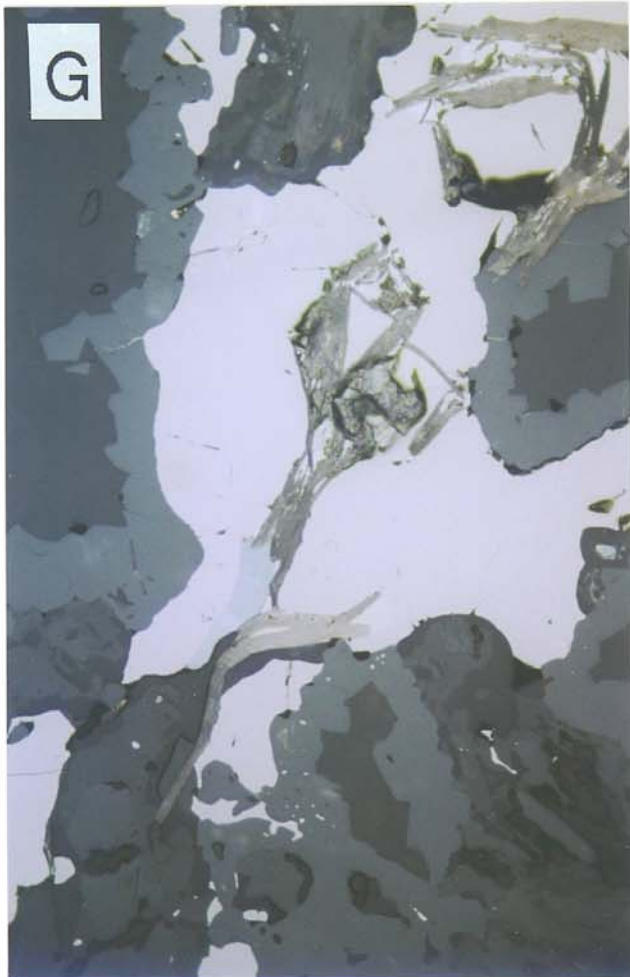
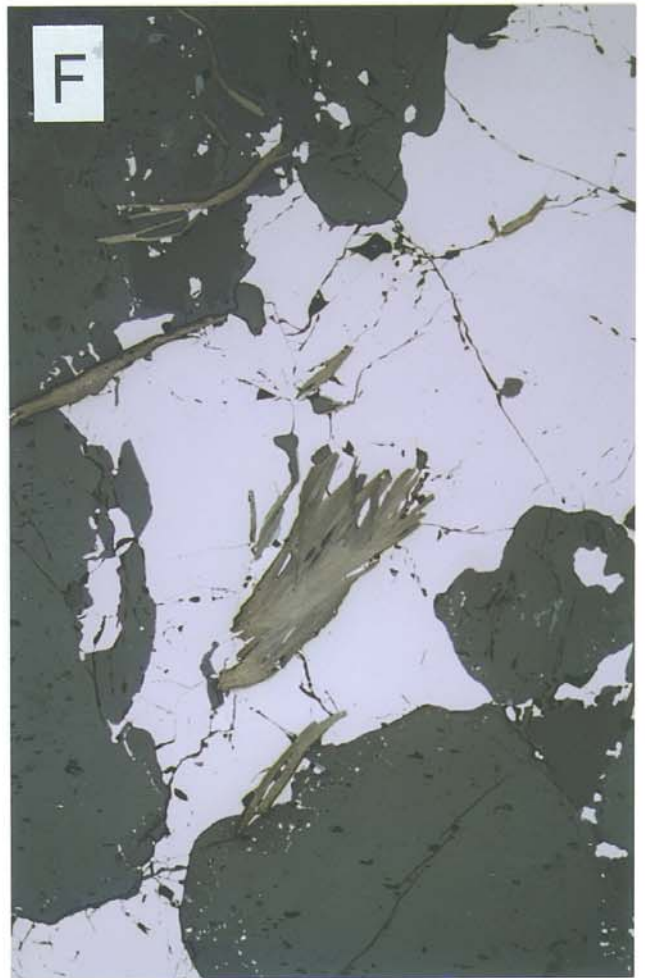
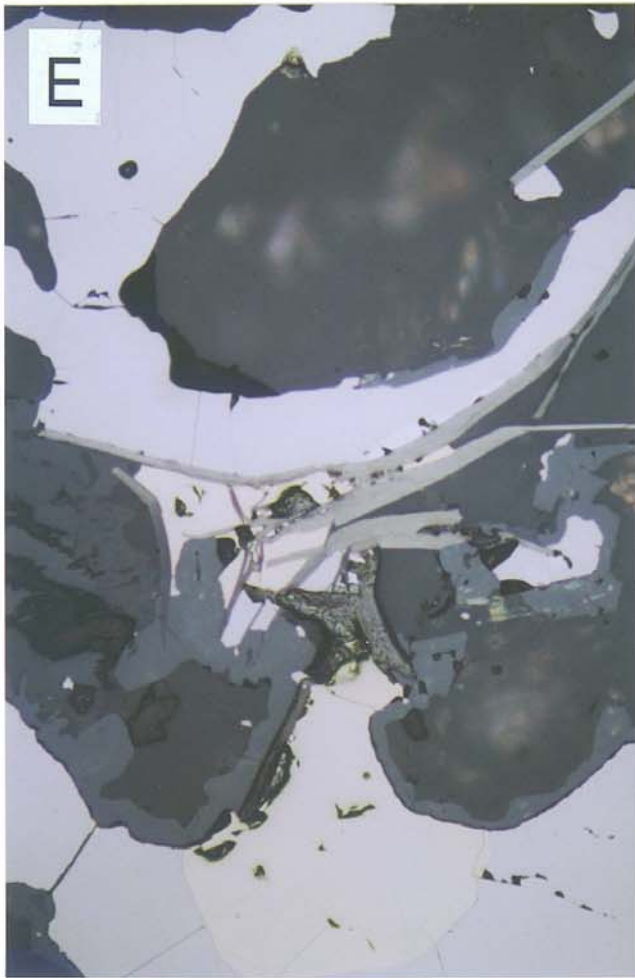
I. Graphite rimming pyrrhotite. X10. Sample 9619545, Ekojoki drill hole EJ17.

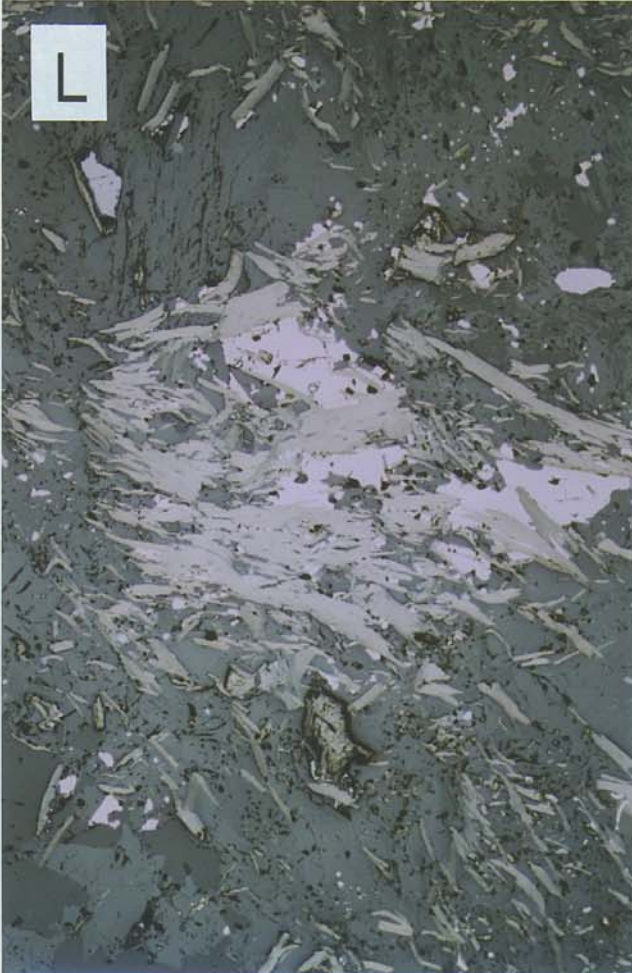
J - Detail of a vein of nickelinite, cobaltite, chalcopyrite and pyrrhotite. X50. Sample 9619325, Bruvann drill hole 235-160.

K - Graphite laths - pyrrhotite association in a silicate matrix (dark grey). X5. Sample 9619387, Bruvann drill hole 235-160.

L - Graphite laths - pyrrhotite association in a silicate matrix (dark grey). Note the very high proportion of graphite. X5. Sample 9619387, Bruvann drill hole 235-160.







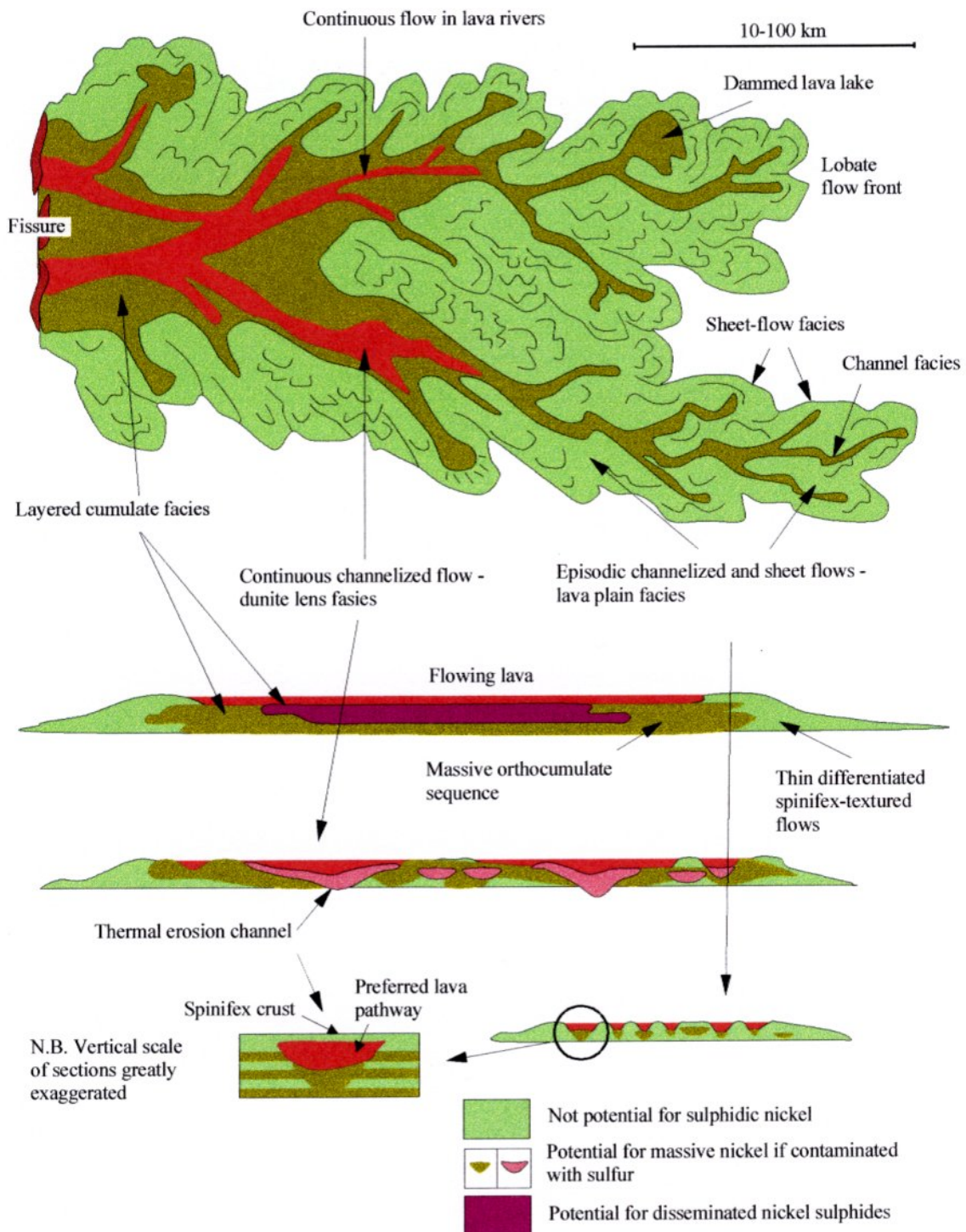


Figure 1.2.2.1 Schematic illustration of a komatiitic volcanic complex. The structures and lava types potential for type 1 (massive) and type 2 (disseminated) sulphide Ni deposits are indicated (modified after Hill et al. 1990).

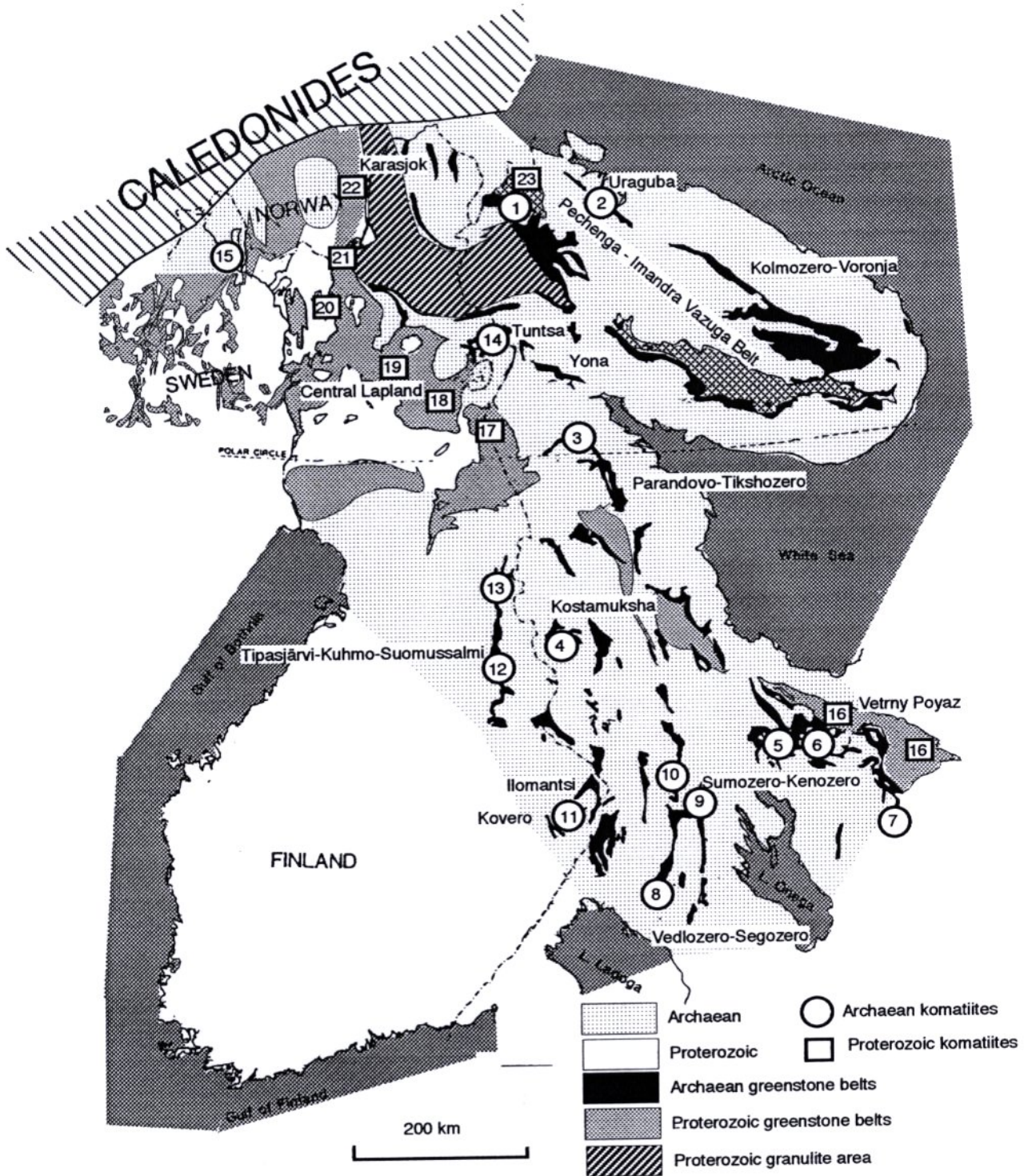


Figure 4.1.1 Archean and Proterozoic greenstone belts of Fennoscandia. Archean komatiite areas: 1. Allarechen, 2. Uraguba, 3. Notozerska, 4. Kostamuksha, 5. Shiloska, 6. Kammenoozero, 7. Tokshinska, 8. Hautavaara, 9. Koikari, 10. Sovdozero, 11. Kovero-Ilomantsi, 12. Tipasjärvi-Kuhmo, 13. Suomussalmi, 14. Tuntsa, 15. Sarvisoaivi. **Proterozoic komatiites:** 16. Vetreny Poyaz, 17. Salla, 18. Kummitsoiva, 19. Sattasvaara, 20. Pulju, 21. Kaamajoki, 22. Karasjok

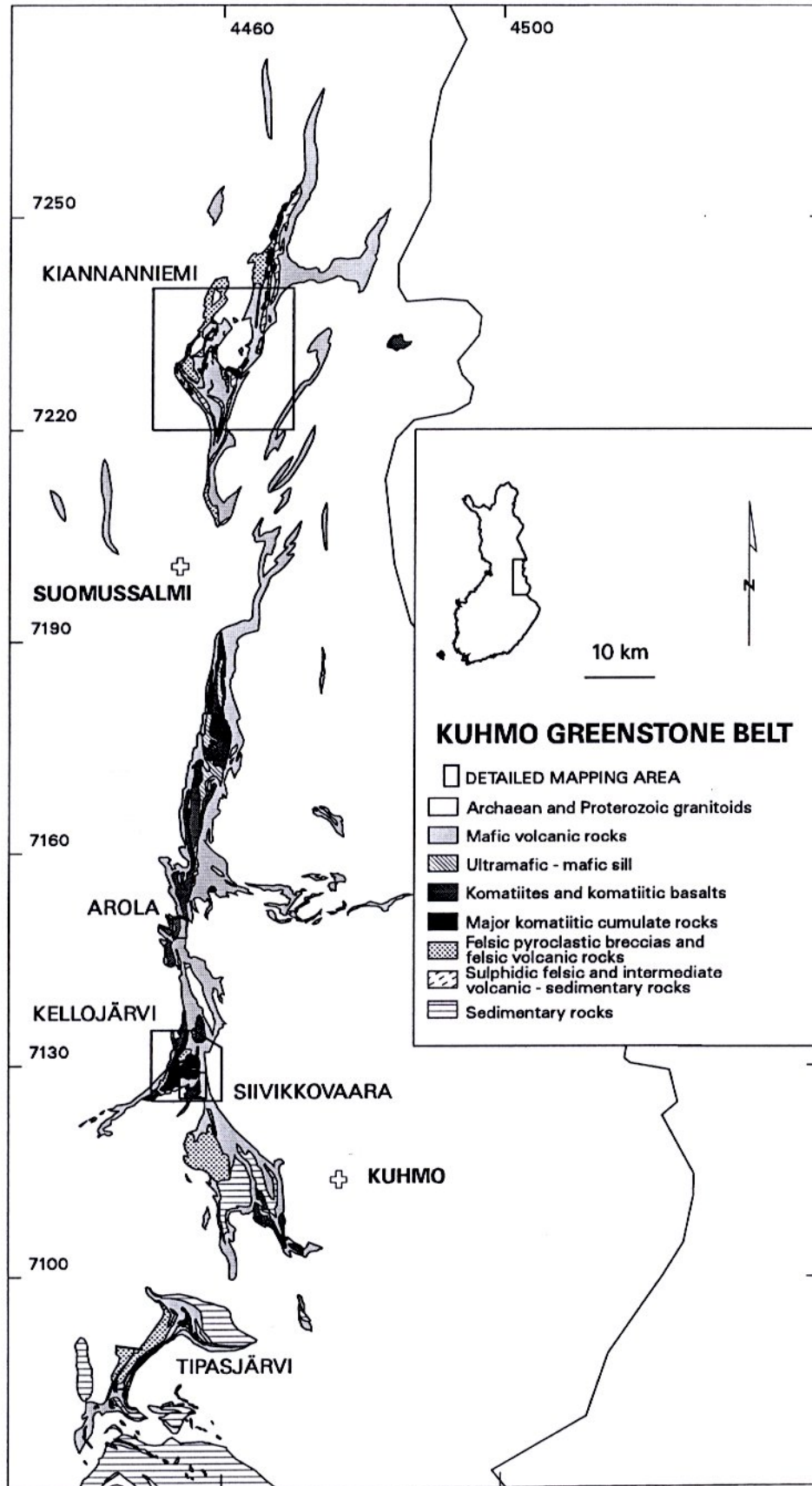
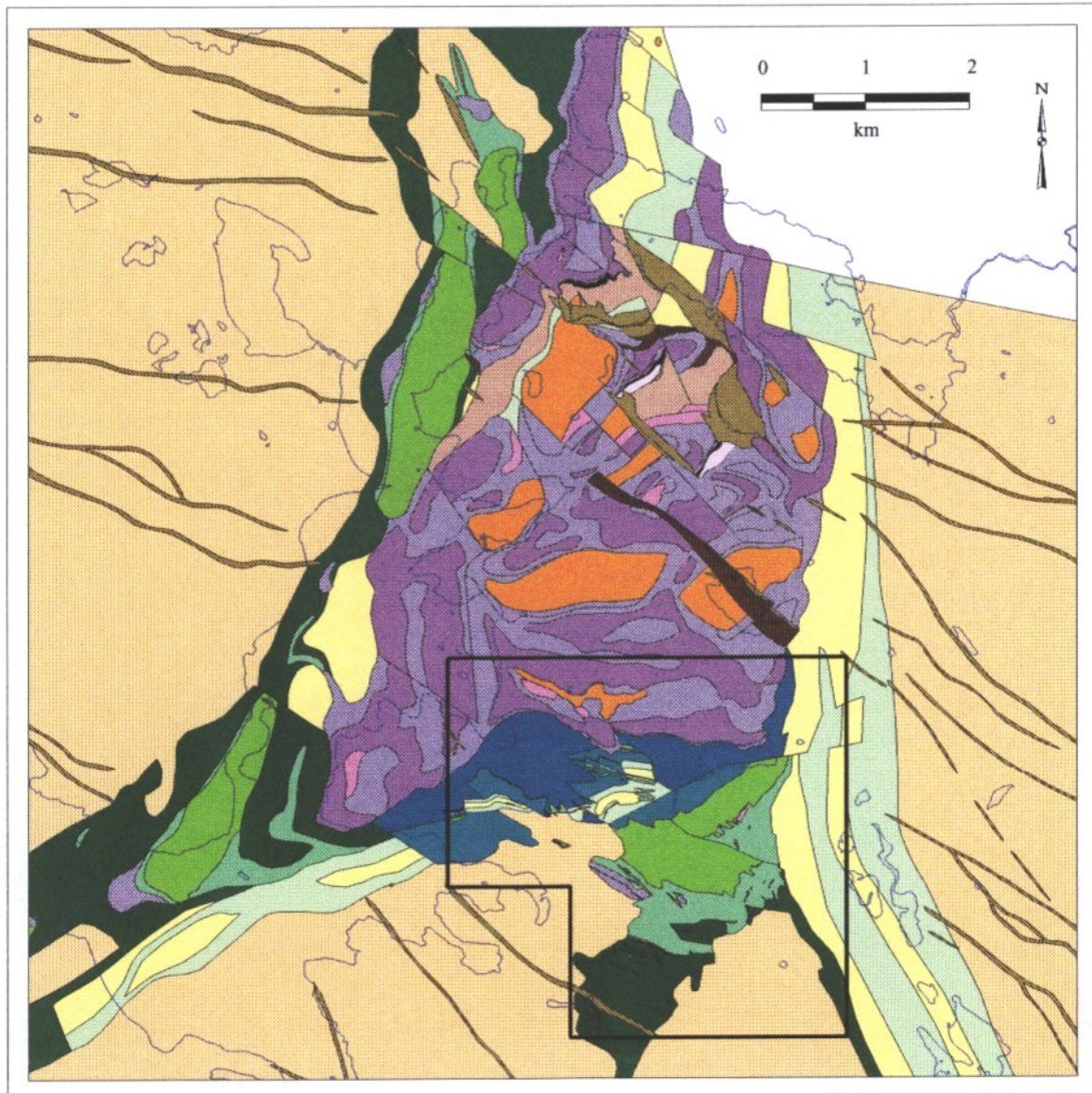


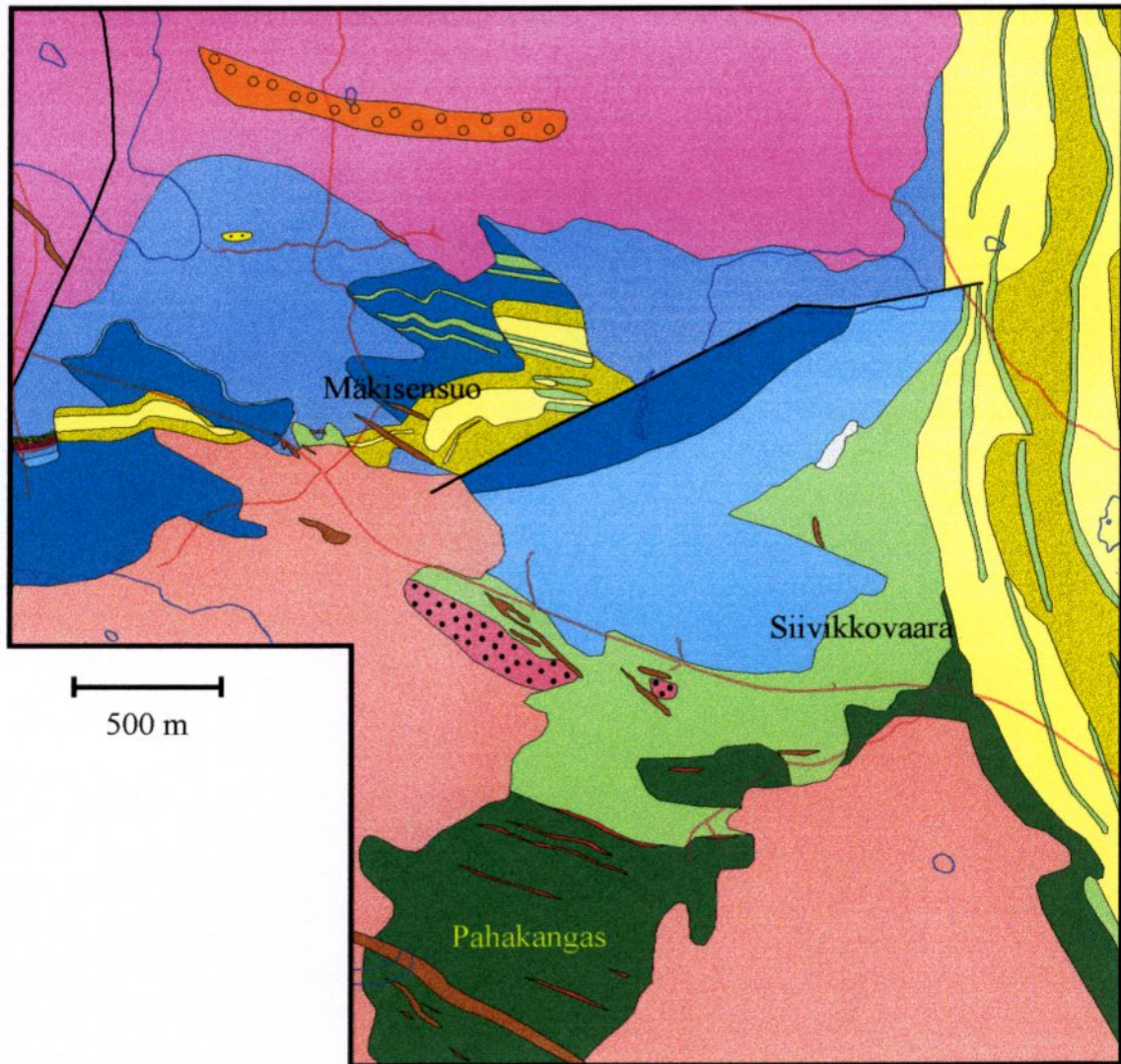
Figure 4.1.2 Generalized geological map of Tipasjärvi, Kuhmo and Suomussalmi greenstone belts. The areas mapped in detail in this study are delineated.



Rock types of the Siivikkovaara - Kellojärvi mapping area

Basement granitoids	Kellojärvi ultramafic complex	Supracrustal rocks younger than Kellojärvi ultramafic complex
Granodioritic basement	Olivine adcumulate	Komatiitic basalt
Plagioclase porphyrite	Olivine meso-orthocumulate	"High-Cr-basalt" (Cr 1300-4500 ppm)
Supracrustal rocks older than Kellojärvi ultramafic complex	Olivine augite ad-mesocumulate	"Medium-Cr-basalt" (Cr 450-1300 ppm)
Calc-alkaline mafic volcanic rocks	Plagioclase augite adcumulate	Pyroclastic felsic volcanic rocks
Calc-alkaline felsic volcanic rocks	Pyroxene cumulate, marginal zone	Proterozoic dykes
Tholeiitic basalt	Komatiite flows and thin orthocumulates	Wehrlitic and pyroxenitic dykes
BIF or black schist		Gabbroic dykes

Figure 5.1 Generalized geological map of the Kellojärvi - Siivikkovaara area, Kuhmo. The Siivikkovaara area presented in Fig. 5.2 is delineated.



T. Halkoaho 1998

Rocks older than the komatiitic sequence

- Tholeiitic basalt (Pahakangas type) with thin banded iron formation interlayers
- Calc-alkaline bimodal felsic to mafic volcanic and sedimentary rocks

Rocks of the komatiitic sequence

- Medium-Cr basalt
- High-Cr basalt
- Komatiitic basalt (high-Mg basalt)
- Olivine orthocumulate (mainly thin komatiite flows)
- Olivine mesocumulate lens of lava flow facies
- The Kellojärvi ultramafic complex

Rocks younger than the komatiitic sequence

- Polymictic lahar-type volcanic sedimentary rocks
- Phyllite and felsic to mafic sedimentary rocks
- Homogeneous granodiorite or granodioritic dyke
- Pyroxenitic dyke
- Gabbroic dyke

- Major fault
- Road

Figure 5.2 Geological map of the Siivikkovaara area.

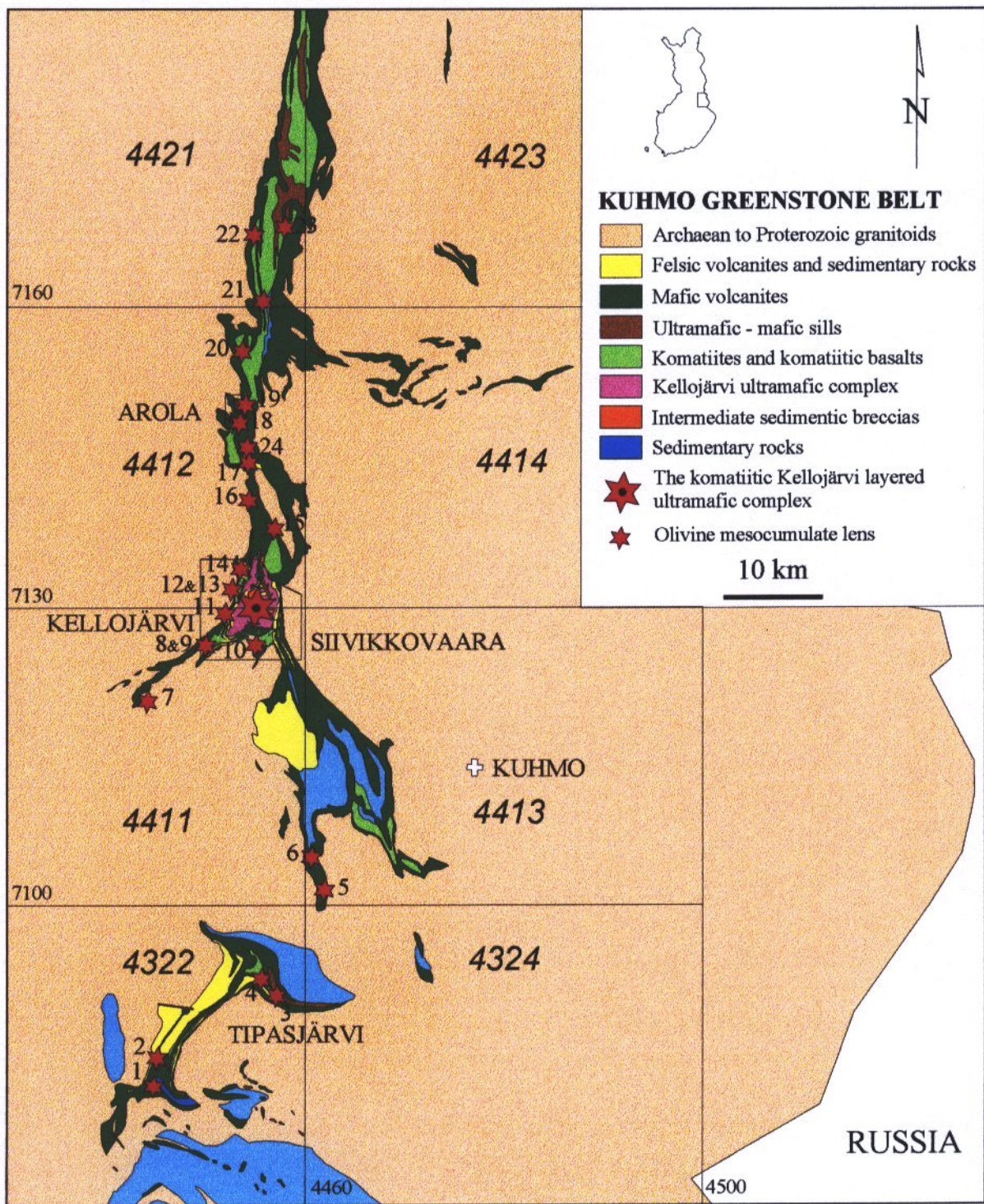


Figure 5.3 Generalized geology of the southern part of the Kuhmo greenstone belt. Olivine cumulate lenses are indicated and the numbers refer to Table 1 (map modified after Luukkonen 1991, and Taipale et al. 1993).

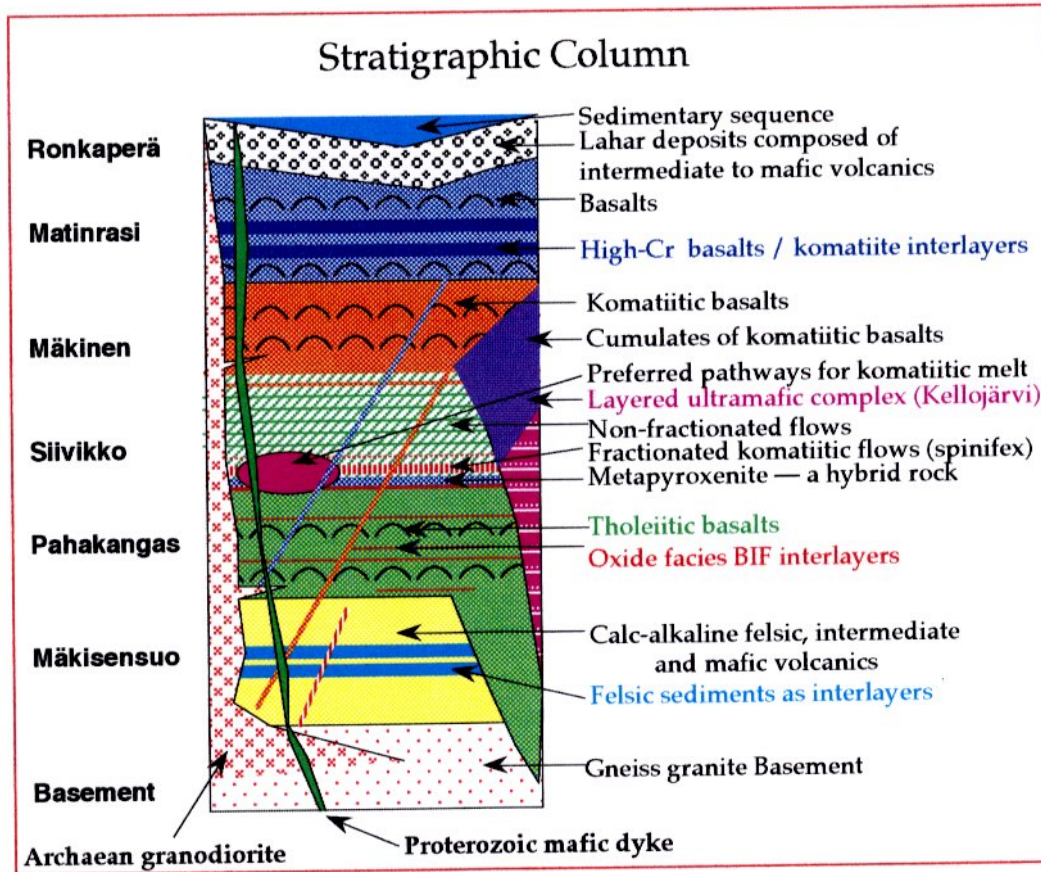


Fig. 5.1.1.1 Stratigraphy of the Siivikkovaara-Kellojärvi area

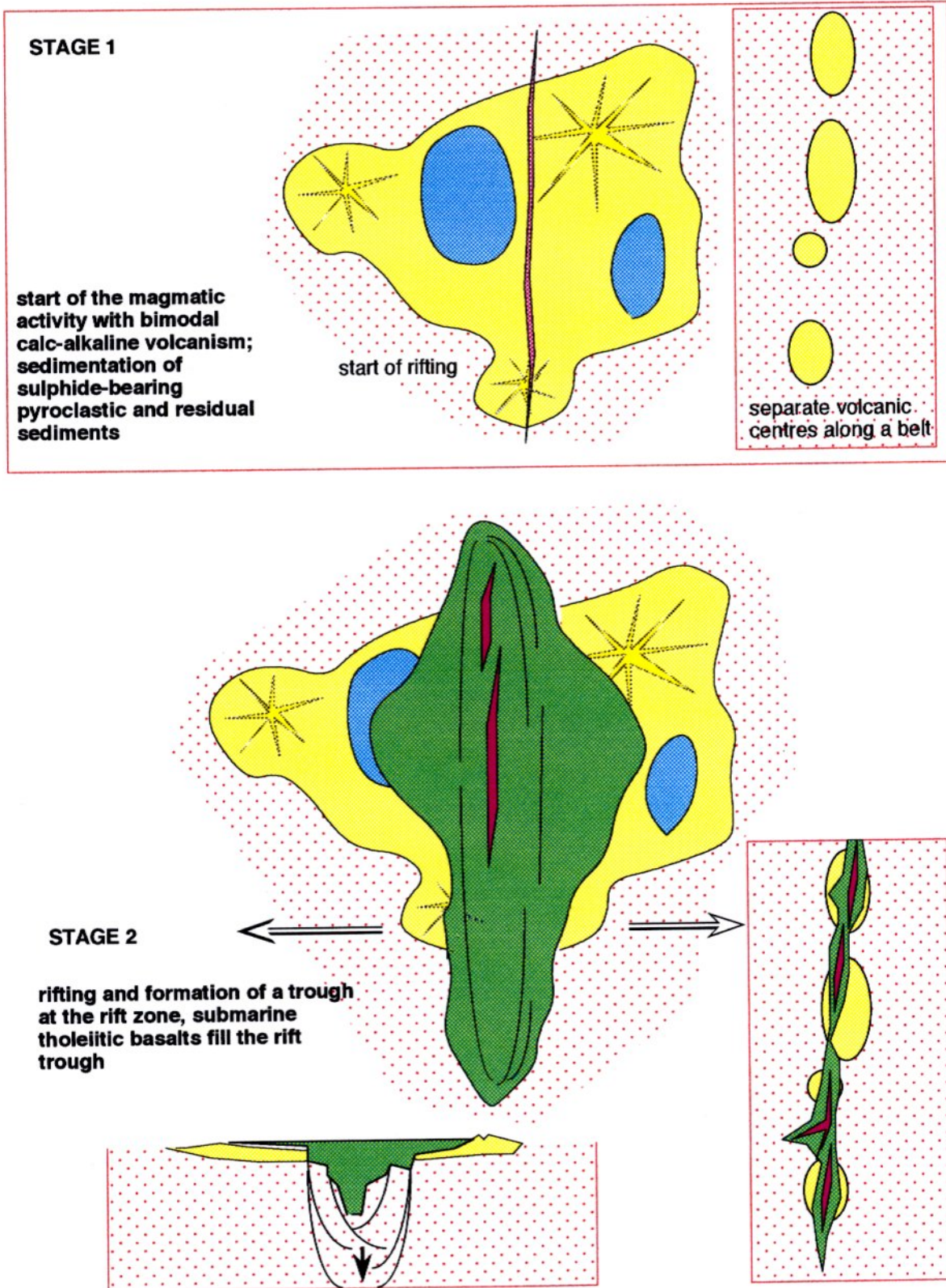


Fig. 5.1.1.2 Schematic illustration of the volcanic and sedimentary evolution of the Kellojärvi- Siivikkovaara supracrustal complex: stages 1 and 2 indicate of incipient rifting and tholeiitic magmatism in the rift basin

STAGE 3 — komatiitic flows, pooling of komatiite magma in the deep portion of the rift and deposition of olivine and clinopyroxene cumulus in the melt conduit

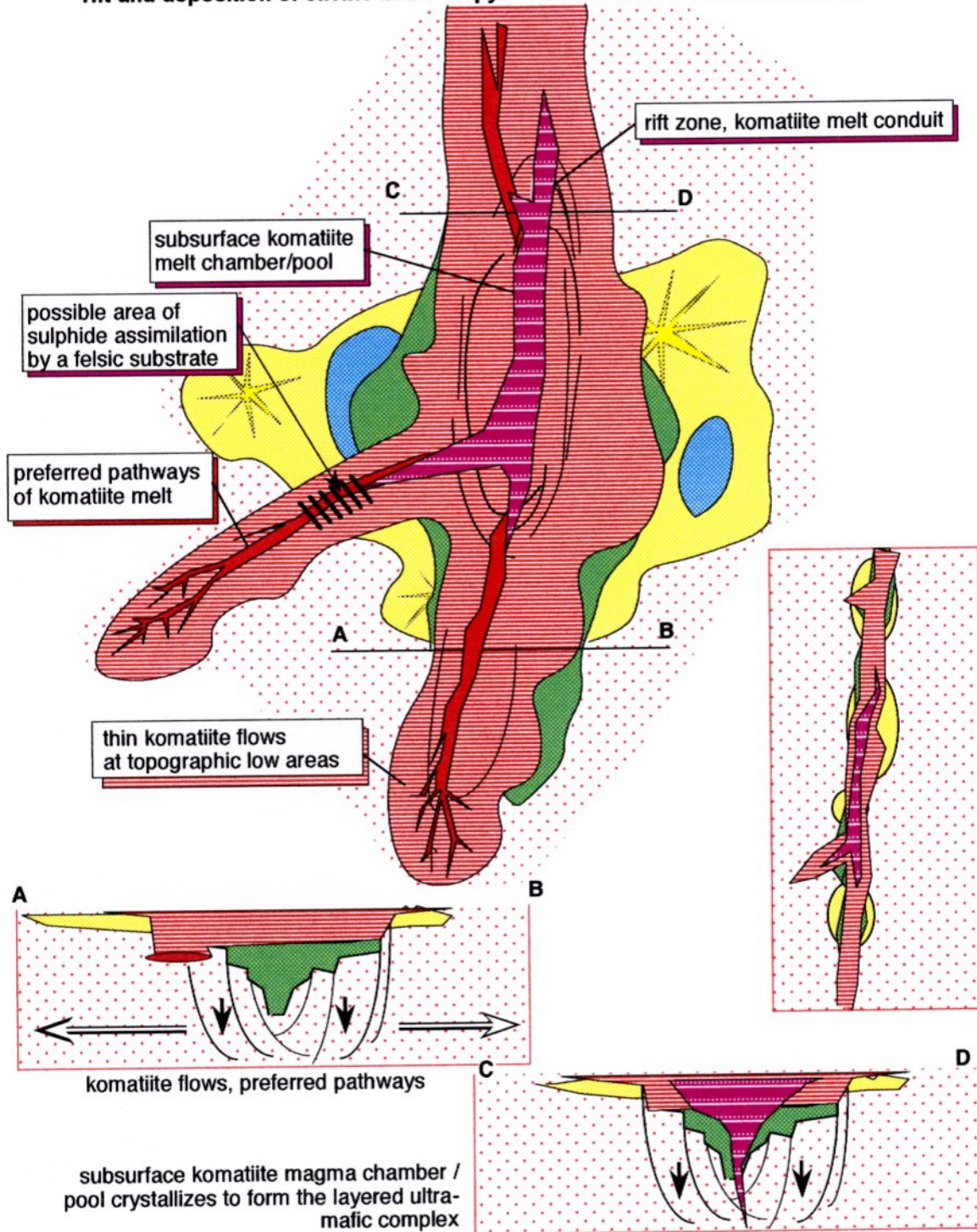


Fig. 5.1.1.3 Schematic illustration of the volcanic evolution of the Kellojärvi-Siivikkovaara complex: Stage 3 — komatiitic magmatism

STAGE 4

submarine extrusion of komatiitic basalt pillow lavas (remelting of the crust and komatiites assimilate crustal material and fractionate (?) to form komatiitic basalts)

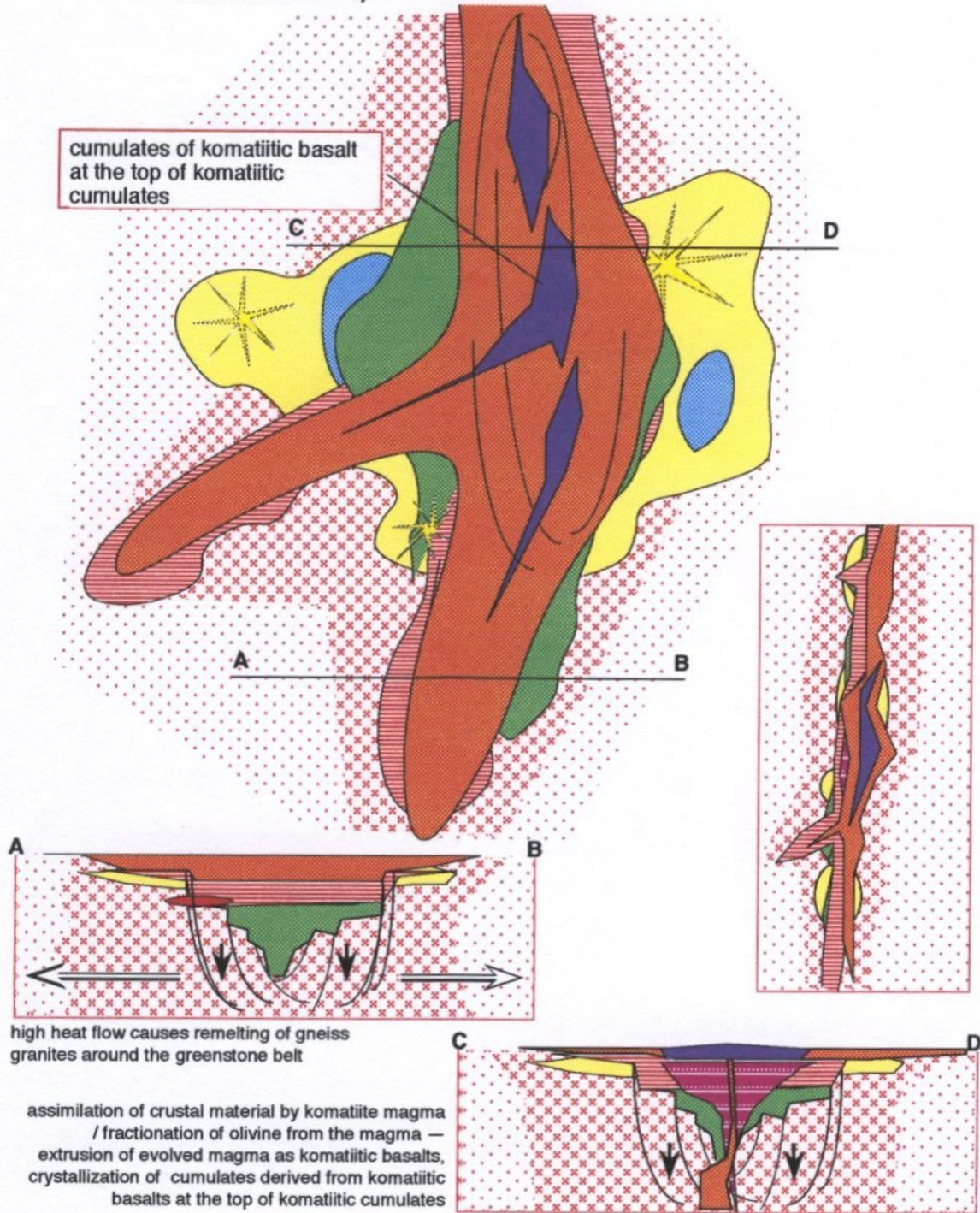


Fig. 5.1.1.4 Schematic illustration of the volcanic and sedimentary evolution of the Kellojärvi - Siivikkovaara supracrustal complex: stage 4 — evolution and eruption of komatiitic basalt (crustal contamination and/or fractionation), crystallization of cumulates

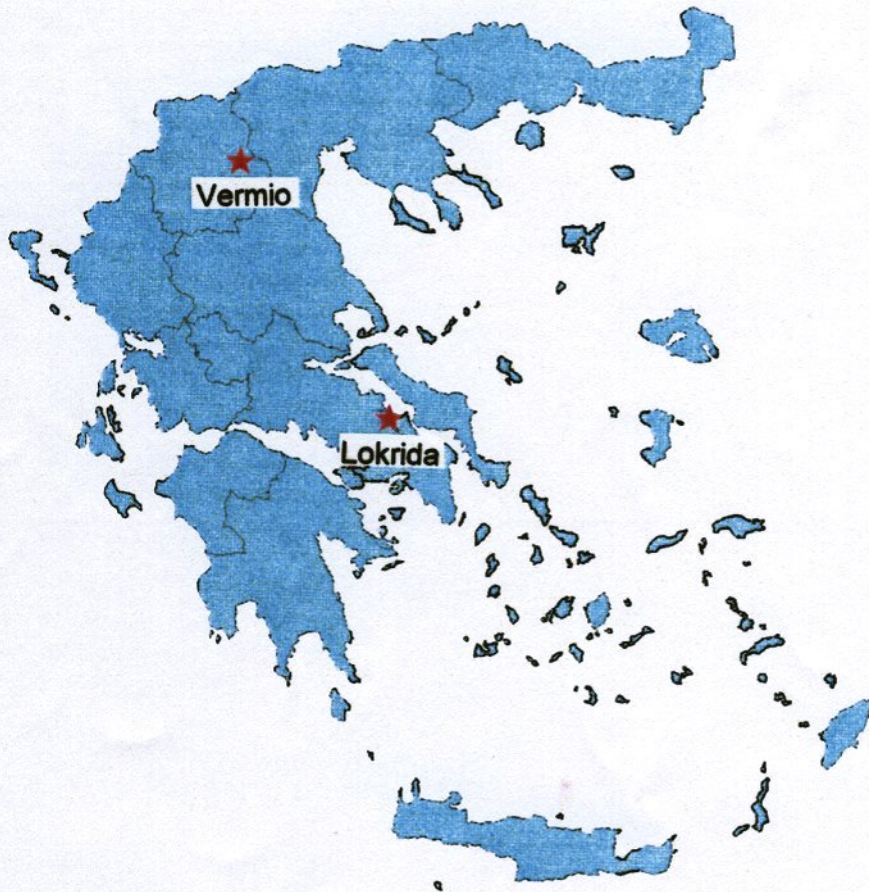


Plate 14: Geonickel WorkPackage 1, Task 3 : General map of Greece showing the areas of Lokris and Vermion.

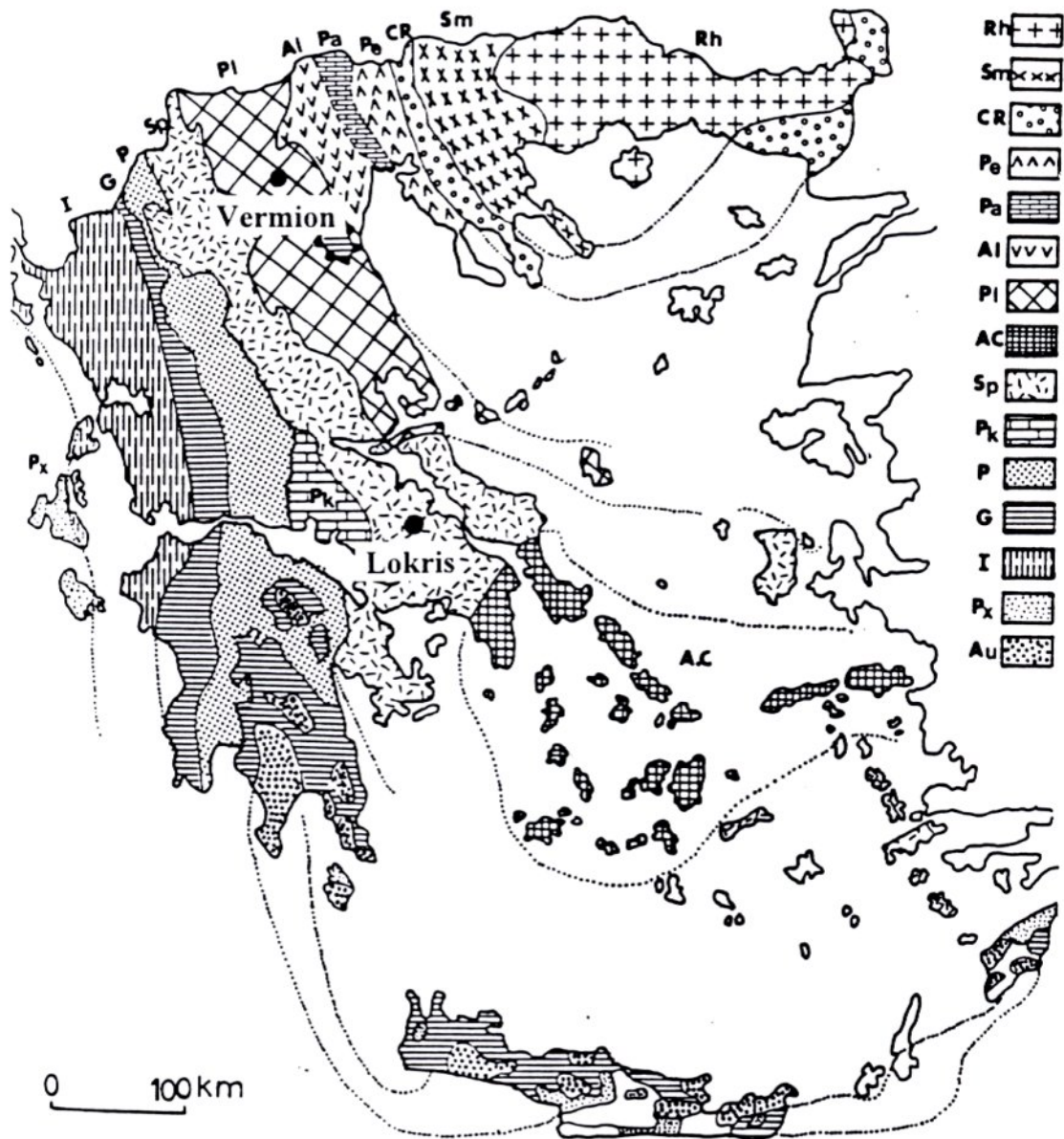


Plate 15: Geonickel WorkPackage 1, Task 3 : Geotectonic map of Greece. Rh=Rhodope; Sm=Serbomacedonian; CR=Circum Rhodope; (Pe-Peonias, Pa-Paikon, Al-Almopias)=Axios Zone; Pl=Pelagonian; AC=Atticocycladic; Sp=Subpelagonian; Pk=Parnassos; P=Pindos; G=Gavrovo-Tripolis; I=Ionian; Px=Paxos (Mountrakis, 1994).

Also shown, the studied areas of Lokris and Vermion.

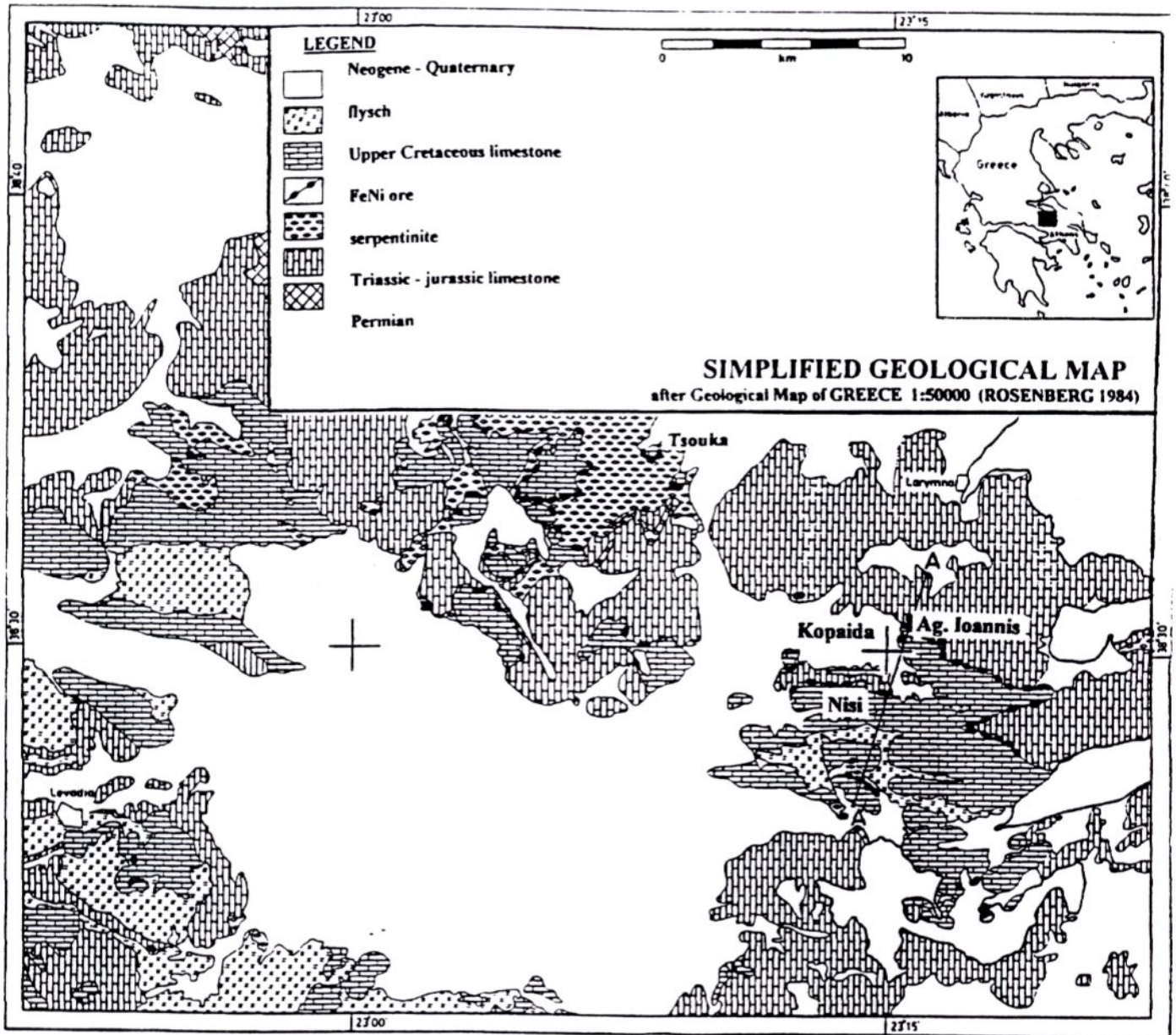


Plate 16: Geonickel WorkPackage 1, Task 3: Simplified geological map of Lokris showing the Ni-laterite deposits of Nisi, Kopaida and Tsouka.

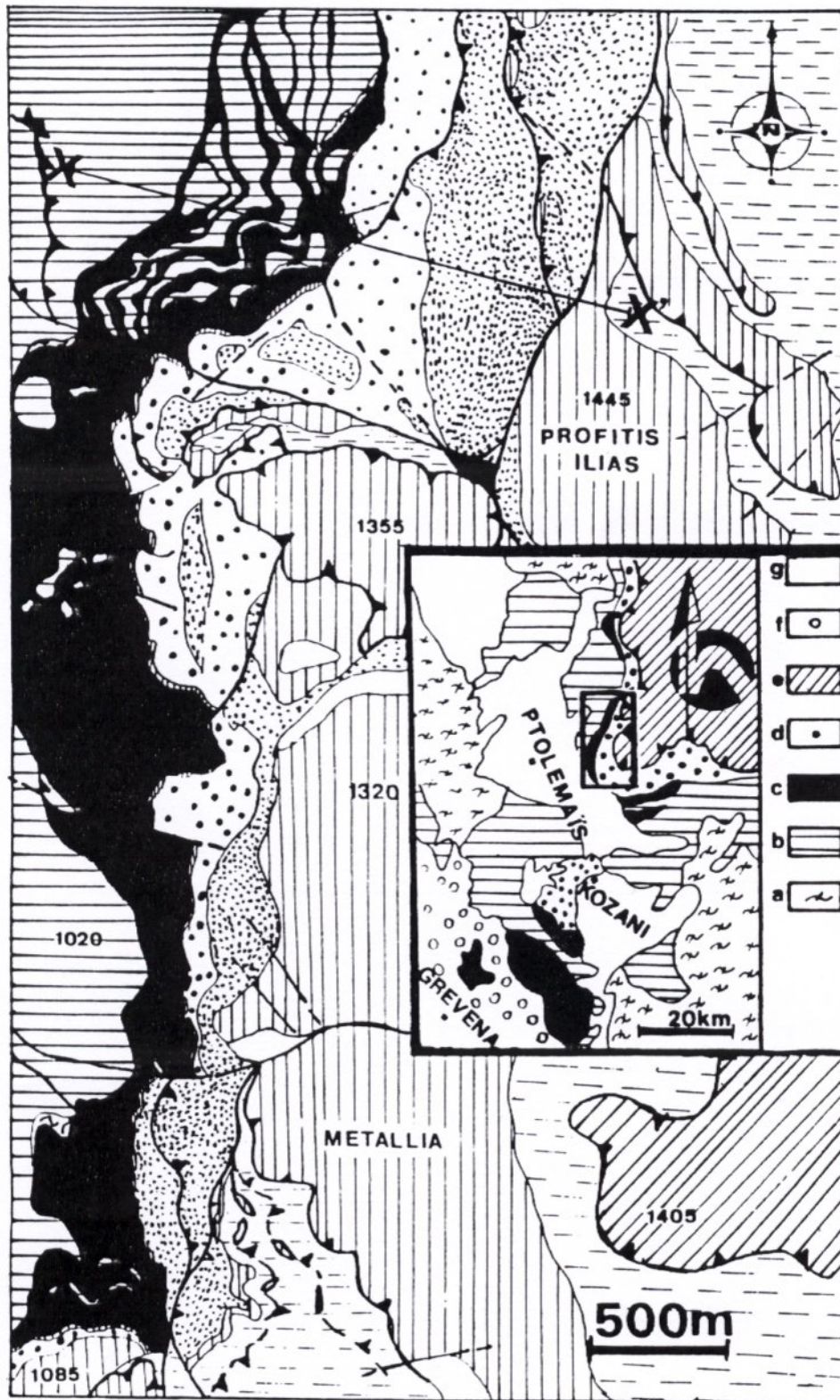


Plate 17: Geonickel WorkPackage 1, Task 3: Geological map of West Vermion showing the Profitis Ilias and Metallia deposits. a: gneiss; b: limestones; c: ophiolitic rocks; d: carbonate ophiolitic cover; e: Upper Vermion cover; f: flysch formation; g: Quaternary formations.

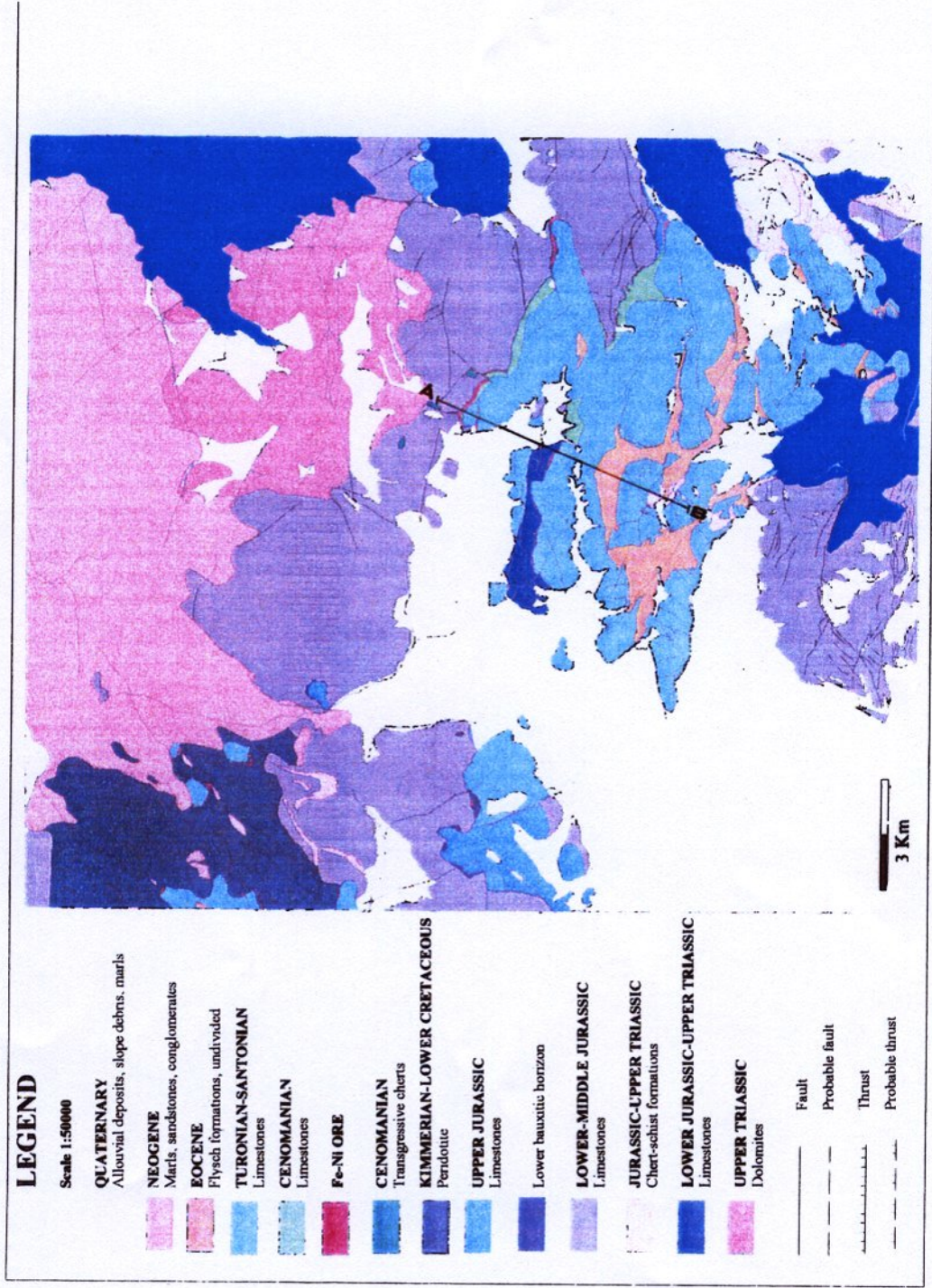
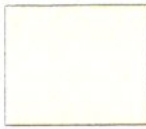


Plate 18: Geonickel WorkPackage 1, Task 3: Geological map of Lokris area, in 1:50 000 scale

LEGEND



Slope debris

LOWER SENONIAN - MIDDLE CONIACIAN



Flysch formation: marly and siltstone formation rich in sandstone horizons. It is characterised by grey transition marly limestone beds towards its base with *Globotruncana*

UPPER TURONIAN - LOWER CENONIAN



Limestone with *Rudists*: Medium laminated-nodular, mostly dark colored, bituminous with or without *Rudist* debris and *Orbitoides* are developed towards the Coral limestone with *Rudists*, which subsequently are developed to thin laminated light colored pelagic limestone with *Globotruncana*. Thickness 100m.

TURONIAN



Clastic series: Flow debris developing a sandstone flyschoid formation locally rich in reworked material with several alternations of micro-conglomeratic brecciated limestone horizons of Turonian age. Towards the top light colored micro-conglomeratic brecciated limestone is dominated. Thickness 100m.

LOWER CRETACEOUS - CENOMANIAN



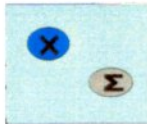
Conglomeratic limestone: Mainly consists of conglomeratic limestone horizons of varying thickness with limestone components of varying diameter (2-25cm) within red limestone and pelitic matrix. They are unconformably developed on the Fe-Ni horizon or on the ultrabasic rocks through a clayey-hematitic horizon. Thickness 80m.

UPPER JURASSIC - LOWER CRETACEOUS



Fe-Ni horizon: Massive lateritic horizon of red-violet to brownish colors, rich in Fe-Ni mineralisation, locally exhibiting pisolitic texture. It often contains reddish jasper breccia and quartz veinlets. Towards its lower parts the hematitic-siliceous material of the lateritization consists the matrix to the underlain peridotite blocks. Thickness 5-10m.

PRE - TITHONIAN (PRE - UPPER JURASSIC)



Ophiolites: Mainly consist of superposed units of serpentine sheets rich in harzburgite and dunite. Their base and top are intensively mylonitized forming serpentine rhawacke that is highly cemented due to the dolomitic grid. The serpentine unit at its upper part contains altered limonitic concentrations with nickel mineralisation. Thickness 100-150m.

MIDDLE JURASSIC

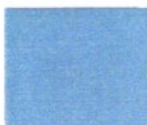


Meta-sediments: Brown meta-pelitic schists, which toward to their top are developed to chlorite schists with lenses of meta-volcanic rocks and towards their lowest parts to calc-schists progressively. They exhibit parallel bedding to the underlain pelagonian marbles.

TRIASSIC - JURASSIC



Pelagonian marbles: They consist of banks of 10-15m thick. The upper members exhibit pseudobedding and contain nodules of white chert. In general, the marbles have inclined folds of extensive length accompanied by flow schistosity caused by the upper Jurassic tangential phase.



Almopian dislodged slices



Thrust



Fault



Unconformable tectonic contact

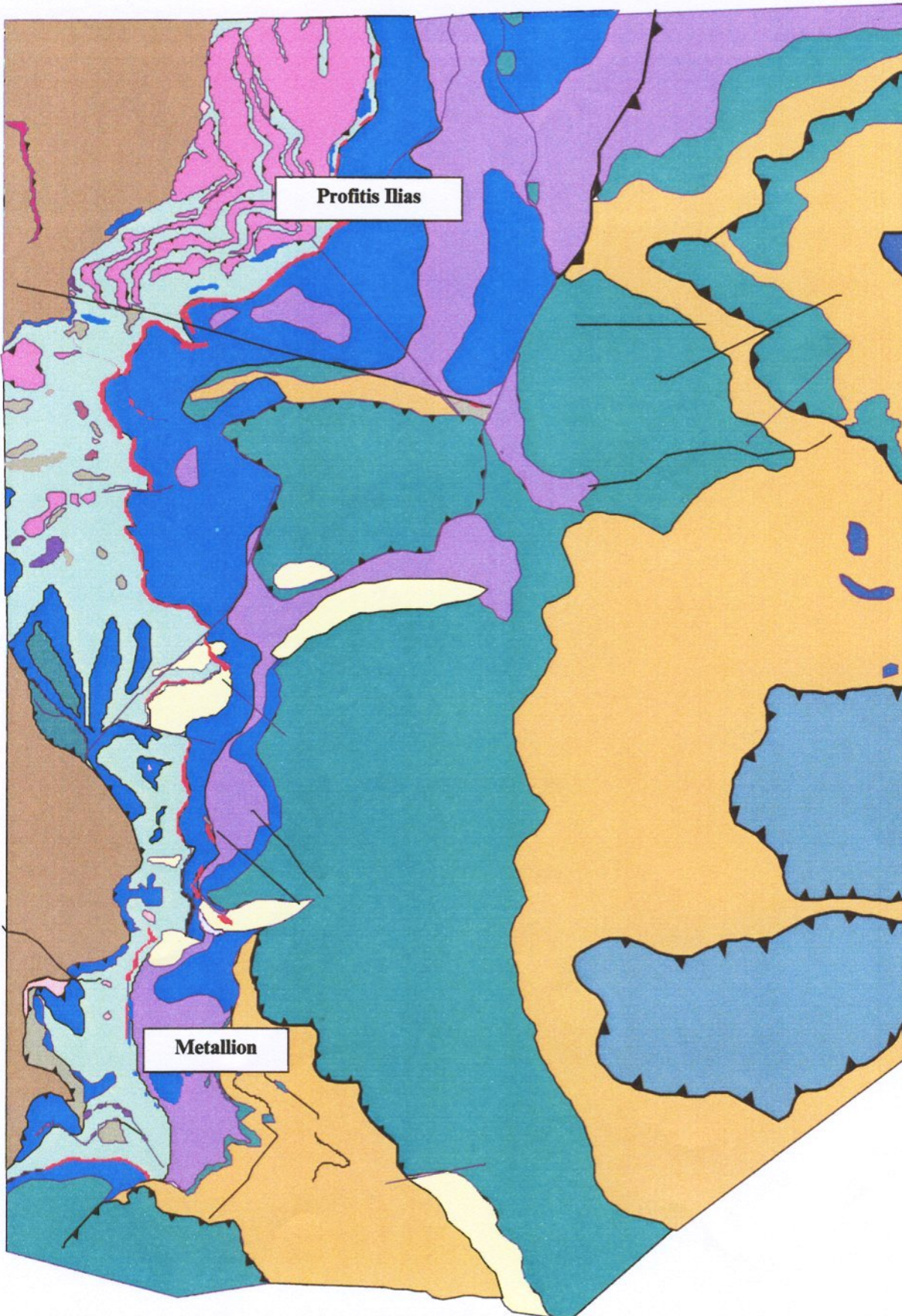


Plate 19: WorkPackage 1, Task 3 : Geological Map of West Vermont in 1 : 5.000 scale
(By Grigoris P. and Photiadis A. 1998)

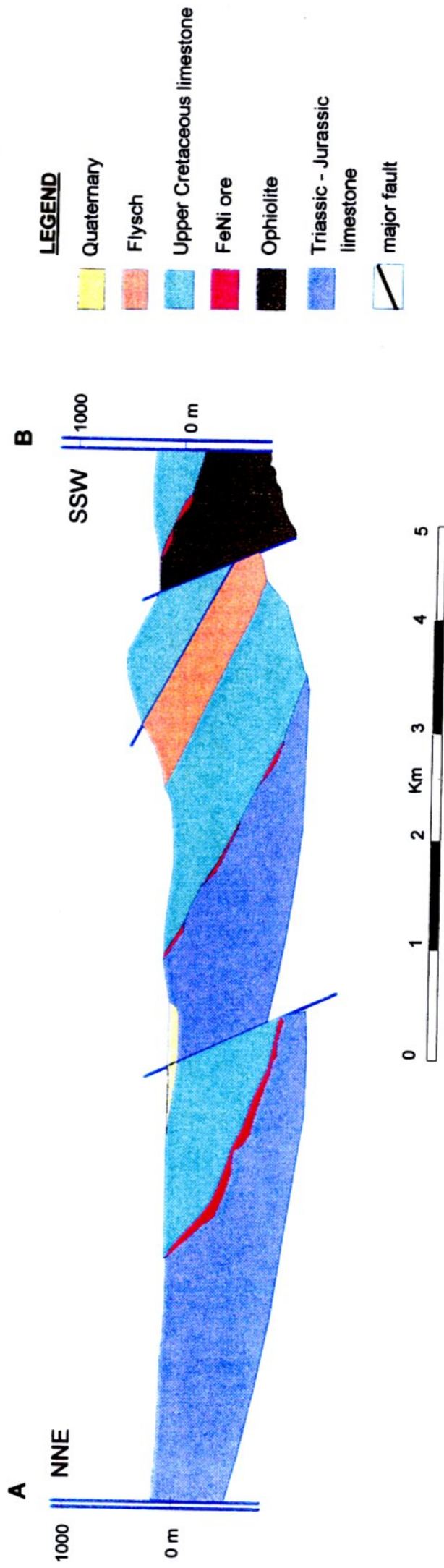
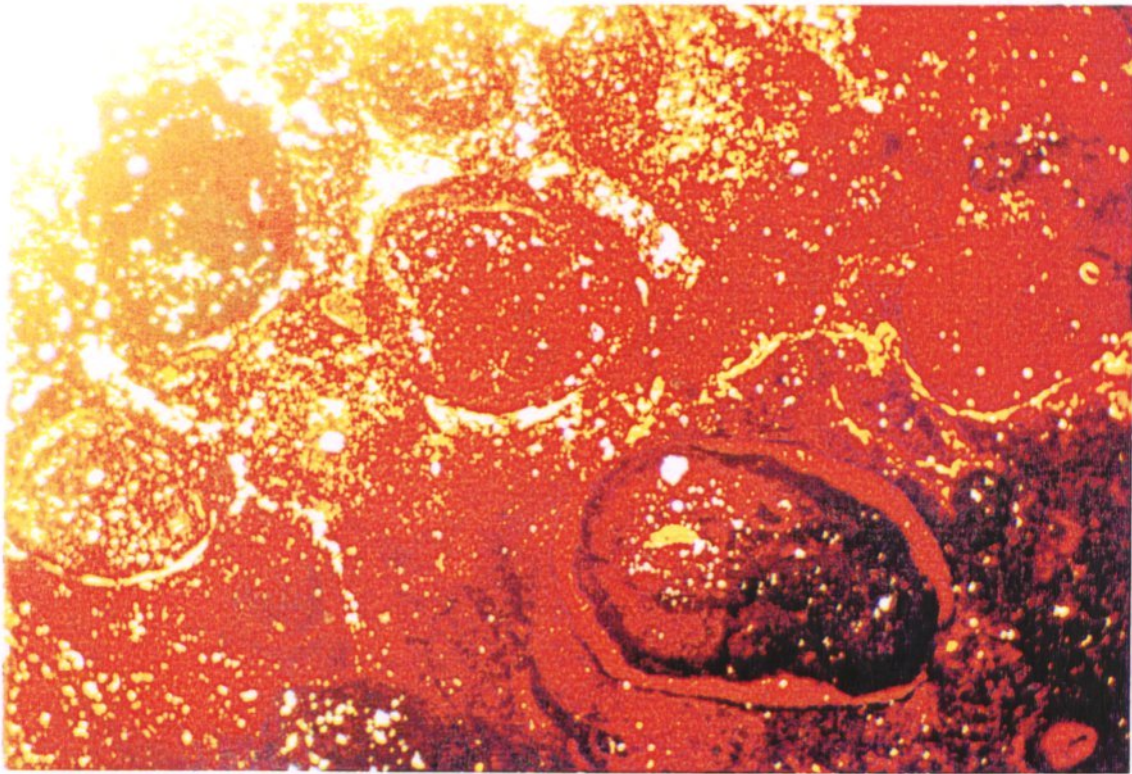
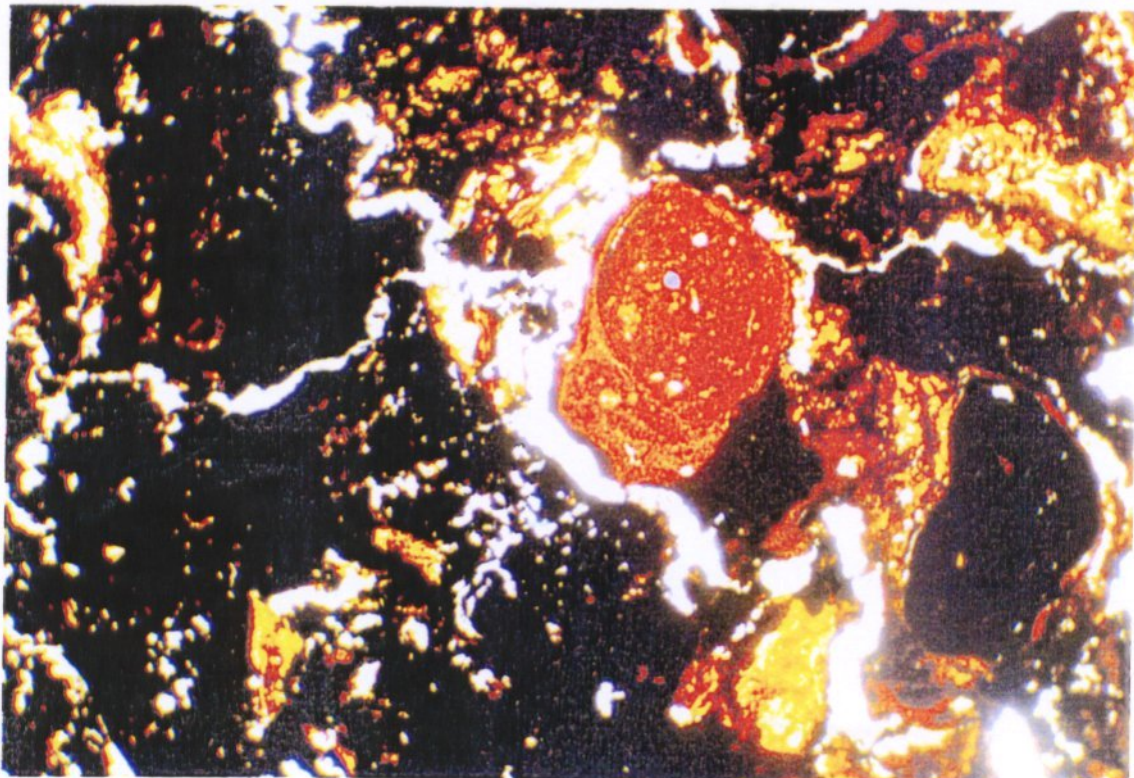


Plate 21: Geonickel WorkPackage 1, Task 3: Geological cross-section (AB, Plate 18) of Lokris area.

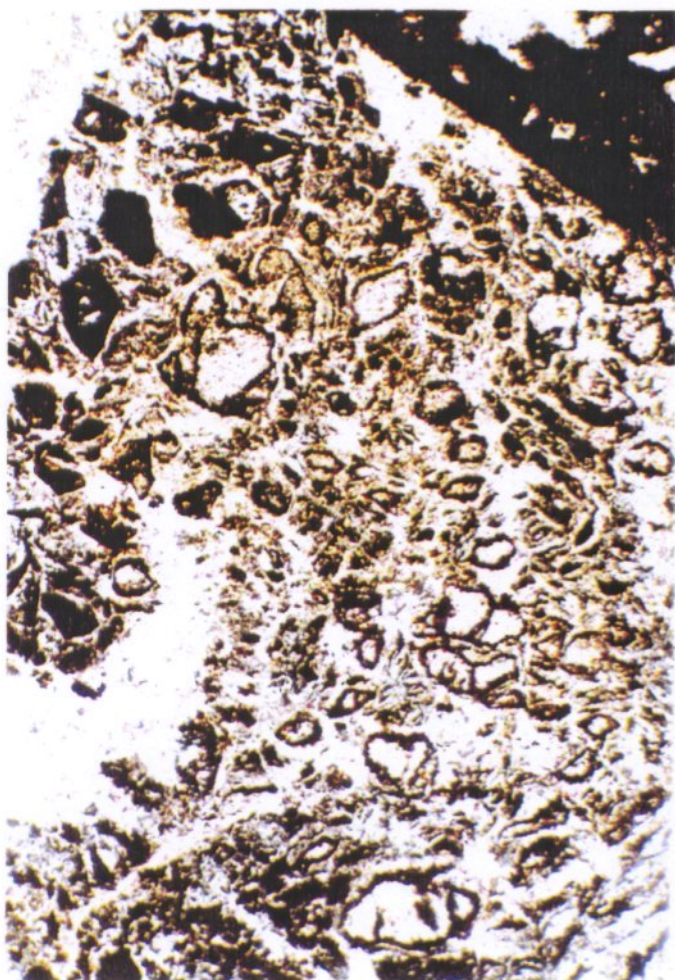


1



2

Plate 22: Pissolithic (1) and pisolithic to massive Fe-Ni ore (2), from Larymna, Lokris area. Transmitted light, // nicols X 40



1



2

Plate 23: Geonickel WorkPackage 1, Task 3: Intensive silicification, where the initial cellular structure has been maintained (1), and quartz islands (initial olivine) surrounded by garnierite aureoles in compact iron oxides (2). Profitis Ilias Fe-Ni deposit, Vermion, Greece

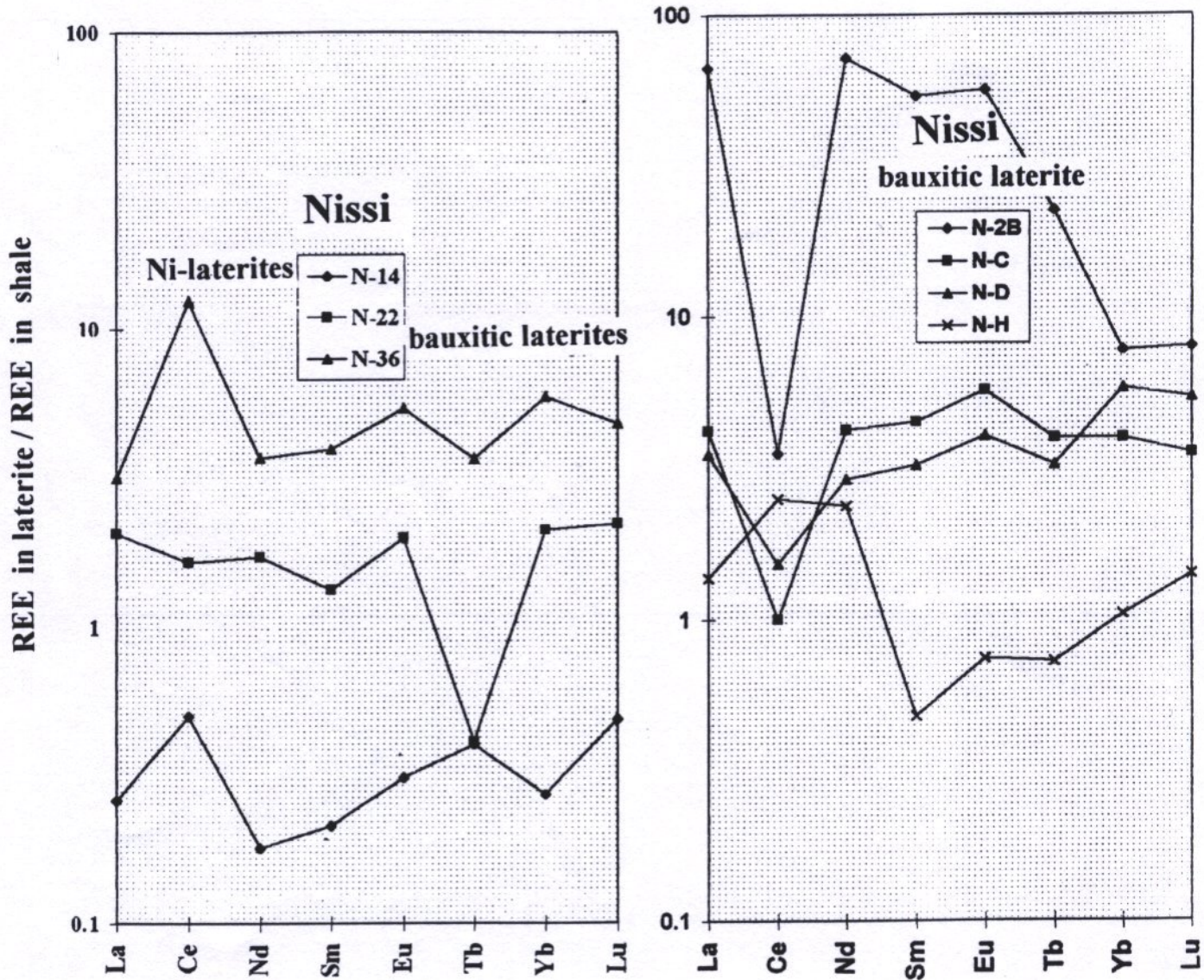


Plate 24: Geonickel WorkPackage 1, Task 3: REE in laterite/ REE in shale from the Nissi Ni-laterite and Bauxitic-laterite deposits.

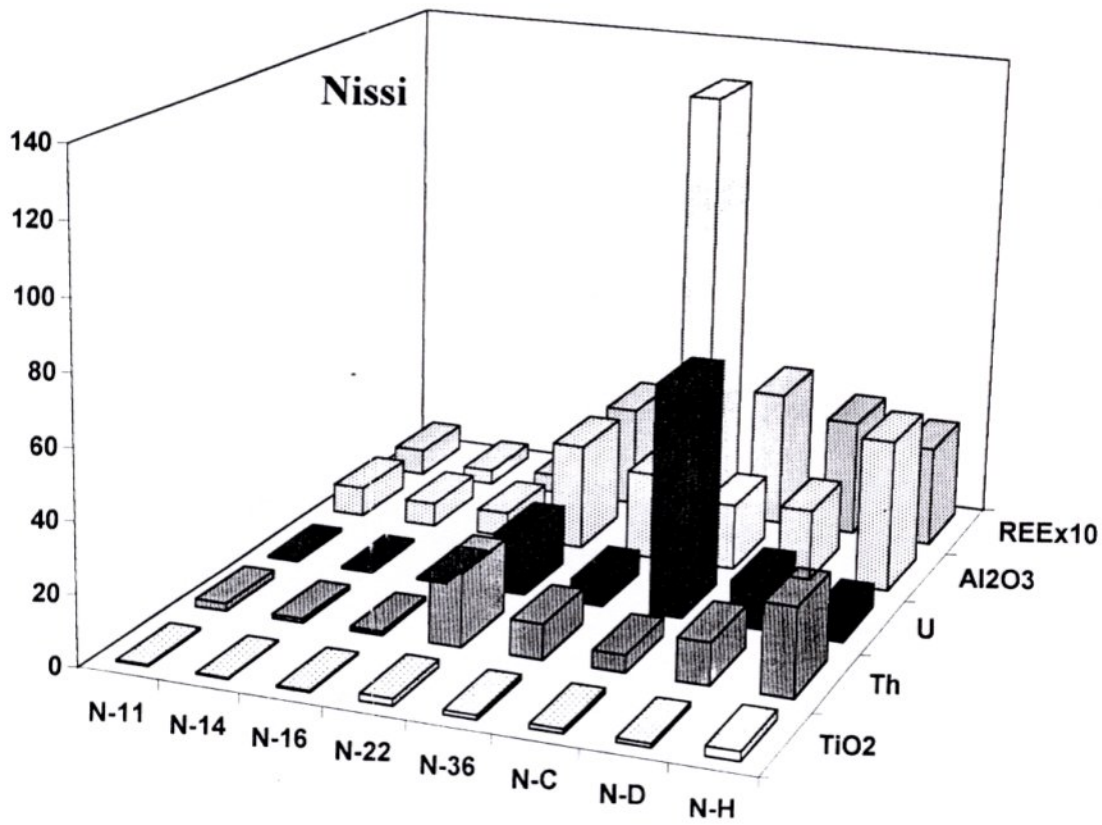
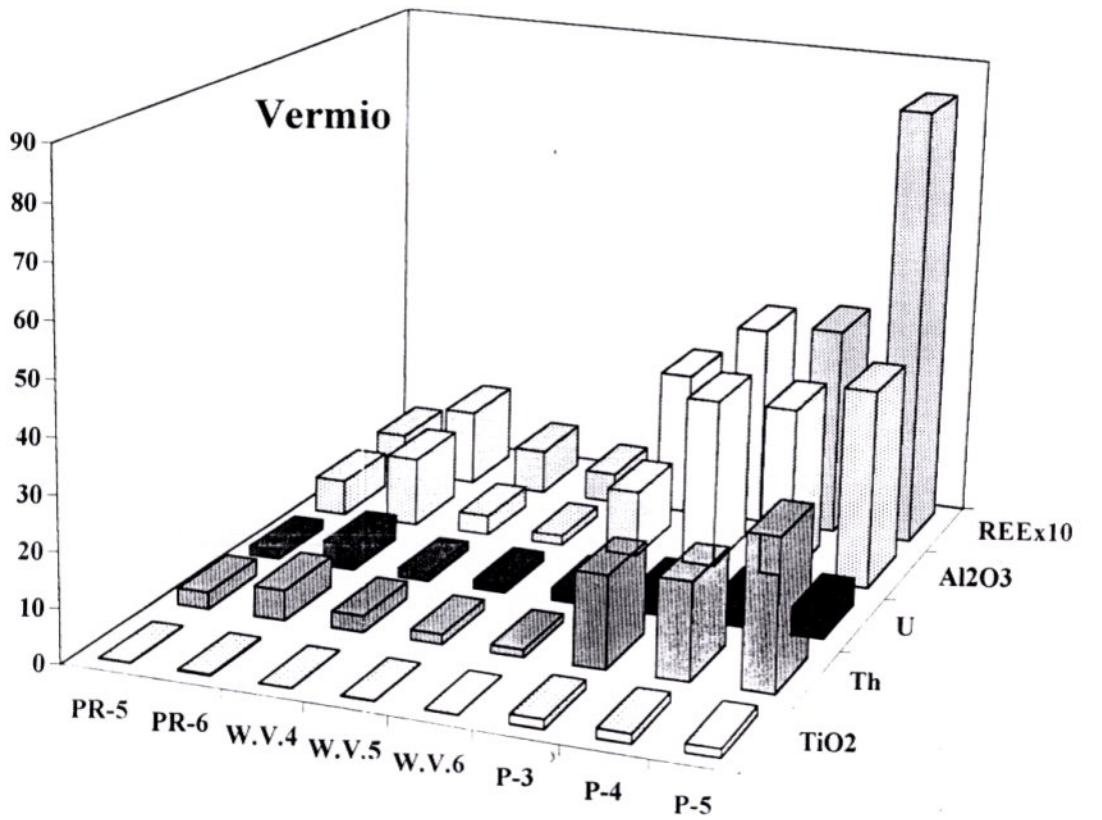


Plate 25: Geonickel WorkPackage 1, Task 3: Interelement correlation of REE, Al₂O₃, U, Th and TiO₂ in the Profitis Ilias (Vermion) Ni-laterite deposit and the Nissi bauxitic-laterite deposit

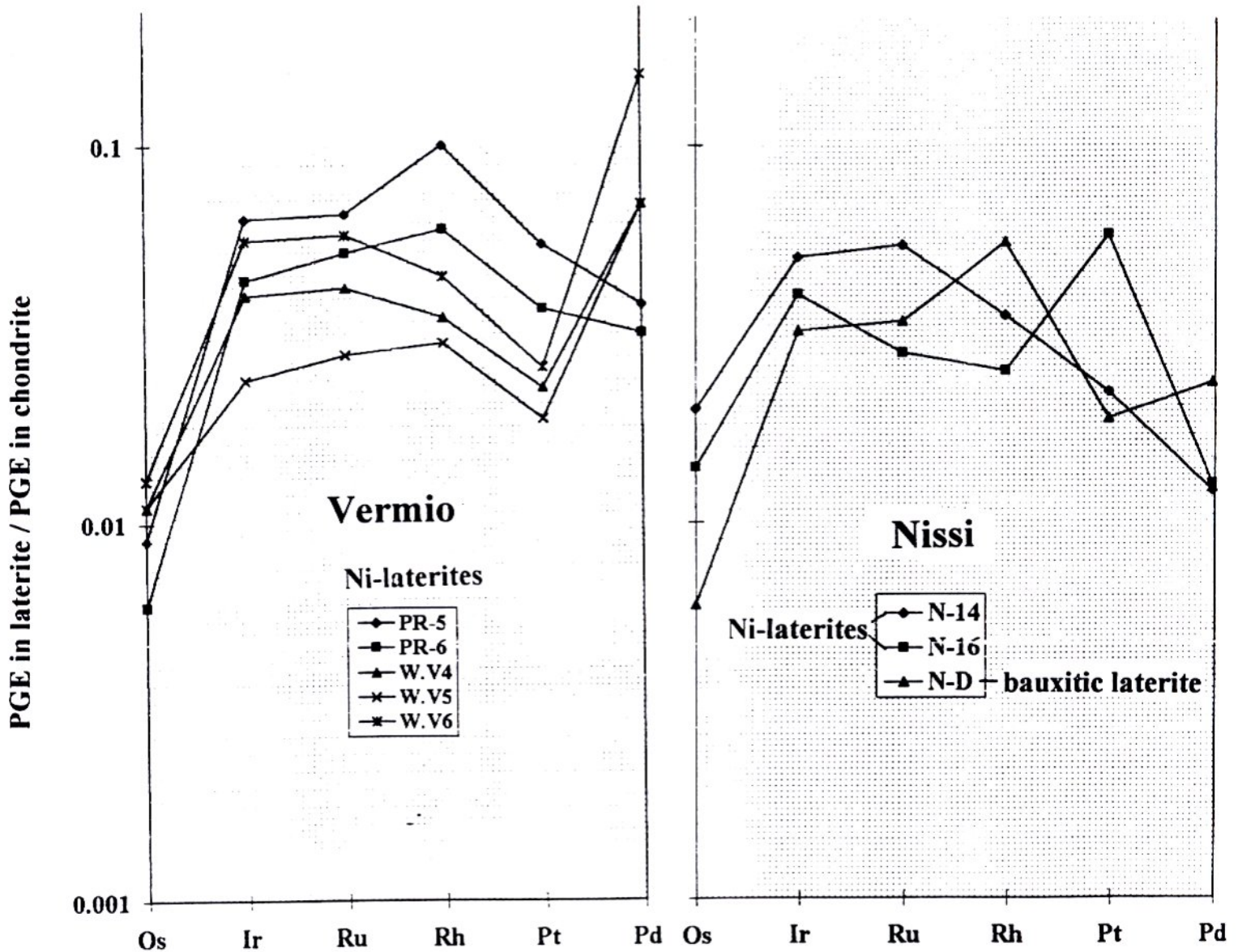


Plate 26: Geonickel WorkPackage 1, Task 3: PGE in laterite/PGE in chondrite for the Profitis Ilias Ni-laterite deposit (Vermion) and the Nissi Ni-laterite and Bauxitic-laterite deposits

GeoNickel

Annex 3

FINAL TECHNICAL REPORT

ANNEX 3

WP3 IMAGE PROCESSING / PATTERN RECOGNITION

~~CONFIDENTIAL~~

CONTRACT NO: BRPR-CT95-0052 (DG12 – RSMT)
PROJECT NO: BE – 1117
TITLE: Integrated Technologies for Minerals Exploration,
Pilot Project for Nickel Ore Deposits
GeoNickel

WP3
RESPONSIBLE: NCSR DEMOKRITOS,
Greece

PARTICIPATING
PARTNERS:

LARCO	General Mining and Metallurgical Company SA, Greece
IGME	Geological Survey of Greece Greece
OUTOKUMPU	Outokumpu Mining OY, Finland
GSFIN	Geological Survey of Finland Finland

STARTING DATE: 1st January 1996 DURATION: 36 MONTHS



PROJECT FUNDED BY THE EUROPEAN
COMMISSION UNDER THE BRITE/EURAM
PROGRAMME

Date: February 28, 1999

CONTENTS

WP3 EXECUTIVE SUMMARY	3-3
PROJECT STAFF.....	3-4
3. IMAGE PROCESSING AND CLASSIFICATION SOFTWARE.....	3-5
3.1 Objectives.....	3-5
3.2 Means Used to Achieve the Objectives.....	3-5
3.3 Scientific and Technical Description.....	3-7
3.3.1 Data Acquisition, Quality Evaluation and Preprocessing.....	3-7
3.3.1.1 Lateritic Data.....	3-7
3.3.1.2 Sulphidic Data.....	3-8
3.3.2 Software Overview.....	3-8
3.3.3 Artificial Neural Network – Fuzzy Classif. Methods & Software.....	3-9
3.3.3.1 Program Structure and Assumptions.....	3-9
3.3.3.2 Program Operation.....	3-10
3.3.3.3 Description of Classification Methods Included in ANNGIE.....	3-10
3.3.4 Advanced Statistical Methods and Software.....	3-12
3.3.4.1 Program Structure and Assumptions.....	3-13
3.3.4.2 Tasks of ASM.....	3-13
3.3.4.3 Restrictions.....	3-14
3.3.4.4 Missing Values.....	3-14
3.3.4.5 Description of the Statistical Methods.....	3-15
3.3.5 Delineation of Lineaments.....	3-19
3.3.6 Evaluation of the Software.....	3-21
3.3.6.1 Evaluation on Lateritic Data.....	3-21
3.3.6.2 Evaluation on Sulphidic Data.....	3-21
3.4 Initially Planned Activities and Work Accomplished.....	3-23
3.5 Conclusions.....	3-23
3.6 Acknowledgments.....	3-23
3.7 References.....	3-24
ANNEXES:	
Reports Issued (Excluding Reports to the Commission).....	3-27
Doctoral Theses.....	3-27
Conference Presentations.....	3-27
Demonstrations.....	3-28
Prototypes.....	3-28
Pictures 1-10.....	3-29

EXECUTIVE SUMMARY

Effort has been concentrated in developing advanced image processing, classification and pattern recognition techniques that can be used in order to assist geoscientists to locate important geological features related to Ni deposits.

As a result of this work, two software prototypes have been developed. Both packages receive as input ancillary data (geophysical, geological, satellite images) in the form of gridded data or images and can produce maps that classify each picture element or grid point into classes (bedrock type, type of ore, etc). Innovative methods recently developed by the information science partners are included in the software.

The first prototype (ANNGIE-Artificial Neural Networks for Geological Information Extraction) comprises a number of different algorithms and methods originating from the field of neural networks and fuzzy processing in order to carry out the classification task. A wide selection of both supervised and unsupervised methods is provided for the benefit of the end user, as well as a module that can combine results from different classifiers, in order to take advantage of their benefits and improve individual results. In addition, a module has been incorporated into ANNGIE that can be used to locate important linear structures (lineaments).

The lineament detection module utilizes the results of classification methods and postprocesses them using new image processing techniques in order to identify the required lineaments.

The second prototype (ASM-Advanced Statistical Methods) is also used for classification purposes and achieves its goal by employing advanced methods of statistical nature. A wide selection of supervised classification methods is provided by this prototype. Algorithms for efficiently performing Discriminant Analysis (DA) are incorporated in this module, including Empirical DA, Linear DA, Quadratic DA, Flexible DA and Penalized DA.

Both systems have been developed as a result of close collaboration between information scientists and geologists, and appropriate user interfaces have been designed and implemented to help the users select methods and related parameters in their effort to identify features of geological importance. Several of the methods included in the software prototypes are applied for the first time to data of geological interest. The software modules have been evaluated by the geo-expert partners, using appropriately preprocessed satellite, geological and geophysical data from selected areas of interest in Finland and Greece.

PROJECT STAFF**NCSR DEMOKRITOS**

Stavros J. Varoufakis
Stavros J. Perantonis
Nikolaos Vassilas
Nikolaos Ampazis
Eleni Charou
Vassilis Virvilis
Constantine Seretis
Theoharis Tsenoglou

Geological Survey of Finland

Nils Gustavsson
Markku Tiainen
Ilkka Suppala

IGME

Martha Stefouli
Anthony Angelopoulos

Outokumpu Mining OY

Jussi Aarnisalo.

LARCO:

Athanassios Apostolikas
Michael Melakis

FINAL TECHNICAL REPORT

Annex

WP3:Image processing/pattern recognition

3. IMAGE PROCESSING & CLASSIFICATION SOFTWARE

3.1. Objectives

The objectives of WP3 were to develop, implement and test conventional and new pattern classification and image processing techniques. These were to be used for processing of multisource (satellite, geophysical etc) data and applied for extracting and locating significant geological features related to Ni deposit detection. In particular, of interest were the identification of lithological regions and mineral alteration zones, as well as the delineation of lineaments. The workpackage activities focus on

- Collection of multisource information (remotely sensed, geophysical etc) from the selected test areas.
- Processing of collected information.
- Software development for classification of multisource data and lineament detection.
- Application of the software to the collected data.

3.2. Means Used to Achieve the Objectives

One of the most important phases of WP3 was the specification of the requirements for the image processing and pattern recognition software (ANNGIE and ASM). The decision on the selection of the individual modules that had to be included in the software was based on information about the particular characteristics of the nature of the problem. Following an extensive review in the literature covering already available methods, the major contribution to the acquisition of this information was a result of sessions between image processing and pattern recognition experts of NCSR Demokritos with geo-experts. These requirements consisted of the general knowledge about the Ni exploration task, the specification of available data types (satellite images, geophysical data, etc), and the process of how experts elaborate on these data in order to favour the existence or not of Nickel ore deposits.

During the sessions it was realized that the software should have been able to handle all the available data types, and to provide the users with a large variety of different pattern recognition methods (classifiers), since some methods were expected to perform well for a particular region covered by a particular data type (e.g satellite data), while others had the potential to produce better results for a data type (e.g geophysical data) covering a different region. Due to this variety of possibilities it was also decided that the software had to provide

the users with a multimodular classifier module that would be able to combine the results of individual classifiers in order to assist them in making their final decision.

Moreover, the needs of the users were taken as far as possible into account in the design of the user interface so that the user is able to access intermediate results (e.g. viewing of image histograms to aid the selection of thresholds in the lineaments detection phase) before the initiation of the next module. All this functionality is easily used and is integrated with the rest of the tools developed within GEOSIS, the geoinformation database system developed in WP4. What is more, a training set selection and extraction tool was jointly developed between NCSR and SOFTECO so that user sessions requiring definition of new training sets and recalculation of results are fully integrated and can be executed within the same session when deciding to switch between new training and test phases.

We achieved our final goals in the development of the software by following a *cyclic prototyping methodology* during the development phase. The first ANNGIE prototype had been released to users as early as the end of the first year. Our approach has resulted to many intermediate releases of ANNGIE that were important in order to decide which further tools had to be developed. For example, the development of the lineament extraction module was greatly affected by getting feedback from the users concerning the classification results of geophysical data. All these releases were tested, validated, and finally integrated with GEOSIS. This resulted in having the system evolved to something that could better suit the needs of its users. In retrospect, collaboration with the users enabled to refine the software. However, more regular data flow for testing the system in the intermediate stages would have helped increase its functionality.

To enable our approach to software development, we employed rapid development tools that still offered the flexibility we needed:

- C and Visual C++: ANNGIE makes use of these well known programming languages for Windows95/NT. All the individual classifier modules have been implemented in C which is probably the most suitable language for developing scientific computing applications. In addition the training set extraction tool was developed using Visual C++ in order to achieve rapid integration of the tool within GEOSIS.
- TCL/TK: The GUI (Graphical User Interface) of ANNGIE has been implemented with this versatile script language that allows efficient development of interfaces comprising menus, submenus, dialog and check boxes, graphics, help etc, so that the user is presented with a friendly and productive environment.
- ASM has been written in Fortran90 under Digital Visual Fortran Version 6.0A on Windows95/NT. The dialog boxes and graphics windows are generated using the non-standard *QuickWin* facilities of Digital Visual Fortran. Also some of MS-Windows API functions have been employed to improve the user-friendly behaviour of the program particularly in file selections. All graphics are generated with a few routines from the free graphics library PGPLOT.

The developed software belongs to the category of integrated image processing and pattern recognition systems, combining a wide range of geological and geophysical data. It can be used in conjunction with other information processing systems developed within *GeoNickel* for exploring Ni ore deposits and, to a greater extent than existing systems, since it places special emphasis to the integration of the different disciplines. It comprises a generic mechanism for the processing of the available data, provided, of course, that the user becomes familiar with the majority of processing options offered by the software.

3.3. Scientific and Technical Description

3.3.1. Data Acquisition, Quality Evaluation and Preprocessing

Effort has been concentrated on acquiring, evaluating and processing multisource data concerning areas with lateritic Ni deposits from Greece and with sulphidic Ni deposits from Finland. The data thus collected are used as input for evaluating the classification, pattern recognition and image processing algorithms developed in subsequent tasks.

3.3.1.1. Lateritic Data

Image processing techniques have been applied to Landsat TM, SPOT, ERS / SAR, images of the two test areas of study, Vermio and Lokris for: Removal of artifacts related to atmosphere. Rectification of the images. Reduction of the high inter-band correlation inherent to the reflected part of the spectrum through the decorrelation stretching of bands. Map variations in ferric - iron and clay mineral content after the assessment of ratio, IHS. and PCA / DPCA images. Filtering and edge detection techniques (high, low, edge, mode filters). Interpolation and co-registration of all data sets. Image integration.

Remotely sensed imagery have been interpreted in terms of geologic structures, lithology and mineralogical variations of the two test areas of study, Vermio and Lokris. The interpretations have been verified with the 1:50,000 scale geologic /topographic maps, and in the field. Maps of the interpreted lineaments have been produced, while directional / statistical analysis of the mapped patterns has been included.

The contribution of the remotely sensed data to the geologic and structural mapping of the pilot project areas is indicated with the processed satellite imagery. More structural features are depicted on the satellite images than the general 1:50,000 scale geologic maps. Generally, the use of the remotely sensed images in geologic map updating up to scales 1:25,000 lies in the fact that various geologic and mainly structural features can be mapped quickly for large areas. The time which is needed to delineate the general structure of the area and to mark lithological mineralogical features of interest is minimum relatively to that needed for the construction of a geological map and field mineralogical / lithological observation collection.

3.3.1.2. Sulphidic Data

The well-studied Vammala area in southwestern Finland was selected as one of the main test areas in the **GeoNickel** project. The test area covers 30 km x 40 km including the well-known Proterozoic intrusive type nickel deposits Vammala and Kylmäkoski. The Vammala nickel mine produced 7,6 Mt of ore grading 0,67 % Ni and 0,42 % of Cu during 1974 – 1994. The regional mapping data from the test area include geophysics, geochemistry, and Landsat TM data, compiled by GTK for software development purposes of the GeoNickel project. These data were distributed to all GeoNickel partners in *geosoft* (.grd), *geotiff* (.tif), Landsat bil (.bil) and ASCII formats depending on the original type of data. The geophysical data set includes airborne magnetic, electromagnetic in-phase and out-of-phase components, radiometric potassium, thorium, uranium and total components both in *geosoft* and *geotiff* formats. The Landsat data include six channels in .bil format, and the geochemical data are in ASCII format and consist of 33 elements (Ag, Al, As, Au, Ba, Ca, Co, Cr, Cu, Fe, K, La, Li, Mg, Mn, Mo, Na, Ni, P, Pb, Pd, Sb, Sc, Sr, Te, Th, Ti, V, W, Y, Yb, Zn, Zr) analyzed from the fine fraction of 294 composite till samples (sampling density 1 sample/4 km²).

3.3.2. Software Overview

In the context of GeoNickel, software has been developed for the classification of objects of geological interest and for the delineation of lineaments.

Classification methods are useful for grouping objects of data sets into unknown and given classes. In the context of **GeoNickel** the objects to be classified are grid points or pixels. In general a pattern is the vector of values of variables associated to an object. A supervised classifier attempts to assign objects (e.g. pixels) into previously defined classes and an unsupervised classifier groups the objects into previously unknown classes. Supervised methods force patterns into classes (bedrock type, type of ore, etc.) defined by user while unsupervised methods reveal the natural groups of the patterns and the classes are designed during the run. The supervised methods need a training set in which class representatives are assigned to respective classes.

For the delineation of lineaments, new image processing methods have been developed in the course of the project.

As mentioned before, two software packages have been produced in the course of GeoNickel WP3. The first system (ANNGIE – Artificial neural networks for geological information extraction) implements classification techniques based on neural networks and fuzzy classifiers and also incorporates the new methodologies for the delineation of lineaments. The second system (ASM-Advanced Statistical Methods) comprises advanced statistical classification methods. Both modules are invoked from GEOSIS, the integrated software developed in Work Package 4.

3.3.3. Artificial Neural Network – Fuzzy Classification Methods and Software

3.3.3.1 Program Structure and Assumptions

The classification part of the ANNGIE software includes data type converters, feature extraction modules, individual classifiers and a module for combining the power of individual classifiers. A graphical representation of the methods included in this software is shown in Figure 1. Documentation is available for the ANNGIE software in the form of a user’s manual that describes the various techniques and their use, the parameters that the user has to provide as well as useful tips for optimal utilization of the routines. Only general aspects are mentioned here.

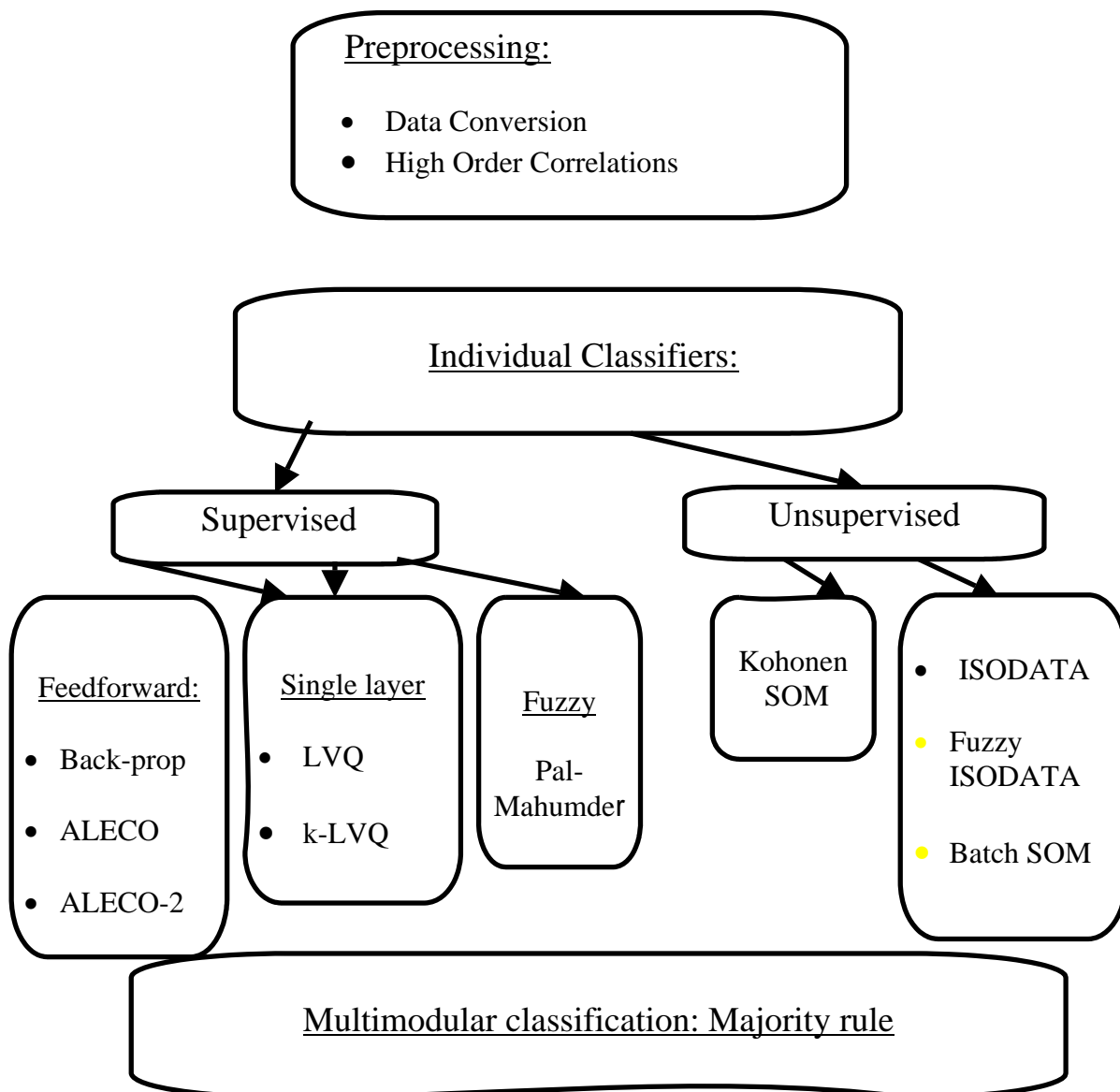


Figure 1: Diagram of the methods included in the neural networks based classification software.

ANNGIE classifies only pixels (image elements). The patterns to be classified consist of intensity values input from image files which are all assumed to cover exactly to the same area. There is no control for this requirement in the software, except that ANNGIE reports a severe error and stops if the number of pixels in consecutive input files is unequal in either dimension.

For the application of supervised classification methods, the training data set is also composed of data generated from images only through training areas defined in GEOSIS. For the selection of training sets, a training set selection module has been incorporated in GEOSIS. It is based on the mouse driven selection of polygons on an image and the specification by the user of the category (e.g. lithology) to which pixels in each polygon belong.

3.3.3.2. Program Operation

The program proceeds in two phases (training or testing phase). In the training phase:

- (1) the training data set (one file) is read (only for supervised methods);
- (2) Preprocessing of the data set may be selected (e.g. using high order correlations)
- (3) the classification method and respective configuration parameters are chosen from dialog boxes;
- (4) the selected classifier is trained using the specified configuration;

In the testing phase:

- (1) A set of images (different bands from the same geographical area), part of which may have been used for training, is selected and possibly preprocessed; In this stage, ANNGIE handles TIFF, PGM and GRD image types.
- (2) The trained classifier is used to classify data from the specified image and produces a file, which contains the class indices in PGM format (same as in ANN).
- (3) For improving individual results, different classifiers can be combined using a multimodular classification option.

A screenshot of ANNGIE in operation is shown in Picture 1.

3.3.3.3. Description of Classification Methods Included in ANNGIE

Individual classification modules include both supervised and unsupervised algorithms. A new feature for achieving orders of magnitude of speedup at the classification stage (especially when repetitive classification is necessary for fixing the optimum number of clusters) is provided through an optional output file format (CGF format) used for indexed representation of the original data in compressed form.

The following unsupervised classification methods are included in the ANNGIE software:

Variants of the Learning vector quantization (LVQ)

The original learning vector quantization paradigm was proposed by Kohonen (1989). A new family of algorithms supported in the current version of the software, namely the k -LVQ algorithms, generalizes the LVQ algorithm by adapting at each iteration the k -nearest reference vectors to the input pattern, provided not all k reference vectors (for $k > 1$) belong to the same class for stable learning (Vassilas et al., 1997). Classification of a new pattern is performed by assigning to it the label of the majority of its k -nearest reference vectors. The LVQ algorithm is the special case with $k = 1$.

Variants of the Backpropagation algorithm

These types of algorithms are used to train feedforward multilayer neural networks. Apart from the original Backpropagation algorithm introduced by Rumelhart et al. (1986), two improved algorithms (ALECO and ALECO-2), which are based on constrained optimization techniques, are included. These usually achieve much faster and more efficient performance in large-scale classification problems (Perantonis and Karras, 1995; Karras and Perantonis, 1995).

Pal-Majumder fuzzy classifier

This type of classifier has been proposed by Pal & Majumder (1977). A comprehensive description can be found in Pao (1989). This is a non-adaptive (one-step training) classification algorithm whereby, the training set is fuzzified using a (user selected) parametric bell-shaped membership function and then, new, similarly fuzzified, test patterns are classified to that category to which their fuzzy similarity score (computed from class similarities relative to each dimension of the pattern space) is maximum.

Multimodular classification

After individual supervised classification methods have been applied, a multimodular classification architecture becomes available to the user. This has been developed for the integration of the individual decisions is based on voting schemes that use absolute or relative majority rules. This architecture allows the combination of classification results from many individual classifiers, so that the final classification is made more accurate and trustworthy.

The following unsupervised classification methods have been also included in ANNGIE:

Classification based on self organizing maps (SOM)

This is a module based on the Self Organizing Map (SOM) neural algorithm for vector quantization (Kohonen, 1989; Kohonen, 1995) followed by neuron clustering using either a hierarchical min-max procedure (Duda & Hart, 1973) or the Fuzzy ISODATA algorithm (Bezdeck, 1976) before the final classification result is produced. The SOM is an adaptive-competitive algorithm used to optimally quantize the pattern space through 1-D or 2-D lattices of neurons, whereby, a sequence of inputs is randomly presented to the network (map) and its synaptic weights are then updated so as to reproduce the input probability distribution as closely as possible. The weights self-organize in the sense that neighboring neurons respond to neighboring inputs (the space is given topological properties through the Euclidean

distance similarity metric) and tend toward asymptotic values that quantize the input space as well as possible. Following quantization, the user can apply the clustering algorithms on the relatively few prototypes (assigned to the neurons of the map) rather than to the original voluminous data set. In this way, even the highly demanding hierarchical min-max algorithm can be used for clustering. This algorithm would require more than 100 years to run directly on a 3-band, 512x512 image, on a SUN Sparc II workstation.

Fuzzy ISODATA algorithm

This method (Bezdeck, 1976; Pao, 1989) is an iterative algorithm that can be used as an independent automatic classification method although much slower and memory demanding than the method using the SOM. This algorithm produces a fuzzy partition of the data space by assigning each input pattern (or data point) to several clusters through the degrees of membership to those clusters. This partition is represented in the form of a fuzzy partition matrix.

Batch SOM algorithm

This method (Kohonen, 1995) includes as a special case the standard ISODATA algorithm (Duda & Hart, 1973). The Batch SOM algorithm can be considered as a combination of the SOM algorithm and the standard Isodata. This iterative algorithm, assumes progressively less overlapping clusters until the final crisp partition, whereby, the cluster centers correspond to the reference vectors associated with the units of a 1-D or 2-D map. At no cluster overlapping, this algorithm is transformed to the standard Isodata algorithm.

An example of supervised classification of lithological units (using ALECO-2 applied on satellite data) from the Vermion area is shown in Picture 2.

3.3.4. Advanced Statistical Methods and Software

The objective of work in *GeoNickel* related to the statistical methods was to complement the ANN- and fuzzy methods with probabilistic methods considering the random fluctuation of measurements. The goal was to prepare existing code and write some totally new code for integration in GEOSIS. The ASM software generated for GeoNickel must, however, be considered a prototype in the sense that the graphics and user interface are not fully developed and tested, but the software body handling the methods is running satisfactorily.

ASM includes five methods for solving the supervised classification problem:

- the linear discriminant analysis (LDA)
- the quadratic discriminant analysis (QDA)
- the penalized discriminant analysis (PDA)
- the flexible discriminant analysis (FDA)
- the empirical discriminant analysis (EmpDA)

Each method has advantages and disadvantages depending on the dimension of patterns and the amount of training data. EmpDA, for example, uses all the training data as parameters in

the classifier and therefore large training sets yield slow classification. All methods can, however, be run in almost all situations. Depending on the current classification problem the user is recommended to choose the method according to the following scheme:

Table I: Methods recommended in various classification problems.

<i>Dimensionality</i>	<i>Amount of training patterns</i>	<i>Recommended method(s)</i>
Low	Small	LDA, QDA, PDA, FDA, EmpDA
Low	Large	LDA, QDA, PDA
High	Small	PDA, EmpDA
High	Large	PDA

If two or more variables are strongly correlated neither LDA nor QDA are recommended. The other methods are insensitive to correlation conditions.

3.3.4.1 Program Structure and Assumptions

Details of the program structure and assumptions of ASM can be found in the User's Manual of ASM (Gustavsson & Suppala, 1999) (deliverable from *GeoNickel*). Only general aspects are mentioned here.

Similarly to ANNGIE, ASM classifies pixels (image elements). The patterns to be classified consist of intensity values input from image files, which are all assumed to cover exactly to the same area. There is no control for this requirement in the software, except that ASM reports a severe error and stops if the number of pixels in consecutive input files is unequal in either dimension.

The training data set is also composed of data generated from images only through training areas defined in GEOSIS. As a consequence ASM handles only those image file types which are specified for the training data generation: TIF, PGM, GRD. ASM as integrated to GEOSIS always assumes that the training data file exists and has a specific format (See the ANNGIE manual).

Browsing directories, and selecting and saving files, are done using MS-Windows API functions and therefore they behave exactly as in any MS-Windows program.

The program proceeds as follows:

- (1) the training data set (one file) is read, checked and statistics are reported by class;
- (2) the raw data set (one variable/file) to be classified is selected and briefly checked;
- (3) the classification method and respective parameters are chosen from dialog boxes;
- (4) A set of output files specific to the selected method are created, one of which contains the class indices in PGM-format (same as in ANNGIE).

3.3.4.2 Tasks of ASM

ASM proceeds with the following steps:

- open the handshaking dialog box and provides alternatives for training data input;
- search and analyze the training data

- report the class specific statistics
- select the raw data input files (one file/variable) of types: TIFF, PGM, and GRD;
- select a classification method among Empirical Discriminant Analysis (EmpDA), Linear Discriminant Analysis (LDA), Quadratic Discriminant Analysis (QDA), Flexible Discriminant Analysis (FDA), and Penalised Discriminant Analysis (PDA);
- choose appropriate output files (depend on methods selected);
- view the classification result.

3.3.4.3 Restrictions

Most arrays are dynamically allocated implying that the actual memory of the computer will cause restrictions. The array containing the training patterns is held in the memory (and may be swapped). Some of the arrays are not dynamically allocatable and have been restricted according to method (see method descriptions). The restrictions mentioned in Table II are due to definitions in the source program. The source must be modified recompiled and linked if any of these restrictions are changed.

Table II: Restrictions in the ASM software (releasing needs changes in code).

<i>Method</i>	<i>Max. number of variables</i>	<i>Max. number of training patterns</i>	<i>Max. number of classes</i>	<i>Max. number of input files</i>
LDA, QDA, PDA, FDA	36	10000	15	36
EmpDA	20	30000	10	20

3.3.4.4. Missing values.

All patterns are not necessarily complete because some measurements may fail or be invalid. A missing value is introduced by a dummy value given by the user at run-time or defined in the header description of an input file. Even one missing value in a pattern causes the pattern to be skipped in the classification.

A skipped pattern is labeled 0 in the resultant class file allowing the user to separate between unknowns and unclassified items on viewing the results.

Internally all missing values are coded according to the IEEE 1985 standard for quiet NaN (not a number) in real 4-byte presentation. All input data are transformed to 4-byte reals independent of original type (incl. signed and unsigned integers).

No procedure for filling in values for missing data has been implemented. If the number of missing values becomes disastrous for the classification, something should be done with the data: reducing ill-behaving variables, screening out bad training areas or subsets, or inserting values using an auxiliary program.

3.3.4.5. Description of the Statistical Methods

The statistical methods implemented in ASM are all supervised and need a training (design) set of patterns for teaching the classifier making it able to recognize similar patterns in unknown data sets. Before classifying unknown patterns the user must define a training set containing a reasonable number of representative patterns for each class. The supervised classification procedure proceeds as follows:

- choice of classes and collection of training sets
- checking the quality of the training data
- teaching the classifier to recognize patterns in the classes
- checking the performance of the classifier using a test set or subsets of the training set
- classification of unknown patterns.

Empirical Discriminant Analysis (EmpDA)

EmpDa is a nonparametric and nonlinear supervised method based on the Bayes classification rule where prior probabilities are involved and misclassification is penalised with a loss value for each class. The Bayes rule minimizes the expected overall loss and is optimal in that sense. The conditional probability density of a class is estimated from the training data by the kernel method (Parzen's window). Early descriptions of EmpDA, also called Kernel Classifier, Potential Function Method, or Parzen's Classifier, were reported by Specht (1967). Applications in the geosciences are reported by Howarth (1971), Howarth (1973), and Gustavsson&Björklund (1976). Specht (1990) noticed that EmpDA can be defined as a probabilistic neural network. A thorough theoretical description of this and other statistical pattern recognition methods can be found in Fukunaga (1990).

The only assumption for EmpDA is that the variables must be numeric and scaled on the ratio scale permitting arithmetics of the values. Because EmpDA is nonparametric nothing is assumed about the conditional density and normality, for example, is not required even if the kernels may be Gaussian. The conditional density distributions may be even multimodal. Nothing is assumed about the shapes of the classes or if they form connected clusters. This means that that classes can be folded in each other and may consist of multiple subgroups scattered anywhere in the variable space. This is not true for the linear discriminant analysis, for example.

The prior probabilities must be known or somehow estimated. Usually they are assumed equal, but can be proportional to the number of training patterns per class or subjectively entered by user knowing them from earlier experience.

Few assumptions are an advantage in practical applications where the data rarely behave according to theoretical laws. On the other hand, few assumptions may lead to weak classification performance because the data are free to vary. In the kernel method all the training data are parameters in the estimates of the class densities making the classification of large data sets computationally heavy. Powerful computers have made EmpDA a more attractive choice than in the 1970's.

For the implementation of the Bayes decision criterion, estimation of prior probabilities and conditional densities must be carried out. The prior probabilities can be known from earlier experience, assumed equal, or estimated as simple proportions $P_i = n_i / n$ where n_i is the number of training patterns in class i and n the total number of training patterns. For the estimation of conditional densities, a kernel method is used, with a Gaussian kernel density centered at each training pattern with a given spread or uncertainty characterized by the standard deviation σ . The software provides two methods for estimating this parameter, namely:

- σ is entered by the user (knowing the uncertainty of the data);
- σ is derived through an iterative procedure where the classifier is applied repeatedly on the test set or the unknown set and the percentage of unclassified is retained; at every step σ is increased until the number of unclassified is less than a given percentage.

Estimating the performance of the classifier. The performance of the classifier is here tested using the training set by the *leave-one-out method* explained in Fukunaga (1990) or Blayo et al. (1995), for example. In the leave-one-out method the classifier is designed using $n-1$ of the n training patterns and the one left out is classified. Each training pattern is left out in turn and the average classification rates are presented in the *confusion matrix*. Also the total *error rate* is reported. The confusion matrix shows how the misclassified patterns are distributed and which classes are more confused than others. If a test set is available the confusion matrix is computed from the test patterns.

Another matrix showing the confusion between the decision by EmpDA and the class of the nearest training pattern is also generated with the final classification of the unknown set.

Variants of Discriminant Analysis by Multivariate Regression

This work is based on the papers published by Hastie, Tibshirani and Buja: *Flexible Discriminant Analysis by Optimal Scoring* (1994) and *Penalised Discriminant Analysis* (1995). They combine parametric/nonparametric regression techniques with discriminant analysis. Linear discriminant analysis (LDA) is a simple and well known and understood method. The basic idea is to find a low dimensional projection of the original data such that in resulting space the ratio of between-class variation and within-class variation is the largest. It assumes that the classes are multivariate Gaussian populations with the same within-class covariance structure. The decision boundaries in classification are linear. Regardless of its limitations it is one suitable statistical feature extraction and dimension reduction method. It has been used to preprocess the raw data before actual classification (e.g. Blayo et al. 1995). It could be used also as a visualizing and image processing tool like principal component analysis (PCA).

Regression analysis is one choice to solve a classification task. Important is that new advanced nonparametric regression methods have been published to handle more realistic problems (e.g. Friedman, 1991; Kooperberg et al., 1997). In statistical literature methods have been changed to be adaptive, nonparametric and learning, they have similarities with neural networks methods.

Hastie et al. (1994, 1995) pointed out the relationship between LDA, canonical correlation

analysis and optimal scoring. Optimal scoring contains linear least squares regression as a building block. They generalized LDA by using (in optimal scoring) other types of regression. For example using multiresponse nonparametric regression in their procedure (below) one can handle better complex and nonlinear class boundaries. Hastie et al. call the method Flexible Discriminant analysis (FDA).

Procedure for FDA by optimal scoring

Measurements $\mathbf{x} = (x_1, \dots, x_p) \in R^p$ is presumed to be a member of one of J groups (classes) $\mathbf{x} \in \{G_j\}_1^J$. Let \mathbf{X} be $n \times p$ matrix of observations, and let \mathbf{Y} be $n \times J$ indicator matrix, the ij th element of \mathbf{Y} is 1 if the i th observation falls in class j , and 0 otherwise.

1. Initialize: Θ_0 is $J \times K$ matrix $K \leq J$ satisfying the constraints $\Theta_0^T \mathbf{D}_p \Theta_0 = \mathbf{I}_K$ ($K \times K$ identity matrix), $\mathbf{D}_p = \mathbf{Y}^T \mathbf{Y} / n$, a diagonal matrix of sample class proportions n_j / n . $\Theta_1 = \mathbf{Y} \Theta_0$.

2. Multivariate nonparametric/parametric regression: Fit a multiresponse regression of Θ_1 on \mathbf{X} , fitted values $\Theta_1^* = \mathbf{S}(\lambda^*) \Theta_1 = \mathbf{n}(\mathbf{X}) = \mathbf{h}(\mathbf{X}) \mathbf{B}$ (in linear regression $= \mathbf{X} \mathbf{B}$).

3. Optimal scores: Obtain the eigenvector matrix Φ of $\Theta_1^T \Theta_1^* = \Theta_1^T \mathbf{S}(\lambda^*) \Theta_1$.

4. Update: The final model is attained (from step 2) using the optimal scores:
 $\mathbf{n}(\mathbf{x}) = \boldsymbol{\eta}(\mathbf{x}) \Phi$.

5. Classify: Assign an observation \mathbf{x}_i to the class j that minimises $\delta_\pi(\mathbf{x}_i, j) = \|\mathbf{D}(\mathbf{n}(\mathbf{x}_i) - \bar{\mathbf{n}}^j)\|_2 - 2 \log \pi_j$, \mathbf{D} is the diagonal matrix of scale factors, $\bar{\mathbf{n}}^j = \sum_{G=j} \mathbf{n}(\mathbf{x}_k) / n_j$ and π_j is the prior of class j .

Linear discriminant analysis (LDA)

The programmed methods (LDA, QDA, PDA, FDA) follow the above simplified procedure. LDA is done by fitting in step 2 a multiresponse linear least squares regression of Θ_1 on \mathbf{X} . The model of fitted values is now $\Theta_1^* = \mathbf{X} \mathbf{B}$. The matrix of linear coefficients \mathbf{B} ($p \times K$) is solved using the LAPACK Fortran subroutine *dgels* (Anderson et al., 1992). It computes the minimum norm solution to the linear least squares problem using the singular value decomposition (SVD).

Restrictions in the program are not caused by this option. If the design matrix \mathbf{X} is (nearly) singular it is better to use option PDA, but in principle that case can be handled by SVD.

Quadratic discriminant analysis (QDA)

The basic ideas in all these methods are the same and already mentioned: maximize the between-class scatter while minimizing the within-class scatter. In QDA we presume that the class populations are again multivariate Gaussian but now they can have different covariance structures. The class boundaries are quadratic. Here QDA is done by augmenting the predictor set to include also quadratic and bilinear terms and then performing the LDA in the enlarged space. Linear coefficients \mathbf{B}_q ($p_{\text{new}} \times K$) are solved by SVD (*dgels*).

If p is large the dimension of \mathbf{B}_q ($((1+p+p+p!)/((p-2)! \times 2!)) \times K$) can cause problems.

Numerically that case could be handled by SVD, but there could be too many parameters to fit to get meaningful classification results. It could need some regularisation like in PDA. In program the allowed maximum value of p_{new} is set (incidentally 121). LDA and QDA are so called conventional statistical methods. If the model assumptions are somehow met they will work well. But it is easy to generate problems where they are worse than some new “advanced” method.

Penalised discriminant analysis (PDA)

In ill-posed linear inverse problems (like in regression analysis) some kind of regularization has been long used to get acceptable result (see O’Sullivan, 1986). Regularization means (e.g.) that some constraints are applied in inversion to reduce the generalization error. Problem can be in the same manner ill-posed in LDA, if we use many highly correlated predictor variables and not enough observations. E.g. Friedman (1989) uses ridge-type regularization to stabilize the within-class covariance matrix. The use of regularization in classification is even more obvious if we use regression in classification like in the FDA-procedure above.

Hastie et al. (1995) use in PDA penalised regression (inversion) with Laplacian penalty. They classify one channel image data (hand written characters) and profile data (speech frames), so they want spatially smooth prototypes penalising with second derivatives (differences). Here the option PDA use in step 2 only ridge-type penalty (penalising with $\lambda \|\mathbf{B}\|^2$). In ridge regression the design matrix \mathbf{X} is first decomposed by SVD ($\mathbf{X}=\mathbf{U}\mathbf{D}\mathbf{V}^T$ by Lapack, *dgesvd*) so that the solution is easily calculated using different λ values: $\mathbf{B}(\lambda) = \mathbf{V} (\mathbf{D}^2 + \lambda\mathbf{I})^{-1} \mathbf{D} \mathbf{U}^T \mathbf{\Theta}_1$. Optimal λ could be find using test data set. Hastie et al. use instead of λ a more meaningful parameter that is the effective degree of freedom (*df*) (see Buja, Hastie and Tibshirani, 1989). Loosely speaking it measures how many parameters (degrees of freedom) have been fitted to the data (Frank and Todeschini, 1994). If \mathbf{X} is a $n \times p$ matrix, then $0 \leq df \leq p$. Buja et al. (1989) define $df(\lambda) = \text{tr}(\mathbf{D}^2 + \lambda\mathbf{I})^{-1} \mathbf{D}$.

Restrictions in the program are not caused by this option.

The default degrees of freedom are estimated from the dimension of the problem. The default value usually gives satisfactory results.

Flexible discriminant analysis (FDA/MARS)

The actual FDA uses in step 2 some multiresponse nonparametric regression method. Hastie et al. (1994) use BRUTO and MARS. BRUTO is an additive-spline model with smoothness penalty in data space, so it corresponds to a form of penalised discriminant analysis. Here is used only MARS, that is a procedure of Multivariate Adaptive Regression Splines presented by Friedman (1991). The procedure is explained also by Hastie et al. (1994) and Kooperberg et al. (1997). In short it first tries to overfit the data building adaptively by forward stepwise process a piecewise linear spline model. Then the backward pruning procedure is applied to the model removing the least important terms one at a time. Kooperberg et al. (1997) have made a POLYMARS algorithm, which should be much faster than what here is used.

The model of fitted values is now $\Theta_1^* = \mathbf{h}(\mathbf{X})\mathbf{B}$, where the basis expansion $\mathbf{h}(\mathbf{X})$ is build up adaptively by MARS. In MARS model ($\mathbf{h}(\mathbf{X})\mathbf{B}$) maximum interaction allowed between the variables is controlled by the parameter *degree*. A first-degree model is additive (no interaction terms), a second-degree model allows pair-wise interactions between variables, and so on. Maximum *degree* allowed in program is 3. It is possible to get information about importance of variables from the MARS model (Friedman, 1991), but we haven't yet tried to utilized that. Keeping the degree 1 or 2 makes the interpretation easier and probably makes the model to generalize better.

FDA/MARS is computational much more expensive than LDA, QDA and PDA. Restrictions in the program are mainly put considering the space and CPU time that FDA/MARS option can need. The program has been tested using ELENA test data *satimage* (Blayo et al., 1995), which have specified the maximum values of dimensions and parameters. The preliminary *satimage* results using FDA/MARS are substantially equal good as the best ones in that report. Better results are nevertheless published by Hastie and Tibshirani (1996), who use their Discriminant Adaptive Nearest Neighbour classification method.

3.3.5. Delineation of Lineaments

A novel method for the delineation of lineaments has been incorporated into ANNGIE. Starting from images corresponding to ancillary data from the areas of interest, we first perform an unsupervised classification using a self organizing map. As was observed using images obtained from gridded magnetic and electromagnetic (real and imaginary) data, categories with a relatively small number of pixels correspond to significant linear formations. Therefore, a threshold is imposed on the classification map. In the resulting black and white image, only categories with a small number of pixels are kept as foreground, with the rest of the categories considered as background. At this stage, usually many linear formations are present, along with regions that do not correspond to linear formations.

At this stage, further processing is needed, whose task is to extract the significant information corresponding to lineaments from the unwanted information corresponding to correlated or uncorrelated noise. To this end, we have originally applied variants of the Hough transform (Duda and Hart, 1972), which is a well known method for detecting linear formations in the presence of noise and has been applied with some success to the delineation of lineaments (Wang and Howarth, 1990). However, we noted that in most data sets related to this project, interference from unwanted pixels was very prominent.

A novel method which has been developed at NCSR for detecting linear formations in highly noisy images proved much more successful for the delineation of lineaments. According to this method, the image is decomposed into connected regions following a fast, one pass, label assignment procedure which is outlined in Sonka, Hlavac and Boyle (1994). While in the original Hough transform all foreground pixels contribute the same amount to all accumulator array points that correspond to lines passing through them, our method achieves preferential weighting of certain pixels by introducing a suitable voting kernel, which depends on shape descriptors of the connected regions of the image. In particular, to form the voting kernel, we take into account the elongation of each connected region, its area and the angle formed by a

candidate linear formation and the principal axis of the region. The method is successful in removing both correlated and uncorrelated noise and find lines and prevalent orientations in very noisy images (Perantonis et al., 1998).

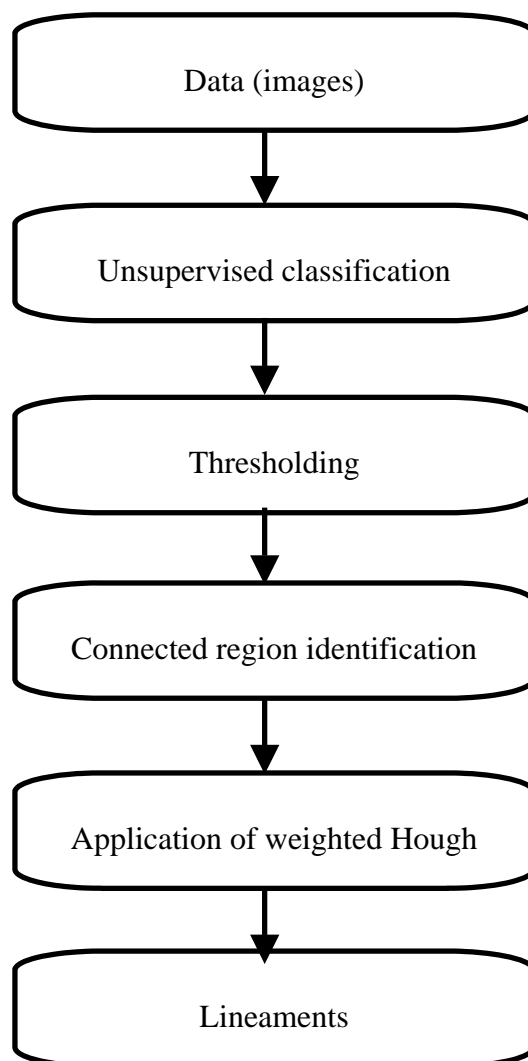


Figure 6: Outline of the procedure for the delineation of lineaments.

The whole procedure for the delineation of lineaments (application of self organizing map for unsupervised classification, suitable thresholding and application of the novel line detection method-see Figure 2) has been programmed in C and compiled using Microsoft Visual C++. It has been integrated into ANNGIE and can be executed by the end users using a friendly menu driven graphical user interface programmed in Tcl/Tk. Documentation is also provided for the use of the corresponding routines.

The method has been applied with success starting from different combinations of geophysical (airborne magnetic and electromagnetic) data from the Vammala area. In Picture 3, the lineaments found by our method are seen superimposed on classification results obtained using unsupervised SOM classification of geophysical data.

3.3.6. Evaluation of the Software

3.3.6.1. Evaluation on Lateritic Data

The lateritic data used in evaluating WP3 software are 50 m resolution Landsat TM images, for the Lokris area of study. Although a complete evaluation of supervised algorithms was not performed, training sets were selected, using the *Training Set Definition* tool of GEOSIS, from the above data in order to test if the developed classification techniques are running well under GEOSIS. All algorithms (supervised & unsupervised) are running well and the output is produced in TIFF (8bit gray level) and PGM formats.

A single run of the ANNGIE unsupervised techniques has been included during the evaluation sub-task. Processing times are short, and well within the limits of similar algorithms running on other image processing systems. The result is shown in Picture 4. The result has been imported to an external image processing system for adding a color palette, geo-referencing and comparison with the information depicted on the 1:50,000 scale geologic map. The created color maps of the result of the unsupervised techniques are shown in Picture 5, while those overlaid by the geologic map in Picture 6. A qualitative comparison shows that the most meaningful results have been obtained with the SOM classifier (Lower right image of Pictures 7 to 9).

3.3.6.2. Evaluation on Sulphidic Data

Test configuration

Both supervised and unsupervised classification/pattern recognition methods have been evaluated by an exploration geologist with airborne geophysical data sets, that have been used in nickel exploration applying conventional image processing methods. The tested methods have been developed by NCSR and GSF, and integrated to GEOSIS. The methods were developed to classify TIFF images in non-earth referenced coordination. The training sets were defined by the Training set definition tool of Geosis, that is based on the polygon drawing tool of MapInfo.

This discussion is an evaluation of the methods from the end user's viewpoint and is based on classifications of airborne geophysical magnetic and electromagnetic in-phase and out-of-phase data sets on the 30 km x 40 km (601 x 801 pixels) Vammala area that include two old intrusive type nickel mines and several uneconomic Ni deposits. The training sets were selected for five main lithological types and a mineral deposit type in the area: mica gneiss, graphite-sulphide bearing schists, granitoids, gabbro, peridotite and nickel deposit. They were selected according to the geological maps from the surroundings of the Vammala Ni deposit. The same training sets were applied for all supervised classification methods. The data sets were classified into six classes also by unsupervised methods to compare the classification results with the supervised methods.

Methods

Supervised Classification methods. ANNGIE includes three types of classification methods,

LVQ, Multilayer neural networks and Fuzzy classifiers. ASM includes LDA, PDA, QDA, FDA and EmpDA methods.

The classification results of LVQ (Picture 7), Fuzzy classifiers and EmpDa (Picture 8) resemble each other. LVQ and EmpDA have perhaps more clear lithological patterns, whereas LVQ classifies mainly anomalies that differ clearly from the data, like graphite-sulphide bearing schists. The results of QDA and FDA (Picture 9) are quite similar to each other and the classification patterns of QDA and FDA resemble the patterns of LVQ.

The study area can be classified applying supervised classification methods with airborne magnetic and electromagnetic data sets into ore geologically interesting and less interesting areas by using lithological training sets, some classifiers produce classification patterns, but with these data sets and training sets the lithological classifications are not reliable. More work in the selection of the training sets and classification parameters are needed than was done in this test. Only graphite-sulphide bearing schists are reliably shown by most methods. The use of gravity data in addition to these data sets would already lead to more meaningful results.

Unsupervised classification methods. ANNGIE includes three unsupervised classification methods: Kohonen SOM, Fuzzy ISODATA, and Batch SOM algorithm. By classifying the three data sets into six classes the most obvious lithology, graphite-sulphide bearing schists were defined. The result of Kohonen SOM by six classes (Picture 10) resembles that of PDA of ASM. By increasing of number of classes in Kohonen SOM classification, probably more interesting results in the viewpoint of nickel exploration would be achieved. More detailed testing of the unsupervised classification methods with different options, for example changing the number of classes, requires however more time than was possible to use for this test. The results of these short tests indicate that by using some other data sets in addition to the used data sets, like geochemistry and gravity data and geologically significant derivatives calculated from the original data, more interesting classes could be defined.

Conclusion

The classified data sets are too few to get results that correlate with the known geology. The graphite bearing sulphide schists are the only lithological unit that can be found by all methods. The petrophysical properties of all other lithologies in the study area are so much overlapping with each other that the classification results cannot be geologically reliable. The use of more training data polygons around the whole area and with more detailed lithological classification of the training sets would enable better results by supervised methods. Also the use of more classes about fifteen classes or more, the unsupervised methods would give more interesting results than with the used six classes. The use of gravity data, its derivatives and other geological variables like metamorphic grade as additional variables would probably lead to clearly better lithological classification results. The developed methods are interesting new tools for the exploration geologist. There is still room for refinement by more closely complying to specialized requirements of the end users, exploration geologists. It should be possible to use normal georeferenced geodata formats in addition to TIFF. The classification of point data could be made possible. For example geochemistry data include tens of variables and it would be very interesting to apply these new methods with that data set. Legends and

reports that explain the classification results would make easier for the geologist to interpret the classification results.

3.4. Initially Planned Activities and Work Accomplished

There were no substantial deviations from the original plan.

3.5. Conclusions

Two software prototypes have been developed for assisting geologists to identify important geological features related to Ni deposits. These prototypes have been integrated into GEOSIS and can be applied for rock type classification and geomorphological structure identification.

Regarding the methods used to achieve the objectives of the project, the first prototype (ANNGIE-Artificial Neural Networks for Geological Information Extraction) comprises a number of different algorithms and methods originating from the field of neural networks and fuzzy processing. Innovative algorithms recently developed by the information science partners are included in the software. In addition, a module has been incorporated into ANNGIE that can be used to locate important linear structures (lineaments). The second prototype (ASM-Advanced Statistical Methods) is also used for classification purposes and achieves its goal by employing advanced methods of statistical nature. Close collaboration between information scientists and geologists led to the design and implementation of the user interfaces for selecting methods and related parameters for each task.

The software modules have been evaluated by the geo-expert partners, using appropriately preprocessed satellite, geological and geophysical data from selected areas of interest in Finland and Greece. Several methods included in the software were applied for the first time to the geoscientific field. It was found that the developed methods are interesting new tools for the exploration geologists and are able to extract information useful to the exploration of Ni deposits. Evidently, there is still room for future refinement of the prototype software. Significant improvements could be made by adding the true georeferencing of data, extending the allowed geodata formats to those normally used in GIS and image processing systems, and by adding also point data to the suite of data types allowed in the classification. Application of the novel methods to real exploration problems also calls for further familiarization of the geologists with the newly developed tools. It is important, however, that ANNGIE and ASM are advanced new information science products, now available to the geoscientists and capable of processing the ever increasing amount of remotely sensed data in regional and local scale.

3.6. Acknowledgments

Our thanks to all the partners, geo-scientists and computer scientists that collaborated for building ANNGIE and ASM.

3.7. References

- Anderson, E., Bai, Z., Bischof, C., Demmel, J., Dongarra, J., Du Croz, J., Greenbaum, A., Hammarling, S., McKenney, A., Ostrouchov, S., and Sorensen, D., 1992: *LAPACK Users' Guide*, SIAM, Philadelphia, 235 p.
- Bezdeck, J.C., 1976: A physical interpretation of fuzzy ISODATA, *IEEE Transactions on Systems, Man and Cybernetics*, Vol. 6, pp. 387--389.
- Blayo, F., Cheneval, Y., Guérin-Dugué, A., Chentouf, R., Aviles-Cruz, C., Madrenas, J., Moreno, M., and Voz, J.L., 1995: ELENA, Enhanced Learning for Evolutive Neural Architecture. *ESPRIT Basic Research Project Number 6891*. Deliverable R3-B4-P, Task B4: Benchmarks.
- Buja, A., Hastie, T., and Tibshirani, R., 1989: Linear smoothers and Additive Models (with discussion), *The Annals of Statistics*, 17, 453B555.
- Duda, R. D. and P.E. Hart., 1973: *Pattern Classification and Scene Analysis*. Wiley: New York.
- Duda, R. D. and P.E. Hart., 1972: Use of the Hough transform to detect lines and curves in pictures, *Commun. ACM*, Vol. 15, pp. 11-15.
- Frank, I.E., and Todeschini, R., 1994: *The data analysis handbook*, Amsterdam, Elsevier, 365 p.
- Friedman, J., 1989: Regularized discriminant analysis, *Journal of the American Statistical Association*, 84, 165B175.
- Friedman, J., 1991: Multivariate Adaptive Regression Splines (with discussion), *The Annals of Statistics*, 19, 1B141.
- Fukunaga, K., 1990: *Introduction to Statistical Pattern Recognition*. Second Edition. Academic Press, Inc.. 1990.
- Gustavsson, N., Björklund, A., 1976: Lithological classification of tills by discriminant analysis. *Journal of geochemical exploration* 5 (3), p. 393-395.
- Gustavsson, N. and Suppala, I., 1999: Documentation of Software for Advanced Statistical Classification Methods (ASM). User's Manual. *Unpublished deliverable in the GeoNickel Project BRPR CT 0052 (DG 12 RSMT)*.
- Hastie, T., Tibshirani, R., and Buja, A., 1994: Flexible Discriminant Analysis by Optimal Scoring, *Journal of the American Statistical Association*, 89, 1255-1270.
- Hastie, T., Buja, A., and Tibshirani, R., 1995: Penalized discriminant analysis, *The Annals of Statistics*, 23, 73B102.

- Hastie, T., and Tibshirani, R., 1996: Discriminant Adaptive Nearest Neighbor Classification, *IEEE Trans. Pattern Analysis and Machine Intelligence*, 18, no. 6, 607B615.
- Howarth, R.J., 1971: An Empirical Discriminant Method Applied to Sedimentary-Rock Classification from Major-Element Geochemistry. *Math. Geol.* Vol 3., No. 1, 1971.
- Howarth, R.J., 1973: FORTRAN IV Programs for Empirical Discriminant Classification of Spatial Data. *Geocom Bull.*, 6: 1-31.
- Karras, D.A. and S. J. Perantonis, 1995: An efficient training algorithm for feedforward networks, *IEEE Tr. Neural Networks*, Vol. 6, pp. 1420-1434.
- Kohonen, T., 1989: *Self-Organization and Associative Memory*. Springer-Verlag: Berlin-Heidelberg-New York-Tokyo, 3 ed..
- Kohonen, T., 1995: *Self-Organizing Maps*. Springer-Verlag: Berlin-Heidelberg-New York-Tokyo.
- Kooperberg, C., Bose, S., and Stone, C.,J, 1997: Polychotomous Regression, *Journal of the American Statistical Association*, 92, 117B127.
- O'Sullivan, F., 1986: A Statistical Perspective on Ill-posed Inverse Problems, *Statistical Science*, 1, 502B527.
- Pal, S. K. and D. D. Majumder, 1977: Fuzzy sets and decision making-approaches in vowel and speaker recognition, *IEEE Transactions on Systems, Man and Cybernetics*, Vol. 7, pp. 625-629.
- Pao, Y.-H., 1989: *Adaptive Pattern Recognition and Neural Networks*. Addison-Wesley.
- Perantonis, S.J. and D. A. Karras, 1995: An efficient learning algorithm with momentum acceleration, *Neural Networks*, Vol. 8, pp. 237-249.
- Perantonis, S. J., N. Vassilas, Th. Tsenoglou and K. Seretis, 1998. Robust line detection using weighted region based Hough transform. *Electronics Letters* 34(7), 648-650.
- Rumelhart, D.E., J.E. Hinton and R.J. Williams, 1986: Learning internal representations by error propagation, in *Parallel Distributed Processing: Explorations in the Microstructures of Cognition*, vol. 1, Foundations, D. E. Rumelhart and J. L. McClelland, Eds. Cambridge, MA: MIT Press, pp. 318-362.
- Sonka, M., V. Hlavac, and R. Boyle, *Image Processing, Analysis and Machine Vision*. London: Chapman and Hall, 1993.
- Specht, D.F., 1967: Generation of polynomial discriminant functions for pattern recognition: *IEEE Trans. Electr. Computers*, Vol. 16, p. 308-319.

Specht, D.F., 1990: Probabilistic neural networks. *Neural Networks*. Vol 3, 109-118.

Vassilas, N., E. Charou and S. Varoufakis, 1997: Fast and efficient land-cover classification of multispectral remote sensing data using artificial neural network techniques. *In Proc. 13th Int'l Conference on Digital Signal Processing (DSP97)*: Santorini, pp. 995-998, June 1997.

Wang and P. J. Howarth, 1990: Use of the Hough transform in automated lineament detection, *IEEE Transactions on Geoscience and Remote Sensing*, Vol. 28, No. 4, pp. 561- 566.

ANNEXES

Reports Issued (Excluding Reports to the Commission)

1. Varoufakis, S. J., Vassilas, N., Perantonis, S.J., Ampazis, N., Virvilis, V., Charou, E., Seretis, K., and Tsenoglou, Th., 1998: Documentation for ANNGIE Classification and Lineament Detection Software, User's Manual.
2. Varoufakis, S. J., Vassilas, N., Perantonis, S.J., Ampazis, N., Virvilis, V., Charou, E., Seretis, K., and Tsenoglou, 1997: NCSR Maps of ANNGIE Classification Results and Extracted Lineaments from Geonickel Areas of Interest.
3. Gustavsson, N. and Suppala, I., 1999: Documentation of Software for Advanced Statistical Classification Methods (ASM). User's Manual.
4. Stefouli, M., 1997: Preliminary Report, WP3 (Task 3.1, Satellite and Other Data Acquisition, Quality Evaluation and Image Processing).
5. Stefouli, M., 1999: Technical report. WP3 Image Processing/Pattern Recognition, Satellite and Other Data Acquisition, Quality Evaluation and Image Processing.
6. Stefouli, M., 1999: WP3 Evaluation Report.
7. Tiainen, M., 1999: Evaluation of the Classification and Pattern Recognition Methods by an Exploration Geologist.

Doctoral Theses

1. E. Charou, 1999: Design and Exploitation of Advanced Methods for the Extraction of Lineaments and Land Cover Classification from Satellite Images. University of Athens, Department of Geology, in progress.

Conference Presentations

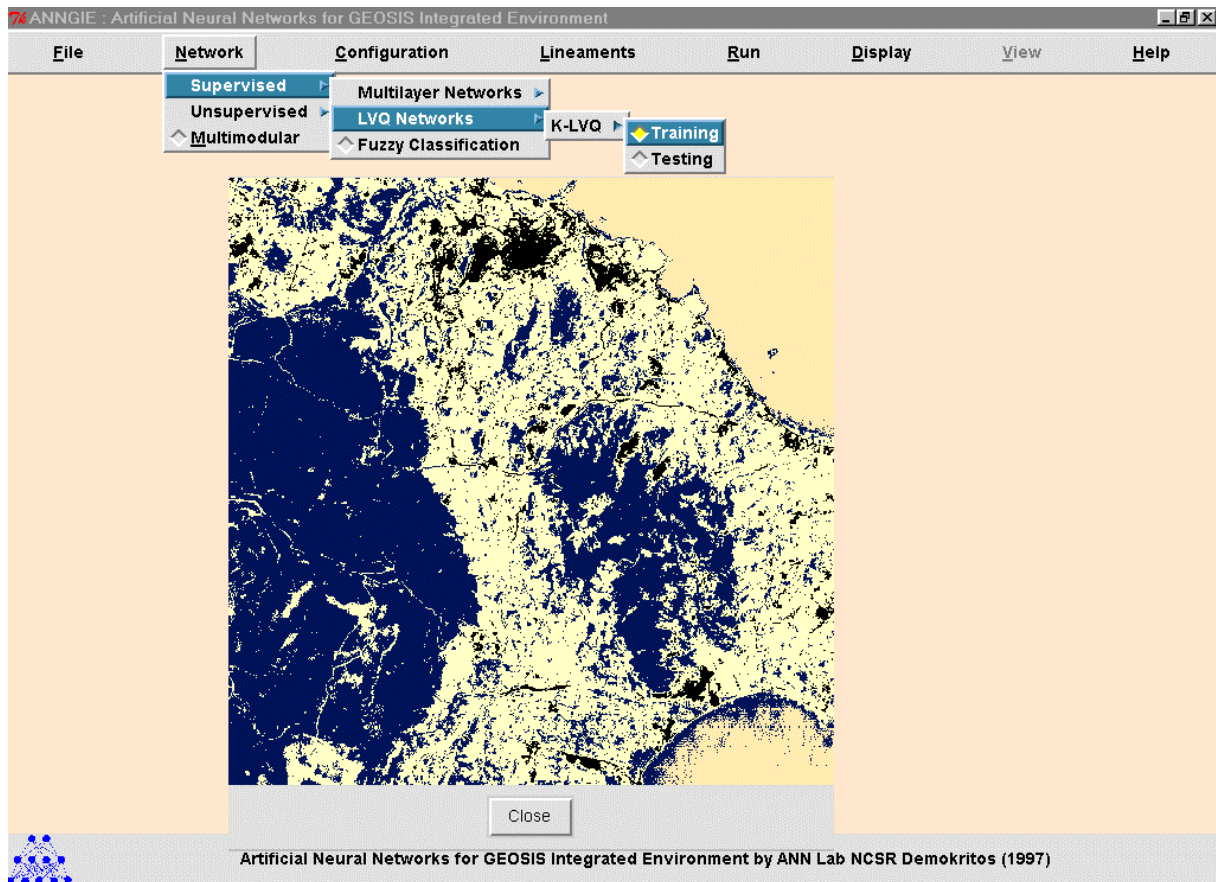
1. Vassilas, N., Charou, E. and Varoufakis, S., 1997: Fast and Efficient Land-Cover Classification of Multispectral Remote Sensing Data Using Artificial Neural Network Techniques, in *Proc. 13th Int'l Conference on Digital Signal Processing (DSP97)*, Santorini, pp. 995-998.

Demonstrations

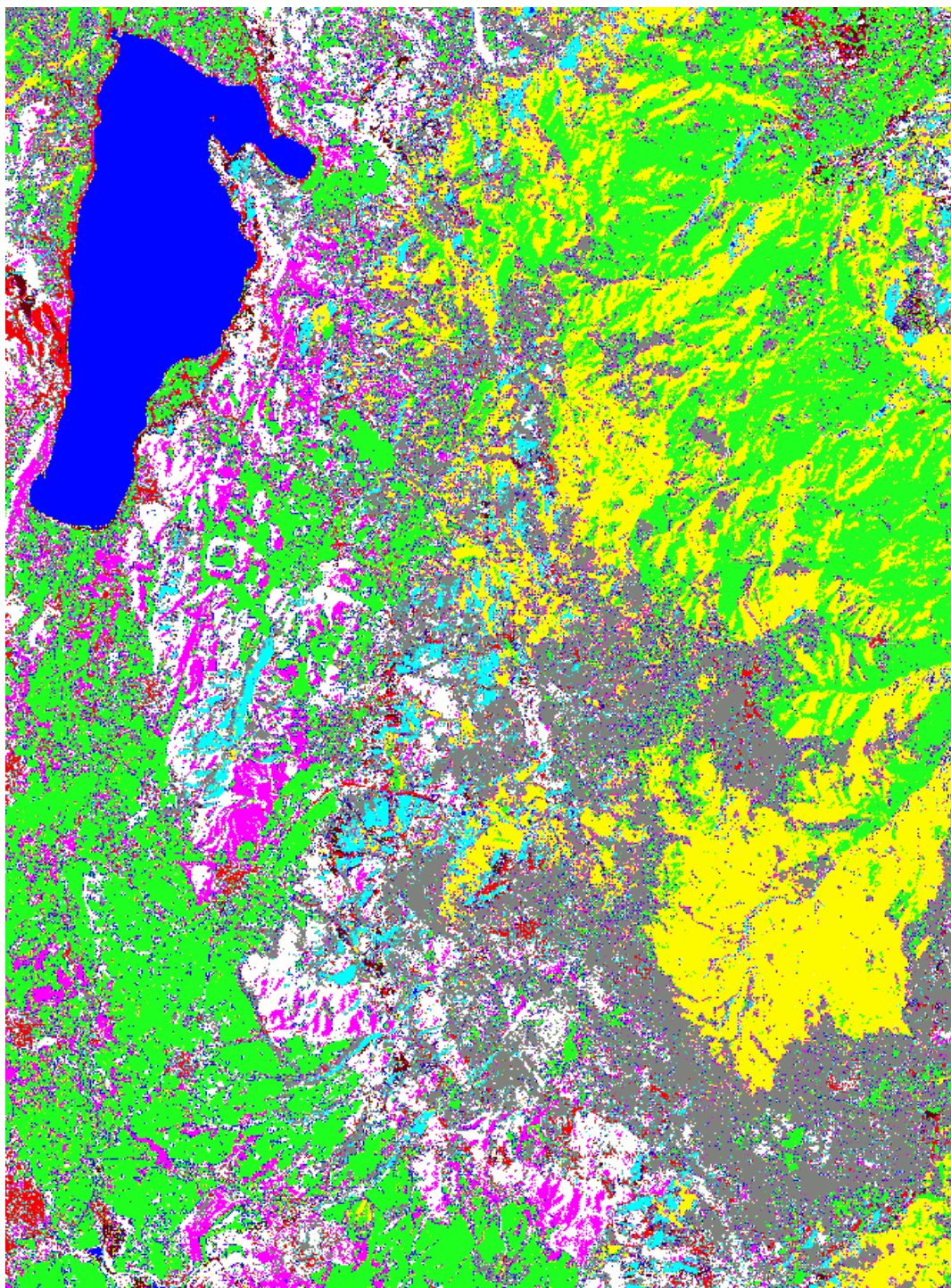
1. Presentation at INFOWORLD'98 Exhibition, Athens, May 1998.

Prototypes

1. ANNGIE software prototype– Artificial Neural Networks for Geological Information Extraction
2. ASM software prototype – Advanced Statistical Methods



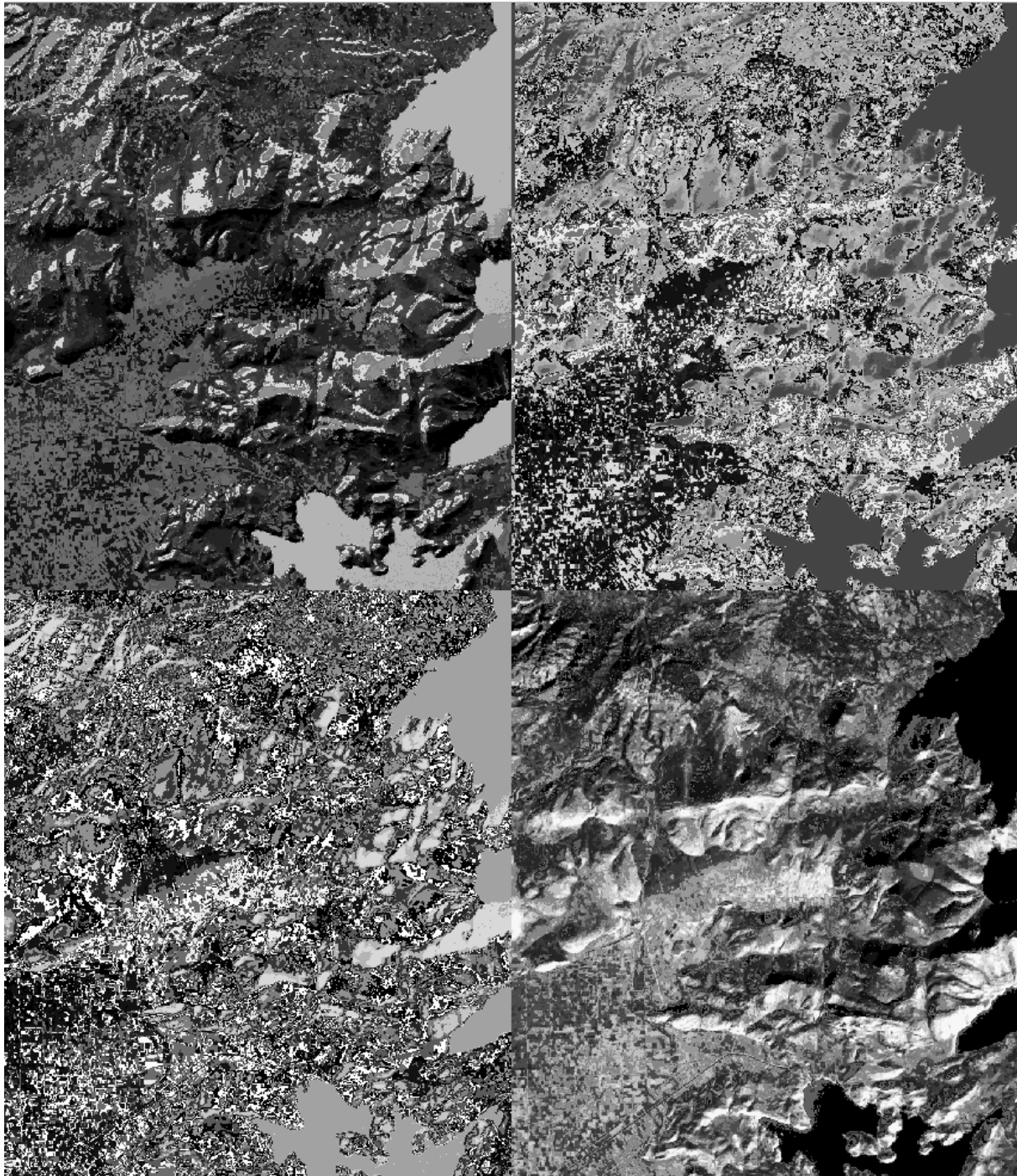
Picture 1: A screenshot of ANNGIE in operation. The algorithm selection menu is activated.



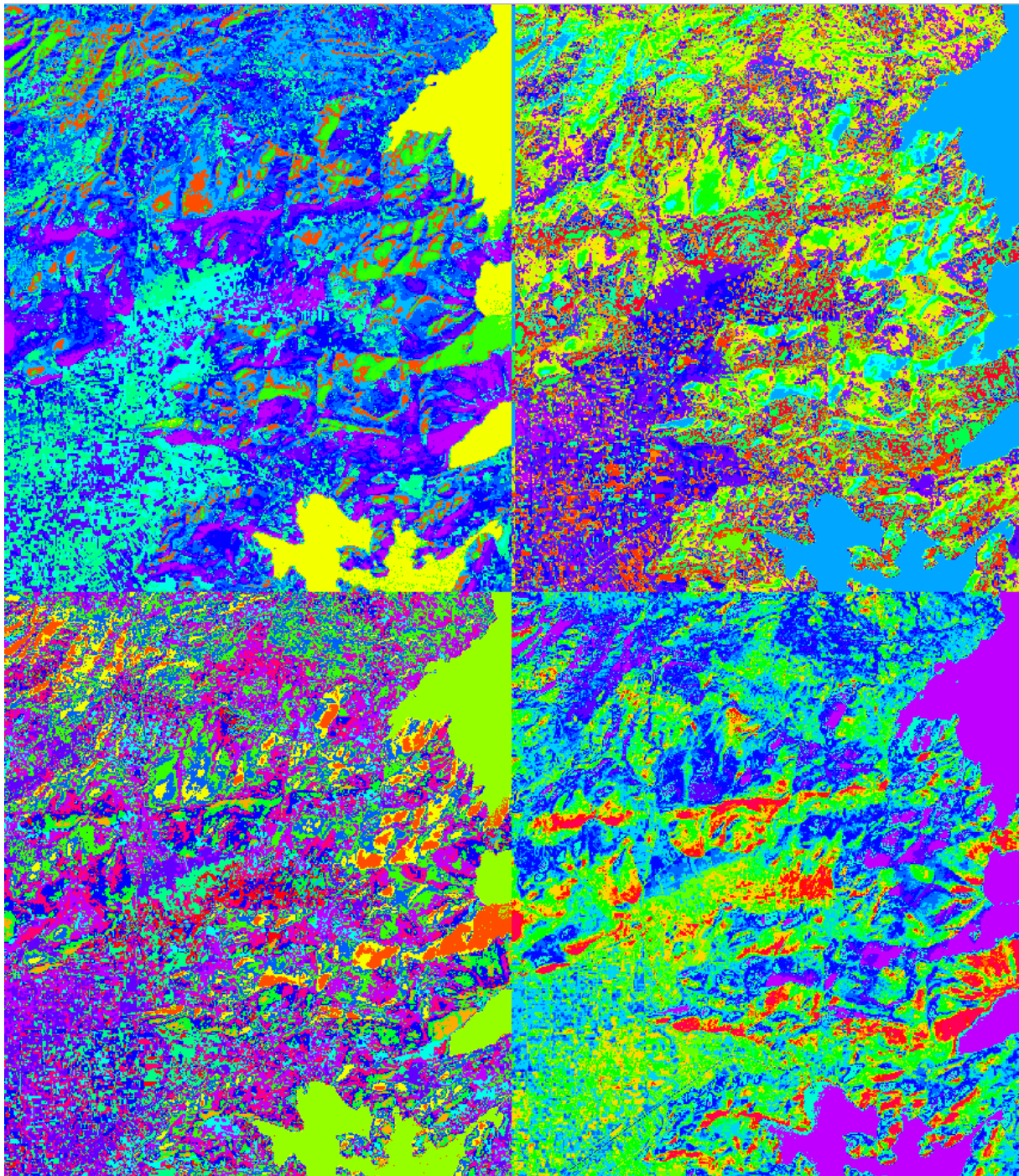
Picture 2: Supervised lithological classification of Vermion area from satellite data using the ALECO-2 algorithm available in ANNGIE.



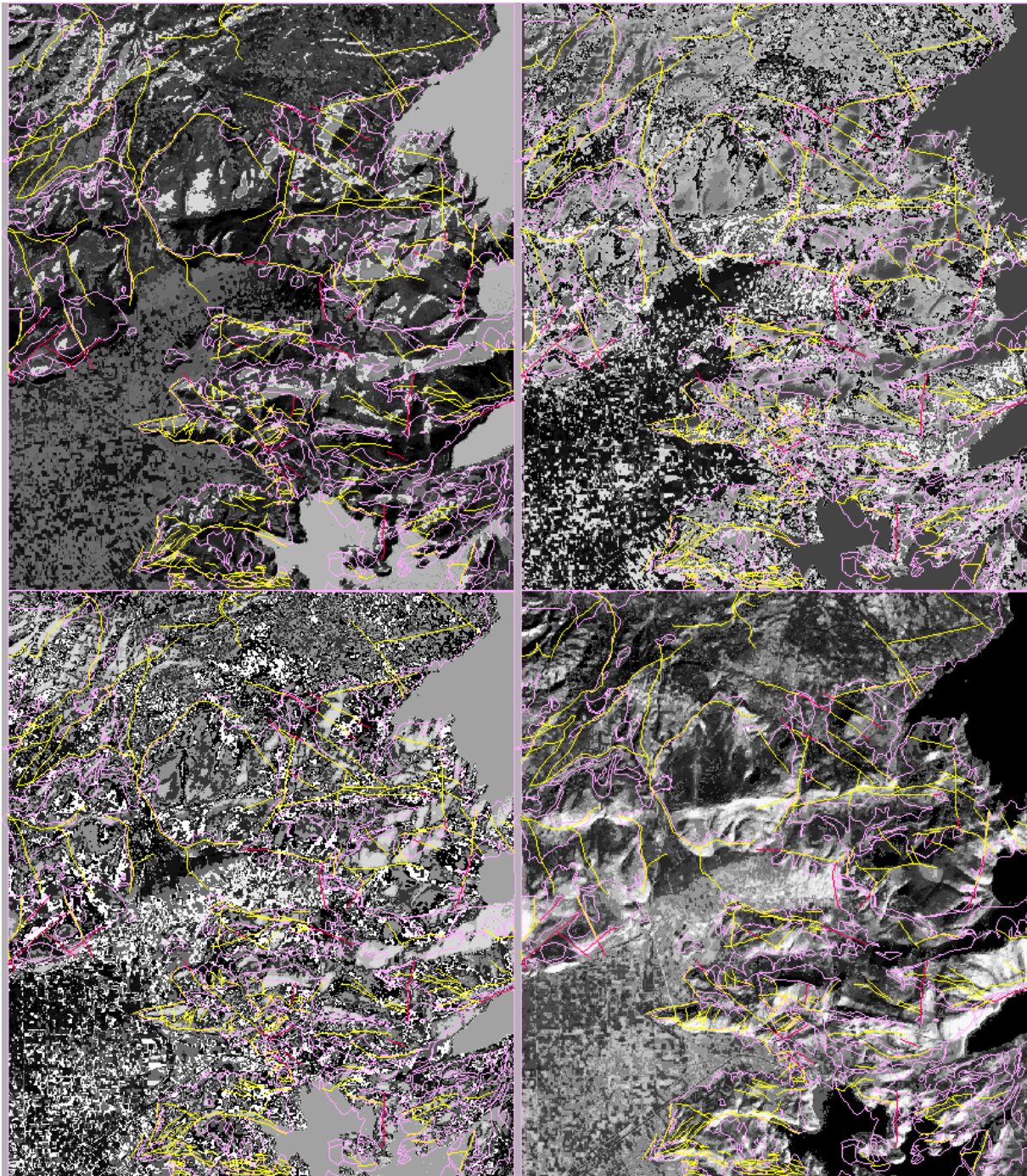
Picture 3: Lineament detection from the Vammala area, superimposed on thresholded version of unsupervised SOM classification. ANNGIE was used to obtain the result.



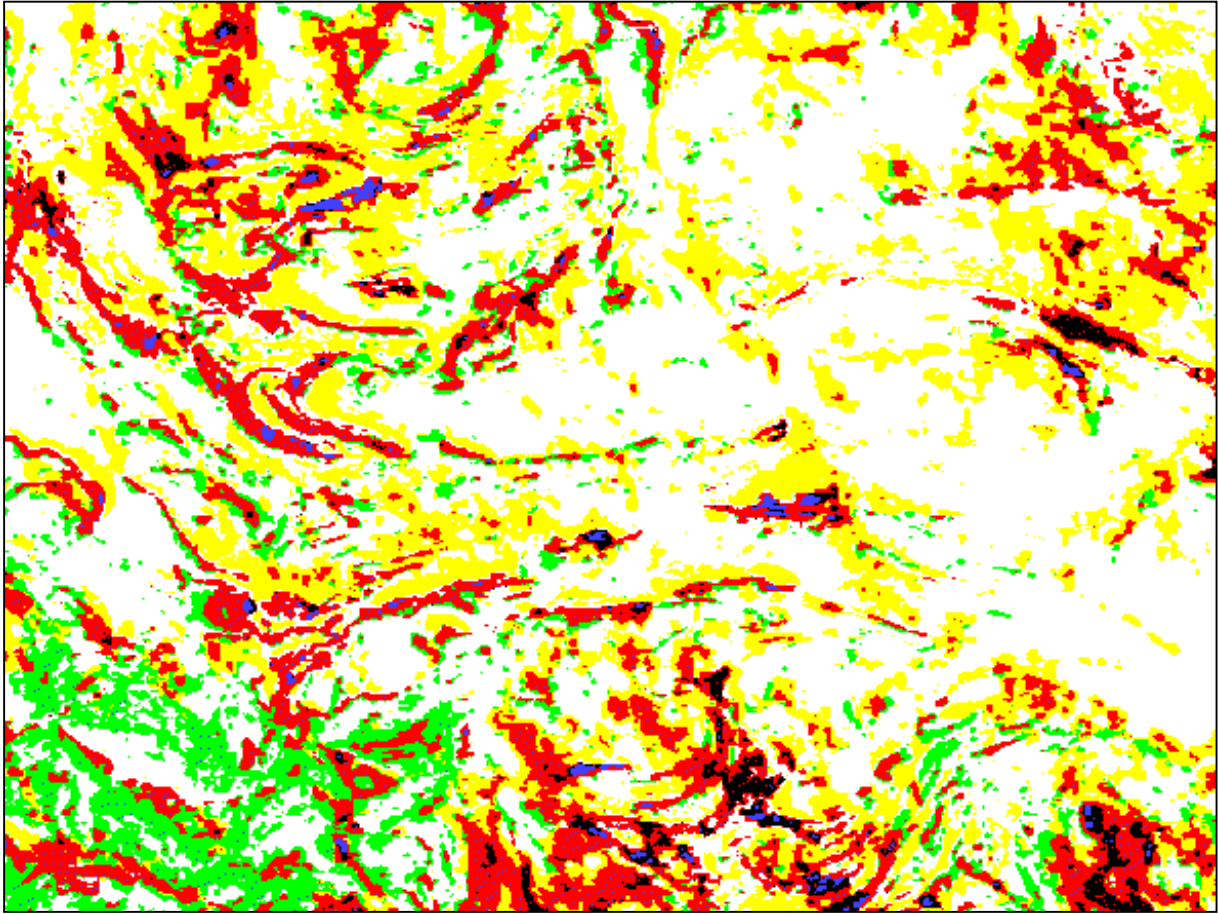
Picture 4: Image results obtained after the testing of the available four ANNGIE unsupervised classifications on the Landsat TM image with the 50 m resampling.



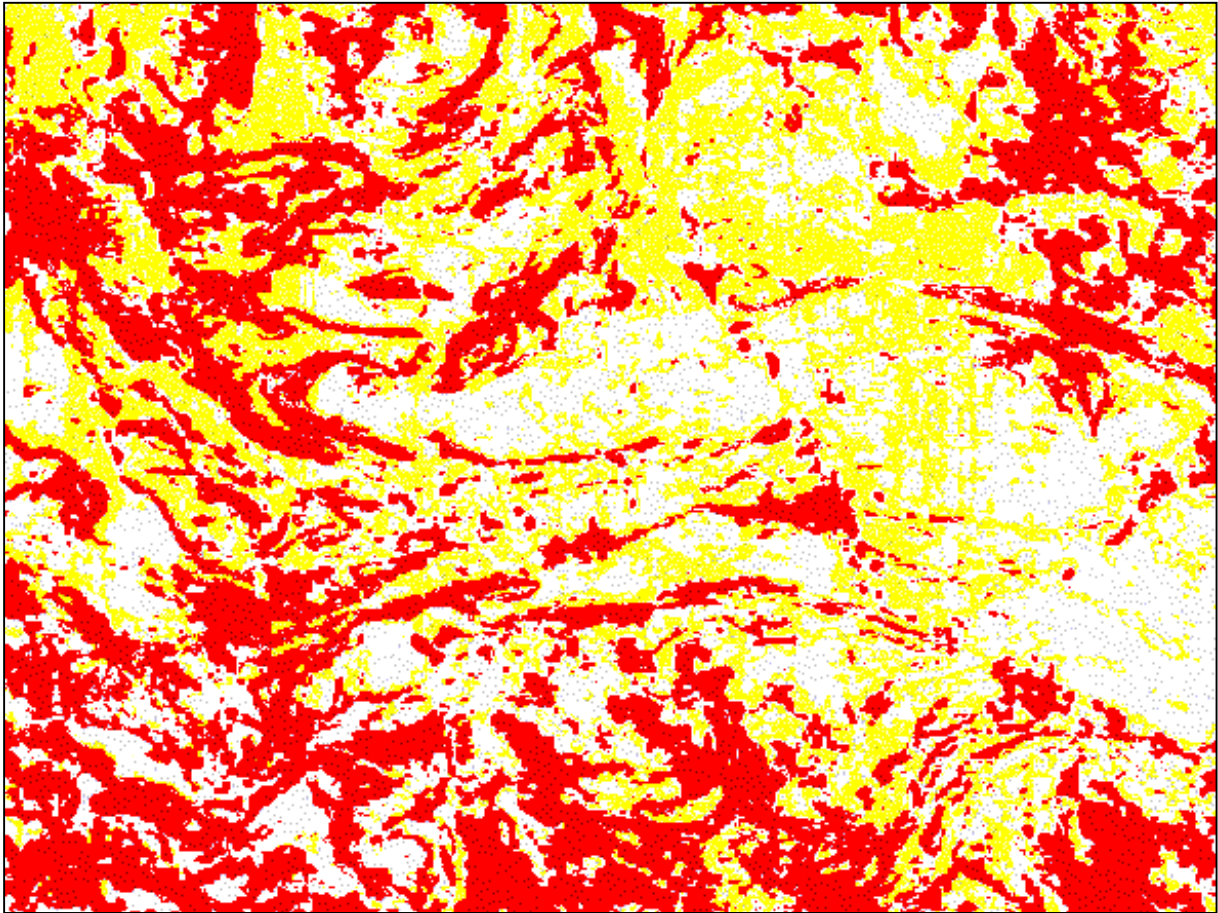
Picture 5: The same image results shown as color maps. Classes seem to be recognized more easily.



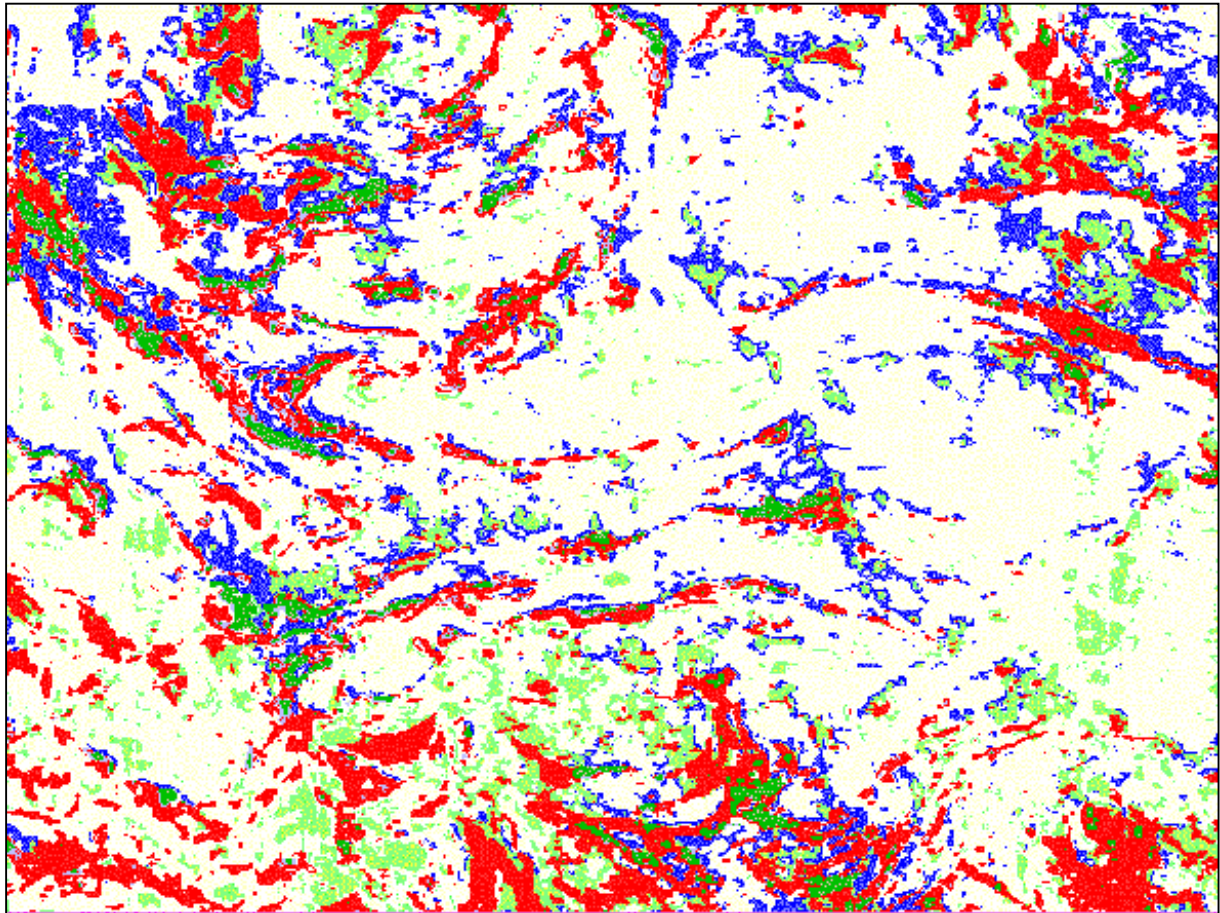
Picture 6: The same “image” results overlaid by the boundaries of the geologic features shown on the 1:50,000 scale map.



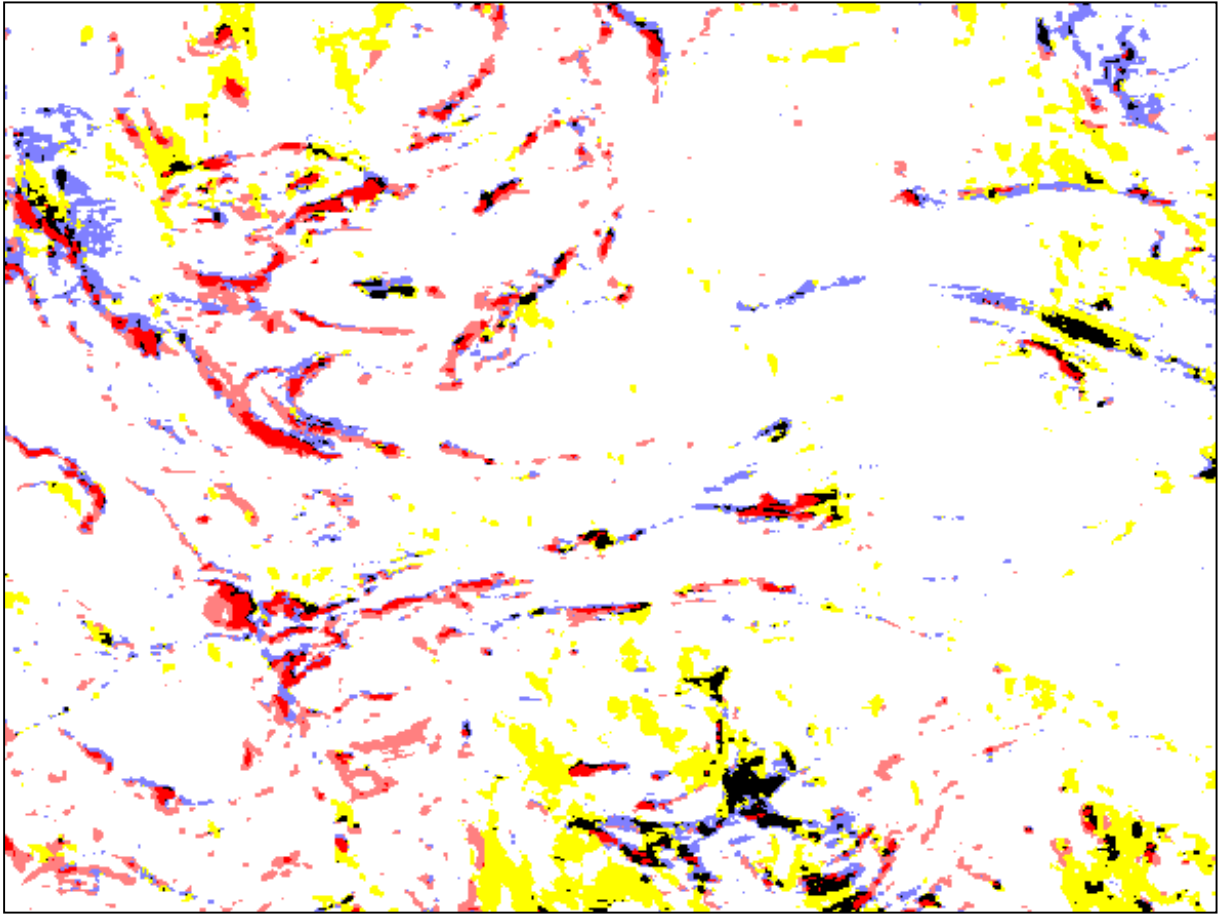
Picture 7: Image results obtained after the testing of the LVQ classifier on the Vammala area



Picture 8: Image results obtained after the testing of the Empirical Discriminant Analysis classifier on the Vammala area



Picture 9: Image results obtained after the testing of the Flexible Discriminant Analysis classifier on the Vammala area



Picture 10: Image results obtained after the testing of the Kohonen's SOM classifier (with hierarchical clustering algorithm) on the Vammala area

GeoNickel

Annex 4

**FINAL TECHNICAL REPORT
ANNEX 4**

WP4 GEOSIS DESIGN AND GIS TOOLS DEVELOPMENT

~~**CONFIDENTIAL**~~

CONTRACT NO: BRPR-CT95-0052 (DG12 - RSMT)
PROJECT NO: BE – 1117

TITLE: Integrated Technologies for Minerals Exploration,
Pilot Project for Nickel Ore Deposits
GeoNickel

PROJECT
COORDINATOR: OUTOKUMPU Outokumpu Mining OY
Finland

PARTNERS: LARCO General Mining and Metallurgical Company
SA,
Greece
BRGM Bureau de Recherches Géologiques et Minières
France
GSFIN Geological Survey of Finland
Finland
SOFTECO Softeco Sismat Spa
Italy
IGME Geological Survey of Greece
Greece
IRIS Iris Instruments SA
France
NCSR 'D' National Center of Scientific Research
'Demokritos', Greece

STARTING DATE: 1st January 1996 DURATION: 36 MONTHS



PROJECT FUNDED BY THE EUROPEAN
COMMISSION UNDER THE BRITE/EURAM
PROGRAMME

Date: February 28, 1999

FINAL TECHNICAL REPORT ANNEX 4

WP4 GEOSIS DESIGN AND GIS TOOLS DEVELOPMENT

CONTENTS

1	EXECUTIVE SUMMARY	3
2	OBJECTIVES	4
3	MEANS USED TO ACHIEVE THE OBJECTIVES	4
4	SCIENTIFIC AND TECHNICAL DESCRIPTION OF THE PROJECT	5
4.1	The work performed	5
4.2	GEOSIS architecture	6
4.2.1	GEOSIS main modules	11
4.3	Database architecture	14
4.4	GEOSIS interface	16
4.4.1	The data management	16
4.4.2	Reports on the stored data	21
4.4.3	The analysis and the elaboration of map images and data	22
5	COMPARISON OF INITIALLY PLANNED ACTIVITIES AND WORK ACTUALLY ACCOMPLISHED	27
6	CONCLUSIONS	28
7	ANNEXES	28
8	PROJECT STAFF	28

1 EXECUTIVE SUMMARY

The work performed in WP4 was focused on the development of a geo-scientific information system: GEOSIS. This system supports the management and the analysis of the complex data sets which are used in the nickel exploration and integrates the advanced analysis tools developed in the other Workpackages of the project.

GEOSIS has been developed after an extensive work of analysis performed with the co-operation of experts coming from different disciplines, and using up-to-date software analysis and development tools. It is based on reliable software environments, available on the market at low cost: the operating system Windows, the database ORACLE and the GIS MapInfo.

The initial work was focused on the analysis and the definition of the requirements. This analysis work proved to be one of the most complex activities because of the great complexity of data and analysis methodologies used in the nickel exploration, and was successfully carried out with the co-operation of geo-experts and software engineers.

The development of the software has been carried out within the timing foreseen in the project programme, mostly by taking advantage of object oriented technology and by including in GEOSIS all the GIS and data management functions available in the software environments used. Also the other software analysis modules developed in the project, the expert system, the neural network classification methods, and the advanced statistical methods, have been integrated in GEOSIS as foreseen in the initial programme.

The prototype developed has been validated and tested by the end user partners. The software has been improved on the basis of the results of the first tests and a final test has been performed with real data in Greece and Finland. In the final test data coming from real explorations and referring to different scientific disciplines (geology, geophysics, geochemistry etc.) have been loaded into the database and analysed with the available methodologies. The results of the test have confirmed the validity of the approach followed in the project. The software developed has proved to be easy to use and stable enough to support the real work of the experts during the explorations. The data management allows dealing with the high complexity of the data. The new analysis techniques developed seem promising tools for the mineral explorations. The mapping capabilities of MapInfo can support a large amount of the analysis work which needs to be performed (some specific analysis, for instance three-dimensional modelling, needs to be done with separate tools, but the communication of data with these specific tools is straightforward).

After the positive results obtained in the validation and test phase, and taking into account the industrial criteria which have been at the basis of the software development, the partners are planning to proceed into the exploitation phase of the prototypes developed in the project. An analysis of the market opportunities and of the investment required to develop a first release of software products is in progress.

2 OBJECTIVES

The final objective of WP4 was the development of a Geoscientific Information System (GEOSIS), to support the experts in the mineral explorations. This system must have the capability to work both in the lateritic and in the sulphidic nickel ore, and to be flexible enough to incorporate other methods and techniques, as future need arise.

The software system needs to allow the management of the complex and large data sets which are used in the nickel explorations, and to support the analysis tools which are used to elaborate the data. The data management is one of the most difficult tasks performed during the nickel explorations: an information system which supports the management of all these data, needs to include data coming from different scientific disciplines and to support complex data entry, data browsing and data downloading operations.

The information system also needs to support the different elaborations performed on the data, which include standard analyses and statistical computations, but also new methods and tools specifically developed during the project (the expert system GEOES, the neural network classification tool ANNGIE, and the advanced statistical methods ASM). GEOES, ANNGIE and ASM can be accessed directly from GEOSIS and the input and output data to and from these tools can be handled.

The main objective of WP4 have been achieved with the completion of all the software tools defined in the programme, but what perhaps is more important is that the results of the final test are very promising. The software developed has proved to be quite reliable, it has been developed with up to date tools and environments and it may constitute a good basis for the development of future products. The experts have been able to load into the database a set of real data and the data management, one of the most complex activities, has resulted to be quite easy to use and effective. The analysis of the data performed with the new modules developed in the project has given interesting results and indications. MapInfo is a very good and widely diffused platform for most of the mapping activities that are commonly performed in mineral explorations.

3 MEANS USED TO ACHIEVE THE OBJECTIVES

The objectives of WP4 have been achieved with a careful and extensive work of analysis and specification, with the use of up-to-date software technologies and with the co-operation of experts coming form different disciplines.

Formal analysis tools (such as SADT) have been used to perform the requirement analysis which was quite complex and which was one of the most relevant activities performed. Reliable and innovative software tools available on the market (such as ORACLE and MapInfo) have been used as a support for the development of the software.

Object Oriented techniques have been applied to develop all the software modules in order to cope with the complexity of the system and to obtain an easy integration with other software packages.

Advanced tools and methodologies have been applied successfully to manage the design and the development of the software but the most critical aspect have been solved thanks to the wide and active co-operation among different geo-experts and software experts which have been working together in the project.

4 SCIENTIFIC AND TECHNICAL DESCRIPTION OF THE PROJECT

4.1 The work performed

The work performed for the development of GEOSIS and the integration of the other software modules, has mostly followed the scheduling defined in the project programme. Some modifications to the original scheduling have been done to take into account unforeseen difficulties which have arisen, mostly because of the complexity of the data.

The initial work was focused on the definition of the software tools used to support the development of the software and on the analysis of the requirements. The partners decided to develop the software modules on a PC and Windows platform considering its wide diffusion, in spite of some initial doubts about the robustness of the platform, which anyway has improved its reliability since the beginning of the project, and can be considered now quite mature.

Two powerful software packages: ORACLE, for the management of the database, and MapInfo for the management of all the mapping function, have been chosen to support all software developments. This choice allowed to integrate all the functions already available with these packages, and to focus the development of the software on the most advanced features. We also decided to develop the software using C++ and MapBasic, the language available with MapInfo.

The next step in the WP4 was the analysis of the requirements of the end user partners (Task 4.1). This analysis has been performed in the initial part of the project with the co-operation of all the end users, and using a formal functional analysis methodology. Several meetings, where the requirements of the different users have been discussed and analysed, were held to perform the functional analysis. The results of this task was a detailed knowledge of the different functions which needed to be implemented in the system, and allowed to define a complete set of functional specifications. These requirements were the basis for the following phase of system design.

The design of GEOSIS (Task 4.2) was a complex phase of the project. The first step, the definition of the database scheme, required more effort than originally planned. The amount and the diversity of data which need to be taken into account in an exploration is very large,

and each data set has its own characteristic which requires a specific structure. Moreover the analyses and elaboration performed on the different data sets are completely different and require a different data management. For this reason, and also considering the great relevance of the availability of an efficient data management, the design of the database has undertaken a constant revision and improvement throughout most of the project. The final revision was completed in the Refinements and Consolidation Task 6.2, in the last months of the project.

The design of GEOSIS was completed by month 14th of the project, and, although improvements and revisions have been successively done, on the basis of the first tests and of the problems encountered, the following phase of software implementation followed this architecture. The architecture of GEOSIS is based on a client-server object oriented approach. It has been developed using object oriented language (C++) and following the main indication of object oriented architecture, thus allowing a consistent time saving in the software development, and with an “open architecture” which allows easy integration with other software modules.

The work in WP4 proceeded with the implementation of the database (Task 4.3) and the Integration and Development of GIS Tools (Task 4.4). These two tasks required a consistent development of software code, which was performed taking into account the high reliability required by the following phase of intense testing performed by the end users. The software was also developed with the objective to be completed and improved successively into a product ready for the market.

After the completion of the software system the end users began a phase of Validation and Testing (Task 4.5). In the WP4 only the first part of the validation and testing was performed. These activities continued in the WP6 (Final Integration) where the software developed in the other WPs was integrated. At the end of this activity the Geoscientific Information System (GEOSIS), with the advanced data analysis and elaboration modules: GEOES, ANNGIE and ASM, was available for the final testing. Throughout all this final phase the software has been frequently upgraded and modified in order to fix problems reported by the end users and improve the performances of the system. The results of the final tests confirm the validity of the approach followed in the project and open interesting opportunities of future development.

4.2 GEOSIS architecture

The following figure 4-2-1 shows the internal architecture of GEOSIS as it has been defined after the analysis performed in the first months of the project

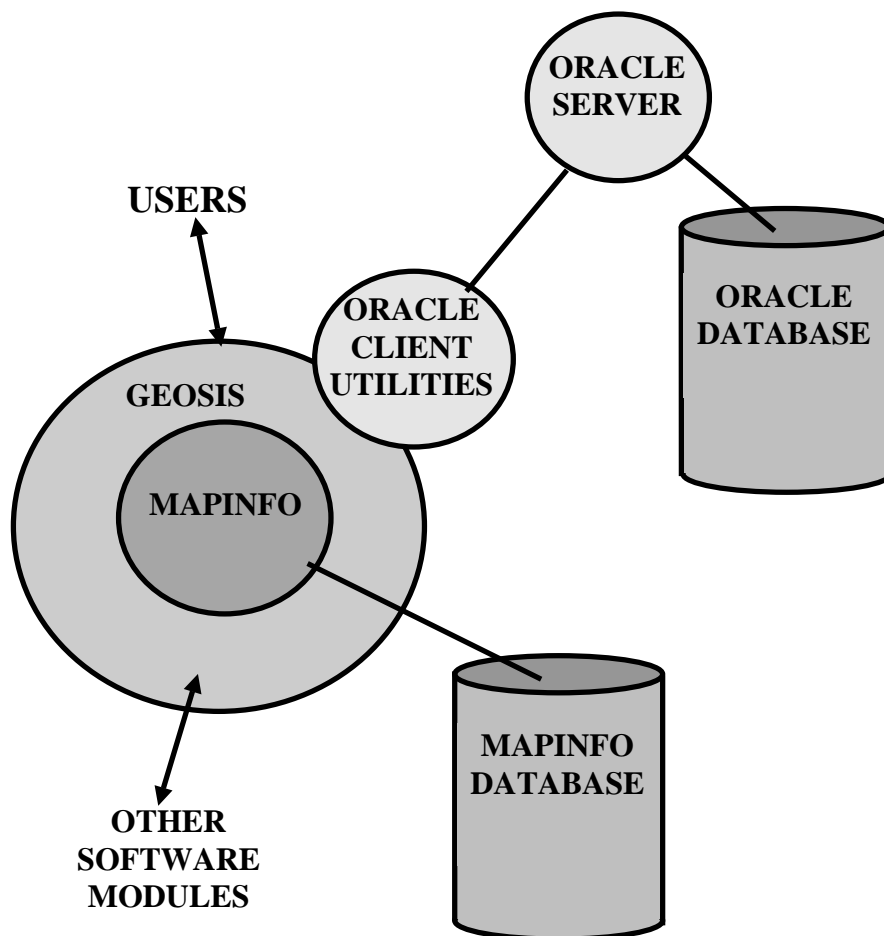


Figure 4-2-1. The internal architecture of GEOSIS

GEOSIS is based on MapInfo. This architecture assures the integration of all the capabilities of MapInfo into GEOSIS using updated and powerful integration techniques. It also assures the possibility to modify and improve the capabilities of MapInfo using its specific software development tools (MapBasic), and avoids the rebuilding of software modules already available in the market.

GEOSIS uses client server database architecture based on ORACLE, which assures the capability to deal with large and complex data sets. GEOSIS has its own interface that guides the user to access all the functions of the system (GIS functions, data management functions, new analysis functions...)

GEOSIS allows easy data import and export to other software packages. It is possible to perform an exploration using different analysis software through standard file formats.

One of the most complex tasks, which GEOSIS needs to perform, is the data management. We defined the conceptual architecture of the database that can be seen in figure 4-2-2:

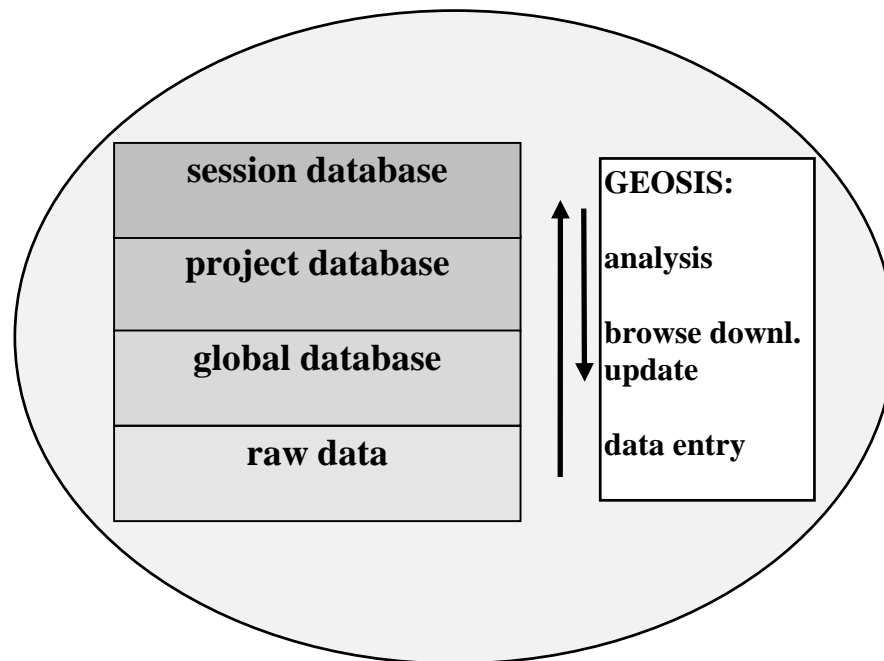


Figure 4-2-2. The conceptual architecture of the Database

GEOSIS supports the **data entry** of new **raw data** into the **global database**. The data coming from geological observations, geophysical acquisitions, or other data sources can be entered into the database with an easy to use interface. Among the data stored in the global database, the GEOSIS interface allows the data **browsing** and selection: the user is able to define his own data and to **download** them into his **project database**. In his project database he will perform all the **analyses** required for his exploration. The user can perform analyses with the expert system, the neural networks, or the other analysis modules developed in the project, which will store their internal data into their **session database**. After the completion of the work the user will be able to **update** the global database with the results of his work.

The internal data structure of GEOSIS can be further detailed as shown in the figure 4-2-3:

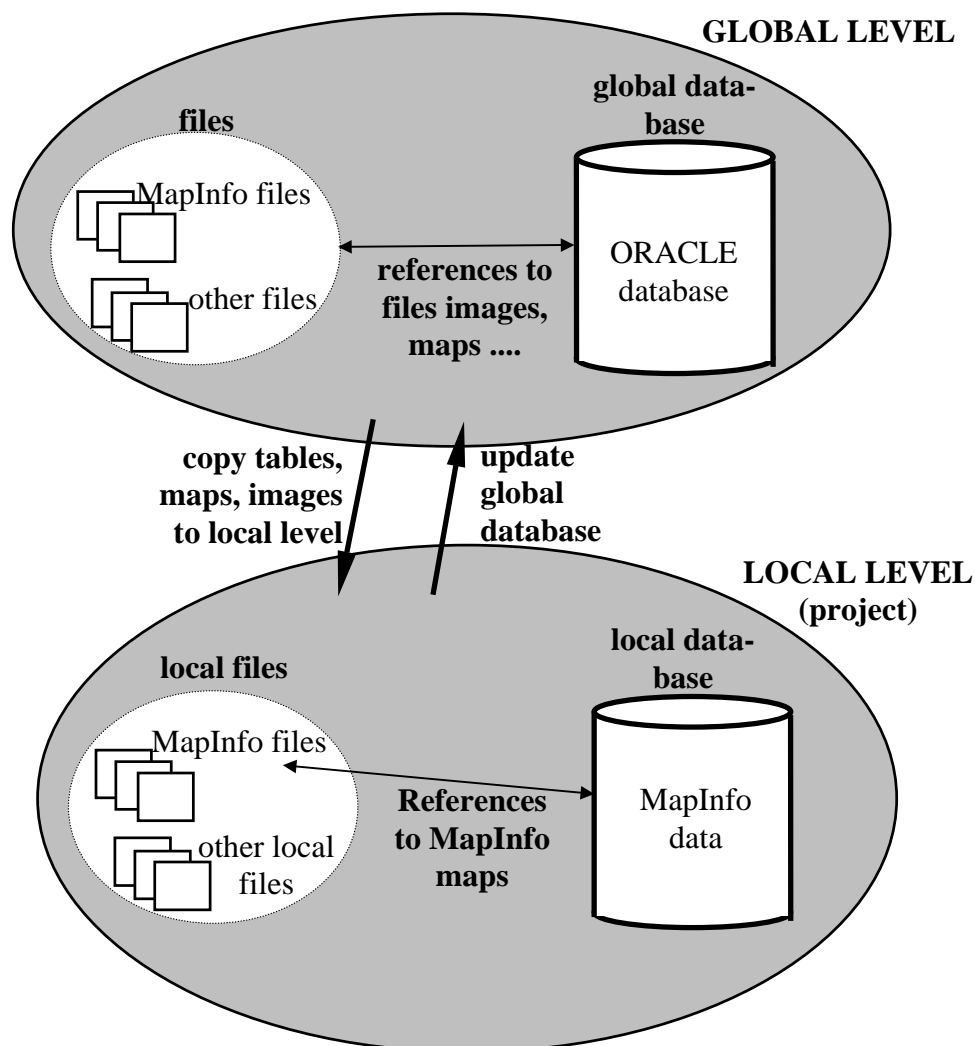


Figure 4-2-3. The internal data structure of GEOSIS

The data structure of GEOSIS is divided into a **global level** and a **local level (project)**. The global level is based on the ORACLE database, all the data are stored in its tabular structure and also the reference to all the vector, raster, annotation files and maps contained in the MapInfo files structure will be stored in tables in the ORACLE database.

In the local level the user will copy all the data which he needs for his exploration (a project). In the local level the tabular data are copied into the MapInfo tables and the user will be able to link them to maps. All the files needed for the exploration are copied into the local directory of the user. The user may update some data or create new data and he will be able, with the appropriate permissions, to update the global database.

After the definition of the workflow and the main tools to be developed we have performed a detailed analysis. On the basis of this analysis we have defined the internal architecture of GEOSIS as it is shown in the following figure 4-2-4, which details the architecture defined in figure 4-2-1:

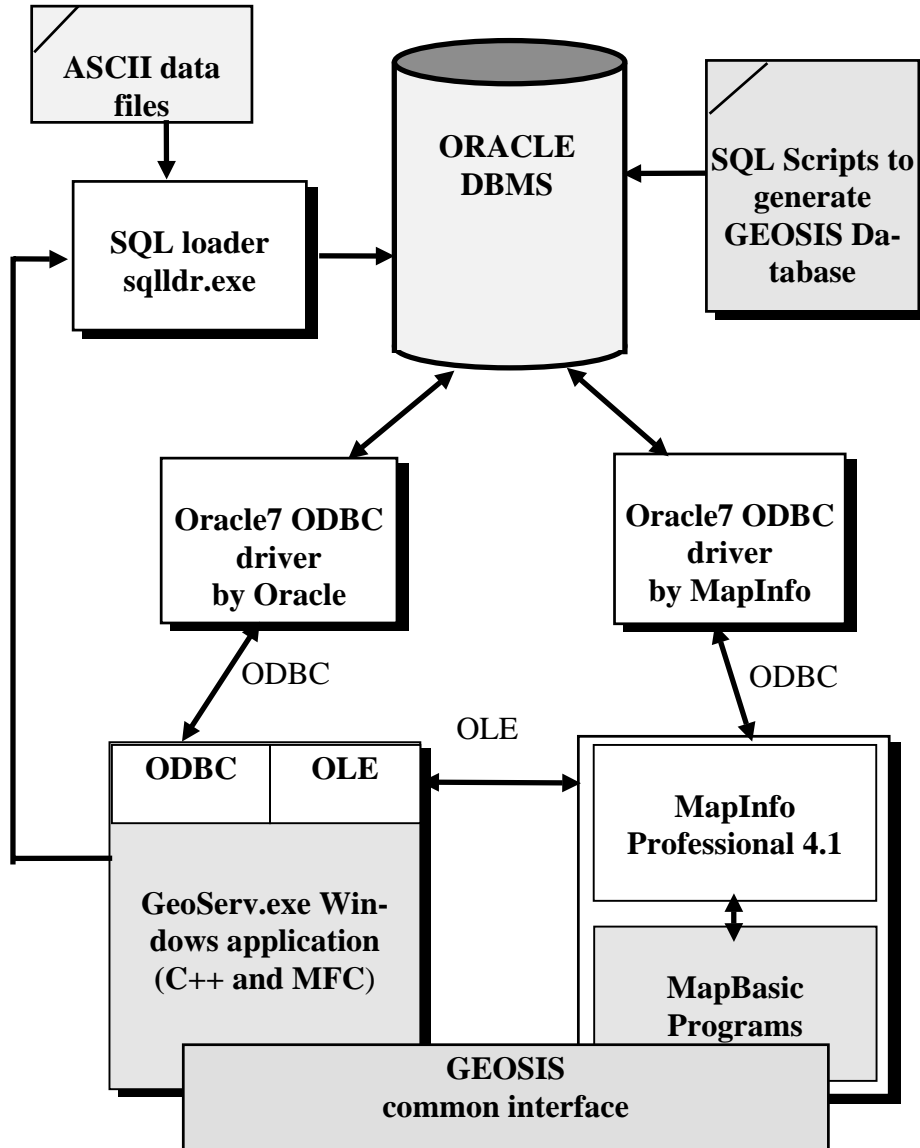


Figure 4-2-4. A more detailed architecture of GEOSIS

The shaded boxes in figure 4-2-4 refer to modules which have been specifically developed, while the white boxes refer to external modules available on the market.

As you can notice GEOSIS is based on a client-server and object-oriented architecture. Two external applications: ORACLE and MapInfo Professional will act as GEOSIS servers. ORACLE allows the management of the Database, through the use of ODBC drivers. MapInfo Professional allows the management of the GIS functions, through the use of OLE services.

The ORACLE Database contains all the tables with the Geological, Geophysical, Geochemical and other data sets which will be used for the mineral explorations. The Database is generated with a script written in SQL, which builds up the tabular structure of the Database.

A seamless interface allows access to all the GEOSIS services (which include all the MapInfo functions). This interface was developed with the Microsoft C++ environment and MapBasic, and complies with the Microsoft Windows standards.

One of the most important functions implemented with the C++ module manages the communications with ORACLE through the ODBC driver and with MapInfo, through the OLE services, and allows an easy integration of the external software modules.

The advanced GIS functions available in GEOSIS have been implemented using MapBasic, the software development language of MapInfo, and are based on the standard functions of MapInfo.

The data entry function of GEOSIS manages the generation of the appropriate script for the ORACLE SQL loader, which will import the ASCII file containing the new data which need to be entered into the Database.

4.2.1 GEOSIS main modules

In the following paragraphs we give a brief description of the main modules which compose GEOSIS

Data handling

The Data Handling (DH) module has been designed to assist the users in the management of all kinds of different information stored in the ORACLE database. It provides tools for data entry, data view and editing, both at the global level, for administration purposes, and at the local level, to work on a project. The data handling can be performed through a set of windows which guide the user and allow complete access to all the complex data stored in the database.

Database

In the database module 4 basic types of data will be used:

- Numeric data
- Maps
- Images
- Text data

The **numeric data** are the result of measurements or analysis performed on the ground (by direct ground analysis or by airborne remote analysis) with many different instruments and methodologies, and a possible subsequent elaboration of these data. Numeric data may be

seen as two- or three-dimensional graphics or profiles but the basic data are always a set of numbers, which are usually disposed in tables.

The **maps** are two-dimensional data set (**points**, **lines** and areas delimited by **polygons**) generally related to an area or to a region of the earth. The maps contain symbolic two-dimensional or three-dimensional elements; numeric data and attributes are associated to the elements. The attributes can be numerical values, text and so on. More detailed maps or multimedia can be connected to certain geographical features. The maps have the georeference (geographic location and projection) and the scale as a basic characteristic.

Point data consist of separate points that have geological, geophysical and/or other attributes. Typical attributes of point data are values of chemical analysis, geophysical measurements and so on, but also texts like geological description and images (photographs) can be connected to a point. Geophysical measurements along lines are a special case of point data. The points are connected together ("connected points") along the line, but the observations do not form a line in the meaning of GIS. However the point coordinates of the geophysical observations form a line (measurement line) that has attributes (like the number of the line).

Line data in GIS consist of points (nodes and vertexes) that are to be topologically considered together. The line has attributes like name, width, length, height (contour) classification and so on. The points of the line show the ends (nodes) and shape (vertexes) of the line.

Polygon data consist of border lines, that have nodes and vertexes. Polygons have attributes like lithology or other geographical area features.

The **images** are two-dimensional data sets which contain visual information. The images may come from camera acquisitions or from numerical data processing, either in grayscale or colour coded (one image), or composites (2 or 3 images composed).

Although the images are always two-dimensional, they may be obtained from volume three-dimensional information (as slices or projections). The image description is usually stored in a header before the pixel values (as defined in the standard formats, for instance TIFF). Raster data or images are two-dimensional arrays of pixels containing both spatial and spectral information. The images may come from multispectral or conventional camera acquisitions (hyperspectral, satellite, airphoto, photograph data) or from numerical data processing including statistical and image processing. The images are single images or composites of several images and either binary (black and white), colour (pseudo, RGB, CMY) or grayscale coded using different look-up tables. The images used in different projects are usually enhanced or classified derivatives of the original data.

The text data are description, notes and comments. The text data are in a free format. Textual notes, comments, papers may be connected to a map, a point, a line or an area.

All the data defined originate from very different sources (maps, images, measurements, chemical or spectroscopic analyses ...) and have different characteristics and meaning, but they are all geographically referenced; they refer to a specific location on the earth (x,y,z). Drilling data have location at a certain depth from the earth surface, flying data have certain

flying altitude, gravity data also have their height value and so on. So there are several types of z-values, which are specific to the data.

GIS functions

GEOSIS is based on MapInfo, and has all the capabilities of MapInfo. Moreover more specific functions are implemented with MapBasic (the software development language of MapInfo), and with standard software development tools (C++).

The vector maps can be imported through a standard vector format. The user is able to open and display a vector map, to open a database table with numerical or alphanumerical data, and to link lines (lines or polylines) or areas (polygons) of the vector map to one or more records of the table.

An appropriate and user-friendly set of windows and menus allows the import of maps, the selection of the data tables and the building of the links between graphic objects in the vector maps and records in the database. The linked data are stored into the MapInfo tables. The records of the database that contain the geographical co-ordinates are directly mapped into the maps by MapInfo, which displays the appropriate symbol in the corresponding coordinate of the map. The vector maps, with their links to the numeric or alphanumeric data, are stored in MapInfo format.

The relational database (ORACLE) stores in a table the list of the vector maps and the reference to the vector map files stored in MapInfo format. The user can browse through the maps stored and select the maps he needs for his exploration. These maps can be visualised with MapInfo and the user will be able to perform analysis or queries on them. The queries allow to select vector objects in the map and display the associated data, or to perform more complex search on the maps and their associated data.

The user can also analyse maps and data with the MapInfo functions, or export the vector, numeric, or alphanumeric data to external software packages through standard formats. The raster images or grid data will be imported and displayed with MapInfo standard functions. Since the image processing capabilities of MapInfo are rather limited, all the most complex analysis on images or grid data will be done with external software packages. Also the three-dimensional data analysis will be done with external software packages.

The following standard formats are supported:

- GEOSOFT standard ASCII and grid geophysical data format
- Excel and Lotus 1-2-3 data
- DXF, MIF (Mapinfo Interchange Format), ARC/INFO and AtlasGIS (option of MapInfo) standard vector data format
- GIF, JPEG, TIFF, PCX, BMP, Targa (.TGA), SPOT (.BIL), standard image data format

4.3 Database architecture

As we have mentioned in the previous chapters the database is one of the most critical components of GEOSIS. The database is logically organised in a hierarchical structure. The main layers of the structure are the following:

Area and **Target tables** are the first (higher) level of tables in the database structure. Each entry in the Area table describes a large geographical area. Each entry in the Target table describes a smaller area. Each area can have one or more targets or, in other words, each target belongs to an area. Area and Target must be defined before any other kind of data is stored into the database, because all the data in the tables belonging to the underlying layers (see below) are bound, either directly or indirectly, to a specific target in a specific area.

Header tables represent the second level of tables. In a header table you describe the object of your acquisition as a whole, and specify which target and area it belongs to. These tables correspond to the main subjects of investigation in the different geo-science disciplines: they can be geophysical surveys, drilling holes, sets of geological observations, and so on. For example: one entry in the *Diamond Drill Hole* header table describes one drill hole; one entry in the *Geophysical Ground Survey* header table describes one ground survey; the same applies to the remaining header tables.

Each entry in all these tables is uniquely identified by a 15 character string (which is generally called *header ID* hereafter). In the GEOSIS user interface, these identifiers are given different and appropriate names (*Hole_ID*, *Survey_ID*, *Obs_Set_ID*, etc.) according to their actual meaning, that is to the type of objects they identify (drill holes, geophysical surveys, geological observation sets, etc.).

In every *header* entry the fields specific to a particular data type and some general pieces of information common to all types are stored: geographical location (area and target), acquisition and recording date, the observer's name, and so on.

Data tables which are a third level of tables. For each header table there may be one or more data tables. In a data table, data acquired from the objects described in the relating header table are stored. For example: in the Drill Lithology data table we may have the lithological descriptions of different hole sections, at different depths, for the holes registered in the Diamond Drill Hole header table.

In a *data table*, a *data set* is a set of records which refers to a single header entry (uniquely identified by its *header ID*). In our example, the lithological description of a drill hole (*Hole_ID*) is made of a set of records in the Lithology data table, each one containing the attributes of a specific hole section at a specific depth: this set of records is the lithological *data set* for the hole *Hole_ID*.

Subdata tables are defined in only one particular case, the *Geological and Lithochemical Observation Set*. In our structure, they belong to the third and fourth hierarchical level. In a *subdata table*, a *data set* is just a set of records which must be consistent with the records

stored in its parent table (according to the relationships defined within the database to maintain referential integrity of data in related tables).

Analyses and *Assay tables* are used to store results of studies and analyses made on samples collected from various sources and disciplines (petrophysical observations, drill holes, geological and lithochemical observations, overburden geochemical observations). These tables constitute a separate group, with their own hierarchy and relationships. However they are related to some of the tables in the data and sub-data levels, as explained below.

When a sample is collected, a record describing its characteristics (in terms of geographical coordinates, attributes, etc.) can be stored in the appropriate data table, which hereafter we will call *source* table for that sample. The following tables behave as sample *sources*, because they contain data on the collection of samples:

Petrophysical Observation Set:

- *Observation*

Diamond Drill Hole:

- *Sample*

Geological and Lithochemical Observation Set:

- *Rock Chip and Slush*
- *Boulder and Outcrop*
- *Geological Field Observation – Rock Type – Sample*

Overburden Geochemical Observation Set:

- *Till Observation*
- *Humus and Peat Observation*
- *Lake Sediments Observation*
- *Heavy Minerals Observation*
- *Stream Sediments and Waters Observation*
- *Ground Water Observation*

Each sample, regardless of what the type of the *source* table where its description is stored is, is given an identifier which must be unique within the whole database. This identifier is called *SAMPLE_NO*, and it is used by GEOSIS to automatically register the sample in a private table, not accessible by users. Once a sample is present in one of the *source* tables, and then internally registered by GEOSIS, its *SAMPLE_NO* is made available by the system for adding records to the following Analysis and Assay tables:

- *Mineralogical Analysis*
- *Lithochemical Assay*
- *Overburden Geochemical Assay*

These tables are the upper level of the Analysis and Assay hierarchy and have a *SAMPLE_NO* column used to establish the link between the study results (stored here) on a certain sample and its collection (described in one of the *source* data tables).

Please note that: one *SAMPLE_NO* can be used only once, in only one of the *source* tables listed above, but many records bearing the same *SAMPLE_NO* can be stored at a time in all

of the three analysis and assay tables. This means that one *SAMPLE_NO* cannot identify two samples of two different types, but one sample can have more than one kind of analysis/assay.

4.4 GEOSIS interface

The design of an easy to use interface, to allow the management of the database and the analysis and the elaboration of maps images and data, was a critical task in WP4. We have organised the interface with a set of windows which guides the user through the different available functions, and allows a complete control of the data sets and the analysis methods.

4.4.1 The data management

In GEOSIS, the data management is handled via the Data Manager window, that can be opened through the *Manager* item in the *Database* menu, or from the *Database Manager* button in the *Database* button-pad.

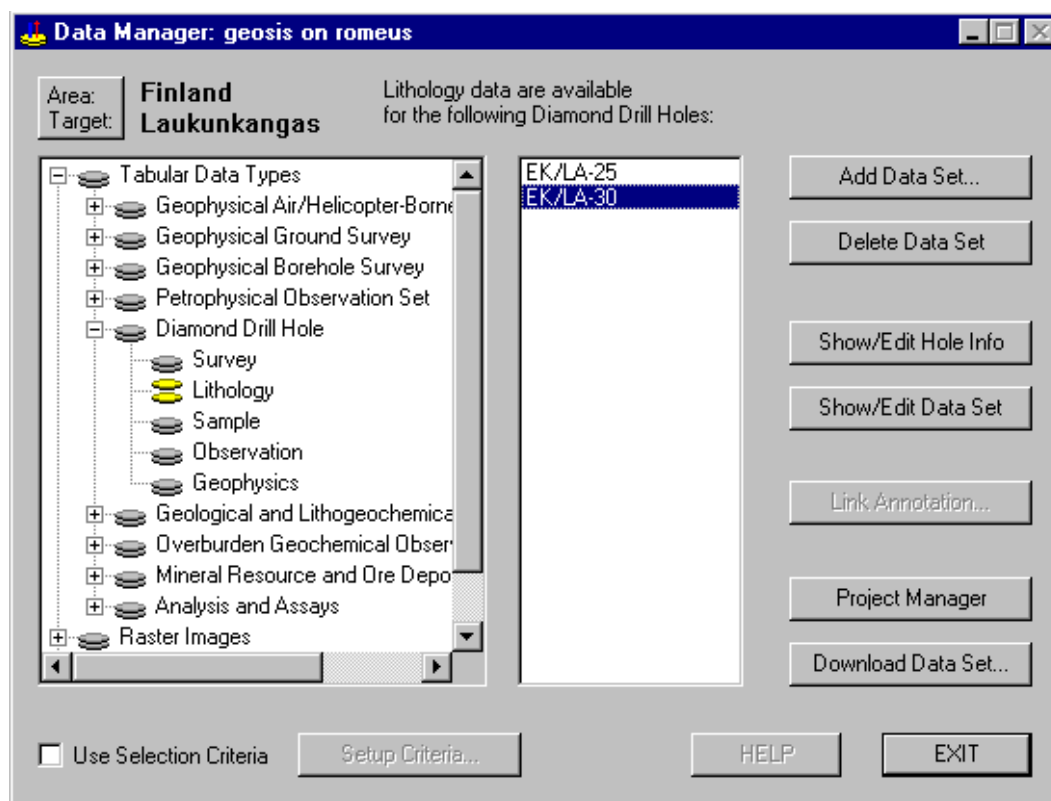


Figure 3-4-1-1. The Data Manager window

The Data Manager window (Figure 3-4-1-1) is the starting point for every operation on the GEOSIS ORACLE DB. The box on the left side provides a user-friendly, graphical and logical representation of the GEOSIS database structure, where tables of the database map to leaves in a hierarchical visual tree.

This representation does not match completely the physical structure of the GEOSIS relational database but, because of the hierarchical nature of its design, it is quite close to it. Each leaf in the *data type* tree either refers directly to a table in the database, or simply clusters a group of related leaves.

When you start the Data Manager, the four root-leaves of this *data type* tree are shown (*Tabular data*, *Raster Images*, *Vectors/Maps*, *Annotations*); these are not selectable and are used only to group the *data types* into four main categories.

The user can expand them to navigate through the database structure (Figure 4-4-1-2):

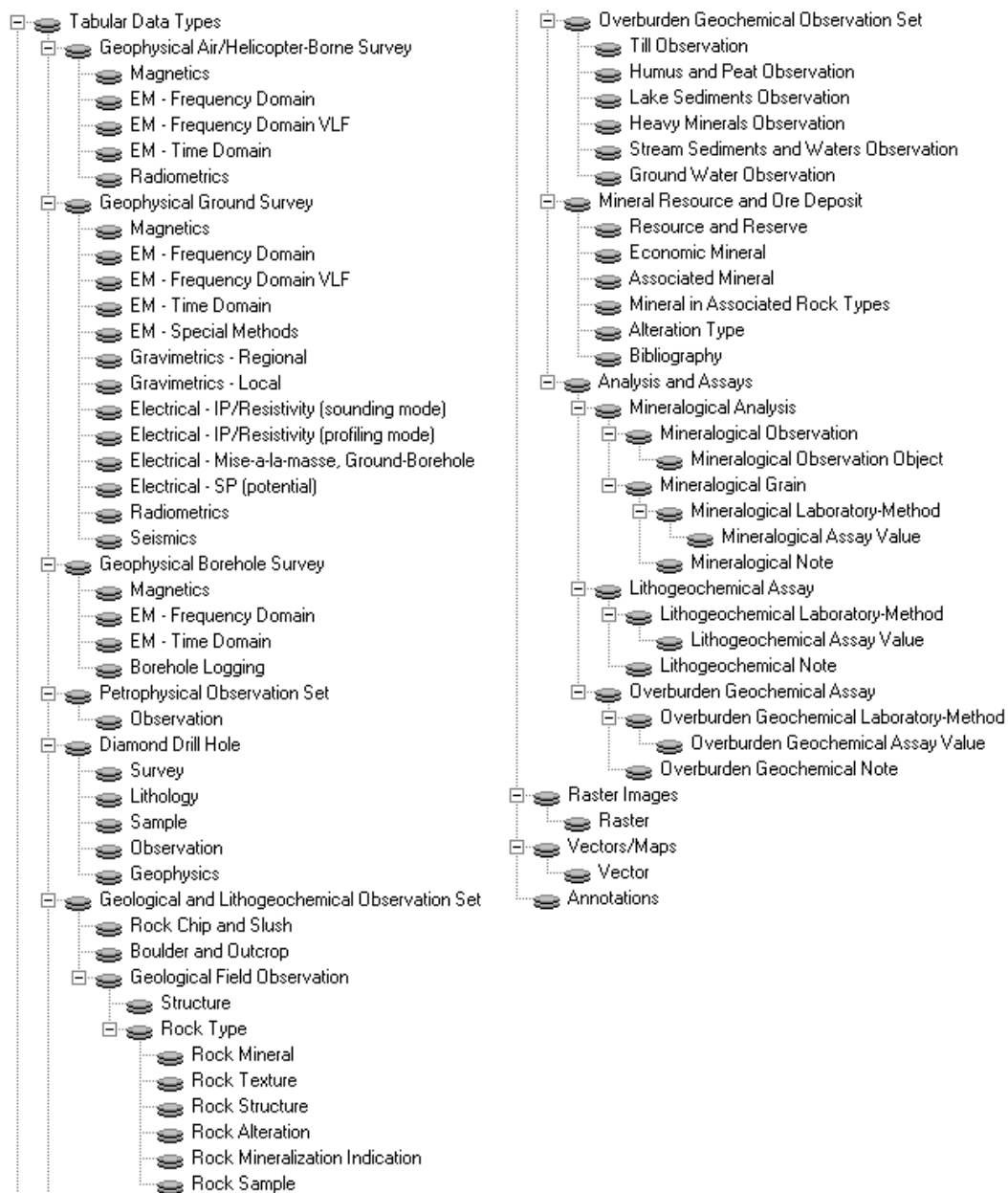


Figure 4-4-1-2. The *data type* tree fully expanded

Below the **Tabular data** group, tables belonging to the header, data, sub-data levels and to the analysis and assay branch are organised in layers of leaves. All the leaves in the first layer refer to different geo-science disciplines and activities. Each of them (except for the *Analyses and Assay* one) refer to a *header* table in the database, where specific acquisition objects in that discipline are described. All the leaves in the second layer map to tables of the data level. The *Analyses and Assay* leave represent a separate branch of tables with their own relationships and behaviour. Their contents are not accessible via any *header ID*, and they have no heading description. Below the **Raster images** and **Vector/Maps** groups, you find just one leaf each. These leaves map directly to the header tables where raster images and vectors are described (file name, path, format, date, and so on). The **Annotation** leaf is not accessible at present.

The list-box in the centre of the Data Manager window shows the list of *header IDs* available in the database within the data type selected on the tree-view, and bound to the current Area and Target. Each *header ID* of the list allows direct access to its related *data set* and its heading description. This list-box is not used (and it is empty) when the selected leaf refers to any table of the *Analyses and Assay* branch, or to a table belonging to the subdata level.

Once the user has selected a *data type* from the tree, and he has chosen a *header ID* from the list (when possible), or has defined some selection criteria he can ask the Data Manager to perform one of the functions available through the buttons on the right side of its window.

The main available functions are described in the following paragraphs.

The **Area and Target Selection** window (Figure 4-4-1-3) is accessible via the Area Target button in the top left corner of the Data Manager window. This tool is provided by GEOSIS for selecting, adding, deleting and editing Area/Target entries. Each *header ID*, identifying a *header* entry and one or more *data sets*, is always bound to one Target in one Area.



Figure 4-4-1-3. The Area and Target selection and management window

Show Heading Information: this window (figure 4-4-1-4 shows an example) can be displayed clicking the *Show/Edit <object> Info* button and is available only for *data types* which include heading information (whose data sets are accessible through *header IDs*). The Heading Information window shows the header entry describing the object (survey, drill hole, observation set, ore deposit) identified by the selected *header ID* (Survey_ID, Hole_ID, ObsSet_ID, Deposit_ID).

field	value
AREA_ID	Finland
TARGET_ID	Laukunkangas
NAT_ID	
ORG_ID	
COORSYS	
ACQDATE	1/7/1998
DECDATE	7/7/1998

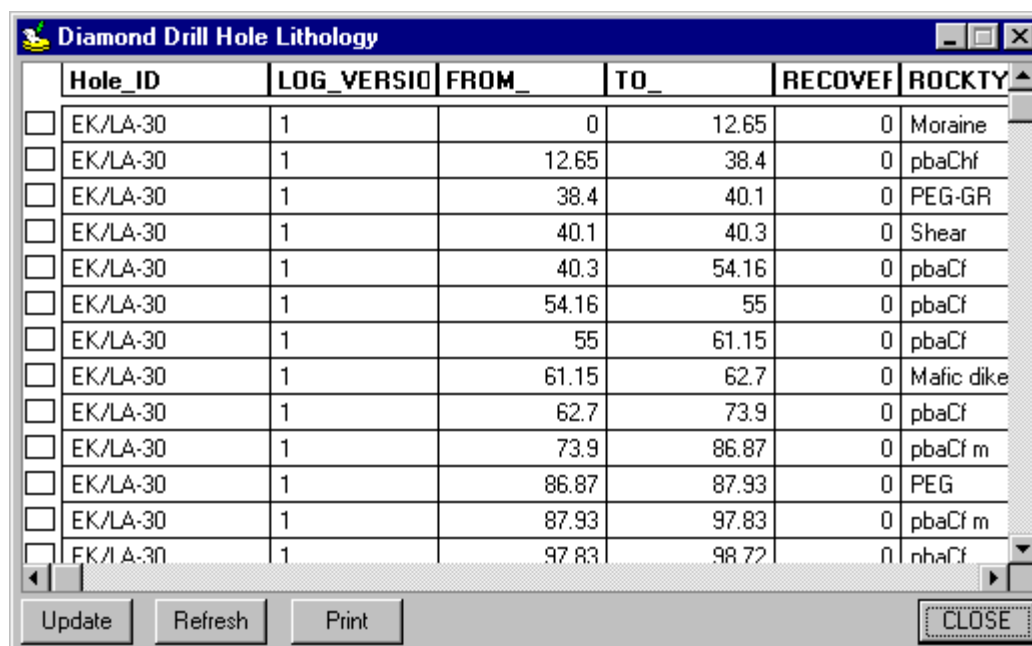
field	value
Hole_ID	EK/LA-30
EASTING	4300000.000000
NORTHING	7120000.000000
T_CODE	
YEAR	1998
SYSTEMME...	
COORDINATE...	

Update
Refresh
CLOSE

EASTING 4300000.000000

Figure 4-4-1-4. The Heading Information window for data browsing

Showing and editing data sets: the button *Show/Edit Data Set* allows the user to display the records of a *data set* and, if he has write and delete permissions on the database (super-user), to edit the values of its columns or delete data records. The *data set* records are shown in a tabular form inside a Data Editing window like the one in the picture below (figure 4-4-1-5). There can be many Data Editing windows open at a time, each displaying records of a different *data type*, whose name is printed in the title bar. The tabular view inside the Data Editing window is a MapInfo table linked to the GEOSIS ORACLE database, so the user can do with it most of the operations he would do in a MapInfo browser window, including modifying the values, removing records and manually add new records. Moreover, since the table is linked to the database, the user can send any change (records added, modified, deleted) to the database, or discard them.



Hole_ID	LOG_VERSION	FROM_	TO_	RECOVER	ROCKTY
EK/LA-30	1	0	12.65	0	Moraine
EK/LA-30	1	12.65	38.4	0	pbaChf
EK/LA-30	1	38.4	40.1	0	PEG-GR
EK/LA-30	1	40.1	40.3	0	Shear
EK/LA-30	1	40.3	54.16	0	pbaCf
EK/LA-30	1	54.16	55	0	pbaCf
EK/LA-30	1	55	61.15	0	pbaCf
EK/LA-30	1	61.15	62.7	0	Mafic dike
EK/LA-30	1	62.7	73.9	0	pbaCf
EK/LA-30	1	73.9	86.87	0	pbaCf m
EK/LA-30	1	86.87	87.93	0	PEG
EK/LA-30	1	87.93	97.83	0	pbaCf m
EK/LA-30	1	97.83	98.72	0	nhaCf

Figure 4-4-1-5. The Data Editing window

Data Entry: The data entry to the database, which is one of the most critical functions, is performed by clicking the *Add Data Set* button on the Data Manager window. This button starts a data entry guided procedure, through which he can store a new *data set* of the type specified by the selection in the tree-view. Presently two file formats are supported: the *ASCII User Defined File Format*, where the user can define its format for the data entry, and the standard *GeoSoft Line XYZ file format* (see figure 4-4-1-6).

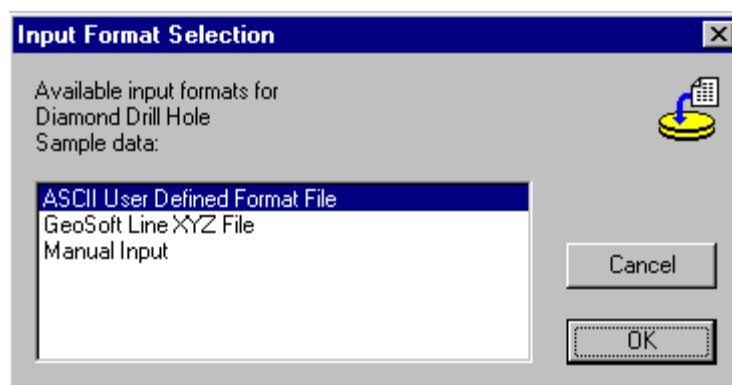


Figure 4-4-1-6. The input File Format Selection window for the data entry

The *ASCII User Defined File Format* has been defined within the GeoNickel project, in order to give a flexible way to fill text files, with data from the different geo-science disciplines. It is a plain text file, editable through any text editor, which contains one input *data set* of one *data type*. Its syntax is defined by the user, but must comply with certain rules. The data entry procedure guides the user through a set of windows to perform the data

entry into the database, and gives the user a complete report if errors occur during the data loading.

Download Data Set: after the user has selected some data, browsing through the database with the available tools, he may need to download these data to his project directory through the *Download Data Set* button. “To download a data set to a project directory” means that a copy of the selected data set is created in the current specified Project Directory. Thus, when the user works on a table or on a map, in the MapInfo environment, he uses his personal copy of it. Data stored in the global database are therefore preserved from intentional or unintentional modifications: if you don’t have super-user rights on the GEOSIS database and you want to work with a *data set*, you have first to download it to your *project’s* directory.

In this description we have included only the main features of the data management available in GEOSIS. A complete description of the software may be found in the GEOSIS user manual (deliverable of WP 6.1)

4.4.2 Reports on the stored data

The GEOSIS Reporting Tool has been designed to achieve two main tasks:

1. To give a friendly, easy and flexible way to access data in the Analysis & Assay branch of the database.

The hierarchy of the analysis & assay tables (as they are presented in the data type tree of the Data Manager window) is highly “normalised”. This means that data storage is optimised to reduce tablespace usage and to maximise flexibility: in particular chemical elements or compounds and their values are listed by rows (instead of by columns) in the assay tables, to let each preparate have a different and variable list of analysed elements.

For the above mentioned reasons, data of this kind are not easy to browse through, retrieve and interpret. The Reporting Tool is intended to overcome this limitation. Reports belonging to this category, according to the type of analysis/assay they map to, are called respectively: Mineralogical Analysis Reports, Lithochemical Assay Reports and Overburden Geochemical Assay Reports.

2. To build any kind of join on all the database tables (including the Analysis Reports), in order to give the expert user maximum flexibility in querying the database.

Reports of this category are called **User Defined Reports**. The user defined report engine provides a means both for creating synthetic views, in which information spread over more tables can be presented in a compact and easy-to-read way, and to store pre-defined queries (also on single tables), which can be reused to retrieve specific pieces of information. The Reporting Tool is integrated within the already known GEOSIS user interface. Mineralogical Analysis, Lithochemical Assay and Overburden Geochemical Assay Reports appear as leaves at the bottom of the data type tree in the Data Manager window (see figure 4-4-2-1).

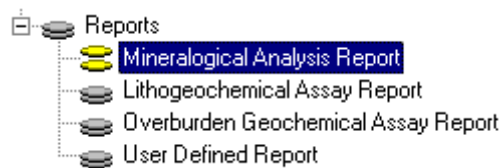


Figure 4-4-2-1. The Report leaves in the data type tree

Please note that these are *read-only* data types: each report definition results in a set of read-only data records, and no data entry can be performed through a report.

The operations available for all the report types are: defining a new report, editing an existing report definition, showing and downloading the resulting data set, deleting a report definition.

The definition of a new report allows defining format and content of the report. This is done through a proper user interface. Every *report definition* can be given a unique identifier and be permanently stored in the database, in order to be reused any time when that report is needed.

When one of the four report leaves is selected in the data type tree, the listbox in the Data Manager window displays the identifiers of all the reports already defined within that report type.

Through the buttons in the Data Manager the user can:

- Create a new report definition (*Add New Report* button).
- Select an existing report definition (in the ID listbox).
- Edit the selected definition (*Show/Edit Report Def* button).
- Browse through the data records resulting from the selected report definition (*Show Data Set* button).
- Download these data records to a MapInfo permanent table (*Download Data Set* button). A default name for the MapInfo file is suggested, but it can be overridden.
- Delete the selected report definition (*Delete Report* button).

The reports are among the most relevant features of GEOSIS since the complexity of the data sets stored in the database. With this tool the user is able to consult the database and to select those data which are needed for the specific analysis that he is performing.

4.4.3 The analysis and the elaboration of map images and data

MapInfo provides a built-in set of basic mapping mechanisms and tools, like geocoding (*“Geocoding...”*, from the *“Table”* menu), mapping points (*“Create Points...”*, from the *“Table”* menu), and thematisms (*“Create Thematic Map...”*, from the *“Map”* menu). Not all of them are useful for geological mapping purposes: geocoding by address or ZIP code is not likely to be used in a geological project. On the other hand, more specialised tools are needed in order to build geological maps: the geologist needs to link data to existing vectorial objects (contained in a DXF file, for example), or to draw new vectorial objects, such as polylines and polygons (not only points).

We have developed a set of customised GIS Tools that improve (and do not overwrite) the standard MapInfo tools, in order to accomplish more specialised tasks. These tools have been written in MapBasic Professional, which is the developing language for applications under MapInfo Professional. In order to work, the GEOSIS GIS Tools require a dedicated layer to display the geographical content of a specific table containing data, this layer is called the *Objects* table, and is used to store the graphical objects drawn by the user or mapped from data. It also contains extra information that is used by the GIS Tools to handle links between data and graphical objects.

The GEOSIS GIS Tools may be grouped in 4 categories:

- Tools for handling GEOSIS maps (GEOSIS Map tools);
- Tools for handling the *Objects* table (Linking tools);
- Tools for retrieving links (Selection tools);
- External tools(GEOSIS External integrated modules).

In the following paragraphs we are giving a short description of these 4 categories of tools:

Tools for handling GEOSIS maps (GEOSIS Map tools)

A map is the result of the overlaying of different layers, each one mapping data from a table. In MapInfo there is not a specific file format designed to store maps. The MapInfo “workspace” can be used to store maps. Quoting the *Glossary of terms* in MapInfo Professional - User’s Guide, the workspace is “a saved configuration of open MapInfo tables and windows”: it is used to preserve the user’s set-up from session to session, in order not to start each session by opening again all the tables, and rearranging the windows on the screen.

We have used a restricted concept of workspace for storing GEOSIS maps: a GEOSIS map is a workspace with only an open Map window, without any open Browser windows, and with at least the *Objects* table open (which is a mandatory table). GEOSIS maps have extension .GS.

New commands have been added to the standard MapInfo “*File*” menu to manage GEOSIS maps:

- “*New Geosis Map...*”: it asks the user to locate and name the new map;
- “*Open Geosis Map...*”: it asks the user to locate the map to open and opens it.
- “*Save Geosis Map...*”: it asks the user to locate and name the map to save and saves it.

Tools for handling the Objects table (Linking tools)

The Object table is used to store the graphical objects drawn by the user or mapped from data. These tools constitute the kernel of the GEOSIS GIS Tools; they are grouped in a dedicated button pad, the “*GIS Tools*” button pad, where they are divided into three groups:

Managing tools, used to manage graphical objects in the *Objects* table. The user can link a set of records of a table to a graphical object. He can also copy a graphical object into a set of records and delete graphical object from a set of records.

Mapping tools, used to map data into graphical objects, starting from coordinates values contained in the data table.

Join/Split tools, used to join points into a polyline, or to split an extended object into its nodes.

Tools for retrieving links (Selection tools)

These tools are activated by two buttons which have been added to the “*Main*” button pad, where the MapInfo standard selection tools are available. They are complementary tools that allow retrieving links between data records and graphical objects in the *Objects* table.

As they are MapInfo Toggle buttons, they are used to enter a selection modality, and they remain pressed until the same button is pressed again (to exit the selection modality), or the complementary button is pressed (and the selection modality is changed).

GEOSIS External integrated modules

The following external modules have been integrated in GEOSIS:

1. The GEOES expert system (developed by S.K.E. Lab NCSR Demokritos), which is composed by two applications: Spatial GEOES (for spatial explorations) and Interactive GEOES (for punctual explorations).
2. The ANNGIE neural network (developed by A.N.N. Lab NCSR Demokritos).
3. The ASM package of advanced statistical methods (developed by GSF).

For each of them a button pad has been defined. The buttons activate the GEOSIS procedures that allow the user to prepare input data for the module, to run it, and to display its results. The button pads can be popped up from the correspondent submenu in the second section of the *Tools* menu.

In the second section of the *Tools* menu, the submenu *Training Set* is also present. It enables the button pad with the Training Set definition tool for the definition of a training set on a map. Though this tool is not to be properly considered an external module, it is described in this paragraph, since it allows the user to prepare input data (the training set) for ANNGIE and ASM. Moreover, it exploits an external routine for the conversion of the drawn polygons to a training set, which is provided by A.N.N Lab NCSR Demokritos.

In the following paragraphs, instructions are given on how to prepare data to be used by the external modules, on how to start them from the GEOSIS interface, and on how to display their results. For the instructions on how to use the single modules, refer to their specific manuals.

The expert system, GEOES, can be managed with some specific button pads. The *GEOES* button pad contains three groups of buttons, one for **Spatial GEOES**, one for **hybrid GEOES** and one for **Interactive GEOES**.

Spatial GEOES is a standalone application that requires input data (observations) on a grid of points, each with its own spatial coordinate, and produces results (evidences) which can be displayed on a map. The input data are the result of analyses and elaboration performed on raw data, and are loaded into some specific tables in the GEOSIS database (called the GEOES Intermediate Tables) which contains all the input observations required by the expert system.

With a specific button the user can export to GEOES the input data and start the expert system. The results of the elaboration are evidences which show the evaluations performed by the expert system on the grid of points in the different domains where the expert systems works (Geology, Geophysics, Geochemistry, Pedo-Geochemistry, Litho-Geochemistry) and also an overall evaluation which takes into account all the different domains. High evidence means favourable conditions for the presence of ore bodies. The results will be displayed in the active map window, the figure 4-4-4-3 shows an example.

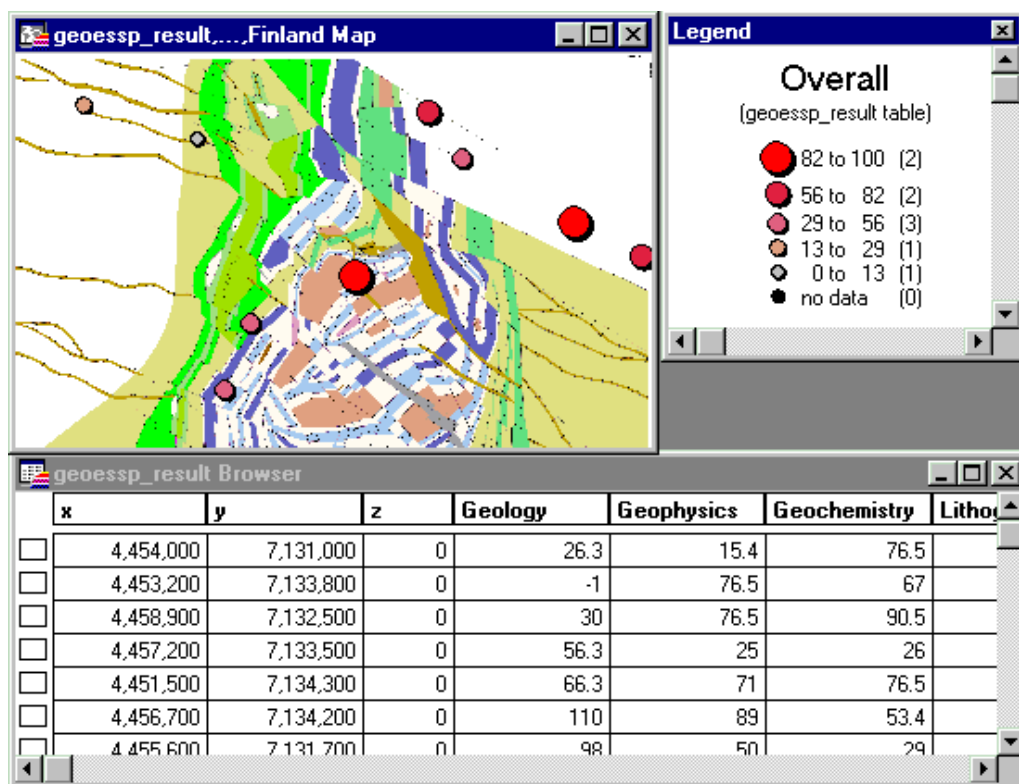


Figure 4-4-4-3. Results from Spatial GEOES

After the user has confirmed the map window on which the results must be shown, the results are displayed. In the example the results are shown on a map of an area of Finland. The results will also be displayed in a Browser window, in order to see their numerical values. For each point at Longitude/Latitude (x, y and eventually z) position, the result of the evidence is given (in percentage) for each domain of the exploration, plus an Overall domain that summarises the exploration. For each domain, each point of observation is represented by a unique symbol, whose size and colour represent the importance of the evidence. A Legend window shows the symbols and the correspondence between the

symbol size, the symbol colour and the range of evidence values. These correspondences have been assigned by GEOSIS as defaults. They can be modified through the standard MapInfo *Modify Thematic Map* window, just double clicking on one of the symbols in the Legend window.

Once the user has the results of spatial GEOES on a wide area, he will focus his analysis on the more promising points. Spatial GEOES is able to analyse a very large amount of data, thus allowing a relevant time saving, but in the more interesting areas the user will perform an in-depth analysis.

After the user has selected a point in the map where the evidence resulting from the spatial GEOES elaboration is shown, he can press a button to start a session of GEOES (called **hybrid GEOES**) on that specific point, and perform a what-if analysis. When the user clicks on a point in the map where an evidence is shown, GEOSIS passes to GEOES the coordinate of the point and the input data (the observations) referring to that point. Then he starts GEOES which perform its elaboration on that point and the user can modify or complete the input data and see how the results change.

Interactive GEOES is a standalone application that does not need any input data, and does not produce any result to be displayed as output in the MapInfo environment. Therefore, a unique button is needed, just to start the program. The user must manually input the data into GEOES.

ANNGIE is a standalone application, which allows performing image classification with neural network analysis. It may require training sets as input data, and produces image results to be displayed as output. The training sets may be defined with the *Training Set* tool. Therefore, the *ANNGIE* button pad contains only two buttons, one to run ANNGIE, and one to display its results.

The advanced statistical methods **ASM** is a standalone data analysis application that may require training sets as input data. The training sets may be defined with the *Training Set* tool. Therefore, a unique button is needed, just to start the program.

Note: a detailed description of GEOES, ANNGIE and ASM can be found in the chapters of the report which refers to WP5, and WP3.

The Training Sets can be defined with the specific definition tool: the *Training Set* button pad which contains two buttons, one to start the tool, and one to start polygon drawing. The first time the start button is pressed, the definition procedure starts performing the following steps.

1. In order to define a training set, at least one raster image must be already open.
2. GEOSIS will ask for a table name where to store the polygons that are going to be drawn.
3. GEOSIS will then ask for the number n of images the user wants to relate to the training set he is going to define.
4. If the chosen raster is registered in Earth coordinates, then it will be temporarily removed from its Map window and it will be mapped into a new Map window as a Non-Earth image.

5. The *Draw Polygons* button is now enabled and the user can press it to start drawing.

The second time the button is pressed, the definition procedure ends: the Map windows configuration is reset as it was before the definition procedure started, and the polygons are converted into a training set.

The *Draw Polygons* button becomes enabled after the user has completed the definition phase described above. After the user has pressed the button, the mouse pointer switches from the standard arrow to a cross when passing on a Map window, suggesting the user to click in a Map window for drawing purposes.

The drawing procedure for a polygon runs the following steps.

1. Every click on the image becomes a vertex of the polygon; to end the polygon, define the last point with a double click. When the user has finished to draw the polygon, the new polygon is checked with eventual previously drawn polygons for overlapping.
2. If the new polygon has been accepted, the user is asked to give it a class name.
3. The user can start drawing a new polygon or end the training set definition procedure, by pressing again the *Polygon/Training Set definition* button.

5 COMPARISON OF INITIALLY PLANNED ACTIVITIES AND WORK ACTUALLY ACCOMPLISHED

On the whole all the activities initially planned have been performed, even if some modification in the time scheduling have been done, and the results which where in the original scope of the project have been obtained.

The most relevant modifications were caused by the need to allocate more resources in the analysis of the data, their structure and the interface needed for their management.

The database management proved to be very complex and required more efforts both in the design and development phase (task 4.2 and 4.3), in the test and debug phase (task 4.5), and also in the WP6 for the final refinement and consolidation. The extra effort required was compensated by the exploitation of object-oriented software development tools and methodologies, which allows to speed up the development process, and by the reduction of cost of the hardware platforms.

The validation and testing activity performed by the end user partners in the final phase of the project allowed to assess the performance of the software and confirms its correspondence with the initial objectives of the project.

Also the future exploitation of the results seems feasible on the basis of the reports of the end users.

6 CONCLUSIONS

The WP4 was focused on the software development of the geoscientific information system, quite a complex task which required a great deal of effort in the requirement analysis and specification phase, and required also the finding of a common language between geo-experts and software engineers. The final results of this effort, the actual GEOSIS with the integrated advanced analysis tools, although a prototype, seems to satisfy the requirements of the end users and it has proved to be a useful tool in the test nickel explorations.

7 ANNEXES

List of deliverable of WP4:

- T4.1 - GEOSIS Functional Specifications - Document RS/9601-TR/GEO/EM
- T4.2 – GIS and Relational Databases Scheme - Document RS/9602-TR/GEO/EM
- T4.2 – GEOSIS Design - Document RS/9701-TR/GEO/EM
- T4.3 – GIS and Relational Databases - Database
- T4.5 – Software Report - Document RS/9702-TR/GEO/EM and Software

Also in WP5 SOFTECO issued the

- T5.3 - GEOSIS User Interface – Software

And in WP6

- T6.1 – GEOSIS User Manual - Document RS/9801-TR/GEO/EM

In the table with type and number of project outputs SOFTECO has: one prototype

8 PROJECT STAFF

Mainly the following persons have been working in WP4

Marco Boero	SOFTECO
Enrico Morten	SOFTECO
Marco Boero	SOFTECO
Enrico Morten	SOFTECO
Paolo Venturini	SOFTECO
Davide Defini	SOFTECO
Jussi Aarnisalo	Outokumpu Mining Oy
Pertti Lamberg	Outokumpu Research Oy
Markku Tiainen	Geological Survey of Finland
Nils Gustavsson	Geological Survey of Finland
Costas Ripis	IGME
Michael Melakis	LARCO G.M.M.C
Athanasios Apostolikas	LARCO G.M.M.C
Costas Maglaras	LARCO G.M.M.C

GeoNickel

Annex 5

**FINAL TECHNICAL REPORT
ANNEX 5**

**WP5 KNOWLEDGE BASED SYSTEM
(GEOES)**

~~**CONFIDENTIAL**~~

CONTRACT NO: BRPR-CT95-0052 (DG12 – RSMT)
PROJECT NO: BE – 1117
TITLE: Integrated Technologies for Minerals Exploration,
Pilot Project for Nickel Ore Deposits
GeoNickel

WP5

RESPONSIBLE: NCSR «D» National Centre for Scientific Research
«Demokritos»,
Greece

PARTICIPATING
PARTNERS:

LARCO General Mining and Metallurgical Company
SA,
Greece
SOFTECO Softeco Sismat Srl
Italy
IGME Geological Survey of Greece
Greece
OUTOKUMPU Outokumpu Mining OY,
Finland
GSFIN Geological Survey of Finland
Finland

AUTHORS: Dr. Costas Spyropoulos, Yannis Stavrakas
STARTING DATE: 1st January 1996 DURATION: 36 MONTHS



PROJECT FUNDED BY THE EUROPEAN
COMMISSION UNDER THE BRITE/EURAM
PROGRAMME

Date: February 28, 1999

CONTENTS

EXECUTIVE SUMMARY	5-3
PROJECT STAFF.....	5-5
1. THE OBJECTIVES OF GEOES.....	5-6
2. MEANS USED TO ACHIEVE THE OBJECTIVES.....	5-6
3. SCIENTIFIC AND TECHNICAL DESCRIPTION OF GEOES.....	5-8
3.1 Specifications on the Mineral Deposits Exploitation Task.....	5-8
3.2 Knowledge Acquisition Process.....	5-10
3.3 GEOES Design Specifications.....	5-11
3.3.1 Overall Architecture.....	5-11
3.3.2 User Interface Principles.....	5-13
3.3.3 Knowledge Representation.....	5-14
3.3.4 Assessment Process.....	5-16
3.3.5 Integration with GEOSIS.....	5-18
3.4 Implemented GEOES Modes.....	5-19
3.4.1 The Interactive GEOES.....	5-19
3.4.2 The Spatial GEOES.....	5-20
3.4.3 The Hybrid GEOES.....	5-20
4. INITIALLY PLANNED ACTIVITIES AND WORK ACCOMPLISHED	5-21
5. CONCLUSIONS.....	5-21
6. ACKNOWLEDGEMENTS.....	5-22
7. ANNEXES.....	5-23
7.1 Publications and conference presentations.....	5-23
7.2 Reports.....	5-23
7.3 Prototypes.....	5-23
8. REFERENCES.....	5-24
LIST OF SCREEN-SHOTS	
Screen-shot 5.3.4.1-1 : Interactive GEOES.....	5-25
Screen-shot 5.3.4.2-1 : Spatial GEOES.....	5-26
Screen-shot 5.3.4.2-2 : Results of Spatial GEOES, displayed in GEOSIS.....	5-27

WP5 KNOWLEDGE BASED SYSTEM (GEOES)

EXECUTIVE SUMMARY

GEOES is the expert system developed within GeoNickel to facilitate and promote the process of identifying Ni-ore deposits. It has been designed and implemented in close cooperation with geo-experts, whose knowledge of the domain has been encoded and transferred into the system. That knowledge is now available in a structured form for every geo-scientist to use, through an interactive and friendly Windows 95 / NT interface. A key advantage of GEOES is its ability to process in a batch mode large quantities of geo-data, and produce results that embody expert opinions, in a small fraction of the time that would be required if the computations were performed by hand.

At the heart of GEOES lie the knowledge base and the inference engine. The knowledge base keeps estimations and facts that reflect the knowledge and experience of geo-experts in a formal, organised fashion. The inference engine is a software module able to apply the knowledge base to input data and draw conclusions. Input data are mostly measurements concerning a certain number of specific factors / subfactors / observations that relate to the existence of Ni deposits. The conclusions reveal to the user the degree that input data are supportive of Ni existence.

GEOES can handle three different geological models for komatiite, intrusive, and lateritic deposits. For every model there are three exploration stages, namely «explore area», «identify potential zones», and «select target». Those stages cover the whole process of exploration, starting from a wide geographical area, going through the identification of zones of interest, and ending at specific small target areas. For each model / stage combination, there is a distinct set of factors and sub-factors that can be assigned a value either directly by the user or by input data. Factors are grouped by geo-science to facilitate scientists. After the system has run for a data set, it gives in pictorial way an overall result and how much each geo-science has contributed to the overall result, plus a consultation that provides an answer as to how the system has reached those conclusions.

To better support the needs of geo-scientists in their work to identify favourable Nickel ore deposits, GEOES is released in three modes of operation:

- Interactive GEOES: is a flexible version of the expert system, perfect for training and familiarising the end user with GEOES, but not suitable for large quantities of real

data.

- Spatial GEOES: produces results from large data sets in a form that can be drawn on a map, making it easy to observe interesting spots and geological anomalies.
- Hybrid GEOES: gives the opportunity to further explore a specific spot on the Spatial GEOES results map, and allows the user to engage in what-if scenarios.

All modes of GEOES are fully integrated within GEOSIS, which automatically provides GEOES with input data and shows the results on maps.

FINAL TECHNICAL REPORT ANNEX 5

WP5 KNOWLEDGE BASED SYSTEM (GEOES, AN EXPERT SYSTEM FOR IDENTIFYING Ni DEPOSITS)

PROJECT STAFF

The following people worked in the various tasks of “WP5 Knowledge Based System “.

Dr. C. Spyropoulos	NCSR	WP Leader
Dr. G. Vouros	NCSR	
Dr. Maria Katzouraki	NCSR	
Dr. S. Kokkotos	NCSR	
Dr. C. Koutras	NCSR	
Mr D. Katsoulas	NCSR	
Mr. Y. Stavrakas	NCSR	
Mr. Costas Ripsis	IGME	
Mr. Demetrios Eliopoulos	IGME	
Mr. Anthony Angelopoulos	IGME	
Mr. Vasilios Noutsis	IGME	
Vasilios Klentos	IGME	
Mr. Michael Melakis	LARCO	G.M.M.C
Mr. Athanasios Apostolikas	LARCO	G.M.M.C
Mr. Costas Maglaras	LARCO	G.M.M.C
Davide Defini	SOFTECO	
Enrico Morten	SOFTECO	
Paolo Venturini	SOFTECO	
Jussi Aarnisalo	Outokumpu Mining Oy	
Leo Grundström	Outokumpu Mining Oy	
Jarmo Lahtinen	Outokumpu Mining Oy	
Risto Pietilä	Outokumpu Mining Oy	
Aimo Hattula	Outokumpu Mining Oy	
Kaarlo Mäkelä	Outokumpu Mining Oy	
Erkki Ilvonen	Outokumpu Mining Oy	
Martti Kokkola	Outokumpu Mining Oy	
Pertti Lamberg	Outokumpu Research Oy	
Markku Tiainen	GSF	
Hannu Makkonen	GSF	
Erkki Luukkonen	GSF	
Heikki Papunen	UT	
Tapio Halkoaho	UT	
Jyrki Liimatainen	UT	

1. THE OBJECTIVES OF GEOES

The objectives of WP5 were to elicit knowledge from geo-experts, specify the functional requirements, and design and implement GEOES, the GEOSIS Expert System. Structured interviews with geo-experts was the driving force for integrating different data sources, elaborating on them during all stages of exploration, and combining results from different disciplines (geology, geophysics, geochemistry etc.) is the most cumbersome and difficult task that geo-scientists face. Geo-experts need assistance to perform this task effectively and efficiently.

More exactly, the objectives of WP5 can be interpreted as:

- to gather and encode in a structured fashion the knowledge of expert geo-scientists from all the different fields (geology, geochemistry, geophysics) that contribute to Ni exploration
- to specify the requirements for a novel expert system that will consult this knowledge and be able to automatically draw reliable conclusions from it
- to cover the required geological models (komatiite, intrusive, lateritic)
- to support three stages of Ni exploration process (wide area selection, identification of potential zones, target selection)
- to develop a friendly user interface for the expert system
- to integrate completely the system with GEOSIS
- to provide many modes of operation for the expert system

It is worth noting that not all of those targets were clear since the beginning of the project, but became clearer as GEOES evolved.

2. MEANS USED TO ACHIEVE THE OBJECTIVES

The first and most important phase of WP5 was to specify the requirements for GEOES. They have been produced as a result of knowledge acquisition sessions that NCSR Demokritos had with geo-experts. The requirements are distinguished as follows: general knowledge about the Ni exploration task, requirements concerning data and methods used for Ni ore exploration, requirements about the overall functionality of GEOES, and the process of how the experts elaborate on the existing data in order to favour the existence or not of Nickel ore deposits.

During the knowledge acquisition stage, it has been realised that GEOES should cover geological models for lateritic, komatiitic and intrusive Ni-ore deposits and should provide extensive assistance to users during all the phases of their work. These phases are: area selection, identification of potential zones, target selection and evaluation of target prosperity.

For each combination of model and phase there is a different set of factors that contribute in

deciding the favourability of Ni ore existence. Those factors (of geological, geophysical, pedogeochemical, mineralogical and lithogeochemical type) are grouped together according to the scientific field of their origin and specifying their relationships to each other. In this way each geo-scientist is easily oriented when using the system and gets involved with the domain category corresponding to his expertise.

All this functionality is easily used and is integrated with the rest of the tools developed within GEONICKEL. What is more, the system is easy to evolve and change, in order to adapt to new requirements. There are mainly two reasons why new requirements emerged during the development of GEOES:

- during the sessions we had with geo-scientists their knowledge and experience took a more formal shape, and this fact helped them afterwards realise other elements related to our discussion, that did not seem relevant at the beginning
- the trials of the GEOES prototype software by the geo-scientist partners that started at a very early stage of the development, gave birth to new requirements, as users realised the weaknesses as well as the potential of the system

We achieved our final GEOES goals by following a *cyclic prototyping methodology* during the acquisition / development phases. The first system prototype has been released to users as early as the end of the first year. Our approach has resulted to many intermediate releases of GEOES that were tested, validated, and finally integrated with GEOSIS. As a result, we had a system evolved to something that better suited the needs of its users.

To enable this evolutionary approach to software development, we employed rapid development tools that still offered the flexibility we needed:

- SICSTUS Prolog: a well known version of the Prolog language for Windows95/NT. Prolog is probably the most suitable language for developing expert system. We used Sicstus Prolog for the development of the knowledge base and the reasoning engine.
- Tcl/Tk: a versatile scripting language that allows rapid development and interfaces well with Sicstus Prolog. We used Tcl/Tk to develop the user interface as well as various types of functionality tied to the Prolog module

In conclusion, we think that what has been achieved is better than it was expected. The GEOES knowledge-based system belongs to the category of integrated expert systems, combining a wide range of geological, geophysical, geochemical and geographical information. However, it is dedicated for exploring Ni ore deposits and, to a greater extent than existing systems, it places special emphasis to the integration of the different disciplines. It comprises a generic mechanism for knowledge exploitation, provided that domain knowledge is structured according to some simple rules. Thus, this mechanism can be used for the exploration of other types of ore-deposits.

3. SCIENTIFIC AND TECHNICAL DESCRIPTION OF GEOES

The scientific and technical description of GEOES is presented by:

- giving specifications on the mineral deposits exploitation task;
- describing the knowledge acquisition process followed;
- specifying the overall architecture, the user interface and integration design principles, as well as the knowledge representation and the assessment process, and
- describing the implemented three modes of GEOES.

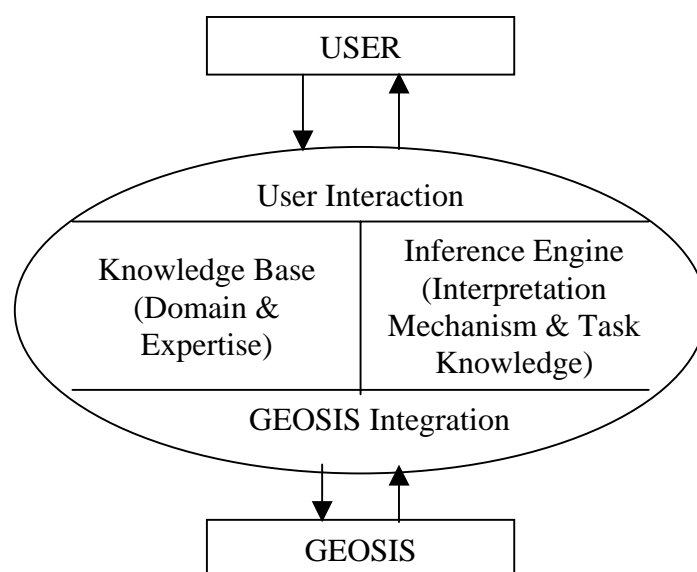


Figure 5.3-1: GEOES view.

As an expert system, GEOES in principle conforms to the view showed in Figure 5.3-1.

3.1 Specifications on the Mineral Deposits Exploitation Task

Assessment of mineral and other types of resources, requires associating observations with the features of a mineral deposit model. Observations can be either features obtained by interpreting data from various origins (e.g. geology, geochemistry, geophysics, pedogeochemistry, lithogeochemistry, and mineralogy), or direct indications acquired from field work.

A mineral deposit model is “a systematically arranged information describing the essential attributes of a class of mineral deposits”. Such a model can be a descriptive, a generic, or a combination of them. In particular, a descriptive model provides the essential features that a

class of mineral deposits must possess. It is the use of descriptive models that have increased the capability of interpreters to perform mineral resource assessments. A genetic model, also relates these features among themselves, to the host strata, and to the geologic evolution of deposits, aiming to bring coherence to the particular set of features postulated. Mineral deposit models guide the exploration at the planning and at the interpretation stages [Cox].

Exploration of mineral deposits requires the collaboration of geo-experts from different disciplines, and involves acquiring and interpreting a sheer amount of data that come from different origins. Geological, geophysical, mineralogical, and geochemical data can be acquired by applying various methods. Data contributed from geo-experts aim to provide as much as possible evidence towards the truth of model's features. Combination of data, and mainly, of observations coming from these data, is a very complicated task that requires experience from all the contributing parts and should be done efficiently and accurately.

During the exploration task, geo-experts (geologists, geophysicists, geochemists, etc) identify an area of potential favourability. Favourability is a hypothesis that is justified by the observations acquired. In other words, observations provide evidence towards the truth of the favourability hypothesis. Such observations may come from different geoscientific domains:

- (a) Geology
- (b) Geochemistry
- (c) Mineralogy
- (d) Geophysics
- (e) Litho-geochemistry
- (f) Pedo-geochemistry

As the exploration task continues, explorers circumscribe even narrower areas for exploration and apply their methods more intensively. This task continues until they find a mineral deposit or until they decide that their hypothesis concerning favourability is not valid. The major stages of an exploration project are the following:

- (a) Select a region, then
- (b) Within the selected region select a cluster or zone that seems promising, and
- (c) Within the selected cluster/zone identify an area that may host a mineral deposit.

Exploration is a combination of data acquisition and interpretation. Interpretation is a combination of data abstraction and model-guided reasoning tasks. Abstraction involves combining data towards intermediate conclusions. Such conclusions form evidence that justify more abstract conclusions and so on, until the truth - or a certain degree of favourability - of features comprising a model is assessed. According to model-guided reasoning, experts are guided by mineral deposit models to form and discriminate hypothesis. The latter involves gathering observations that provide evidence towards the truth of this hypothesis. During interpretation, experts may provide an overall geological story, bringing coherence to the observations postulated. The interpretation task is performed for every exploration stage and for all data acquired.

The ordering of data acquisition, abstraction, hypothesis formation and hypothesis discrimination is not fixed. For instance, new evidence may strengthen or weaken a previously formed conclusion, or give priority to a previously underestimated hypothesis. Also, hypothesis formed drives the acquisition and interpretation of data.

To perform the interpretation task, a geo-expert must have detailed knowledge concerning alternative reasonable aggregations of observations (things that she/he expects to «see») and of their supported features. *Observations* and their immediate conclusions play the role of evidence for justifying more abstract conclusions, which in their turn justify mineral model's features. Intermediate conclusions and model features are called *factors*. The combination of observations and factors towards hypothesis truth forms causal dependencies among them. These causal dependencies do not affect only a specific domain model and the overall hypothesis, but might affect other domain models positively or negatively.

Assessment of model features involves uncertainties that make the task more subjective, and therefore, less accurate and more complicated. On the other hand, limited exploration budgets may prohibit the application of resource-demanding data acquisition methods. In such cases, experts should make the best evaluation of the known data and should only apply methods that help to assess the essential features of models. As indicated in [Cox], we can never “acquire” a complete model. We can approach a complete understanding of a model only asymptotically.

Therefore, the exploitation interpretation task accommodates uncertainties that might be categorised as:

- Uncertainty associated with factual knowledge. Observations may be difficult to acquire. They may be ill defined, and data may have been measured with unreliable techniques or equipment. They may even be unavailable.
- Uncertainty in the interpretation phase. Interpretation depends on the experience of human experts. Uncertainties related to an interpretation that specifies the degree by which an expert believes a step to be valid.
- Human experts belief in a conclusion or in a piece of evidence.

3.2 The Knowledge Acquisition Process

During knowledge acquisition we have followed a stratified approach: First, we have contacted an overview of the most important expert systems for the assessment of deposits [Vour96]. This overview, in conjunction with the first discussions with the geo-experts, helped us to identify the major aspects of the interpretation task, the attributes-characteristics of that task and understand the rationale behind it. Also, this process has helped us to identify the major types of knowledge elements utilised. Moreover, considering the way geo-experts co-operate towards assessing model's features, we have specified the model of co-operation between GEOES modules. The result was a knowledge level description of GEOES.

The abstract description of the interpretation task, as well as, the major types of knowledge identified, provided the appropriate templates that guided subsequent knowledge acquisition sessions.

Second, we specified in detail the types of knowledge utilised by the interpretation task. Types of knowledge include causal dependencies between factors, the primitive inferences, as well as, conceptual dependencies between observations and factors. Such conceptual dependencies are mostly, instance-of and type-of relations. These types of knowledge were acquired by extensive knowledge acquisition sessions, where geo-experts from different domains contributed their own experience. This process provided us with extensive insight into the cooperation process between geo-experts, as well as, into the interpretation task, since experts usually recalled known cases and the factors that played a major role in assessing the existence of Ni-ore deposits.

Finally, we have implemented and released a number of prototypes that were demonstrated to experts during knowledge acquisition sessions. The cyclic prototyping approach helped both, knowledge engineers and the geo-experts, to have a common language, refine their thinking, and helped each part to examine the outcomes that the other part expected.

3.3 GEOES Design Specifications

In the design specifications of GEOES we emphasize on the overall architecture of the system. Then we proceed to describe shortly the design principles of the user interface. Two issues that need clarification and special attention, namely the knowledge representation and the assessment process, are presented in the corresponding sections. Finally, the issue of integration between GEOES and GEOSIS is examined.

3.3.1 Overall Architecture

The overall architecture of GEOES is depicted in Figure 5.3.3.1-1. GEOES comprises of a models knowledge base, a generic inference engine and a set of modules with heuristics on mineral explorations knowledge (strategies), together with the user interface and GEOSIS integration components. The heuristics on mineral explorations modules are grouped so that they correspond to each of the geo-domains concerned and they participate in the corresponding assessment as well as in the overall assessment of the system.

GEOES contains one domain module for each of the specialities that contribute in assessing the existence of mineral deposits. *In the final version these are the geological, geophysical, geochemical, pedogeochemical, lithogeochemical, and mineralogical modules.* It must be pointed that there is not an overall manager or a central module that co-ordinates the work of the different modules. This reflects and models the distributed and collaborative work of geo-experts, who gather data and interpret them from their own point of view, taking into consideration conclusions, observations and requests coming from other geo-experts. Then, conclusions coming from different domains are evaluated to provide an overall assessment concerning the existence of mineral deposits. This is exactly how the different modules of GEOES perform

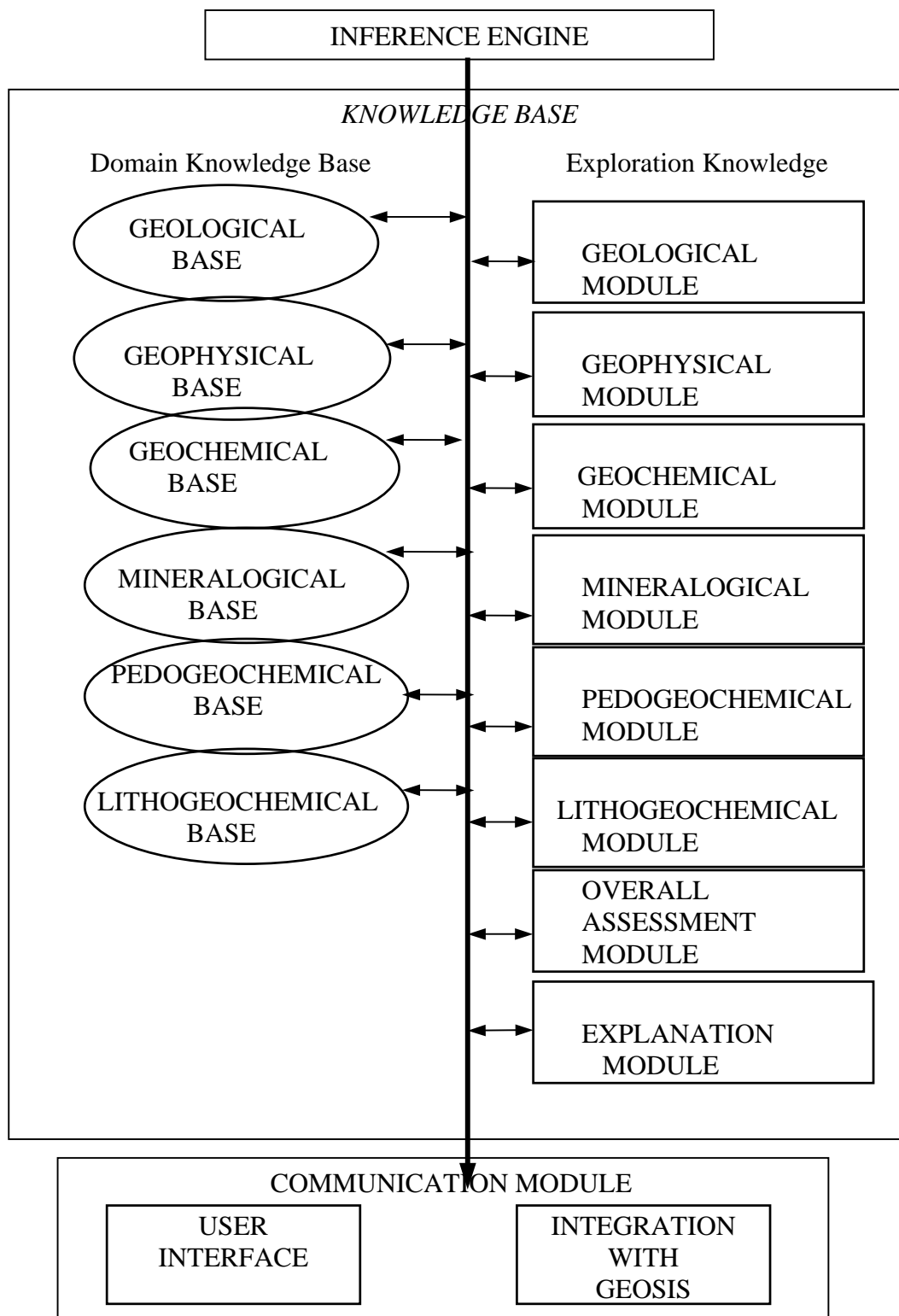


Figure 5.3.3.1-1: GEOES overall architecture.

and collaborate. Specifically, the main task of each domain module is to interpret observations that belong to its own domain. To perform the interpretation task, each module identifies and assimilates important pieces of evidence, draws conclusions concerning the existence of important features of descriptive models, suggests and focuses the attention of users to important features whose assessment is weak.

Each domain module is associated mainly with a GEOES domain knowledge base that stores observations, factors assessed within the corresponding domain, the evidence degree of factors, and pieces of evidence that contribute to its truth. Each domain knowledge base can be accessed from any domain module.

Concerning the collaboration of modules, each module with the support of the inference engine:

- manipulates observations, and assessed factors from domain knowledge bases, and
- places requests to other GEOES modules (this is done in case that it needs evidence which can not be found in the corresponding domain knowledge bases).

The main task of the overall assessment module is to mesh observations and factors coming from different domains and provide an overall conclusion. To perform this task, the overall assessment module:

- consults observations, and assessment of factors recorded in all internal GEOES domain knowledge bases,
- ranks the different mineral deposit models based on the available evidence, and
- places requests to other GEOES modules (it is the responsibility of the other modules to provide such information or notify the user for the lack of evidence).

The explanation module provides explanations concerning the inference steps performed and the decisions taken by the system. Explanation concerns conclusions formed by each of the domain modules involved in decision making, as well as by the overall assessment module. The explanation module indicates important missing information that GEOES needs to strengthen its judgements.

3.3.2 User Interface Principles

GEOES comes in three different modes, each using the same underlying knowledge base and inference engine but having different user interface and functionality. Those three modes are the interactive, the spatial and the hybrid GEOES (see Section 5.3.4 and Screen-shots 5.3.4.1-1, 5.3.4.2-1, and 5.3.4.2-2). In all three versions however there is a similar design philosophy behind the user interface. The *context* of operation, which consists of the model (komatiite, intrusive or lateritic), the exploration mode (select area, potential zones or select target), and the domain (geology, geophysics, geochemistry, pedogeochemistry, lithogeochemistry or mineralogy) appear on the left part of the GEOES window. In interactive GEOES, the user can select the context in full, while in spatial and in hybrid the user may select only the domain – the model and the exploration mode depends on the selected input data.

Once the context is set, the user will normally make three steps:

- set various options, data values and interpretation parameters
- invoke the expert system to process the data
- view, save or print the results

The first step is the most important one. Parameters can be set for each factor / subfactor through the *Observations* window that shows all factors / subfactors / observations for the specified context. The user may select a factor and open another window presenting the choices that are available for the manipulation and interpretation of the factor, or for the values this factor can be assigned.

Various other options are available to the user, such as the ability to alter internal parameters of the inference engine, to save them and to restore them, or to save and restore values assigned to factors.

The implementation of the user interface has been done using Tcl/Tk, a powerful, portable scripting language. It runs on the Windows 95 and Windows NT operating systems. The main reasons for choosing Tcl/Tk are:

- speed of development, which is an important factor in an evolutionary development approach where a prototype system must be ready as quickly as possible, and
- support for Sicstus Prolog, which was used for the development of the knowledge base and the inference mechanism.

3.3.3 Knowledge Representation

Knowledge in the GEOES knowledge base is represented by causal diagrams. Those causal diagrams are directed acyclic graphs that represent how factors / subfactors are predicted from other factors, or directly from observations. Arrows in such diagrams represent primitive inference steps towards assessing models' features. The information that arrows carry in these graphs encode conditional interdependencies between factors / subfactors / observations [Shaf96][Char91][Gas82]. Specifically, each arrow is related with a set of quantities, or qualities, that express the dependency degree of a factor / subfactor / observation from its parents. Additionally, each factor / subfactor, given the occurrence of its parents, is independent from its predecessors. Therefore, to predict the occurrence of a factor in such diagrams, one needs the evidence degree of its immediate predecessors and factor's causal dependencies from them. An instance of such a diagram is shown in Figure 5.3.3.3-1. It must be noted that the diagram in Figure 5.3.3.3-1 is a 2-level one. In general, there may be many levels of subfactors between factors / subfactors and observations. Moreover, it should be noted that observations are the terminal nodes of the diagram. Such nodes may also be factors and subfactors that are not analysed in further detail. Finally, a single subfactor or observation may contribute to the assessment of more than one factors or subfactors.

A causal dependency in GEOES is represented by a pair of numbers (S_G , N_G) associated with each link of a diagram:

(a) S_G represents the sufficiency of evidence E to establish the hypothesis H. In particular, S_G indicates the degree of E's suggestiveness to H, given that the truth of E is supported. Dealing

with sufficiency, imposes considering the causal diagram in an bottom-up way, in a way that is analogous to the abstraction task during human interpretation.

(b) N_G represents the necessity of evidence E to establish hypothesis H. In particular, N_G indicates the degree of E's presence given that the truth of H is supported. In other words, necessity expresses the effect of E's absence to the truth of H. Necessity encourages considering the causal diagram in a top-down direction. This is analogous to the model-guided task during human interpretation.

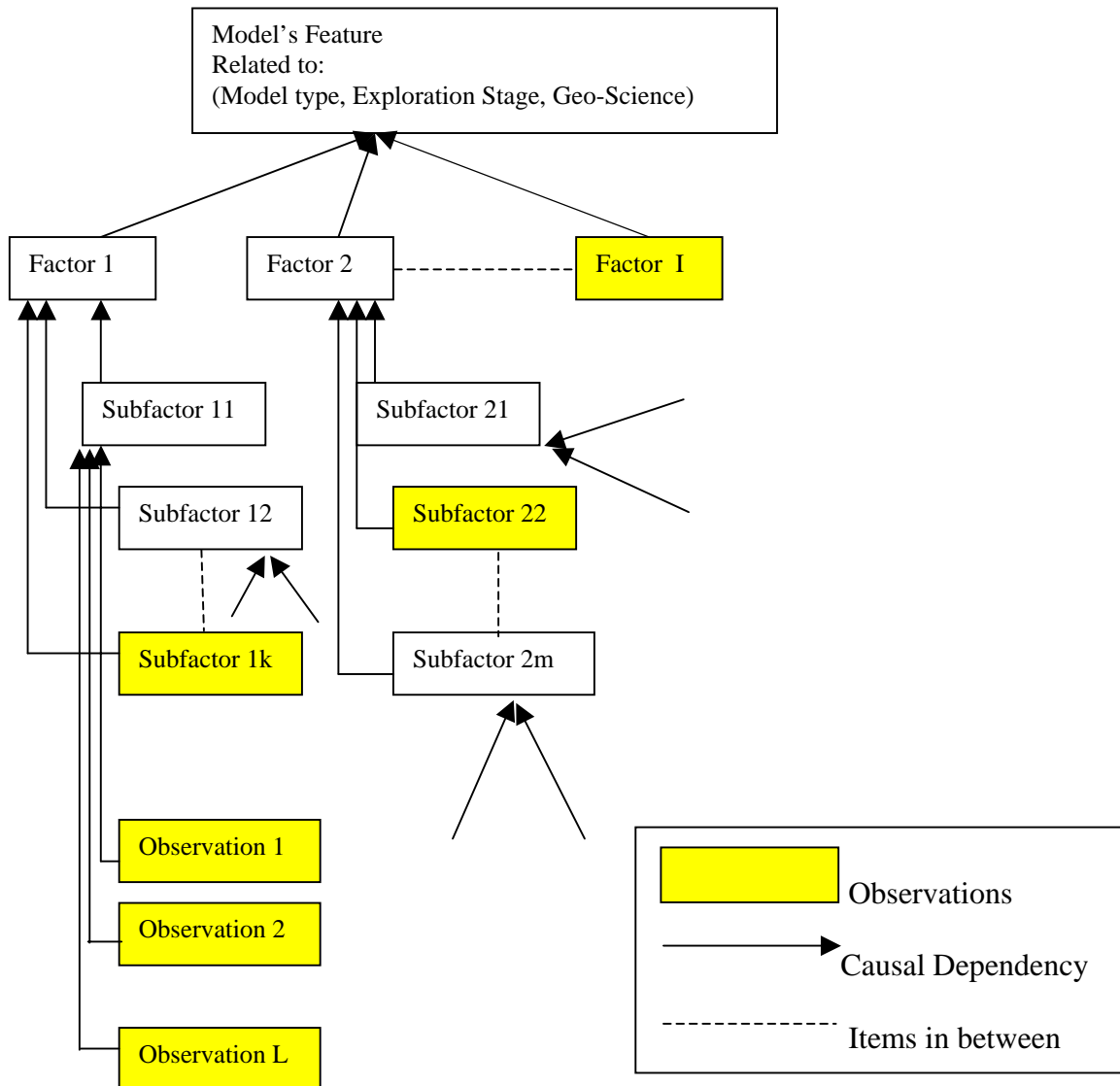


Figure 5.3.3.3-1 : A generic GEOES causal diagram.

We have utilised such a representation of uncertainties because:

- It enables acquisition of knowledge: It supports and guides human interpreters to effectively unfold the causal diagram they have in mind and evaluate the representation with known cases. The representation is made more comprehensive to human interpreters.

- It supports assessment of factors that resembles the human way of thinking. Conclusions are supported with the degree that a human expert would support them, given the same pieces of evidence and the same uncertainties associated.
- It provides the means for an accurate representation of the way geo-experts think nature works, and yet, it reflects the fact that models can be completed only asymptotically. Modelling of ignorance facilitates the latter.
- It supports computational efficiency
- It gives the opportunity to the user to specify what-if scenaria before he/she finalises a causal dependency, or have different causality behaviour in different regions or exists a different human opinion.

3.3.4 Assessment Process

To compute the degree by which pieces of evidence force the truth / falsity of a hypothesis, GEOES utilises both degree of necessity and sufficiency. Necessity and sufficiency allow specifications of disjunctions and conjunctions of factors towards hypothesis, without stating explicitly AND / OR connectives between these factors. When two pieces of evidence E_1 and E_2 should be combined with an AND connective, then their necessities should be as high as possible and their sufficiencies must approach zero. This indicates that both of them are necessary but none of them can force by itself the truth of a hypothesis H . Also, when two pieces of evidence E_1 and E_2 should be combined with an OR connective, then their necessities must be low but their sufficiencies high. This indicates that each piece of evidence is sufficient to support in a high degree the truth of a hypothesis H , but none of them is necessary. It must be pointed out that this representation of an OR connective does not exclude the case that both pieces of evidence support the truth of the hypothesis.

Suppose that a piece of evidence E is related to a hypothesis H , with degrees N_G and S_G for necessity and sufficiency, respectively. E has been assigned an evidence degree W_E that indicates the evidence contributing to its truth. In case E is an observation, W_E is provided by the user and expresses the belief of the user to the presence of E . In case E is a factor that contributes to more abstract hypotheses, then W_E is computed by combining the pieces of evidence to E . This is a real number from -1 to 1 . Values assigned to W_E correspond to the certainty levels given in Table 5.3.3.4-1.

Degree of Evidence	Verbal Description
0.83 – 1	Supported
0.57 – 0.82	Highly Supported
0.30 – 0.56	Moderately Supported
0.13 – 0.29	Weakly Supported
0 – 0.12	Absence of Evidence

Table 5.3.3.4-1: Verbal descriptions of certainty levels

Let $T_{E,K}$ be the highest possible evidence that forces the truth of E . The subscript K indicates the number of children of E . In case E is an observation, then $T_{E,0} = 1$. Otherwise, $T_{E,K}$ can be

any positive real less than or equal to 1. $T_{E,K}$ is computed by forcing the evidence degrees of E's children to be equal to 1, and each dependency to have sufficiency degrees equal to 1. The calculation is performed using the formula for evidence combination described below. For example, when $k=1$, then $T_{E,K}=0.73$. For $k=2$, $T_{E,K}=0.88$ etc. It should be pointed out that W_E can not be greater than $T_{E,K}$. Given W_E , the number $T_{E,K}-W_E$ gives the lack of evidence for supporting the truth of E. Table 5.3.3.4-2 gives some sample values for W_E , $T_{E,K}$ and $T_{E,K}-W_E$.

$T_{E,K}$	W_E	Verbal Description for evidence towards E	$T_{E,K}-W_E$	Verbal Description for lack of evidence towards E
1	1	Supported	0	absent
1	0	Absent	1	supported
1	0.2	weakly supported	0.8	highly supported
1	0.5	moderately supported	0.5	moderately supported

Table 5.3.3.4-2: Evidence and lack of evidence towards supporting E's truth

Let us recall that S_G indicates the degree of E's suggestiveness to H, given all the evidence needed to force the truth of E. Therefore, given that the current degree of evidence towards E is W_E , then $(S_G * W_E / T_{E,K})$ expresses the degree by which E supports the truth of H. Moreover, since N_G indicates the degree of E's presence when the truth of H is supported, then $N_G * (T_{E,K} - W_E) / T_{E,K}$ represents the degree by which absence of evidence towards E affects the truth of H, when the evidence for E is W_E . This can be modelled by a switch that spends W_E time units to E and $T_{E,K} - W_E$ time units to E's lack of evidence. To have all the evidence that is needed to force the truth of H, there is a necessity of $T_{E,K} - W_E$ time units, that "cost" $N_G * (T_{E,K} - W_E) / T_{E,K}$.

Therefore, there is a factor $S_G * W_E$ that contributes towards the truth of H in a positive way, and a factor $N_G * (T_{E,K} - W_E)$ that contributes towards the refutation of H. Finally, the computation for the evidence towards the truth of H, that is W_H , is done by a sigmoid function used for the forward activations flow in a backpropagation network:

$$W_H = \left(\frac{1}{1 + e^{-((S_G W_E) - (T_{E,K} - W_E) N_G) / T_{E,K}}} \right)$$

In case hypothesis H is supported by more than one pieces of evidence, $\{E_i, 1 \leq i \leq n\}$, then:

$$W_H = \left(\frac{1}{1 + e^{-\sum_i [(S_{Gi} W_{Ei}) - (T_{Ei,K} - W_{Ei}) N_{Gi}] / T_{Ei,K}}} \right)$$

Moreover, since results provided to users should be in [0,1] and in order for these to correspond to the certainty levels specified in Table 5.3.3.4-2, W_H is normalised to $W'_H = W_H / T_{H,K}$. Where $T_{H,K}$ is the highest degree of evidence for supporting H, in case H has exactly k children.

The sigmoid function has been chosen due to the following reasons: it provides a natural normalisation of results between 0 and 1, included. The results calculated have been proven to be intuitive to human experts, and it enables learning, that is, adaptation of uncertainties to handle cases that cannot be handled effectively.

The development of the knowledge base and the inference engine was done in Sicstus Prolog. Prolog in general is the language of choice for expert systems because of its strong support of logic concepts. Sicstus Prolog is a well known implementation of prolog, with good support and interfaces to other languages, such as Tcl/Tk and Visual Basic.

3.3.5 Integration with GEOSIS

Integrating GEOES with GEOSIS was an important part of WP5. Integration concerns mainly the spatial and hybrid GEOES modes, and to a smaller extend the interactive mode. The integration consists actually of three issues:

- GEOSIS provides the data that spatial GEOES use as input
- GEOSIS shows the results of spatial GEOES on a map
- GEOSIS initializes hybrid GEOES with the required parameters

Therefore, it is clear that spatial and hybrid GEOES depend heavily on GEOSIS for their complete functionality. Technically, there are a number of options to consider when two or more programs must interact with each other. We used intermediate files to exchange information between GEOES and GEOSIS, as this technique is simple, safe, and does not require additional tools.

A communication protocol between GEOES and GEOSIS defines who creates each file and when, and who updates or deletes each file and when. Also the location and structure of each of the files used for information exchange is strictly defined, so that GEOES can read information produced by GEOSIS and vice-versa.

3.4 The Implemented GEOES Modes

The GEOES system gives emphasis on the integration of a variety of different approaches for the Ni exploration tasks, combining a wide range of data and knowledge from all the geo-domains involved. It covers geological models for *lateritic*, *komatiitic* and *intrusive* Ni-ore deposits and provides assistance to users during all the phases of their work. Those exploration phases include:

- *Area selection*, where wide areas are examined for the existence of Ni-ore deposit.
- *Identification of potential zones*, where zones within a given area are examined.
- *Target selection*, where a restricted small area is examined.

For each combination of the above models and phases, there is a number of *observation entities*, grouped in specific geo-domains such as geology, geochemistry, geophysics, pedogeochemistry, lithogeochemistry, and mineralogy. The observation entities correspond to factors and sub-factors which are connected with the favourability of existence of Ni-ore deposits. The user provides qualitative data measurements for the observation entities, that feed the expert system. Based on those data, GEOES is able to assess the favourability of existence of Ni-ore deposit, provide a consultation that presents arguments to that assessment, even graphs that depict the contribution of each scientific geo-domain to the final result.

To accomplish the requirements we have implemented three modes of GEOES. All of them are based on the same knowledge bases - dependent on the context - and inference engine. However, each one is contributing from a different point of view, and they are going to be exploited complementary to each other. Therefore, there are three different communication modules, that correspond to the three distinct modes of operation of GEOES, each having its own user interface, its own communication protocol for integrating with GEOSIS, and its own functionality suitable for applying it to specific situations.

3.4.1 The Interactive GEOES

The interactive version of GEOES was developed in the early stages of the project in order to help the knowledge acquisition process and test the knowledge engine against real geo-data. Those tests were vital for the development of GEOES, which followed an iterative evolutionary approach with the end users playing a significant role in testing and improving the system.

The user interface gives access to all the functionality of the underlying system: it is possible to select various combinations of geological models and exploration phases, fill in values to the corresponding *observations*, and get the result of the expert system in the form of a verbal *consultation*, and in the form of a graph (see Screen-shot 5.3.4.1-1). Based on those results the user can experiment and engage in what-if scenarios by changing the values of a few observations and then check on the difference at the final results. Experimentations are supported at an even deeper level, as the user can set some of the internal parameters of the knowledge engine, namely the *necessity* and *sufficiency* values for each observation.

Through the menu, the user has access to various other useful options, such as:

- the print menu item for printing the histogram and the consultation

- the save / restore menu items for the necessity and sufficiency setting of the knowledge base
- the save / restore menu items for the observation values

Although interactive GEOES gives unrestricted access to all the functionality of the knowledge engine, it requires that each set of input values must be given to the system by the end user. This is very flexible when someone wants to experiment and very suitable for geoscientists who want to become familiar with GEOES, but it clearly becomes impractical when one is going to use it in a real situation.

3.4.2 The Spatial GEOES

The spatial version of GEOES was developed to remedy this drawback. Furthermore, with spatial GEOES, the integration with GEOSIS becomes tighter. Our goal was threefold:

- First, to make it possible for GEOES to exploit the GEOSIS database and avoid manual data entry.
- Second, to run the knowledge engine in a batch mode for many sets of data at once (each data set corresponds to a cell of a map).
- Third, to present the results in a way that makes more sense to the users.

For this we used intermediate tables that are provided by GEOSIS. Each line in those tables contain measurements that correspond to one cell of a map. The intermediate tables are used as input for spatial GEOES, which runs the knowledge engine until all data have been processed. The output is recorded in again another intermediate table used by GEOSIS to present the results on a coloured map (see Screen-shot 5.3.4.2-2).

In contrast to the interactive version, spatial GEOES has functionality that makes it easier to deal with a lot of data. The user has absolute control on the way the knowledge engine assesses the data. It is possible to see the lowest and highest values for each observation, to set the lowest and highest admissible value, to select a method for evaluating the measurements from linear, exponential, logarithmic, or user-defined (see Screen-shot 5.3.4.2-1).

With the spatial version, GEOES becomes a truly useful and powerful tool in the GEOSIS toolbox. However, because spatial GEOES runs the knowledge engine in a batch mode for many data sets, it is not possible to get a consultation as in the interactive version.

3.4.3 The Hybrid GEOES

This problem is solved with the introduction of the hybrid GEOES version. The hybrid version completes the spatial GEOES, by elaborating on the results of the spatial version and combining the flexibility of the interactive version. Once the user has used the spatial version to produce a map coloured according to the results (Screen-shot 5.3.4.2-2), he/she may wish to select a map cell and get more information on the specific cell, or even try some what-if scenarios on that cell.

The hybrid version runs when the user selects a cell, loads automatically the data concerning

that cell, and offers the flexibility of the interactive version: it is possible to view consultation and histograms, change the values and compare as many times as needed. All the functionality of the interactive GEOES is available in the hybrid mode, but the user does not have the burden of entering manually the observation data.

4. INITIALLY PLANNED ACTIVITIES AND WORK ACCOMPLISHED

The initially planned activities for GEOES, although not so clear at the beginning, have been clarified during the project and have been accomplished quite well. Towards the final success it helped very much the early and subsequent GEOES prototypes that were released to the geo-expert users for evaluation and subsequent successful knowledge acquisition process.

To achieve reliability of GEOES and the requirement for realisation of three GEOES modes together with the integration in the GEOSIS environment, we had a very hard task till the end of the project.

The final GEOES prototype modes support Ni exploration professionals in all the stages of the exploration task as well as during the training or familiarisation process of young or unfamiliar professionals, respectively. The capability of Spatial GEOES to deal with bulk of input data, that could correspond to large region areas, potential zones, or target areas, in a very small time frame, is very promising.

This achievement is even greater, since the system consultation results appear on a map where it is possible to instantiate Hybrid GEOES for further work on specific points, which was well-accepted by geo-experts.

Finally, the expression of interest by a well-known company in geo-informatics, on the resulting software tools from the GeoNickel project is another evidence of the value of the accomplished work.

5. CONCLUSIONS

GEOES belongs to the class of integrated systems. To a greater extend of already known systems integrates information from many geo-domains in order to assess the existence of Ni-ore deposits. The GEOES knowledge based system is the result of a multidisciplinary approach to the problem of mineral exploration. It utilises knowledge and information from diverse domains (geological, geophysical, geochemical, pedogeochemical, lithogeochemical, mineralogical) and combines them to provide an overall conclusion concerning the assessment of Ni-ore deposits in certain areas.

Knowledge is exploited by a very generic inference mechanism that calculates the favourability of hypothesis with pictorial and text consultation. The explicit representation of the different types of knowledge using specific structures contributes to the development of a knowledge base that can be expanded and maintained with efficiency, effectiveness and safety. A key feature in this dimension is the effectiveness with which knowledge can be enriched so as to include more detailed and subtle issues concerning the assessment of the existence of Ni-ore deposits.

Furthermore, the generic mechanism that exploits the represented knowledge can be transferred to the exploration of other types of ore-deposits (except Ni deposits). Knowledge concerning these types of ore-deposits has to be structured using the knowledge structures mentioned above.

GEOES offers a complete suite of expert tools to geo-scientists, since it is designed to support all the stages of Ni exploration, from wide area selection to potential zones and further to target selection. In addition it comes in three modes of operation, interactive, spatial, and hybrid, that are adapted to be used for different but complementary purposes.

A crucial feature of the system is its complete integration with the overall GEOSIS system. Integration of these systems helps geo-experts to manage their exploration data more effectively and contributes to the identification of further (geological, geophysical, geochemical etc.) features, as well as to refine knowledge concerning the importance of known features to the assessment of Ni-ore deposits.

6. ACKNOWLEDGEMENTS

Dr. Spyropoulos would like to thank all the partner professionals and especially those from OUTOKUMPU, LARCO and IGME that contributed very seriously during the phases of acquisition and validation of GEOES, and without their sincere participation GEOES would not have been realised. Also, Dr. Spyropoulos expresses great «thanks» to all his colleagues that participated in the realisation of GEOES, namely, Dr. Maria Katzouraki, Dr. G. Vouros, Dr. S. Kokkotos, Dr. C. Koutras, Mr D. Katsoulas and Mr. Y. Stavarakas.

7. ANNEXES

7.1 Publications and conference presentations

C.D.Spyropoulos, “Intelligent techniques for identifying Ni-ore deposits”, Technical Workshop, Mantoudi, Evia, Greece, 1998.

C.D.Spyropoulos, Y.Stavrakas, D.Katsoulas, G.Vouros et. all, “Integrated technologies for mineral exploration: pilot project for Nickel ore deposits”, Eurothen Conference, 1998.

7.2 Reports

G.Vouros, «Expert Systems for Exploration of geological deposits», GEONICKEL Internal Paper, 1996.

G.A.Vouros, C.D.Spyropoulos, M.Katzouraki, “Requirements Specification in GEOES”, internal technical report, 1996, NCSR “D”.

G.A.Vouros, M.Katzouraki, C.D.Spyropoulos, “GEOES knowledge base”, internal technical report, 1997, NCSR “D”.

G.A.Vouros, “Knowledge representation and reasoning in GEOES”, internal technical report, 1998, NCSR “D”.

G.A.Vouros, “Expert systems for exploration of geological deposits”, internal technical report, 1996, NCSR “D”.

C.Koutras, C.D.Spyropoulos, G.A.Vouros, “GEOES knowledge base: necessity / sufficiency measures for lateritic, Komatiite, and intrusive models”, technical report, 1998, NCSR “D”.

G.A.Vouros, C.D.Spyropoulos, M.Katzouraki, C.Koutras, “The GEOES knowledge based system for Ni-ore deposits exploration”, internal unpublished paper, 1998, NCSR “D”.

G.A.Vouros, C.D.Spyropoulos, M.Katzouraki, “Functional Specifications for GEOES”, internal technical report, 1996, NCSR “D”.

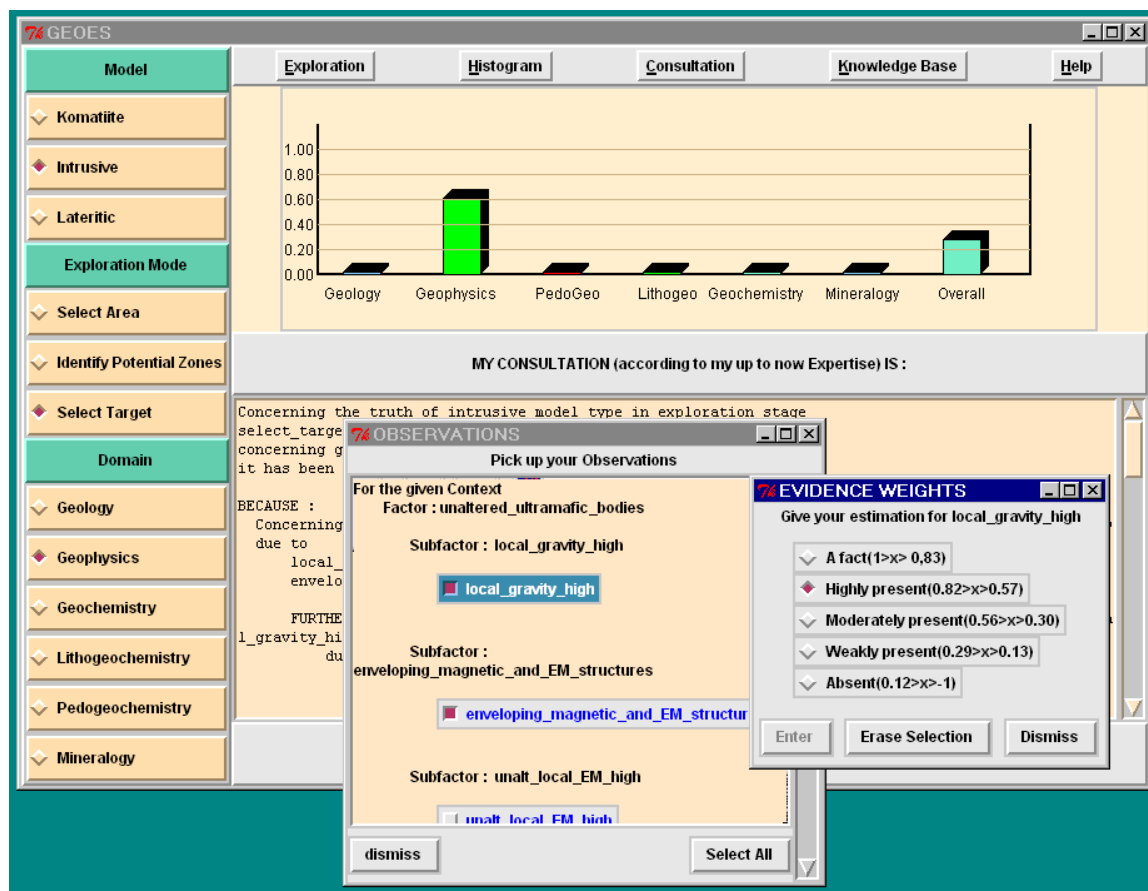
7.3 Prototypes

GEOES Prototype Software: a user-friendly expert system for identifying Ni ore deposits, in three modes of operation (Interactive, Spatial, and Hybrid) for the Windows 95 / NT operating systems.

8. REFERENCES

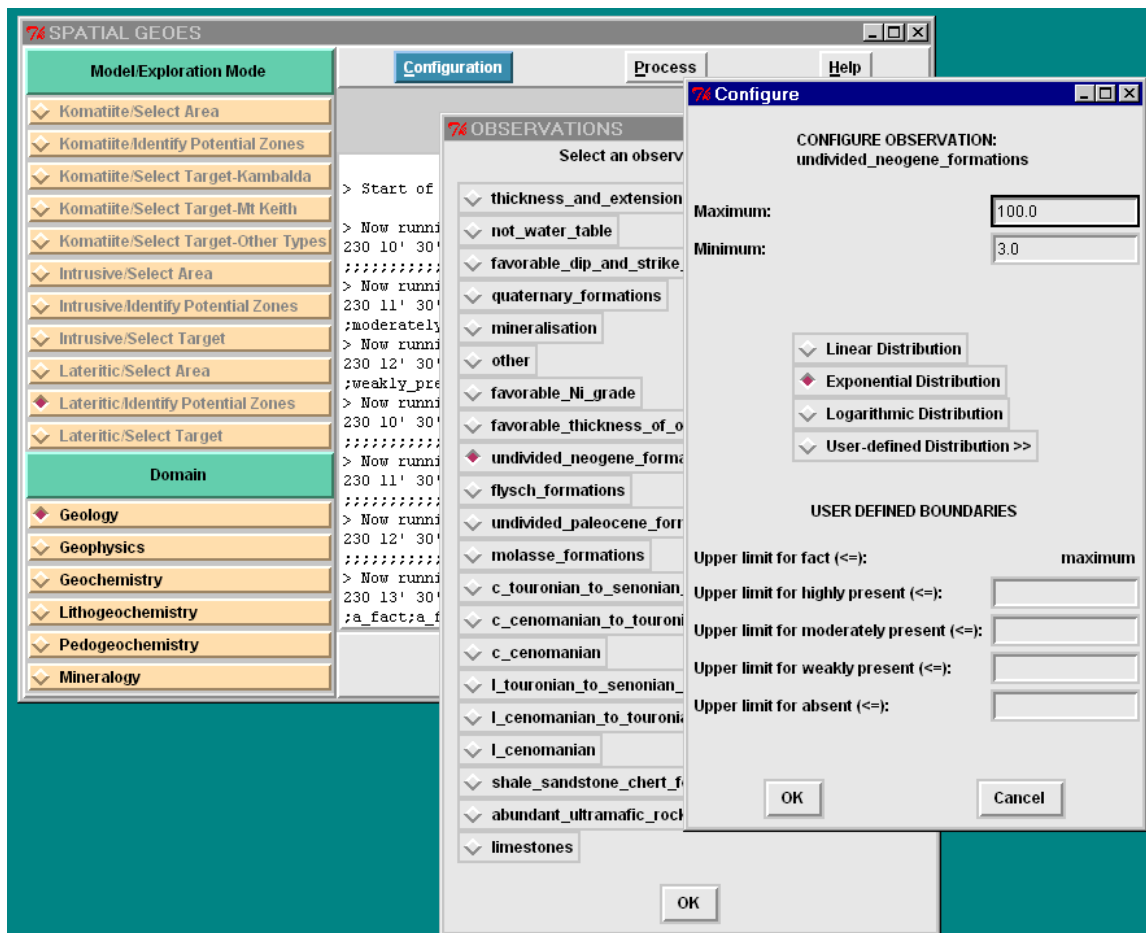
- [Vour96] G.Vouros, «Expert Systems for Exploration of geological deposits», GEONICKEL Internal Paper, 1996.
- [Cox] D.P.Cox, D.A.Singer, «Mineral Deposit Models», U.S. Geological Survey Report.
- [Mart87] L.Martin «Expert Systems and their use as exploration assistants», Exploration '87 Proceedings «modern computer based methodologies: their coming role in exploration», pp 826-834, 1987.
- [Cam94] R.B.McCammon, «Prospector II: Towards a Knowledge Base for Mineal Deposits», Mathematical Geology, Vol 26, No 8, 1994, pp. 917-936.
- [Gas82] J.Gaschnig «PROSPECTOR: an expert system for mineral exploration», in Michie D. (ed.) Introductory readings in Expert Systems, Gordon and Breach Science Publishers, Inc., 1982, pp 47-64.
- [Char91] E.Charniak, «Bayesian Networks without Tears», AI Magazine, Winter 1991, pp 50-63.
- [Shaf96] G.Shafer, «The Art of Causal Conjecture», The MIT Press, 1996.
- [Vour96b] G.A.Vouros, C.D.Spyropoulos, M.Katzouraki, “Requirements Specification in GEOES”, internal technical report, 1996, NCSR “D”.
- [Vour97] G.A.Vouros, M.Katzouraki, C.D.Spyropoulos, “GEOES knowledge base”, internal technical report, 1997, NCSR “D”.
- [Vour98b] G.A.Vouros, “Knowledge representation and reasoning in GEOES”, internal technical report, 1998, NCSR “D”.
- [Spy98d] C.D.Spyropoulos, “Intelligent techniques for identifying Ni-ore deposits”, Technical Workshop, Mantoudi, Evia, Greece, 1998.
- [Vour96a] G.A.Vouros, “Expert systems for exploration of geological deposits”, internal technical report, 1996, NCSR “D”.
- [Kout98a] C.Koutras, C.D.Spyropoulos, G.A.Vouros, “GEOES knowledge base: necessity / sufficiency measures for lateritic, Komatiite, and intrusive models”, technical report, 1998, NCSR “D”.
- [Vour98c] G.A.Vouros, C.D.Spyropoulos, M.Katzouraki, C.Koutras, “The GEOES knowledge based system for Ni-ore deposits exploration”, internal unpublished paper, 1998, NCSR “D”.
- [GEONICKEL98e] C.D.Spyropoulos, Y.Stavrakas, D.Katsoulas, G.Vouros et. all, “Integrated technologies for mineral exploration: pilot project for Nickel ore deposits”, Eurothen Conference, 1998.
- [Vour96c] G.A.Vouros, C.D.Spyropoulos, M.Katzouraki, “Functional Specifications for GEOES”, internal technical report, 1996, NCSR “D”.

Screen-shot 5.3.4.1-1 : Interactive GEOES.



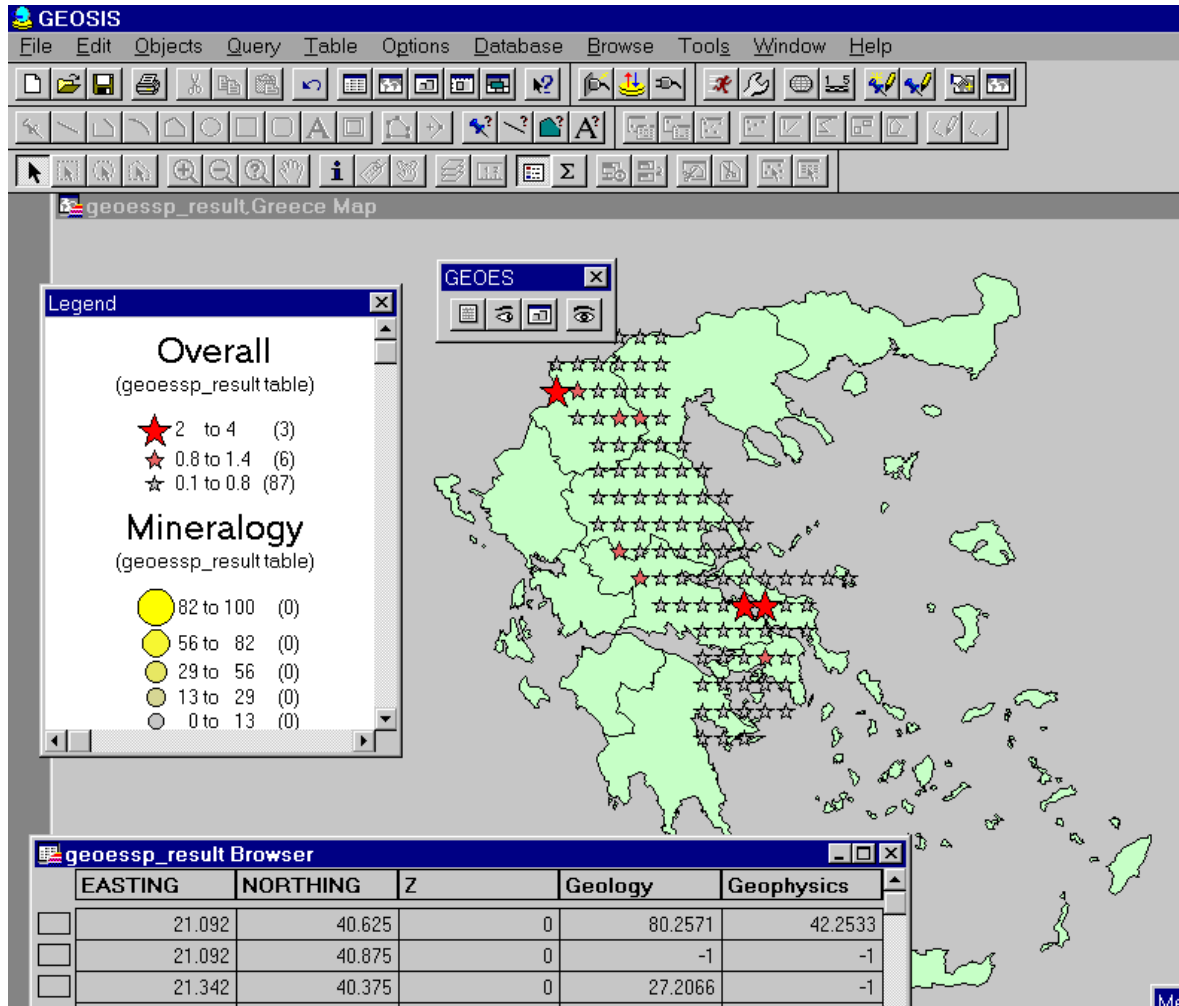
In Interactive GEOES, the user selects a context (model, exploration mode, and domain). Then by using the Observations window, the user sees the factors – subfactors - observations linked to a context, and selects the observations to which values can be assigned. Values are qualified evidence weights: fact, highly present, moderately present, weakly present, or absent. Then the user can view the consultation on a histogram showing the contribution of each domain towards the favourability of Ni ore existence, or on a text form explaining how the system reached those conclusions.

Screen-shot 5.3.4.2-1 : Spatial GEOES.



In Spatial GEOES, the system decides automatically the model and exploration mode by the category of data, that appear on the intermediate tables of GEOSIS. Those data, in contrast to Interactive GEOES, are of a quantified form. They are not entered manually by the user but instead are downloaded from the GEOSIS database, and concern many points of the area under consideration. The user may select the domain and in the Observations window the relevant factors that quantified in the intermediate tables are displayed. For each factor the user may see the minimum and maximum values present, and has an option to choose between linear, exponential, logarithmic, and user defined methods for classifying the data values. At this point the Spatial GEOES can run, and the results are displayed on a map opened from within GEOSIS.

Screen-shot 5.3.4.2-2 : Results of Spatial GEOES, on the area of Greece for the «lateritic / select area» context.



By clicking on one of the map cell, the user can initiate an Interactive session, based on the previous computations of Spatial GEOES. This is what we call the Hybrid GEOES, a mode that combines the versatility of the Interactive mode with the results of the Spatial mode. The hybrid mode enables the user to view histograms and consultations for interesting points, and engage him in what-if scenaria to further explore the favourability of Ni ore existence.

GeoNickel

Annex 6

**FINAL TECHNICAL REPORT
ANNEX 6**

**WP6 FINAL INTEGRATION,
Task 6.2 Validation and testing**

~~**CONFIDENTIAL**~~

CONTRACT NO: BRPR-CT95-0052 (DG12 - RSMT)

PROJECT NO: BE-1117

TITLE: Integrated Technologies for Minerals Exploration,
Pilot Project for Nickel Ore Deposits
GeoNickel

PROJECT

COORDINATOR: OUTOKUMPU Outokumpu Mining OY Finland

PARTNERS: LARCO General Mining and Metallurgical Company
SA, Greece
BRGM Bureau de Recherches Géologiques et
Minières, France
GSFIN Geological Survey of Finland, Finland
SOFTECO Softeco Sismat Srl, Italy
IGME Geological Survey of Greece, Greece
IRIS Iris Instruments SA, France
NCSR National Center of Scientific
Research 'Demokritos', Greece

STARTING DATE: 1st January 1996 DURATION: 36 MONTHS



PROJECT FUNDED BY THE EUROPEAN
COMMISSION UNDER THE BRITE/EURAM
PROGRAMME

Date: February 28, 1999

CONTENTS

EXECUTIVE SUMMARY	4
PROJECT STAFF	7
1. OBJECTIVES	8
1.1 Task 6.2	8
2. MEANS USED TO ACHIEVE THE OBJECTIVES	8
3. GEOSIS TESTS AND VALIDATION FOR SULPHIDIC NICKEL DEPOSITS	9
3.1 Introduction	9
3.2 Comments on the final testing of GEOSIS database	9
3.3 Testing of GEOES in the Intrusive Area Selection mode	10
3.4 Testing of APE and GEOES in the Identify Potential Zones and Target Selection modes	11
3.4.1 Northern Bothnia test area, intrusive case	11
3.4.1.1 Data acquisition for lithochemical studies	13
3.4.1.2 APE testing	14
3.4.1.3 Data acquisition for GEOES testing in the Northern Bothnia test area	17
3.4.1.4 Testing of the spatial GEOES	17
3.4.2 Pulju test area, komatiite case	19
3.4.2.1 Geological description of the Pulju greenstone belt	19
3.4.2.1.1 Location and general description	19
3.4.2.1.2 Stratigraphy	21
3.4.2.1.3 Lithology	21
3.4.2.1.4 Tectonic-metamorphic evolution	22
3.4.2.2 Geological research in the Pulju greenstone belt	22
3.4.2.3 APE testing	23
3.4.2.4 Data acquisition for GEOES testing in the Pulju test area	24
3.4.2.5 Testing of the spatial GEOES	25
3.5 Evaluation and discussion	25
3.5.1 APE	25
3.5.1.1 Evaluation of APE from the research point of view	25
3.5.1.2 Evaluation of APE from practical komatiite nickel exploration point of view	26
3.5.2 GEOSIS and GEOES	26
4. SCIENTIFIC AND TECHNICAL DESCRIPTION OF TESTS FOR THE LATERITIC NI DEPOSITS	27
4.1 Introduction	27
4.2 Evaluation and test	28

4.2.1	Area selection.....	28
4.2.2	Identification of potential zones.....	29
4.2.3	Target selection	30
5.	COMPARISON OF INITIALLY PLANNED ACTIVITIES AND THE WORK ACTUALLY ACCOMPLISHED.....	30
6.	CONCLUSIONS AND SUGGESTIONS	30
7.	ANNEXES	33
7.1	List of publications, conference presentations, and patents resulting from the project.....	33
7.2	Task 6.2 outputs	33
8.	REFERENCES.....	34

EXECUTIVE SUMMARY

The objective of Task 6.2 was to test the developed systems against real known cases. In the earlier phases of the project GEOSIS and GEOES programs were first tested with virtual data. Malfunctions were encountered but once corrected, the programs functioned properly in virtual testing and the real case testing was initiated.

Real case testing for the exploration of sulphidic Ni deposits related to intrusives was done in the Northern Bothnia test area, Central Finland, where nickel mines and prospects occur in mafic-ultramafic intrusives. Existing data were collected from databases. Since the lithochemical data did not cover all of the prospective areas of mafic rocks, additional sampling was carried out, and lithochemical and mineralogical analyses were done on the 45 samples collected. Finally, a total of 1278 analyses from 61 targets were processed with APE.

Komatiites were tested on the Pulju greenstone belt (PGB), Finnish Lapland. PGB is composed of felsic metavolcanites and metasediments overlain by flow and cumulate (up to 50% MgO) komatiites, which in turn are topped by mafic metavolcanites. The succession underwent polyphase deformation. A total of 653 XRF-analysed samples were processed with APE with the purpose of identifying the nickel potentiality of PGB and classifying heavily altered rock types on the basis of the whole rock analyses. As a result, Ni-potential komatiites were identified from less potential ones. Komatiite cumulus phases were classified and coherent naming was established.

APE was found to be a tool suitable for geologists dealing with lithochemical data.

In WorkPackage 6, the “Database and GIS” GEOSIS is integrated with advanced data analysis tools developed in the other WorkPackages of GeoNickel: the Expert System (GEOES), the Neural Network Analysis Module (ANNGIE) and the Advanced Statistical Methods (ASM). This leads to the expanded meaning for term GEOSIS: the whole software system developed during the project and integrated to operate through the common user interface.

“Database and GIS” GEOSIS and GEOES modules were tested for both sulphidic and lateritic Ni deposit exploration environments with virtual and real case data during the different phases of the software development. This facilitated an interactive, cyclic development process, where problems encountered were solved and corrected by the software developers, and new versions of both GEOSIS and GEOES were delivered for further testing. For instance, the interactive GEOES developed in the early phase of the project was tested extensively and systematically in order to locate the errors and unbalanced parameters in the system. After a fine-tuning and correction phase, the next version of interactive GEOES was tested against known Ni deposits and real exploration targets in collaboration with Ni exploration geologists.

For the sulphidic Ni exploration, the database modules of GEOSIS were first tested in WorkPackage 4 using the data collected in the WorkPackage 3 from Vammala and Enonkoski areas. GeoNickel tools GEOSIS, GEOES and APE were also used in Task 2 of WorkPackage 1. Final testing of the prototype, GEOSIS database modules revealed technical features that should be developed further if commercialisation takes place. The most important area to be renewed in the software are the input and output tools. These processes should be developed from the simple prototypes to versatile and user friendly software modules that would facilitate easy data entry to database and easy and fast access to all the data stored, with flexible reporting tools for data querying and output.

GEOES is an Expert System aimed to facilitate exploration performed by geoscientists. It is integrated within the GEOSIS system and can be used in three different modes (Interactive, Spatial and Hybrid), sharing the knowledge base but each one having a different role. The system gives emphasis on the integration of a variety of different approaches for the nickel exploration tasks, combining a wide range of data and knowledge from all geo-domains involved. It covers geological models for lateritic, komatiitic and intrusive types of nickel deposits and provides assistance to users during the different phases of their exploration work. These include “Area Selection”, where wide areas are examined for the existence of nickel ore deposits, “Identification of Potential Zones”, whereas zones within a given area are examined, and “Target Selection”, where restricted areas are examined.

The tests of the three modes of GEOS were made on data collected from the selected test areas; sulphidic exploration models were tested in Finland and the lateritic model in Greece. In both countries, the first step involved the testing of the Area Selection models using data covering most parts of the countries; Intrusive mode was tested in Finland and Lateritic mode in Greece. In both countries the test result showed that, based on input data, GEOES was able to locate the major zones and areas that host the modelled types of Ni deposits. In Greece the “Laterite Area Selection” mode was also tested in the areas of Lokris, Euboea Island, Vermion and Kastoria. In three cases the results were well related to the real assessment and encouraging, but in the other two, they were not in agreement with the known geology of the areas. In both cases, the discrepancy may be attributed to limitations in geophysical data.

The “Identification of Potential Zones” and “Target Selection” modes for Intrusive and Komatiite models were tested in two test areas in Finland, the Northern Bothnia test area and Pulju Komatiite Belt, respectively. The corresponding lateritic tests were carried out in four different test areas: Lokris, Euboea Island, Vermion, and Kastoria.

The tests for “Identification of Potential Zones” for both Intrusive and Komatiite models resulted in detecting the known areas potential for hosting nickel deposits. Further, they revealed interesting targets not recognised earlier. The data preparation procedure indicated, however, that the quality and coverage of the data and the objectivity of the preprocessing measures used in extracting information for the observations needed in spatial GEOES analysis, are of utmost importance for reliable results.

The identification of potential zones for lateritic Ni deposits was tested in the Lokris area and Pyrghoi in Vermion. In the Lokris area, three nickel ore potential zones were defined. Results in geochemistry, mineralogy and geophysics correlated well with the existing background information, but the results for geology were weak in one of the studied map sheets. In the Vermion area, GEOES suggested a zone where the mineralised horizon is hosted, and geo-

chemical, mineralogical and geophysical data corresponded with the background information.

The target selection mode of spatial GEOES for intrusives was tested in the Northern Bothnia area using a large data set (6043 grid cells) collected digitally from the existing data. Several tests with different input data and evidence weight configurations were conducted in order to see how these affect the results. This also gave the possibility to evaluate, how the user can control the system for different exploration scenarios and “what if?” simulations. The tests conducted generally revealed three to six of the seven Ni deposits and occurrences used as reference targets in the test area, and a reasonable amount of other anomalies in geologically sound locations were detected. The tests also showed that the system can be well controlled by changing the evidence weights and/or selecting input data. In Greece, the target selection mode for the lateritic Ni deposits was evaluated mainly in the Lokris area. The results corresponded with the existing data for the area.

In general it is apparent that GEOES is a complete and powerful exploration tool for the Area Selection, Identification of Potential Zones, and Target Selection, covering and compiling geological data from diverse origin (geology, geophysics, mineralogy and geochemistry). It corresponds well to results obtained using conventional exploration methodologies. However, the developed prototypes in the GEOSIS system (GEOSIS database and GIS modules, GEOES, ANNGIE and ASM) at present form a conglomerate of complex software that has been developed in different environments and need different third party programs to be run. If commercialisation of the GEOSIS system takes place, the integration of these programs should be carried further than is the case in the prototypes.

Though nickel exploration was the primary target for GeoNickel, it is evident that most of the developed instruments and software are of generic nature. Consequently, they can be applied to a great variety of base metals deposits other than the "nickel family" (Ni, Co, Cu and PGE). Most of them can be used to aid mineral exploration genetically related to magmatic, or even sedimentary rocks in various geotectonic environments.

One of the powers of the GEOES Expert System is the systematic approach needed from the data acquisition to the output of results. It gives the exploration staff a good opportunity to systematically examine all of the available data, estimate its homogeneity and validity, showing where more information is required for well-balanced reasoning results. Ultimately, the most important feature in using such an expert system may be the fact that it forces different specialists in an exploration team to work more closely and coherently, enhancing the strengths of teamwork in mineral exploration.

PROJECT STAFF

The main activists in WP6, Task 2 were the following.

Validation and testing of GEOSIS system for the exploration of sulphidic Ni deposits:

Jussi Aarnisalo	Outokumpu Mining Oy
Leo Grundström	Outokumpu Mining Oy
Jukka Jokela	Outokumpu Mining Oy
Jarmo Lahtinen	Outokumpu Mining Oy
Pertti Lamberg	Outokumpu Research Oy
Jukka Ojalainen	Outokumpu Mining Oy
Risto Pietilä	Outokumpu Mining Oy
Jukka Välimaa	Outokumpu Mining Oy
Markku Tiainen	GSF

Validation and testing of GEOSIS system for the exploration of lateritic Ni deposits:

Costas Ripis	IGME
Michael Melakis	LARCO G.M.M.C
Athanasios Apostolikas	LARCO G.M.M.C
Demetrios Eliopoulos	IGME
Anthony Angelopoulos	IGME
Costas Maglaras	LARCO G.M.M.C
Vasilios Noutsis	IGME
Vasilios Klentos	IGME

1. OBJECTIVES

1.1 Task 6.2

The objective of task 6.2 was to test the developed systems against real known cases.

2. MEANS USED TO ACHIVE THE OBJECTIVES

The Geoscientific Information System, GEOSIS, developed in the WorkPackage 4 of the project. It includes database and GIS functionality and allows the management of a considerable variety of data, maps and images (geological, geophysical, geochemical and other scientific data) which are currently used in the Ni exploration. The data management is based on a relational database (Oracle) and MapInfo Professional allows the management of GIS functions through the use of OLE services.

In WorkPackage 6, the “database and GIS” GEOSIS is integrated with advanced data analysis tools developed in the other WorkPackages of the GeoNickel: the Expert System (GEOES), the Neural Network Analysis Module (ANNGIE) and the Advanced Statistical Methods (ASM). This leads to the expanded meaning for term GEOSIS: the whole software system developed during the project and integrated to operate through the common user interface.

The technical testing of database and GIS functionality in GEOSIS, as well as the technical testing of the other developed tools (GEOES, ANNGIE and ASM) were conducted within the corresponding WorkPackages during the development of the software. The validation and testing of GEOSIS system in WorkPackage 6 aims to the functionality of the integration of the different software modules, especially GEOES, and to their use in real exploration cases.

GEOES covers geological models for intrusive, komatiitic and lateritic types of nickel deposits and comprises three different levels: area selection, identification of potential zones, and target selection. Moreover, GEOES can be run either in interactive, spatial or hybrid modes, sharing the knowledge, yet each having a role of its own.

To achieve the objectives (validation and testing of the GEOSIS system) test areas were selected for each geological model. In Finland, intrusive and extrusive (komatiitic), and in Greece lateritic nickel deposit models were tested. As each model could be applied to three exploration levels (area selection, identification of potential zones, and target selection), separate data sets for the Spatial GEOES had to be produced from test areas for them.

The data sets were input to the Intermediate Tables in the GEOSIS database and retrieved through MapInfo tables to GEOES for the analysis with the Spatial GEOES. The results were imported back to the MapInfo tables for graphical display, evaluation and study with the Hybrid GEOES.

3. GEOSIS TESTS AND VALIDATION FOR SULPHIDIC NICKEL DEPOSITS

3.1 Introduction

GEOSIS and GEOES modules were tested with virtual data during the software development phase. Several problems and malfunctions were encountered in them and were corrected by the software developers. For instance, interactive GEOES developed in the early phase of the project was tested extensively and systematically in order to locate the errors and unbalanced parameters in the system. After the consequent fine-tuning and correction phase, the next version of interactive GEOES was tested against the known sulphidic Ni deposits and real exploration targets in collaboration with Ni exploration geologists. In generally, first when the programs worked properly in virtual testing, testing was changed to the second stage, where real cases were used. The results of the final tests are briefly discussed in the following.

3.2 Comments on the final testing of GEOSIS database

For the sulphidic Ni exploration, the database modules of GEOSIS were first tested in WorkPackage 4 using the data collected in the WorkPackage 3 from Vammala and Enonkoski areas. GeoNickel tools GEOSIS, GEOES and APE were also used in Task 2 of WorkPackage 1. The tests were conducted in several phases during the development of the software. Errors were reported to the developers as soon as recognised, the software developers made corrections and suggested changes, and new versions of GEOSIS were delivered to the geoscientists for further testing.

Final testing of the GEOSIS version 1.8 database modules was carried out in WorkPackage 6 in December 1998 using the above mentioned data sets and data for the GEOES intermediate tables. As the results of these tests cannot be implemented during the GeoNickel project, the major findings on features to be further developed are listed in the following:

- Report tool has a limit of only 40 samples. Often when working with geological data, hundreds or thousands of assay results are needed in one report.
- Large GeoSoft (.xyz) files (>28 columns) don't fit to preview window when inputting data into database. You should, however, be able to look at the column names and file contents.
- It is not possible to resize GEOSIS program window by dragging from corners as in any other Windows application.
- If you wish to delete a *data set*, you have to delete the corresponding assay values and other linked data first. This should be automatic. When you choose to delete something,

you should be able to delete also the linked data in other tables (with confirmation dialogues). This should apply to Area and Target deletion, too.

- It should be possible to have also other conditions than "AND" between selection criteria clauses.
- In table D0BB_GPGR_EMFRQ we are able to input data of 5 different frequencies, but it is possible to input only one frequency in the Header table (H0B_GPGR). This still needs further rethinking by the geophysicists.
- Mise-a-la-masse table (D0BJ_GPGR_ELMIS) needs also to be rechecked. It is not possible to input GeoSoft file into GEOSIS database, because in this case you have to associate a column from file for a mandatory data table field LINE_HOLE. But the LINE_HOLE information is not in columns but in rows in the GeoSoft file. However, when uploading other data from GeoSoft files the line id is read into database from the appropriate row.
- Choosing Area/Target doesn't apply when opening or downloading an assay values table, for example. The entire table is downloaded, despite the target selection.
- It should be possible to pick up as many Targets/Data sets/Observation sets as you like from data manager, not just one or all.
- The present data input and output modules do not allow for addressing several drill holes at one time. This is due to the structure of diamond drilling tables. The input and output modules have to be developed further to overcome this serious constraint in the prototype software. For instance, it should be possible to input tabular data into Header table (H0E_DIDR).

3.3 Testing of GEOES in the Intrusive Area Selection mode

The Area Selection phases of spatial GEOES are aimed at the study and evaluation of vast regions, countries or even continents, in order to locate areas most potential for nickel deposits. In many regions this may produce difficulties in collecting the necessary data, since pedogeochemical, lithogeochemical and geophysical data may be sparse and inhomogeneous, and the publicly available geological information may be outdated. In this sense Finland is one of the best testing grounds for GEOES, as the whole country is covered with up-to-date pedogeochemical and geophysical data. Geological map of Finland has been recently redrawn and other necessary data are well organised and filed in the databases of the Geological Survey of Finland.

The compilation of a detailed data set covering the entire country was considered as too large a task within the limited time and resources of the project. Instead, a test data set was created using the uniform, scaled-down maps and information provided by the Geochemical Atlas of Finland, Part 2: Till (Koljonen 1992). The maps published in the said Atlas included data for most of the observations needed in the compilation of the intermediate tables for GEOES. Only some of the geological and geophysical observations had to be derived from other sources.

The area of Finland was divided into 50-km x 50-km grid cells. Geological, geophysical, lithogeochemical and pedogeochemical observations for each cell were derived from the appropriate maps by visually evaluating the data and giving each datum relative weightings between 0 and 10. This procedure was considered to homogenise the input data that differ in nature and intensity ranges. The observations were input to a spreadsheet and transferred into GEOSIS intermediate tables using the developed data input tools.

As MapInfo does not recognise null values, but fills the missing data points with 0, the table exported to GEOES had to be edited in an external text editor in order to remove such false values. During the testing this was found to be crucial to achieve acceptable results. If the zeros were left unedited, GEOES treated them as “absent” level information, which drastically reduced the overall results.

The Spatial GEOES was run using the default values, and the results were visualised in MapInfo with standard MapInfo/GEOSIS tools. Plate 6.2-1 depicts the output and shows clearly that GEOES - using the data given - was able to recognise the two major nickel belts in Finland. The highest overall scores were obtained in two areas: the Kotalahti Ni Belt with the Kotalahti and Enonkoski Ni deposits, and the Pori-Kylmäkoski Ni Belt with Vammala and Kylmäkoski nickel deposits, eastern and southwestern Finland respectively.

The test results obtained indicated that the reasoning engine of GEOES functioned properly and produces results well in accordance with the conventionally-known existence of nickel deposits of the intrusive type in Finland. The technical functioning of the integrated software was good after some errors were identified and corrected. The only major problem remains with MapInfo, which cannot handle the null values indicating missing data.

3.4 Testing of APE and GEOES in the Identify Potential Zones and Target Selection modes

Real case testing were performed in two test areas. Intrusive Target Selection level and Intrusive Identify Potential Zones level tests were conducted in the Northern Bothnia test area, and Komatiite Identify Potential Zones test on the Pulju greenstone belt. As appropriate data for the Komatiite Target Selection level and Area Selection level were not available, they could not be tested at this stage.

3.4.1 Northern Bothnia test area, intrusive case

The Northern Bothnia test area is located on seven 1:100 000 map sheets: 2342, 2431, 2344, 2433, 2434, 3411 and 3322 (Fig. 6.2-1). The Hitura nickel mine is on the area (map sheet 2344).

The test area belongs to the Raahe-Ladoga zone that has been recognised as a major tectonic, ore-bearing structure in Finland. According to Vaasjoki and Sakko (1988), the main geological feature of the zone is the transition from predominantly Archaean rocks in the Northeast to a Proterozoic domain in the Southwest over a zone a few tens of kilometres wide. It is characterised by a succession of NW-SE trending faults associated with pairs of similarly trending

gravimetric minima and maxima. Several economic and subeconomic base metal deposits lie within the Raahe-Ladoga zone (Kahma 1973; Mikkola 1980 and Isohanni et al. 1985) and are hosted by metavolcanic and metasedimentary rocks emplaced during the lower Proterozoic Svecokarelian orogeny (Simonen 1980). Three of the exploited base metal deposits are found within the selected test area: Vihanti Zn deposit in the northern part of the area, and Makola and Hitura Ni deposits in the central southern part of the area (Plate 6.2-2). Moreover, several studied and diamond drilled base metal mineralisations are known in the test area; five of the most prominent Ni occurrences are shown in the maps showing the test results (Plates 6.2-3 – 6.2-7).

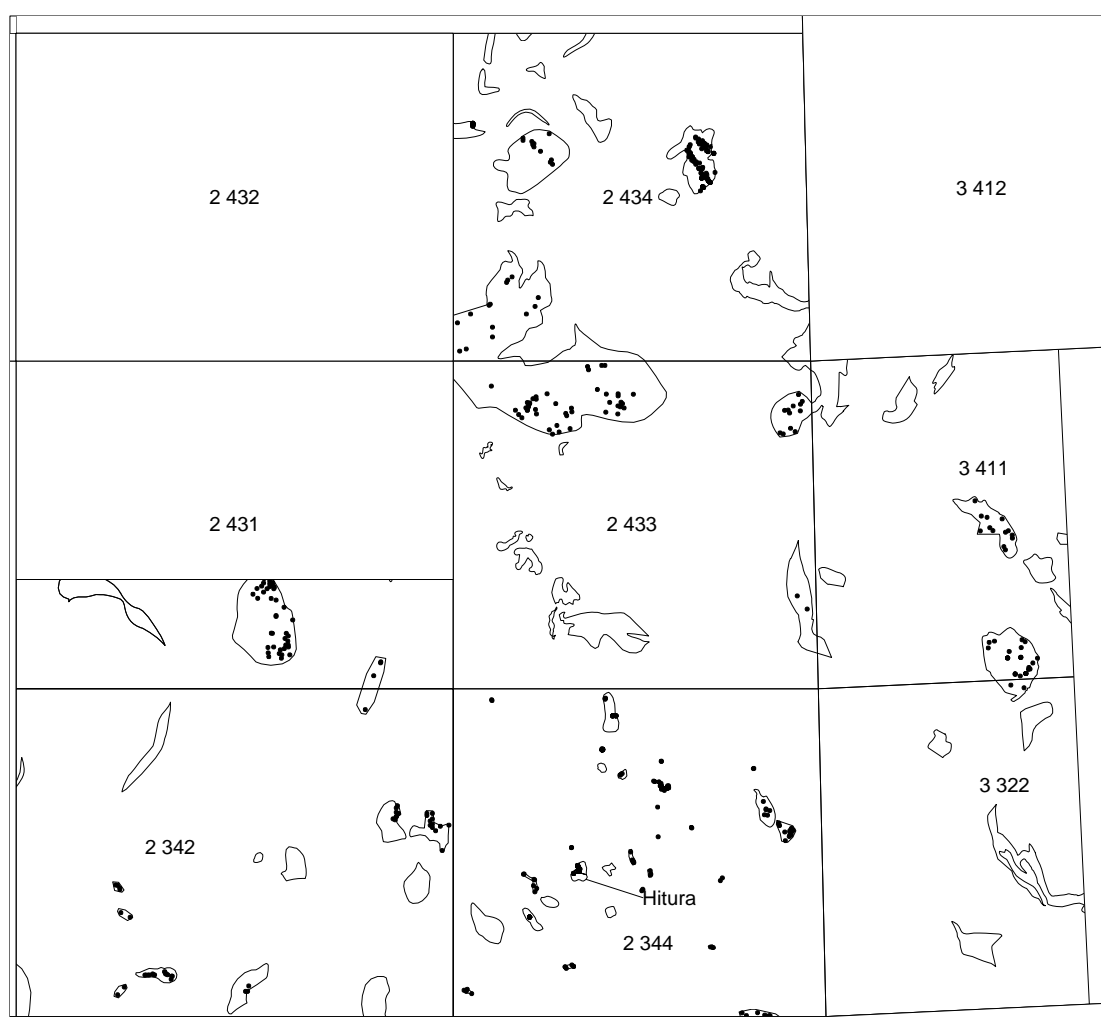


Fig. 6.2-1. WP6 Northern Bothnia test area. Intrusion polygons and analysed samples shown.

The main rock types in the area comprise intensely metamorphosed geosynclinal metasediments, intervening metavolcanics and extensive felsic intrusives (Isohanni et al. 1985). The

volcanic rocks have been formed in at least two cycles of activity (Vaasjoki and Sakko 1988). The first one, associated with the base metal ores, was extensively deformed during the Sve-cokarelian orogeny (Rouhunkoski 1969; Rauhamäki et al. 1978). According to Vaasjoki and Sakko (op. cit.), early tectonic gabbros and syntectonic granitoids penetrate the lower volcanic sequence, while the emplacement of hypabyssal plagioclase porphyrites terminated the younger volcanic sequence. There are also a few apparently post-tectonic granites in the district. The lower volcanic unit comprises rocks mostly dacitic in composition that are, at Vi-hanti, intimately associated with the pyritic and sphalerite-galena orebodies (Rouhunkoski op. cit.; Rauhamäki et al. op. cit.).

In the southern half of the test area, the prevailing rocks are migmatitic micagneisses with intercalations of graphite and sulphide bearing gneisses and amphibolites (Isohanni et al., op. cit.). In addition, east and northeast of Hitura mine there are nebulitic and schollen migmatitic gneissose granites that are interpreted originating from greywackes, quartzofeldspathic schists and mica schists (Plate 6.2-2). The oldest suite of intrusive rocks in the area consists of the ultramafic and mafic intrusives that host the exploited Hitura and Makola Ni ores as well as several smaller nickel occurrences. These intrusives occur in the gneissose granites and in the migmatitic mica gneisses but not in the sequence of supracrustal rocks stratigraphically above the mica gneisses (Isohanni et al., op. cit.). The syntectonic intrusive series, younger than the ultramafic and mafic intrusives, is composed of gabbros (some of them layered), diorites, quartz diorites, granodiorites, tonalites and granites.

The terrain in the Northern Bothnia test area is generally flat and outcrops are sparse as Pleistocene glacial drifts and bogs cover large parts of the area. Numerous Ni-Cu ore boulders discovered in the glacial drift since the early 1930's have revealed the area potential for nickel deposits. The area has therefore been the target of wide variety of explorational activities by the Geological Survey (GSF) and Outokumpu Oy. However, the nickel exploration has been concentrated mostly in the vicinity of the Hitura and Makola mines in the southern parts of the test area and in the Ylivieska layered gabbro in the western part, where GSF has discovered an uneconomic nickel occurrence. Northern half of the test area has been explored mostly for massive sulphide deposits, even though there exist some weakly mineralised nickel boulders and sporadic outcrop observations of nickeliferous mafic and ultramafic rocks in the extensive layered gabbro complexes.

3.4.1.1 Data acquisition for lithochemical studies

From the bedrock outcrop databases, rock types more mafic than diorites were selected and drawn as maps. The rock types were classified to the following groups: (a) Peridotite class, (b) Pyroxenite class, (c) Gabbro class, and (d) Diorite class. From the lithological maps and the above-mentioned data, all of the gabbroic and more mafic intrusions were outlined by creating "Target polygons" with MapInfo (Fig. 6.2-1).

The existing rock analyse data were collected from the exploration databases. A total of 1278 samples analysed and 61 targets were included. Exporting the analyse data from GEOSIS proved to be clumsy. Therefore, a reporting tool was added in the final GEOSIS.

The retrieved analyse data was found to be unevenly distributed in the test area. Most of the samples were collected from the studied exploration targets and only a minority represented

the extensive layered gabbros in the region. This is partly due to the fact that bedrock in the test area is very poorly outcropped, being covered almost totally by metres of moraine that is overlain by flat-lying swamps and peat-bog. Thus bedrock sampling is impossible without mechanisation, justifying the conducted light mechanised sampling within the selected mafic intrusions in the test area. The sampling served not only the modelling of Ni-deposits in intrusive rocks (WP1), but also the GEOSIS testing and database evaluation (WP4), and validation and testing of GEOES (WP5). Consent for the additional mechanised sampling on selected targets was obtained also from the GeoNickel partners. Targets and sample points were selected by applying GEOES. A total of 45 samples from four targets (Matkaniva, Korkatti, Rimpineva, and Porkkala) were collected. The sample points are shown in Figs. 6.2-2.

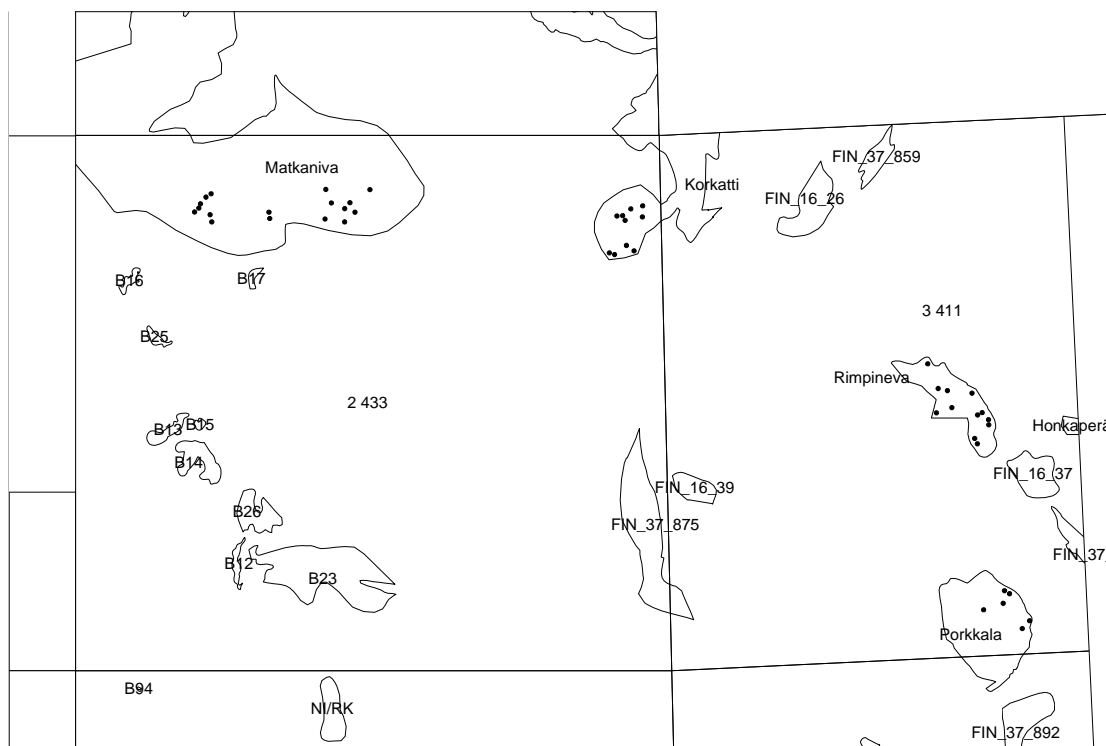


Fig. 6.2-2. Rock sampling points for targets Matkaniva, Korkatti, Rimpineva and Porkkala.

3.4.1.2 APE testing

A litho geochemist working with GEOES on the exploration of nickel deposits related to intrusives should pay attention to the following factors.

- Primitivity of parental magma.
- Existence of favourable differentiation series and cumulates.
- Contamination features.
- Nickel depletion and sulphur saturation features.

APE was used to determine the evidence weights of the factors. A total of 1278 samples from 61 targets were processed. Tools existing in APE were useful in studying the data, but the fi-

nal determination of key figures proved to be laborious and time demanding. To fasten this stage *Population analysis* module was developed in APEStat. This enables the running of statistical analyses from populations (i.e. intrusions=targets). User can write macros, and save them for further use. Table 6.2-1 provides an example of Population Analysis macro.

Table 6.2-1. An example of *Population Analysis* macro in APEStat.

Macro row					Explanation
Target analysis #1					
Delete	CalcSF	Sulphide%	>	10	Select all samples from target Delete samples containing more than 10% sulphides
Analyse	MinTraceNi	Olmg%	max		Analysis from remaining samples maximum MinTraceNi.Olmg%
Store	ParentalMagma	Max_Fo_ana			Store the value in field Parental-Magma.Max_Fo_ana
Target analysis #2					
Delete	CalcSF	Sulphide%	>	5	Analysis 2. Start by selecting all the samples of the target Delete samples containing more than 5% sulphides
Delete	RockName	CRGN	<>	"C"	Delete other but cumulates
Analyse	CalcVSF	MgO_n%	max		Analysis from remaining population maximum MgO_n%
Store	ParentalMagma	Max_MgO_n%			Store value in Parental-Magma.Max_MgO_n%

After the development of the population analysis module, key figures of studied targets were determined by writing macros as follows:

1. Primitive_parental_magma

- Maximum forsterite% (analysed, calculated).

2. Contamination_features

- Contamination features come from percentage of samples contaminated (number of samples containing anomalously high vanadium content vs. total number of samples).

3. Existence_of_favourable_differentiation_series_and_cumulates

- Average of maximum olivine (CIPW) content and average of orthopyroxene/pyroxenes ratio (in percent) in cumulates.

4. Ni_depletion_and_sulfur_saturation_features

- Average sulphide content of non-ore bearing cumulates * a

- if olivine analyses not available, then a =1

- if standard deviation > absolute value of average, then a = standard deviation

- if standard deviation < absolute value of average, then a= 0.2* standard deviation.

Returned raw data had to be classed in five groups (absent, weakly present, moderately present, highly present, fact) for GEOES. Grouping was done with APEStat, as illustrated in Fig. 6.2-3.

Several errors were corrected in APE during the testing. The *Population analysis* module improves the performance of APE especially when the number of targets (intrusions) becomes large (>20). After corrections and the development done in WorkPackage 6, APE is an effective study and data processing tool especially in select target stage of Ni exploration.

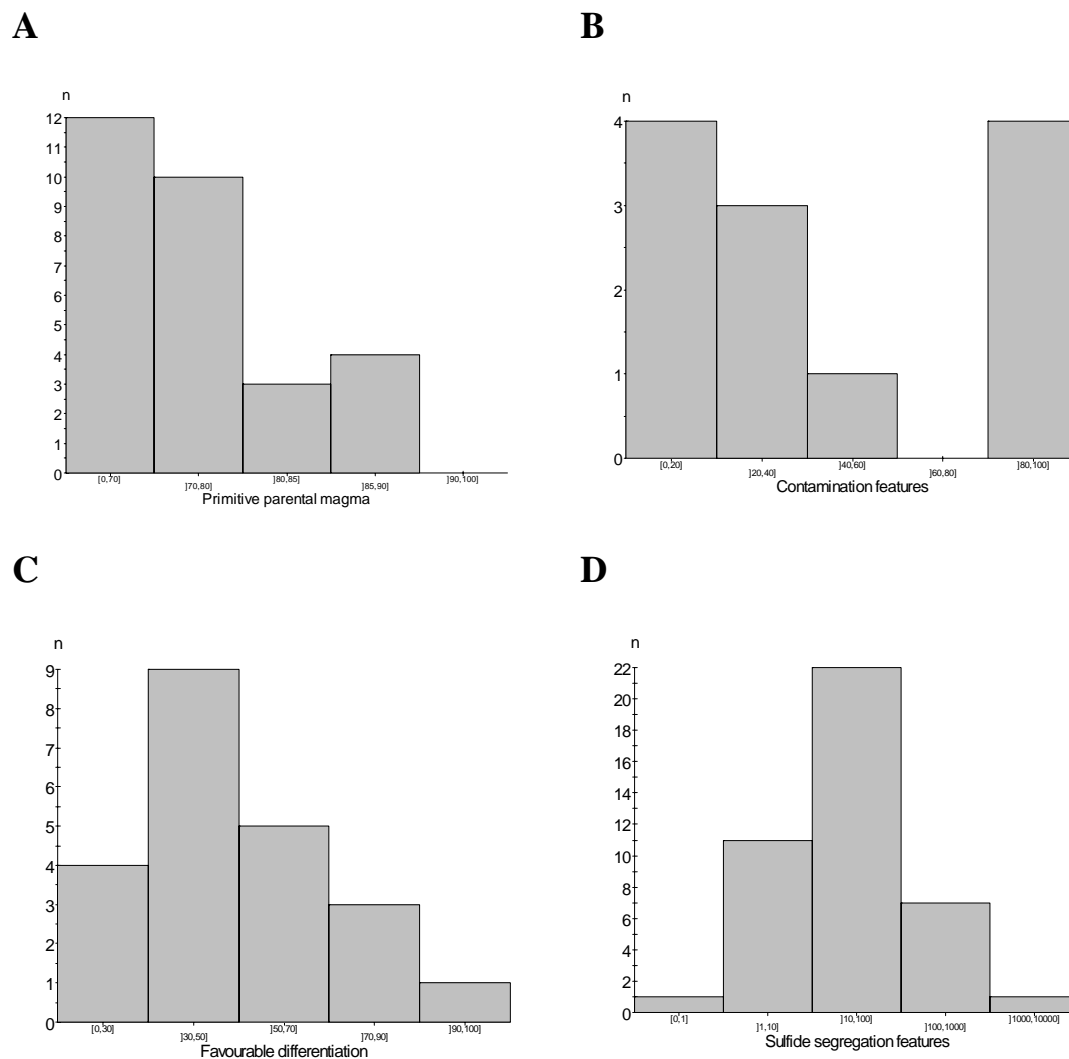


Fig. 6.2-3. Grouping and distribution of evidence weights in the Northern Bothnia test area. Intrusive Ni exploration, Select target, Litho geochemistry and mineralogy.

3.4.1.3 Data acquisition for GEOES testing in the Northern Bothnia test area

The Northern Bothnia test area is covered with uniform low-altitude airborne geophysical data set and with regional till data (sample density 1 sample/ 4 km²), both provided by the Geological Survey of Finland. The regional geological map of the area has been recently updated (Mid-Norden Project 1996). Further, the digital database of Outokumpu Mining Oy, Exploration contains a wealth of different detailed exploration data from the area. Also the lithochemical data analysed with APE adds to the available information.

As all the necessary data for preparing the intermediate tables were available in digital format, the construction of the tables was made using tools available in MapInfo and in an external image processing system (TNT-mips). The data preparation process showed that the pre-processing of the necessary data to the format required by the intermediate tables and GEOES is a crucial and complex step in the whole process. Most of the observations in GEOES do not use the exploration data in its original form, but asks for interpreting or pre-processing of the data into a format not earlier used. For example, geophysical domain includes observations incorporating concept of “local anomaly”. This calls first for the definition of both “local” and “anomaly”, before the procedure for extracting these digitally from the original data can be developed. In the Northern Bothnia test area, this was solved using the image processing, vectorising and vector morphology tools available in TNT-mips.

In order to transform the exploration data available either as digital maps, or as point data, into the format required by GEOES, all the data was input into MapInfo. Some of the point data were given an influence area with diameter of one kilometre, while others were interpolated into grids. A sampling grid (1 km x 1km cell size) was created as a polygon layer and the required information within each cell from the input data layers was read into appropriate columns in the result table using the SQL geographic operators of MapInfo. This procedure made possible to complete the data acquisition for all 6043 grid cells and 26 observation columns for “Identify Potential Zone”-data, and 34 columns for “Target Selection”-data, in a time frame available in the project. The process, although now carried out interactively, can be automated in the future to facilitate fast and much user-friendlier approach to the time consuming and complicated process of feeding the necessary data into the intermediate tables for GEOES. As the GEOSIS prototype input tools do not allow direct input into GEOSIS database from the MapInfo tables, the completed result tables had to be first exported into ACII format for loading the data into the intermediate tables in GEOSIS database.

3.4.1.4 Testing of the spatial GEOES

Once the data preparation and input was completed, several tests were run on the spatial GEOES using different combinations of input data and observation evidence weight configurations. This was done to find out how GEOES behaves both technically and “explorationally” in different situations. During the testing process, a few technical errors were still located; software developers corrected them and provided the end user with new versions for continued tests.

A result of the GEOES spatial mode process in Intrusive Identify Potential Zones phase is shown in Plate 6.2-3. The Northern Bothnia test area belongs to the Raahe-Ladoga zone also visible in the result of the spatial GEOES Intrusive Area Selection phase process (see Plate 6.2-1), running from Lake Ladoga to Bothnian Bay. This wide zone transects the Northern

Bothnia test area approximately from its southeastern corner to Northwest. The spatial GEOES result reveals the zone as divided into two subparallel narrower belts, the southern one including the exploited Makola and Hitura Ni ore deposits and four of the five studied Ni occurrences in the area. However, the scores in the northwestern part of the northern belt are higher even though no known Ni mineralisations exist there. The highest anomalies are in the southern contact zone of the Matkaniva gabbro complex (see Plates 6.2-2 and 6.2-3, and Fig. 6.2-2). Furthermore, five high score clusters are found in the areas of extensive gabbros north of this belt.

Without going into details of the possible reasons for the detected anomalous features it can be said that the spatial GEOES could locate two different belts within the previously known wide ore potential zone, and some interesting anomaly clusters north of the belts. The data preparation procedure has shown, however, that the quality and coverage of the data and the objectivity of the preprocessing measures used in extracting the required information for the observations needed in GEOES analysis, are of utmost importance for the reliable results.

The Intrusive Target Selection phase of GEOES was also tested using the prepared data set from the Northern Bothnia test area. Several tests with different input data and evidence weight configurations were conducted in order to see how these affect the results. This also gave the possibility to evaluate how the user can control the system for different exploration scenarios and “what if?” simulations. Two pairs of test results are shown in Plates 6.2-4 - 6.2-7.

In the first two tests the default linear configuration of spatial GEOES was used to give the evidence weights for observations. The first test was run using the complete data set (Plate 6.2-4). Study of the results show that scores are divided in two groups – a few quite high values and large amount of lower values. About a hundred points of the lower values are separated slightly above the remaining ones that form the background for the result. The high scores are situated in groups indicating some local reason. For instance, it may due to only one point data source given the one kilometre influence diameter. Only one of the Ni occurrences have clearly high scores, but all except Makola seem to have been detected with low-level anomalies differing slightly from the background.

In the second test, all the ore deposit, mineralisation and erratic boulder data were removed from the geological observations in the input data (Plate 6.2-5). The high score points of the first test were mostly removed, indicating that they probably were caused by erratic boulder data. Also the low-level anomalies around the known mineralisations were subdued so that only three out of seven targets were recognised. On the other hand, the change in the input data caused many of the other low-level anomaly scores to increase, bringing them up more in the result map (Plate 6.2-5).

It is quite common that in geodata sets the frequency distribution of intensity values is not linear or symmetrically distributed. Much more typical are exponential, skewed and/or clustered intensity distributions. In these cases the linear configuration of evidence weights will not give the best results, but the configuration must be customised according to the observation data distributions or known models. The second pair of the test shows the spatial GEOES results processed using an experimental customised configuration for the evidence weights of the observations (Plates 6.2-6 and 6.2-7).

The test using all the data brings out quite clearly five of the seven known Ni deposits or occurrences; even Makola area has now weakly anomalous scores (Plate 6.2-6). In addition, over ten high score clusters are revealed in geologically quite reasonable and interesting locations. Just as in the first pair of tests, the high score values were dropped markedly when all the ore deposit, mineralisation and erratic boulder data were removed from the geological observations in the input data (Plate 6.2-7). Again only three of the seven known deposits or occurrences were detected at least as weak anomalies. This points to the possibility that the sufficiency/necessity values are not in balance and the direct mineralisation indications get too strong weighting in the process. On the other hand, as the exploration model should be a fact in those cases, the scores should also be high by default. One could now ask if the known direct mineralisation data should be avoided in the input data, if new previously unknown targets are sought. This problem clearly calls for more experiencing, but it also show how delicate the process is for the right types and combination of data.

The tests have shown that the system can be quite well controlled by changing the evidence weights and/or by selecting input data. The GEOES works well in all the different phases of Intrusive model and the processing time for the data sets of 6043 observations in 26 and 34 columns was about two hours in a Pentium II 233 MHz PC with 64 Mb RAM. This was considerably faster than anticipated after the first tests with slower PC. This point to the fact that the process is demanding, requiring quite heavy processing power for practical work on large data sets.

3.4.2 Pulju test area, komatiite case

3.4.2.1 Geological description of the Pulju greenstone belt

3.4.2.1.1 Location and general description

The Pulju greenstone belt (PGB) is located in Lapland, in the northern part of the Fennoscandian Shield. The PGB strikes N-S for c. 70 km in Finland and continues for c. 160 km to the north into Norway where it is called the Karasjok greenstone belt. To the north, the Karasjok belt is covered by Caledonian metasediments. The Karasjok belt was described by Often (1985), Barnes and Often (1990) and Davidsen (1994). In the south, the PGB is surrounded by granitoids of the Hetta type.

Neither definite observations of Archaean basement rocks nor any radiometric age determinations exist from the PGB. Its Proterozoic age is obvious as well as the correlation with the Karasjok belt and the Central Lapland greenstone belt (CLGB) occurring in the Kittilä, Sodankylä, Savukoski and Salla areas of Finland. Numerous age determinations have been conducted by the Geological Survey of Finland (GSF) on the CLGB, described by Lehtonen et al. (1998). The lower age boundary of the CLGB is that of the Koitelainen layered intrusion, 2.440 Ga. The youngest rocks in the Sodankylä area are komatiites of the Sattasvaara type, c. 2.050 Ga old. They are correlated with the PGB where only minor volcanic-sedimentary units exist

Stratigraphy of PGB and correlation with CLGB			
PULJU	CORRELATION WITH CENTRAL LAPLAND		
Lithology	Lithology	Type formation	AGE (Ma)
Greenstones	Greenstones		c. 2 012
Mafic metavolcanics (lavas and tuffites); intermediate tuffites; metapelites	?	?	?
Metasediments (interflow sediments) Komatiites, metalavas and - cumulates Komatiites, mainly metacumulates / channel facies (Hotinvaara type)	Komatiitic metavolcanics	Sattasvaara Formation	> 2 050
Cherts; skarns; quartz-feldspar schists; felsic tuffs - tuffites; black shales; sulphide-graphite schists; metapelites; mafic metavolcanics (lavas and tuffites);	Phyllite; black schist; dolomite; tuff; tuffite; BIF	Matarakoski Formation	> 2 130
Mafic metavolcanics (mainly lavas); intermediate metavolcanics	Mafic to felsic metavolcanics; albitised metasedimentary rocks	Honkavaara Formation	> 2 210
Orho quartzites; arcose quartzites; metapelites; intermediate tuffites	Quartzites; mica schist; mica gneiss; conglomerate	Virttiövaara Formation	> 2 210
Felsic - intermediate metavolcanics ?	Intermediate to felsic metavolcanics	Rookkiaapa	c. 2 500
Granitic-granodioritic-tonalitic gneisses	Granitic gneisses	POC	Archaean ?

Figure 6.2-4. The stratigraphy of the PGB and its correlation with the CLGB.

stratigraphically above the komatiites. A Sm-Nd age determination for a komatiite in the Karasjok belt has given an age of 2.085 ± 0.085 Ga (Krill et al., 1985).

The general geological picture of the PGB belt was obtained through exploration carried out by Outokumpu Mining Oy from 1978 to 1998 and from geological research by the University of Turku (Papunen et al., 1977) from 1974.

3.4.2.1.2 Stratigraphy

Especially in the south and west, the PGB is surrounded by granites of the Hetta type which in many areas cut across the above mentioned supracrustal rocks. Zircon ages for Hetta granites range from 1.810 to 2.366 Ga reflecting the polyphase development of these rocks and possibly indicate that they originate from partly remobilised older material. The stratigraphy of the PGB and its correlation with the CLGB is depicted in Fig. 6.2-4.

3.4.2.1.3 Lithology

Gneissic granitoids and migmatites outcrop only in a few parts of the schist belt. Such gneisses are considered part of the basement group.

The lowermost stratigraphic unit of the volcano-sedimentary succession, felsic-intermediate metavolcanics, is poorly developed in the PGB but is clearly present at Pokka (CLGB) to the east.

The quartzite unit is composed of arenitic metasediments. The quartzites are mostly arcose but in places ortho-quartzites are also common. Arcose quartzites grade into metapelites rich in Al and contain silicates such as andalusite, sillimanite and kyanite. Hornblende and mica-banded arcose gneisses, interpreted to indicate incipient volcanism in the succession, occur in the top of the quartzite unit.

Mafic metavolcanics and minor intermediate metavolcanics consist mainly of amygdaloidal or massive metalavas and in some cases of banded metatuffites. This unit usually overlies the quartzites or the banded arcose hornblende-mica gneisses.

The most complex of the units in the PGB is a heterogeneous group of metavolcanics and metasediments equivalent to the Matarakoski formation of the CLGB. This unit is called the Chert Formation and is characterised by sulphides which are disseminated, but massive pyrrhotite-dominated varieties also occur. It consists of various types of chemical, argillic and arenitic metasediments (chert, skarn, iron formation, black schist, metapelite, quartz-felspar schist). Mafic metavolcanics consist of a succession of variable metalavas, metatuffites and metatuffs. Felsic metavolcanics are mostly reworked metatuffites as well as metatuffs in a few places.

Komatiites are widespread in the PGB the Sattasvaara komatiites being the dominant type. They include flows, hyaloclastic rocks, pillow lavas, breccias and minor cumulates. Their volatile-free MgO-content ranges from 20 to 25 %. The Hotinvaara komatiites are composed mostly of cumulates and occur in long, narrow belts interpreted as magma flow channels. Their volatile-free MgO typically ranges from 40 to 50%.

The uppermost stratigraphic unit consists of mafic metalavas and metatuffites, intermediate metatuffites and metapelites. This unit is poorly exposed and further studies are needed to define its accurate stratigraphic position.

3.4.2.1.4 Tectonic-metamorphic evolution

The polyphase tectonic-metamorphic evolution of the PGB contains four ductile folding phases and at least of two younger, more brittle fault systems. Hydrothermal alteration processes occurred at several stages of the tectonic-metamorphic history.

The tectonic - metamorphic evolution of the PGB began with horizontal - subhorizontal isoclinal folding (F1) and overthrusting structures. Some observations indicate that the D1 overthrust is N-NW vergent. The thickening of crust caused a peak in regional metamorphism while D1. D1-metamorphism took place under medium grade conditions. The main schistosity of supracrustal rocks in the PGB is S1, and all of the peak metamorphic index minerals are syn-D1 minerals.

The second deformation phase (D2) equals the main folding phase in the PGB. Tight to isoclinal F2 folding was intense. Usually F2-folds are flat-lying but a series from vertical axial planes to recumbent structures can be followed in several profiles across the PGB. F2 fold axes mainly plunge gently SW. Axial planes mainly dip gently SW-E (in places also NW). Sheared, mylonitic zones in the limb areas of F2-folds indicate strong overthrust and displacement during this deformation phase. Observations from the entire PGB indicate that D2 overthrusting is NW to W verging. Metamorphic mineral growth during D2 is retrograde, even if axial plane cleavage S2 is intensive in places. Small granitic to tonalitic intrusions and veins are associated mainly to D2.

Two younger folding phases (F3-F4) are observed in the PGB. Both of them have vertical-subvertical axial planes and gently dipping fold axes. F3-folds trend c. E-W and younger F4-folds c. N-S. In places these younger deformation phases appear as culminations of older structures. The metamorphic events for D3-D4 are retrograde.

Brittle fault and fracture systems are the youngest deformations in the PGB. Several faults cut it in a NW-SE direction. Subparallel to the PGB, there are mylonitic faults that trend NE-SW.

3.4.2.2 Geological research in the Pulju greenstone belt

Geological fieldwork for GeoNickel consist geological mapping and was focused mainly on the northern part of the Pulju greenstone belt (PGB). The purpose of the mapping was to collect material for the recognition of the nickel potential of komatiite types in the northern part of PGB, and to determine the stratigraphy in PGB.

Selected samples were whole rock analysed with XRF. These data, combined with analytical data from other sources (such as drilling and mapping samples in the southern part of PGB), were used as test material for the APE program. The purpose was to identify nickel potential in Hotinvaara type of komatiites and to find other Ni-ore potential indications.

3.4.2.3 APE testing

The APE program was tested with komatiite nickel exploration data from the PGB. Since APE was developed for intrusive rocks, some problems were faced with CIPW and B-norm calculation routines. After these were corrected all calculation routines were successfully passed in APECalc.

A total of 653 samples were processed with APE. An important questions faced by petrologists in the Pulju case was the proper naming of rocks. Task 2 had developed a relatively straightforward naming of volcanites and their cumulates. A procedure was built in APE-Graph to discriminate different volcanics and cumulates according to chromium and magnesium contents (Fig. 6.2-5). When these trendlines had been created, classification was fast and easy to do. Saving this classification to a PictureBook-file of APE allows also other users to run same procedures with different data.

The Pulju sample set included anomalous samples in terms of titanium and aluminium contents. These samples could easily be identified from the data set with APEGraph, and the characteristics of these groups could be studied with APEStat and APEGraph. Practically all samples poor in titanium and aluminium proved to be rich in normative pyroxenes. Therefore a hypothesis was set, that these samples are actually pyroxene cumulates after komatiitic magma and do not represent olivine-liquid systems. Another explanation for such features is, that samples are altered (SiO₂ was introduced). The two alternative hypotheses can easily be tested with APE.

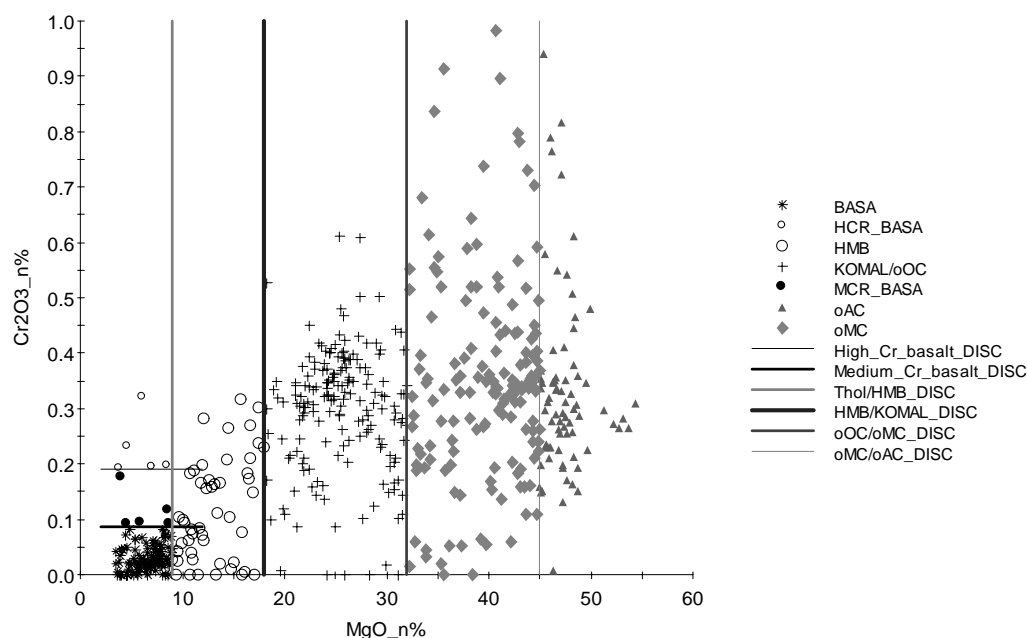


Fig. 6.2-5. Grouping and naming of volcanites according to criteria of Turku University and applying APE discrimination properties.

The next test was to study nickel depletion features. Trendlines after Duke (1984) were digitised and stored in APE database. From the Pulju data, only komatiitic lavas and orthocumulates were included. Most of the samples plot on trendline indicating fractional crystallisation of olivine under sulphide undersaturation. However, a group of samples plots clearly in the field of sulphide saturation, a positive sign from nickel exploration point of view (Fig. 6.2-6).

APE testing with data from the PGB indicated that APE is suitable for handling Ni exploration data also in komatiites. With the help of APE the analysis described above could be done in two hours. With pre-GeoNickel techniques such an analysis would have taken days.

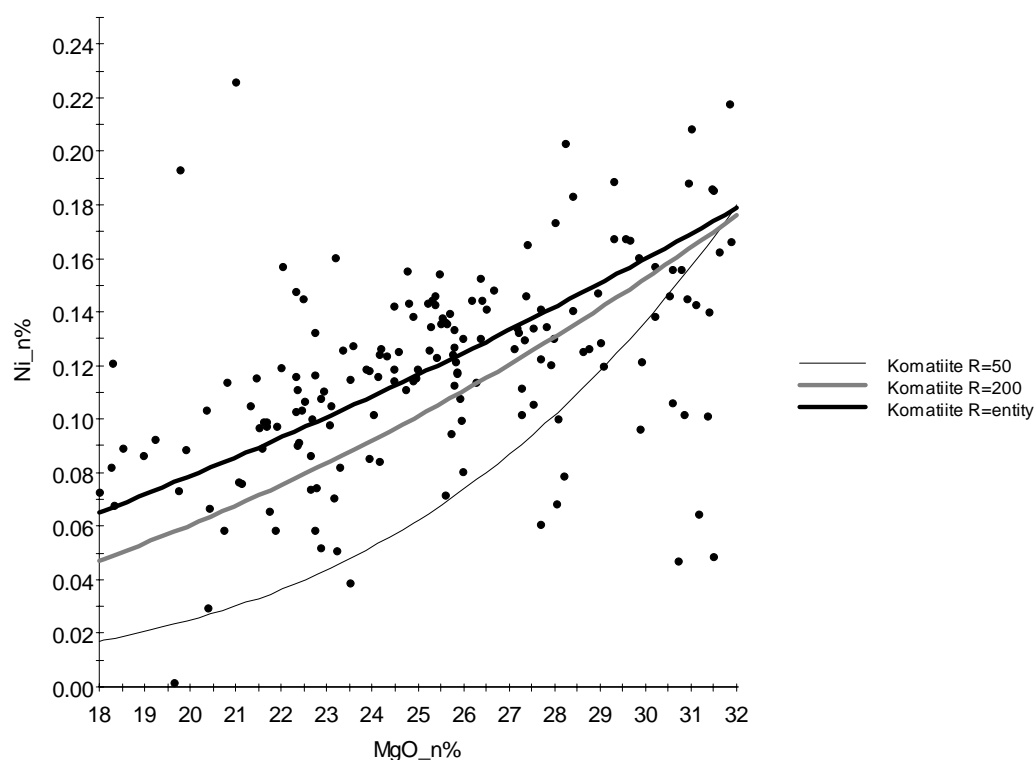


Fig. 6.2-6. Nickel depletion study of komatiitic lavas and oOC in the PGB.

3.4.2.4 Data acquisition for GEOES testing in the Pulju test area

The Komatiitic Identify Potential Zones phase was tested in the Pulju test area. Data acquisition by interviewing the Ni exploration geologists was considered as the most efficient way to obtain the information into the intermediate tables for the spatial GEOES analysis in the Pulju test area. This was because the available exploration data was only partly digital, partly only in the experience and knowledge of the geologists, and the existing geological maps did not cover most of the Pulju greenstone belt. The test area was chosen to cover the entire known greenstone belt from Pulju north to the border of Norway. The area was divided into 2 km x 2 km grid which was drawn both manually on transparent mylar and digitally on the geophysi-

cal and other data available in digital format. Then the Ni exploration geologists studied all the necessary existing maps and data using these grids and gave each of the grid cells rating between 0 and 10 for all the necessary 28 observations in the Komatiite Identify Potential Zones phase. These values were stored into a spreadsheet table and transferred to GEOSIS intermediate table when completed. The created data grid consisted of 364 cells which was still a reasonable amount for the interview method and manual input into the spreadsheet table.

3.4.2.5 Testing of the spatial GEOES

The spatial GEOES was run in the Komatiite Identify Potential Zones phase using the collected intermediate table. An error in the processing of the geophysical observations was still found during the GEOES process. This caused the geophysical data sets to be omitted from the input data and the final test was carried out using geological, lithochemical and petrochemical observations. The result of the analysis is shown in Plate 6.2-8. The evidence weights for all the observations were given by the default configuration of GEOES. The result brings out some known and a few new targets for komatiite Ni exploration. It also indicates that in the north the eastern branch of the belt might be more interesting than the western one.

The data export from GEOSIS to spatial GEOES was fluent except for the MapInfo derived problem on editing the missing values in text editor before entering the input table to GEOES. The results of the GEOES process could be directly transferred into MapInfo table and symbol maps overlaid on desired maps or images.

3.5 Evaluation and discussion

3.5.1 APE

3.5.1.1 Evaluation of APE from the research point of view

APE made it possible to have all the tools a researcher needs under the same software. It was built with standard tools on Windows 32-bit platform, which makes the interaction between APE and other Windows software, e.g. Excel or any spreadsheet, just a breeze. The logic of APE is relatively easy to adopt but may require some guidance first. APE is definitely designed for a researcher, and an exploration geologist as well, who is analysing his/her lithochemical data in great detail, but uses relatively large datasets. The great advantage is the combination of the database, spreadsheet and visualisation tools in the same software. All this and the geology-oriented special features (certain type of diagrams, calculations, normalisation etc.) makes APE a special tool, which does not have real competitors in the market.

A minor defect with APE is a bit confusing GUI, which requires one to become customised before it becomes familiar. This is due to the many button-based controls, which are difficult to avoid in this sort of application. Nevertheless APE has been mainly built up as standard Windows software and after a short period of getting acquainted with the user interface and the data managing procedures any user should be able to learn the basics. For advanced users APE software will give many possibilities to analyse their data. Clearly the capabilities of APE will show up to the user after certain amount of work with it.

An open interaction between different applications is an essential feature in APE. It is important to be able to communicate with different types of data sources, even though input data can be premodified by APE to become feedable. Correspondingly, the output figures must be exportable into graphics software packages.

In general terms, APE has features to become a suitable tool for geologists dealing with litho-geochemical data. With the mineralogical data included, APE becomes even better.

3.5.1.2 Evaluation of APE from practical komatiite nickel exploration point of view

The APE program is in use on Outokumpu Mining Oy's komatiite exploration projects in Finland. Experiences of applying APE in practical exploration appear good.

It is important to classify rock types in komatiite nickel exploration areas and targets. Often classification can be done directly, on the basis of drill core logging or field observations. However, as in the PGB, komatiites are so heavily altered that one cannot recognise primary textures. In such case analytical data, normally whole-rock XRF assays, are the only key to identify original rocks. For the identification of primary rock types, original mineral compositions, cumulus and intercumulus minerals, and even the crystallisation paths of magmas, APE provides an excellent tool.

Advantages of APE include the following.

1. A flexible program digests XRF data in original or volatile-free form, in percent and ppm.
2. There are possibilities for filtering, queries and classification of material.
3. It is possible to make various trend lines and compositional areas in library for the comparison of targets.
4. APE is handy for displaying 2-axis or triangular diagrams.

All these, and many other good properties, make APE a practical tool to identify original rock types, to classify them as nickel potential or less potential ones, and to compare the analytical data of current project with those of known areas or economic deposits. In the PGB, it was possible to separate the Ni-potential Hotinvaara type of komatiites from other less potential ones.

APE is a petrological tool made by a geologist for geologists. It can be applied in many kinds of exploration projects and is at its best in those where it is important to recognise original features under heavy alteration. APE itself is not able to show where a nickel ore deposit is located, but the application of APE will point to the potential rock types.

3.5.2 GEOSIS and GEOES

Final testing of the prototype, GEOSIS database modules revealed technical features that should be developed further if commercialisation takes place. The most important area to be renewed in the software are the input and output tools. These processes should be developed from the simple prototypes to versatile and user friendly software modules that would facilitate easy data entry to database and easy and fast access to all the data stored, with flexible reporting tools for data querying and output.

The developed prototypes in the GEOSIS system (GEOSIS database and GIS modules, GEOES, ANNGIE and ASM) form at the present a conglomerate of complex software that has been developed in different environments and need different third party programs for to be run. If commercialisation of the GEOSIS system takes place, the integration of these programs must be carried further than in the prototypes. The entire system should be written in the same development environment, using the same standard Windows tools. This would ensure easier installation and would obviously provide more stable system free of technical hardware related compatibility problems.

The preparation of the large real case data set for the Northern Bothnia test area showed that the quality and coverage of the data, and the objectivity of the preprocessing measures used in extracting the required information for the observations needed in GEOES analysis, are of utmost importance for reliable results. This calls for the systematic approach from the data acquisition to the output of the results. The exploration staff has to examine systematically all the available data and estimate its homogeneity and validity, deciding where more information is required for well-balanced reasoning results. Ultimately, the most important feature in using such an expert system may be the fact that it forces different specialists in an exploration team to work more closely and coherently, enhancing the strengths of teamwork in mineral exploration.

4. SCIENTIFIC AND TECHNICAL DESCRIPTION OF TESTS FOR THE LATERITIC Ni DEPOSITS

4.1 Introduction

The GEOES is an Expert System aiming to facilitate the exploration process performed by geoscientists and it is integrated within GEOSIS, the software toolbox of the Geonickel project. The system gives emphasis on the integration of a variety of different approaches for the nickel exploration tasks, combining a wide range of data and knowledge from all geo-domains involved. It covers geological models for lateritic, komatiitic and intrusive type nickel deposits and provides assistance to users during different phases of their exploration work, including:

- Area selection, where wide areas are examined for the existence of nickel ore deposits
- Identification of potential zones, whereas zones within a given area are examined
- Target selection, where restricted small area is examined

Within GEOSIS there are three modes of GEOES, namely Interactive, Spatial and Hybrid, sharing the knowledge but each one having a different role.

For the validation and test of the Expert System the principles briefly described above were taken into consideration. Data used for the evaluation was retrieved from the Intermediate tables created.

Prototype software was developed at IGME (Noutsis & Angelopoulos 1998) that automati-

cally estimates the Power Spectrum. Auto-correlation function (Spector and Grand, 1970) was used to retrieve information related to the intensity, wavelength, lateral extension and direction from the 2d signal (gravity and magnetic anomalies). These parameters are estimated for 64x64 grids at the center of 1:50000 map sheets but the same is applicable for every 2D exploratory data set. This approach had very effective results for objective evaluation of the geophysical data and formulation and compilation of the intermediate tables necessary for the Expert System.

All data-existing and obtained during the project was digitized according to the format agreed, and then used as input to the GEOSIS.

4.2 Evaluation and tests

The Interactive version of GEOES was developed during the early stages of the project in order to help the knowledge acquisition process and test it against real geodata. The tests were successful and already submitted to the NCSR DEMOKRITOS in June 1998. The results of these tests were used for the development and further improvements of the succeeding modes of GEOES.

The tests of the Spatial GEOS and the Hybrid Version were made in combination to Area Selection, Identification of Potential Zones and Target Selection using data from known cases and are as follows:

4.2.1 Area selection

The Area Selection tests were made in two steps. The first step covered the largest part of the mainland of Greece. 88 map sheets cover this part in 1:50000 scale and regional scale geological, geophysical, mineralogical and geochemical information was processed from the Intermediate Tables. The results of these tests showed negative results (areas with no interest et. all) in 55 sheet maps, low interest for 8 sheet maps, and very positive results (areas of high interest) for 25 sheet maps. These map sheets coincide geographically with the areas of Sub-Pelagonian and Pelagonian geotectonic zones of Greece. These tectonic zones are characterised by the presence of large ophiolite complexes which are the host rocks of the Ni-laterite deposits of Greece (Plates 1, 2 and 3).

Based on the results taken from the first step the areas of Lokris, Euboea Island, Vermion and Kastoria were selected for evaluation and testing of the system for Area Selection, Identification of Potential Zones and Target Selection. The selection of the above areas made based also on the geoscientific information available, since all areas have not been explored at the same level.

The best area for GEOES evaluation and testing is the Lokris in central Greece including three different case studies namely Kopais, Nissi and Tsouka. These case studies represent three different Ni-laterite deposits under exploitation by LARCO and the degree of geological information covers a wide spectrum from surface to drill-holes data, and consequently tests made covered the Area Selection, Identification of Potential zones and Target Selection.

The results of the validation process in the Lokris area can be summarised as follows:

- In the Thiva Sheet map 1:50 000 scale (23.342, 38.375) the geological rating given through the Hybrid mode (histogram) is low, whereas the geophysical data is highly rated (histogram) resulting to the rate increase in the OVERALL assessment. The results obtained are well related to the real assessment made for the area using conventional exploration and mining methodologies.
- In the Larymna Sheet map 1:50 000 scale (23.342, 38.625) the geological and geophysical data evaluated by the system coincide again with the results from the conventional methodologies used. This coincidence is very encouraging for the system evaluation since in the Larymna area the large and significant Ni-laterite deposits of LARCO are hosted and are under exploitation at present.

For the Euboea Island tests the results are summarised as follows:

- In the Psachna Sheet map 1:50 000 scale (23.342, 38.625) although geology is highly rated (histogram) the geophysical data receives negative evaluation (-1) from the system. This has a negative effect on the OVERALL rating thus receiving low score (Plate 3). These results are not agreement with the geological information for the area, since it is hosting the largest Ni-laterite deposits in the Euboea Island. After a series of tests, it is believed that this discrepancy may be attributed either to the limited geophysical data for the area or to the large grid used for geophysical measurements.

For the Vermion area, case study Profitis Ilias, the results are as follows:

- In the Pyrghoi Sheet map 1:50 000 scale the evaluation for the geology and geophysics is high and corresponds to the geological data available for the area. Geological data includes large mineralised horizons, high nickel content, extended alteration zones etc. It is worth to mention that the evaluation results for this area are similar to those of the Tsouka area in the Larymna Sheet map. The Profitis Ilias, the Tsouka and the Kastoria deposits are lying on ophiolitic rocks, whereas the deposits studied in the rest cases are transported. Similar evaluation is given for the geophysical data for the Profitis Ilias and the Tsouka deposits also corresponding to the results obtained by the conventional geophysical research.

For the Kastoria area, the evaluation is:

- In the Mesopotamia Sheet map 1:50 000 scale (21.092, 40.625) the rate for the geology is low and it is not corresponding at all with the results obtained by the classical geological methods. The area is well explored and a LARCO's mine is in operation. Geophysics, although not present, since it is not available for the area, receives negative rating. This negative rate decreases the OVERALL rate and the area is evaluated by the system as not interested for further research.

4.2.2 Identification of potential zones

For the evaluation tests concerning the Identification of Potential Zones the Lokris area and Pyrghoi in Vermion have been selected. Both areas are suggested by the results obtained in

Area Selection and the fact that geological information existing is sufficient to make comparison between the systems evaluation and results from conventional exploration methods.

The results of the validation process in the Lokris area can be summarised as follows:

- Three potential zones are defined in the Thiva, Larymna and Livanates map Sheets (Plates 4 and 5). These areas correspond to the Kopais, Nissi and Tsouka deposits that have been discovered in the past using classical mineral and mining exploration methodologies. The low score (histogram) that was given for the geology in Area Selection is also given for geology in the Identification of Potential Zones for the Thiva map sheet, whereas rating for geochemistry, mineralogy and geophysics are high and correlate well with the existing background information.

For the Vermion area, results are as follows:

- The zone of the Profitis Ilias is suggested where the mineralised horizon is hosted. Geochemical, mineralogical and geophysical data correspond with the background information. Results for this area are not further evaluated, since drill-hole operations are lacking in the area and any correlation will not be objective.

4.2.3 Target selection

Evaluation tests were made mainly in the Lokris area, where background information exists for both surface and underground. Results obtained from geology, mineralogy, geochemistry and geophysics correspond with the existing data for the area (Plates 7, 8 and 9).

5. COMPARISON OF INITIALLY PLANNED ACTIVITIES AND WORK ACTUALLY ACCOMPLISHED

Despite the collection of 45 additional samples from the Northern Bothnia test area for intrusives, WP6 generally advanced as initially planned.

6. CONCLUSIONS AND SUGGESTIONS

Real case testing for the exploration of sulphidic Ni deposits were performed in the Northern Bothnia test area for intrusives, and komatiite test were carried out on the Pulju greenstone belt. The corresponding testing for the lateritic Ni deposits was carried out in the areas of Lokris, Euboea Island, Vermion and Kastoria.

For the sulphidic cases, data were acquired from existing files and in the field. The whole-rock and mineralogical analyse results were processed with APE. This facilitated fast and versatile analysis of the available litho-geochemical and petrological data for both the intrusive and the extrusive case studies. Litho-geochemical factors important in the exploration of Ni

deposits related to intrusives are readily calculated and transformed into input data for GEOES. In komatiite case APE was also used for renaming and classifying rocks into coherent types by comparing the chemistry and (calculated) mineralogy to rocktype names given to the rocks in the field.

APE made it possible to have all the tools a researcher needs under the same software. It was designed for researchers and exploration geologists, who wish to analyse lithochemical data in detail, but use large datasets. The advantage in APE is the combination of the database, spreadsheet and visualisation tools in the same software. All this and the geology-oriented special features (certain type of diagrams, calculations, normalisation etc.) make APE a special tool, which does not have real competitors in the market. In general terms, APE has enough features to become a suitable tool for geologists dealing with lithochemical data. When the mineralogical data are included, APE becomes even better.

The APE program is in use on Outokumpu Mining Oy's komatiite exploration projects in Finland. Experiences of applying APE in practical exploration are good. Advantages of APE include the following.

1. Flexible program digests XRF data in original or volatile-free form, in percent and ppm.
2. There are possibilities for filtering, queries and classification of material.
3. It is possible to make various trend lines and compositional areas in library for the comparison of targets.
4. APE is handy for displaying 2-axis or triangular diagrams.

Such properties make APE a practical tool to identify original rock types, to classify them as Ni-potential or less potential ones, and to compare the analytical data of current project with those of known areas or economic deposits. On the Pulju Greenstone Belt, it was possible to separate the Ni-potential komatiites from less potential ones.

Final testing of the prototype GEOSIS database modules has revealed some technical features that should be developed further if the commercialisation takes place. The most important area to be developed is the input and output tools in the software. These processes should be developed from the simple prototypes to versatile and user friendly software modules that would facilitate easy data entry to database and easy and fast access to all the data stored, with flexible reporting tools for data querying and outputs.

The developed prototypes in the GEOSIS system (GEOSIS database and GIS modules, GEOES, ANNGIE and ASM) form at the present a conglomerate of complex software that has been developed in different environments and need different third party programs for to be run. If the commercialisation of the GEOSIS system takes place, the integration of these programs must be carried further than in the prototypes. The entire system should be written in the same development environment, using the same standard Windows tools. This would ensure easier installation and would obviously provide more stable system free of technical hardware related compatibility problems.

In general it is apparent that GEOES is a complete and powerful exploration tool for the Area Selection, Identification of Potential Zones and Target Selection, covering and compiling geological data from diverse origin (i.e. geology, geophysics, mineralogy and geochemistry) well corresponding to results obtained using conventional exploration methodologies. Consultation

and suggestions given by the Hybrid mode of the system are indeed very constructive in all evaluation steps.

However, in case of commercialisation of the product, the following suggestions are given for improvements and refining:

- Data entry to the intermediate Tables from GEOSIS database is very difficult and cumbersome due to their different structures. It is suggested the development of a methodology to automate the process of fill out the intermediate Tables.
- In the testing of Interactive GEOES for the lateritic model, separate processing of the various data sets (i.e. geology, geophysics, mineralogy and geochemistry) gives results corresponding exactly with the background information. However, in Spatial GEOES if a data set is absent, i.e. geophysics, then the system instead of ignoring this data set, gives negative score for geophysics and thus the OVERALL rate is low, even in cases where geological factors are strongly present.
- After the completion of a data set processing in GEOSIS, there are two directories on the hard disk where some files have been created. These files if they will not be deleted or transferred from these directories namely C:\TEMP and C:\GEODATA, create problems to the GEOES performance, since the application *overwrite* of new data on the old one is not functioning properly. Therefore the number of the system routines is doubled and the results obtained are not correct. We solved the problem during the tests by transferring the files in new directories and keeping the initial ones empty.
- After the data import into the system some names do not appear in the expected order and the user has to search again the relevant column for the proper linking of the corresponding fields. Also, the text spaces of the same window are very narrow. The left column, accommodating long names, does appear on the screen completely and thus proper selection for the next step is difficult.
- The addition of the Hybrid mode of GEOES in the final version of the expert system was very helpful. Its contribution for the evaluation of the data sets on the maps is commendable.
- Finally, it is suggested that the end users would be provided with a CD-ROM containing all the installation procedures automated. Installation of so many software packages necessary for the complete performance of the system and interference of so many files and directories create difficulties not only to the end users but also sometimes to the system itself.

Even though nickel exploration was the primary target of the GeoNickel project, it is evident that most of the developed instruments and software are of generic nature. Consequently, they can be applied to a great variety of base metals deposits other than the "nickel family" (i.e. Ni, Co, Cu and PGE). Most of them can be used to aid exploration of commodities genetically related to magmatic, or even to sedimentary rocks in various geotectonic environments.

One of the powers of GEOES system is the needed systematic approach from the data acquisition to the output of the results. It gives the exploration staff a good opportunity to

sition to the output of the results. It gives the exploration staff a good opportunity to examine systematically all the available data, estimate its homogeneity and validity, showing where more information is required for well-balanced reasoning results. Ultimately, the most important feature in using such an expert system may be the fact that it forces different specialists in an exploration team to work more closely and coherently, enhancing the strengths of teamwork in mineral exploration.

7. ANNEXES

7.1 List of publications, conference presentations and patents resulting from the project

Eliopoulos D., Aarnisalo J., Papunen H., Apostolikas A., Economou M., Bourgeois B., Angelopoulos A., Gustavsson N., Stefouli M., Varoufakis S., Morten E., Ripis C. and Spyropoulos C., 1998: Integrated Technologies For Minerals Exploration: Pilot Project For Nickel Ore Deposits. In: A. Kontopoulos, I. Paspaliaris, A. Adjemian and G. Katalagarianakis, eds, *Proceedings of the first annual workshop (Eurothen '98), Athens, Greece, 12-14 January 1998*. European Commission, Industrial and Materials Technologies Programme (BRITE-EURAM III). Lab. Metall., Nat. Tech. U Athens, pp. 24-32.

Aarnisalo J., Lamberg P., Papunen H., Mäkelä K., Eliopoulos D., Ripis C., Dimou E., Maglaras K., Apostolikas A., Melakis M., Economou-Eliopoulos M., Bourgeois B., Elo S., Pietilä R., Varoufakis S., Vassilas N., Perantonis S., Ampazis N., Charou E., Gustavsson N., Stefouli M., Morten E., Spyropoulos C., Vouros G., Stavrakas Y. and Katsoulas D., 1999: Integrated Technologies For Minerals Exploration: Pilot Project For Nickel Ore Deposits. In: *Eurothen '99. Eurothen '99 workshop. Preprints of the second annual workshop (Eurothen '99), Cagliari, Sardinia, Italy, 18-20 January 1999*. European Commission, Industrial and Materials Technologies Programme (BRITE-EURAM III). Pp 3-27.

7.2 Task 6.2 outputs

	Number
Reports issued	0
Publications	0
Doctoral thesis	0
Master thesis	0
Conference presentations	2
Demonstrations	0
Prototypes	0
Patents	0

8. REFERENCES

- Chai, G. and Naldrett, A.J., 1992: The Jinchuan ultramafic intrusion: Cumulate of a high-Mg basaltic magma. *J. Petrology*, 33, 277-303.
- Barnes, S.-J. & Often, M., 1990 : Ti-rich komatiites from northern Norway. *Contributions to Mineralogy and Petrology*, vol. 105, no 1, 42-54.
- Daividsen, B. ,1994: Stratigrafi, petrologi og geokjemi med vekt på komatiittiske bergarter innen den nordligste del av Karasjok grønnsteinsbelte, Brennelv, Finnmark. In Norwegian. Unpublished master thesis, Institutt for Biologi og Geologi, University of Tromsø, Norway. 380 p.
- Irvine, T.N., 1970: Crystallization sequences in the Muskox intrusion and other related intrusions. 1. Olivine-pyroxene-plagioclase relations. *Geol. Soc. S. Afr. Spec. Publ.*, 1, 441-476.
- Isohanni, M., Ohenoja, V. and Papunen, H. ,1985: Geology and nickel-copper ores of the Nivala area. In: *Papunen, H. and Gorbunov, G. I.: Nickel-copper deposits of the Balti Shield and Scandinavian Caledonides. Geol. Surv. Finland Bull.* 333, 211-228.
- Kahma, A. ,1973: The main metallogenic features of Finland. *Geol. Surv. Finland Bull.* 265, 28 p.
- Koljonen, T. (Ed.) ,1992: The geochemical atlas of Finland, Part 2: Till. *Geol. Surv. Finland, Espoo* 218 p.
- Krill, A.G., Bergh, S., Lindahl, I., Mearns, E.W., Often, M., Olerud, S., Olesen, O., Sandstad, J.S., Siedlecka, A., & Solli, A. ,1985: Rb-Sr, U-Pb and Sm-Nd isotopic dates from Precambrian rocks of Finnmark. *Norges Geologiske Undersøkelse, Bulletin* 403, 37-54.
- Lehtonen, M., Airo, M-L., Eilu, P., Hanski, E., Kortelainen, V., Lanne, E., Manninen, T., Rastas, P., Räsänen, J., and Virransalo, P. ,1998: Kittilän vihreäkivialueen geologia. Lapin vulkaniittiprojektin raportti. In Finnish. Geological Survey of Finland, Report of Investigation 140, 144 p. English summary : The stratigraphy, petrology and geochemistry of the Kittilä greenstone area, northern Finland. A report of the Lapland Volcanite Project.
- Mid-Norden Project ,1996: Bedrock map of Central Fennoscandia. Scale 1 : 1 000 000. Compiled by the Geological Surveys of Finland, Norway and Sweden.
- Mikkola, A. ,1980: The metallogeny of Finland. *Geol. Surv. Finland Bull.* 305, 22 p.
- Often, M. ,1985: The Early Proterozoic Karasjok Greenstone Belt, Norway; a preliminary description of lithology, stratigraphy and mineralization. *Norges geologiske undersøkelse, Bulletin* 403, 75-88.
- Papunen, H., Idman, H., Ilvonen, E., Neuvonen, K., Pihlaja, P., and Talvitie, J. ,1977: Lapin ultramafiiteista. In Finnish. Geological Survey of Finland, Report of Investigation 23, 87 p. English summary: The Ultramafics of Lapland.
- Rauhämäki, E., Mäkelä, T., and Isomäki, O-P. ,1978: Geology of the Vihanti mine. In: *Metallogeny of the Precambrian, IGCP Project 74/1/91 Excursion Guide*, 35-56. *Acad. Finland.*

- Rouhunkoski, P. ,1968: On the geology and geochemistry of the Vihanti zinc deposit, Finland. Bull. Comm. Geól. Finlande 236, 121 p.
- Simonen, A. ,1980: The Precambrian in Finland. Geol. Surv. Finland Bull. 304, 58 p.
- Vaasjoki, M. and Sakko, M. 1988: The evolution of the Raahe-Ladoga zone in Finland: isotopic constraints. In: *Korsman, K. (Ed.): Tectono-metamorphic evolution of the Raahe-Ladoga zone. Geol. Surv. Finland Bull. 343, 7-32.*

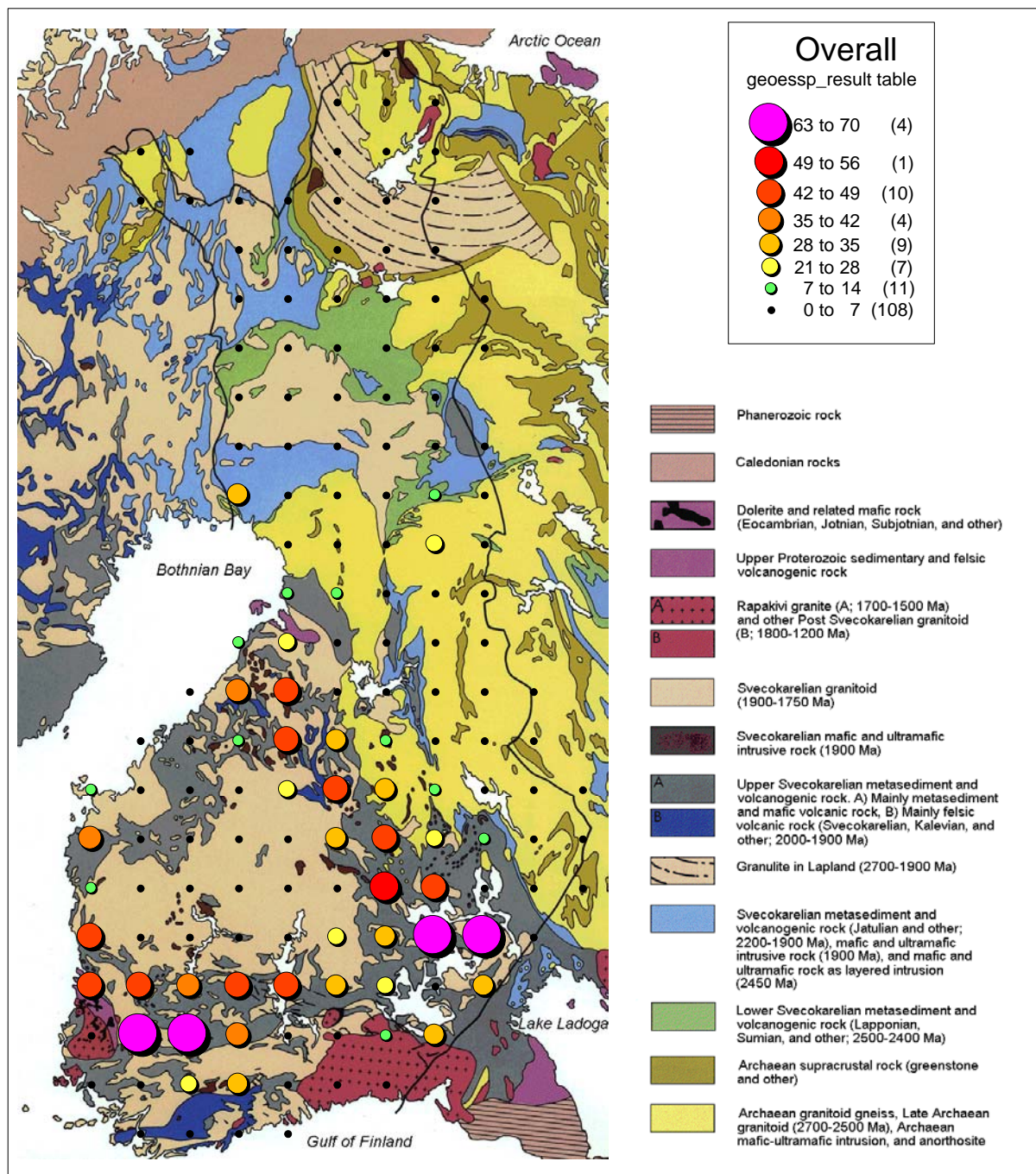


Plate 6.2-1 An overall result of GEOES spatial mode process in Intrusive Area Selection phase. Geological map extracted from the Map of Prequaternary Rocks of the Fennoscandian Shield (Koljonen 1992).

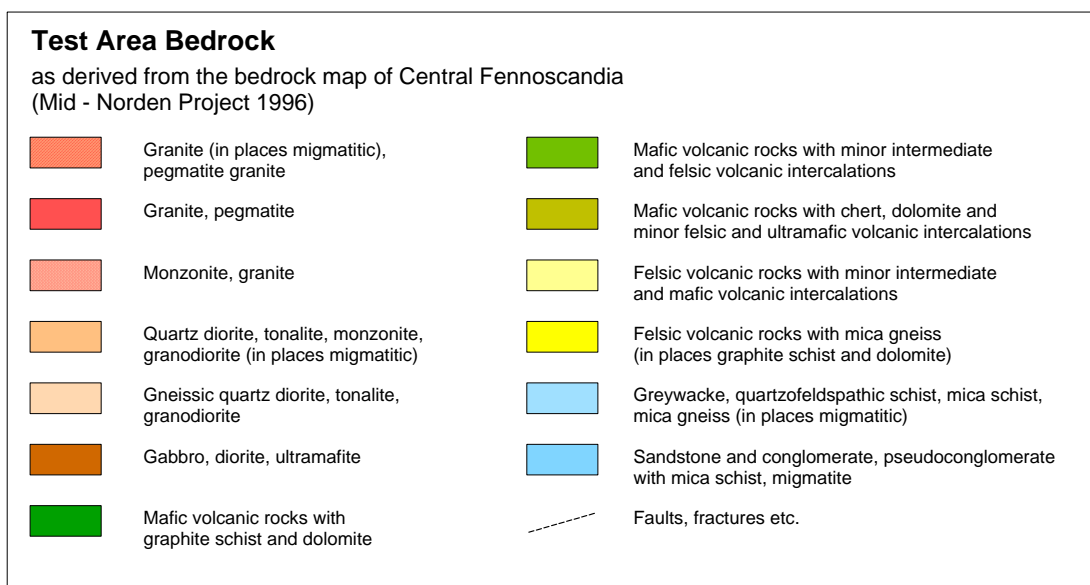
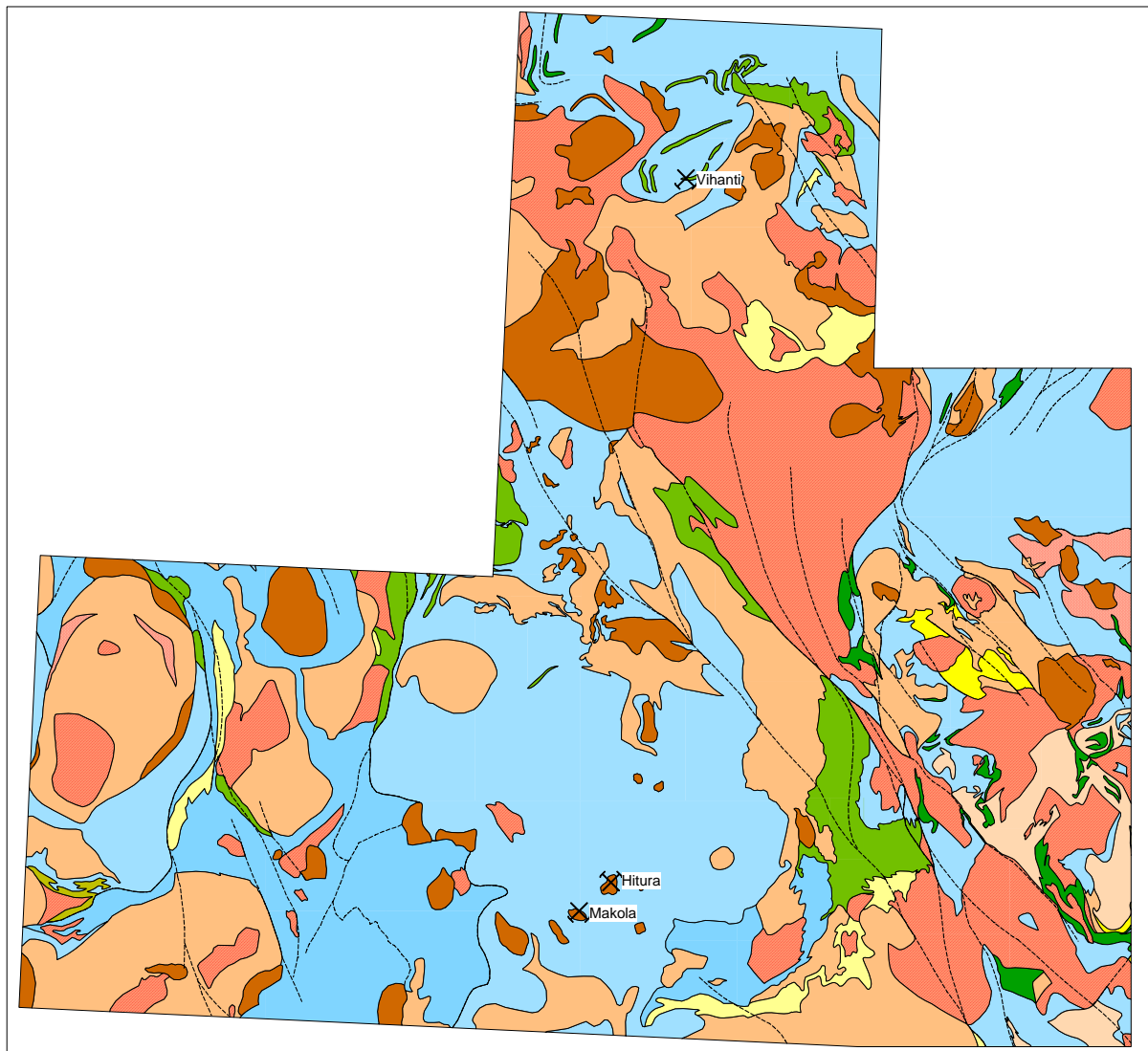


Plate 6.2-2 Bedrock map of the Northern Bothnia test area.

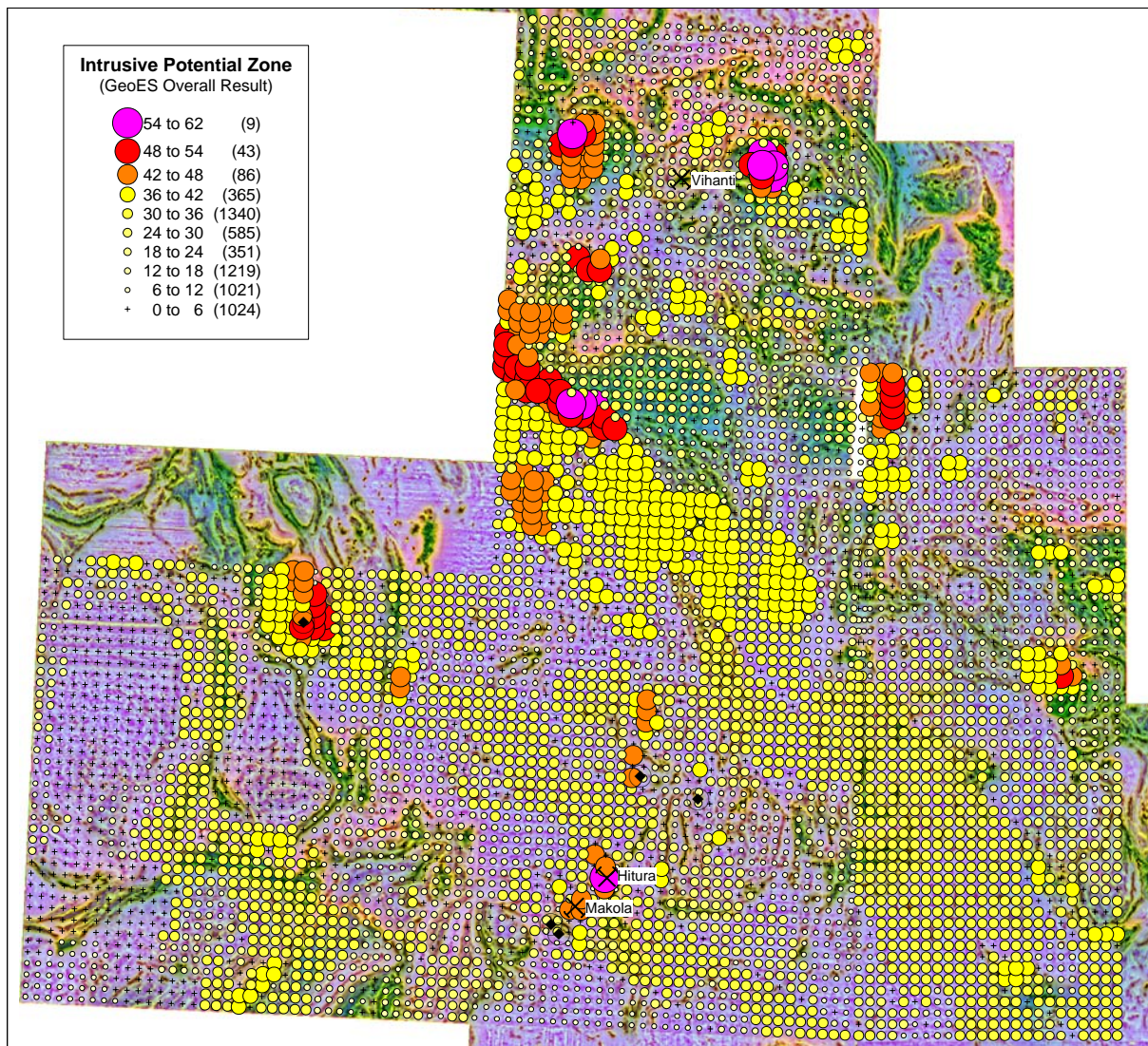


Plate 6.2-3 An overall result of GEOES spatial mode process in Intrusive Identify Potential Zone phase, Northern Bothnia test area. The background image was processed at Outokumpu Mining Oy from the low-altitude airborne magnetic data provided by Geological Survey of Finland. Evidence weights for the observations were given using the default linear configuration available in GEOES.

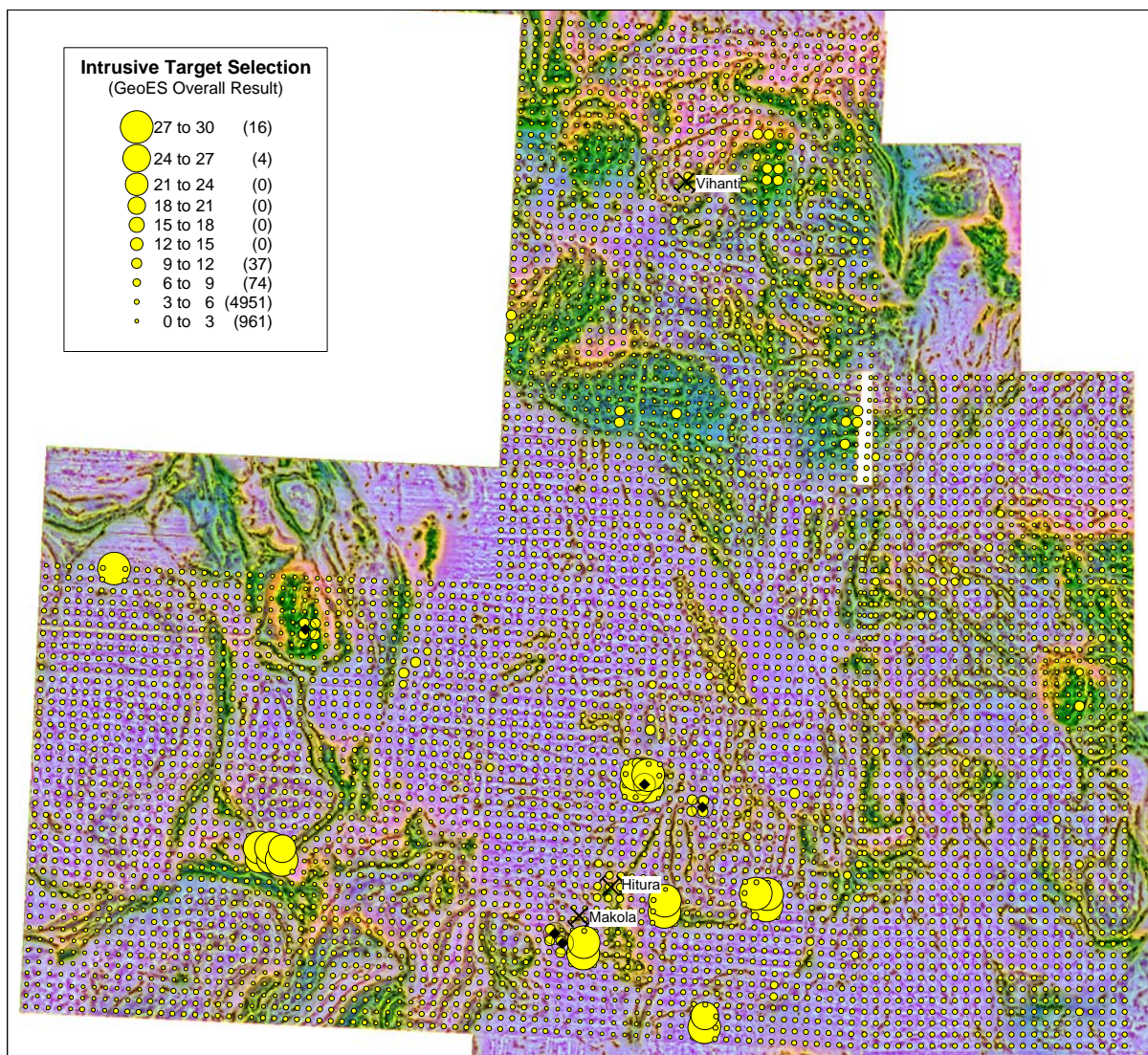


Plate 6.2-4 An overall result of GEOES spatial mode process in Intrusive Target Selection phase, Northern Bothnia test area. Background as in plate 6.2-3. Evidence weights were given using the default linear configuration available in GEOES.

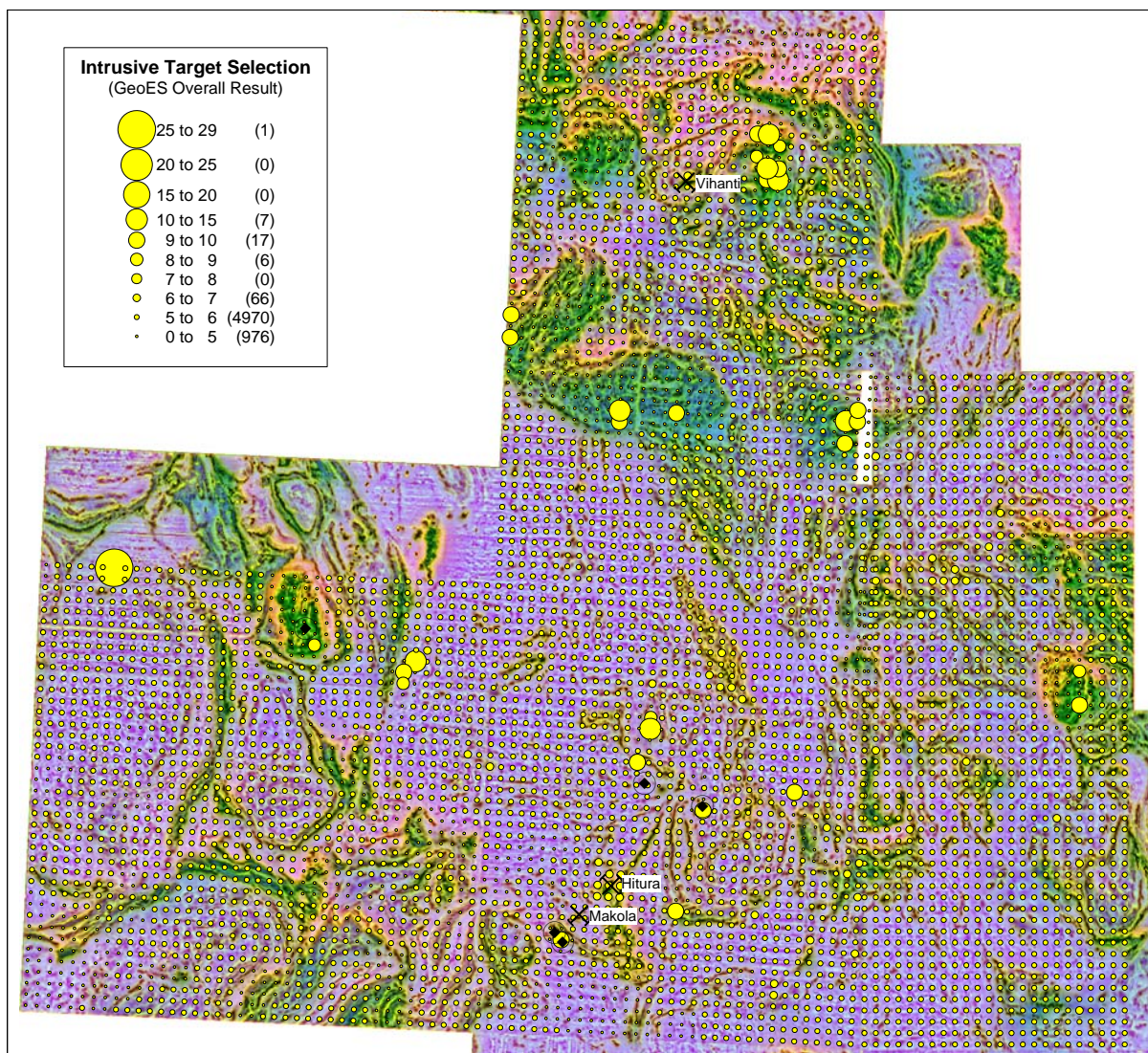


Plate 6.2-5 An overall result of GEOES spatial mode process in Intrusive Target Selection phase, Northern Bothnia test area. Background as in plate 6.2-3. Ore deposit, mineralisation and erratic boulder data were removed from the input data set. Evidence weights for observation were given using the default linear configuration available in GEOES.

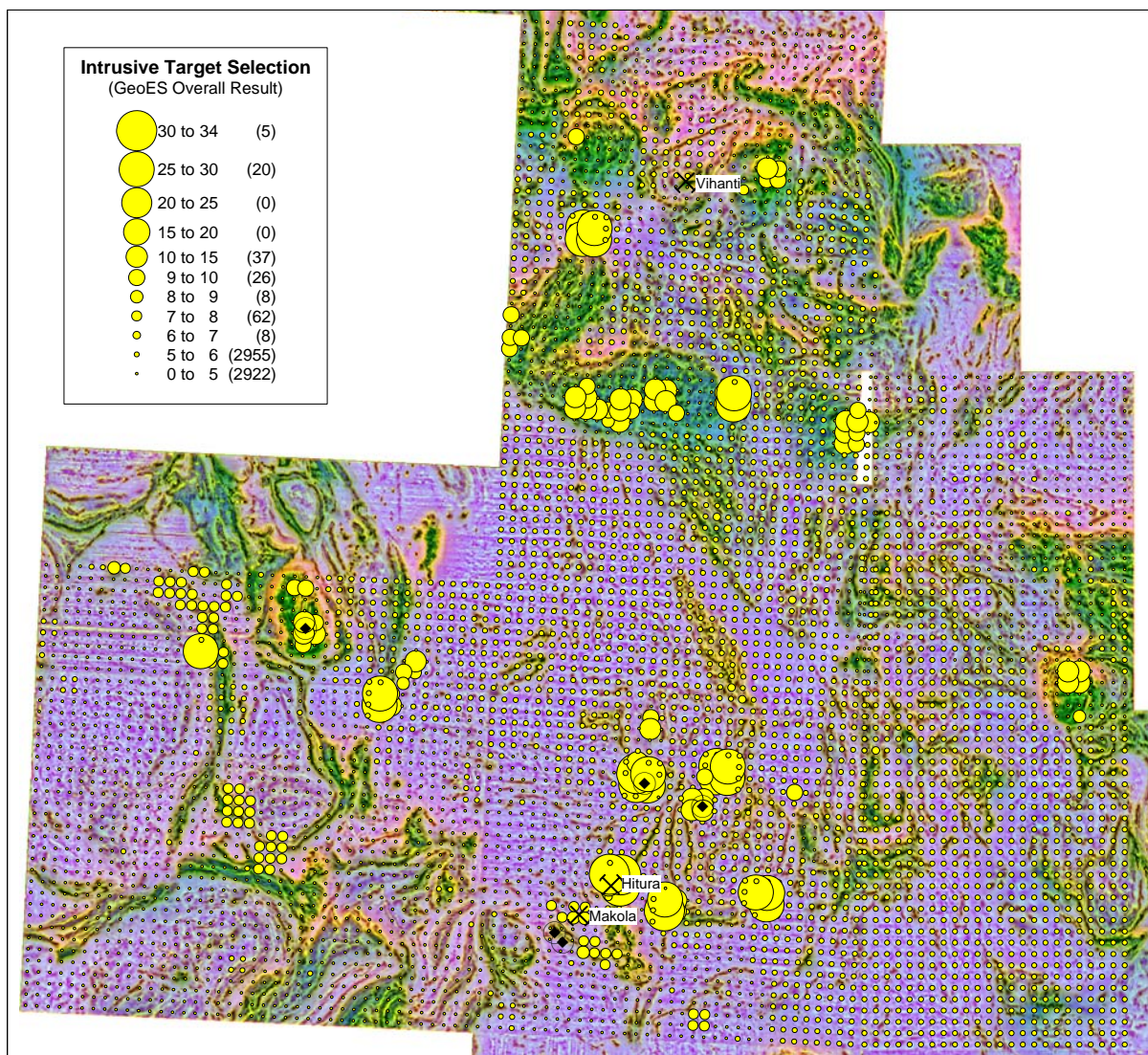


Plate 6.2-6 An overall result of GEOES spatial mode process in Intrusive Select Target phase, Northern Bothnia test area. Background as in plate 6.2-3. Evidence weights for the observations were given by the user as customised configuration.

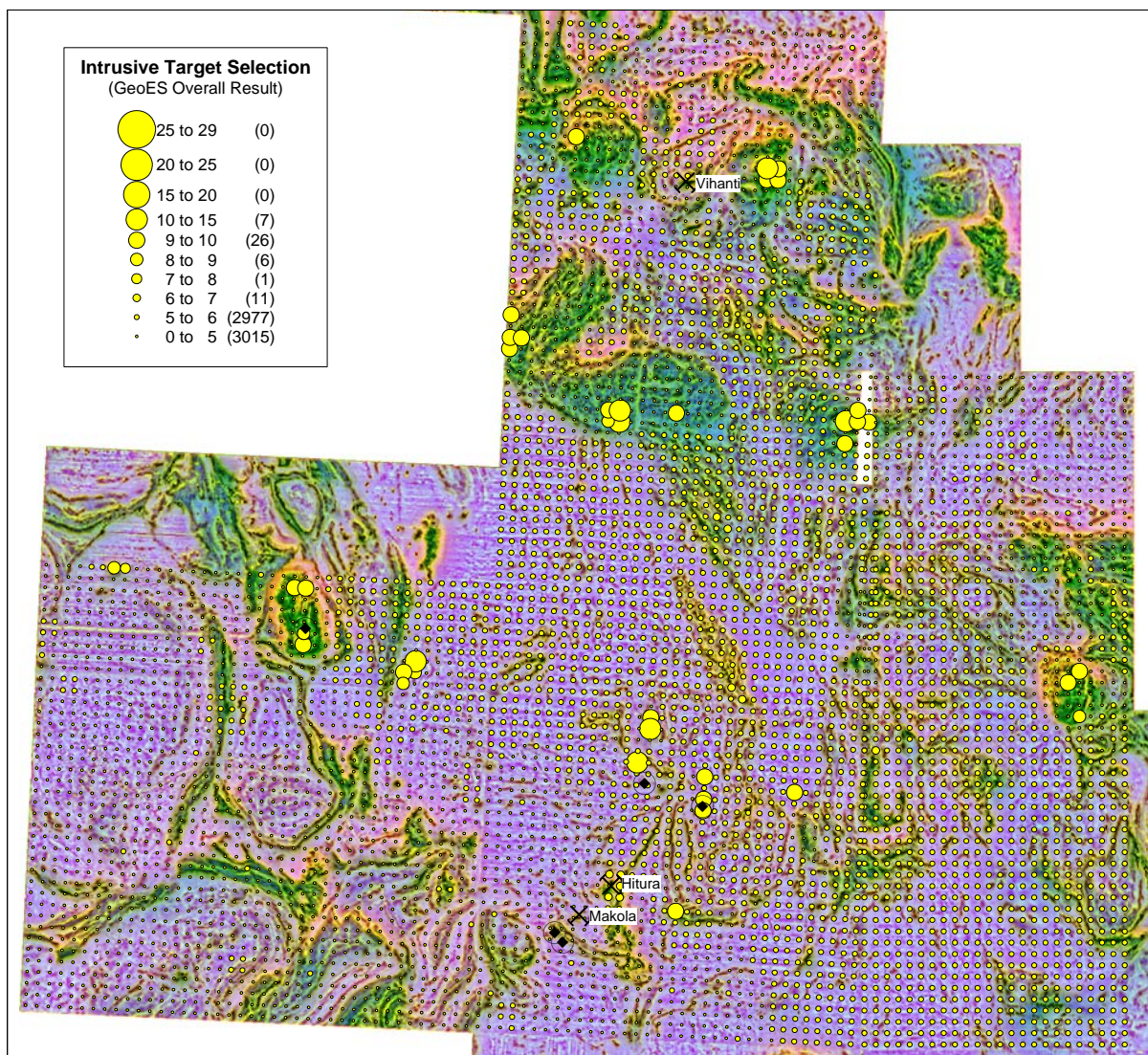


Plate 6.2-7 An overall result of GEOES spatial mode process in Intrusive Target Selection phase, Northern Bothnia test area. Background as in plate 6.2-3. Ore deposit, mineralisation and erratic boulder data were removed from the input data set. Evidence weights for observations were given by the user as customized configuration.

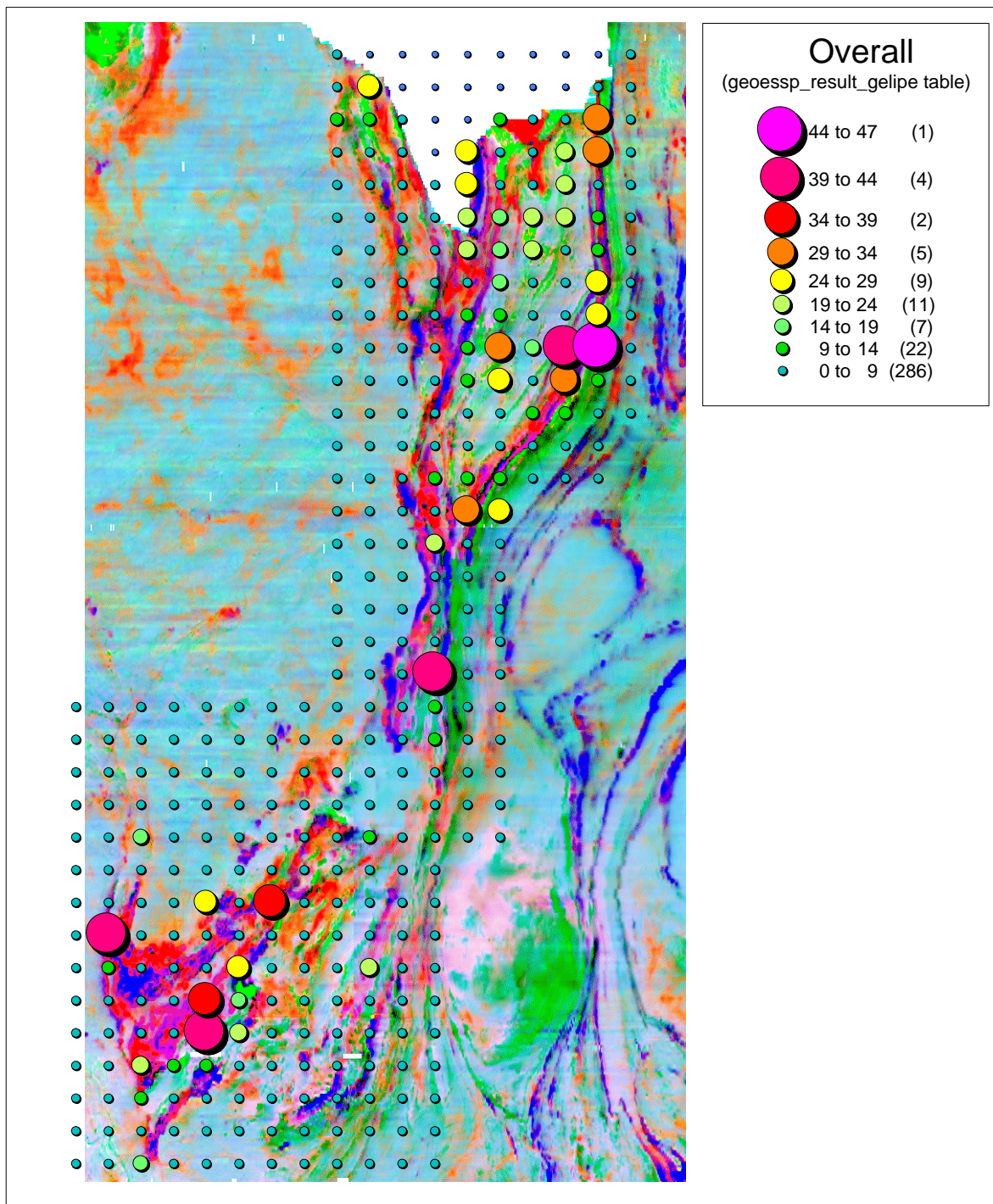


Plate 6.2-8 An overall result of GEOES spatial mode process in Komatiite Identify Potential Zones phase, Pulju test area. Background image is a color composite of PCA images derived at Outokumpu Mining Oy from low-altitude airborne magnetic and electromagnetic data provided by the Geological Survey of Finland. The processed observations consist geological, lithogeochemical and pedogeochemical data. Evidence weights for the observations were given as default configuration available in GEOES.

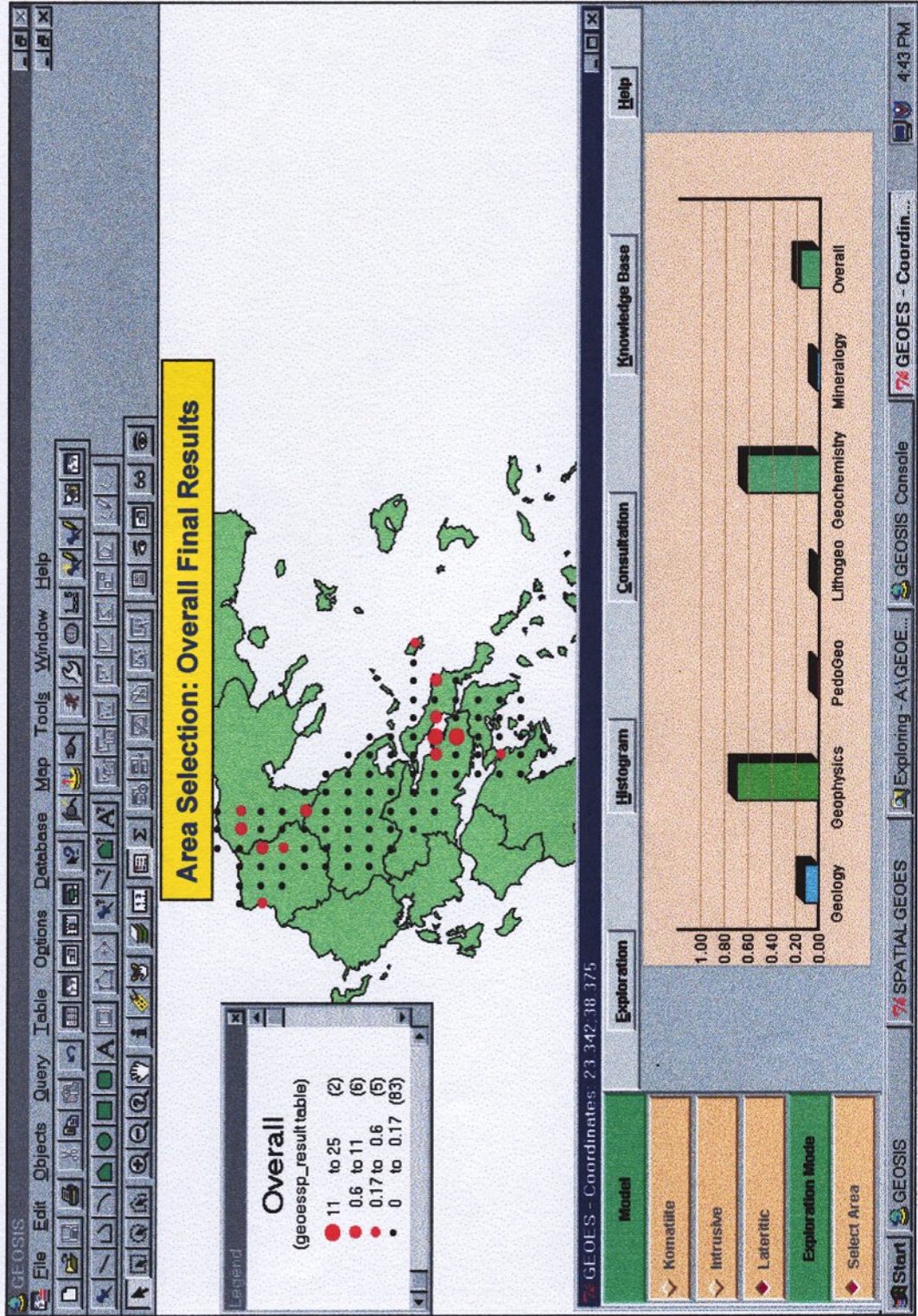
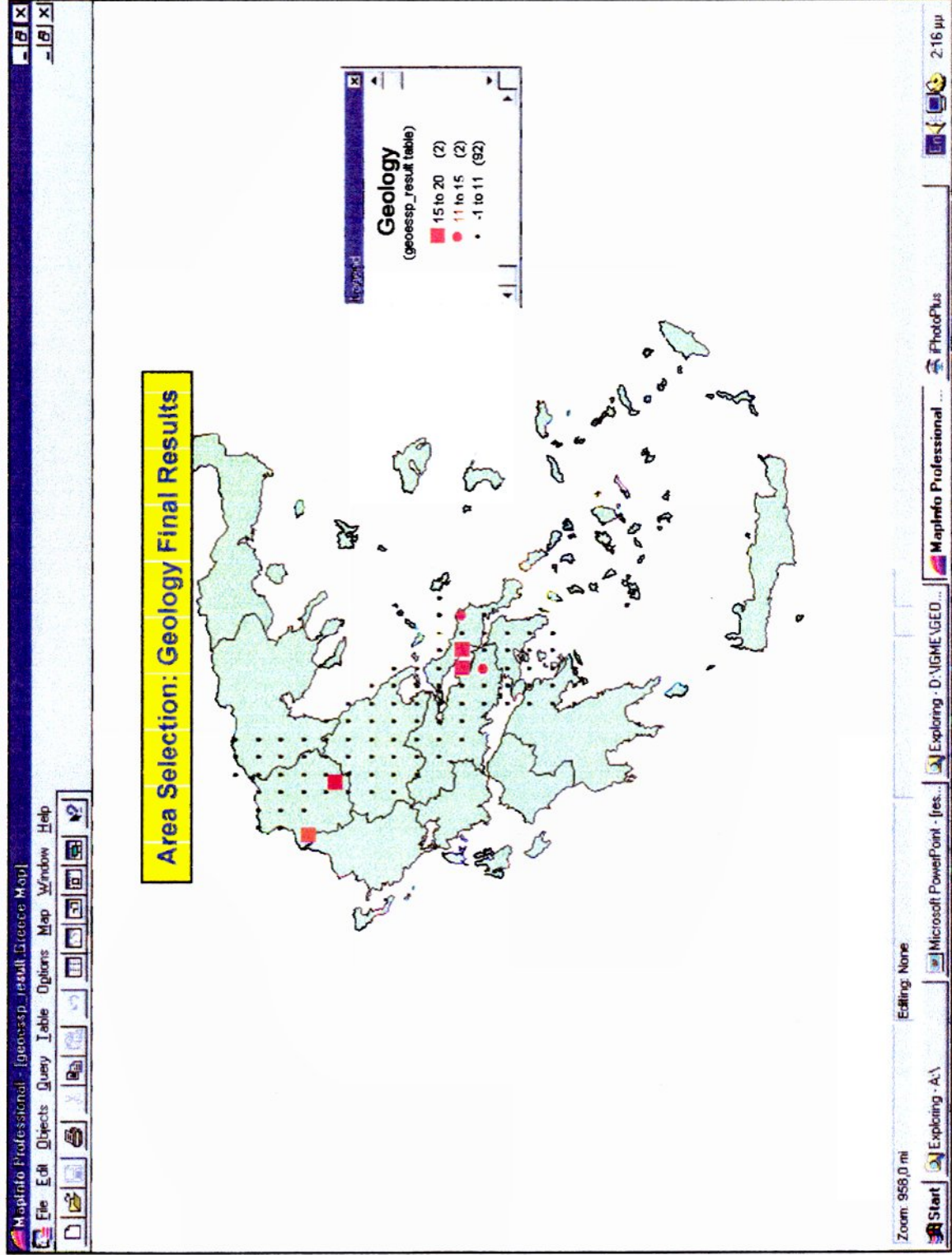


Plate 1: WorkPackage 6, Task 6.2: Area Selection, Overall Final Results



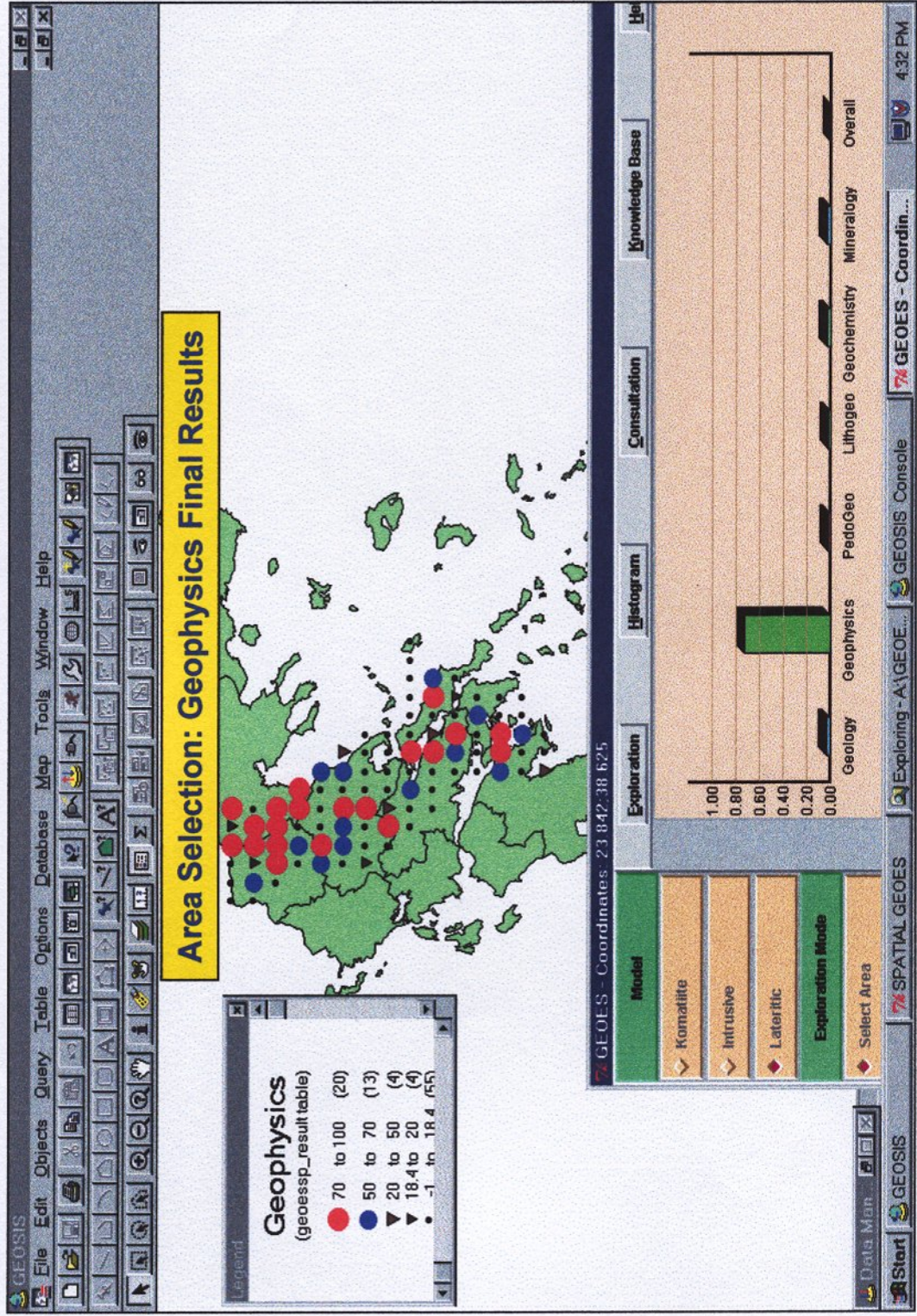


Plate 3: WorkPackage 6, Task 6.2: Area Selection, Geophysics Final Results

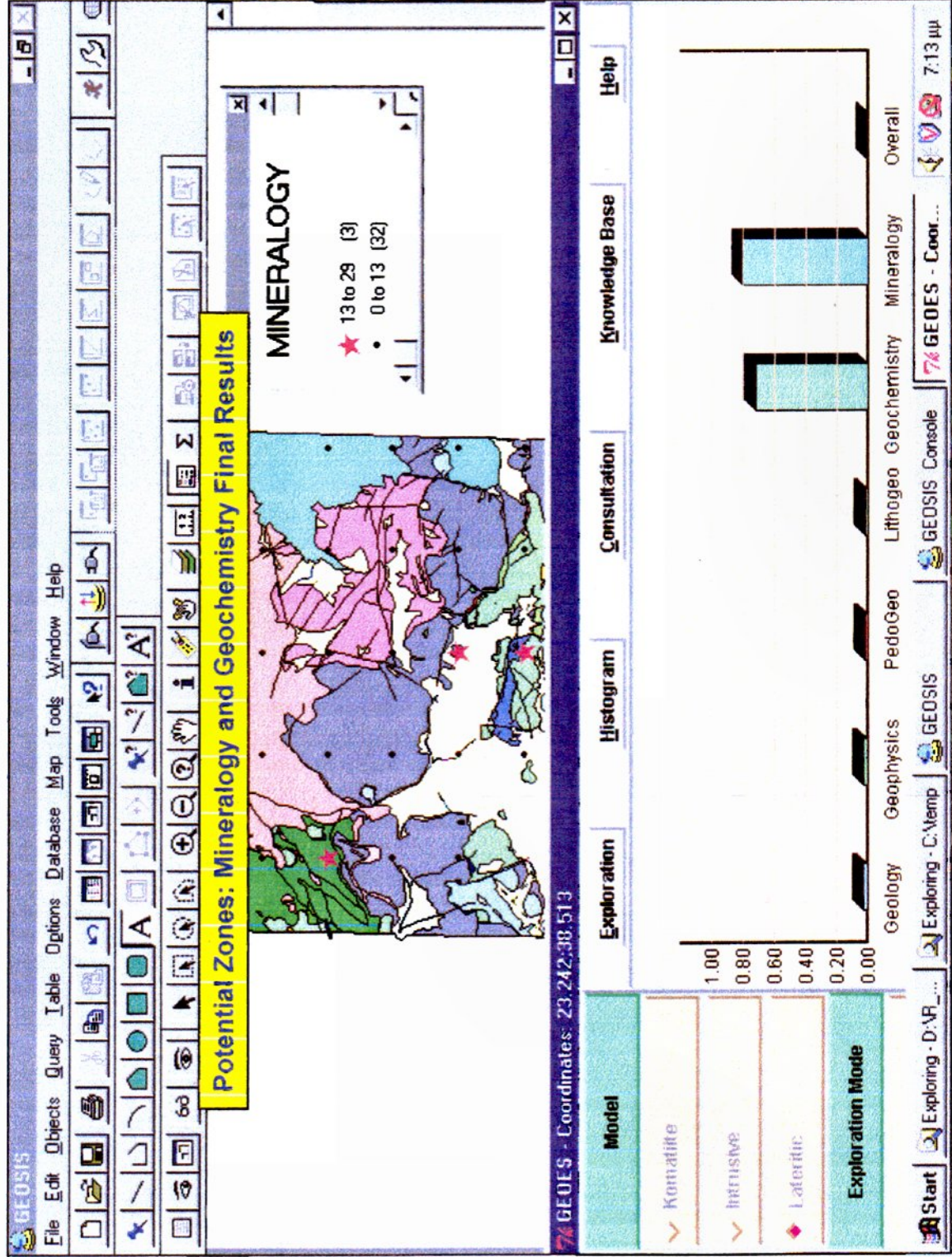


Plate 4: WorkPackage 6, Task 6.2: Identification of Potential Zones, Mineralogy and Geochemistry Final Results

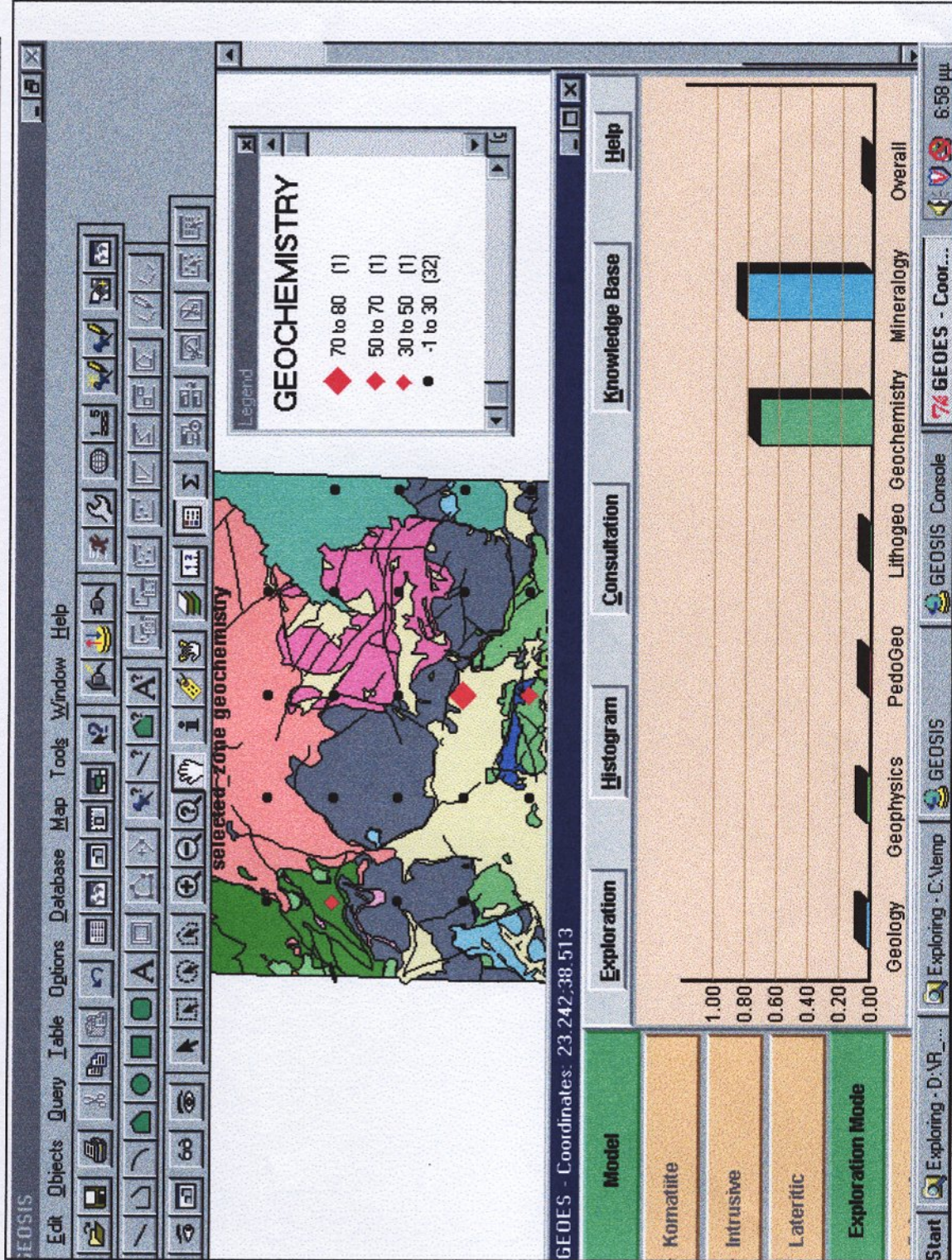


Plate 5: WorkPackage 6, Task 6.2: Identification of Potential Zones, Geochemistry Final Results

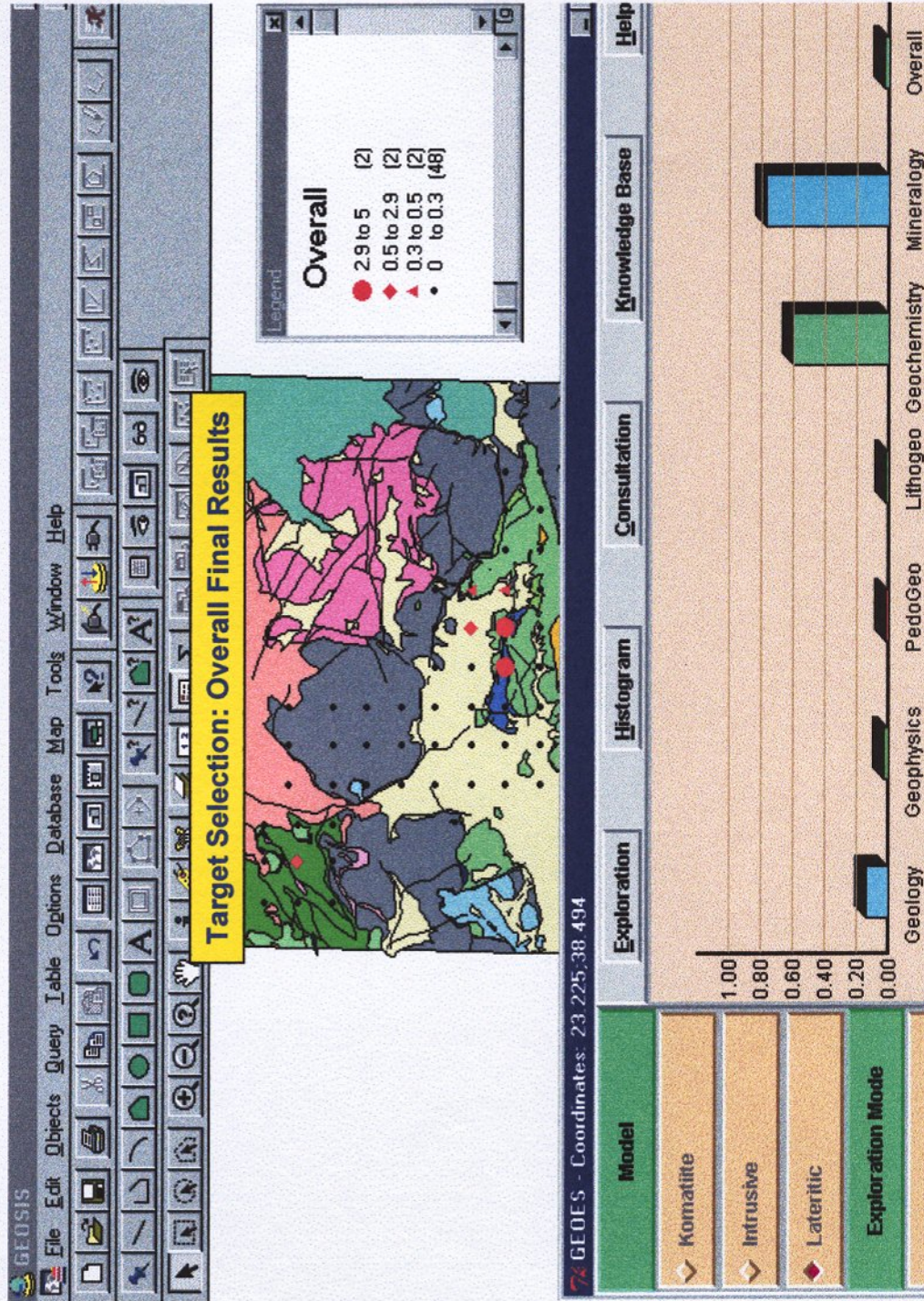
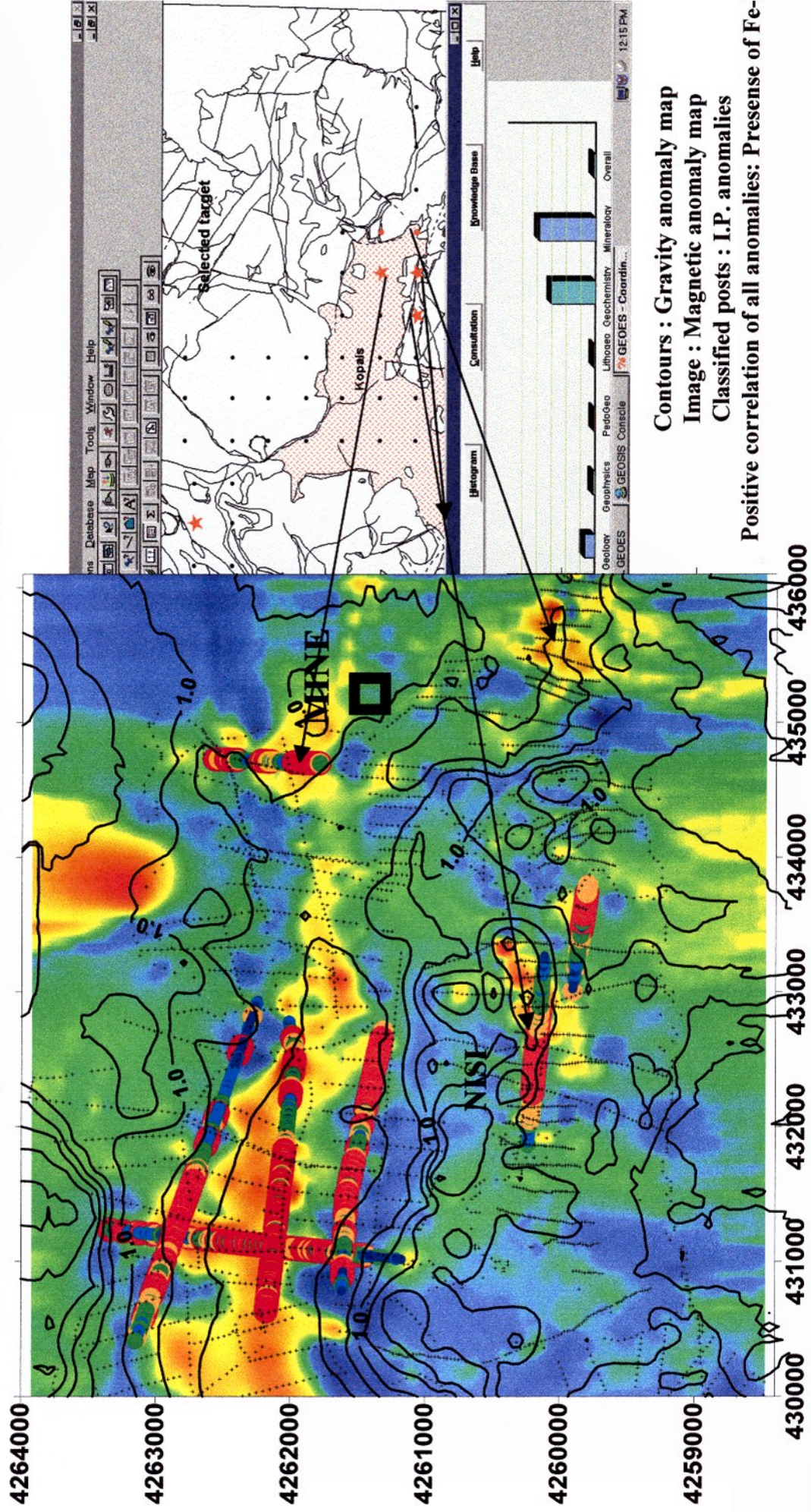


Plate 6: WorkPackage 6, Task 6.2: Target Selection, Overall Final Results



Contours : Gravity anomaly map
Image : Magnetic anomaly map
Classified posts : I.P. anomalies

Positive correlation of all anomalies: Presence of Fe-Ni

Plate 7: WorkPackage 6, Task 6.2: Target Selection, Overall Final Results

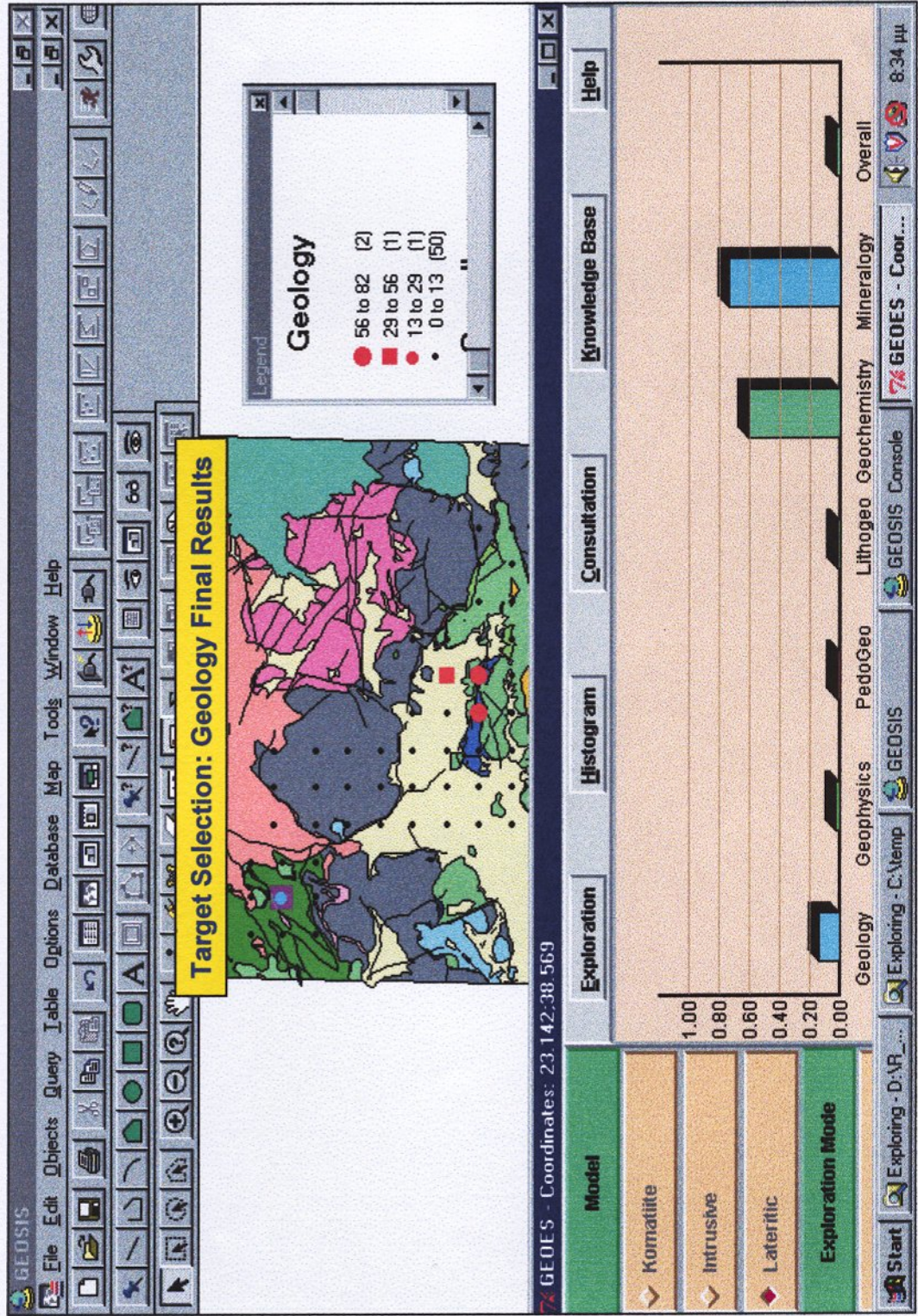


Plate 8: WorkPackage 6, Task 6.2: Target Selection, Geology Final Results

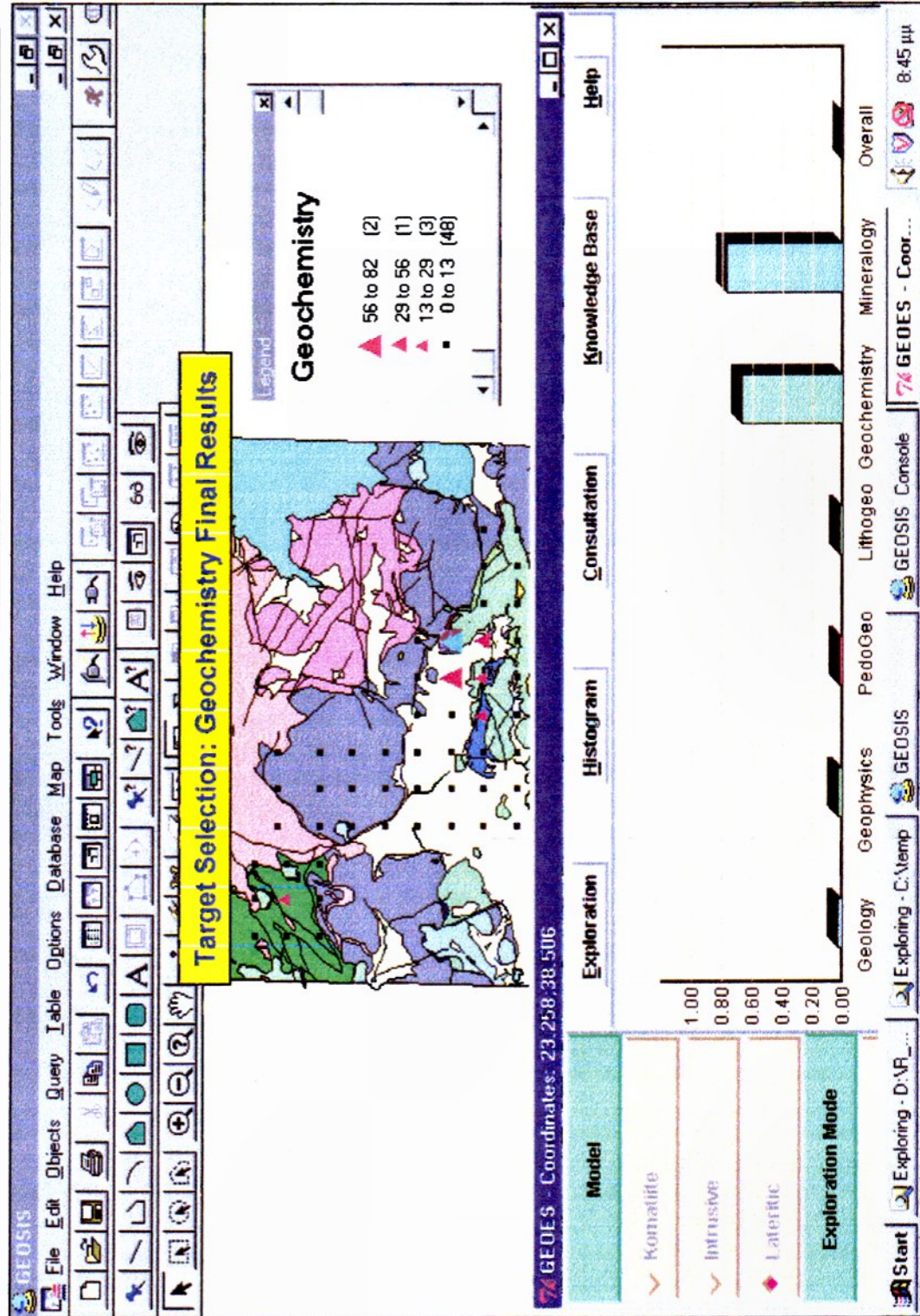


Plate 9: WorkPackage 6, Task 6.2: Target Selection, Geochemistry Final Results

GeoNickel

FINAL TECHNICAL REPORT

VOLUME 2

FINAL TECHNICAL REPORT

VOLUME 2

INTEGRATED TECHNOLOGIES FOR MINERALS EXPLORATION, PILOT PROJECT FOR NICKEL ORE DEPOSITS

~~CONFIDENTIAL~~

CONTRACT NO: BRPR-CT95-0052 (DG12 - RSMT)

PROJECT NO: BE – 1117

TITLE: Integrated Technologies for Minerals Exploration,
Pilot Project for Nickel Ore Deposits
GeoNickel

PROJECT

COORDINATOR: OUTOKUMPU Outokumpu Mining OY

Finland

PARTNERS: LARCO General Mining and Metallurgical Company
SA

Greece

BRGM Bureau de Recherches Géologiques et Minières
France

GSFIN Geological Survey of Finland
Finland

SOFTECO Softeco Sismat Srl
Italy

IGME Geological Survey of Greece
Greece

IRIS Iris Instruments SA
France

NCSR 'D' National Center of Scientific
Research 'Demokritos', Greece

STARTING DATE: 1st January 1996 DURATION: 36 MONTHS



PROJECT FUNDED BY THE EUROPEAN
COMMISSION UNDER THE BRITE/EURAM
PROGRAMME

Date: February 28, 1999

FINAL TECHNICAL REPORT VOLUME 2

INTEGRATED TECHNOLOGIES FOR MINERALS EXPLORATION, PILOT PROJECT FOR NICKEL ORE DEPOSITS *GeoNickel*

VOLUME 2:

Annex 2 WP2 DEVELOPMENT OF GEOPHYSICAL TECHNOLOGY

VOLUME 1:

Executive Summary	3
1. Objectives	11
2. Means used to achieve the objectives	11
3. Scientific and technical description of the project.....	13
4. Comparison of initially planned activities and the work actually accomplished.....	14
5. Conclusions for WP1-5.....	16
6. Conclusions and suggestions for WP6.....	22
7. Acknowledgements	24
8. Annexes.....	25
8.1 Publications.....	25
8.2 Conference presentations	25
8.3 Patents	27
8.4 Summary of GeoNickel output.....	27
8.5 Final Technical Reports of the GeoNickel WorkPackages.....	28
Annex 1 WP1 MINERALOGY AND MODELLING OF NI ORE DEPOSITS	
Annex 3 WP3 IMAGE PROCESSING / PATTERN RECOGNITION	
Annex 4 WP4 GEOSIS DESIGN AND GIS TOOLS DEVELOPMENT	
Annex 5 WP4 GEOSIS DESIGN AND GIS TOOLS DEVELOPMENT	
Annex 6 WP6 FINAL INTEGRATION, Task 6.2 Validation and testing	

GeoNickel

Annex 2

FINAL TECHNICAL REPORT

ANNEX 2

WP2 DEVELOPMENT OF GEOPHYSICAL TECHNOLOGY

~~CONFIDENTIAL~~

CONTRACT NO: BRPR-CT95-0052 (DG12 - RSMT)

PROJECT NO: BE – 1117

TITLE: Integrated Technologies for Minerals Exploration,
Pilot Project for Nickel Ore Deposits
GeoNickel

PROJECT

COORDINATOR: OUTOKUMPU Outokumpu Mining OY
Finland

PARTNERS: LARCO General Mining and Metallurgical Company
SA

Greece

BRGM Bureau de Recherches Géologiques et Minières
France

GSFIN Geological Survey of Finland
Finland

SOFTECO Softeco Sismat Srl
Italy

IGME Geological Survey of Greece
Greece

IRIS Iris Instruments SA
France

NCSR National Center of Scientific
Research 'Demokritos', Greece

STARTING DATE: 1st January 1996 DURATION: 36 MONTHS



PROJECT FUNDED BY THE EUROPEAN
COMMISSION UNDER THE BRITE/EURAM
PROGRAMME

Date: February 28, 1999

CONTENTS

EXECUTIVE SUMMARY 3

PROJECT STAFF 8

OBJECTIVES 10

MEANS USED TO ACHIEVE THE OBJECTIVES 11

**SCIENTIFIC AND TECHNICAL DESCRIPTION OF
THE PROJECT 13**

**COMPARISON OF INITIALLY PLANNED ACTIVITIES
AND WORK ACTUALLY ACCOMPLISHED 103**

PLATES 214

FINAL TECHNICAL REPORT ANNEX 2

WP2 - DEVELOPMENT OF GEOPHYSICAL TECHNOLOGY

EXECUTIVE SUMMARY

The objective of WP 2 was to develop and improve several Geophysical methods intervening at the three basic stages of nickel exploration:

Regional scale exploration: Combine GPS elevation measurements and digital Gravity measurements to obtain accurate and cost-effective regional gravity surveying.

Site scale exploration: a) Apply spectral IP method to Ni exploration, in particular develop specific measurement procedures. b) Develop software for fast (approximate) interpretation of ground EM methods. c) For the lateritic Ni, field-test existing geophysical methods to detect, map and outline the lateritic FeNi bodies.

Deposit investigations: Develop the cross-hole (tomography) and single-hole (borehole Slingram) EM methods (with 3-component receiver) for locating missed targets and possibly outlining intersected orebodies. The task involves development of prototype equipment suited to slim exploration boreholes, processing and interpretation software, methodology and field tests.

With the objective of serving all the above applications, the compilation of a petrophysical database of Ni deposits and host-rock was also in the programme.

The results for each task in WP2 is summarized hereafter.

Task 2.1. *Integrated GPS-Gravity system.* A ready-to-use prototype of real-time GPS-gravity system and associated software were assembled for exploration-oriented regional, semi-regional and local gravity surveys. Altogether 18 separate field campaigns were carried out in Finland, Greece, Norway and France by GTK, Outokumpu Oy, BRGM, IGME, and LARCO to test the conditions in which the GPS yields the expected vertical accuracy of a few centimetres, to find out the advantages and disadvantages of gps-gravity surveys, and to set guidelines for future work. Permanent routes were established for repeated testing of various

GPS equipment and software. Knowledge was obtained of how to transform in real-time GPS coordinates into local coordinate systems, and, especially, how to model local geoid undulations in order to transform heights above ellipsoid into heights above sea level. The sub-project has also greatly helped and accelerated general efforts to utilise rapidly developing GPS technology in various geophysical and geological applications.

Task 2.2.1. *Development of spectral IP method for Ni exploration.*

The objective in spectral IP development is to study the applicability of spectral IP method to Ni exploration and to develop proper data acquisition techniques. Although the spectral IP method has been extensively studied for base-metal exploration, the case of Ni-ores had not been thoroughly investigated. Moreover, there were still questions in the precise field measurement procedures needed to acquire reliable spectral data in an extended frequency range.

Laboratory determinations of resistivity spectra from sulphidic nickel deposits and their environments were carried out. Relationships between the measured spectra and textural features of the samples are studied from thin sections by using image processing techniques which make it possible to analyze rapidly large amount of samples. More than 500 samples were measured.

In the interpretation of spectral IP data it is crucial to have a mathematical model which depicts the behaviour of the spectra. Based on the laboratory spectral measurements, the mathematical models to describe the behaviour of the spectra were constructed. The problem of the phase-spectra asymmetry has been solved by using a generalised Cole-Cole spectrum or by fitting the sum of several Cole-Cole spectra.

The problem of electromagnetic coupling was addressed by developing a non-collinear electrode array which minimises the primary coupling of the layered host. By using such optimal array, the highest available frequency can be increased at least one decade over the maximum frequency given by standard collinear dipoles (up to several kHz). This considerably improves the capability of mineral discrimination of the method.

Field-tests were carried out at several exploration sites.

Task 2.2.2. *Development of interpretation software for ground EM methods.* An interactive interpretation program (*EMPLATES*) has been developed for the ground electromagnetic (EM) dipole-dipole measurement systems operated in frequency domain (Slingram, Sampo and Melis). The *EMPLATES* program combines an approximate forward computation, based on thin plate models in layered conductive space, with an automatic optimisation and a user-friendly interface under Windows 95. Forward computation usually takes only a few minutes, inversion takes less than one hour.

The final report (ANNEX WP2.2.2) describes the basic theory and equations that form the approximate computational method and the inversion procedure used in the software. The results from *EMPLATES* were compared to those from a 3D integral equation software used

by GSF (MARCO). When a MARCO forward model is inverted with EMLATES, the XY location and 3D attitude of the initial plate are well retrieved, but its depth and conductivity are always over-estimated (strongly for the conductivity).

Task 2.2.3. – 2.2.6. Geophysical methodology for lateritic Nickel ores. Gravity (with and without GPS), magnetics, induced polarisation (IP), transient EM, and high resolution seismics were all successfully tested in carbonated and ophiolitic environments. The most effective methods to detect the ore at a few tens of meters below the surface revealed to be gravity and IP, as well as high-resolution seismics for accurate determination of the geometry at depth.

Task 2.3. Development of 3-component borehole EM methods. The task 2.3 consisted in developing two new configurations of the 3-component downhole EM method of mineral exploration, the 'cross-borehole' (or tomographic) configuration, where a magnetic dipole transmitter (Tx) is in one hole and the 3-component magnetic receiver (Rx) is moved in another hole, and the 'single-borehole' configuration, where the dipolar source and the 3-D receiver are moved together in the same hole at a fixed separation. The latter configuration is sometimes called 'Borehole Slingram' for its analogy with the well-known dipole-dipole surface EM profiling method.

The technical report successively presents the methodology study performed at both BRGM and GSF, the development of a prototype equipment (the 'SlimBoris' system) by IRIS Instruments, the software development made at BRGM, and the field campaigns performed in Finland for testing the new equipment and methods (involving BRGM, IRIS, OMR and GSF).

An extensive set of 3-D numerical modelling for the new 'single-' and 'cross-borehole' EM methods was performed at BRGM and GSF. The objectives were: a) to understand the physics of the EM response of a conductive target, b) to optimize the instrument design and field configuration, and define practical limitations for the new methods, and c) to give interpretation guidelines for certain simple geometries.

Concerning the physics, the two types of EM responses of a conductive target (inductive and galvanic) that can appear according to the coupling with the transmitter were thoroughly analysed. Their respective signatures are now clearly identifiable on a 3-component EM log. They are first distinguishable by very different spatial geometries, the inductive response being equivalent to the field of a magnetic dipole whereas the galvanic response is equivalent to the field of an electric dipole. The two responses also have very distinct spectral behaviours, with very different resonance frequencies.

Regarding the instrument design and practical limitations, it appears that the magnetic moments provided by the downhole transmitter should enable an investigation radius of about 50 m in the 'single-hole' configuration and a separation of about 100 m between boreholes in the 'cross-hole' configuration. In the 'single-borehole' configuration, a Tx-Rx spacing of about 100 m will be best suited in order to obtain the expected investigation radius of about 50 m.

Elementary rules for localizing the target according to the signs of the anomalies on the transverse components were derived for simple targets in the 'single-borehole' configuration. However, it was also shown that this rules can be misleading. They should be only used to get a rough idea of the location of a target. Precise localization, e.g. for siting a new borehole, should be sought by inverse modelling (filaments, plates, or more complex models).

A second set of modelling in the borehole Slingram configuration was performed after the different field tests to check whether the high responses observed in this mode (several hundreds of percents of the free-space primary field¹) were geophysically relevant, or if some malfunctioning was to be suspected on the SlimBoris prototype.

This second modelling study showed that confined conductive targets close to a borehole can produce anomalies up to several hundreds of percents, when the spacing is equal to the extension of the target parallel to the borehole (i.e. its height in most cases). This result is opposed to what is generally believed for surface Slingram, where a theoretical limit of about 100% is assumed (or almost dogmatized) by several users —may be wrongly however. Certain concepts have thus to be revised and care must be exercised when extrapolating surface Slingram knowledge to borehole Slingram.

A versatile prototype equipment for 3-component downhole frequency EM measurements has been developed by IRIS Instruments. The 'SlimBoris' system covers the three configurations that can be envisioned in boreholes, i.e. the two configurations using downhole transmitter developed in this project, plus the classical surface-to-hole configuration where the transmitter is a large loop at the surface.

External diameter of the probes is 42.5 mm for use in slim exploration boreholes, most of which are drilled in 46 mm. The probe envelopes are pressure tested to 200 bars, corresponding to 2000 m in water. The frequency range is 35-8960 Hz, with nine frequencies in geometric progression of ratio 2. The transmitted magnetic moments are about 250 A.m² at low frequency, down to 50 A.m² at the highest frequency. The system uses standard 4-conductor logging cables. Due to power losses in the cable, the transmitter power supply is limited to only 1000 m of such a cable. However, the Tx probe could probably be operated down to 2000 m using a 7-conductor cable (not tested).

In the Slingram configuration, the two probes are separated by a fixed length of connecting cable. Three spacings are available: 25, 50 and 100 m, enabling pluri-decametric investigation around the borehole.

After fixing several problems found during the first field tests, especially on the single-hole configuration, the instrumentation and driving software (BORISLOG) are now operational.

Four PC software were developed for recording, processing and interpreting the data:

1) BORISLOG drives the SlimBoris equipment from a PC, enabling real-time graphic visualization of the log being recorded.

¹ Much greater indeed than in the surface Slingram, where a limit of about 100% is generally observed.

2) BOREM is a data handling software which proposes basic processing such as a) projection of the measured components onto a fixed coordinate system ('derotation'), b) borehole trajectory calculation (for both transmitter and receiver boreholes), and c) primary field reduction, either in free-space, in homogeneous space or by the low-frequency field. The projection system is either the current geographic system (e.g. North, East, Down) or the standard reference system used in gimbal-mounted probes.

3) REDSTRAT is a tool for simulating the primary field created in a layered half-space by an arbitrarily oriented magnetic dipole (or by a large horizontal loop of current).

4) OPTEM is an inversion software developed for rapid interpretation of 3-component borehole EM data, performing non-linear least-square fitting with Marquardt-Levenberg algorithm. It is based on very simple models such as EM dipoles or current filaments, the calculation of which takes only a fraction of a second on a standard (e.g. 486) PC. Thanks to the speed of the forward calculation, the whole inversion process is performed in only a few seconds.

The validity of such simple models have been studied on synthetic data generated by 'exact' 3-D modelling software. The results are very satisfying: the 3-D attitude of the target is always well retrieved and its 3-D location is as accurate as a few percents of the target-to-borehole distance.

Two field tests have been performed in Finland during spring and autumn 1998. Due to a malfunctioning in the single-hole configuration, unnoticed during preliminary testing in France, the data acquired in this configuration during the first field test (April 1998) are inconsistent and cannot be used. All other configurations (cross-hole and surface-to-hole) worked properly and the data have been successfully processed. In particular, at one site, a surface-to-hole recording enabled the localization of an off-hole conductor in excellent agreement with interpretation of time-domain data recorded in the same hole (Pietila and Bourgeois, 1999).

After IRIS fixed the problem concerning the single-hole configuration, a second test specific for this mode took place in late September 1998. The data recorded on the above site are very good: the responses have correct amplitudes, and are consistent with the known geology and with the interpretation of surface-to-hole logs (Bourgeois and Alayrac, 1999). However, on another site where the borehole water is very conductive (around 1 Ω .m) below 250 m depth, inconsistent responses were observed below this depth, in the conductive water.

This new problem has been investigated during the last three months of the project. It has been reproduced in plastic pipes filled with saline water and has finally been worked out. A last test of the borehole Slingram configuration is programmed in Finland in spring 1999, thus outside the administrative frame of the project. No doubt that it will be successful !

Task 2.4. *Compilation of a petrophysical data base.* The petrophysical database concerning the density, magnetic and electrical properties of the Ni bearing lithology has been established and documented. The database includes petrophysical parameters of both magmatic and lateritic deposits. Laboratory measurements and statistical analysis of the samples related to WP1 deposits have been performed as well.

Statistical analysis has been applied to get correlation between different rock types, petrophysical parameters and chemical assays. Factor analysis appeared to be a very useful tool to analyse the inner variance of nickel ore.

PROJECT STAFF

The main activists in WP2 were as follows:

Task 2.1

Elo, Seppo	Geological Survey of Finland
Soininen, Heikki	Geological Survey of Finland
Lehtimäki, Jukka	Geological Survey of Finland
Hattula, Aimo	Outokumpu Mining Oy
Sandgren, Eero	Outokumpu Mining Oy
Lehtonen, Tapio	Outokumpu Mining Oy
Bureau de Recherches	Géologiques et Minières
Bureau de Recherches	Géologiques et Minières
Angelopoulos, Anthony	Geological Survey of Greece

Task 2.2.1

Soininen, Heikki	Geological Survey of Finland
Vanhala, Heikki	Geological Survey of Finland
Lerssi, Jouni	Geological Survey of Finland
Sandgren, Eero	Outokumpu Mining Oy
Hattula, Aimo	Outokumpu Mining Oy
Lehtonen, Tapio	Outokumpu Mining Oy

Task 2.2.2

Hattula, Aimo	Outokumpu Mining Oy
Pietilä, Risto	Outokumpu Mining Oy
Lehtonen, Tapio	Outokumpu Mining Oy
Pirttijärvi, Markku	University of Oulu
Hjelt, Sven-Erik	University of Oulu
Bourgeois, Bernard	Bureau de Recherches Géologiques et Minières
Soininen, Heikki	Geological Survey of Finland

Task 2.2.3-2.2.6

Antonis Angelopoulos, WP2 Lateritic Leader, IGME
Athanasios Apostolikas, Ec.Geologist, LARCO
Michalis Nicolaidis, Geophysicist, IGME
Pavlos Alexandridis Geophysicist Larco / IGME

Sotiris Nikolaou, Eng. Geophysicist, Vermion Area, IGME
Evangelos Markogiannakis, Geophysicist Vermion Area, IGME
Anastasios Tsoygiannis, Electr. Tech.Eng., IGME
George Lontos, Electr. Tech.Eng., IGME
Vasilios Klentos, Electr. Tech.Eng., IGME
Theodoros Theodoridis, Electr. Tech.Eng, Vermion Area, IGME
Spiros Ioannidis, Electr. Tech.Eng, Vermion Area, IGME
Sotiris Babalukas, Electr. Tech.Eng., IGME
Vasilios Noytsis, Programmer, IGME
Panagiotis Tsailas, Technician, IGME
Ioannis Pavliotis, Surveyor, LARCO
Ioannis Nikas, Surveyor, LARCO
Antonis Sigalas, Geologist, LARCO
Dimitrios Triantafillou, Geology Student, LARCO/IGME

Task 2.3

Bourgeois, Bernard	Bureau de Recherches Géologiques et Minières
Lebert, François	Bureau de Recherches Géologiques et Minières
Valla, Pierre	IRIS Instruments
Bernard, Jean	IRIS Instruments
Alayrac, Christophe	IRIS Instruments
Abdelhadi, Abderraman	IRIS Instruments
Soininen, Heikki	Geological Survey of Finland
Mononen, Risto	Geological Survey of Finland
Poikonen, Ari	Geological Survey of Finland
Oksama, Matti	Geological Survey of Finland
Hongisto, Hannu	Geological Survey of Finland
Pietilä, Risto	Outokumpu Mining Oy
Hattula, Aimo	Outokumpu Mining Oy
Sandgren, Eero	Outokumpu Mining Oy

Task 2.4

Pietilä, Risto	Outokumpu Mining Oy
Hattula, Aimo	Outokumpu Mining Oy
Sandgren, Eero	Outokumpu Mining Oy
Jääskeläinen, Petri	Helsinki University of Technology, Outokumpu Mining
Peltoniemi, Markku	Helsinki University of Technology
Angelopoulos, Anthony	Geological Survey of Greece

OBJECTIVES

Task 2.1.

One of the aims of the GeoNickel project is to use GPS to obtain, in both horizontal and vertical positioning, an accuracy of a few cm, compatible with semi-detailed and even detailed gravity surveys that are needed in partner's countries. The novelty in the GeoNickel project versus previous state of the art consists of studying the field and processing procedures giving such an accuracy and the way of solving problems in conditions specific to European countries.

Task 2.2.1.

The objective in spectral IP development was to study the applicability of spectral IP method to Ni exploration and to develop proper data acquisition techniques. Although the spectral IP method has been extensively studied for base-metal exploration, the case of Ni-ores had not been thoroughly investigated. Moreover, there were still questions in the precise field measurement procedures needed to acquire reliable spectral data in an extended frequency range. That is why the applicability of spectral IP to Ni exploration was to be studied and proper data acquisition techniques to be developed in GeoNickel.

Task 2.2.2.

The objectives of Task 2.2.2 were to improve 3D modelling software, to develop inversion algorithms for frequency domain ground EM methods, and to create interfaces for SLINGRAM, SAMPO (Gefinex 400S) and MELIS systems.

Task 2.2.3-2.2.6 Lateritic

The main objectives of these sub-tasks are to acquire and compile all existing geophysical information, along with the results obtained from the methodologies applied in the lateritic environment for the first time, in order to model the detected and imaged ores, determine their shape and size and introduce this information as interpreted results to the GEOSIS database, ready for processing by the Knowledge Based System. Gravity, magnetic and IP surveys were expected to produce appreciable anomalies in the carbonaceous hosting environment (Lokris). IP/Resistivity and time domain EM methods were expected to identify the FeNi laterites hosted by ophiolites (Vermion). IP may discriminate on areas of higher concentration of ore and map their extension.

Task 2.3.

The main objective for Task 2.3 were to develop and test a prototype for 3-component frequency EM measurements in boreholes, using a downhole transmitter either in the same

borehole (fixed spacing dipole-dipole profiling) or in another borehole (EM tomography). Linked objectives were the necessary methodology study and software development for the new methods.

Task 2.4.

The objectives of Task 2.4 were to compile density, magnetic and electrical parameters of nickel ore formation and host rocks for use in quantitative geophysical interpretation and to develop interfaces between mineralogy and petrophysics.

The final objective was not only to run basic descriptive statistics and plot correlation charts but also to implement the factor analysis to the data sets in order to find correlations between petrophysics and the occurrence of nickel and other associated chemical elements.

MEANS USED TO ACHIEVE THE OBJECTIVES

Task 2.2.2

Electromagnetic (EM) methods are widely used in geophysical prospecting. Although several computational methods have been developed during the last few decades, geophysicists are still looking for practical interpretation tools. This study concentrated yet another method created for approximate interpretation of EM frequency domain profile data. The method uses a lattice structure to model the EM response of thin plate-like conductors embedded in conductive earth. The new computational method, parametric inversion and graphical user interface were combined in the *Emplates* program.

Task 2.2.3-2.2.6 Lateritic

The implementation for the objectives of the task two areas were chosen for investigation with different degree of background information. The first area is the Ag.Ioannnis mine in Lokris and the second is the West Vermion Mountain in Western Macedonia where geologic mapping revealed target FeNi orebodies (Plate 2.2.3-1).

During the course of the project great effort was dedicated to the LOKRIS area for operational (high degree of available information) and logistic purposes. Most of the equipment belonging to IGME was used, like Lacoste & Romberg gravity meter G856 Geometrics magnetometers, Geometrics Strata View seismograph and in house created made Buffalo Gun, Sirotem II TEM system was used. For the IP method a multi channel receiver (SCINTREX IPR12) and the IRIS SYSCAL R2 system were purchased in the name of the project. Software for inverting the IP/Resistivity method (from New Jersey Geological Survey

modified in house to fit our requirements) and for processing High Resolution seismic data (Winseis package from Kansas Geological Survey) were also purchased.

Computer interface for the throughput of the IP data and its presentation was developed in house . In addition prototype software (Based on power spectrum & auto correlation function for statistical evaluation of potential field data was developed to compile intermediate tables necessary for the knowledge base system).Topographic corrections were also made by in house prototype software .For the presentation and enhancement of the data, Golden ,TNT MIPS Image Processing ,GEOSOFT OASSIS & MapInfo software were used.

Positioning for field measurements was provided from Larko's personnel by means of an electronic Theodolite (providing ± 5 cm accuracy in z). For detailed magnetic coverage a Magellan single frequency differential GPS system was used(providing sub meter accuracy in x & y co-ordinates).It was purchased from Larko. More than 4500 magnetic and 2500 gravity measurements were acquired in both areas . IP/Resistivity lines were measured for more than 15 Km and ~ 25 VES IP/resistivity while about 8 line Km were covered for TEM

Initial test lines and petrophysical parameters were also measured . The USGS Saki software was used for modelling gravity and magnetic data while IP/resistivity profiles are inverted using software developed by Dr P. Tsourlos (Kindly provided by the author).

Task 2.3

1D and 3D numerical modelling. Software and Hardware development. Field testing.

Task 2.4

The first part of the work was to measure magnetic susceptibility, magnetic remanence and density of rock samples from nickel deposits in Finland and Norway and to create a digital database. Also a number of laterite samples from Greece were included to the study as well as an update of the previous database compiled by Niemi (1989). The second step was to study the electrical conductivity and contrast of nickel ore in relation to host and country rocks.

Petrophysical measurements were followed by XRF assaying which was made by the Geoanalytical Laboratory of Outokumpu Research.

SCIENTIFIC AND TECHNICAL DESCRIPTION OF THE PROJECT

2.1. Task 2.1: Regional Surveys - Test and design of an integrated GPS-gravity system (Seppo Elo, 10.2.1999)

2.1.0. Introduction

Three years ago at the outset of the GeoNickel project, the use of regional geophysics in prospecting for Ni-bearing mafic and ultramafic intrusions was considered well-established in Finland. Airborne magnetic and electromagnetic methods were quite adequate due to improved system designs using new positioning techniques. However, the gravity method needed improvement, mainly due to difficulties in measuring the elevations above sea level, which are necessary in order to reduce measured gravity values into geologically meaningful gravity anomalies. This was particularly true for regional gravity surveys where sparse data coverage (2 to 6 points per sq.km) makes optical or hydrostatic levelling too slow and expensive. Although barometric altimeters have been extensively used, they do not guarantee good quality even with necessary frequent ties (repetitions). In Finland, the problem also existed for semi-detailed gravity surveys (10 to 20 points per sq.km) due to the impracticality of optical levelling among forests and small-scale topographic relief.

The introduction of GPS surveying to civilian use beginning at 1980's started a rapid development of techniques, which still goes on. GPS (Global Positioning System) implemented by the U.S. Department of Defence uses satellites with known trajectories to continually transmit codes on two separate frequencies, which enable a GPS receiver on Earth's surface with an open view to the sky to locate itself. The accuracy of standard positioning service (SPS) in civilian use is restricted to about 30 meters (rms) horizontally and about 50 metres (rms) vertically, which is very far from the required vertical accuracy in gravity surveys. Carrier-phase differential measurements (that is two receivers, one of which on a known fixed location, measuring carrier-phase in addition to receiving codes from the same satellites at the same time) were developed to overcome this restriction, and it became possible to determine the position of a roving receiver in relation to a fixed one very accurately. At first, the required occupation time per one measurement was quite long, but differential methods were continuously improved to reduce the occupation time to even under one minute. Extensive amount of literature, e.g. Hofmann-Wellenhof et al. (1997), Langley (1995,1996,1998), Poutanen (1998), and Internet web-sites, e.g. <http://www.utexas.edu/depts/grg/gcraft/notes/gps/gps.html>, describe GPS technology for professionals, teachers, students and common users.

Already three to five years ago, it appeared possible that GPS would enable an accuracy of some centimetres in three-dimensional positioning rapidly enough by means of either post-processed or real-time-kinematic (RTK) carrier-phase differential measurements. However, at that time, the performance of such procedures in various applications and geographical

conditions was not well known. Consequently, the objectives of the work package 2.1 were set as (1) extensive testing of GPS for elevation measurements in gravity surveys in order to determine the reliability and productivity of GPS in varying seasonal and geographical conditions, and (2) to design and assemble a working gps-gravity system that provides real-time Bouguer anomalies with an accuracy of better than 0.1 mGal (better than 0.5 m in elevation) for several types of gravity surveys. For a background, Table 2.1.-1 shows rms errors achievable by various methods to measure elevation above sea level.

Table 2.1.-1. Achievable errors in measuring elevation above sea level.

Method	Error/rms/m	Comments
barometric altimeters	<1.0	requires closures (e.g. every 2 hours)
inertial surveying	<0.5	requires stopping (e.g. every 5 minutes)
photogrammetric	<0.5	requires post-processing
tachymeters	<0.1	requires line of sight
chain levelling	<0.05	requires closures but not line of sight
optical levelling	<0.01	still the most accurate method
GPS (SPS)	<50.0	standard positioning service
GPS (CPD)	<0.05	carrier-phase differential
laser ranger+inclinometer	<0.10	over short distances (e.g. < 100m)

2.1.1. Testing an integrated GPS-gravity system

2.1.1.1. Selection and purchase of initial equipment

The first task was to select the initial equipment to be used. Inquiries were sent to various manufacturers, actual users of GPS equipment were interviewed, technical exhibitions were attended, and literature was consulted. UNAVCO (University Navstar Consortium) GPS Receiver/Antenna Test Report (November 1995), whose summary sheet considered 140 different points, was taken into account. Three manufacturers (Ashtech, Trimble, and Sercel) entered the final stage. Table 2.1.-2 contains some basic information on these three GPS receivers at the beginning of 1996. The Ashtech equipment was selected. In technical terms Trimble and Ashtech were about equal and better than Sercel, but the pricing of Ashtech was more competitive, and auxiliary equipment, software (including source code of RTK control software) and support provided by the Ashtech representative in Finland were more versatile and adaptable.

The selected gravimeter was Scintrex Autograv CG-3M, which was the only fully automated digital gravimeter available for field use. Its main competitors were LaCosteRomberg and Worden gravimeters. The advantages of CG-3M include automatic measurements, automatic tilt, temperature, drift and tide corrections, nearly linear drift, and digital recording. The main disadvantages of CG-3M are its size and weight which make it a little cumbersome to handle. Table 2.1.-3 gives some background information on gravimeters.

Evaluation, selection and purchase of initial equipment was completed by 30.5.1996.

Table 2.1.-2. Basic information on three GPS receivers (1996)

	Ashtech	Trimble	Sercel
Base station	Z-12	Site Surveyor Ssi	NDS 100 MKII
Size (cm)	W22 L21 H10	W25 L28 H10	W40 L45 H20
Weight (kg)	3.1	3.6	13.7
Operating temp.	-20 to +55 °C	-20 to +55 °C	-20 to +55 °C
Rover	”	”	NR 202-K
Size (cm)	”	”	W13 L27 H28
Weight (kg)	”	”	3.5
Operating temp.	”	”	-20 to +55 °C
Power consumption	10.5 W	12 W	10 W
Radio link	Satellite-2ASx	Satellite-2ASx	NDR104
frequency	420-470 Mhz	420-470 Mhz	405-470 Mhz
range	1 ... 10 km	1 ... 10 km	1 ... 15 km
RTK operating mode	Yes	Yes	Yes
Initialization			
OTF	Yes	Yes	Yes
Warm start	< 1 min	< 1 min	3 to 10 min
Cold start	< 2 min	< 2 min	3 to 15 min
Tracking			
Channels	12	9	10
Phase	L1+L2	L1+L2	L1
Code	L1/L2-Y,L1/L2-P	L1-C/A, L1/L2-P	L1-C/A
Accuracy			
Fine X,Y	±1cm + 2 ppm	±1cm + 2 ppm	< 2 cm
Fine Z	±2cm + 2 ppm	±2cm + 2 ppm	< 3 cm
Control Unit	Husky FS/2	Husky FS/2	Trimble S.C.
Source Code	Yes	No	No
Radio link	Satellite-2ASx	Satellite-2ASx	NDR104
Frequency	420-470 Mhz	420-470 Mhz	405-470 Mhz
Range	1 ... 10 km	1 ... 10 km	1 ... 15 km

Table 2.1.-3. Basic information on three gravity meters (1996)

	Scintrex CG-3M	LaCoste-Romberg G Model	Worden Standard Master
Sensor	fused quartz		fused quartz
Size (cm)	W24 L31 H32	W18 L20 H25	D18 H36
Weight including battery with a carrying case	11.4 kg 15.0 kg	5.5 kg 10.0 kg	4.4 kg 8.2 kg
Operating range	8000 mGal	7000 mGal	4000 mGal
Range without resetting	8000 mGal	~200 mGal	~210 mGal
Reading resolution	0.001 mGal	0.005 mGal	~0.01 mGal
Temperature Control	Yes	Yes	Yes
Automated operation	Yes	No	No
Automated corrections	Yes	No	No
Digital recording	Yes	No	No

2.1.1.2. Field tests

The following objectives were set for GPS test measurements: (1) to gain sufficient knowledge of the different types of GPS surveying, (2) to test the conditions in which GPS yields the expected vertical accuracy, (3) to find out advantages and disadvantages of gps-gravity surveys, (4) to modify field procedures to suit our requirements, (5) to provide typical examples of GPS-gravity surveys, (6) to set guide-lines for the use of GPS in gravity measurements, and (7) to establish sites for future testing of various GPS equipment and procedures.

The typical procedure in the test measurements was as follows. At first, high-quality benchmarks were located. If these were not suitable for gps-gravity measurements, a network of new base stations was determined starting from available benchmarks using post-processed static methods with observation times of approximately 30 minutes per one vector. GPS-antennas were fastened by means of tribrachs on tripods and located with an accuracy of about 1 mm above the benchmarks. The results were processed in WGS84-coordinate system and transformed afterwards into the national or local coordinates. The gps-gravity measurements were then conducted in real-time or for post-processing. The base station GPS-antenna was mounted as in the network measurements with an accuracy of about 1 mm. The roving antenna was either on a 2 to 3 metre fiberglass mast for a walking person and for a snowmobile, or on a 0.5 metre short mast on the top of a cross-country vehicle for a car application. As to the radio communication link, at the base station a directional antenna was mounted on a 4.5 metre fiber-glass telescope mast. For a walking person and a snowmobile a similar mast was used together with the gps-antenna. A ground-plane whip on the top of a car was used when driving. At first, many mistakes were made, but gradually the field practice developed towards a satisfactory one. Most of the problems were not related to the GPS itself, but to the cables, connectors, batteries, radio link, quality control, transforming the

coordinates into national or local coordinates, and modelling local geoid undulations. Occasionally, there were problems with visibility and geometry of satellites, but these problems could (and can) be eliminated with a good planning and flexible working hours. In the following, mainly the vertical accuracy is considered because GPS-measurements are more accurate horizontally than vertically and because in gravity measurements the height above sea level is the critical parameter, not the horizontal coordinates.

As listed in the table 2.1.-4, altogether 18 separate field campaigns were conducted in Finland, Greece, Norway and France by GTK (GSF), OUTOKUMPU, BRGM, IGME, and LARCO.

Table 2.1.-4. List of field tests 1.6.1996-31.6.1998

Field campaign	Date	Organisations
1. Kauhajoki, Finland	Jun 1996	GTK
2. Moisiovaara, Finland	Jun 1996	GTK, Outokumpu
3. Hyvinkää, Finland	Jul 1996	GTK
4. Vammala, Finland	Jul-Sep 1996	GTK, Outokumpu
5. Moisiovaara, Finland	Sep 1996	GTK
6. Hyvinkää, Finland	Sep 1996	GTK
7. Hyvinkää, Finland	Oct 1996	GTK
8. Ballangen, Norway	Mar 1997	GTK, Outokumpu
9. Hyvinkää, Finland	Mar 1997	GTK
10. Savitaipale, Finland	Mar 1997	GTK
11. Orléans, France	Apr 1997	BRGM
12. Argentat, France	June 1997	BRGM
13. Hyvinkää, Finland	Sep 1997	GTK
14. Hyvinkää, Finland	Nov 1997	GTK
15. Ag. Ioannis Mine, Greece	Mar 1998	GTK, IGME, LARCO
16. Vermion, Greece	Mar 1998	GTK, IGME
17. Hyvinkää, Finland	June 1998	GTK, Haines Surveys
18. Kemi Open Pit Mine, Finland	June 1998	GTK, Outokumpu

In the following, the tests are very briefly described with some relevant data tables and figures to give an idea of the work carried out during the testing phase.

2.1.1.2.1. Kauhajoki test, Finland, June 1996, GTK

The first realistic experience in using RTK GPS was in the Kauhajoki area (map sheet 1234) in June 1996. There was a lot to learn, and the measurements succeeded only partially. The aim was to measure a 4 km profile in a forest with exactly a 100 meter station interval. Only 33 % of the measurements succeeded with a rms error better than 5 cm, 45 % with a rms error better than 1 m, and 22 % of the measurements did not succeed in a reasonable time. As a side benefit, the coordinates of one drill-hole were accurately re-established.

2.1.1.2.2. Moisiovaara test A, Finland, June 1996, GTK and Outokumpu

New base points were measured using a post-processed static procedure with a network adjustment. Estimated rms height errors in this survey were of the order of 4 cm. A bad

trigonometric height value of a benchmark used as a starting point was located. Using new base locations, altogether one hundred twenty-one new gravity stations with a 200 - 250 m station spacing were measured using RTK GPS among forests and fields. A couple of unacceptably large errors, which were not indicated by error estimates in RTK GPS software, caught us unprepared and pointed out, as was fully understood only afterwards, that more careful planning and quality control was needed also in sparse forests. Fig. 2.1-1 shows a typical walking arrangement.



Figure 2.1-1. Real-time GPS-gravity measurements in Moisiovaara, the roving GPS receiver and the gravimeter.

2.1.1.2.3. Vammala test, Finland, July-September 1996, GTK and Outokumpu

Four hundred and twenty-eight new gravity stations with approximately 200 m station spacing were measured using RTK GPS in a typical Finnish southwestern rural landscape. Nineteen points were rejected due to unacceptably large errors which were not indicated by the error estimates in RTK GPS software. Problems were encountered in locations obstructed by foliage and at the limits of the radio link. The radio modem with a 0.5 W output carried comfortably approximately 2 km. There were no problems to establish a good network of gravity stations with the given station spacing.

2.1.1.2.4. Hyvinkää test A, Finland, July 1996

A 15 km long profile of 79 stations was measured along small roads by car, partly in real-time, partly for post-processing, across a gabbro body, which is considered to be a host of ore mineralizations. An example of a post-processed survey results is given in Table 2-1.4. In this example, on the average the occupation time was 5.8 minutes, the number of tracked common satellites 7, the baseline length 4.8 km, the dilution of precision 2.9, and the standard error* of the vectors estimated by the PNAV software 0.019 m (*excluding the station where the ambiguity was not fixed). At the time, the memory of the roving gps-receiver allowed only 20 second interval when recording satellite data for the entire working day. Stations along roads

were often obstructed by trees, the roving receiver every now and then lost some satellites, and it was rather difficult to estimate how many common satellites with the base station the rover was connected to, especially because the base station had a few obstructions itself, see Fig. 2.1-2. As usual in the post-processing mode, one did not exactly know, how long one should stay on each station so that in post-processing ambiguities could be reliably fixed. To work efficiently, a crew obviously must be well trained and experienced.

Table 2.1-4. A summary of an post-processed GPS-gravity survey

Ashtech, Inc., Program: PNAV, Version: 2.4.00M								
Processing direction: Backward								
Processing mode: SURVEY								
Data sample period (sec): 20.00								
Data being processed: PL1-code/PL2-code/PL2-phase/CAL1-phase/								
Ambiguity search algorithm: Min QF search								
Ambiguity	BASE	ROVR	LENGTH (m)	Std (m)	Time (min)	SVs	DOP	Comment
FIXED	9555	0070	7383.658	0.017	4.7	6	2.6	
FIXED	9555	0069	7220.789	0.018	4.3	6	2.7	
FIXED	9555	0068	6994.273	0.023	4.0	6	2.9	
FIXED	9555	0067	6755.430	0.021	4.3	7	4.0	
FIXED	9555	0066	6412.966	0.021	4.7	6	3.6	
FIXED	9555	0065	6126.490	0.021	5.3	7	3.5	
FIXED	9555	0064	5834.067	0.020	5.3	7	3.8	
FIXED	9555	0063	5573.666	0.014	4.0	9	1.8	
FIXED	9555	0062	5246.624	0.012	4.3	8	2.1	
FIXED	9555	0061	5026.008	0.015	4.7	8	2.2	
FIXED	9555	0060	4750.545	0.016	7.7	8	2.2	
FIXED	9555	0059	4562.463	0.015	9.0	9	2.0	
FIXED	9555	0058	4345.880	0.015	6.3	10	1.9	
FIXED	9555	0057	4170.160	0.031	5.0	8	2.5	
FLOAT*	9555	0056	4071.050	0.992*	5.3	7	2.4	
FIXED	9555	0055	3497.370	0.022	11.7	5	5.6	
FIXED	9555	0054	3363.699	0.028	5.7	5	5.0	
FIXED	9555	0053	3179.179	0.013	5.7	7	2.3	
FIXED	9555	0052	2660.101	0.035	9.7	6	3.4	cycle slips
FIXED	9555	0051	2929.528	0.025	4.7	6	3.2	
FIXED	9555	0050	2900.560	0.015	4.7	7	2.3	
FIXED	9555	0049	2714.667	0.012	5.3	7	2.4	
FIXED	9555	0048	2466.776	0.013	6.7	6	3.0	
Mean			4816.035	0.019*	5.8	7	2.9	



Figure 2.1-2. A GPS base station with minor obstructions.

Fourteen permanent benchmarks maintained by the National Land Survey, with eleven levelled and three high-accuracy GPS heights, and baselines up to 14 km, were measured to be repeatedly used to test post-processing systems. Because the approximately 10 km wide Hyvinkää gabbro causes a gravity high of about 30 mGal and a corresponding local geoid undulation, the area is also very suitable for testing how accurate various geoid models actually are. The GPS gives coordinates in earth-centered coordinate system. Heights above the reference ellipsoid can be calculated, but to transform GPS heights to elevations above sea level the geoidal undulations must be modelled and subtracted. Most of the locations had obstructions and were not by no means ideal for GPS measurements. It was predicted that some of these locations would be much easier to measure in winter time.

In addition, ten permanent benchmarks of the National Board of Public Roads with baselines up to 2.2 km were measured to be repeatedly used to test various GPS equipment and software. Four of the benchmarks are in heavily obstructed locations. There are forests and small but steep hills, which impair real-time radio communication.

2.1.1.2.5. Moisiovaara test B, Finland, September 1996, GTK

One hundred twenty-six stations were measured partly in a full-grown sparse forest with station spacing varying from 10 to 40 m to provide four half a kilometre profiles across a Ni-ore body. A 1.27 km profile with an average station interval of 35 m was measured for post-processing. A 1.06 km profile with an average station spacing of 25 m was measured in real time. A number of drill-hole locations were determined and the results were compared to the coordinates obtained with a tachymeter.

2.1.1.2.6. Hyvinkää test B, Finland, September 1996, GTK

An 1.8 km profile was measured in real-time with a station interval of approximately 20 m in with forests and fields alternating. There were problems with one poor base station location. At two stations cm-accuracy was not achieved in less than 10 minutes because they were occupied at unsuitable times. Again it was quite evident, that measurements during a poor satellite availability should only take place in open terrain, if at all, and not in forests. It was concluded, that with a proper planning and experience two persons can measure at least a 1 to 2 km profile with approximately 20 meter station spacing (50 to 100 stations) during one shift in partly forested terrain of this type.

2.1.1.2.7. Hyvinkää test B, Finland, October 1996, GTK

The performance of Trimble 4400 Total Station of the Geostar company and of Ashtech RTZ-12 of the GeoNickel project was compared to each other both in real-time and with post-processing along the previously measured test line. At the same time a new digital hydrostatic levelling device LEVA20 was tested with a thought that the most efficient method doing accurate gravity surveys in densely forested areas would be to combine GPS measurements and chain-levelling. In this test, two different base stations were alternatingly used. The following results were obtained as shown in Table 2.1-5 on the next page. The various gps measurements were internally consistent with a standard error of about ± 0.019 m. On the average, the GPS measurements reproduced the elevations of the National Board of Public Roads with a systematic error of $+0.027$ m and a standard error of ± 0.016 m. The internal estimates include the uncertainty in the base station coordinates, the uncertainty in the gps-antenna heights of the base and roving stations, and the errors of the gps measurement itself. The external estimate also includes the errors of the reference values.

2.1.1.2.8. Ballangen test, Norway, March 1997, GSF and Outokumpu

Two hundred stations were measured with a station spacing of approximately 100 m in post-processing mode in the Norwegian mountains shown in Fig. 2.1-3, where Outokumpu Oy operates a Ni-ore mine. The operation was facilitated by seven layers of clothing with a raincoat on top. Severe storms occurred after which half a metre of light new snow and steep slopes proved to be a real test of the skills of the snowmobile driver. Together the old and new snow cover with ice layers in-between was unfathomable with a 3 metre metal measuring rod. There were no problems with satellite visibility, at this time of the year not even among mountain birches.

Table 2.1-5. GPS test Hyvinkää 30OCT96, Ashtech RTZ-12 and Trimble 4400 total station comparison.

Id.	(1) NBPR	(6)-(1)	(2) Ashtech RT	(2)-(6)	(3) Trimble RT	(3)-(6)	(4) Ashtech PP	(4)-(6)	(5) Trimble PP	(5)-(6)	(6) Mean of 2345
953	114.260	+0.028	114.279	-0.009	114.280	-0.008	114.298	+0.010	114.295	+0.007	114.288
9515	104.013	+0.033	104.046	+0.000	no data	no data	104.056	+0.010	104.035	-0.011	104.046
9516	103.747	+0.023	103.764	-0.006	no data	no data	103.781	+0.011	103.766	-0.004	103.770
9517	102.673	-0.005	102.685	+0.017	102.657	-0.011	102.649	-0.019	102.681	+0.013	102.668
9518	102.511	+0.035	102.543	-0.003	102.561	+0.015	102.507	-0.039	102.571	+0.025	102.546
9519	103.322	+0.025	103.345	-0.002	103.333	-0.014	103.342	-0.005	103.368	+0.021	103.347
9520	113.614	+0.017	113.627	-0.004	113.632	+0.001	113.617	-0.014	113.647	+0.016	113.631
9521	114.014	+0.059	114.095	+0.022	114.055	-0.018	114.073	+0.000	114.067	-0.006	114.073
9522	116.622	+0.033	116.603	-0.052	116.650	-0.005	116.645	-0.010	116.722	+0.067	116.655
9523	127.393	+0.023	127.417	+0.001	127.419	+0.003	127.399	-0.017	127.429	+0.013	127.416
mean		+0.027		-0.004		-0.005		-0.007		+0.014	
std		±0.016		±0.020		±0.011		±0.016		±0.022	
total		0.031		0.020		0.012		0.017		0.026	

Elevations in metres, RT= Real Time, PP = Post-processed,

NBPR = National Board of Public Roads Benchmark Class 5, with the exception of class 4 Benchmark Id. 953.

Ashtech rover gps antenna mast was held in hands, Trimble rover gps antenna mast was supported by two extra legs.

The gravity measurements were difficult because of the stormy weather. Two different Norwegian coordinate systems (NGO and UTM) and the local system of the mine caused some confusion, and a lack of accurate advance information prevented real-time measurements. During the one week of the measurements, a scheme to deal with situations, where accurate coordinate transformation formulas are not available, was developed. This scheme was tested later on in Greece. The gps-gravity system worked very well in these difficult conditions. Even with an allowance for post-processing, an experienced crew of two should measure at least 50 to 100 stations per one shift with station spacings of the order of 100 metres.



Figure 2.1-3. Gps-gravity measurements in Ballangen, Norway, the roving gps receiver and the gravimeter.

2.1.1.2.9. Hyvinkää test D, Finland, March 1997, GTK

GPS was used to provide ties approximately every kilometre along a 15 km gravity profile for hydrostatic levelling. GPS was deemed to substantially improve the efficiency and quality of chain-levelling.

Thirty-nine stations with an average station spacing of 100 metres were measured in real-time to test the efficiency of car transport along a narrow dirt road in a forest, again it became evident that one must be in the right place at the right time, comfortable range of the radio link varied from from 2.5 to 3.0 km in a difficult hilly terrain, at the limits of the range reliability depended much on the tuning and the directional gain of the antennas.

Measurements at fifteen levelled benchmarks were repeated in winter for post-processing. Some of the difficult sites in summer/autumn proved to be easy in winter (an improvement of 22 percentage units). Three geoid models have been tested with this data as shown in Tables 2.1-6 and 2-1-7. The most accurate available geoids available in Finland (NKG and FIN95)

Table 2.1-6. GPS test 19MAR1997 Hyvinkää, Post-processed Survey. Base station at the benchmark 959547.

	(1)		(2)		(3)	NKG	(4)		FIN95	(5)	FIN95	
Id.	NLS	Type	HAE1 fixed	(2)-(1)	HASL1 fixed	(3)-(1)	HASL1 float	(4)-(1)	N	HASL2 fixed	(5)-(1)	Baseline (km)
9554	104.972	gps	123.480	18.508	104.980	+0.008	105.081	+0.109	18.936	105.005	+0.033	5.150
0001	82.632	lev	101.093	18.461	82.607	-0.025	81.443	-1.189	18.939	82.615	-0.017	5.163
3725	96.280	lev	114.644	18.364	96.255	-0.025	96.625	+0.345	18.847	96.258	-0.022	2.594
3726	84.745	lev	103.144	18.399	84.788	+0.043	84.249	-0.496	18.813	84.792	+0.047	1.370
0002	81.354	lev	99.789	18.395	81.408	+0.014	82.088	+0.694	18.837	81.413	+0.059	2.044
5387	84.179	lev	102.615	18.436	84.161	-0.018	84.698	+0.519	18.910	84.166	-0.013	4.907
5386	91.540	lev	109.991	18.451	91.510	-0.030	91.150	-0.390	18.931	91.521	-0.019	6.613
5385	93.539	lev	no value	no value	no value	no value	94.888	+1.358	18.971	no value	no value	7.903
5384	113.155	lev	131.663	18.508	113.093	-0.062	112.247	-0.728	19.025	113.098	-0.057	9.789
5383	108.168	lev	126.874	18.706	108.278	+0.110	107.830	-0.338	19.053	108.282	+0.114	11.149
5382	131.265	lev	149.862	18.597	131.274	+0.009	131.575	+0.310	19.046	131.277	+0.012	11.929
5381	100.651	lev	no value	no value	no value	no value	101.267	+0.616	19.052	no value	no value	12.914
0953	114.260	lev	132.781	18.521	114.284	0.024	113.954	-0.306	18.926	114.316	+0.056	5.643
9555	123.460	gps	142.006	18.546	123.511	0.050	123.271	-0.189	18.927	123.540	+0.080	5.980
5185	99.209	lev	117.699	18.490	99.241	0.032	98.584	-0.625	18.870	99.290	+0.081	8.779
mean				18.491		+0.010		-0.020			+0.027	+6.795
std			±0.092		±0.044		±0.664			±0.051	±3.561	

NLS=National Land Survey height, lev=optically levelled reference height, heights are given in metres.
FIN95=Finnish Precision geoid. NKG=Nordic geoid.

Table 2.1-7. Solution of a local geoid model for the test Hyvinkää 19mar1997.

Linear equation matrix							Model Model				
Id.	a	b	c	d	e	f N(obs)	geoid	residual			
0001	.129735E+09	.231899E+08	.548501E+08	.113901E+05	.481559E+04	1.	18.461	18.458	-0.003		
0002	.152456E+09	.608952E+08	.963525E+08	.123473E+05	.780354E+04	1.	18.395	18.390	-0.005		
0953	.265853E+09	.310472E+08	.908514E+08	.163050E+05	.557200E+04	1.	18.521	18.520	-0.001		
3725	.134367E+09	.555119E+08	.863654E+08	.115917E+05	.745063E+04	1.	18.364	18.364	+0.031		
3726	.160639E+09	.715331E+08	.107196E+09	.126744E+05	.845772E+04	1.	18.399	18.392	-0.007		
5185	.443126E+09	.539040E+08	.154552E+09	.210505E+05	.734194E+04	1.	18.490	18.499	+0.009		
5382	.287761E+08	.134412E+06	.196668E+07	.536434E+04	.366622E+03	1.	18.597	18.589	-0.008		
5383	.470911E+08	.818029E+05	.196270E+07	.686230E+04	.286012E+03	1.	18.706	18.660	-0.046		
5384	.590366E+08	.190437E+07	.106032E+08	.768353E+04	.137999E+04	1.	18.508	18.591	+0.083		
5386	.759759E+08	.202262E+08	.392008E+08	.871642E+04	.449735E+04	1.	18.451	18.432	-0.019		
5387	.105066E+09	.306564E+08	.567534E+08	.102502E+05	.553682E+04	1.	18.436	18.417	-0.019		
9554	.220191E+09	.267748E+08	.767826E+08	.148388E+05	.517443E+04	1.	18.508	18.512	+0.004		
9555	.288457E+09	.328182E+08	.972967E+08	.169840E+05	.572871E+04	1.	18.546	18.526	-0.020		
Elevations in metres							mean +0.000				
							std ±0.031				

Model is a two-degree polynomial $N = ax^2 + by^2 + cxy + dx + ey + f$

Least-squares coefficients:

a= 1.848433E-009
b= 1.058398E-008
c= -9.877103E-009
d= 2.317382E-005
e= -4.030551E-005
f= 18.444188E+000

Residuals include reference point, geoid modelling,
and GPS errors. Estimated error of the local geoid
model is approximately 0.024 m.

delivered by the Finnish Geodetic Institute reduced the vertical standard error (as compared to levelled heights) from 0.092 m (with no geoidal correction) to respectively 0.044 m and 0.051 m. A two-degree polynomial model (Table 2.1-7) of geoidal undulations solved from the data reduces the vertical error to 0.031 m, which still includes reference point and GPS measurement errors. Because of the gravity anomaly due to the gabbro body and associated volcanic rocks, the local geoid warping in the test area is greater than normal. The results suggest that with two-degree polynomial models, easily adaptable to real-time work, local geoid undulations can be modelled with an accuracy of 0.010 ... 0.025 m.

2.1.1.2.10. Savitaipale test, Finland, March 1997, GTK

Fifty-two real-time GPS-gravity measurements were accomplished on the ice of a lake with rather difficult movements and vibrations. GPS made the navigation on the ice easy, even in a heavy snowstorm. Almost ideal results were obtained. Standard deviation of height measurements was 0.043 m, which includes GPS error, antenna height variations due to the variable attitude and delayed response of snowmobile suspension system to varying load, and fluctuation of ice surface elevation.

2.1.1.2.11. Orléans test, France, April 1997, BRGM and GTK

The Orléans test is described in more detail in Debeglia et al., 1998. This important test consisted of measuring 29 optically levelled points along a loop, which was approximately 3 km in diameter, with the Ashtech and Sercel GPS receivers both in real time and with post-processing. The Sercel equipment had a considerably longer initialisation times than the Ashtech equipment, in accordance to Table 2.1-1. At two locations radio communication was lost by the Ashtech system, in which the transmitting power was only 0.5 W. The standard deviation of the measured elevations was 0.032 m, which also includes the unknown local geoid undulations and levelling errors. This is very consistent with the results obtained in Finland.

2.1.1.2.12. Argentat test, France, June 1997, BRGM

The Argentat test is described in more detail in Debeglia et al., 1998. Altogether 169 gravity stations over an area of 406 km² with 23 repetitions were measured in two weeks with the Ashtech GPS receivers and a LaCoste-Romberg gravity meter. Two days of the field work were devoted to the calibration of two new gravity bases and to the installation of a GPS base station. Within a radius of about 20 km, an altimetric precision of 5 cm could be assured by 10 minutes of recording (in 50% of the cases in less than 5 minutes). Thus, for regional gravity mapping, GPS positioning can provide not only a considerable increase in precision, but also greater flexibility and a better yield.

2.1.1.2.13-14 Hyvinkää tests E and F, Finland, September and October 1997, GTK

In the Hyvinkää E and F tests, measurements on permanent benchmarks were repeated in autumnal conditions. A laser ranger with an inclinometer was tested as an auxiliary device to GPS receivers, and altogether 12.6 km of gravity profiles were measured with various combinations of hydrostatic chain-levelling, laser&inclinometer and GPS measurements.

2.1.1.2.15. Ag. Ioannis Mine Test, Greece, March 1998, IGME and LARCO and GTK

The first test in Greece was conducted in the surroundings of Ag. Ioannis lateritic Ni mine. It consisted of a network measurement to tie the GPS coordinates to the local system, a regional survey and detailed profile measurements above a known Ni ore. The Helmert transformation

parameters were solved in one day with a standard error of 0.04 m. The transformation was used in real-time for detailed profile measurements. The Greek crew had no difficulties in adopting the new technique. A typical profile of 51 observations with approximately 15 m station spacing was measured in an easy terrain in two and a half hours by two persons using the system for the first time. The measured data was of very high quality as shown in Fig. 2.1-4. The regional and detailed measurements proved to be much easier than in Finland because of open views to sky on the mountains as well as on the plains. The system performed very well in this area. Altogether 137 regional and profile gps-gravity observations were made during the four days of measurement including the determination of the coordinate transformation parameters. The output power of the radio modem transmitting real-time corrections from the base to the rover had been increased earlier to 10 W. Corrections could be received at the other end of the plain at a distance of about 10 km.

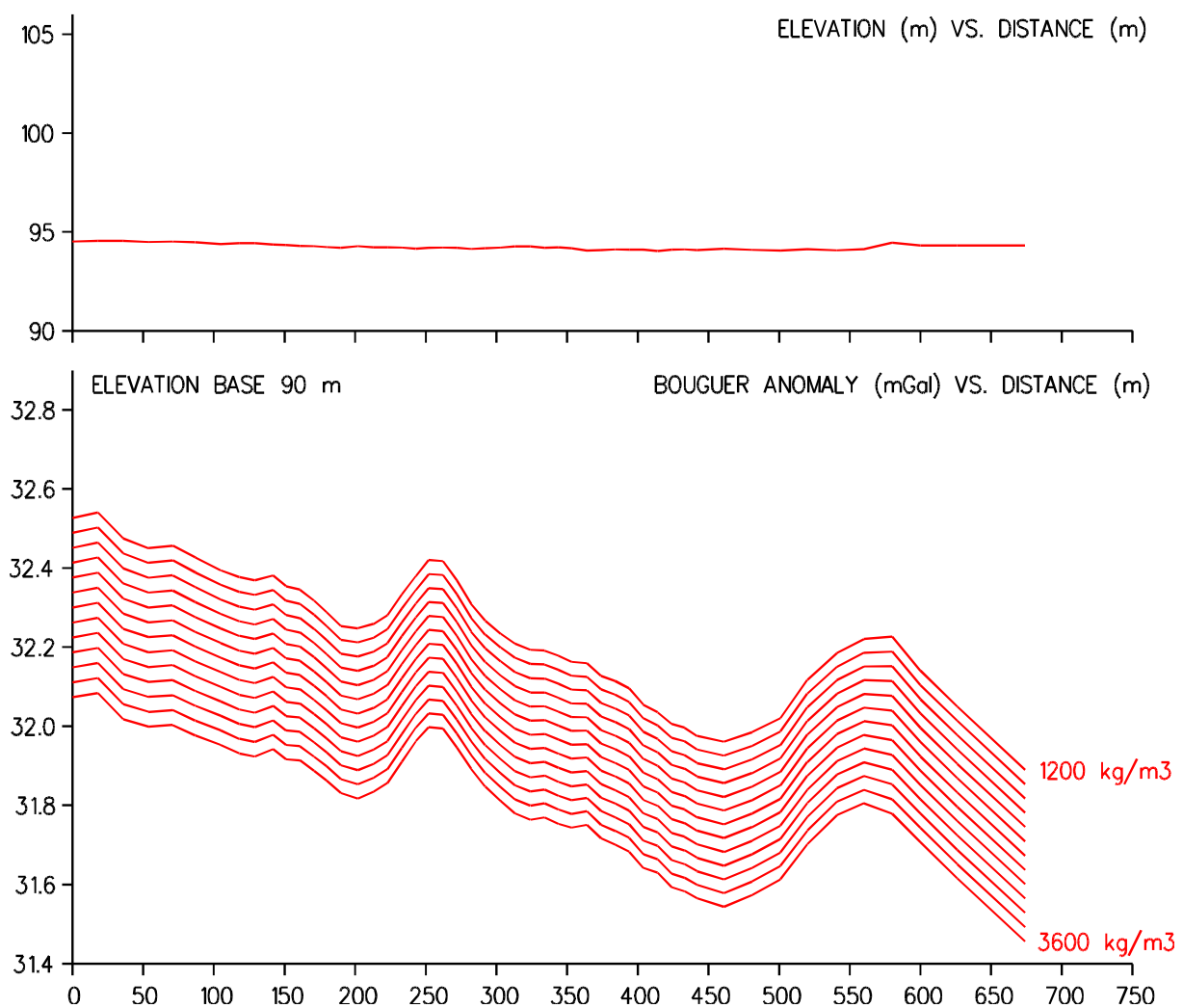


Figure 2.1-4. A GPS-gravity profile over a lateritic Ni-ore in Ag. Ioannis Mine area.

2.1.1.2.16. Vermion test, Greece, March 1998, IGME and GTK

The second Greek test took place in an Ni-exploration area on the remote Vermion mountains in northern Greece. The system worked with the expected accuracy and efficiency in this area, too. Solving experimentally the coordinate transformation parameters took one day.

During the remaining four days, altogether 107 regional and profile gps-gravity observations were made in this hard to access area during an unusually cold spell of weather.

2.1.1.2.17. Hyvinkää test G, Map sheet 2042, Finland, June 1998, GTK and Haines Surveys

The GeoNickel GPS equipment was compared to the equipment of the Haines Surveys from Australia. In this test, the GeoNickel equipment performed better and was more versatile than the Australian one.

2.1.1.2.18. Kemi Open Pit Mine test, Map sheet, 2541, June 1998, GTK and Outokumpu

This test is described in more detail in Elo, 1998. At first, coordinate transformation parameters between the GPS and the mine coordinates were experimentally solved. Detailed gravity profiles were measured across a 150 meter deep open pit mine to estimate the amount of the remaining ore. Outside the mine, elevations were measured by hydrostatic levelling. In the mine, the GPS-gravity equipment proved to be very efficient. In four days altogether 230 real-time stations were measured in an operating mine. Fourteen gravity stations were established in an underground tunnel. With the GPS-gravity equipment five of these locations were occupied at the bottom of the mine pit, from 200 to 260 metres above the tunnel, and based on the results anomalous vertical gradients of gravity were calculated.

2.1.2. Design of an integrated GPS-gravity system

2.1.2.1 RDGPS (Real-Time Differential GPS) Seminar

In April, 1998, a two-day RDGPS seminar was arranged for the partner organisations at the Geological Survey of Finland. The purpose was to review the the state-of-art knowledge on different aspects of real-time GPS surveying before embarking on the final stage of the work package 2.1. The talks, listed in Table 2.1-8, were followed by short discussions, and the following summary papers: Somersalo, 1998; Ollikainen, 1998; Vermeer, 1998; Ruotsalainen, 1998; Elo, Bourgeois, and Angelopoulos, 1998; together with brochures and booklets of Ashtech GPS+GLONASS technology, Sateline Radio modems and ComAnt VHF and UHF antennas were handed out to the participants.

In this connection, the following literature is also recommended: DMA, 1989; May, M.B., 1996; NIMA, 1997; Langley, R.B., 1997a and 1997b; Levy, L.J., 1997; Ollikainen, 1997; and Snyder, J.P., 1987. In general, the Innovation Column of the GPS WORLD magazine contains easy to read introductions to various aspects of GPS surveying.

Table 2.1-8. RDGPS (Real-time Differential GPS) SEMINAR, Titles of talks.

-
- I. Koskelo (NavData Oy): Infrastructure development. Future trends in precise satellite positioning with GPS, GLONASS and geostationary (GEO) satellites. The European Radio Navigation Plan.
 - I. Koskelo (Navdata Oy): Technology development. Performance characteristics of single frequency GPS-Glonass receiver in Real-Time-Kinematic applications compared with dual-band GPS receivers. Global Navigation Satellite System (GNSS) receiver architecture.
 - E. Somersalo (Institute of Mathematics, Helsinki University Technology): Introduction to Theory and Practice of Kalman Filtering.
 - M. Ollikainen (Finnish Geodetic Institute): Basic definitions of and transformations between WGS84, EUREF and European national coordinate systems.
 - M. Vermeer (Finnish Geodetic Institute): European and national geoid models and their role in vertical GPS positioning.
 - P. Aura (Satel Oy): Wireless data transfer for portable applications.
 - A. Alonen (Completech): Practical antenna applications for telemetry environment.
 - H. Ruotsalainen (Finnish Geodetic Institute): GPS positioning in the gravity measurements of Finnish Geodetic Institute
 - S. Elo (GTK), B. Bourgeois (BRGM), A. Angelopoulos (IGME) : GPS equipment and experiments of the GeoNickel Project.
 - J. Lehtimäki and T. Ruotoistenmäki (GTK): An antarctic experience.
 - S. Elo (GTK): Practical demonstration of real-time GPS-gravity measurements in the vicinity of the Geological Survey of Finland.
-

2.1.2.2. Components of the GPS-gravity system

The main components of the GPS-gravity system of the GeoNickel project at the end of 1998 were as follows:

- 1a) Two Ashtech RTZ-12 GPS-receivers for dual-frequency carrier-phase differential real-time cm-accuracy positioning (one base and one rover, both with 3 Mb memory).
- 1b) Three Sateline 2ASx 430 MHz radio modems to provide a real-time link between the GPS base station and rover.
- 1c) One Satelgain UHF Booster to increase the output power of the base station radio modem from 0.5 W to 10W.
- 1d) Husky FS/2 control unit with 4Mb memory for real-time measurements.
- 2) One Geolaser ranger plus inclinometer device to obtain coordinates of obstructed locations in relation to unobstructed GPS sites.
- 3) Scintrex CG-3M automated gravity meter to be used together with the roving GPS receiver.
- 4) Several auxiliary pieces of equipment such as
 - * tripods, tribrachs, and antenna masts for GPS-antennas,
 - * directional antennas and antenna masts for radio modems,
 - * gravity meter tripods and backpacks,
 - * devices for fastening equipment to masts and vehicles,

- * batteries and battery chargers,
- * cables and connectors
- 5) Portable computer for processing results in the field camp.
- 5) Ashtech PRISM and WINPRISM software for planning GPS surveys and processing survey results.
- 6) Husky F/S control software for real-time gps-gravity measurements including coordinate transformations.
- 7) PC-software for integrating GPS and gravity results and for solving and calculating coordinate transformations and gravity anomalies.

2.1.2.3. Current status

Test routes have been established for repeated testing of various gps receivers and software.

When there is an open view to the GPS satellites, measurements with a vertical positioning accuracy of better than 5 cm can be effectively made

- * in real-time with station intervals from some meters to few hundred meters and baseline lengths up to 3 - 10 km,
- * using post-processing with station intervals from a few hundred meters to a few kilometres and baseline lengths less than 20 km.

In full-grown forests, or other similar areas with obstructed view to the sky, when using station spacings substantially less than say 200 metres GPS must be augmented by e.g. a hydrostatic chain-level or a laser ranger plus inclinometer. Moreover, detecting errors caused by multipath and obstructed view to satellites requires prolonged observation times. On the other hand, GPS makes the use of other devices much more effective than previously.

Laser ranger plus inclinometer can be used to transfer an accurate elevation measured by GPS at a GPS-wise good location to an obstructed location with an accuracy of better than 10 cm for distances up to 100 m.

The effects of local geoid undulations can be modelled with standard errors of 0.010 to 0.025 metres by measuring a GPS network on optically levelled benchmarks and fitting a two-degree polynomial to the results.

If formulas are not available, the Helmert transformation parameters from GPS horizontal coordinates to local horizontal coordinates can be similarly solved with cm-class standard errors by measuring a GPS network on benchmarks whose coordinates are accurately known in the local system.

Once the transformation and geoid model parameters have been solved, the Husky control software can make the corresponding corrections and transformations in real time.

The range of radio link for real-time corrections depends on terrain and national radio traffic regulations. Directional antennas have to be used to obtain maximum range under given conditions and regulations.

The residual drift of Scintrex Autograv gravimeter after automatic linear drift correction is small enough to facilitate accurate real-time calculation of Bouguer anomalies.

2.1.2.4. Exploitation plans

According to the original project plan, the GPS-gravimeter system will remain in the possession of the Geological Survey of Finland. The GPS-gravity system assembled during the project will be exploited by the GSF both in scientific research and commercial applications. The GSF is open to suggestions how to best exploit the experience and equipment together with the partner organisations. The work done certainly has helped to accelerate the adoption of GPS in other applications. Based on the test results, more complete technical reports, including geophysical interpretations of the results, and papers to be presented in international meetings are under preparation. The GPS-gravity system and associated software will be further developed at the Geological Survey of Finland.

2.1.3. Acknowledgements

Several tens of persons at the Geological Survey of Finland, Outokumpu Oy, BRGM, IGME and LARCO contributed substantially to the WP2.1. To all of them we present our sincere thanks. Representatives of the various equipment at Navdata Oy, Satel Oy, Completech Oy, Geostar Oy and Miranet deserve also our thanks. Personnel at the Outokumpu and LARCO mines welcomed us to do our tests and showed interest in our results. Heikki Soininen and Bernard Bourgeois as leaders of the Work Package 2 helped to realise the work. The persons without whom important parts of the work would not have been at all possible include Seppo Elo, Heikki Forss, Aimo Hattula, Eero Sandgren, Pasi Kråknäs, Nicole Debeglia, Evgeni Burov, Antonios Angelopoulos and Dimitrios Eliopoulos. Geophysicists and geophysical field crews at the Geological Survey of Finland, Outokumpu Oy, BRGM and IGME gave invaluable help and enthusiastic support. Technicians at the Geological Survey willingly manufactured auxiliary equipment as needed. Martin Vermeer, Matti Ollikainen, and Hannu Ruotsalainen of the Finnish Geodetic Institute provided solid geodetic background for coordinate transformations and geoid modelling.

2.1.4. References

- Debeglia, N., Burov, G., Lebert, F., Besse, A., 1998. GEONICKEL Project Task WP2: Development of geophysical techniques, GPS and Gravity module. BRGM R39920. 41 p.
- DMA, 1986. The Universal Grids: Universal Transverse Mercator (UTM) and Universal Polar Stereographic (UPS). DMA Technical Manual DMATM 8358.2. 39 p.
- Elo, S., 1998. GPS-gravimetraus ja gravimetriset profiilimittaukset Elijahärven kaivoksella 9-17.6.1998. Geologian tutkimuskeskus, Raportti 13.10.1998. 21 s.
- Elo, S., Bourgeois, B., and Angelopoulos, A., 1998. GPS equipment and experiments of the GeoNickel Project. RDGPS Seminar, GeoNickel Project, Geological Survey of Finland, 6-7 April, 1998, 12 p.

- Hofman-Wellehof, B., Lichtenegger, H., and Collins, J., 1994. GPS: Theory and practice. Springer-Verlag, 355 p.
- Langley, R.B., 1995. GPS and the Internet. GPS WORLD, November 1995, 59-63.
- Langley, R.B., 1996. The GPS User's Bookshelf. GPS WORLD, January 1996, 56-63.
- Langley, R.B., 1997a. The GPS Error Budget. GPS WORLD, March 1997, 51-56.
- Langley, R.B., 1997b. GLONASS: Review and Update. GPS WORLD, July 1997, 46-51.
- Langley, R.B., 1998. RTK GPS. GPS WORLD, September 1998, 70-76.
- Levy, L.J., 1997. The Kalman Filter: Navigation's Integration Workhorse. GPS WORLD, September 1997, 65-71.
- May, M.B., 1996. Gravity and GPS: The G connection. GPS WORLD, 53-57.
- NIMA, 1997. Department of Defense World Geodetic System 1984. Its definition and Relationships with Local geodetic Systems. NIMA STOCK NO. DMATR83502WGS84. 174 p.
- Ollikainen, M., 1993. GPS-koordinaattien muuntaminen Kartastokoordinaateiksi. Tiedote 8, Geodeettinen laitos. 32 s.
- Ollikainen, M., 1997. Determination of orthometric heights using GPS levelling. No. 123, Publications of the Finnish Geodetic Institute. 143 p.
- Ollikainen, M., 1998. Basic definitions of and transformations between WGS84, EUREF and European national coordinate systems. RDGPS Seminar, GeoNickel Project, Geological Survey of Finland, 6-7 April, 1998. 12 p.
- Poutanen, M., 1998. GPS-paikanmäärittäminen. URSA. 269 s.
- Ruotsalainen, H., 1998. GPS-positioning in the gravity survey of Finnish Geodetic Institute. RDGPS Seminar, GeoNickel Project, Geological Survey of Finland, 6-7 April, 1998, 19 p.
- Somersalo, E., 1998. Introduction to Theory and Practice of Kalman Filtering. RDGPS Seminar, GeoNickel Project, Geological Survey of Finland, 6-7 April, 1998, 18 p.
- Snyder, J.P., 1987. Map Projections - A Working Manual. U.S. Geological Survey, Professional Paper 1395. 383 p.
- Vermeer, M., 1998. National and international geoid models and their role in vertical GPS positioning. RDGPS Seminar, GeoNickel Project, Geological Survey of Finland, 6-7 April, 1998, 18 p.

2.2. Task 2.2.1: Development of spectral IP method for Ni exploration

2.2.1. Introduction

The induced polarization method (IP) is based on the concept that, in the linear regime (sufficiently low current densities), the resistivity of earth materials is a frequency-dependent and therefore complex quantity. The standard IP method measures the response at a fixed frequency (usually $f < 10$ Hz) or over a narrow frequency range. The IP method is well suited to mineral exploration especially for disseminated occurrences. The IP method has been a standard exploration tool from the early fifties.

In the spectral IP method (SIP), the complex resistivity spectrum of the earth is measured over a wide frequency range (e.g. 0.001 Hz - 5000 Hz).

The resistivity spectra of rock types differ from each other, and consequently, SIP is a method for discriminating between different mineralization types. Better understanding of the concepts of the linear systems theory in description of the electrical behaviour of a rock have markedly improved the applicability of the method. Development of better numerical methods for computing IP anomalies has greatly increased the power of quantitative interpretation.

There are accurate instruments available on commercial basis for the measuring of signals at wide frequency band. However, the high accuracy needed in field measurements has made reliable data acquisition difficult. Moreover, too little is known about the spectral behaviour of different rocks.

In the GeoNickel project SIP method has been developed specially for nickel exploration. The emphasis is put to the data acquisition and interpretation of spectral laboratory and field data. Elimination of EM coupling from the field measurements is a crucial improvement to measure reliable resistivity spectra. Progress has also being made for understanding the relationship between the spectral IP behaviour of a rock and its mineral composition and texture. Altogether 650 core samples were measured in the laboratory. Finally, the geological interpretation which can be made from the measured spectra is studied in field tests.

2.2.2. Transformation from true to apparent spectrum

In field measurements, the recorded resistivity spectrum is an apparent spectrum that depends on the true spectra of the target and the host but also on the electrode array and the geometry of the target. Therefore, the problem is how the true spectrum (or the parameters describing it) is transformed into an apparent spectrum (or equivalent parameters).

In the numerical modelling carried out it is assumed that the resistivity spectrum of the rocks can be depicted by means of the Cole-Cole dispersion model (Pelton, et al., 1978). By application of such a mathematical model makes the analysis easier because the characteristic features of the spectrum can be represented solely by means of finite number of parameters. The Cole-Cole model has four parameters R_0 resistivity at zero frequency; m chargeability; τ time constant and c frequency effect.

The behaviour of the apparent spectra for different basic situations can be summarized in the following way.

The functional form of the Cole-Cole spectrum of a polarizable body situated in an unpolarizable host is preserved well in the transformation from the true to the apparent spectrum.

For this reason, the Cole-Cole dispersion model can also be fitted into an apparent spectrum. Of the parameters inverted from apparent spectra, the apparent frequency dependence preserves well its true value. The apparent time constant remains somewhat smaller (generally, however, less than a decade) than the petrophysical time constant. From the practical standpoint of mineral discrimination, however, the apparent time constant is generally sufficiently close to its true value.

The effect of a polarizable environment on an apparent phase spectrum can be readily approximated by summing the petrophysical phase spectrum of the host medium with the apparent phase spectrum caused by the model in an unpolarizable environment. Thus the spectral parameters can be inverted from the apparent phase spectrum by fitting into it the sum of two Cole-Cole phase spectra. This can be done with the inversion software INVELOG developed in the project. Inversion is based on the Marquardt-Levenberg method. In the case of several polarizable bodies, the apparent spectrum is built up in a complex way, and it can no longer be described simply as the sum of the spectra of its components.

The aim of spectral measurements is often to map different parts of a formation that differ in their time constant. By measuring a profile crossing over the formation, the components that differ in time constant can be separated from the apparent spectra.

2.2.3. Removing of EM coupling

A major problem in spectral IP field measurements is the frequency-dependent electromagnetic coupling between the transmitter and receiver. This coupling is especially strong at high frequencies and with large collinear arrays. This is readily seen in Fig. 2.2.1-1a where inductive phase shift anomaly is calculated for homogeneous half-space. The calculation is based on the expression for mutual coupling between a pair of grounded wires (Sunde, 1949). As an example let us consider the following case with $a=20$ m, $n=5$, $f=1000$ Hz and $\rho=100$ Ω m. The response parameter $a^2f/\rho=4000$ Am/Vs gives the value of -123 mrad for phase shift. In practical measurements disseminated magnetite could cause similar response at high frequencies.

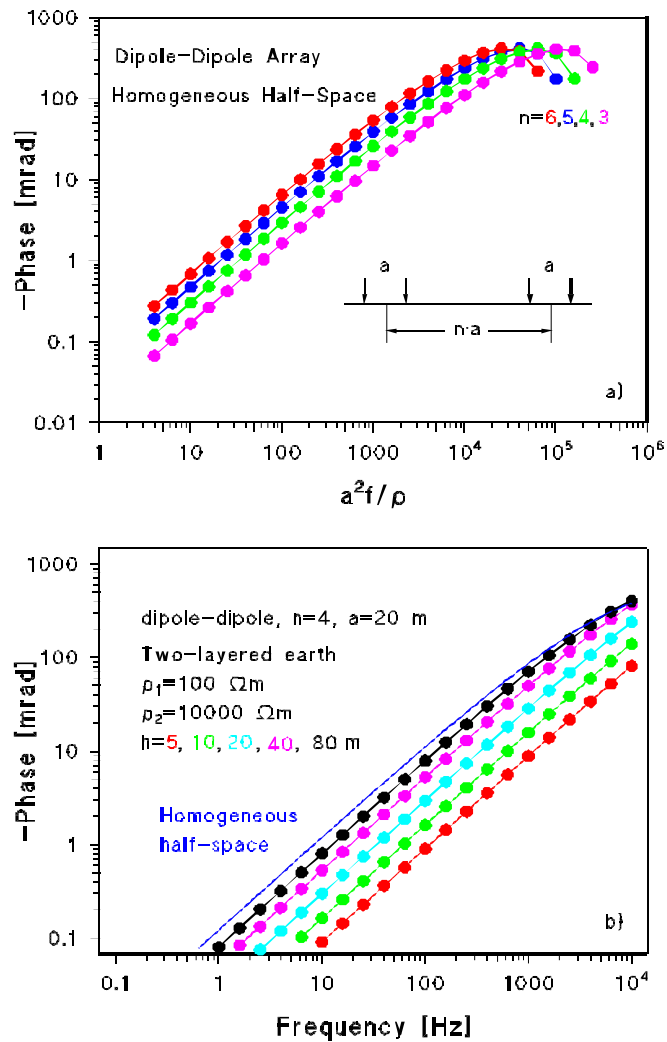


Fig. 2.2.1-1. a) Inductive coupling for a homogeneous half-space.
 b) Inductive coupling for two-layered earth.

Fig. 2.2.1-1b shows the inductive coupling in the case of a two-layered earth. The upper layer (overburden) has the resistivity of $100 \Omega\text{m}$ and the resistivity of the basement has the value of $10000 \Omega\text{m}$. The figure shows phase shifts as a function of frequency for different thicknesses

h of the first layer. When the thickness increases from 5 m to 80 m the phase shift increases and approaches to the value of homogeneous half-space.

In the GeoNickel project a two-stage EM-coupling removing scheme is developed. A major portion of the coupling, due to the environment, is minimized by using a non-collinear dipole-dipole array (Fig. 2.2.1-2). Such an array minimizes the inductive electric field but still gives a measurable galvanic effect. The problem is that the optimum geometry of the electrode array depends on each particular environment. In this study two models of the host are examined; homogeneous half-space and two-layered half-space. Due to inhomogeneities and three-dimensional effects there still remains secondary coupling after using optimal electrode array. This remaining EM coupling, whose spectrum is characteristic, will then be removed by a mathematical spectral analysis method. With these techniques, it is possible to obtain a measurable IP spectrum up to frequencies of several thousands of Hertz.

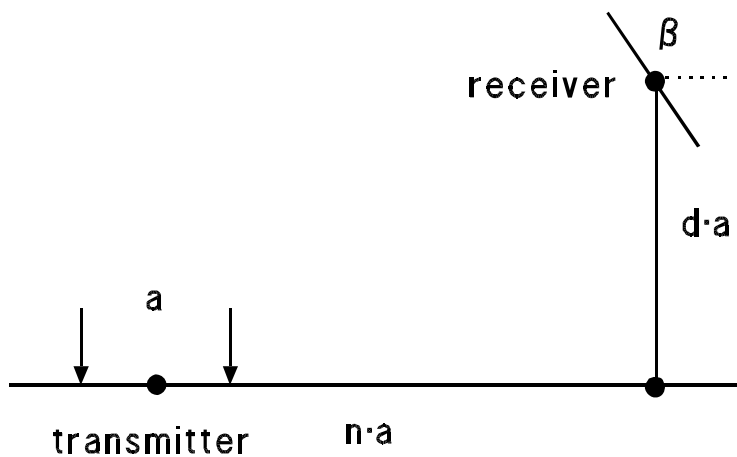


Figure 2.2.1-2. Non-collinear electrode array

2.2.3.1. Homogeneous half-space

When the polarizable body is embedded in a homogeneous half-space the inductive coupling of the half-space can totally be removed by using a perpendicular dipole-dipole array (in Fig. 2.2.1-2 angle of rotating $\beta=90$ deg.). The problem is that if the receiver is rotated in collinear dipole-dipole array the inductive but also galvanic coupling is zero when $\beta=0$. To increase the galvanic coupling receiver dipole should be off from the measuring line. It can be derived analytically that the array which has $d=n/2$ gives the maximum galvanic coupling with zero inductive coupling. In this case the galvanic signal is 43 % of the signal for corresponding collinear array.

2.2.3.2. Two-layered half-space

The choice of optimal electrode array is more complicated if the host geometry differs from homogeneous half-space. In practice important case is a two-layered earth because then the effect of overburden can be taken into account. In this case the optimal rotation angle β is no longer 90 degrees for an optimal array but depends on the resistivities and thickness of the overburden. Fig. 2.2.1-3 shows a calculated two-layer case with $\rho_1=100 \Omega\text{m}$ (overburden),

$\rho_2=1000 \Omega\text{m}$ and thickness of the overburden $h=10 \text{ m}$. Figure shows the phase spectrum without EM coupling, the phase spectrum with EM coupling and the spectrum for a non-collinear array with $\beta=106 \text{ deg}$. The frequency range which can be measured without a disturbing EM coupling has been increased from about 100 Hz to 3000 Hz.

In practice a recommendable procedure for field work is to measure along measuring profiles using two perpendicular transmitter dipoles and two perpendicular receiver dipoles. The optimal angle in this case $\beta=\arctan(0.5)$ - β can be found in data processing phase by rotating mathematically the measured spectrum. This can be done with the developed TURNSIP software.

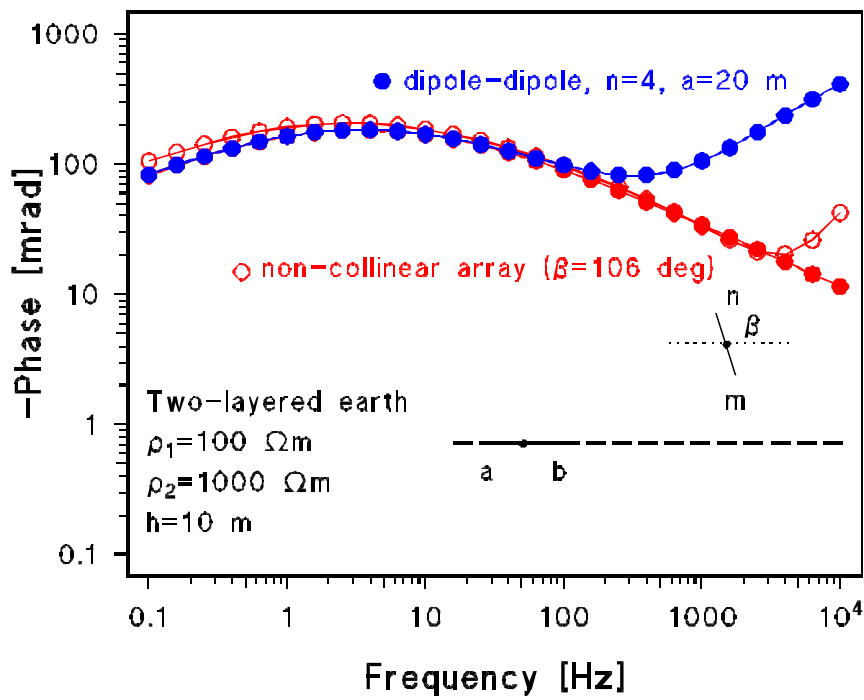


Fig. 2.2.1-3. Removal of inductive coupling by using non-collinear electrode array in a two-layered case.

2.2.3.3. Spectral techniques

The disturbing effect of EM coupling can be reduced by using an optimal electrode array as described above. In most cases this gives reasonable result, but if the EM coupling which still remains should be smaller the following technique can be used. It is assumed that the EM coupling has a characteristic functional form. In terms of Cole-Cole parameters the frequency effect has a value $c=1$ and time constant is small. This assumption has been tested by numerical modelling.

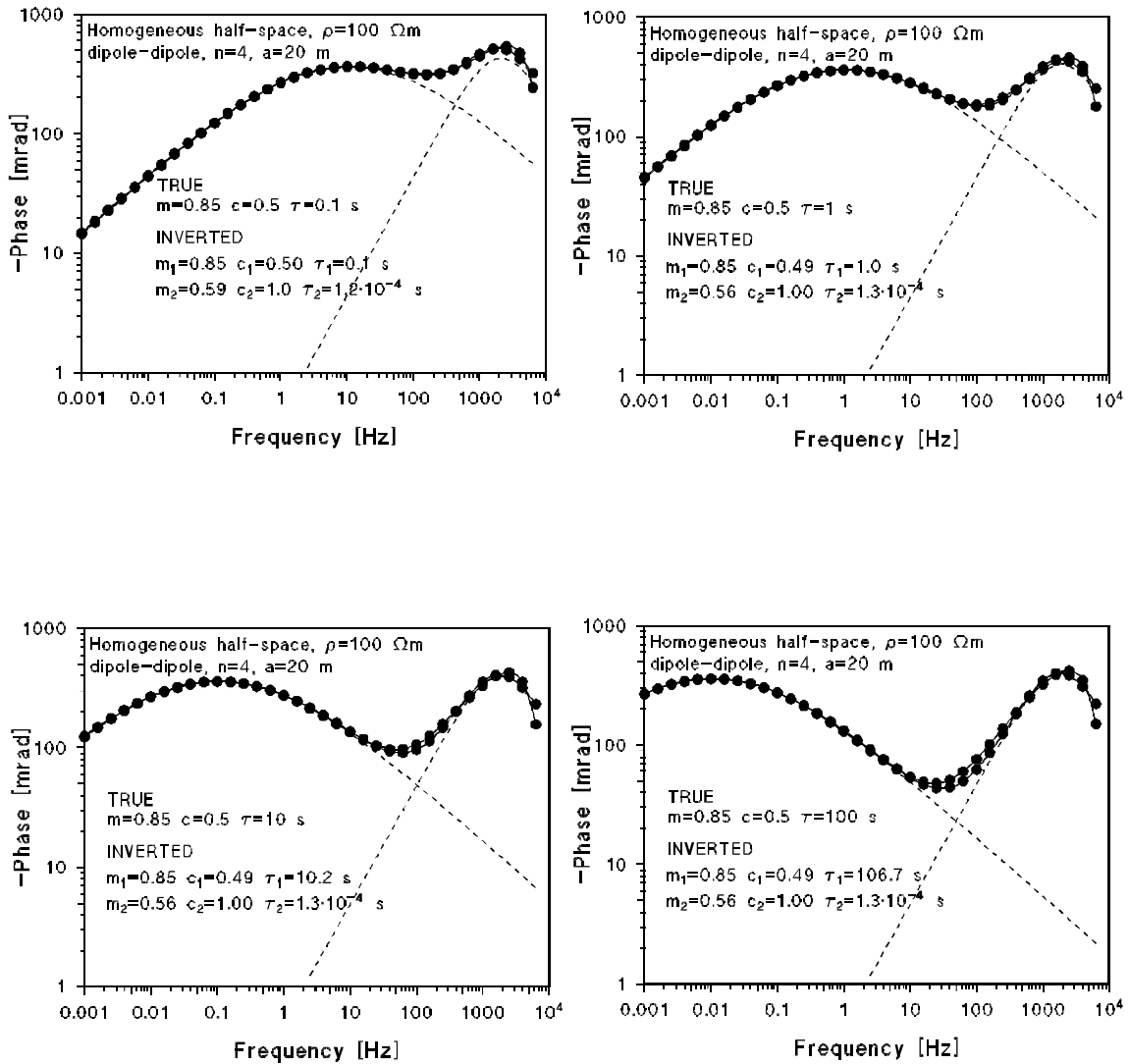


Fig 2.2.1-4. Two Cole-Cole dispersion models fitted into the apparent spectra for removing EM coupling

Fig. 2.2.1-4 shows apparent phase spectra for a homogeneous polarizable half-space model with $R_0=100 \Omega.m$, $m=0.85$ and $c=0.5$. Time constant has varied having the values of $\tau=10$ s, 1 s and 0.1 s. Forward modelling is carried out with MARCO software (Raiche et al., 1998).

EM coupling distorts the spectra at high frequencies. The sum of two Cole-Cole spectra is fitted to the calculated spectra. All spectral parameters are kept free in the inversion. In all three cases the functional form of the phase spectra can well be described by the sum of two Cole-Cole models. Moreover, the inverted Cole-Cole parameters for the half-space are the same or very close to the true values of these parameters. The second dispersion describes the inductive part. The frequency effect is in all cases $c_2=1$. The further modelling which has been performed suggests that inversion scheme presented can be used if the dispersion of the target is simple enough and can be described by a single dispersion model.

2.2.4. Petrophysical studies of rock samples

The objective of the petrophysical studies was to determine the relationships between the resistivity spectrum and the textural and mineralogical features of Ni ores and their host rocks. The methods used were laboratory SIP measurements of core samples, derivation of the Cole-Cole parameters from the complex resistivity data, thin section studies and ore-grain analysis based on digital thin section images. The results are presented in terms of the relation between the ore textures and the electrical parameters. A database having geological, petrological, mineralogical, chemical, textural and electrical properties of each sample was compiled.

2.2.4.1. Laboratory system

The laboratory SIP measurements were carried out using the technique and equipment described in detail by Vanhala and Soininen (1995). This system (Fig. 2.2.1-5) is built around a two-channel frequency response analyzer (HP 35665A). A four-electrode system is used to measure the voltage signal across the sample. Into the analyzer the signal is input through a differential pre amplifier (constructed in GSF). The phase accuracy of the system depends on the sample and frequency: The analyzer by itself reach a very high phase accuracy of 0.1 mrad in the whole frequency range (0.0156 - 51 000 Hz). With geological samples - mainly due to noise from the sample-electrode contacts - the phase accuracy decreases, and is at it's best around 1 mrad. The noise level is lowest when the sample resistance is from some tens of ohm-meters to some kilo ohm-meters, and when the frequency is between 0.1 Hz and 1000 Hz. At higher frequencies, especially when the resistance of the sample is high, capacitive coupling effects cause additional impedance which is difficult to remove exactly. At the lowest frequencies the noise originates from the rock-electrode interface. During the long time needed to measure the lowest frequencies moisture conditions, for example, may change near to electrodes giving rise - in addition to other noise sources - to a very low-frequency noise component. New solid AgCl potential electrodes, tested and installed during the project, showed a very low noise level at the highest frequencies. The new electrodes are originally developed for sub-marine electric field measurements.

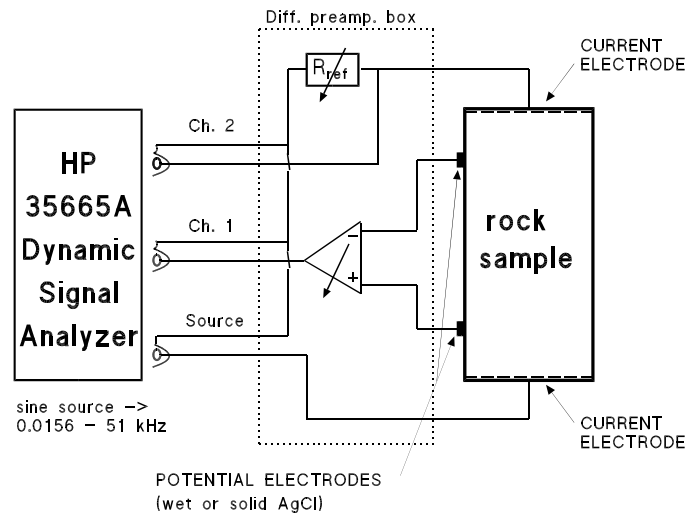


Fig. 2.2.1-5. The laboratory system.

2.2.4.2. Test sites and samples

Almost all the rocks studied in the laboratory were drill core samples having a diameter of 4 cm and a length of 5-10 cm. Some outcrop samples were measured also. Before measurements the samples were immersed into a 70 Sm tap water for 40-60 hours. The measured laboratory resistivity data is presented in graphs which include the phase spectrum, value of the amplitude at 1 Hz frequency, Cole-Cole model spectrum and the Cole-Cole parameters.

The rock type for each sample and a macroscopic describing of the ore minerals were given by the local exploration geologist. Closer mineralogical and textural determinations were made from polished thin sections and a detailed ore-mineral grain size distribution calculated from digital thin section images.

The image processing procedure developed in this project started with a scanning of the thin section with a high resolution slide scanner (2700 pixel/inch). The three-component image was then classified into 2-bit image (ore minerals and silicates). From these images, several parameters describing the shape and size of the ore minerals were calculated; the surface-area, perimeter, ellipse axis ratio (fitted to surface), and direction of ellipse axis.

The number of ore grains detected in a thin section was typically few thousands, but some thin sections of fine-grained textures had as many as 16 000 ore particles. In thin sections from coarse grained textures only few hundred ore particles were detected.

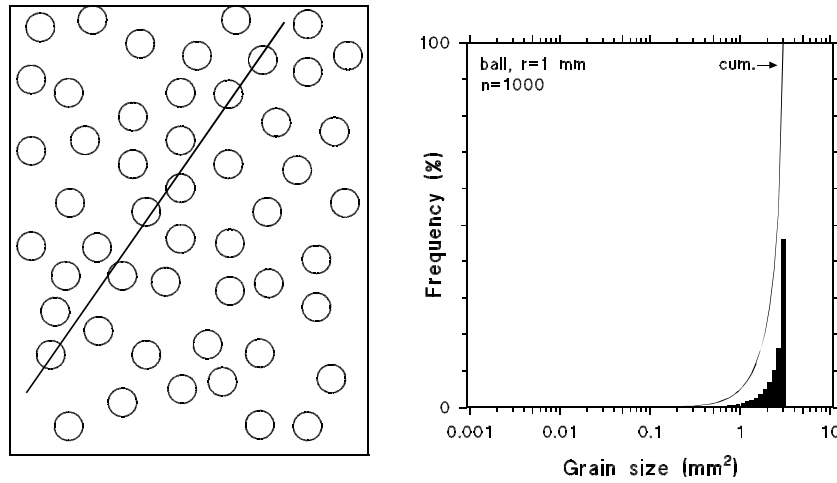


Fig. 2.2.1-6. A model simulating disseminated texture (even-grained spheres) and the theoretical grain-size distribution calculated for a plain section.

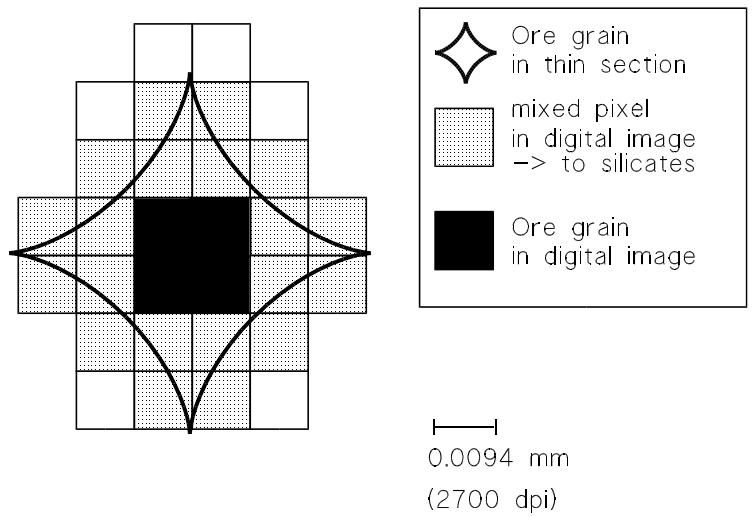


Fig. 2.2.1-7. Actual size and shape of an ore grain and the same grain in a digital image. The size is reduced because the ore-silicate mixed pixels are classified into silicate.

A plane section, as a thin section, gives not the accurate grain size distribution from a 3D texture. However, as the Fig. 2.2.1-6 shows, the calculated grain-size distribution for a model texture simulating a disseminated ore indicates very well the true grain-size maximum. A more difficult problem arises with grain sizes near to the scanners resolution. There the classification procedure reduces the true size of the ore particles significantly (Fig. 2.2.1-7). The mixed pixels will be classified into silicates in the case of larger ore grains also, but the relative error is meaningful only with small grains. For network textures this procedure, and any analysis based on a plane section, gives erroneous information about how largely the ore grains are electrically connected.

Material for laboratory studies was collected from Ni deposits related to Archaean green stone belts and from deposits related to Proterozoic basic-ultra basic intrusions (Fig. 2.2.1-8, Table 2.2.1-1).

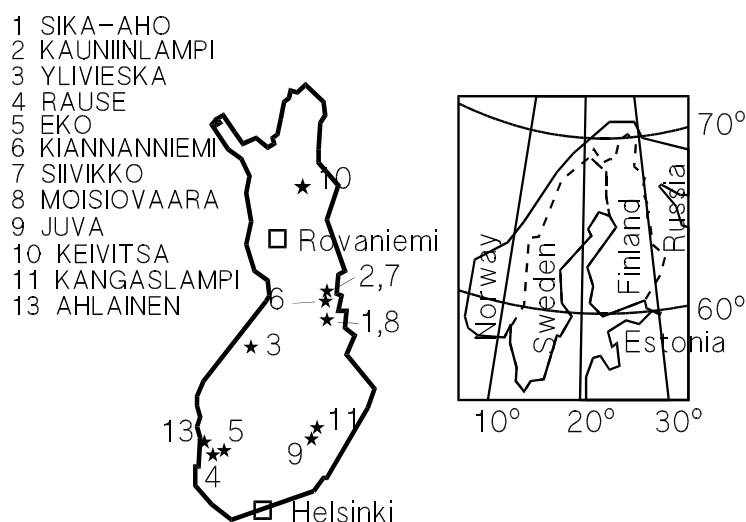


Fig. 2.2.1-8. Location of spectral IP test sites

Table 2.2.1-1. Spectral IP test sites and laboratory and field measurements.

Test site	geology	field SIP (number)	RES/IP sound (line meters)	lab. SIP (number)	thin sections	digital images	6.	7.
1. Sika-aho	Arc.	32	3150	81	19	19	x	x
2. Kauniinlampi	Arc.	112	6000	126	25	25	x	x
3. Ylivieska	Pro.	45	100	31	4	4	x	
4. Rausenkulma	Prt.	56	2100	3				
5. Eko	Prt.		400	33	12	2		
6. Kiannanniemi	Arc.	93	4200	3				
7. Siivikko	Arc.	75	900	3				
8. Moisiovaara	Arc.		520					
9. Juva	Pro.	39	.	28	14	11	x	
10. Keivitsa	Pro.			160	35	15	x	
11. Kangaslampi	Pro.			33	22	2		
12. Savukoski	Pro.			12	4			
13. Ahlainen	Pro.	12	2300	40				x
SUM		464	19670	553	135	78		

Legend: Column 6= density and susceptibility measured in the laboratory; Column 7= ground and bore-hole geophysics; Arc= late Archean deposit (about 2.8 Ga); Pro= Proterozoic deposit (1.8-1.9 Ga, besides Keivitsa which is 2.04 Ga).

The green-stone deposits (with core samples) are the Sika-aho and Kauniinlampi. In the former target the exploration problem was how to discriminate the conductive ore from conductive graphite bearing phyllites. At Kauniinlampi the Ni sulphides showed a

disseminated texture and the problem was how to discriminate them from the disseminated magnetite. Within the Proterozoic intrusions the geological problems were the same. Juva and Ylivieska are basic - ultra basic intrusions having a variable magnetite dissemination and weak sulphide showings at certain parts. The deposits of Ahlainen, Kangaslampi, Eko and Rausenkulma include the both problems; sulphide vs. graphite and sulphide vs. magnetite. The Keivitsa layered intrusion had a different kind of problem: Most of the mineralization is disseminated pyrrhotite without pentlandite, some portions show a similar dissemination but composed mainly of pentlandite. Savukoski is an oxide mineralization with an even-grained dissemination, processed for grain-size estimation purposes only. Only little geological information was available from the Siivikko, Kiannanniemi and Moisiovaara test areas.

In Ni exploration the basic aim is to find the massive part of the mineralization. However, also the disseminated portions can be economically important. The role of SIP in Ni prospecting lies just in mapping the disseminated and net-textured parts of an ore formation. Fig. 2.2.1-9, as a working hypothesis, indicates the relations between the time constant and typical ore textures of Ni deposits. The targets for SIP inside a Ni-containing formation are to discriminate the fine-grained magnetite from a sulphide dissemination, or to discriminate the disseminated sulphide from a net-textured sulphide. Idea to use SIP also for research of massive ores was presented by Pelton et. al (1978) but the later papers do not support this (e.g., Vanhala and Peltoniemi, 1992). In addition to problems stated in Fig. 2.2.1-9, SIP also has a role in discriminating pyrite-, pyrrhotite- and graphite-bearing meta sediments from those ore types.

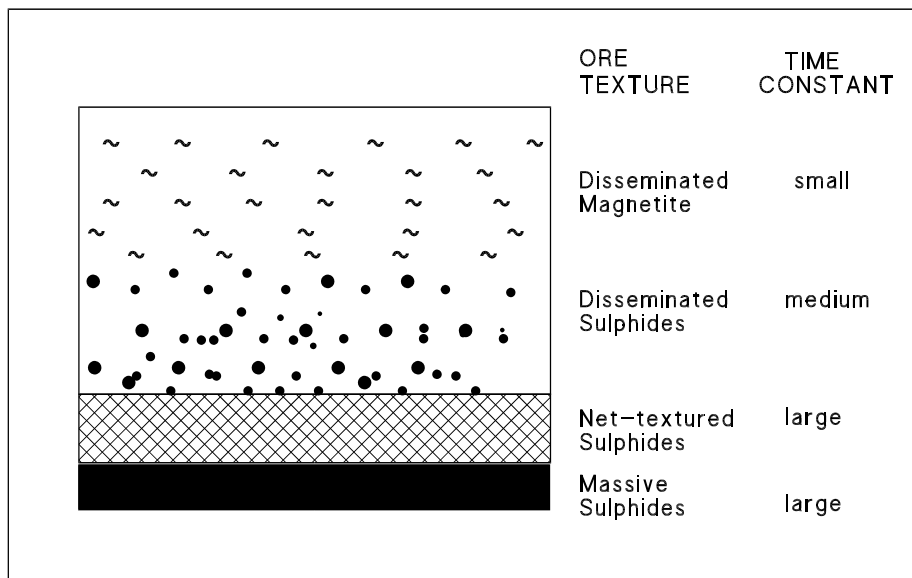


Fig. 2.2.1-9. A model for the ore textures in a Ni-Cu deposit related to an ultra mafic intrusion or extrusion, and the predicted electrical response.

2.2.4.3. Laboratory results

Figure 2.2.1-10 presents one of the most important results of the study. The grain sizes calculated from the electrical data show a close relationship to the petrographic grain size. The distribution in the figure, however, do not follow the theoretical trend (solid line); in the case of large grains the Cole-Cole grain sizes are larger than the petrographic sizes, and in small sizes, vice versa. The reason for this is that with coarse-grained (net-textured) textures a plane section always shows only a part of the possibly very complicated grain form. The data from the Juva, Ylivieska and Keivitsa deposits show some obscure features which may be due to very high resistivity of these samples (see Fig. 2.2.1-11). The above result indicates that the theoretical relation between the Cole-Cole time constant and grain size has to be corrected.

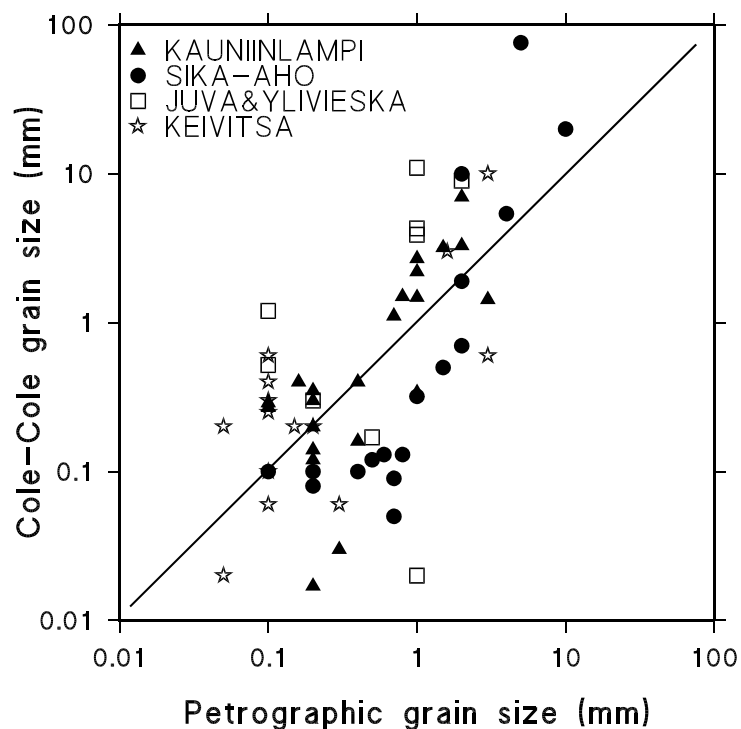
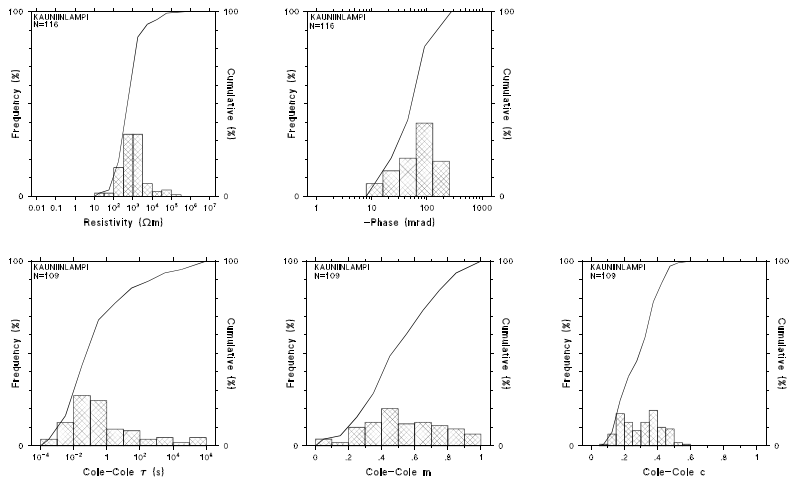


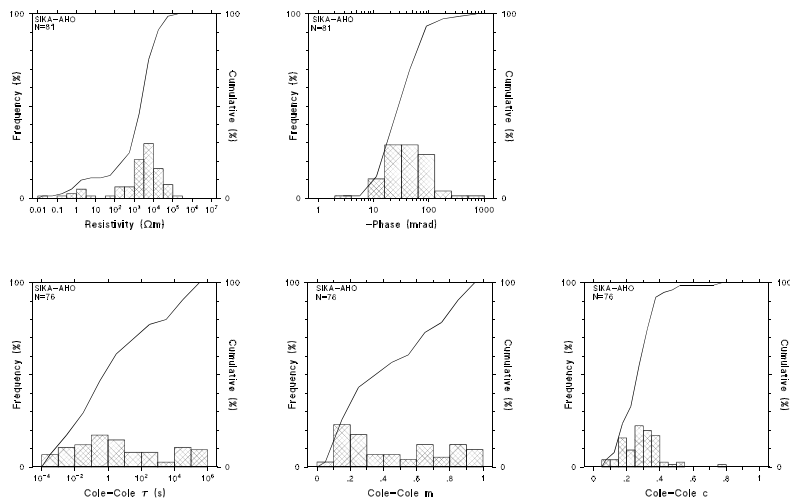
Fig. 2.2.1-10. Relation between petrographic and Cole-Cole grain size at five test sites in Finland. Grain size is the diameter of a sphere grain. Petrographic grain size is calculated from digital images (the grain area is seen as a sphere). The Cole-Cole grain size is based on Cole-Cole time constant, and R_0 , surface impedance parameters (here fixed) and volume percentage of ore grains (see Vanhala and Peltoniemi, 1992).

Figure 2.2.1-11 and 2.2.1-12 show the distribution of low-frequency resistivity and phase shift and Cole-Cole parameters for five test sites. An unexpected and important feature is the large number of short time constants in the Kauniinlampi and Sika-aho sample material (Archean green stone belt deposits). Also the high Cole-Cole c value of this material is a feature not reported before. In fact, the real c -value could be even somewhat higher (see the results in section of development of the electrical model).

a) Kauniinlampi



b) Sika-aho



c) Ylivieska

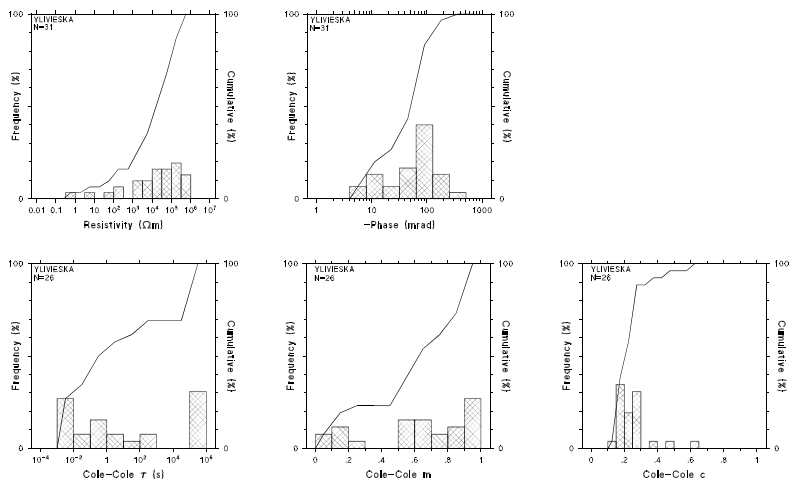
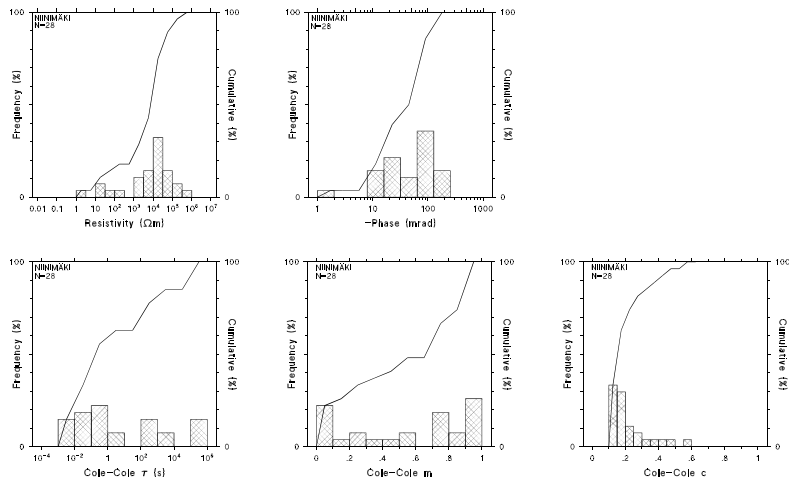


Fig. 2.2.1-11. Histograms of electrical parameters of three test sites, a) Kauniinlampi, b) Sika-aho, and c) Ylivieska (continues at the next page).

Characteristic features for the samples from the Proterozoic basic and ultra basic intrusions (Ylivieska, Ahlainen, Juva) are the very high resistivity, around tens of thousands of ohm meters, and the low Cole-Cole c value (around 0.2).

a) Juva, Niinimäki



b) Ahlainen

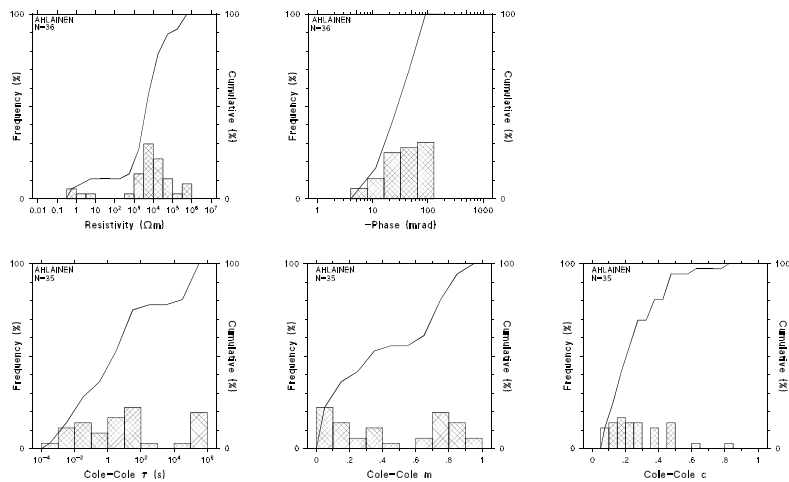


Fig. 2.2.1-12. Histograms of electrical parameters of two test sites, a) Ahlainen and b) Niinimäki (Juva).

In this project, the laboratory material was utilized in the interpretation of the field SIP data (see Table 2.2.1-1). A closer description of the results is presented in separated reports together with the field results. The reports are named according to the names of the test sites. The reports include a general explanation of the geology of the sites, the description of the mineralogical and textural features of each thin section (also thin section photos and digital

images) and all the measured phase spectra with Cole-Cole fittings. Relations between different parameters are also presented. All material is combined into a data base (today an Excel file) which gives an easy way to utilization. An example of this is presented in Fig. 2.2.1-13, where time constants and Cole-Cole c parameters of pyrite and pyrrhotite dominating samples are compared. The Figure suggest a larger time constant and smaller c value for pyrrhotite dominating rocks.

The laboratory data collected to the data base include 553 resistivity spectra (in the form of resistivity and phase at 1 Hz frequency, and Cole-Cole m , c and J). Every sample has been classified according to a formation, rock and texture type (for example: Proterozoic intrusion/gabbro/net-textured). The grain-size information is from 78 samples. In addition to this, the data base include the Ni content and petrophysical magnetic and density data for about 60 % of the samples.

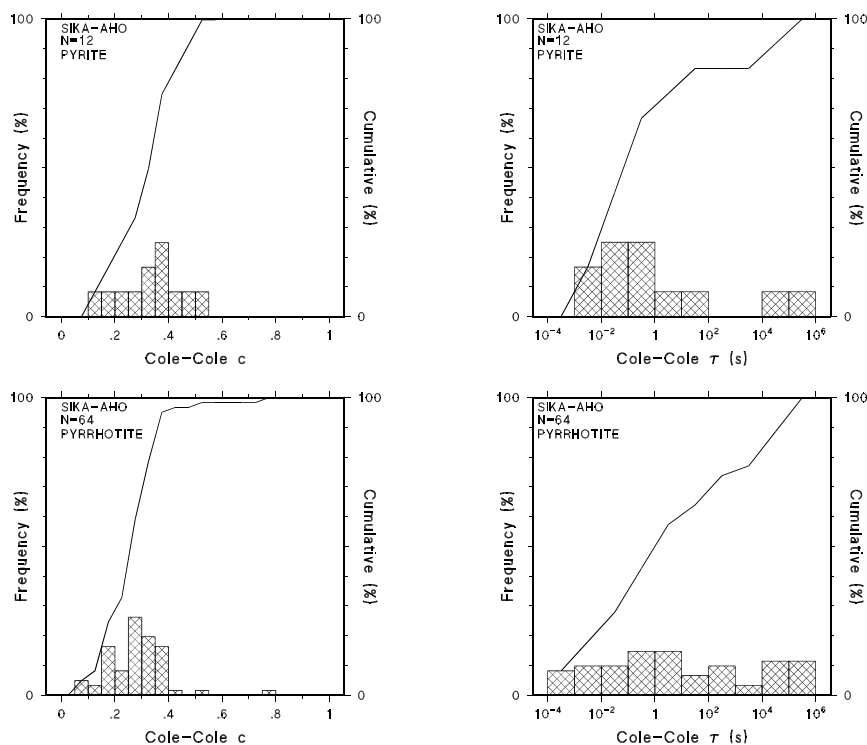


Fig. 2.2.1-13. Cole-Cole c and Cole-Cole time constant distributions at the Sika-aho deposit. Distributions are calculated for pyrite dominated samples and for pyrrhotite dominated samples.

2.2.4.4 Conclusion

The main results from the petrophysical studies is the data base of Ni ores, host rocks and rocks favorable for Ni deposits, to be used in the interpretation of IP and spectral IP field

data. The special reports include a closer description of the relations between the resistivity spectra and the properties of the samples.

2.2.5. Development of the electrical model

The Cole-Cole model has been used as a standard mean to parameterize and present complex resistivity frequency- and time-domain data. There has been, however, some problems in the use of this model. The most serious problems are the following: (1) All spectra of natural rocks do not obey the Cole-Cole model, (2) electrical noise present in field and laboratory data and the information of the spectra which have their phase peak outside the measured frequency range.

The objective of this chapter is to test a generalized Cole-Cole model and to determine the limits of error for noisy data and for phase spectra having no phase peak in the measured range.

2.2.5.1. Generalized Cole-Cole model

Many fine-grained and fairly conductive samples showed a phase spectrum with a distinct phase peak at the middle frequencies and a strong decrease in the phase-shift value towards low frequencies, so that at 0.0156 Hz the phase shift is near to zero. This kind of phase spectrum points the low-frequency end of the relaxation, and show that the low-frequency part of the relaxation is measured completely.

The laboratory data indicated that the more completely the low-frequency end of the relaxation is measured the unsatisfactory is the Cole-Cole fitting. This kind of phase spectra show a flat part at the middle frequencies, but a very rapid decrease towards the low frequencies. At the highest frequencies the phase shift always increases.

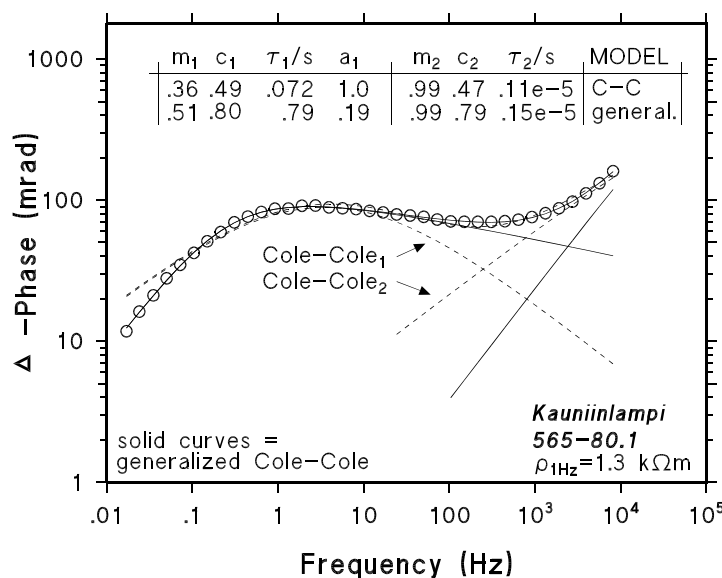


Fig. 2.2.1-14. Fitting of Cole-Cole model and Generalized Cole-Cole model.

An asymmetric shape of phase spectrum is previously related to membrane polarization of clay-containing sediments (Klein and Sill, 1982). They introduced the generalized Cole-Cole model for parameterizing the SIP data of sedimentary rocks. Compared to the Cole-Cole model, the generalized Cole-Cole model have one more parameter (a) and an asymmetric phase spectrum.

In addition to Cole-Cole model, the generalized Cole-Cole model was fitted to laboratory data. Practically in every case the latter gave a better fitting result (Fig. 2.2.1-14).

It seems that the form of a resistivity spectrum of a mineralized rock obeys the generalized Cole-Cole model rather than the Cole-Cole model. The problem is, however, that the generalized Cole-Cole time constant differs from the Cole-Cole time constant and the parameter a , which have no textural or geological equivalent.

2.2.5.2. Noisy resistivity data

In the case of phase spectrum such as in Fig. 2.2.1-14, the normal electrical noise is no problem - the time constant and other parameters can be determined accurately. At many sites, however, the phase peak is situated lower than the lowest measured frequency (0.0156 Hz).

A critical examination of the accuracy of the Cole-Cole fitting was conducted using the field data from the Sika-aho, Kauniinlampi and Ylivieska test sites. The results showed that it is not only the lowest frequencies affect the time Cole-Cole time constant, but also the noise at the highest frequencies.

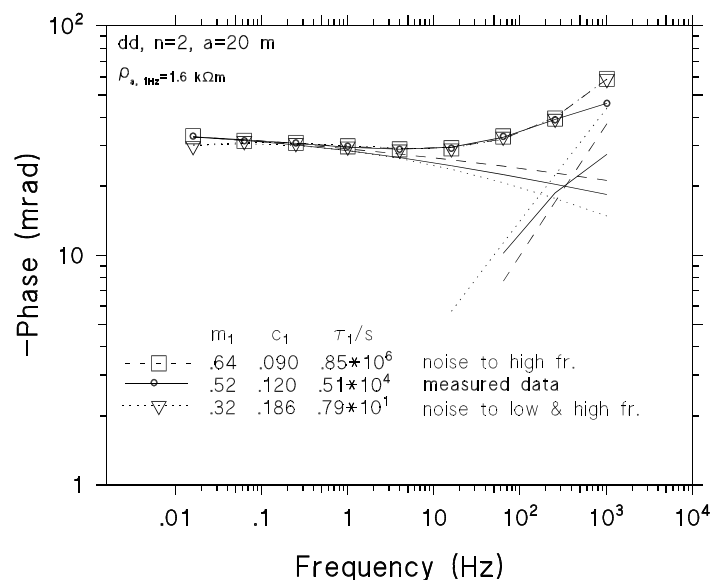


Fig. 2.2.1-15. Field phase spectrum from the Sika-aho test site and two spectra with additional synthetic noise. Note the change in time constant due to noise.

Figure 2.2.1-15 is an example of a field spectrum and two spectra to which noise has added, first to high frequencies only, and then to both high and low frequencies. Especially the latter case changed the low-frequency time constant dramatically.

Figure 2.2.1-16 is an example from Sika-aho. The low-frequency part of the phase spectrum is exceptionally noisy. Fitting to the whole data gives a time constant of longer than 240 000 seconds. The removing of the lowest frequency decreased the time constant to 510 seconds. Giving a fixed value to parameter c_1 ($c_1=0.24-0.16$) and excluding the lowest phase value caused change from 18 seconds to 3400 second in the time constant. The example clearly shows the insensitivity related to noisy data and spectra having no phase peak (at the measured frequency range).

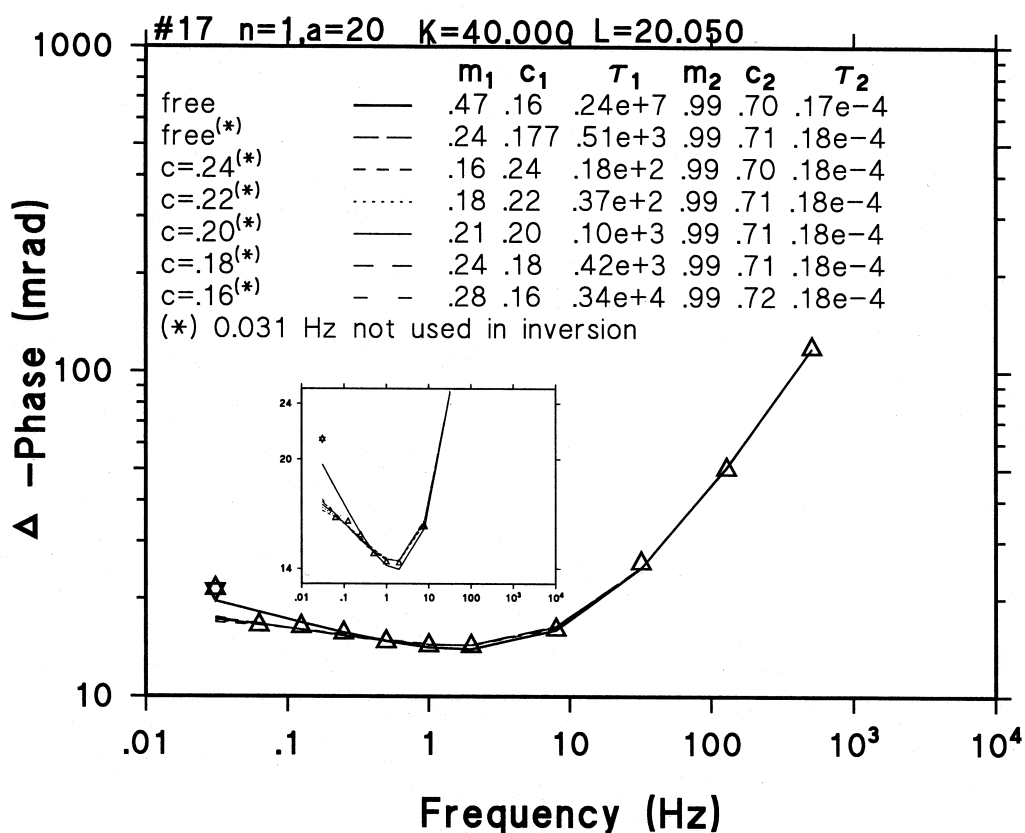


Fig. 2.2.1-16. A field phase spectrum from the Sika-aho test site. The time constant varies between 18 and 240 000 seconds depending on the fitting procedure.

Figure 2.2.1-17 shows the insensitiveness of the Cole-Cole fitting in the case of noise-free data, but no indication of the phase peak. A free fitting gave an unreasonable high time constant, 57 000 seconds. A slightly increased c value led to more realistic time constant, 180 seconds.

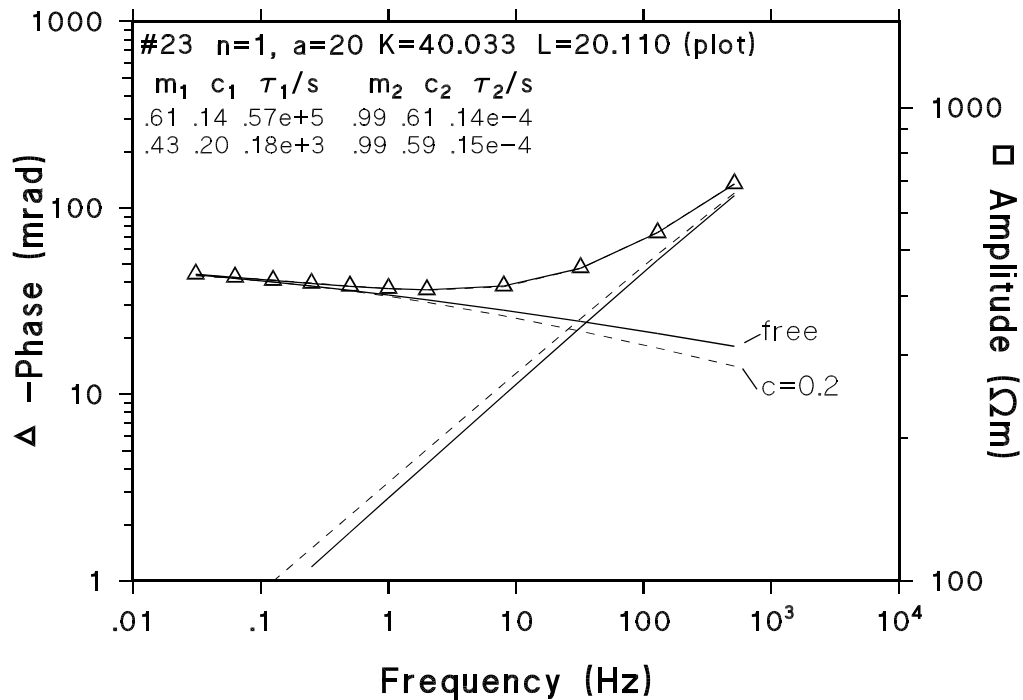


Fig. 2.2.1-17. A field phase spectrum from the Sika-aho test site. Two cole-cole fittings are shown, one with fixed c_1 ($c_1=0.2$), the other is a normal fitting with no fixed parameters.

The results presented in the section 2.2.5.1 and in this section lead to a conclusion that if the phase spectrum show no phase peak, only an estimate for maximum time constant value can be given. In figure 2.2.1-18, this conclusion is examined in terms of Cole-Cole and generalized Cole-Cole spectra. The data, indicated by circles and squares, are Cole-Cole spectra with parametric values indicated in the figure. The Cole-Cole "fittings" are the solid curves and the arrows indicate the phase peaks for the fitted Cole-Cole spectra (0.0001 Hz and 0.00004 Hz). The generalized Cole-Cole fittings were made with a large (fixed) c value ($c_1=0.70$). The large c in the generalized Cole-Cole fitting moves the phase peak as close to the "measured" frequency range as possible (0.01 Hz and 0.001 Hz). The Figure 2.2.1.4-5 indicates that in the case of the flat phase spectrum (Cole-Cole $c_1=0.11$) the phase peak is at least one decade lower than the lowest measured frequency, and in the case of the spectrum with c value of 0.36 at least two and half decades lower.

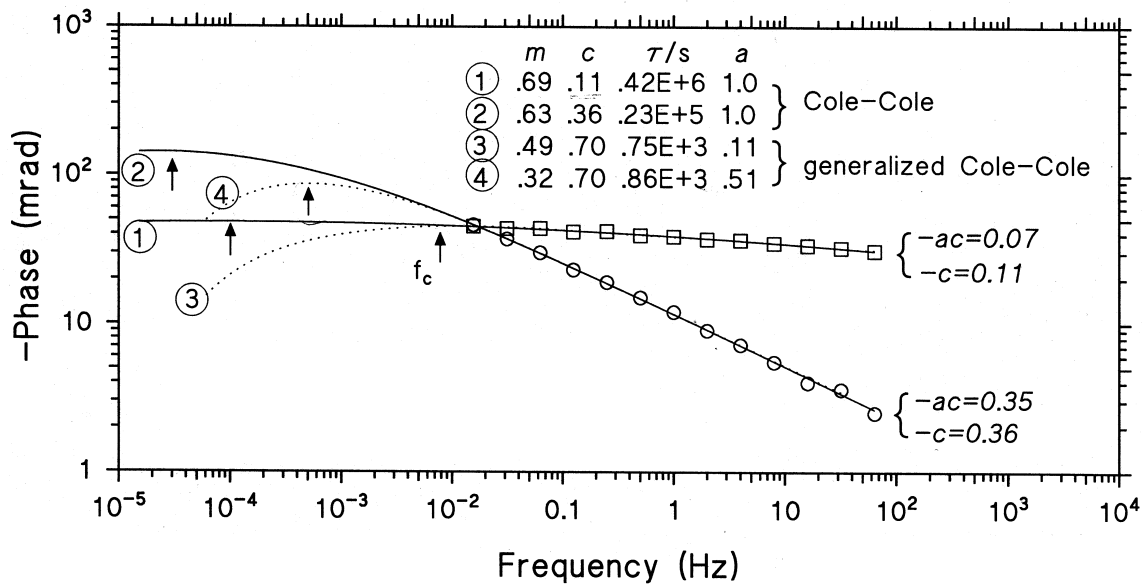


Fig. 2.2.1-18. The dependence of the inverted phase peak (arrows) on the shape of the measured phase spectrum (in the case when the measured spectrum has no phase peak).

2.2.5.3. Conclusion

The suitability and advantages of the generalized Cole-Cole model for parametrizing resistivity spectra of Ni ores and their host rocks was documented. The Cole-Cole model is today a standard mean to present the complex resistivity data, but it is reasonable to use the generalized model at least side by side the conventional model.

2.2.6. Field tests

The objective of the field measurements was to test and develop the SIP method in real exploration circumstances. A part of the test sites was well studied by drilling and field geophysical methods (e.g. Sika-aho, Kauniinlampi, Eko).

The field test sites and the measurements are presented in Table 2.2.1-1. In order to construct the electrical 2D models for the test areas multi-dipole (n=1-7) resistivity-IP soundings were conducted at each site. The SIP measurements were then directed to the most interesting locations. The electrical models of the targets and test areas also give the formation resistivities needed in grain-size calculations.

The field SIP measurements were conducted by the Phoenix IPV-5 receiver and IPT-1 transmitter. External preamplifier was used to minimise capacitive coupling effects. The receiver has 6 input channels, but only one was used to acquire as high-quality data as possible. The data processing technique was the same as in the laboratory studies, i.e., a product of two Cole-Cole spectra was fitted to the measured phase spectrum. The results are presented in terms of phase shift at 1 Hz frequency, Cole-Cole parameters and grain-size estimates.

The first step in a test area is to determine the response of overburden. Namely, it has been observed that common sediments can have phase spectra similar to apparent spectra of ore bodies. Figure 2.2.1-19 is an example of phase response of clay-till overburden at the Ylivieska test site.

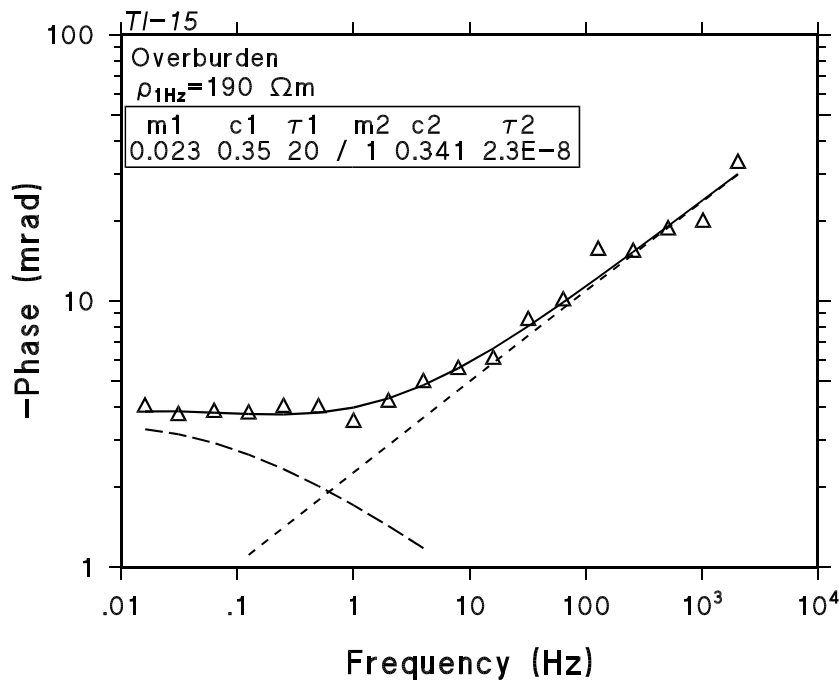


Fig. 2.2.1-19. Phase spectrum of clay-till overburden, Ylivieska.

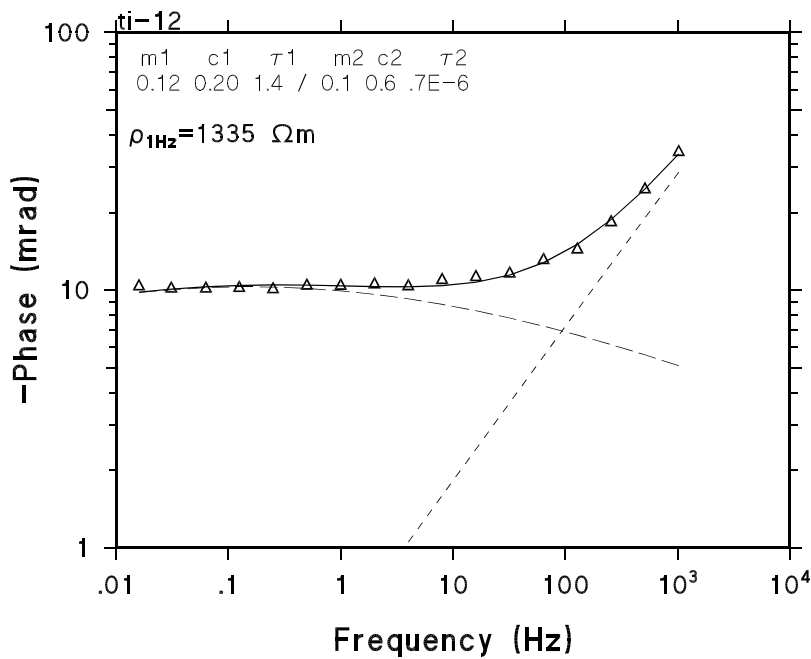


Fig. 2.2.1-20. Apparent phase spectrum of gabbro, Ylivieska (dipole-dipole, a=20 m, n=3).

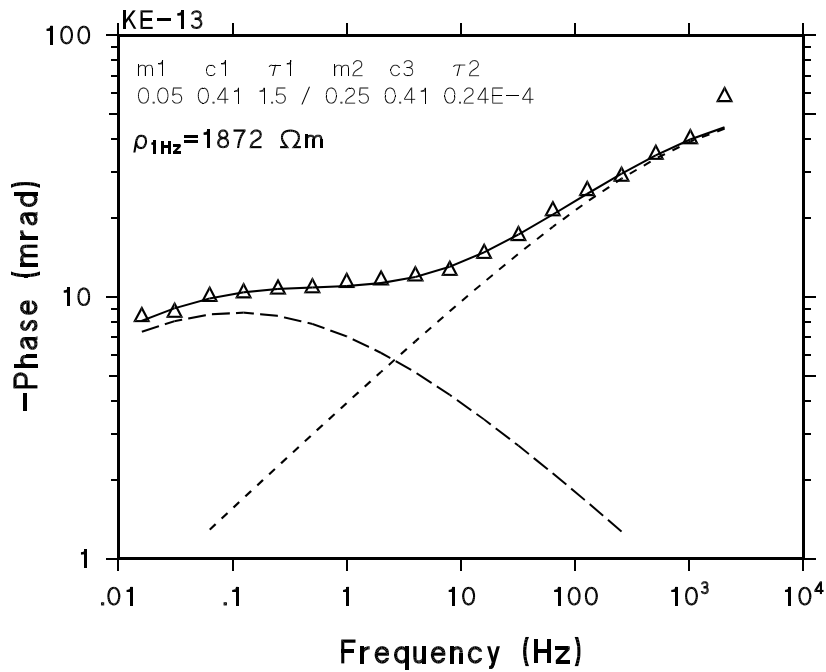


Fig. 2.2.1-21. Apparent phase spectrum of peridotite, Ylivieska (dipole-dipole, a=20 m, n=3)

A comparison between the spectrum of the overburden and the spectra shown in Figures 2.2.1-20 and 2.2.1-21 clearly indicates the importance to know what is the response from the overburden sediments. The low polarizability of the mineralized gabbro and peridotite is due to the conductive 50-10 meters thick clay-till overburden.

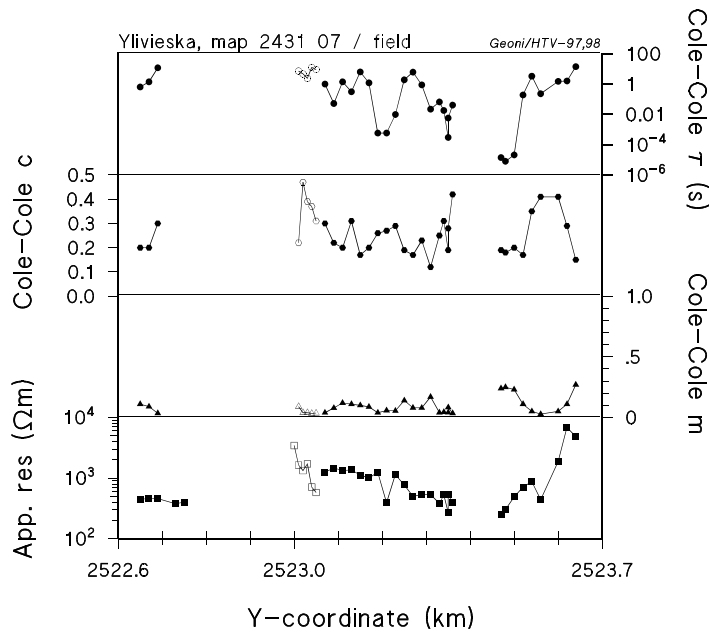


Fig.2.2.2-22. Spectral IP Field data from the Ylivieska test site.

Figure 2.2.1-22 shows the graphic form which is used at every test area. In sites where the geology is known, it is included to presentations. At the Ylivieska site the right end of the profile is gabbro, the middle and left part peridotite. At the area of peridotite the longer time constants are interpreted to contain weak sulphide dissemination.

A comparison between the laboratory and field results (Fig. 2.2.1-23) do, however, support any sulphide mineralization at the test profile.

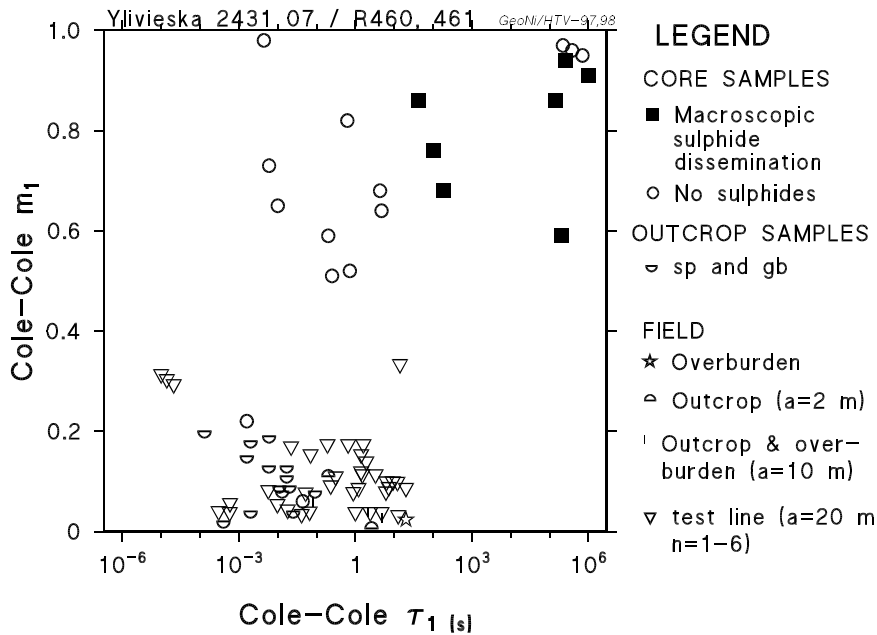


Fig. 2.2.2-23. Cole-Cole m versus Cole-Cole J, laboratory and data, Ylivieska test site.

Table 2.2.1-2. Electrical parameters from the Ylivieska test site.

Figure	Line	Tx	Rx	tx->rx	Resistivity (1Hz) (m)	phase (1Hz) (mrad)	Cole-Cole parameters				
Name	x-coord.	y-coord.	y-coord.	(m)			m ₁	c ₁	1 (s)	c ₂	2 (s)
ma-1	7104	2523.38	2523.34	60	392	-4.8	0.035	0.42	0.041	1	5.00e-06
ma-2	7104	2523.38	2523.32	80	533	-3.3	0.041	0.28	0.0003	1	6.00e-06
ma-3	7104	2523.36	2523.32	60	526	-4.4	0.044	0.31	0.018	1	7.00e-06
ma-4	7104	2523.36	2523.34	40	271	-5.5	0.083	0.19	0.0057	1	1.50e-06
ti-1	7104	2523.36	2523.3	80	382	-3.9	0.04	0.25	0.066	1	5.00e-06
ti-2	7104	2523.34	2523.28	60	535	-8.3	0.17	0.12	0.022	1	4.40e-06
ti-3	7104	2523.32	2523.26	80	532	-6.8	0.079	0.23	0.88	0.65	8.00e-07
ti-4	7104	2523.3	2523.24	80	502	-3.7	0.08	0.17	6.1	0.65	7.00e-07
ti-5	7104	2523.28	2523.22	80	774	-11.7	0.14	0.19	1.9	0.55	8.00e-07
ti-6	7104	2523.26	2523.2	80	1142	-3.4	0.055	0.29	0.0098	1	4.40e-06
ti-7	7104	2523.24	2523.18	80	392	-3.6	0.057	0.27	0.00059	1	3.70e-06
ti-8	7104	2523.22	2523.16	80	1252	-2.5	0.039	0.26	0.00058	1	2.60e-06
ti-9	7104	2523.2	2523.14	80	1002	-7.3	0.087	0.2	1.2	0.6	7.00e-07
ti-10	7104	2523.18	2523.12	80	1122	-7.1	0.1	0.17	6.3	0.55	3.00e-07
ti-11	7104	2523.16	2523.1	80	1367	-9.2	0.11	0.31	0.31	0.65	9.00e-07
ti-12	7104	2523.14	2523.08	80	1335	-10.4	0.12	0.2	1.4	0.6	7.00e-07
ti-13	7104	2523.12	2523.06	80	1465	-6.9	0.078	0.22	0.052	0.72	1.30e-06
ti-14	7104	2523.1	2523.04	80	1252	-4.9	0.039	0.3	1	0.81	6.40e-05
ti-15	7103.97	2523.05	2523.04	20	190	-3.5	0.023	0.35	20	0.34	2.30e-08
ke-1	7104	2522.78	2522.72	80	400	13.8					
ke-2	7104	2522.76	2522.7	80	377	4.2					
ke-3	7104	2522.72	2522.66	80	458	-4.8	0.035	0.3	11.8	0.45	5.50e-07
ke-4	7104	2522.7	2522.64	80	466	-9.5	0.09	0.2	1.4	0.53	1.80e-06
ke-5	7104	2522.68	2522.62	80	441	-10.5	0.11	0.2	0.64	0.57	2.70e-06
ke-6	7104	2523.5	2523.44	80	254	-8.6	0.24	0.19	0.000014	1	1.00e-06
ke-7	7104	2523.5	2523.46	80	304	-94.7	0.25	0.18	0.00001	1	4.00e-06
ke-8	7104	2523.52	2523.48	80	488	-9.2	0.23	0.2	0.000021	1	8.00e-06
ke-9	7104	2523.54	2523.5	80	709	7.8	0.11	0.17	0.00019	1	8.00e-07
ke-10	7104	2523.56	2523.52	80	872	-12.7	0.05	0.35	3.3	0.33	1.70e-04
ke-11	7104	2523.58	2523.54	80	440	-6.8	0.028	0.41	0.23	0.59	5.00e-04
ke-12	7104	2523.6	2523.56	80	2323	-10	0.09	0.29	0.07		
ke-13	7104	2523.62	2523.58	80	1872	-11.3	0.05	0.41	1.5	0.41	2.40e-05
ke-14	7104	2523.64	2523.6	80	6858	-16	0.11	0.29	1.6	0.54	2.60e-04
ke-15	7104	2523.66	2523.62	80	4836	-20.2	0.27	0.15	14	0.44	7.00e-07
		mid point of rx and tx									
to-1	7103.73	2523.23		20	151	-6.3	.05	.30	.08	.58	7.50e-07
to-2	7103.72	2523.22		20	661	-8.8	.03	.51	2.2	.49	3.80e-04
to-3	7103.71	2523.21		20	339	-7.1	.018	.63	4.8	.35	2.50e-05
to-4	7103.72	2523.2		2	1957	-22.9	.11	.46	.2	.8	1.00e-04
to-5	7103.72	2523.2		2	1400	-6.6	.006	1	2.6	.74	1.70e-03
to-6	7103.93	2523.05		40	579	-4.3	.036	0.31	9.2	.76	5.30e-04
to-7	7103.93	2523.04		60	709	-4.5	.033	.37	12.6	.51	3.60e-05
to-8	7103.93	2523.03		80	1715	-8.3	.039	.39	2.4	.39	2.80e-07
to-9	7103.93	2523.02		100	1329	-7.3	.039	.47	4.7	.44	5.70e-05
to-10	7103.93	2523.01		120	1638	-7.5	.089	.22	7.2	1	9.00e-02
to-11	7103.93	2523		140	3453	-11.1					

Table 2.2.1-2 shows the table form used at every test site

The results and conclusions of the field tests are presented in detail in separate reports (one per test site). It is difficult to give any general rule for the interpretation of field SIP data. The electrical SIP properties change from site to site and close co-operation with the local geologist is needed to utilise the SIP data completely.

2.2.7. References

Klein, J.D. and Sill, W.R., 1982. Electrical properties of artificial clay-bearing sandstone. *Geophysics*, 47, 1593-1605.

Pelton, W.H., Ward, S.H., Hallof, P.G., Sill, W.R. and Nelson, P.H., 1978. Mineral discrimination and removal of inductive coupling with multifrequency IP. *Geophysics*, 43, 588-609.

Raiche, A., Sugeng, F. and Xiong, Z., 1998: Final report for AMIRA project P223C full-domain EM modelling. CRC AMET - CSIRO Exploration & Mining, Mathematical Geophysics Group.

Sunde, E.D. 1949: Earth conduction effects in transmission systems. Van Nostrand.

Vanhala, H. and Peltoniemi, M., 1992. Spectral IP studies of Finnish ore prospects. *Geophysics*, 57, 1545-1555.

Vanhala, H. and Soininen, H., 1995. Laboratory technique for measurement of spectral IP responses of soil samples. *Geophysical prospecting*, 43, 655-676.

2.3. Task 2.2.2: Development of interpretation software for ground EM methods

2.3.1. INTRODUCTION

The objective of GeoNickel subtask 2.2.2 was to develop a fast and approximate interpretation program (EMPLATES) for the electromagnetic (EM) dipole-dipole measurements in frequency domain. The model used in the EMPLATES program consists of several more or less arbitrarily oriented rectangular thin conductors embedded in conductive halfspace. Multiple profiles and multiple frequencies can be handled simultaneously. Parameter optimization can be used to computationally find the best fit between the computed response and the measured data. The measurement systems considered in EMPLATES according to the project specifications are: the horizontal coplanar loop (i.e., Slingram) system (e.g., MaxMin), Sampo system (i.e., Gefinex 400S) and BRGM Melis system. The EMPLATES program is run on a PC under Windows NT/95 environment.

2.3.2. THEORY

2.3.2.1. Forward computation

The parameters of the plate model are illustrated in Fig. 2.2.2-1. A thin rectangular conductor is embedded in conductive, homogeneous halfspace. The orientation of the plate is defined by two rotation angles and the position of the plate is fixed to the center of the top side of the plate. Since a thin plate is considered, the effect of currents flowing in the thin direction of the plate are considered to be insignificant.

In order to simplify the theoretical concept, the quasi-static approximation has been used and the magnetic permeability is set to its free space value everywhere ($\mu = \mu_0$). These approximations mean that the effects of varying electric permittivity and magnetic permeability are not taken into consideration. In practice, the quasi-static approximation, which also neglects the effect of displacement currents, is justified when the measuring frequency is relatively low ($f < 10^5$ Hz).

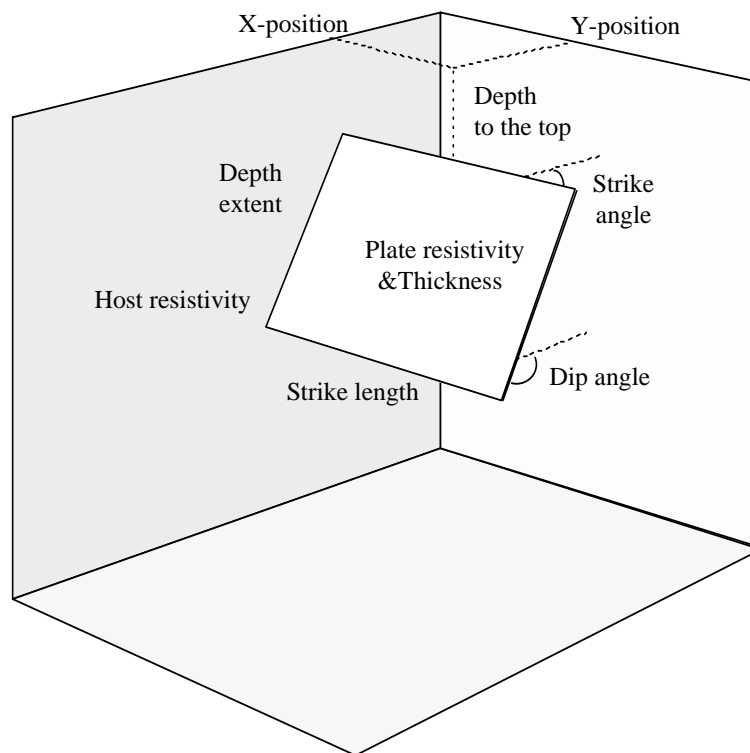


Fig. 2.2.2-1. The parameters of thin plate model.

The computational method is based on the integral equation method. The basic problem can be formulated as a Fredholm's integral equation of the second kind

$$\mathbf{E}(\mathbf{r}) - \int_V G(\mathbf{r}, \mathbf{r}') \cdot \mathbf{J}_s(\mathbf{r}') dV' = \mathbf{E}_i(\mathbf{r}) \quad , \quad (2.1)$$

where $\mathbf{E}(\mathbf{r})$ is the total electric field at the observation point \mathbf{r} , \mathbf{E}_i is the induced electric field generated by the transmitter, \mathbf{J}_s is the scattering current density inside the anomalous volume V' and $G(\mathbf{r}, \mathbf{r}')$ is the Green's function.

The approximate solution used in EMPLATES is based on a variant of surface integral equation method which has originally been presented by Kwan (1989). The idea is to replace the rectangular plate by a lattice structure composed of two dimensional (2-D) surface elements. An example of the lattice model representing the plate is shown in Fig. 2.2.2-2. When the plate is discretized into $n \times m$ loops, the total number of elements is $N = 2 \cdot m \cdot n + m + n$. In each element the current can flow in one direction only. Since the lattice structure forces the current to flow in the network of elements, it can natively describe both the inductive vortex currents and the more or less unidirectional current channeling from the conductive host through the plate.

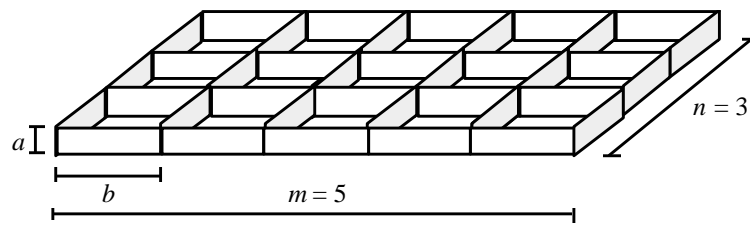


Fig. 2.2.2-2. A schematic view of the lattice model.

The lattice formulation reduces the volume integral equation into a 2-D surface integral equation, which is solved using the method of point collocation. In the discrete form of the equation for the total electric field at element m is:

$$\mathbf{E}_m - \sum_{n=1}^N [\Gamma_{mn} \cdot \mathbf{J}_{sn}] = \mathbf{E}_{im} \quad , \quad (2.2)$$

where Γ_{mn} are the discrete Green's functions between each collocation point. The equation above can be formulated as a matrix form

$$\mathbf{Z} \cdot \mathbf{J}_s = \mathbf{E}_i \quad , \quad (2.3)$$

where \mathbf{Z} is the so called impedance matrix ($N \times N$) the elements of which are

$$Z_{mn} = \frac{\delta_{mn}}{a(\sigma_0 - \sigma_p)} - \Gamma_{mn} \quad , \quad (2.4)$$

where δ_{mn} is the Kronecker's delta function and the denominator represents the anomalous conductivity-thickness product of the plate.

Approximate Green's functions

When the Green's functions for the impedance matrix are computed, the secondary contribution, i.e., the effect of the air-earth interface is not taken into account. This approximation is acceptable when the plate is buried deep. In addition, when determining the impedance matrix, the primary Green's functions are derived using the approximate quasi-static field equations of the electric field of an electric dipole in conductive wholospace (Kaufman & Keller, 1983).

The use of these approximate forms allows analytic solutions for the surface Green's functions to be computed. In addition, the complex Green's functions for the surface elements can be expressed as a sum of static (real) and inductive (imaginary) parts

$$\Gamma_{mn} = R_{mn} + iX_{mn} \quad , \quad (2.5)$$

where $i = \sqrt{-1}$. The static part is generated by line charge distributions at the two ends of the source element and the inductive part is generated by currents in the surface of the source element. When the local coordinate system is made such that plane $z = 0$ is in the center of the

plate and x - and y -axes span the plane of the plate, the approximate equations for an x -directed element are:

$$R_{mn}^{xx} = \frac{1}{4\pi\sigma_0} \left[\frac{xmd \cdot zmc}{xmy \cdot smzm} - \frac{xpd \cdot zmc}{xpy \cdot spzm} - \frac{xmd \cdot zpc}{xmy \cdot smzp} + \frac{xpd \cdot zpc}{xpy \cdot spzp} \right], \quad (2.6)$$

$$R_{mn}^{yx} = \frac{y}{4\pi\sigma_0} \left[-\frac{zmc}{xmy \cdot smzm} + \frac{zmc}{xpy \cdot spzm} + \frac{zpc}{xmy \cdot smzp} - \frac{zpc}{xpy \cdot spzp} \right], \quad (2.7)$$

$$R_{mn}^{zx} = \frac{1}{4\pi\sigma_0} \left[\frac{1}{smzm} - \frac{1}{spzm} - \frac{1}{smzp} + \frac{1}{spzp} \right], \quad (2.8)$$

$$\begin{aligned} X_{mn}^{xx} = \frac{\omega\mu_0}{4\pi} & \left[y \left[-\arctan \left[\frac{xmd \cdot zmc}{y \cdot smzm} \right] + \arctan \left[\frac{xpd \cdot zmc}{y \cdot spzm} \right] \right. \right. \\ & \left. \left. + \arctan \left[\frac{xmd \cdot zpc}{y \cdot smzp} \right] - \arctan \left[\frac{xpd \cdot zpc}{y \cdot spzp} \right] \right] \right. \\ & \left. - zmc \cdot \log \left[\frac{smzm - xmd}{spzm - xpd} \right] + zpc \cdot \log \left[\frac{smzp - xmd}{spzp - xpd} \right] \right. \\ & \left. + 2a \cdot \log \left[\frac{\sqrt{xmy + z^2} - xmd}{\sqrt{xpy + z^2} - xpd} \right] \right], \quad (2.9) \end{aligned}$$

$$X_{mn}^{yx} = \frac{\omega\mu_0 y}{4\pi} \left[\log \left[\frac{smzm - zmc}{smzp - zpc} \right] - \log \left[\frac{spzm - zmc}{spzp - zpc} \right] \right] \text{ and} \quad (2.10)$$

$$\begin{aligned} X_{mn}^{zx} = \frac{\omega\mu_0 y}{4\pi} & \left[xpd(smzm - spzp) - xmd(smzm - smzp) \right. \\ & \left. - zmy \cdot \log \left[\frac{smzm - zmc}{smzp - zpc} \right] + zpy \cdot \log \left[\frac{spzm - zmc}{spzp - zpc} \right] \right], \quad (2.11) \end{aligned}$$

where σ_0 is the conductivity of the host, ω is the angular frequency ($2\pi f$) and μ_0 is the magnetic permeability of the free space,

$$\begin{aligned} x &= x_m - x_n & xmd &= x - d & xmy &= xmd^2 + y^2 & smd &= \sqrt{xmy + c^2} \\ y &= y_m - y_n & xpd &= x + d & xpy &= xpd^2 + y^2 & spd &= \sqrt{xpy + c^2} \end{aligned},$$

where c and d are half of the thickness (a) and the length (b) of the source element, and

$$\begin{aligned} zmc &= (z_m - z_n) - c & smzm &= \sqrt{xmy + zmc^2} & smzp &= \sqrt{xmy + zpc^2} \\ zpc &= (z_m - z_n) + c & spzm &= \sqrt{xpy + zmc^2} & spzp &= \sqrt{xpy + zpc^2} \end{aligned}$$

The last term in Eq. 2.9 is an approximation, which is quite accurate, however. The components of the Green's functions for y-directed source element can be derived from the equations above simply by interchanging the x- and y-coordinates. Note, that since the plate is at plane $z = 0$, only the xx -, xy -, yx - and yy -elements are used in one plate model. For a multiplate model, all Green's functions between the elements of two plates are computed and rotated to the direction of the target element.

Halfspace Hankel transforms

Although the wholespace approximation is used for matrix elements, the effect of the air-earth interface is taken into account when the primary electric field generated by the transmitter and the secondary magnetic field at the receiver are computed. The equations of the electric and magnetic fields of a dipole sources have been presented by Ward & Hohmann (1988), for example. Therefore, only the Hankel transforms used in the EMPLATES program are presented in the following. In EMPLATES the transmitter is represented by a vertical magnetic dipole (VMD) in all the measurement systems considered. When the positive z-axis points downwards, the Hankel transform of the primary electric field inside the Earth in a cylindrical coordinate system is

$$g_{\phi}^{Ep} = \int_0^{\infty} \frac{2\lambda}{\lambda + u_1} e^{-u_1 z} e^{-\lambda h} \lambda J_1(\lambda \rho) d\lambda \quad (2.12)$$

where ρ is the radial distance between the source $(0,0,-h)$ and the computation point (x,y,z) , $J_1(\lambda \rho)$ is Bessel's function of the first order and $u_1 = \sqrt{\lambda^2 - k_1^2}$, where the wave number, k , under quasi-static approximation is defined as $k_1^2 = -i\omega\mu_0\sigma_0$.

In EMPLATES the source and the receiver are always at the same height above or on the surface of the Earth. The two Hankel transforms which are needed to evaluate the radial and vertical component of the primary magnetic field generated by a VMD at the receiver position are

$$g_{\rho}^{Hp} = \int_0^{\infty} \frac{\lambda - u_1}{\lambda + u_1} e^{\lambda(z-h)} \lambda^2 J_1(\lambda \rho) d\lambda \quad \text{and} \quad (2.13)$$

$$g_z^{Hp} = \int_0^{\infty} \frac{\lambda - u_1}{\lambda + u_1} e^{\lambda(z-h)} \lambda^2 J_0(\lambda \rho) d\lambda \quad (2.14)$$

After the matrix equation has been solved, the secondary magnetic field at the receiver is computed using each element as an electric dipole with its dipole moment proportional to the surface current density at the element. The Hankel transforms that are needed to compute the

radial and vertical magnetic field at the receiver position above the ground due to a x-directed horizontal electric dipole embedded in the conductive medium are

$$g_z^{Hs} = \int_0^{\infty} \frac{2\lambda}{\lambda + u_1} e^{-u_1 z} e^{-\lambda h} \lambda J_1(\lambda \rho) d\lambda , \quad (2.15)$$

$$g_{\rho 1}^{Hs} = \int_0^{\infty} \frac{2\lambda}{\lambda + u_1} e^{-u_1 z} e^{-\lambda h} \lambda J_0(\lambda \rho) d\lambda \text{ and} \quad (2.16)$$

$$g_{\rho 2}^{Hs} = \int_0^{\infty} \frac{2\lambda}{\lambda + u_1} e^{-u_1 z} e^{-\lambda h} J_1(\lambda \rho) d\lambda . \quad (2.17)$$

Because of the reciprocity of EM field components, the Hankel transforms in equations 2.12 and 2.15 are the same. In addition, if a horizontal magnetic dipole was used as a source, equations 2.16 and 2.17 would be used to compute the primary electric field.

In EMPLATES the direct computation of Hankel transforms is made using the convolution algorithm developed by Anderson (1983). In order to reduce the computational costs, EMPLATES uses 2-D interpolation of pre-computed Hankel transform tables. When the loop height is zero and the all distances are normalized by the host skin depth, the Hankel transforms in equations 2.15-2.17 can be made independent of host conductivity and frequency. Therefore, only one Hankel transform table file is needed to cover the range of typical host skin depth values.

2.3.2.2 Parameter optimization

The parameter optimization is based on the linearized inversion method. The method used in the EMPLATES is based on the papers by Jupp and Vozoff (1975), Hohmann and Raiche (1988) and Pirttijärvi et al. (1998). The linearized inversion is based on the determination of the partial derivative matrix, i.e., the Jacobian matrix. In EMPLATES the partial derivatives are computed numerically using a forward difference scheme. Parameter steps that reduce the error between the computed and the measured data are computed using the singular value decomposition (SVD) of the Jacobian matrix. A special adaptive damping method is used to stabilize and improve the convergence. In EMPLATES the user must control the iterative parameter optimization process, since it is not implemented as an automatic inversion method.

The objective is to minimize the difference between observed data $\mathbf{d} = (d_1, d_2, \dots, d_N)$ and modeled data $\mathbf{f} = (f_1, f_2, \dots, f_N)$ by adjusting the model parameters $\mathbf{p} = (p_1, p_2, \dots, p_M)$ iteratively. Here N is the number of data values and M is the number of free parameters. In the present problem, N is the sum of the product of the number of profiles and the number of points on each profile multiplied by the number of frequencies. For each iteration parameters steps $\delta \mathbf{p}$ are computed such that the new model $\mathbf{p}^{l+1} = \mathbf{p}^l + \delta \mathbf{p}$ will reduce the error. When singular value decomposition (SVD) is used, the inverse solution for parameter steps $\delta \mathbf{p}$ is

$$\delta \mathbf{p} = \mathbf{V} \mathbf{\Lambda}^{-1} \mathbf{U}^T \mathbf{e} , \quad (2.18)$$

where $\mathbf{e} = (\mathbf{d} - \mathbf{f})$ is the difference between the observed data and the model data. The singular value decomposition, which is made on the Jacobian matrix J is defined as

$$J = U\Lambda V^T, \quad (2.19)$$

where U is an orthogonal $N \times M$ matrix, V is an orthogonal $M \times M$ matrix and Λ is a $M \times M$ diagonal matrix the elements of which are known as singular values. The columns of matrices U and V are known as data and parameter eigenvectors, respectively. The elements of the Jacobian matrix are

$$J_{ij} = \frac{\partial f_i}{\partial p_j}, \quad (2.20)$$

where $i = 1, 2, \dots, N$ and $j = 1, 2, \dots, M$.

To reduce the effects of amplitude variations, the data channels are normalized by their maximums and scaled by using the 10-base logarithm. Since the objective is to allow fast computation, the partial derivatives are computed using the forward difference scheme. Therefore, the evaluation of one column of the Jacobian for one parameter requires one forward computation and the computation of the error requires one additional forward computation. Thus, $p+1$ forward computations are needed to optimize p parameters. Therefore, to reduce the computation time during optimization the discretization should be kept rather coarse and only few frequencies should be used. Good estimates for the position and the orientation of the model plate are likely to be found even with coarse discretization.

Adaptive damping

To make the inversion more stable, the elements of the A^{-1} matrix in Eq. (2.18) are multiplied by damping factors t_j

$$t_j = \frac{s_j^4}{s_j^4 + \mu^4}, \quad (2.21)$$

where $s_j = \lambda_j / \lambda_{max}$ are the normalized singular values and μ is the relative singular value threshold. In the beginning of inversion the least important parameters will be damped and only the most important parameters will get optimized. For the final model all the damping factors should be as close to one as possible.

The problem with undamped inversion is that close to the minimum one or several parameters tend to oscillate. Strong damping, on the other hand, usually leads to small parameter steps and slow convergence. Therefore, the problem is the choice of the threshold value. In the method used in EMPLATES each parameter has a maximum step and initially the threshold is given the minimum value. When new parameter steps are solved from Eq. (2.18), they are compared to these maximum steps. If some parameter step is outside its bounds, the threshold is increased and new parameter steps are computed. This procedure is continued until all the steps are within the allowed range or the maximum threshold value is reached. In the latter

case the parameter step is given its maximum value. The use of maximum steps is generally faster than the conventional Marquardt scheme, since no additional forward computations are needed.

To further improve the inversion performance an additional enhancement is made. The maximum steps are redefined as a function of the threshold value. The maximum steps are large in the beginning of the inversion to allow fast convergence, while closer to the solution they are reduced to damp oscillations. In the present method, when the threshold is at its minimum, the maximum steps are 1/10 of the value that they have when the threshold is at its maximum.

The quality of the fit is based on the visual fit between the two responses and the noise-to-signal ratio (NSR) and standard error $\hat{\sigma}$ (STD), which are defined as (Hohmann and Raiche, 1988)

$$\hat{\sigma} = \left[\frac{1}{N-M} \sum_{i=1}^N (d_i - f_i)^2 \right]^{\frac{1}{2}} \quad (2.22)$$

and

$$NSR = \frac{\hat{\sigma}}{\left[\frac{1}{N-1} \sum_{i=1}^N (f_i - \bar{f})^2 \right]^{\frac{1}{2}}} \quad (2.23)$$

where \bar{f} is the mean of all computed data values. For both the standard error and the NSR a value of few percents usually implies good fit between the modeled and measured data (Hohmann and Raiche, 1988).

2.3.3 THE EMPLATES PROGRAM

The EMPLATES program can be used either for forward modeling or interpretation of measured data. The forward modeling can be used to study the theoretical behavior of EM responses. However, the main objective of the EMPLATES program is in its use in the interpretation of field data. Interpretation is made by fitting the computed data with the measured response by changing the model parameters. Parameter optimization can be used to find the best fitting model in an automated way. In this chapter, the various components of the EMPLATES program will be briefly discussed. The EMPLATES User's Manual is intended for more detailed information about the program usage.

2.3.3.1 Model parameters

The parameters of the plate model are illustrated in Fig. 2.2.2-3. In EMPLATES a rectangular coordinate system is used, where the positive x -axis points to the East and the positive y -axis points to the North. The positive z -axis points downwards and the plane $z = 0$ represents the surface of the Earth. The plate model has two rotation angles: dip and azimuth. Therefore, one side of the plate is always parallel to the Earth's surface. The location of the plate is defined by the center of the upper edge of the plate.

Fig. 2.2.2-3 shows the “Model parameters” dialog box used in EMPLATES and the table below it lists the parameters. The length of the plate the same as the strike length of the plate and the azimuth is the same as the strike direction of the plate. The resistivity of the plate must be greater than the resistivity of the host. The dip must be between 0 and 180 degrees and the azimuth must be between -180 and 180 degrees. When the azimuth is zero, the horizontal side of the plate is parallel to x-axis. When the dip angle is 90 degrees, the plate is vertical. When both the azimuth and dip angle are zero the dipping side of the plate points towards the positive y-axis (North).

Fig. 2.2.2-3. The “Model parameters” dialog box.

Parameters:

P-res.	Resistivity of the plate (Ωm)
Thick.	Thickness of the plate (m)
X-pos.	X-coordinate of the plate position (m)
Y-pos.	Y-coordinate of the plate position (m)
Depth	Z-coordinate of the plate position, i.e., the depth of burial (m)
Dip	Dip angle from xy-plane(deg.)
Azim.	Azimuth angle from x-axis (deg.)
Length	Length of the plate along the horizontal side of the plate (m)
Height	Height of the plate along the dipping side of the plate (m)
Discr.	Discretization in the horizontal and dipping direction of the plate
H-res.	Resistivity of the host medium (Ωm)

The computational method requires that the elements are equally long in the two orthogonal directions. Therefore, either the height or the strike length of the plate is computed automatically. By default the height is computed using the strike length and the element length. The element length, on the other hand, is the strike length divided by the horizontal discretization. The shape of the plate is, therefore, defined by the discretization.

2.3.3.2 System parameters

Fig. 2.2.2-4 shows the “System parameters” dialog box. The EMPLATES program is developed for three measurement systems. The first is the Slingram system (i.e., the

horizontal coplanar loop, HCPL) system. In the Slingram system the transmitter is a vertical magnetic dipole and the response is the real (in-phase) and imaginary (quadrature) component of the normalized vertical magnetic field. The second is the Finnish Sampo frequency sounding system (Gefinex 400 S). In this system the transmitter is a vertical magnetic dipole and the response is the amplitude and the phase of the ratio between the vertical and radial magnetic field. The third is the French BRGM Melis system, which is similar to the Sampo system, except that the transmitter position is fixed. Therefore, the Melis system is a combination of a frequency and a geometric sounding system. By the aid of a transformation table, the quadrature component of the ratio of measured radial and vertical magnetic field is automatically converted to apparent resistivity. The second response component, although seldom used, is the phase of the ratio of radial and vertical magnetic field.

The scaling and normalization affect only the Slingram system, in which the response is presented either as plain numbers or as percentage or as parts per million. There are two ways to normalize the response. The first one defines the response as the ratio H_s/H_0 , where H_s is the vertical magnetic field generated by the plate model alone and H_0 is the free-space vertical secondary magnetic field generated by the source dipole. According to this normalization the response is zero far from the conductor. The second normalization method defines the response as the ratio $(H_s+H_p)/H_0$, where H_p is the vertical magnetic field due to the halfspace. According to this definition, far from the conductor the response is the normalized response of the halfspace. The latter normalization is commonly used in practice, while the first one is sometimes useful in theoretical modeling.

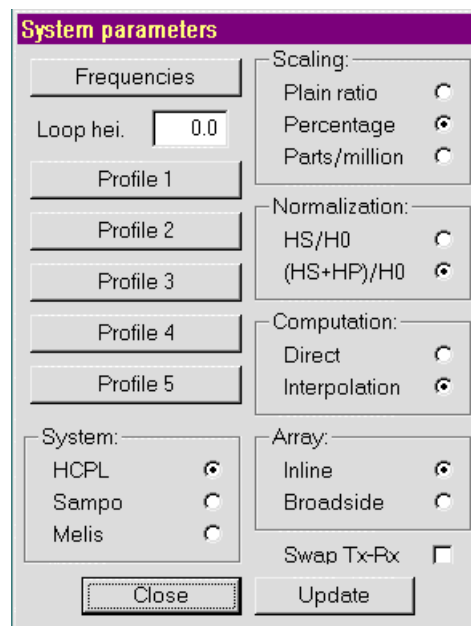


Fig. 2.2.2-4. The “System parameters” dialog box.

For the Slingram and Sampo systems the measurement array is either in-line or broadside. In in-line array the line connecting the transmitter and the receiver is along the profile line, whereas in broadside array they are connected perpendicularly to the direction of the profile.

The position of the transmitter (Tx) and the receiver (Rx) can also be interchanged. By default, in in-line array the transmitter is behind the receiver. In broadside array the

transmitter is to the left of the receiver when looking towards the direction of the profile. This option, on the other hand, has effect only in the Sampo system.

The computation can be performed in two ways. In the first one, the Hankel transforms, which are needed to compute the primary and secondary halfspace fields, are computed using direct filtering methods. In the second one, Hankel transforms are computed using 2-D interpolation (bicubic spline) of a pre-computed Hankel transform table. The second method is faster than the first one. The transform table has been computed using skin depth normalization. Therefore, the interpolation can be used only if the transmitter and receiver are at the surface.

The “Frequencies”-button in the “System parameters”-dialog brings up a dialog which is used to define and include and exclude frequencies from the computation. Up to ten frequencies can be used simultaneously in the computation. Similarly, the “Profile 1-5”-buttons bring up a dialog which is used to define the parameters of each profiles. The maximum number of profiles is five. Each profile is defined by the x- and y-coordinates of its beginning and end. To avoid unnecessary computation, it is also possible to pick a section from the profile by defining the first and the last points of this section measured as the distance from the beginning of the profile.

For the Slingram and Sampo systems the distance between the transmitter and receiver dipoles, i.e., the loop spacing must be defined. In the Melis system the loop spacing defines the offset, i.e., the distance of the first profile point from the center of the transmitter loop. In EEMPLATES the computation is made at constant point interval, whereas the data can have gaps in it.

2.3.3.3 Optimization

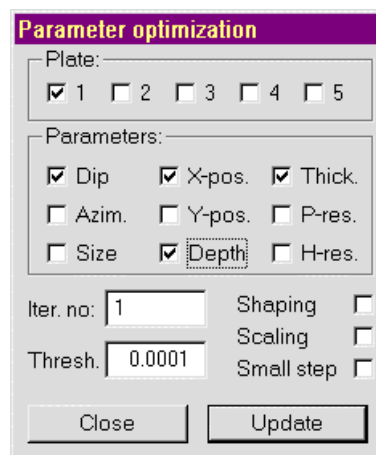


Fig. 2.2.2-5. The “Parameter optimization” dialog box.

Fig. 2.2.2-5 shows the “Parameter optimization” dialog box. The five check boxes near the top of the dialog are used to select the plate or plates for optimization. The nine check boxes in the middle of the dialog are used to select which parameters are used in the optimization. Except for the size of the plate, the parameters are the same as in the “Model parameters”-dialog. Since the strike length and plate height are connected with each other, the

optimization affects them both. Therefore, it is actually the size of the plate which is being optimized.

The two user supplied parameters are the number of iterations and the relative singular value threshold (Eq. 2.21). Usually the threshold can be kept at its default value (0.0001). If problems, such as oscillations in the solution, were to occur, the threshold should be increased to force stronger damping.

The optimization makes use of an heuristic algorithm to determine the shape of the plate. The shaping method varies the discretization and the shape of the plate with large steps and the resulting shape is the one that produces the smallest error. Since the strike length and the height of the plate are coupled, this is the only way to change the shape of the plate.

An alternative method can be used to scale the measured and computed response so that the effect of the differences in the amplitude of various frequency channels is minimized. This method allows the low frequency response to have more importance since each data value is given almost equal weight. The size of the maximum steps which are used to define the optimal damping factors can also be redefined. This method is used to stabilize the optimization.

It is not practical to optimize all the parameters at the same time because of the increased computation time. In the beginning of the optimization only the most important parameters, should be used in the optimization. The least important parameters, such as plate size and azimuth, should be included into the optimization only after the other parameters have been resolved reasonably well. Since the host resistivity is often the most insensitive parameter, it should be optimized alone.

2.3.3.4 Data formats

Before interpretation of measured data can be started, the data must be read into the program. Generalized Geosoft XYZ-format is supported for Slingram and Sampo system data. The Geosoft XYZ-files are simple column-formatted ASCII text files. The first and the second column contain the x- and y-coordinates of each measurement point on the profile. The third and the fourth column contain the response (eg., Slingram's in-phase and quadrature) at the first frequency. The fifth and the sixth column contain the response at the second frequency, etc. The slash-character (/) is used to denote a comment line and multiple profiles are separated either by a LINE-directive or by an empty line.

The Melis system uses a data format of its own, and most of the system parameters are read from the file automatically. Unlike an XYZ-file, an FEM-file contains only one profile. Since an FEM-file does not contain any geographic co-ordinates, EMPLATES will automatically place the transmitter at the origo (x,y = 0,0) and the measurement profile is made along the x-axis.

2.3.3.5 Window components

The two graph windows in the EMPLATES program contain the map/projection view and the response graph. Examples of these windows are shown in Figs. 2.2.2-6 and 2.2.2-7. In the map/projection view, the model geometry, i.e., the profile and plate projection can be

visualized either as a planar map view or as a vertical depth section under current measurement profile.

The map/projection window supports interactive interface for model editing. In the map view a double click with the right mouse button can be used to redefine either the position of the center of the top side of the current plate, the size and the azimuth, or the dip angle of the plate. When changing the size, the aspect ratio of the plate is not altered. In the projection view the mouse can also be used to redefine the depth to the top of the plate and the position of the plate along a line parallel to the current profile.

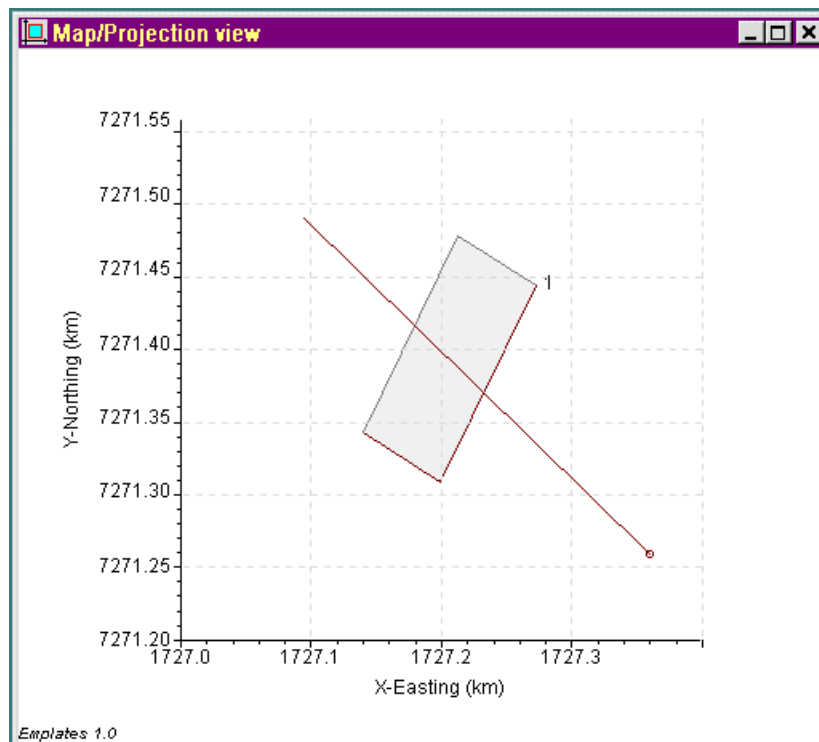


Fig. 2.2.2-6. The "Map/Projection view" window.

Fig. 2.2.2-7 is an example of the response graph for the in-line Slingram system. The measured data is shown by symbols and the computed response is shown by lines. The profile coordinates and the frequency are shown automatically in the graph title. The graph window shows the response of one profile at one frequency. Toolbar buttons (P1-P5 and F1-F0) can be used to change the profile and frequency. In addition, it is possible to include and exclude response components to and from the graph. For example, only the in-phase component of the Slingram response could be visualized. The component selection affects also the optimization; if the channel is excluded from the graph it is excluded from the inversion as well.

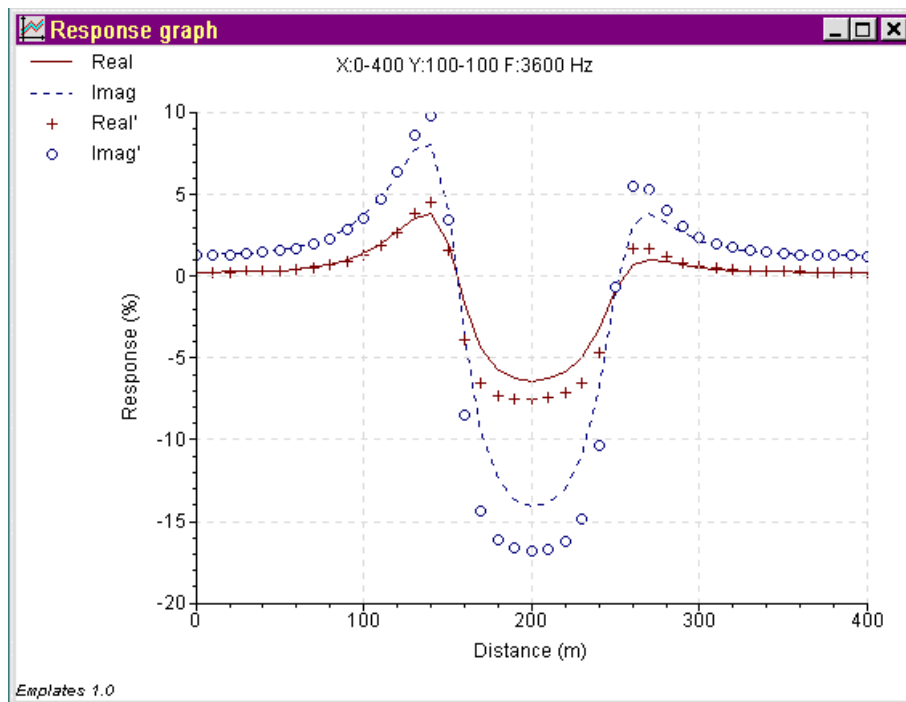


Fig. 2.2.2-7. The “Response graph” window.

2.3.4. JOINT INVERSION OF EM AND MAGNETIC DATA

A well known fact is that the magnetic susceptibility can have large impact on the EM response. As a part of subtask 2.2.2 the magnetic effects were studied. It was found that incorporating the magnetic permeability into the EMPLATES computation would have required a completely new theoretical formulation. Since such a task would have been beyond the scope of subtask 2.2.2, an approximate study was made instead. In the experiment the joint interpretation of electromagnetic and static magnetic field data was studied using the SVD-analysis.

In practice, the inversion code of EMPLATES was modified for the magnetic field data. The algorithm of Hjelt (1972) was modified to compute the forward solution for the magnetic anomaly of a plate-like body. Since the magnetic effects are not taken into account in EMPLATES, the joint interpretation is acceptable only when the susceptibility of the target is not very strong.

The parameters of the model considered in these tests are shown in Table 2.2.2-1. The profile is considered to be along N-S direction (y-axis) and the plate is dipping towards north. Since data is from one profile, the x-position and azimuth of the plate are fixed during the inversion. The x-position is such that the center of the top of the plate is directly below the center of the profile and the azimuth is such that the plate is perpendicular to the profile. Slingram system is used, where the loop spacing is 100 m and the frequencies used are: 3600, 7200 and 14400 Hz. Fig. 2.2.2-8a shows the Slingram response at the frequency of 7200 Hz and Fig. 2.2.2-8b shows its magnetic anomaly.

Table 2.2.2-1

P-res.	1	(Ω m)	H-res.	5000	(Ω m)
Thick.	5	(m)	X-pos.	0	(m)
Y-pos.	0	(m)	Depth	20	(m)
Length	100	(m)	Height	100	(m)
Dip	60	(deg.)	Azim.	90	(deg.)
Susc.	.5	(SI)	T0	52000	(nT)
Incl.	75	(deg.)	Decl.	-5	(deg.)

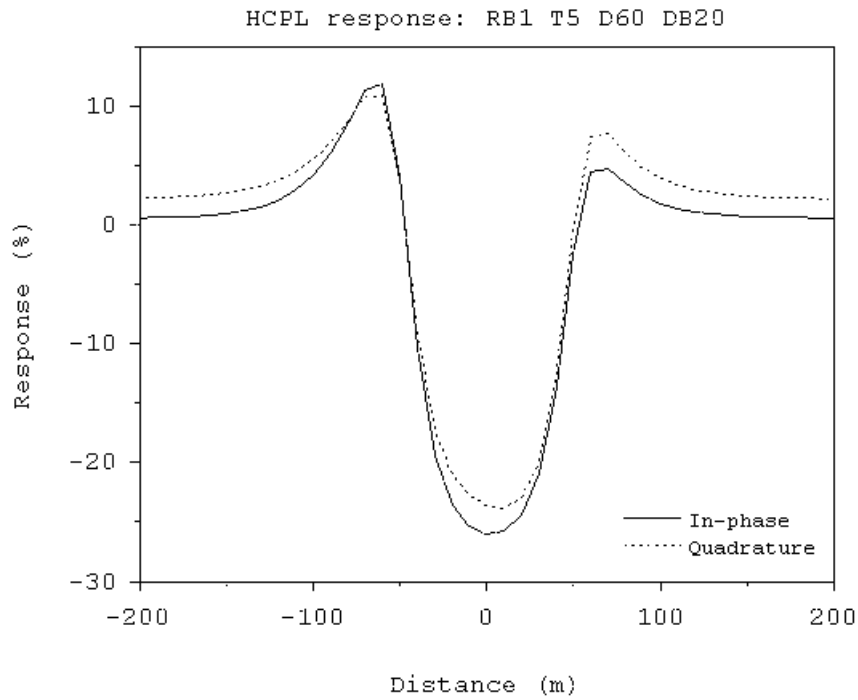


Fig. 2.2.2-8a. Slingram response of a dipping plate model (cf. Table 2.2.2-1) at the frequency of 7200 Hz.

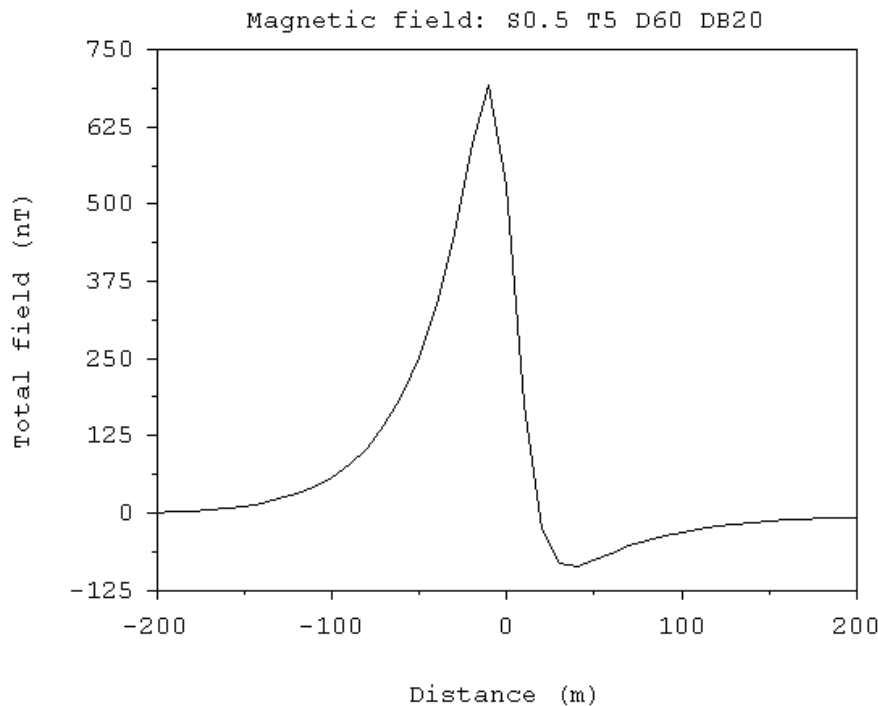


Fig. 2.2.2-8b. The magnetic anomaly of a dipping plate model (cf. Table 2.2.2-1).

Fig 2.2.2-9 shows the parameter eigenvectors for the tested model. The parameter eigenvectors are from top to bottom in the order of decreasing singular values. The normalized singular values (NSV1-7) are shown above each parameter eigenvector and the absolute value of the biggest singular value is displayed inside brackets above the first parameter vector. Fig. 2.2.2-9 shows that the most important parameter is the resistivity of the plate (RB), which is correlated with the thickness of the plate (T). The second most important parameter is the susceptibility of the plate (SU). The third is the depth of burial (DB), which is also correlated with the thickness of the plate. The fourth is the position of the plate along the profile (y-position, YP), The fifth and the sixth eigenvectors are combinations of dip angle (D), depth of burial and plate thickness. The least important parameter is the size of the plate (strike length, SL).

To observe that the plate resistivity and thickness are correlated is not surprising. Similarly, the poor interpretability of the plate size can be expected. On the other hand, to see that plate dip angle is quite difficult to interpret is a bit surprising. In addition, it is interesting to observe that plate susceptibility is not correlated with other parameters and the plate thickness is correlated with so many parameters.

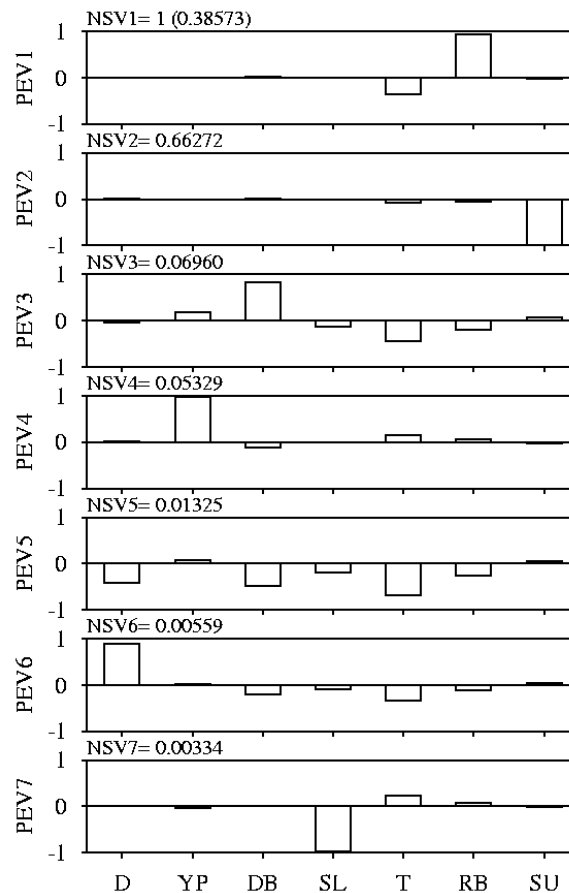


Fig. 2.2.2-9. Parameter eigenvectors and normalized singular values derived from the combined EM and magnetic field data.

One should, however, note that the results mentioned above are valid for this particular model only. The effects of varying model parameters was studied with several additional models. The experiments showed, that the order importance of parameters and the relative size of the singular values varies considerably between different models. For example, increasing the plate resistivity would make it the least important parameter and the plate thickness would be the most important. In addition, decreasing the susceptibility would make it the most important parameter and the relative size of the other singular values would decrease drastically. In practice, this would mean strong decrease in the performance of inversion. This indicates that when joint inversion is applied, special attention must be paid on the scaling and weighting of the two data sets. On the other hand, it also suggests that the parameters should be scaled as well. The simplest scaling would be to use the 10-base logarithm of the parameters.

2.3.5. Conclusion on task 2.2.2

The key elements of the forward computation are the capability to model multiple, more or less arbitrarily oriented thin conductors embedded in conductive host medium, the suitability for microcomputer environment and the capability to handle large conductivity contrasts as well as multiple profiles and frequencies. The parameter optimization enables automated

fitting of the measured and computed data. The method is based on the linearized inversion method, in which a special adaptive damping method is used to speed up the optimization process. The user interface of the program is developed for Windows 95 environment, which allows easy access to parameters and graphical views of the response and the model geometry.

The basic tests indicate that EMPLATES is capable of modeling the behavior of the EM response of a plate model in general. However, the model and the many approximations used in the EMPLATES give rise to several limitations on the applicability of the program. First of all, since only halfspace model is considered, it may be difficult to interpret more complicated geological targets, especially when dealing with multifrequency data. Secondly, the number of elements, i.e., the dimension of the linear system should not become too large. The number of elements that allows practical computation time for interactive work depends mainly on the hardware at hand. Because of this demand, the size of the model plate should not be larger than what is necessary. To model a "large plate" it is enough to have the its size 3×2 times the loop spacing in horizontal and vertical direction. In addition, as a "rule of thumb", the length of the elements should be less than the depth to the top of the plate. This, on the other hand, means that it is difficult to model a large plate close to the surface with sufficient accuracy. Both this and the tendency of EMPLATES to generate maximum currents at plate boundaries makes the depth of burial over estimated for a steeply dipping plate. Furthermore, it must be noted that denser discretization is required to model a horizontal or a gently dipping plate. On the whole, the interpretation of plate position and orientation can be made using coarse discretization which enables fast computation.

The most important restriction concerns the plate thickness and resistivity, the interpreted values of which, although most useful qualitatively, do not directly represent their true physical values. Most likely, this is because the lattice model is different from true three-dimensional model. As a general rule, the plate thickness should be fixed during optimization, which is advantageous also because of the strong coupling between these two parameters. The plate resistivity thus found during optimization is likely to be under estimated (too small) if the plate is very thin and over estimated if the plate is thick. As for the resistivity of the host, there appears to be no restrictions - a wide range of practical host resistivity values can be used in the modelling. However, the more conductive the host is, the denser the discretization should be. As a whole, the EMPLATES program suits for fast and approximate interpretation of data consisting of multiple profiles and frequencies using a model that consists of multiple plate-like conductors embedded in conductive homogeneous halfspace.

There are several ways to improve the EMPLATES software. As mentioned before, including conductive overburden in the computation would be advantageous especially when interpreting data from measurements with wide frequency range (e.g., Sampo and Melis). Furthermore, the interface and the computational method of the EMPLATES program could also be extended for other measurement systems. For example, borehole measurements could easily be modelled if the effect of the surface of the Earth would be neglected, i.e., a conductive wholespace would be considered. As discussed before, great computational savings would be obtained if the lattice elements could be of variable length. In addition, since the solution of the linear equation is the most time consuming task, the use of more advanced algorithms for solving the matrix equation could be of great importance as well.

Finally, since the computational method used in EMPLATES is only approximate, it would be intriguing to add interface for another, more accurate numerical algorithm. The model found after fast EMPLATES optimization would be the initial model for the more accurate computational method. This would enable more precise interpretation of the plate parameters and considerable savings in the total time required for the interpretation.

2.3.6. References

- Anderson, W.L., 1984: Fast Hankel transforms using related and lagged convolutions. *ACM Trans. on Math. Software*, 8, 344-368.
- Hanneson, J.E. and West, G.F., 1984: The horizontal loop electromagnetic response of a thin plate in a conductive earth: Part II - Computational results and examples, *Geophysics*, 49, 421-432.
- Hjelt, S.-E., 1972: Magnetostatic anomalies of dipping prisms, *Geoexploration*, 10, 239-254.
- Hohmann, G.W. and Raiche, A.P., 1988: Inversion of controlled source electromagnetic data. In Nabighian, M.N. (Editor), *Electromagnetic methods in applied geophysics, Volume I, Theory, Soc. Expl. Geophys.*.
- Jupp, D.L. and Vozoff, K., 1975: Stable iterative methods for inversion of geophysical data. *Geophys. J. R. astr. Soc.*, 42, 957-976.
- Kaufmann, A. and Keller, G., 1983: *Frequency and transient soundings*. Elsevier.
- Kwan, C.H., 1989: A novel method of computing the EM response of a conducting plate in conductive medium. *Research in Appl. Geophys.*, No: 45. Dept. of Physics, University of Toronto.
- Pirttijärvi, M. and Hjelt, S.-E., 1993: *Microcomputers in ore prospecting, Final report*. (in Finnish) Department of Geophysics, University of Oulu.
- Pirttijärvi, M., Verma, S.K. and Hjelt, S.-E., 1998: Inversion of transient electromagnetic profile data using conductive finite plate model. *J. of Appl. Geoph.*, 38, 181-194.
- Press, W.H., Flannery, B.P., Teukolsky, S.A. and Vetterling, W.T., 1988. *Numerical recipes, the art of scientific computing*. Cambridge University Press.
- Wait, James R., 1982: *Geo-Electromagnetism*. Academic Press, New York.
- Ward, S.H. and Hohmann, G.W., 1988: *Electromagnetic theory for geophysical applications. Inversion of controlled source electromagnetic data*. In Nabighian, M.N. (Editor), *Electromagnetic methods in applied geophysics, Volume I, Theory, Soc. Expl. Geophys.*.
- Xiong, Z., 1992: *Electromagnetic modeling of three-dimensional structures by the method of system iteration using integral equations*. *Geophysics*, 57, 1556-1561.

2.3.7. Annexes

Products

An interactive interpretation program (*EMPLATES*) has been developed for the ground electromagnetic (EM) dipole-dipole measurement systems operated in frequency domain (Slingram, Sampo and Melis). The *EMPLATES* program combines an approximate forward computation with an automatic optimization and an user friendly interface

Reports

Development of interpretation software for ground EM methods. FINAL REPORT, GeoNickel / WP2 / Subtask 2.2.2. Outokumpu Mining Oy, Subcontracted by Markku Pirttijärvi & Sven-Erik Hjelt, Department of Geophysics, University of Oulu , Finland, 1996 – 1998, pp 91.

Publications / presentations

Markku Pirttijärvi, Sven-Erik Hjelt, Aimo Hattula and Risto Pietilä, 1999: Modeling and inversion of electromagnetic data using approximate plate model, to be held at EAGE Helsinki'99 conference.

2.4. Tasks 2.2.3-2.2.6: Geophysical methodology for lateritic Nickel ores

2.4.1. Introduction

Geophysics is a powerful tool in exploration for base metals . Greek Lateritic FeNi deposits possess, in most cases, physical parameters that significantly differ from those of their host rocks (density ,magnetic susceptibility ,resistivity ,chargeability).

These deposits have been affected by intense tectonism ,which has created over-thrusts, foliation, folds and faults. This has resulted in the transportation of the laterite bodies disrupting their continuity and mixing them with the underlying rocks. Multistage depositional mechanisms ,tectonism and metamorphism almost changed the initial mineralogical composition of the ores. Hematite >51% ,Ni-chloride,Ni-geothite Quartz,Chrome spinel are the main minerals in the FeNi ores. High quality ore reserves were discovered during the past decades (Euboia ,Lokris,Kastoria) by means of geological mapping and drilling operations.

Since the start of this project very little attention was paid towards the application of geophysical methods for the exploration of FeNi laterites .Two attempts (A.Stavrou 1950 IGEY and N.Albandakis 1984 Larko) proved the applicability of magnetic methods for FeNi latterites deposited in Karstified limestones.

Since relevant literature on the geophysical exploration of laterite FeNi ores is scarce it was decided to apply most of the commercially available geophysical methods and techniques in the areas of Lokris and Vermion are presenting two different geologic and tectonic environments.

Geophysical research in both areas followed the following scheme:

Regional scale exploration (strategic phase) . All available airborne, magnetic and gravity data were gathered reprocessed and re-evaluated for the areas under investigation . In the mean time significant anomalies ,of smaller wavelength and size geographically related to FeNi outcrops can be isolated (magnetics).

Site scale (tactical phase) . Local ground geophysical surveys are conducted to increase and further analyse the information gathered from other sources (i.e geology ,geochemistry) and from the regional geophysical surveys. The methods applied at this stage are magnetic ,gravity and IP/Resistivity profiling and soundings, SP & TEM.

Deposit scale (development phase) . Detailed geophysical methods like borehole geophysics and hole to surface techniques i.e :mise alla mase IP are applied.

Field tests . The absence of systematic physical property parameters of the FeNi's made field trials imperative in controlling geologic sections and ore outcrops. In the mean time

petrophysical parameters were measured from FeNi's and their parent rocks from Lokris at Outokumpu Table 3.2.I . One of the test sites is a line T2 in the proximity of Ag.Ioannis Mine, Lokris(see Plate 2.2.3-2) where a number of exploratory holes discovered FeNi ore at shallow depth (10-40 m) confined between Cretaceous and Jurassic limestones . All methods applied recorded clear anomalies.

The second site is located about 10 Km NW of the mine area where an abandoned mine provides good control for tests. The outcrop is trending E-W and two lines parallel and perpendicular to the strike are measured. The foot wall is silicified ophiolite and the hanging wall Cretaceous limestone. IP/Resistivity in gradient and VES configuration ,Transient EM and SP methods are tested. The results from the above tests are summarised in Plates 2.2.3-4 to 2.2.3-6.

Finally a combination of methods which respond positively to the ore and are in agreement with the petrophysical data,is given.

2.4.2. Sub-task 2.2.3: Regional surveys

Both areas chosen for further investigation Vermion & Lokris , (Plate 2.2.3-1), are covered for gravity (1 station /4 km²) and aeromagnetics (300m mean flight altitude 800m mean line spacing & 40m sampling interval) from IGME in previous research during the 70's(Angelopoulos A.,Nikolau S.1984 & Stefouli M., Angelopoulos A., 1990). These data in collaboration with the university of LEEDS (Getech) were reprocessed and produced a digital data base conformable with the specification of West East gravity project and Eastern Magnetic Project to which IGME is affiliated.

The information to be derived from the above data sets refers to the discovery of hidden ophiolites genetically related or hosting FeNi's (long wavelength with lateral development high amplitude anomalies). This information was retrieved from the above data bases by means of prototype software developed in house (Noutsis & Angelopoulos) for PC which automatically estimates the Power Spectrum and Auto-correlation function (Spector ,1968) and gives information related to the intensity, wavelength, lateral extension and direction of the 2d signal (gravity and magnetic anomalies).

These parameters are estimated for 64x64 grids at the centre of 1:50000 map sheets but the same is applicable for every 2D exploratory data set. The same technique is also applicable to the intermediate stage of exploration where anomalies which are directly related to the ore are of interest (small wavelength ,limited lateral development and high amplitude anomalies). This approach had very effective results for objective evaluation of the geophysical information and compilation of the intermediate tables necessary for the Knowledge Based System.

The outcropping ore on the margin of the basin that develops west of the Ag.Ioannis mine in Lokris guided us in examining the aeromagnetic map of the area. Appreciable magnetic anomalies were identified to trend approximately East West and seem to be due to the continuation of the ore westwards. The anomaly ends about 10 Km to the west (Plate 2.2.3-7).

In Vermion Mountain FeNi ore outcrops are reported. In this area the main cause of the magnetic anomalies is attributed to the ophiolites. The FeNi ore, besides its appreciable susceptibility, did not reveal their presence since the line spacing (800m) is not considered appropriate for their size. In any case the identification of ophiolites beneath carbonates is critical for anticipating the presence of FeNi's (Plate 2.2.3-8).

2.4.3. Sub tasks 2.2.6 Magnetic ,gravity and seismic methods

2.4.3.1. Magnetic method

The magnetic method is expected to be an effective exploration tool since Hematite is the main constituent (51%) of the ore in Lokris. The network of measurements for logistics of the project was designed at a step interval of 50 m along roads, irrigation channels and borders of lots spaced \approx 200-300m (Plate 2.2.3-2).

Diurnal and secular corrections for the variation of the Earth's magnetic field recorded at the IGME's Magnetic Observatory in Pendeli ATHENS, were applied to the measurements. The corrected measurements were further checked for uncorrelated spikes which were mostly due to the well casing ,metal pipes etc., used for irrigation. These processed data was later plotted in form of colour contour maps (Plate 2.2.6 1). Signal processing techniques such as low pass and reduction to the pole are applied to the magnetic data to remove spurious noise and transform the bipolar anomalies to symmetrical ones having the peak above the source (Plate 2.2.6-2). For the transformation in house software was used (Angelopoulos and Noutsis, 1988).

The ground magnetic map analyses better the aeromagnetic anomaly which basically has the same form. Amplitudes higher than 500nT are observed and the anomaly trends E-W beneath the lacustrine deposits. As we move to the west, we observe that the anomaly intensity is gradually increasing. A second important anomaly was mapped at NISI to the central south part of the grid where limestones dominate and a third in the SE end of the grid. In both areas known mineralization is reported (Plate 2.2.6-2).

Two lines trending S-N are chosen for numerical modelling and results are shown in Plates 2.2.6-3 and 2.2.6-4. The first profile Km-1 has a maximum at its centre and the anomaly is interpreted as broad $2 \frac{1}{2} D$ body in the middle of the basin. The cross section of the interpreted magnetic body reveals a thick elongated body with its top at shallow depth. The size and depth of burial is not in agreement to the geological model which suggests that FeNi is expected at the bottom of the basin confined between limestones. The second profile Km-2 is cutting the NISI outcrop to the south and ends at the northern rim of the basin. Four bodies are used to model the observed anomalies. In this profile only the first two bodies (related to NISI outcrop) are interpreted to be due to FeNi's presence. The shape, dimension and depth of burial of the next two bodies beneath the basin deposits prohibit any association to FeNi. The only plausible explanation for the nature of these bodies refers to the presence of magnetic material (Hematite) within the basin deposits.

In Vermion (prof. Elias) where FeNi outcrops are reported 12 lines are measured and about 600 stations are occupied (Plate 2.2.3-3). Part of the measurements were taken parallel to gravity survey and the rest along lines crossing at the strike of the ore. Anomalies are detected in the west extremity of the lines where ore is outcropping. The anomalies seem to be related to the ore body but the underlying ophiolites create ambiguities (Plate 2.2.6-5). Finer and wider network of measurements is needed to decipher the nature of the magnetic anomalies.

2.4.3.2. Gravity

Lateritic FeNi ores are considerably denser than the hosting rocks (difference $>0.7 \text{ gr/cm}^3$). The application of the gravity method is attractive since it responds to the excess or deficiency of mass.

Gravity measurements at semi-regional scale were acquired parallel to magnetic measurements but at step interval of 100 m. As for magnetics, positioning was provided by electronic Theodolite, offering accuracy of $\pm 2\text{cm}$ in z. Part of the survey in Vermion was measured with the GSF's real kinematic DGPS system which proved effective while two test lines and a random one were also measured in Lokris. This accuracy is considered critical in gravity exploration since changes of 1m in z correspond to variations of 0.2 mgal and the expected anomalies are of the order of 0.5 mgal .

In Lokris (Plate 2.2.3-2) base stations properly distributed within the surveyed areas ,(980045.718 mgal Base 1, 980042.438 to Base 2 and 980046.630 to Base 3)connected the second order national network through one of its stations in Thiva, allowed quick closures. In Vermion one base station as established (Base 1)in the middle of the area with absolute value 979928.411 Gal connected to the 1st order Gravity net of Greece. Every two hours the drift of the gravity meters was checked. Two Lacoste & Romberg geodetic gravity meters model 203 with the accuracy of 0.002 mgals were used. The second meter was kindly lent to IGME by the Public Petroleum Corporation of Greece DEP-EKY. Conversion constants for the area are 1.04599 and 1.06118 for the IGME's and DEP's meters respectively.

More than 2000 stations distributed along roads and irrigation channels were covered in Lokris while about 300 stations in Vermion. Tidal corrections as well as Free-Air and Bouguer corrections were applied. Corrections are conformable with specifications of the West East Gravity Project to which IGME is affiliated.

Topographic corrections, crucial for mapping low amplitude anomalies e.g.<0.2 mgal were also applied. Fine and coarse DEMs were prepared from the digitisation of 1:5000 and 1:50000 scale maps .Software was developed in house (Vassilis Noutsis IGMEs programmer) based on inspiration of Dr K.Dimitropoulos (Public Petroleum Corporation employee), which calculates the attraction of triangular prisms ,resembling in a finer way the actual topography. Residual map ,after removal of 1st degree plane ,was obtained from the above data only for Lokris. In Vermion the station spacing is not appropriate for producing 2d maps since more stations are needed.

In Lokris the complete Bouguer gravity anomaly map and its derivative,and the residual map,(Plate 2.2.6-6) reflect the morphology of the basins bottom. As it can be seen readily

from these maps the basin is getting progressively deeper westwards. Positive anomalies are identified Westwards, South and SW (NISI) of the mine where the reduced to the pole magnetic map and the residual gravity map correlate well (Plate 2.2.6-2).

A line Kg-1 (Plate 2.2.6-6) approximately in the middle of the surveyed area and along the same route as Km-1 was modelled. The density of 2.67 gr/cm³ was chosen for the limestone and -1 gr/cm³ as contrast for the lacustrine deposits. Plate 2.2.6-3 illustrates the results of the modelling and the quantitative estimation of the basin morphology. In the middle of the profile the basin is getting deeper but not any evidence of dense material or doming is noted. In the same plate we also present the interpretation of magnetic line Km-1 along the same line the interpreted body doesn't show any correlation to gravity. We conclude that the materials which fill up the basin are low density clays and magnetic sands.

In Vermion the measured network (Plate 2.2.3-3) is rather coarse and not advisable to produce 2D maps. Finer and wider coverage is needed to properly evaluate the method there.

2.4.3.3. High-resolution reflection seismics

A multi-purpose high resolution seismic survey test was carried out at the (AG. IOANNIS MINE AREA.) in KOPAIS, LOKRIS.

The aim of the survey was:

- a) To detect and determine the extension of the FeNi horizon, establish its geologic setting within the basin using the seismic and available well data.
- b) To test for Land acquisition techniques using different seismic sources (dynamite, buffalo gun) as well as different methods (Near offset, geophone spacing, recording channel number) for enhancing S/N ratio and suppressing noise such as ground roll and air wave.
- c) To use the optimum processing programs available so specified parameters are compatible with our KANSAS UNIVERSITY processing package for P.C.

Four (4) high resolution seismic reflection lines were shot at two different locations as part of this survey. The shallow high resolution seismic method is used extensively in the study of the subsurface for different targets.

Three of these lines were shot in a grid, two in a N-S direction and one in the W-E direction at right angles and crossing the previous two. The fourth one was shot in the E-W direction much further to the East ($\approx 3,5$ Km). Testing out seismic system capabilities in acquisition and processing was essential to this program, so pitfalls would be avoided in the future.

The survey included four seismic lines T₀, T₂, T₄ and MAKRYNI (Plate 2.2.3-2).

The area in general does not have significant topographical features and is essentially flat at our shooting locations. For equipment and parameters used in the survey, see Table 2.2.6-1. Quality of the seismic data was very good in the MAKRYNI line, fair in the T₀ and T₂ lines and poor in line T₄. Many acquisition parameters were tested. All lines were shot with End-On Geometry.

Table 2.2.6-1. Acquisition parameters

	MAKRYNI	T ₀	T ₂	T ₄
ENERGY SOURCE:	Dynamite		Dynamite	Dynamite BUFFALO GUN
RECEIVERS:	Single geophones 100Hz (vertical)			
Geophone spacing:	2.5 m			
Shot spacing:	2.5 m			
Near offset spacing:	30m			
Record length:	0.5 s			
Coverage (Max. Fold):	6			
Band pass filter:	70 Hz LC	70Hz LC	70Hz LC	70Hz LC

The data was processed using the KANSAS GEOLOGICAL SURVEY Seismic processing software package. Standard processing techniques and available programs were used. Many tests were also run through the programs to increase S/N ratio. Different DECONVOLUTION, F-K Filter, T-Filter, Velocity analysis and Migration parameters were tested for optimum results.

The Basic Data processing flow chart is shown in Table 2.2.6-2

Table 2.2.6-2. Basic Data processing flowchart

DATA REFORMAT (From SEG-2 to SEG-Y)
BULK STATIC CORRECTIONS (For certain records)
GEOMETRY and trace editing (Kill traces and apply first brake mutes)
SORT (GET CDP gathers)
PREDICTIVE DECONVOLUTION (Filter operator 20 ms)
VELOCITY ANALYSIS
NMO CORRECTIONS (Two Locations used)
STACK
BAND-PASS FILTERING (T- FILTER 120-500 was applied)
RESIDUAL STATICS CORRECTION (± 3 ms)
MIGRATION (Migration in time for final section)

1. LINE MAKRYNI (Plate 2.2.6-7) offered the best results. The near offset of 30m was no bother on this line since near surface reflections were of not much importance. We processed down to 350ms with very good frequency content, vertical and horizontal resolution.

MAKRYNI was shot from W-E along strike, basinwards than the other three lines that are situated (3,5Km) to the E.

Five wells were drilled to date along MAKRYNI Line (G-1619, G-1620, G-1621, G-1622, G-1622). Wells 1619, 1621, 1622, 1622_A were incomplete reaching a maximum depth of 138m, 177m, 93m, 159m respectively.

Well 1620 was completed. It reached a depth of 160m and is a good representative for all the wells in the area of MAKRYNI line. The well showed that from 0-108 m clays predominate. From 108-153m clay beds alternating with blue marls containing grains of FeNi and grains of limestone were found. From 153-160m the Jurassic limestones start. The results obtained from the wells do comply with the seismic in MAKRYNI line which shows no significant changes in the closely spaced reflections and the high horizontal resolution indicating non turbulent deposition in the basin.

The horizon of interest (Fe,Ni) is nearly absent, probably faulted out between the 3,5 Km distance of MAKRYNI and the other seismic lines, indicating abrupt change in depositional process between the two areas.

2. LINE T₂ (Plate 2.2.6-8) is oriented in the N-S direction on the shallower part of the basin. T₂ is a dip line shot with dynamite. Results are the same as in the Makryni line.

The geologic cross section with the information from wells M792 and M741 show a major fault and the FeNi deposit at a depth of 35-45 m that matches the migrated seismic section (SPI's 125-150). Evidence of basinal uplift on the upthrown side of the fault followed by erosion of the KARSTIFIED Limestones is evident above the FeNi horizon.

3. T₄ line runs parallel to T₂, is also a dip line and they are only \approx 90m apart. The line tested three different kinds of sources with rather disappointing results.
- dynamite with fair record quality
 - buffalo gun and
 - plain detonator with poor record quality. We will not discuss T₄ further since it is similar to T₂, suffice to say that the line was processed only through stack.

4. Line T₀ is situated along strike and crosses both T₂ and T₄ at right angles. After processing the migrated time sections of T₂ and T₀ gave very good structural ties where they meet, thus making this seismic test project a success.

The results of the high-resolution seismic reflection survey carried out in the AG.IOANNIS MINE AREA in KOPAIS enabled us to detect the FeNi horizon with another geophysical method as well as estimate its extension in the area.

Most of our seismic tests were carried out satisfactorily.

2.4.4. Sub task 2.2.5: IP/resistivity measurements

The IP method intended to be used as a diagnostic tool to the other geophysical methods. Time domain IP proved to be effective in both ore hosting environments. As initially designed all electrode configurations i.e. Schlumberger (VES), Gradient, mise a la masse gradient, pole-dipole and dipole -dipole were effective. In Lokris area parametric measurements over FeNi outcrops gave chargeability values (CH) between 5-12 mV/V while the CH of carbonates and ophiolites was negligible. Superficial lacustrine clays and sands of the Ag.Ioannis area manifest CH values of the order of 2mV/V which can be attributed to the membrane polarisation effect of the clays. These tests demonstrate the direct dependence of the polarisation effect to the FeNi's and constitute an unique tool for their identification . The above contrast combined with the resistivity of the FeNis ranging between 60-100 Om, the 10-14 Om of the lacustine sediments and the much higher >500 Om of the hosting rock (Carbonates or Ophiolites) allowed the registration of indisputable anomalies.

Different electrode configurations used aimed to solve particular needs in the course of the exploration project in both areas of interest .

2.4.4.1. VES IP/Resistivity

This configuration was used at the first stages of the project .In Lokris (Plate 2.2.3-2) the soundings were aiming to check the presence of polarizable material and the depth of the basins basement, while in Vermion (Plate 2.2.3-3) to check the eventual continuation eastwards of the FeNi Horizon and estimate the thickness of the sequence. The inversion of

the data is implemented using the New Jersey Geological Survey software modified in house (V.Noutsis) to fit our requirements. The results in all soundings are considered positive .

In Lokris the resistivity data when inverted, estimates the depth of the basement and in the mean time the IP data reveals the presence of polarisable material from the first 20 m. down to depth of the basin (Plate 2.2.5-1). The soundings located S and SW of the mine are also positive.

In Vermion the VES IP results gave the first positive expectations on the continuation of the ore to the East beneath the carbonates (Plate 2.2.5-1). These results were latter confirmed from IP/Resistivity profiling and the TEM data.

2.4.4.2. Pole-dipole & dipole-dipole profiling

This configuration offers both lateral and in depth scanning of the medium. The 8 channel Receiver resulted very effective and friendly to the user .Production was rather high (more than 1Km /day) and n's levels up #8 were measured . Forty (40) meters dipole lengths were used and current intensity higher than 4Amps was maintained throughout the survey while current pulses were fixed at 2sec.

In Lokris (Plate 2.2.3-2) the pole-dipole configuration was used to increase the emitted current intensity .Four lines (one perpendicular dipole-dipole, and three parallel to the strike pole-dipole) were measured (Plate 2.2.6-1) and n's (apparent depth point levels) up # 8 were used. We were careful to the presence of electrical noise since we operated in the vicinity of the mine. Continuous registration of the electrical activity revealed the presence of noise in the order of 8 mV peak to peak, for certain times of the day .Measurements were made with a single channel graphical recorder and then with a multi channel digital recorder. The noise after repetitive measurements in different times, was interpreted to be the result of massive ground water pumping during the dry season, creating Electro kinetic effects. Part of the noise in the proximity of the mine is due to stray currents diffused in the basin that give the electrical continuity of the ore.

To facilitate the interpretation of the IP data and allow correlation to the 2d gravity and magnetic maps the Chargeability values of the different n apparent depths are projected to the surface plane. IP anomalies are mapped which correlate to the magnetic one but the most consistent ones are those from lines 444, 222, 333 (Plate 2.2.6-1).

The resistivity sections in the basin reveal the faulted nature (presence of abrupt steps) of the resistive basement (Plate 2.2.5-2). The chargeability sections show non consistent anomalies along them as well as from the shallow to the deeper levels . The scattered nature of the anomalies is more evident along the dipole-dipole line cutting N-S the basin (Plate 2.2.5-3). Here the Ch anomalies derived from the lacustrine deposits and correlate with the magnetic anomaly while the resistivity data reveal the presence of highly conductive material. The low resistive nature of materials which fill up the basin are revealed also from the TEM I results.

In Vermion (Plate 2.2.3-3) the dipole -dipole configuration was used since measurements are made on resistive medium (Limestones). Forty meter dipole length was used. Nine lines parallel and perpendicular to the FeNi horizon strike were measured for seven apparent depth

levels. The results for better visualisation are projected on surface plane and plotted on the magnetic map as in Lokris. The IP anomalies correlate to the TEM (see Plate 2.2.6-5).

For the inversion of the IP/resistivity data in pole-dipole and dipole-dipole configuration a fast smoothness constrained algorithm for the 2-D inversion of earth resistivity and IP data was used for interpreting the data (Tsourlos et al., 1998; Tsourlos, 1995). The algorithm is fully non-linear, automated and accelerated by the use of a Quasi-Newton update of the Jacobian matrix. A proven 2.5-D Finite Element Method (FEM) scheme was used as the platform for the forward resistivity calculations. The adjoint equation approach (McGillivray and Oldenburg, 1990) was incorporated into the FEM scheme in order to calculate the Jacobian matrix J (the derivatives of the observations in respect of changes of the model's resistivity) when necessary. In order to tackle the instability of the inverse problem a smoothness constraint was imposed. The technique has been proposed for the geophysical case by Constable et al. (1987). The algorithm proved to be robust noise insensitive and produced good quality inversions. All presented inversions converged after 4-5 iterations and produced low RMS errors. Plates 2.2.5-2, 2.2.5-4 and 2.2.5-5 show the results of representative IP lines from both areas which agrees with geology.

2.4.4.3. Mise a la masse IP/Resistivity

This configuration was designed to cross check IP anomalies detected from other configuration and methods at deposit scale and is only applied in Lokris (Plate 2.2.3-2). This method was introduced by the author and has been used successfully in the past decade for base metal detailed phase exploration (Angelopoulos and Nikolau, 1989). The polarizability values obtained along with the resistivities from parametric measurements of the ore anticipate the applicability of the method in case the ore is hosted between carbonates of different age and ophiolites.

The first trials were made over the NISI ore body in Lokris trending E-W and with inclination $\sim 40^\circ$ to the south. Energising directly the mineralized body known in a well and measuring lines perpendicular to its strike, Time domain current pulses of more than 5 Amps and of duration of 2 sec were used throughout the survey.

Characteristic chargeability anomalies in the order of 13 mV/V are recorded in two lines having the peak above the body (see Plate 2.2.5-6).

Next the method is used to decipher the nature of the magnetic anomaly underlying the basin deposits in its central portion directly above the positive peak. Here, IP anomalous values are recorded from both configurations (VES, dipole-dipole). The metal casing of existing water wells reaching the bottom of the basin was exploited with injection of electrical current at this depth.

The obtained anomalies both in Resistance and CH do not show any major lateral variation of intensity for the measured parameters (slightly above background) which means that no important polarisable material is expected at the basins bottom or directly beneath. It means that the source of the magnetic anomaly is within the lacustrine deposits of the basin (see

Plate 2.2.5-6). The very promising results demonstrate that the method can be effectively exploited in the detailed phases of exploration for FeNi's.

2.4.5. Sub task 2.2.4: transient EM

The Transient EM method was designed to be applied in the prospect areas along with resistivity/IP ones during the reconnaissance and detailed phases of exploration, exploiting the advantages of the TEM method with respect to the galvanic methods.

Also explore the response of the FeNi (lateritic) deposits in the late channels.

The method taking into consideration the resistivity of the ore ~ 70-100 Om that of the carbonates and the ophiolites (>400), the positive results in TSOUKA are applied in both selected areas.

Current higher than 4 Amps is emitted allowing good response both in early and in late channels. Measurements at 25 and 50m step intervals were made with the IGME's SIROTEM II unit in coincident loop mode .

In the area of Ag. Ioannis mine LOKRIS two long sections crossing the basin N-S were measured. Hundred (100)m two turns square loop and 50 m step were chosen (Plate 2.2.3-2). The acquisition speed was high allowing production of more than 1km/day with a crew of 1 observer and 2 -3 assistants.

The lines were designed to cross cut and check the bipolar magnetic anomalies detected in this part of the basin which develop from 20 to about 150m in depth (Depth information from IP/resistivity soundings LARIP 7 is in agreement with the inverted data in the middle of TEMII station 8, Plate 2.2.4-1). Note from the sections obtained ,the differentiation which is observed in the middle of the basin which is attributed to the conductive clays which fill it (Plate 2.2.6-6).

In Vermion five lines were measured for TEM (Plate 2.2.3-3). The geological setting similar to the one encountered in TSOUKA test area ,LOKRIS allowed Fifty (50)m square loops to be deployed at 25 meter step and as above coincident loop configuration. The results of all measured lines presented in Plate 2.2.6-5, show abnormal behaviour (7nt early time channel) which correlates with the IP anomalies.

2.4.6. Validation of geophysical anomalies with drill holes in Lokris

The positive response of Gravity ,Magnetics ,IP in Lokris over known mineralization area (NISI,T2 test line & SE corner of the grid) & TEM in TSOUKA ,validation of the methods applied is considered critical for the their final evaluation .The magnetic and gravity anomalies to the west of Ag.Ioannis mine as we move to deeper parts of the basin we pass from a positive to a negative correlation while the magnetic anomaly becomes progressively higher. The two TEM lines and the resistivity data in the middle of the grid reveal the presence of highly conductive material to the bottom of the basin .In the same area the seismic line revealed the presence of alternating sand and clay layers till bedrock. These facts

raised serious questions about the nature of the source of the high amplitude magnetic anomaly . Four (4) exploratory holes were drilled to check the nature of the coincident magnetic and IP anomalies where no gravity response is recorded . Drill sites are located over the positive lobe of the magnetic anomalies, where 3 IP/Resistivity lines run parallel to the magnetic axis (Plate 2.2.3-2) and a number of IP/Resistivity soundings are made . In all lines IP low amplitude anomalies are recorded. All holes reached bedrock (Jurassic limestones) at depths between 140 and 160m and no ore was found. The overlying limestone beds are composed of alternating layers of sands and clays . These sands as measured manifest high magnetic susceptibility $K \sim .00025$ SI and are composed mainly from grains of Hematite.

These results and all conclusions from the applications of the different methodologies applied, show that the main magnetic anomaly which develops westwards of the mine is not associated to the FeNi horizon. The anomaly is caused from magnetised fluvio-lacustrine deposits which filled up the basin from the Neogene to Quaternary age. Melas river now days flows parallel to the magnetic anomaly and towards the East.

2.4.7. Concluding remarks and achievements

-Magnetic, IP and the gravity proved to be the an ideal combination of geophysical methods for detecting and delineating FeNi laterites hosted within limestones and consequently covered with conductive overburden (~ 10 O m lacustrine clays)in LOKRIS . The same is valid for the case where the ore is confined between Jurassic and Cretaceous limestones (Nisi ore body). The combined interpretation of these data gives useful information that concerns the depositional mechanism of the sands and the paleo environment also.

-IP, Magnetics, Transient EM and/or SP methods cross checked by detailed gravity measurements constitute an effective combination for identification-delineation of ophiolite-hosted FeNi laterites consequently covered by limestone's as in the VERMION case northern Greece and Tsouka Lokris.

-Various electrode arrays and the new IP R12 Scintrex receiver (dipole-dipole ,pole-dipole ,mise alla mass gradient) and IRIS SYSCAL R2 (schlumberger) have been tested . The mise alla mass one results were very effective delineating the extension of already Known mineralisation and checking the bottom of the basin. We recommend the parallel registration of the background electrical noise in similar conditions with the aid of portable digital dataloggers.

-High resolution reflection seismic method (in LOKRIS) gave promising results identifying the carbonates (hosting FeNi's) and lacustrine layer interfaces. Additional information is derived, for the diagnosis and nature of the lacustrine deposits(identification of magnetic sand layers) . This Information proved to be critical in evaluating the magnetic anomaly which develops beneath the basin sediments. The low cost hardware and software used demonstrate that high resolution seismic can be a cost effective tool for FeNi exploration as well as for similar applications.

-Computer software developed in house was used for processing and evaluation of potential field data. Presentation of IP data is also achieved by means of interface software written on purpose to couple the IPR12 receiver and Golden Software. Modeling of magnetic and gravity data was done using free USGS software. Interpretation of Vertical IP & electrical soundings was done with software provided from New Jersey geological survey modified in house to fit our requirements.

**SUMMARY ON THE APPLICABILITY OF
GEOPHYSICAL METHODS FOR FeNi Laterites**

	<i>METHOD</i>	<i>CaCO₃</i> <i>(hosted)</i>	<i>CaCO₃(hosted)</i> <i>+ overburden</i>	<i>OPHIOLITE</i> <i>(hosted)</i>	<i>BEST</i> <i>COMP/ON</i>
1	<i>IP-RES/TY</i>	+	+	+	+++
2	<i>MAGNETICS</i>	+	+	?	++
3	<i>GRAVITY</i>	+	+	+	++
4	<i>TDEM</i>	<i>N.A</i>	--	+	+
5	<i>SP</i>	?	?	+	++
6	<i>SEISMICS</i>	<i>N.A</i>	+	<i>N.A</i>	+

2.4.8. References

Albantakis N., - Coundouros D., (1984): Prospection and localization of nickeliferous iron ore deposits at Kopais with geomagnetic method and drilling. Journal of Mineral Wealth. 32/84.

Angelopoulos A., - Nikolaou S., (1984): Airborne geophysics and mineral exploration in Greece. 27th International Geological Congress Moscow 1984.

Angelopoulos A.- Nikolaou S., (1989): MISE A LA MASSE IP an effective method for mapping metalliferous zones. 1st Hellenic geophysical congress, Florina 19-21/4/1989.

Angelopoulos A.- Noutsis B., (1988): Microcomputer application in applied Geophysics- Spectral analysis of potential field data. Congress on the applications of microcomputers in research-education-industry Patras 3-5/11/1988.

Constable, S. Parker, R., and Constable C., 1987. Occam's inversion: A practical algorithm for generating smooth models from electromagnetic sounding data.

Spector, A., (1968), Spectral analysis of aeromagnetic maps: Ph.D. thesis, department of Physics, University of Toronto.

Stavrou, A., (1950): On the applications of magnetic mapping in the Lokris FeNis. IGEY Internal Report E.139.

Stefouli M., Angelopoulos A., (1990): Integration of Landsat and Aeromagnetic data as aid to the structural analysis of Crete and S.E Peloponessus Int. J. Remote sensing. 1990 Vol. 11#9 1625-1944.

Tsourlos, P., (1995): Modelling, interpretation and inversion of multielectrode resistivity survey data. D. Phil, Thesis, University of York, U.K.

Tsourlos, P., Szymanski, J. and Tsokas G.,(1998). A Smoothness Constrained Algorithm for the Fast 2-D Inversion of DC Resistivity and Induced Polarization Data. Journal of the Balkan Geoph. Soc., 1, 3-13 Geophysics, 52:289-300

2.5. Task 2.3: Development of 3-component borehole EM methods

2.5.1. Introduction

The task 2.3 consisted in developing two new configurations of the 3-component downhole EM method of mineral exploration, the '**cross-borehole**' (or tomographic) configuration, where a magnetic dipole source (Tx) is in one hole and the 3-component magnetic receiver (Rx) is moved in another hole, and the '**single-borehole**' configuration, where the source and the 3-D receiver are moved together in the same hole at a constant separation.

These methods aim at detecting missed targets around barren boreholes or at outlining orebodies intersected by one or several boreholes.

This task comprises four modules:

- a) Methodology study;
- b) Development of prototype equipment;
- c) Development of data processing and interpretation software;
- d) Field tests.

Module (a) was shared between BRGM and GSF. Module (b) was entrusted to IRIS Instruments. Module (c) was the responsibility of BRGM, except for the software driving the equipment, which was a task of IRIS. Module (d) was realised in a close cooperation between BRGM, IRIS, OMR and GSF.

As for module (a), an extensive set of 3-D numerical modelling for the new downhole EM methods was planned with the following objectives: a) understand the physics of the EM response of a conductive target, b) optimize the instrument design and field configuration, and define practical limitations for the new methods, and c) give interpretation guidelines for certain simple geometries.

A second set of 3-D modelling in the borehole Slingram configuration appeared necessary, after the second field tests, to check whether the high responses (several hundreds of percents of the free-space primary field) observed in this new mode were geophysically relevant, or if some malfunctioning was to be suspected on the SlimBoris prototype. The question was raised by the partners experienced in surface Slingram, who expected in boreholes a behaviour similar to what is assumed at the surface, i.e. a limit of about 100%.

As for module (c), different PC software were to be developed for recording, handling, processing and interpreting the numerous and complex data recorded in the various configurations of downhole EM. Note that these software are only research prototypes written in Fortran or Basic languages and working in a DOS Windows.

The first software is a data handling software, BOREM, which proposes the following basic processing tools: a) projection of the measured components onto a fixed coordinate system ('derotation'), b) borehole trajectory calculation (for both transmitter and receiver boreholes), and c) primary field reduction, either in free-space, in homogeneous space or by the low-frequency field. It covers all the three configurations proposed by the SlimBoris system

(surface-to-hole, cross-hole or single-hole), as well as older surface-to-hole formats produced by ARLETT and BORIS systems.

A tool for simulating the primary field created in a layered half-space by an arbitrarily oriented magnetic dipole (or by a large horizontal loop of current) has also been developed in a separate software called REDSTRAT. This tool is particularly useful in cross-hole and surface-to-hole configurations for reducing the measured field by the transmitter's primary field (i.e. subtracting the latter to the former), so as to retain only the secondary field of a target.

Finally, an inversion software (non-linear least-square fitting with Marquardt-Levenberg algorithm) has been developed for rapid interpretation of 3-component borehole EM data. It is based on very simple models such as EM dipoles or current filaments. The validity of such models have been studied on synthetic data generated by 'exact' 3-D modelling software.

Field tests with the SlimBoris prototype were performed in Finland on exploration sites of Outokumpu. Due to some delays in the prototype manufacturing, they did not start in 1997 as planned, but were postponed to 1998. The first field tests were performed on a site where a conductive target was known (or at least strongly suspected) from other geophysical data, in order to assess both the equipment and the methods on a calibrating bench.

Further testing was done on sites with more complex geology, either where the presence of a conductive body is not certain (Mullikorame site), or where several thin conductive veins are probable but are not clearly recognized (Hotinvaara site). The objective in those cases was to help the discovery of new orebodies which could be subsequently used as case histories to promote the new equipment and methods in adequate publications.

The technical content of task 2.3 is justified in next section in terms of its innovative aspects with respect to the state of the art in downhole EM and in corresponding methodology and software.

2.5.2. State of the art

North American instrument manufacturers have put considerable development effort in the last decade into 3-component surface-to-borehole EM methods. Geonics has been promoting a time-domain system (PROTEM) for a few years. Since the beginning of the GeoNickel project in 1996, Crone and Lamontagne have introduced similar systems. IRIS is promoting its BORIS frequency-domain system (53.5 mm) with the methodological support of BRGM.

Much less work has been devoted to 3-component EM tomography (cross-hole) or 3-component borehole EM profiling (i.e. single-hole or borehole Slingram). A large diameter (89mm) tool for both configurations has been developed by EMI (California) for oil field investigation, but it is not suited to the slim holes used in mining exploration. For the single-hole configuration, a Russian prototype has been tested by Outokumpu, giving promising results.

This last configuration looks attractive in mineral exploration for its ease of use and practicality. Unlike the surface-to-hole method, it does not need installation and precise referencing of a large Tx loop. A log can thus be recorded by a single operator. In addition, the

method can sometimes be the sole downhole EM method applicable, e.g. when only one borehole is available and when it is impossible to install a surface loop or when the zone to explore is too deep to get enough primary field from the surface. As for interpretation, the constant Tx-Rx distance makes detection of anomalies much easier than in the surface-to-hole or cross-hole configurations, where the primary field shows rapid variations along the borehole.

The objective of task 2.3 within the GeoNickel project is thus to design, manufacture and assess a prototype of a versatile slim-hole (42mm) frequency-domain 3-component EM system which could be used in the various downhole EM configurations, and to develop the corresponding methodology and software. In particular, the innovative borehole-Slingram configuration has not yet been addressed by abundant literature, and thus needed to be thoroughly studied by modelling and field tests.

For the processing and interpretation of 3-component borehole EM data in frequency domain, no software is currently available in the market. The available 'exact' 3-D forward modelling codes, using integral equations or finite element techniques, are not practical due to their high demand in computer capacity and time (several days for a single model on a fast workstation), which definitely forbids their use in iterative inversion processes requiring at least tens of iterations.

By contrast, very simplified (and thus very fast) forward models such as current filaments are well suited to inversion processes and yet give, with 3-component data, good determination of a target's geometry (3-D location and attitude). This approach was previously used in Australia for the inversion of single-component surface-to-borehole data in time domain. The results were poor due to the lack of transverse components: the XY position of the target and its strike direction were not accessible.

2.5.3. Methodology study (BRGM report)

A first theoretical study based on 3-D numerical modelling for the new 'cross-hole' and 'single-hole' EM methods was performed at BRGM. The objectives of this methodology study were:

- a) to understand the physics of the EM response of a conductive target;
- b) to support the instrument design, optimize field configuration and define practical limitations for the new methods;
- c) to give interpretation guidelines for certain simple geometries.

Calculations were performed with the EM3D software from the University of Utah (Newman and Hohmann, 1988).

2.5.3.1. Model description

The reference model used in this study (Fig. 2.3-1) was defined in common by BRGM, GSF and Outokumpu. It consists of a vertical 25x100x100 m parallelepiped conductor placed at (0, 0, 250) m in a 500 Ω .m homogeneous half-space (5000 Ω .m in some cases). The orebody is either moderately conductive (5 Ω .m) or highly conductive (0.5 Ω .m). In most calculations, the frequency is 2000 Hz, but some results are presented at 60 Hz, 150 Hz, 600 Hz, and 10 kHz. All the boreholes used in this study are vertical. The transmitters are vertical magnetic dipoles (VMD) of unit moments (1 Am²).

In the cross-borehole configuration, the transmitting VMD's are placed at a few discrete depths in one of six transmitter boreholes, shown to the right of the target with labels Tx1 to Tx6. The main transmitting depths used are $Z=250$ m, depth of the target's center, and $Z=200$ m, depth of the target's top. For each transmitter position, calculations in the receiver boreholes (Rx) are carried out from $Z=0$ (surface) to $Z=500$ m, at 10 m interval.

The main receiver borehole used in the cross-borehole configuration is F0 ($X=-50$, $Y=30$ m), located to the left of the target, at about 50 m from its center. In this situation, the receiver is in the shadow of the target, in the so-called transmission geometry, which is known from previous study to be most favourable to response detection, with best secondary to primary ratio (see later). Two symmetrical positions, F'0 ($X=-50$, $Y=-30$ m), in same situation but facing the Tx boreholes, and F''0 ($X=50$, $Y=30$ m), to the right of the target, are also used. Two more distant boreholes, F1 and F2, respectively at 100 and 150 m from target's center (and their symmetrical F'1 and F'2) are also used for testing the inversion procedures.

In the single-borehole configuration, the Tx-Rx pair is moved from the surface to the bottom of the borehole at a 10 m interval, with the Tx placed above the Rx. The Tx-Rx separation is set at either 25, 50, or 100 m, as in the SlimBoris prototype. In this configuration, boreholes Tx1 to Tx6 are used, as well as a few boreholes left of Tx1 and approaching very close to the target (see later). Only the frequency 2 kHz is calculated in this configuration.

N.B.: In single-borehole, the representative point of a measurement will be reported at the mid depth between the transmitter and receiver, as is standard in Slingram methods.

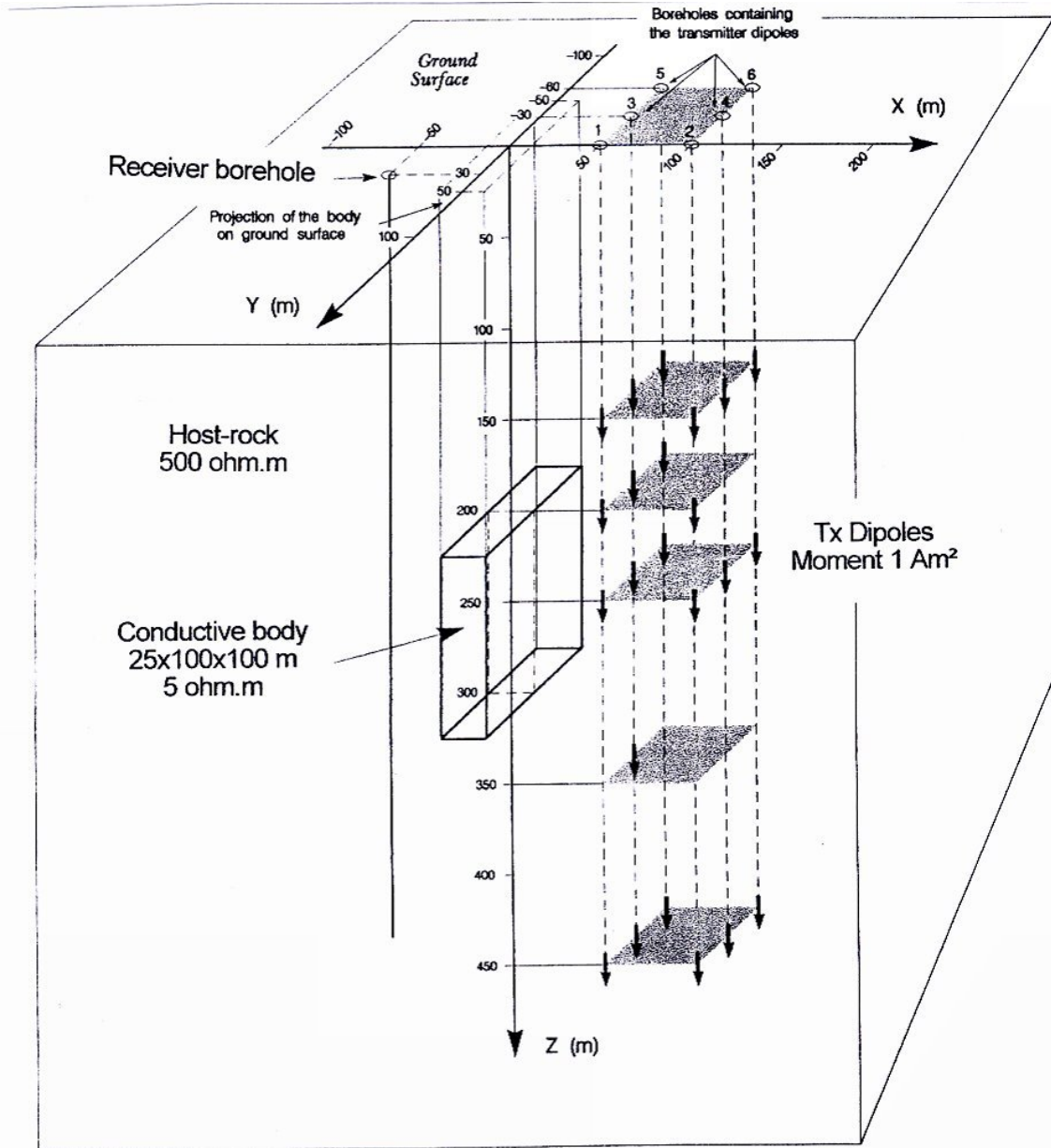
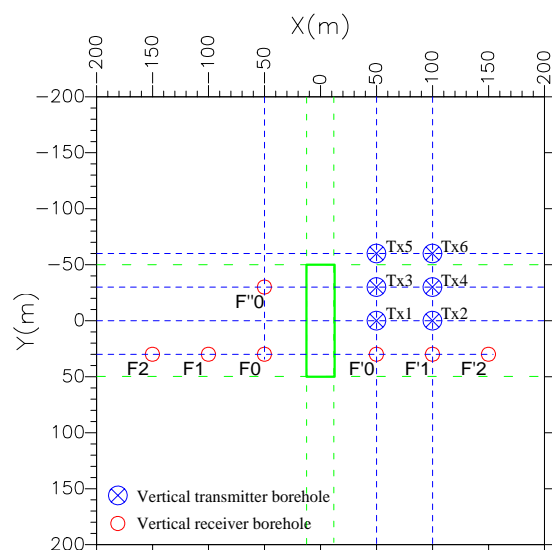


Fig. 2.3-1: 3-D model used for borehole EM calculations, featuring a vertical 25x100x100 m parallelepiped conductor centred at (0, 0, 250) m in a 500 Ω.m conductive half-space. The orebody is either moderately conductive (5 Ω.m) or highly conductive (0.5 Ω.m).



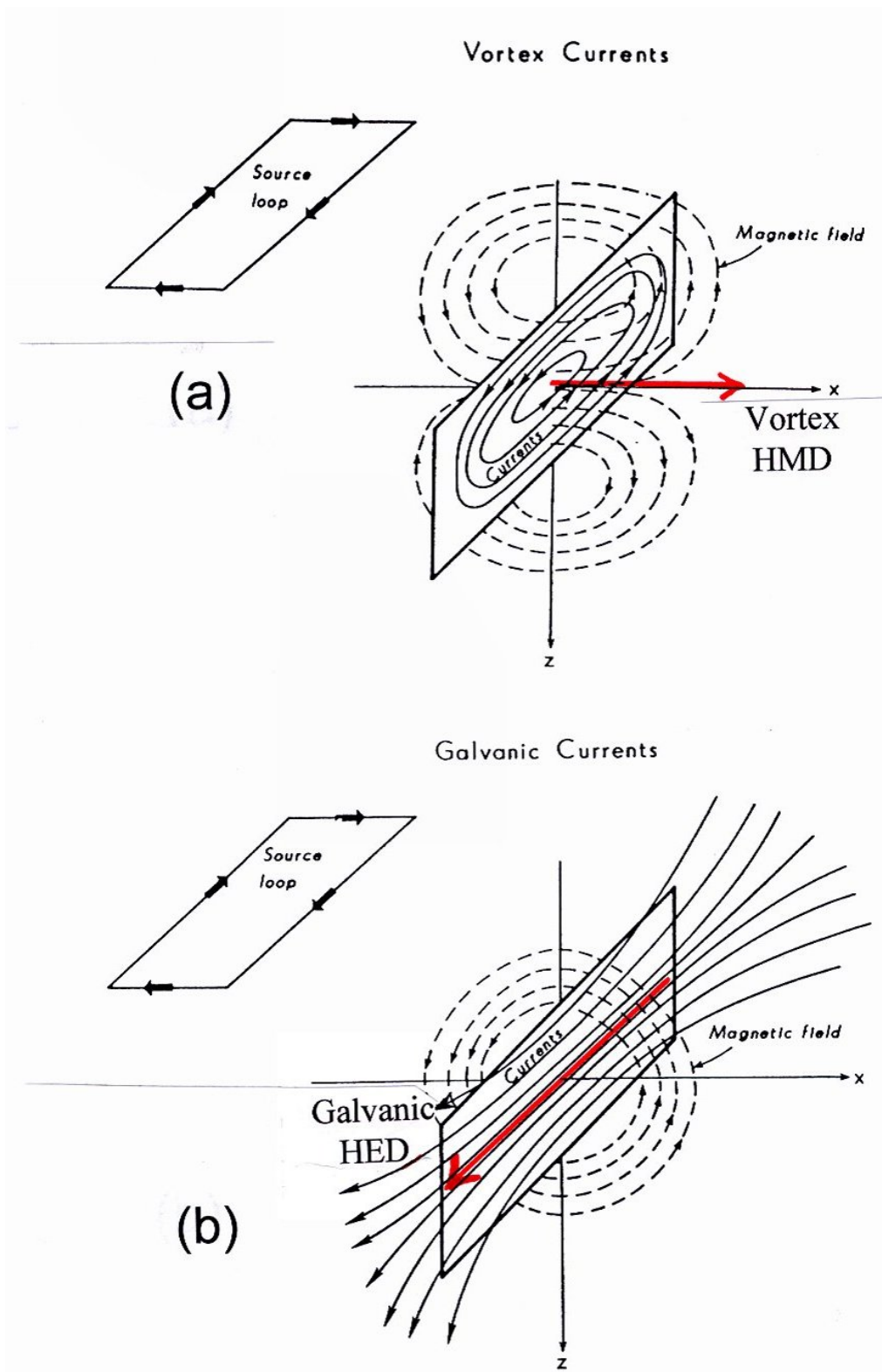


Fig. 2.3-2: Schematic representation of inductive and galvanic effects, showing equivalent .

2.5.3.2. Physics of the EM response

Concerning the physics of the EM response of a conductor, two types of effects (inductive and galvanic) can be present, according to the geometric coupling of the conductor with the transmitter's primary magnetic field and primary electric current density. For each effect, the currents induced within the conductor have very different geometries and spectral behaviours. In turn, the secondary magnetic field scattered by the conductor is very characteristic of each effect.

a) The **inductive** (or vortex) **effect** is the best known and the most intuitive. It appears in any conductor presenting sufficient coupling with the primary magnetic field. It is characterized by electrical currents circulating in closed loops within the conductor (eddy or vortex currents).

The conductor can be either an infinite homogeneous medium (space, half-space) or a limited body embedded in a larger environment. In this last case, the body must be well coupled (i.e. have good cross-sectional area) with the host-rock primary magnetic field, i.e. the magnetic field existing in the host-rock in the absence of the body. The host rock can be either conductive or insulating (e.g. free-space).

The magnetic field created by this effect outside the conductor is approximately equivalent to the field of a closed electrical circuit (current filament). At a larger distance, it is equivalent to the field of a **magnetic dipole** (Fig. 2.3-2a).

b) The **galvanic effect**, also known as current gathering or current channelling effect, is not so well known and understood as the more classical inductive effect. This type of response supposes a finite-size heterogeneity¹ embedded in a conductive host medium², with electrical contact between the target and its host. The target can be either more conductive or less conductive than the host medium.

The host itself must be the seat of induced currents (generally large vortex currents) that can be regarded as the primary electric current density (density existing in the host in the absence of the body). This means that the galvanic effect does not exist in free space or in very resistive host rocks.

The galvanic effect is due to the interaction between the target and the currents circulating in the host medium. These currents are gathered (or channelled) into the body when it is 'conductive' (i.e. more conductive than its host), and diverted away from the body when it is 'resistive' (i.e. less conductive than its host). For a 'conductive' body elongated along the primary current direction, the current density through the conductor can easily reach 100 times or more the primary current density (Nabighian and Macnae, 1991).

¹ Or, more generally, a heterogeneity having smaller dimension than its host (e.g. a plate in 3-D space or a line in a plane,...).

² The host is to be understood in a broad meaning: e.g. a plane-like bearing level containing the orebody and itself contained within a very resistive country rock is a suitable host medium for the appearance of galvanic effects.

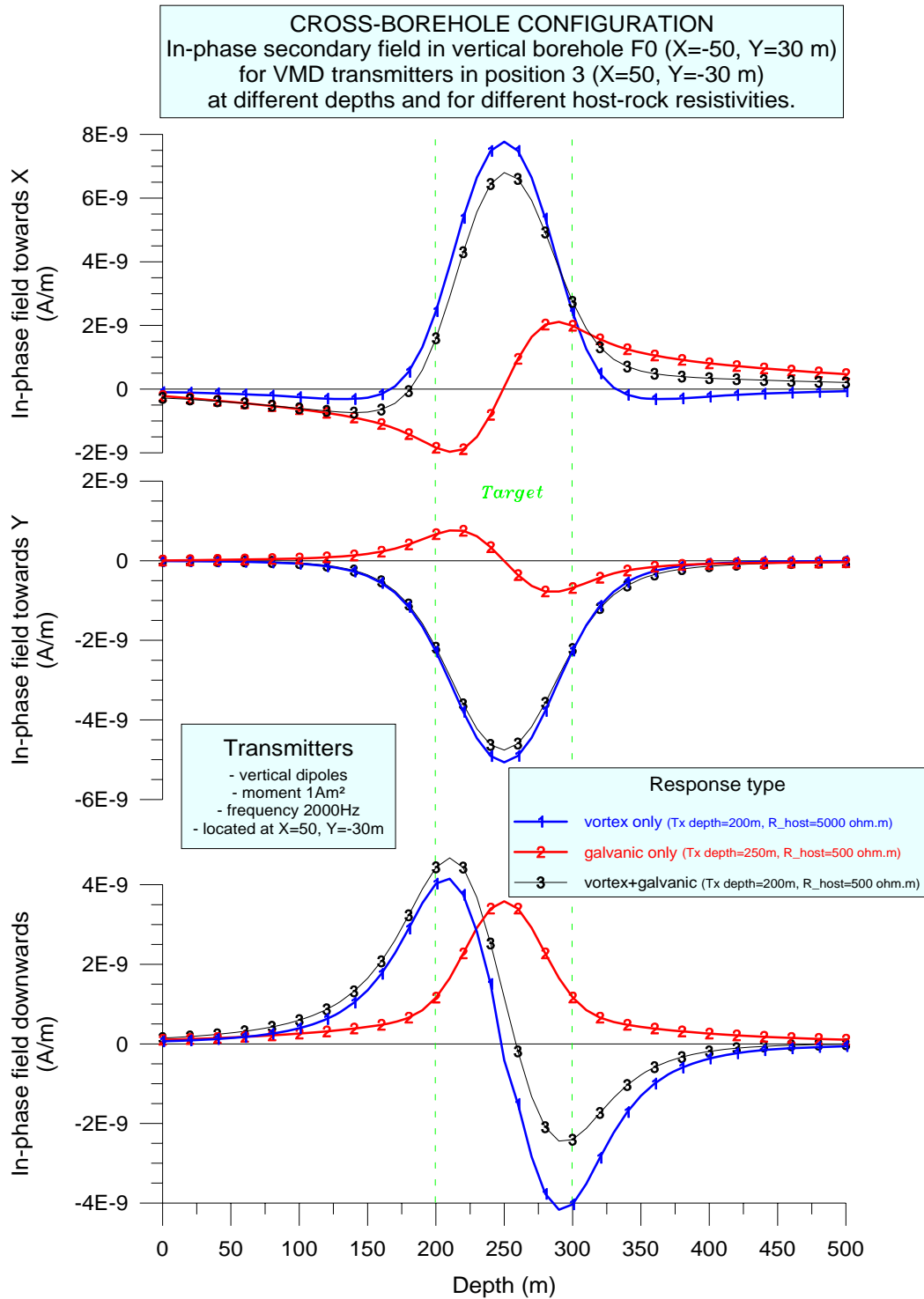


Fig. 2.3-3a: Cross-borehole configuration. In-phase secondary magnetic field scattered, at 2 kHz, by the target defined in Fig. 2.3-1, for fixed VMD transmitters in Tx-borehole 3 (X=50, Y=-30 m) and moving receivers in borehole F0 (X=-50, Y=30 m). The blue curves (labelled 1) represent a purely inductive (vortex) response, which is obtained by setting the host resistivity at 5000 Ω.m with a transmitter well above (or below) the target's center (here Z=200 m). The red curves (labelled 2) represent a purely galvanic response, obtained in a conductive host (500 Ω.m) with a Tx dipole at the level of the target's center (250 m), whatever its XY position. The black curves (labelled 3) represent the general case in a conductive host, with a combination of vortex and galvanic responses. For the in-phase field, the ratio of galvanic-to-inductive response appears to be rather weak. It is much more important for the quadrature field (Fig. 2.3-3b).

The galvanic effect is thus characterized by electrical currents flowing in open paths between two extremities of the body. The magnetic field created by this effect outside the body is approximately equivalent to the field of an open segment of current (electrical bipole). At larger distance, it is equivalent to the field of an **electric dipole** (Fig. 2.3-2b).

Even though the galvanic effect has been known for a long time, its importance in EM is often neglected, as many people have mainly in mind the classical concept of the eddy currents. It is true that this last effect is predominant in very resistive hosts, such as the glacial shields found in Canada and Scandinavia. Nevertheless, even in those resistive hosts, galvanic responses are observed (e.g. in an elongated body embedded in a well coupled plane-like bearing level), and it is thus very important to be able to recognize and understand such responses.

The theoretical study performed in GeoNickel has given clear understanding of both effects and a quantification of their respective amounts in common situations of mineral exploration. Their respective signatures are now clearly identifiable on a 3-component EM log.

These two effects are first distinguishable by very different spatial geometries. For the reference target (Fig. 2.3-1), the inductive response is equivalent to the field of a **horizontal magnetic dipole (HMD)** perpendicular to the strike, whereas the galvanic response is roughly equivalent to the field of a **horizontal electric dipole (HED)** along the strike.

More generally, if the target is flattened as is the case here, the 'inductive' magnetic dipole is perpendicular to the plane of the target, whereas the 'galvanic' electric dipole is horizontal and along the strike of the target.

On the contrary, if the target is compact (e.g. sphere, cube,...), the 'inductive' magnetic dipole lies in the vertical plane joining the target center and the source dipole, whereas the 'galvanic' electric dipole is horizontal and perpendicular to this plane (i.e. tangential).

Figure 2.3-3 compares the responses (secondary magnetic field) from the reference target in two circumstances giving either a purely galvanic or a purely inductive response. An intermediate situation with a combination of both types of responses is also presented. It corresponds to the general case in conductive hosts.

a) The 'purely galvanic' situation is obtained by putting the VMD transmitter (whatever its XY position) at the depth of the target's center ($Z=250$ m). In this case, effectively, the inductive coupling is zero, as the magnetic flux of the vertical dipole on the upper part of the target cancels that on its lower part (Fig. 2.3-4). Consequently, in a conductive host, the response will be limited to the sole galvanic response.

Figure 2.3-5 shows the mechanism of electrical charges created on the surfaces of the conductive heterogeneity and the equivalent HED generated by these charges. The dashed vectors demonstrate the curved nature of the resultant electric dipole; it is in fact a curved line of dipoles, i.e. a curved open electrical current filament. This curved nature is true even for the case of a symmetrical situation, as in Fig. 2.3-5a. This explains why the H_y component of the galvanic response is not uniformly null (see Fig. 2.3-3a or b, curves labelled 2) as would be the case if the HED's were all directed along the strike.

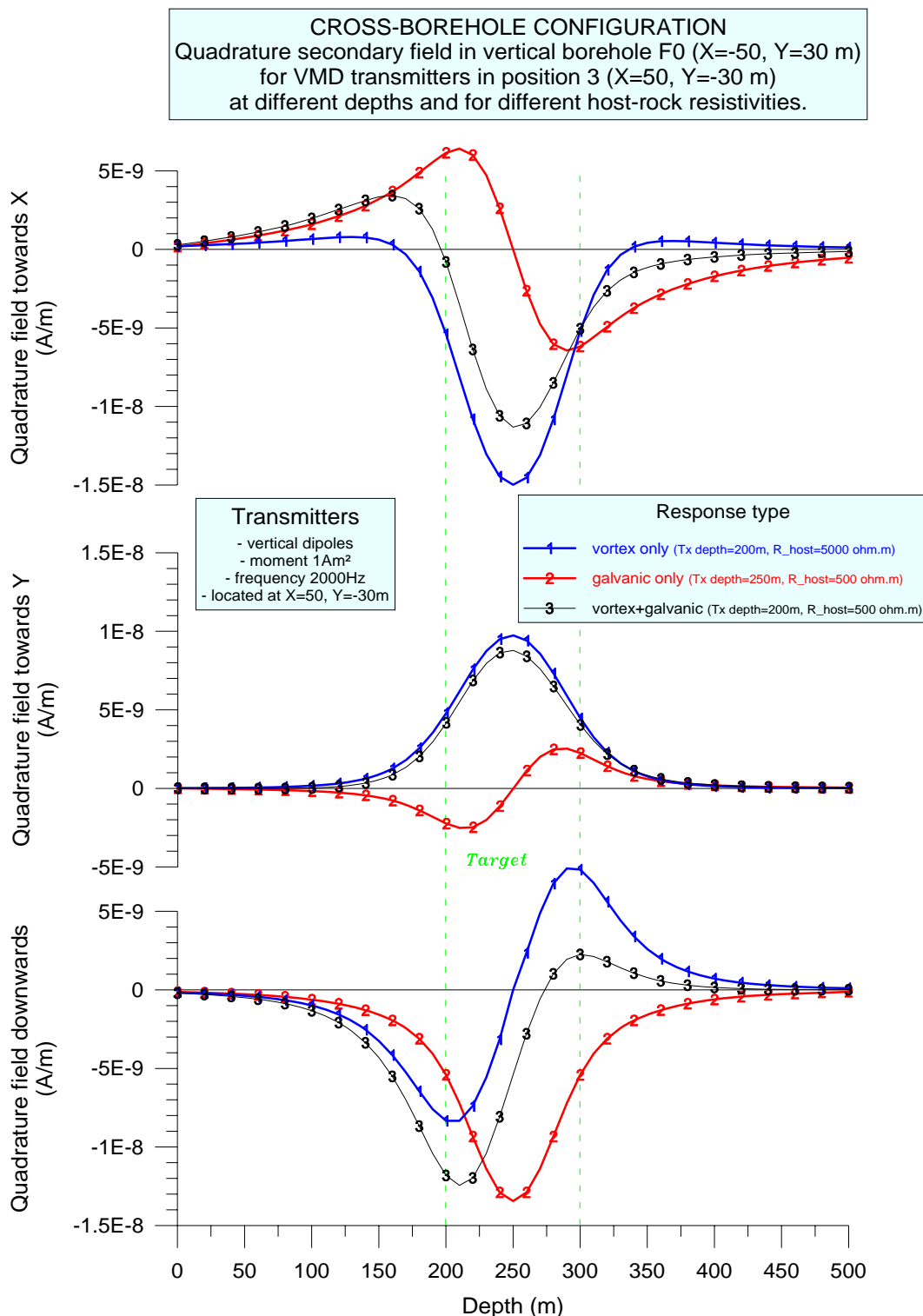


Fig. 2.3-3b: Same as Fig. 2.3-3a with quadrature instead of in-phase field. For the quadrature field, the galvanic-to-inductive ratio for the case of combined effects (black curves labelled 3), appears to be much more important than for the in-phase field. This is because the galvanic effect reacts at lower induction than the inductive effect: in most cases the galvanic is at low induction when the vortex is already close to the resonance. In the complex plane (Fig. 2.3-8), the galvanic secondary vector is closer to the 'Quadrature' axis than the vortex secondary vector, which is often close to the bisecting line. It is important to note that, in the general case of combined effects, the Hy channel is hardly influenced by the galvanic effect, for either in-phase or quadrature, the Hy curves labelled 3 being almost perfectly even.

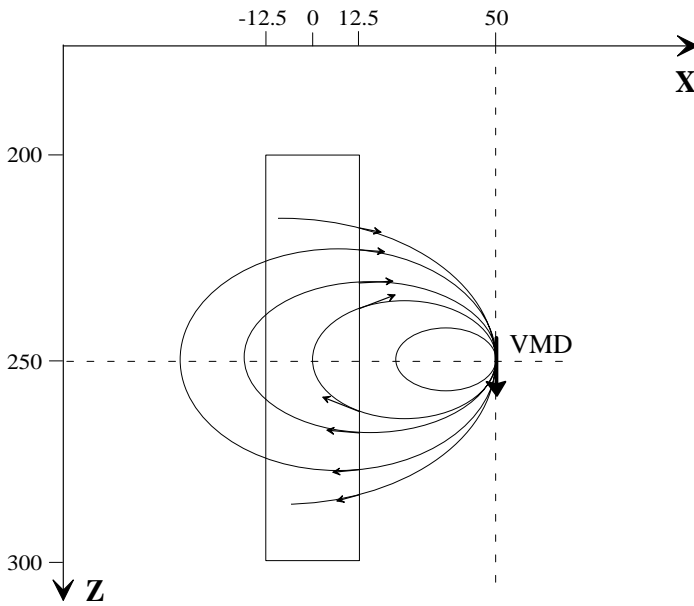


Fig. 2.3-4: Primary magnetic field of a VMD transmitter placed at the depth of the target's center. In this symmetrical situation, the flux on the upper part cancels that on the lower part, which gives zero flux across the target's vertical face and thus a zero inductive coupling. Consequently no vortex reaction will take place in the target.

b) The 'purely vortex' situation, by contrast, needs two conditions: first a resistive host, so that the galvanic effect is negligible³; and also a good inductive coupling, i.e. a good primary magnetic flux across the main face of the conductor. For that, the transmitter must be well above (or below) the target's center (Fig. 2.3-4). Note that, when the Tx VMD is close to the target, i.e. at a horizontal distance which is not greater than 70% of its height, the best inductive coupling is obtained with the VMD at the depth of the target's top, as shown in Fig. 2.3-6a.

Coming back to Fig. 2.3-3, we see that the two types of responses show very different symmetry properties, which are summarized in Table 2.3-1. These properties can be understood with simple representations of the two effects by electric and magnetic dipoles. They can be useful in analyzing the balance between the vortex and galvanic effects.

Field component	Hx	Hy	H _z
Vortex response	Symmetrical (even) (+ - +) or (- + -)	Symmetrical (even) + or -	Anti-symmetrical (odd) (- +) or (+ -)
Galvanic response	Anti-symmetrical (odd) (- +) or (+ -)	Anti-symmetrical (odd) (- +) or (+ -)	Symmetrical (even) + or -

Table 2.3-1: Behaviour of the target's galvanic and vortex secondary magnetic fields as a function of depth in a vertical borehole. The symmetry is considered about the depth of target's center.

We also conclude from Fig. 2.3-3 that, in conductive hosts, the galvanic effect is not a negligible or marginal effect. In a quite standard situation, the galvanic response appears to have the same order of magnitude as the vortex one (Fig. 2.3-3b). This was not so obvious for us before this modelling. It can be conjectured that, in more conductive hosts, the galvanic effect can easily become predominant.

³ A 5000 Ω.m host appears resistive enough to keep the host vortex currents, and their channelling through the target, negligible compared to the vortex currents of the 5 Ω.m target in this configuration.

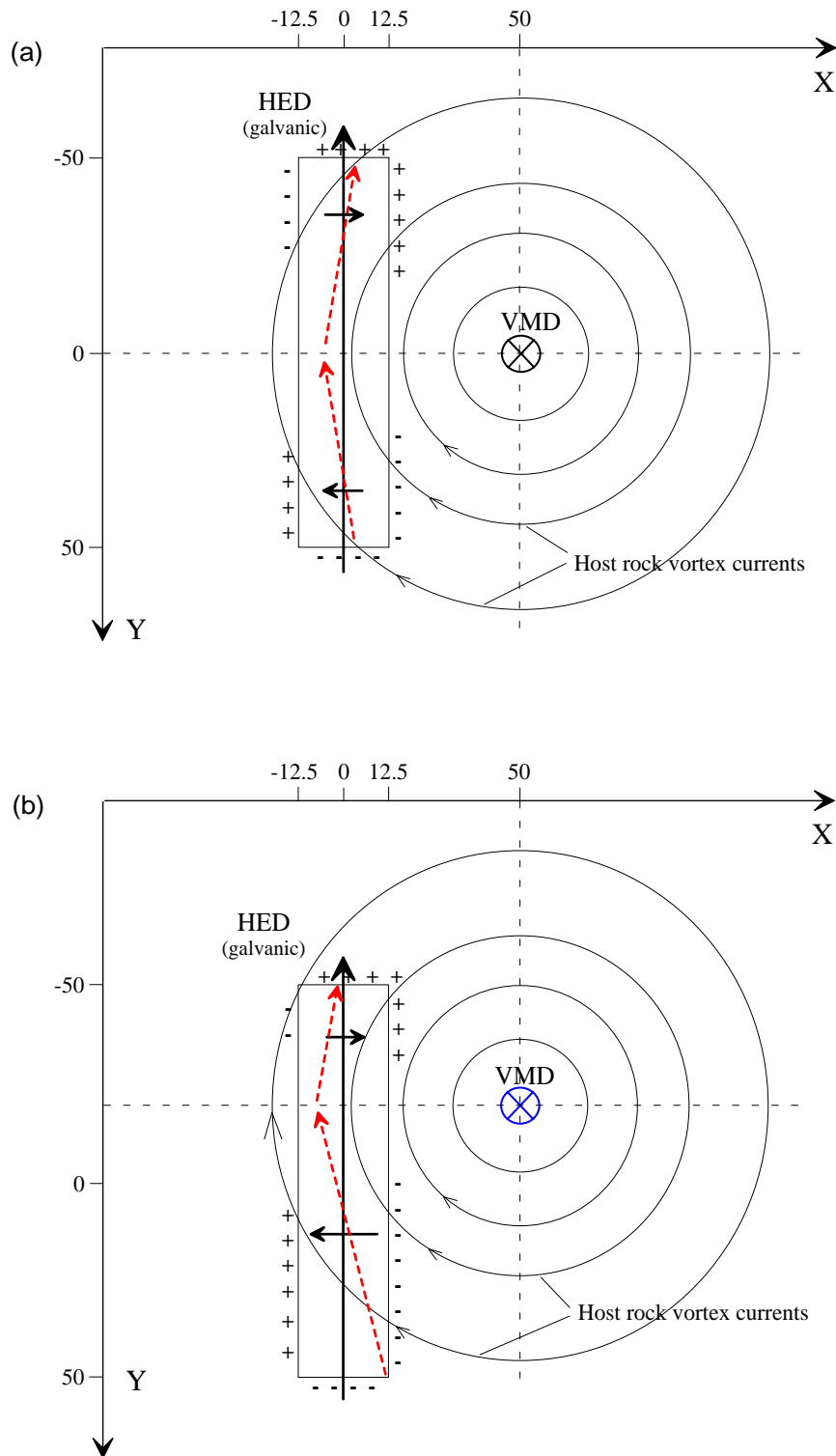


Fig. 2.3-5: Horizontal Electric Dipoles (HED's) equivalent to the galvanic response of the target. The distribution of charges creates a depolarization field which, in turn, produces the channelling of the host-rock vortex currents. The main HED component is along the strike. However, the charges on the lateral faces of the body also create HED components transverse to the strike direction. The resultant HED is oblique (dashed vectors), which explains why the H_y component is not uniformly zero. Case a) corresponds to the symmetrical case of a source VMD in Tx borehole 1, whereas case b) corresponds to the unsymmetrical case of a source VMD in Tx borehole 3, whatever the Tx depth in both cases.

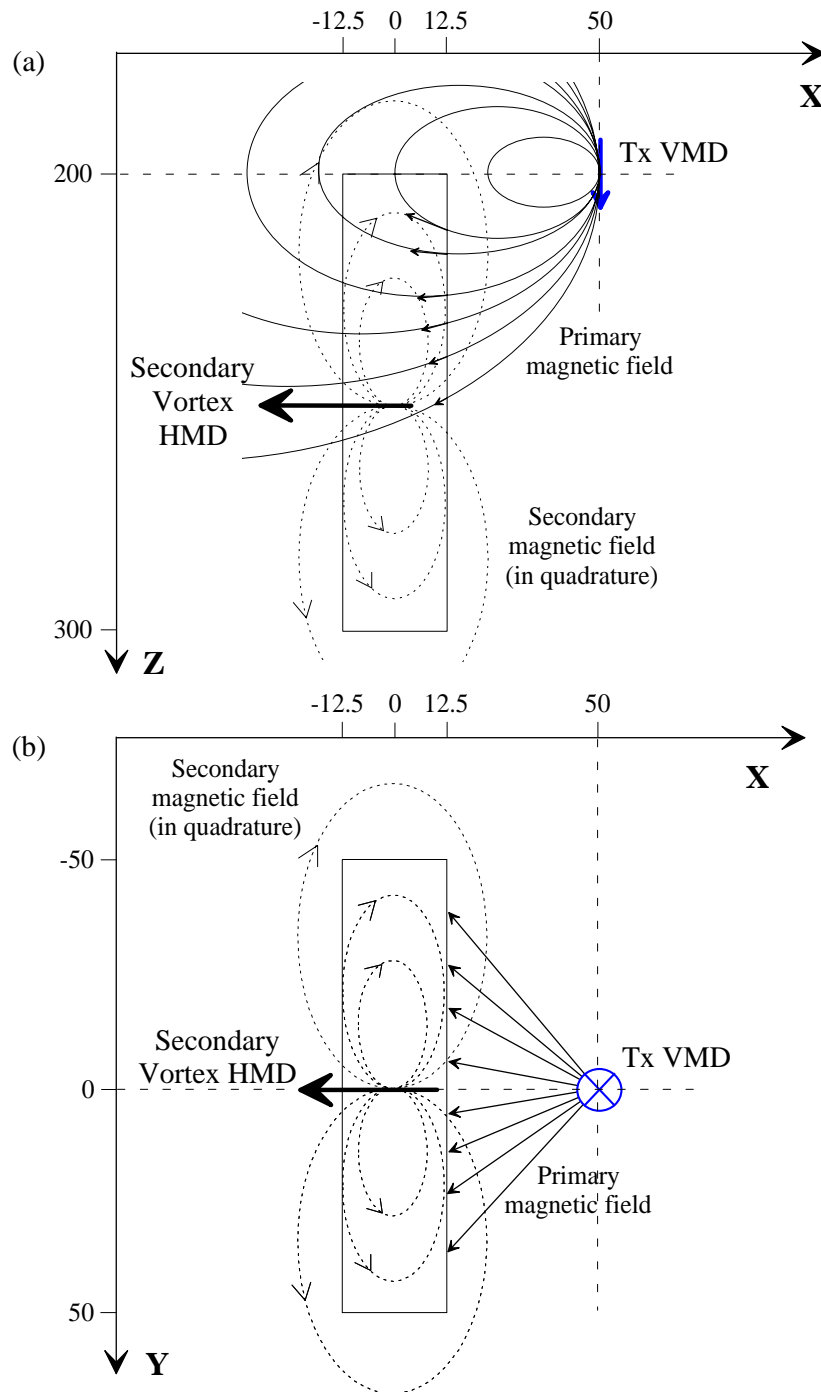


Fig. 2.3-6: Horizontal magnetic dipole (HMD) equivalent to the vortex response of the target. The alternating primary magnetic flux creates eddy currents circulating in closed loops within the conductor. The main circulations are within the plane of the target (YZ plane); their effect can be equated to the field of an HMD directed towards X. The flux across the top and bottom faces of the target being small in this configuration, no significant vortex circulations in the XY plane are expected. Similarly the flux across the front and back faces is not expected to give significant circulations in the XZ plane. Indeed, there is no evidence of distortions created by such effects on Fig. 2.3-3. Only the field of the main, X directed, HMD is clearly visible here.

This situation is partly explained by the fact that the galvanic response, being equivalent to the field of an electric dipole, varies only as $1/d^2$, whereas the vortex response, equivalent to the field of a magnetic dipole, varies as $1/d^3$ and thus decreases much more rapidly than the galvanic response with increasing distance to the target.

In addition to their different spatial geometries, the inductive and galvanic responses also have very different spectral behaviours: for the inductive response, the resonance frequency (frequency at which the quadrature response is maximum) is a function of the size and resistivity of the target, whereas for the galvanic response, it is a function of the distance to the source and host resistivity.

In general, the galvanic response shows a lower induction level than the vortex response, meaning that the resonance of a galvanic effect will be reached at a much higher frequency than for a vortex response.

As a consequence, the two types of responses also have different phase spectra (Fig. 2.3-7).

The spectral behaviour of a confined target **in free space** (i.e. purely vortex response) is well represented by the response of an ideal R-L circuit (Fig. 2.3-8). The phase ϕ varies from -90° at low frequency down to -180° at high frequency. At high frequency ($f/f_r > 10$), the real (or in-phase) part asymptotes to 1, whereas the imaginary (or quadrature) part approaches zero. The representative point never passes above the 'Real' axis (Fig. 2.3-8c).

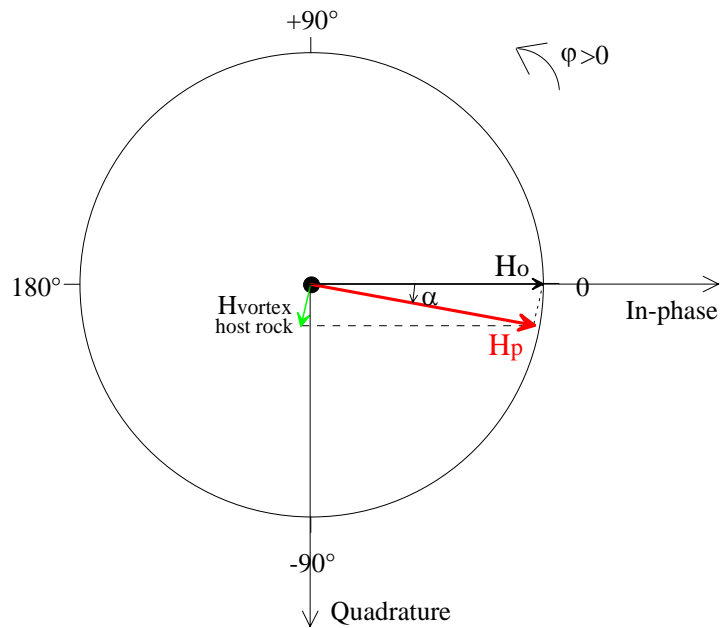


Fig. 2.3-7a: Argand diagram (or complex plot) of the host-rock primary magnetic field. H_p is the sum of the source field in free-space (H_o) and of the vortex response of the conductive host. The case presented corresponds to low induction in the host rock, which is most frequent in common hosts, at ordinary frequencies, and at usual distances from the source.

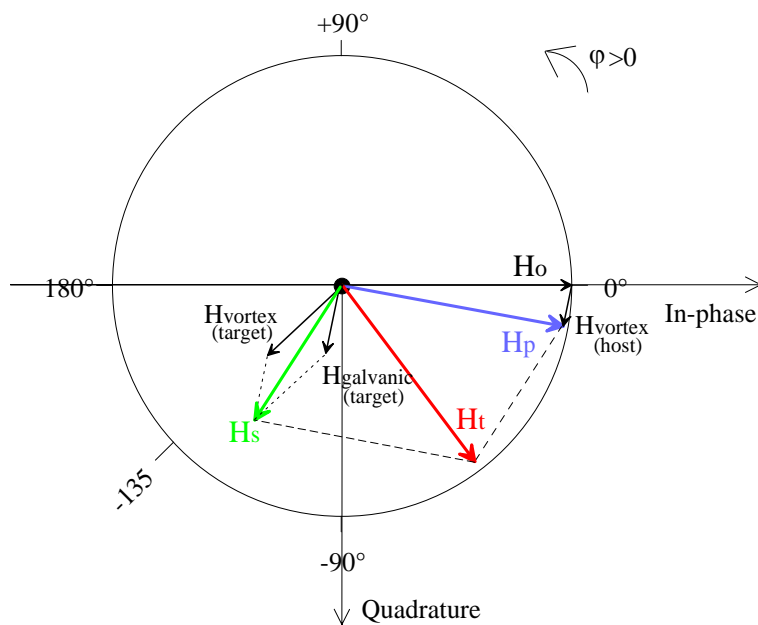


Fig. 2.3-7b: Argand diagram (or complex plot) of the total magnetic field for a confined target within a (less) conductive host. The secondary or scattered field H_s is the sum of the inductive (vortex) and galvanic responses. The field measured is the total field H_t . The case presented corresponds to low induction in the host rock and to resonance (intermediate induction) in the target. Note that the vector $H_{galvanic}$ is parallel to (i.e. in phase with) the vector H_{vortex} of the host.

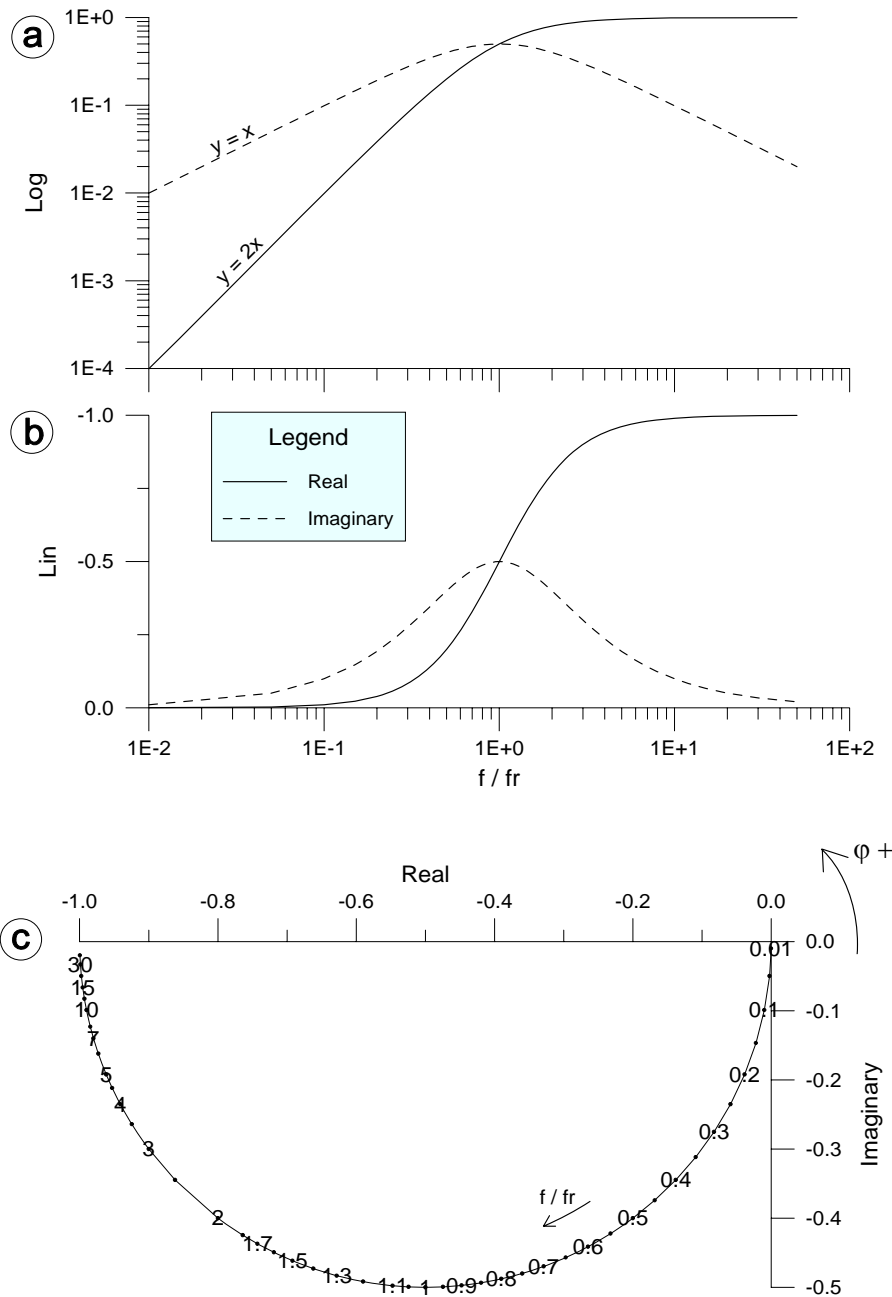


Fig. 2.3-8: Spectral behaviour of the current induced in an ideal R-L circuit (in free space) by an external primary field of flux ϕ_p (vortex response).

The frequency is normalized by the resonance frequency of the circuit (f_r).

The plotted quantity is the dimensionless complex ratio of secondary-to-primary flux i.e. $L \times I_s / \phi_p$.

a) Logarithmic scale; b) Linear scale; c) Complex plot.

2.5.3.3. Equipment design and field configuration

Two main aspects have to be addressed when designing a new method and equipment, as discussed here: a) the detectability of the response over noise and b) the detectability of the response over the primary field. In cross-borehole the second point essentially means the ability of visually separating, on the measured curves, a target response (anomalous field) from the

primary field. In single-borehole, this point also addresses the numerical resolution and the possible need for primary-field compensation for the axial component before A/D conversion.

2.5.3.3.1. Detectability of target responses over noise

The question of the detectability of the EM response (secondary magnetic field) of a target over noise (or response-to-noise ratio) requires to take into account many parameters such as a) the spectral noise density, i.e. internal plus external (magnetotelluric) noise, b) the spectral resolution achieved by the receiver, which itself depends on the sampling parameters – frequency and duration– of the Fourier analysis, and c) the dipolar moments of the transmitter (Tx) probe.

It is also required to define a detectability criterion (or threshold), i.e. a minimum response-to-noise ratio, below which the response is not expected to be sufficiently discernible from noise. This threshold has been taken at 5, which seems a reasonable compromise. The criterion will be considered as achieved if all 3 components of at least one part of the field (i.e. in-phase or quadrature) satisfy the condition simultaneously. This is necessary for further target localization.

In order to translate this noise threshold into a performance criterion, such as a radius of investigation, it is also necessary to define a standard (not too favourable) geoelectric model in which the system is asked to give effective response detection, i.e. response at least five times the noise. Here, the investigation radius was studied with the reference model of Fig. 2.3-1, with either a moderately conductive (5 Ω .m) or a highly conductive (0.5 Ω .m) target in a 500 Ω .m host.

2.5.3.3.1.1. Noise levels

The hypothesis that prevailed for estimating the noise levels is that the total noise density will be limited by the natural magnetotelluric (MT) noise, which supposes that the internal noise of the sensors is kept lower than the MT noise at each frequency. In controlled source methods, this is effectively the way the sensors are devised, as can be seen in Fig. 2.3-51.

The noise levels for each frequency (Table 2.3-2) have thus been estimated from typical MT noise densities, using the sampling frequencies applied by IRIS in the receiver, for two sampling durations: a 'long'⁴ acquisition of 1024 samples (standard case), and a 'short' acquisition of 256 samples.

The noise levels obtained in this way then have to be compared to the target responses given by numerical modelling. This comparison should be done after scaling the modelled responses – which are calculated for a unit transmitter moment (1 Am²)– by the precise dipolar moments produced by the downhole transmitter. In the final prototype, these are about 250 Am² up to 560 Hz, and then quickly decrease down to 50 Am² at 10 kHz –see Fig. 2.3-49.

In fact, it amounts to the same thing to keep the modelling results as they are calculated (i.e. for a unit transmitter moment), and to normalize (divide) the noise levels by the Tx moments. This is what has been done, and the normalized noise levels are plotted against frequency in Fig. 2.3-9. The remarkable feature on this plot is the marked minimum in the 300 - 5000 Hz

⁴ Not too long in fact: at the lowest frequency (35 Hz), the least favourable, the acquisition time of a single measurement of 1024 samples is only 10 sec.

range, which is expected to be a favourable frequency window for measurements⁵. These normalized noise levels will be compared to modelled target responses in subsequent figures.

	Frequency Ft (Hz)	35	140	560	2240	8960
	MT noise density (pT/√Hz)	0.8	0.32	0.074	0.027	0.04
	Sampling frequency Fe (Hz)	8 960	17 920	35 840	35 840	35 840
	Ratio K = Fe/Ft	256	128	64	16	4
N=1024 samples	Ray number R (R=1024/K)	4	8	16	64	256
	Relative resolution 1/R (%)	25 %	12.5	6.25	1.56	0.4
	Spectral resolution Fe/N (Hz)	8.75 Hz	17.5	35	35	35
	MT noise level (μA/m)	1.9	1.1	0.35	0.13	0.19
N=256 samples	Ray number R (R=256/K)	1	2	4	16	64
	Relative resolution 1/R (%)	100 %	50	25	6.25	1.56
	Spectral resolution Fe/N (Hz)	35	70	140	140	140
	MT noise level (μA/m)	3.8 μA/m	2.2	0.7	0.25	0.38

Table 2.3-2: Spectral resolution and natural MT noise for some frequencies (Ft) of the SlimBoris prototype, for a single acquisition of either 256 or 1024 samples. The noise level is obtained by the formula: $\text{Noise_level} = \text{Noise_density} \times \sqrt{\text{Fe} / \text{N}}$, where Fe/N is the spectral resolution.

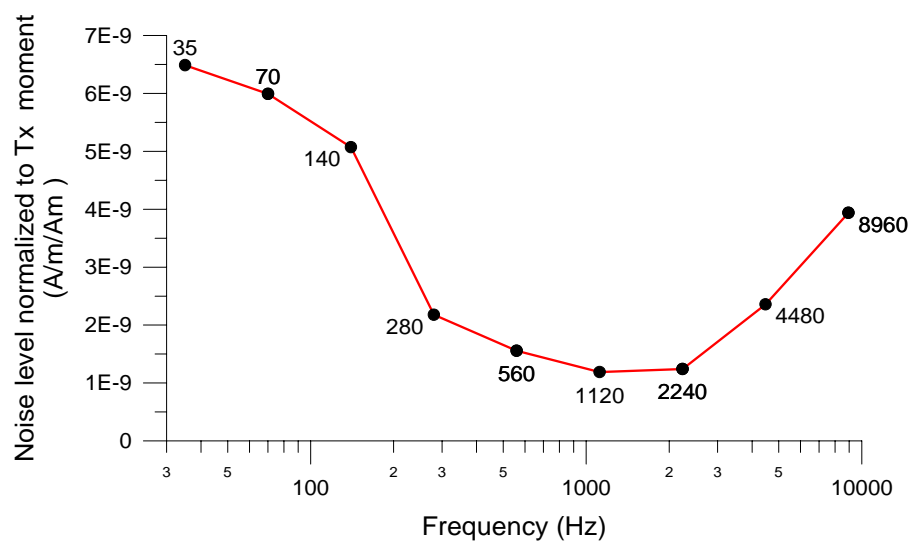


Fig. 2.3-9: Normalized noise levels in the 'SlimBoris' prototype system for a single acquisition of 1024 samples, i.e. noise levels at the receiver normalized by the magnetic moments given by the downhole transmitter (see Fig. 2.3-49). Even though the absolute noise level does not vary much in the 2 – 10 kHz range (see Fig. 2.3-51), the normalized noise level shows a dramatic increase in this range due to the drastic decrease of the transmitter power at high frequency.

Note that a 'short' acquisition of 256 samples would give exactly twice the indicated noise levels.

⁵ Outside this window, it should always be possible (at least theoretically) to decrease the noise by stacking the measurements. Statistically, the noise attenuation expected is equal to $1/\sqrt{N_{\text{stack}}}$. In the current practice of field acquisition, at least 5 to 10 measurements are stacked, making the following discussions concerning the detectability over noise somewhat pessimistic.

Because target responses decrease at least linearly with decreasing frequency, it is possible to anticipate from this curve that frequencies below 280 Hz will not be effective for detecting a target over noise, except possibly in the case of a very conductive target.

2.5.3.3.1.2. Effective detection range in cross-borehole configuration

In the cross-borehole configuration, it is possible to assess the detection range around the reference target by comparing the response logs (secondary magnetic field logs) in a given receiver borehole for several positions of the Tx borehole with the VMD transmitter at a given depth. This is equivalent to analysing, for a given Tx position, the response logs in several receiver boreholes.

This comparison is presented in Fig. 2.3-10, at 2 kHz, for the standard 5 Ω .m target in a 500 Ω .m embedding (Fig. 2.3-1), and for a VMD transmitter at 200 m depth –a situation which corresponds to the general case of mixed vortex and galvanic responses, as discussed above in Fig. 2.3-3. The curve labels (1, 2, 3, 5) refer to the numbering of Tx boreholes defined in Fig. 2.3-1.

Figure 2.3-10 shows that only Tx boreholes 1 and 3 (about 50 m from target's center) satisfy the criterion of a signal-to-noise ratio higher than 5. The criterion is better achieved for the quadrature components, the strongest components in this low-induction situation. Boreholes 2 and 5 (80-100 m from target's center) correspond to the noise limit (response slightly above noise), and boreholes 4 and 6 (not shown on the figure) are below the noise threshold.

With the adopted response-to-noise criterion of 5:1, and for the standard 5 Ω .m target, the detection limit at 2 kHz for a long acquisition (1024 samples) thus appears to be around 50 m from target's center (or 37.5 m from target's closest face), which is in agreement with the initial requirements of the method. A short acquisition (256 samples) gives an acceptable response-to-noise ratio only for Tx borehole 1, and this only for the quadrature components. In the rest of the report, only the standard 1024-sample acquisition will be considered.

Note that the natural MT noise is known to decrease with increasing depth, which can give a slightly increased performance against noise, as the noise would then be strictly limited to the internal noise of the equipment.

Still with the moderately conductive target, another question which naturally arises is at which frequencies, in addition to the previously seen 2 kHz, will an effective detection range of about 50 m from target's center (for both Tx and Rx) be possible.

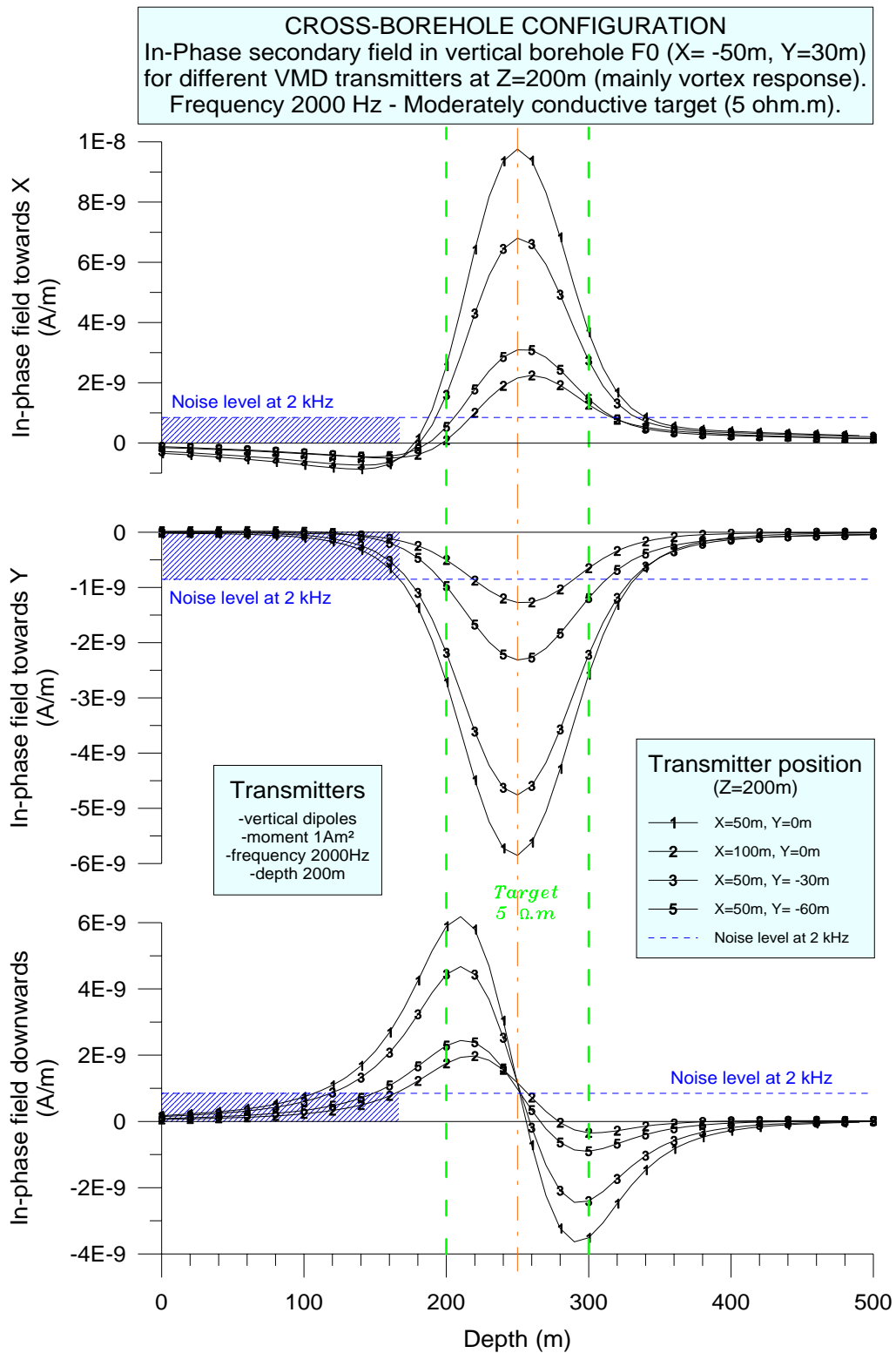


Fig. 2.3-10a: Cross-borehole configuration. In-phase secondary magnetic field scattered, at 2 kHz, by the moderately conductive target (5 Ω.m) for different VMD transmitters at Z=200 m. The receiver borehole F0 (X=-50, Y=30 m) stands at about 50 m from target's center. The situation corresponds to mixed vortex and galvanic responses, with predominance of vortex response for the in-phase field.

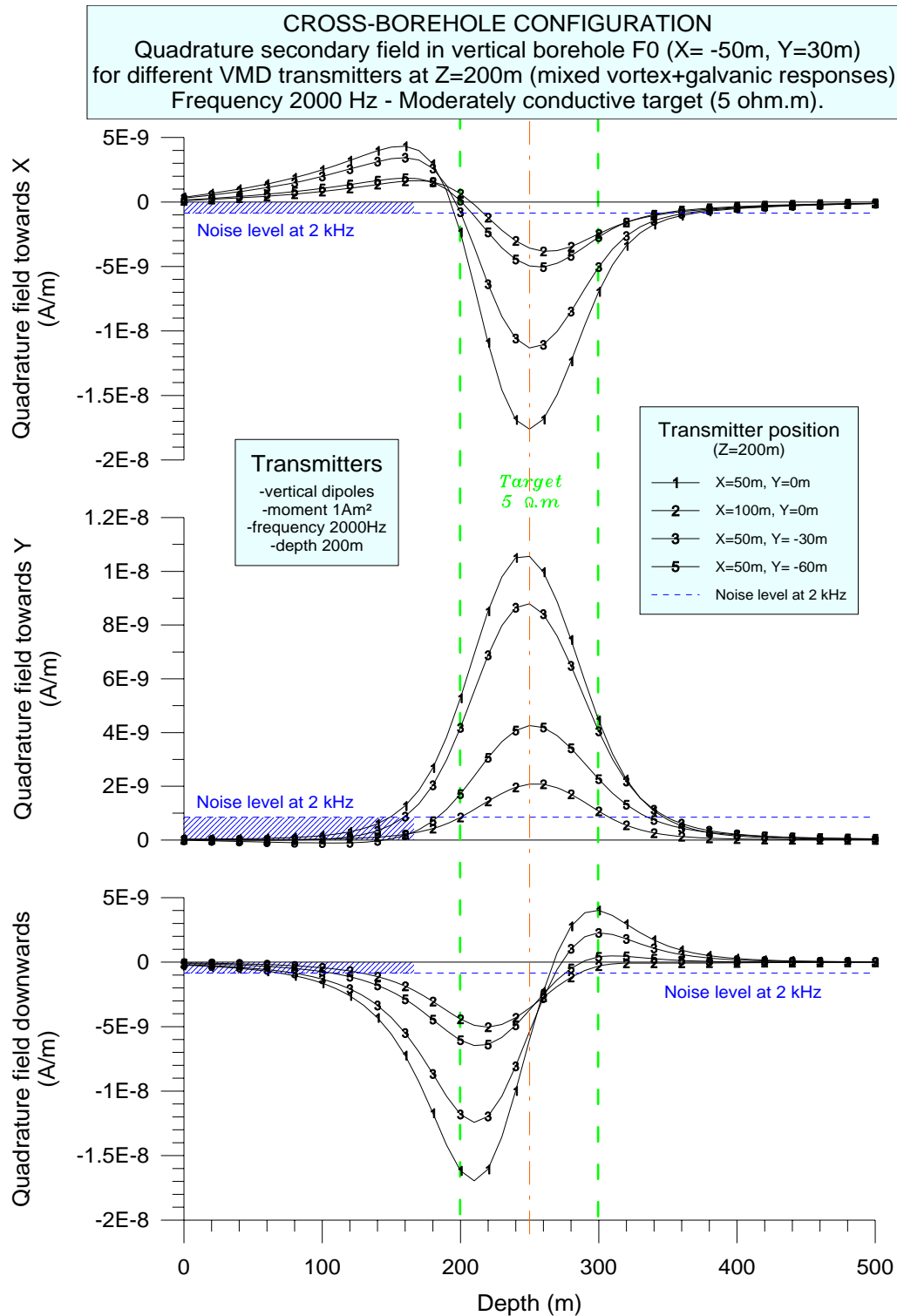


Fig. 2.3-10b: Same as Fig. 2.3-10a with quadrature instead of in-phase field. Vortex effect is still predominant, but as already seen in Fig. 2.3-3b, the balance between galvanic and vortex responses is more equilibrated for the quadrature field than for the in-phase.

N.B.: The noise has been estimated from Table 2.3-2 considering a single standard acquisition of 1024 samples and a transmitter moment of 150 Am² –the theoretical value anticipated at the beginning of the project. The actual Tx moment obtained is somewhat smaller –about 100 Am²– but it can be considered that stacking will in practice compensate the difference. Both noise and responses are normalized to 1 Am² in the transmitter.

Figure 2.3-11 shows the evolution of the target response (compared to noise levels) with varying frequency for the standard 5 Ω .m target. The transmitter and receiver boreholes are located symmetrically at about 50 m from target's center. The VMD transmitter is at 200 m depth.

When passing from 2 kHz (curve 3) to 10 kHz (curve 4), the in-phase target response (the strongest part of the response at high frequency) is significantly increased (Fig. 2.3-11a). Nevertheless, the normalized noise level is also dramatically increased in the same frequency interval (see Fig. 2.3-9), due to the drastic decrease of the transmitter power at high frequency, and thus the detection capabilities of the in-phase field are approximately the same at 10 kHz as at 2 kHz. In the same interval, the quadrature target response (Fig. 2.3-11b) is essentially decreased when passing from 2 kHz to 10 kHz, showing that the latter frequency falls in the high induction domain, i.e. beyond the resonance.

At low frequency, when passing from 2000 Hz to 600 Hz (curve 2), the normalized noise level is almost constant (see Fig. 2.3-9), but the target response decreases rapidly, especially for the in-phase components⁶. As a consequence, the in-phase response at 600 Hz is below the noise level and the quadrature response is only 3 times the noise level –thus the detectability criterion is not satisfied either for the in-phase or for the quadrature fields.

Considering on Fig. 2.3-11 the response extrema (in absolute values) of the three in-phase and quadrature plots at each frequency, it is possible to build Fig. 2.3-12, which compares the frequency behaviours (i.e. the spectra) of target response and of normalized noise levels.

The target response as a function of frequency shows the classical features of EM responses:

- in the low-induction domain (here below 1 kHz), the in-phase response increases rapidly with increasing frequency, varying as the square of the frequency (f^2), whereas the quadrature response increases only linearly with frequency (f).
- at the resonance, or intermediate induction (here around 2 kHz), the quadrature response shows a maximum, whereas the growth of in-phase response begins to slow as it approaches the saturation or conductive limit.
- beyond the resonance, in the high-induction domain (here above 5 kHz), the in-phase response begins to saturate and approaches an asymptotic limit, whereas the quadrature response approaches zero as the inverse of the frequency ($1/f$).

⁶ At low induction, the in-phase EM response is known to vary as the square of the frequency (f^2), whereas the quadrature response varies only as the frequency (f).

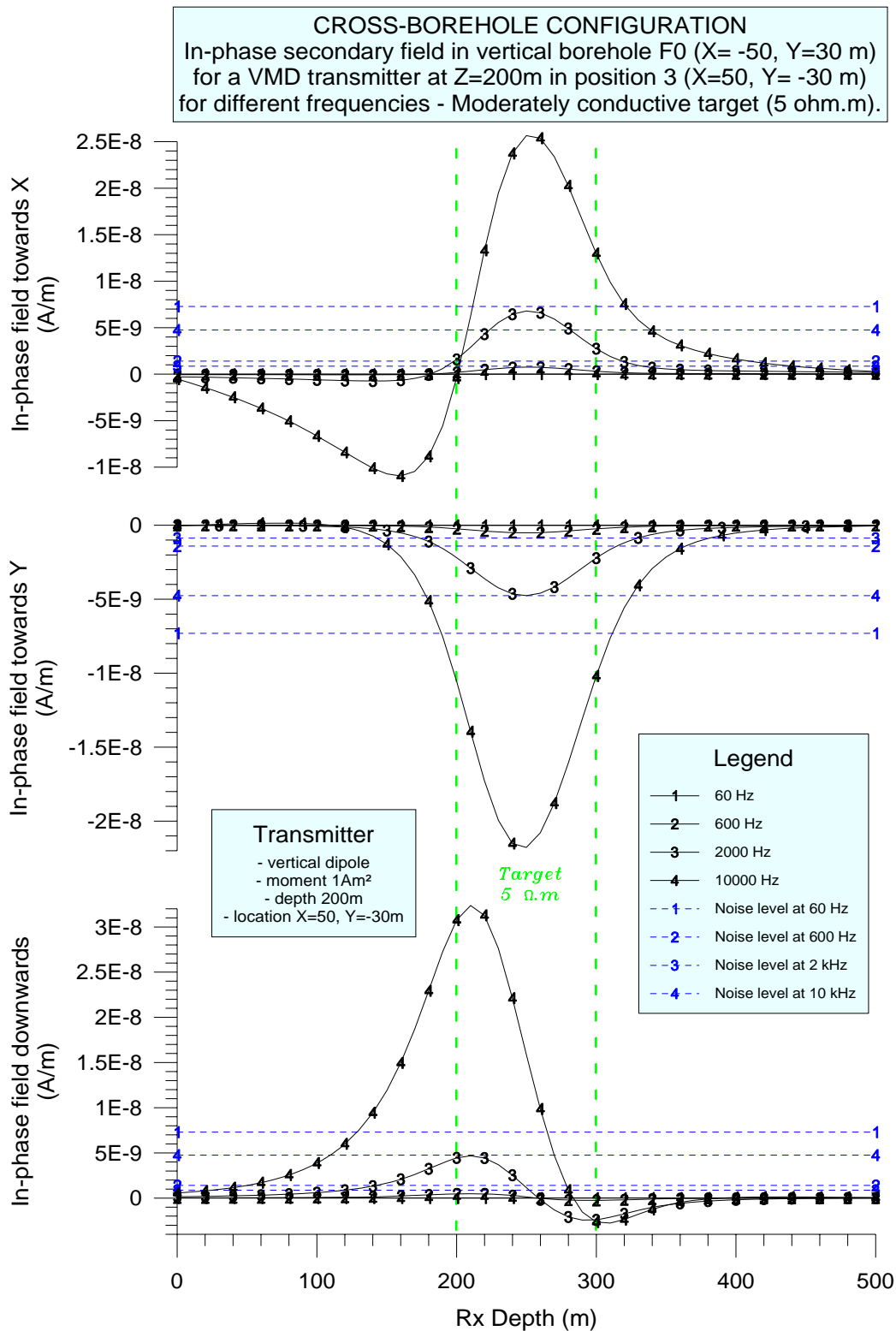


Fig. 2.3-11a: Cross-borehole configuration. In-phase secondary magnetic field scattered at different frequencies by the moderately conductive target (5 Ω.m), compared to normalized noise levels. The receiver borehole is F0 (X=-50, Y=30 m), and the VMD transmitter is at Z=200 m in Tx borehole 3 (X=50, Y=-30 m); the two boreholes stand at about 50 m from target's center. The situation corresponds to mixed vortex and galvanic responses, with marked predominance of vortex effect at low frequency (2000 Hz and below), evolving to predominance of galvanic effect at high frequency (10 kHz and above).

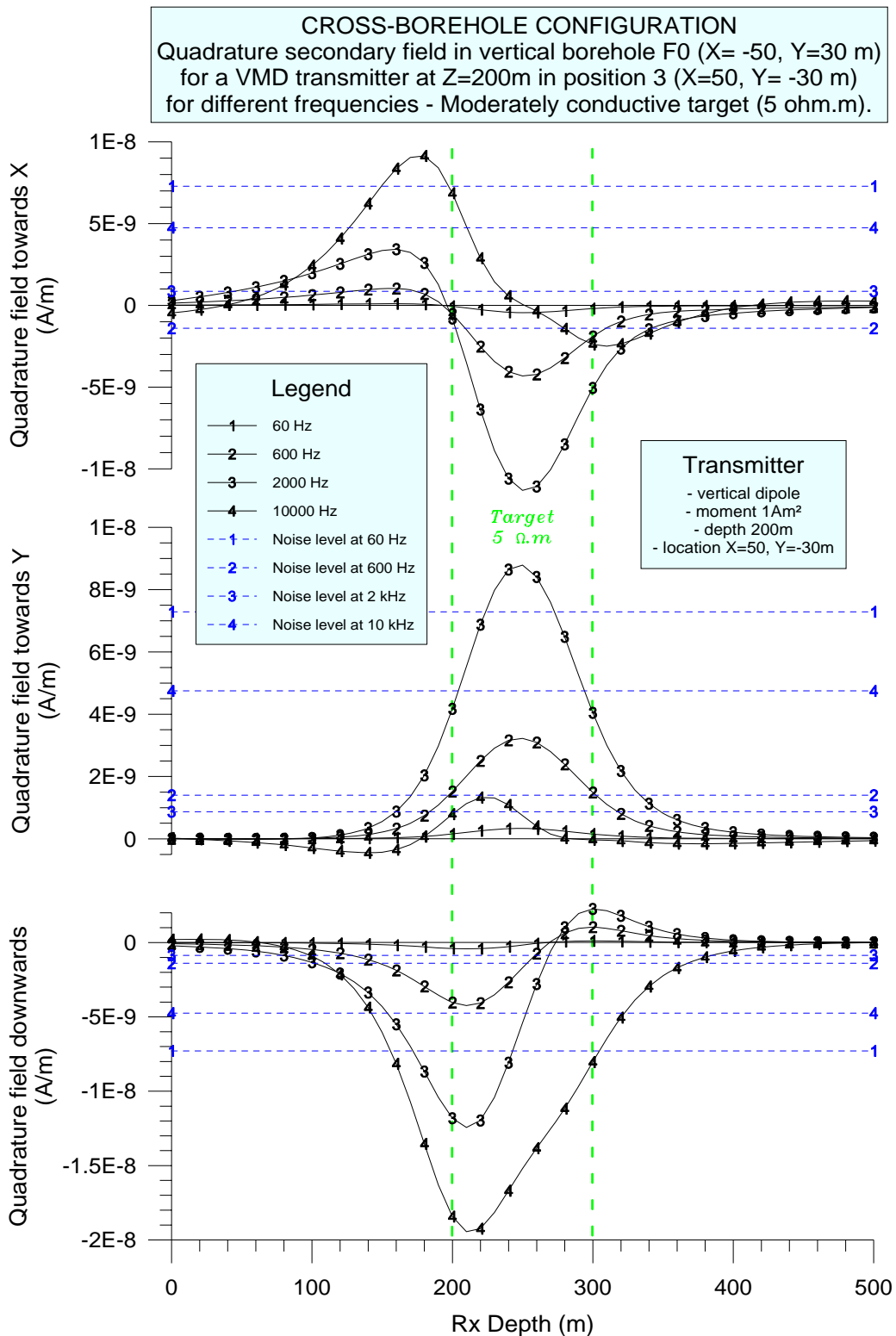


Fig. 2.3-11b: Same as Fig. 2.3-11a with quadrature instead of in-phase field. For the quadrature, the apparent predominance of galvanic effect starts from 2000 Hz and above. The indicated noise levels are those given in Fig. 2.3-9 for a standard acquisition of 1024 samples. Both noise and responses are normalized to 1 Am² in the transmitter.

In fact, only the Hy channel, the least influenced by the galvanic effect (i.e. almost purely vortex), perfectly follows the theoretical behaviour described above for the quadrature field at high induction. On Hx and Hz quadrature channels, the galvanic response, whose resonance is situated at higher frequency than for the vortex response, prevents the normal decrease of the quadrature response at the highest frequency (particularly on the Hz component).

Coming back to our practical considerations, it clearly appears in Fig. 2.3-12 that, for the 5 Ω.m target, the frequency giving the best response-to-noise ratio (obtained in quadrature) is around 2 kHz, due to the concomitance of target resonance (giving quadrature maximum) and of noise minimum. Within a 50 m radius around such a target (for both Tx and Rx boreholes), the lowest frequency at which detection should be possible is about 1 kHz for the quadrature field, and about 2 kHz for the in phase. In overall, the useful frequency window is 1 - 4 kHz.

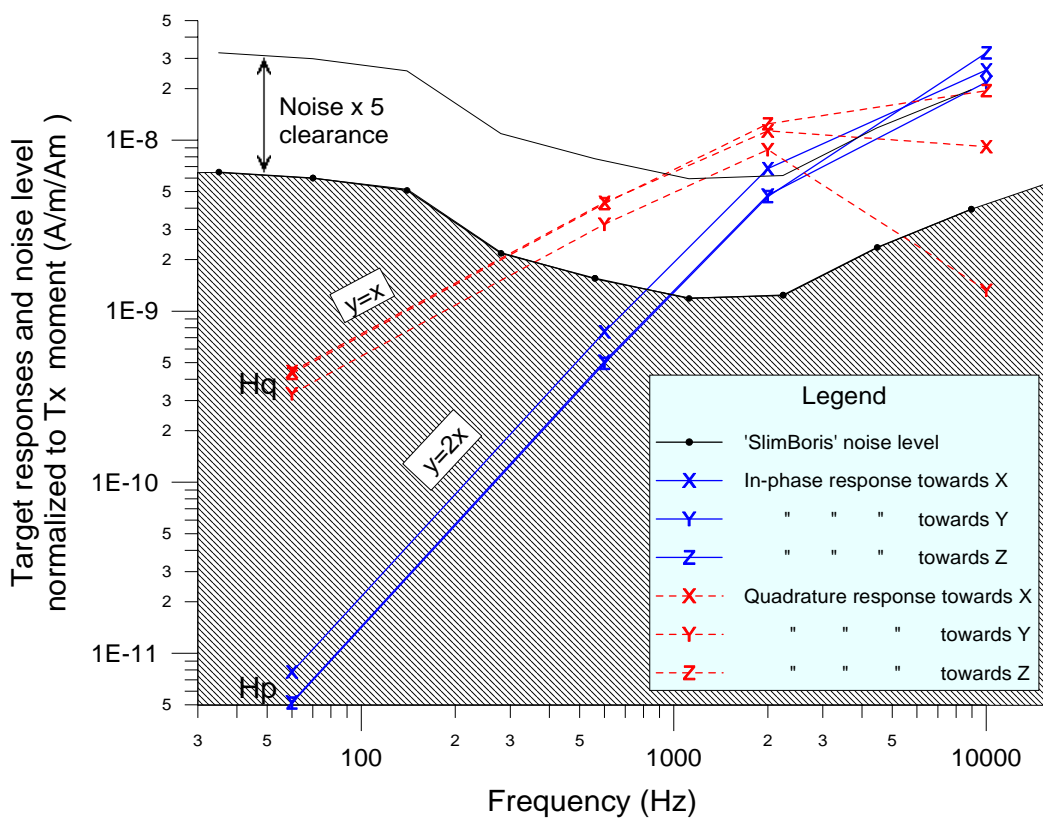


Fig. 2.3-12: Target response maxima as a function of frequency for the 5 Ω.m target in the geometrical configuration described in Fig. 2.3-11, with both Tx and Rx boreholes at about 50 m from target's center. The responses are compared to the normalized noise levels of the prototype EM system. With the adopted response-to-noise ratio of 5:1, it appears that frequencies below 1000 Hz will not be effective for detecting a moderately conductive target over noise within a 50 m radius from both Rx and Tx boreholes.

Let us study now the case of the **highly conductive target** (0.5 Ω.m). It is expected, of course, that target detection will be possible at lower frequencies, or at greater distances from the target.

Figure 2.3-13 shows the evolution of the response from the 0.5 Ω .m target with varying frequency, in the same geometrical situation as in Fig. 2.3-11. The behaviour appears to be extremely complex, due to the superposition of the vortex and galvanic effects, whose resonance frequencies are now more separated than in the previous case with the 5 Ω .m target.

In addition, the quadrature vortex response (Fig. 2.3-13b) shows a change in sign at high frequency, due to additional phase rotation caused by the conductive host (see H_y component). This complex behaviour is worthy of some further clarification. In a conductive host, the target reacts according to the primary field that it receives from the transmitter, and integrally undergoes the phase rotation and amplitude attenuation caused by its host. For example, if the host causes a -40° phase rotation and an extra 0.8 attenuation⁷ of the primary field at the target location, the vortex response will be only 80% of that obtained in free-space and will be -40° phase-rotated compared to its free-space value.

It can be said that the vortex response of a target in a conductive host is approximately equal to its response in free-space multiplied by the complex transfer function of the slice of ground located between the source and the target (Lajoie and West, 1976; West and Edwards, 1985; West and Macnae, 1991).

The attenuation and phase rotation due to the conductive host increase with increasing frequency. Thus, coming back to Fig. 2.3-8, it is easy to understand that the additional, negative, phase rotation⁸ caused by the conductive host will inevitably result, at sufficiently high frequency, in a representative point passing above the 'Real' axis at the inductive limit. This is exactly what we observe in the data of Fig. 2.3-13b, especially on the H_y channel, and also on the H_x channel.

The behaviour of the H_z quadrature response (bottom of Fig. 2.3-13b) is even more complex and not completely understood.

⁷ Attenuation adding to the normal free-space attenuation, which already varies as $1/r^3$.

⁸ With the adopted sign conventions, the filtering due to a slice of ground always results in negative phase rotations.

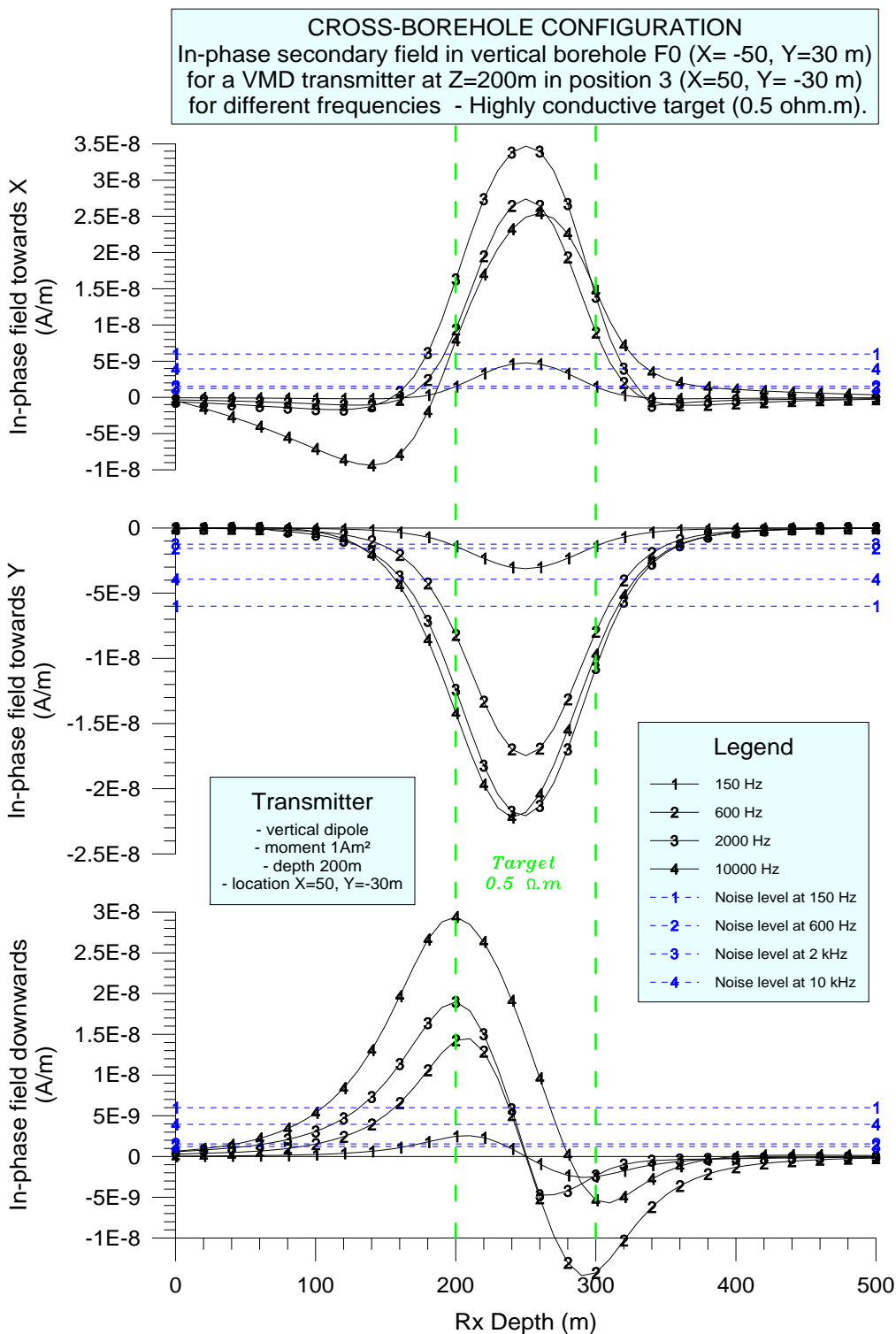


Fig. 2.3-13a: Cross-borehole configuration. In-phase secondary magnetic field at different frequencies from the highly conductive target (0.5 Ω.m), compared to normalized noise levels. The receiver borehole is F0 (X=-50, Y=30 m), and the VMD transmitter is at Z=200 m in Tx borehole 3 (X=50, Y=-30 m); the two boreholes stand at about 50 m from target's center. The situation corresponds to mixed vortex and galvanic responses, with marked predominance of vortex effect at low frequency (600 Hz and below), evolving to predominance of galvanic effect at high frequency (2 kHz and above). Effectively, at high frequency, the in-phase galvanic response, being at low induction, rapidly increases with increasing frequency, while the in-phase vortex response simultaneously decreases, due to additional phase rotation in the conductive host (see text and Fig. 2.3-14a).

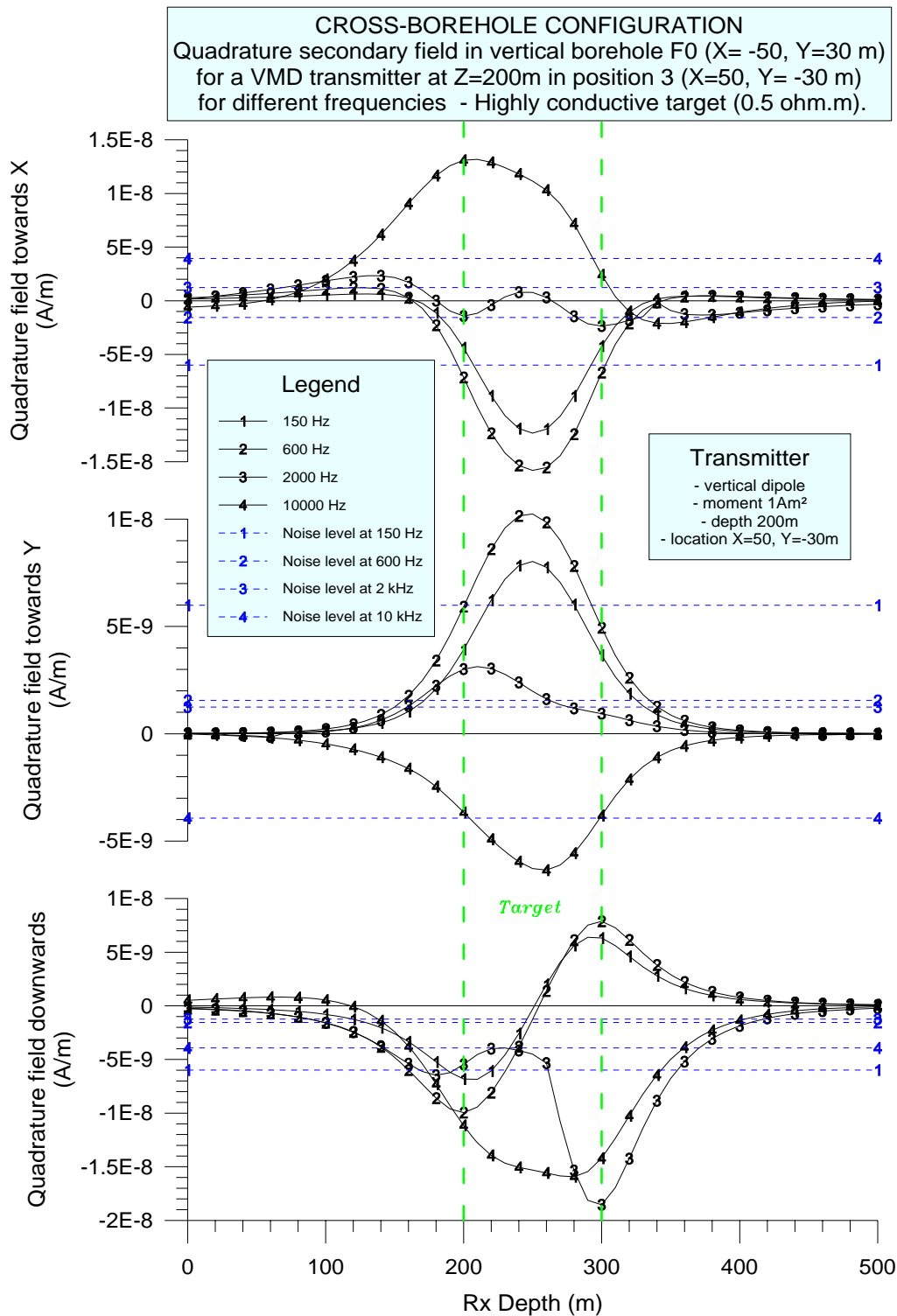


Fig. 2.3-13b: Same as Fig. 2.3-13a with quadrature instead of in-phase field.

At high frequency, the galvanic response becomes predominant because the quadrature galvanic response increases with increasing frequency (being still at low induction), whereas the quadrature vortex decreases to zero (being already at high induction). In fact, the behaviour is even more complex, due to the additional phase rotation induced by the conductive host, which results in a change of sign of the quadrature vortex response at high frequency (see text and Fig. 2.3-14a).

The indicated noise levels are those given in Fig. 2.3-9 for a standard acquisition of 1024 samples. Both noise and responses are normalized to 1 Am² in the transmitter.

Considering on Fig. 2.3-13 the response extrema (in absolute values) of the three in-phase and quadrature plots at each frequency, it is possible to build Fig. 2.3-14. The upper part (complex plot) shows the phase spectrum of the target response, whereas the lower part, similar to Fig. 2.3-12, shows the amplitude spectrum of the response of the highly conductive target compared to the normalized noise spectrum.

The reversal of the quadrature Hx and Hy responses at high frequency appears clearly on the complex plot (Fig. 2.3-14a).

The magnitude of the response (height of the different curves) is about the same as for the moderately conductive target, but the resonance frequency has been shifted by nearly one decade towards low frequencies, in agreement with the EM theory⁹.

This frequency shift results in a wider frequency window in which detection of the target over noise is possible. The frequency window giving the best response-to-noise ratio (obtained now on the in-phase field instead of the quadrature field) is 1 - 2 kHz. Within a 50 m radius around the highly conductive target, the useful frequency window is 300 Hz - 9 kHz.

Figure 2.3-15 shows the in-phase response extrema from the 0.5 Ω .m target at 2 kHz (frequency giving best response-to-noise ratio), as a function of distance between the receiver borehole and target's center, with a transmitter at about 50 m from target's center. The detection range in this configuration appears to be around 100 m from the receiver borehole. This range is confirmed by Fig. 2.6-16, which gives, in the same situation, a contoured presentation of each component of the in-phase target response, in the Y=30 m vertical plane through the target.

From the above results, a rough interpolation enables to state that, for the highly conductive target, the effective investigation radius at 2 kHz in cross-borehole will be about 75 m for both Tx and Rx.

⁹The theory says that the resonance frequency varies as the target's resistivity (when all other parameters are constant), so it should be divided by 10. In fact, the resonance frequency now appears to be around 300-500 Hz which is not exactly one decade below the previous 2 kHz. This slight discrepancy with the theory is probably due to the combination of the vortex and galvanic effects.

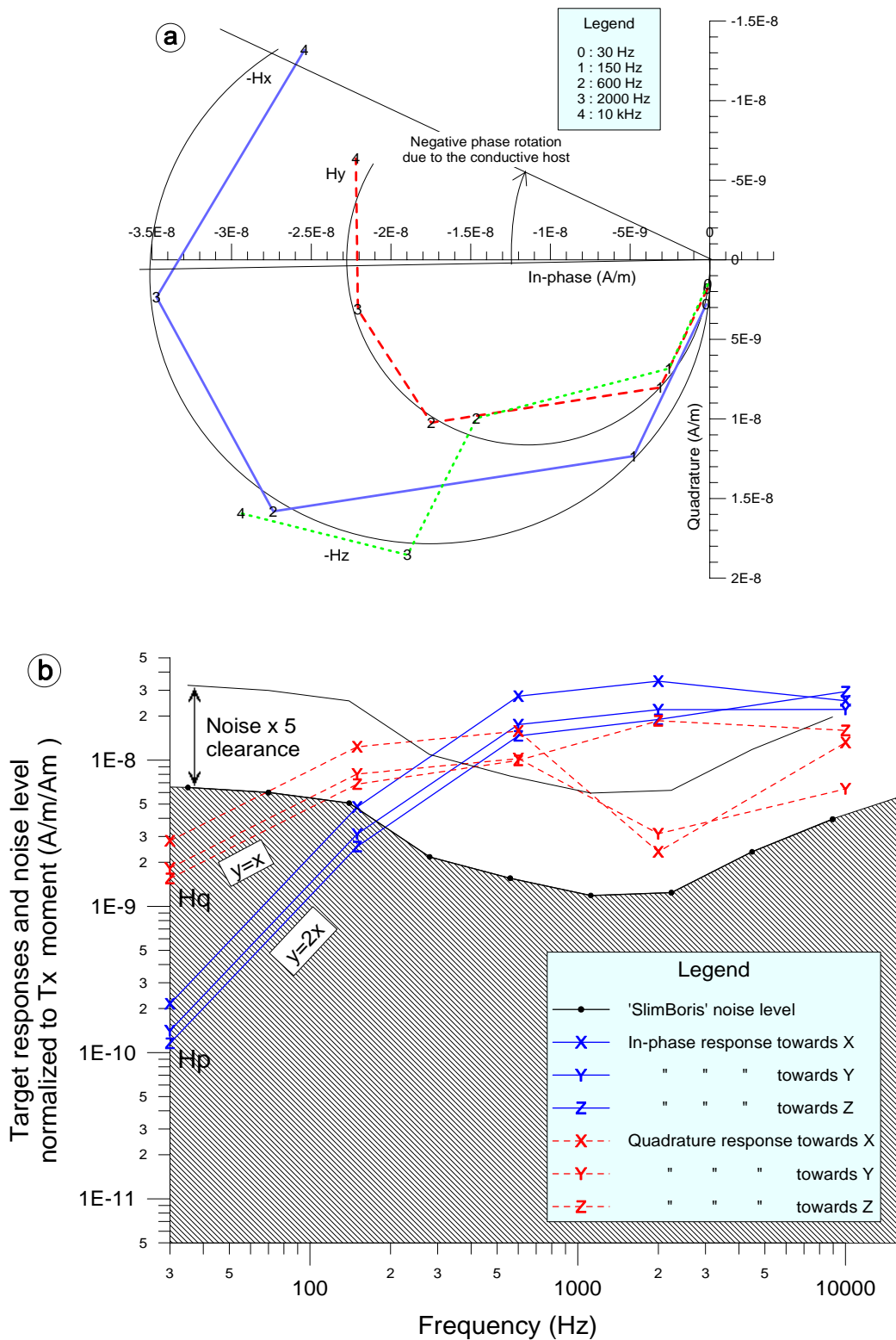


Fig. 2.3-14: Target response maxima as a function of frequency for the 0.5 Ω.m target in the geometrical configuration described in Fig. 2.3-11, with both Tx and Rx boreholes at about 50 m from target's center. a) Complex plot, showing the quadrature reversal at high frequency for channels Hx and Hy. b) Amplitude plot. The amplitudes are compared to the normalized noise levels of the prototype EM system. With the adopted response-to-noise ratio of 5:1, it appears that detecting a highly conductive target over noise in a 50 m radius (for both Rx and Tx boreholes) will be possible down to about 300 Hz, instead of 1000 Hz with the moderately conductive target.

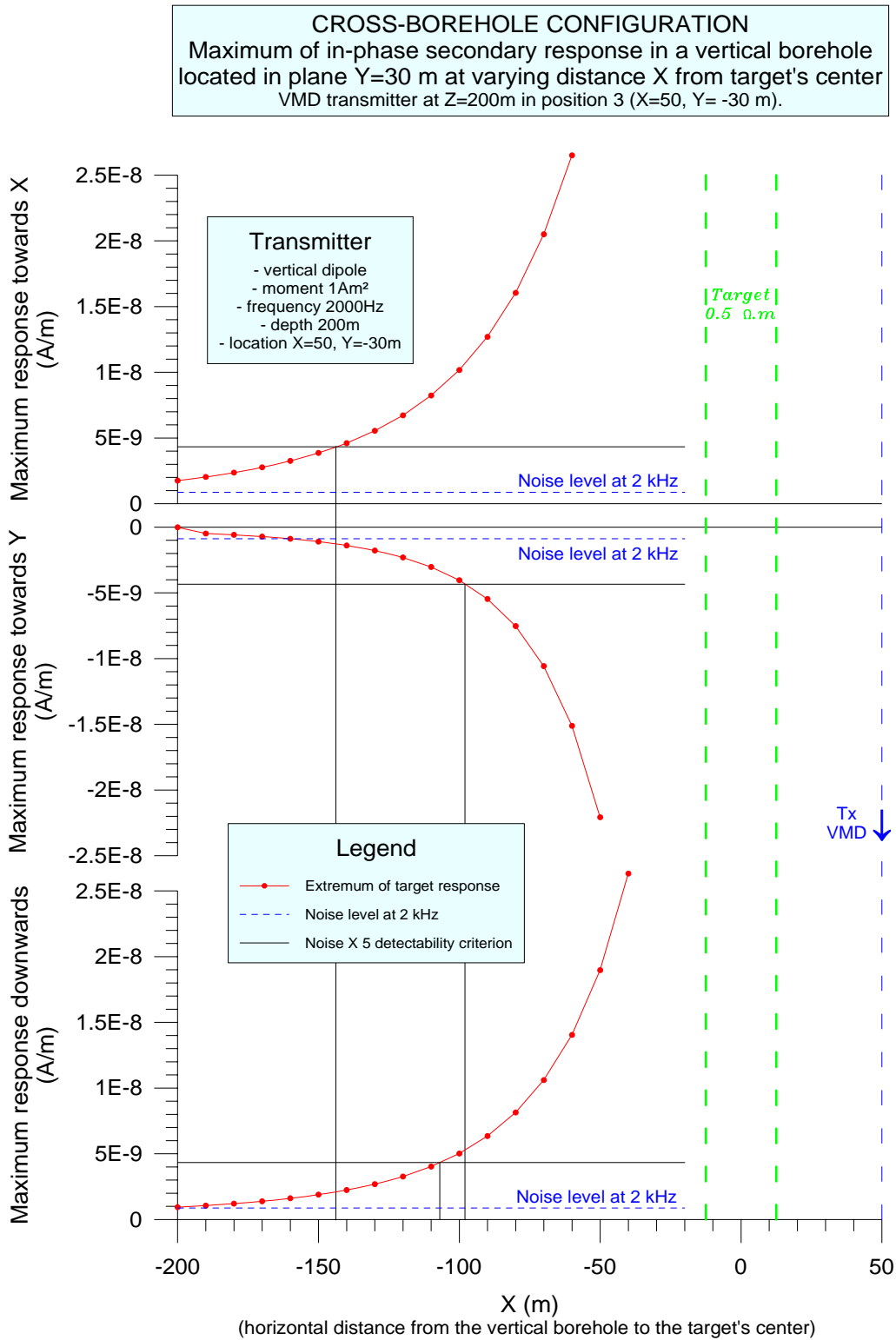


Fig. 2.3-15: Extrema of the three components of the in-phase target response at 2 kHz, as a function of distance (along X axis) between receiver borehole and target's center, for the highly conductive target (0.5 Ω.m). The VMD transmitter is at Z=200 m in Tx borehole 3 (X=50, Y=-30 m) at about 50 m from target's center. Extrema are evaluated in the receiver borehole at Z=250 m for channels Hx and Hy, and at Z=200 m for channel Hz. The noise level (for 1024 samples) and the responses are normalized to 1 Am² in the transmitter. This plot shows that, for the highly conductive target, the detection range at 2 kHz is at least 100 m from the receiver borehole, for a transmitter at about 50 m.

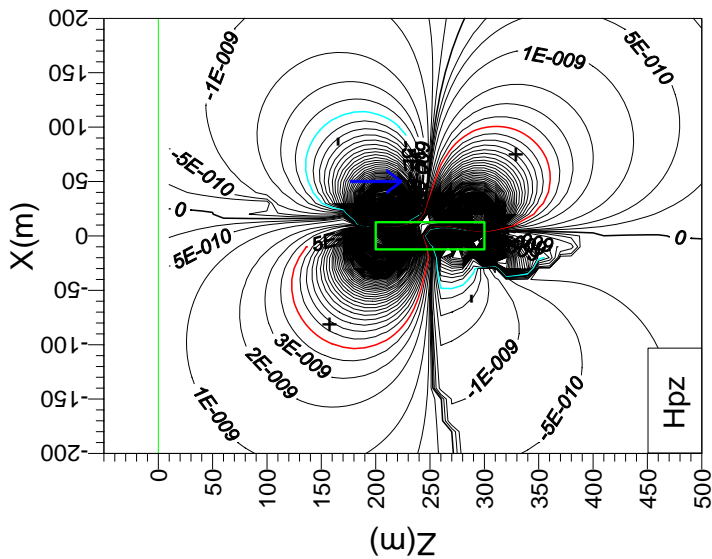
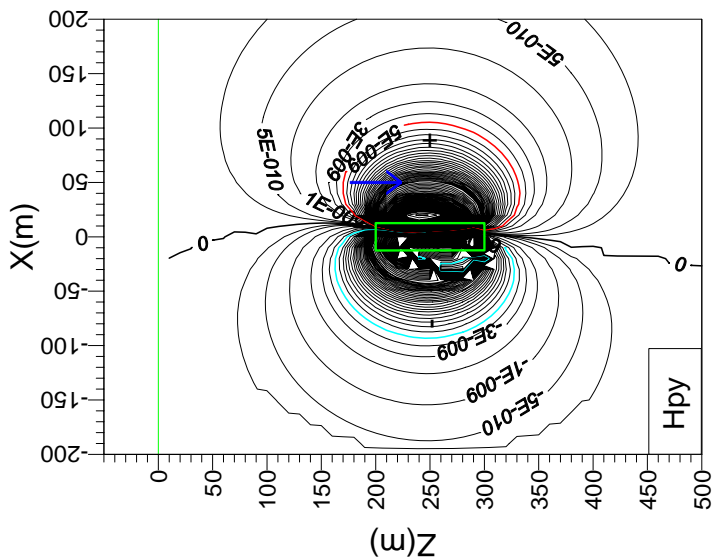
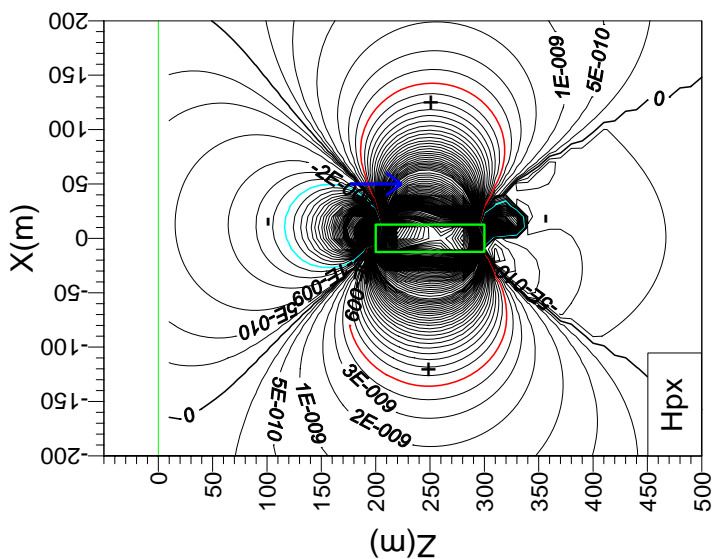


Fig. 2.3-16: Contours of 3-component in-phase response at 2 kHz for the highly conductive target (0.5 Ω.m) with a VMD transmitter at Z=200 m in Tx borehole 3 (X=50, Y=-30 m).



The plane in which data are presented is the Y=30 m vertical plane through the target (plane containing borehole F0, see Fig. 1).

- Bottom: In-phase secondary magnetic field towards X (HpX)
- Center: In-phase secondary magnetic field towards Y (HpY)
- Top: In-phase secondary magnetic field downwards (Hpz).



The thick contour lines represent the normalized noise level at 2 kHz multiplied by 5, thus materializing the detectability criterion.

The various plots confirm an effective detection range of about 100 m around the target in this configuration.

Some numerical instability may be suspected to the left and below the target (especially on Hpz contours).

2.5.3.3.1.3. *Effective detection range in single-borehole configuration*

In the single-borehole configuration, a similar analysis concerning the question of response-to-noise detectability has been performed and it yields the same general conclusions as in cross-borehole. The study is simpler because only one borehole is to be considered. Nevertheless an additional parameter is in play, the Tx-Rx separation.

The longest spacing is the most critical for noise because, for a given target and a given Tx position, the secondary field at the receiver is the smallest, due to the greatest target-to-receiver distance. Consequently, the following discussion about response-to-noise detectability is essentially based on a 100 m Tx-Rx spacing, the longest in the present prototype.

Note that the frequency analysis has not been re-made for the single-borehole case because the frequency behaviour of the target response is supposed to be the same as in cross-borehole. Consequently, all the single-borehole calculations were performed at 2 kHz, the frequency giving the best quadrature response-to-noise ratio for the 5 Ω .m target (see Fig. 2.3-12), and the best in-phase response-to-noise ratio for the 0.5 Ω .m target (see Fig. 2.3-14b).

We first study the evolution of the reference target response for the 100 m spacing when the borehole is 'moved' about the target at a variable distance (ranging from 50 to 117 m) and for a variable azimuth from its center.

Figure 2.3-17 presents the borehole Slingram responses from the moderately conductive target (5 Ω .m) at 2 kHz in boreholes Tx1 to Tx6 (see Fig. 2.3-1) for a 100 m spacing. Only borehole Tx1 (50 m from target's center) satisfies the criterion of a signal-to-noise ratio higher than 5. The criterion is only achieved for the quadrature components, the strongest components in this low-induction field situation, but borehole Tx3 is very close to achieving the criterion for the quadrature field as well.

Similarly, Figure 2.3-18 presents the borehole Slingram responses from the highly conductive target (0.5 Ω .m), all other conditions being the same as in Fig. 2.3-17. As expected in this case, the response-to-noise criterion is satisfied at a greater distance from the target, up to borehole 5, at about 80 m from target's center. The criterion however is only achieved for the in-phase components, the strongest components in this high-induction situation. For the quadrature field, the criterion is not satisfied in any of the boreholes used.

The above observations are consistent with the frequency behaviours shown on Figs. 2.3-12 and 2.3-14b, and confirm that the frequency behaviour of the target response is the same as in cross-borehole.

We note on Figs. 2.3-17 and 2.3-18 that borehole Slingram responses are sharper and more rapidly decaying away from the target than do cross-borehole responses. This is inherent to the moving transmitter configuration: when the measuring system moves away from a target, the secondary field at the receiver decreases not only because the target-to-receiver distance (d_1) increases (giving a variation as approx. $1/d_1^3$), but also because the target-to-source distance (d_2) increases correlatively, making the primary excitation to vary as approx. $1/d_2^3$. As a rule of thumb, we see that the whole variation is roughly as $1/(d_1^3 \times d_2^3)$, which is about the square of what is observed in cross-borehole.

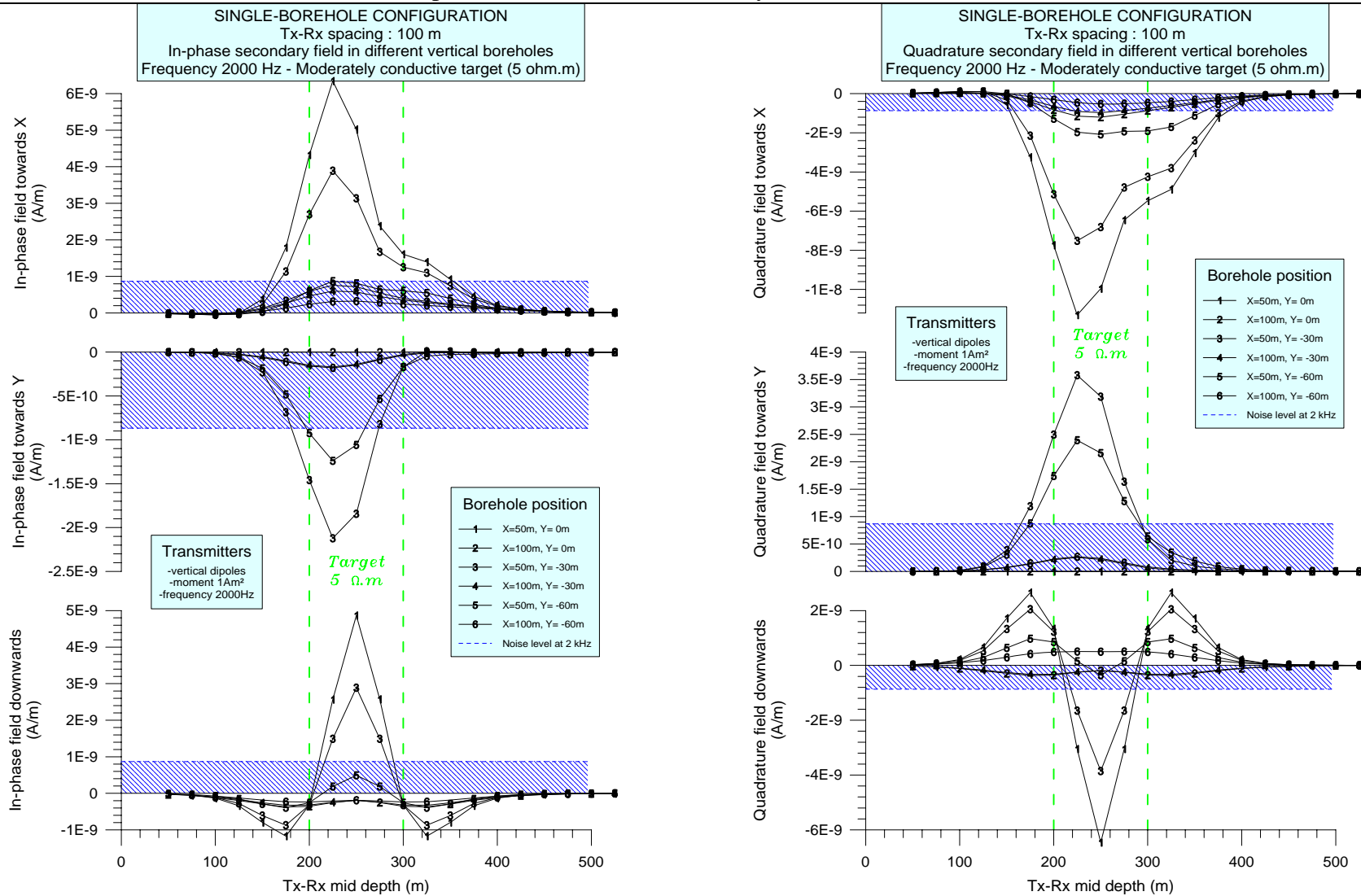


Fig. 2.3-17: Single-borehole configuration. Secondary field logs produced, with a 100 m spacing, in different vertical boreholes by the moderately conductive target (5 $\Omega.m$), at 2 kHz. Labels 1 to 6 refer to Tx1 to Tx6 in Fig. 2.3-1. The indicated noise level is that given in Fig. 2.3-9 for a standard 1024 samples acquisition. Both noise and responses are normalized to 1 Am² in the transmitter. **Left:** In-phase field. **Right:** Quadrature field.

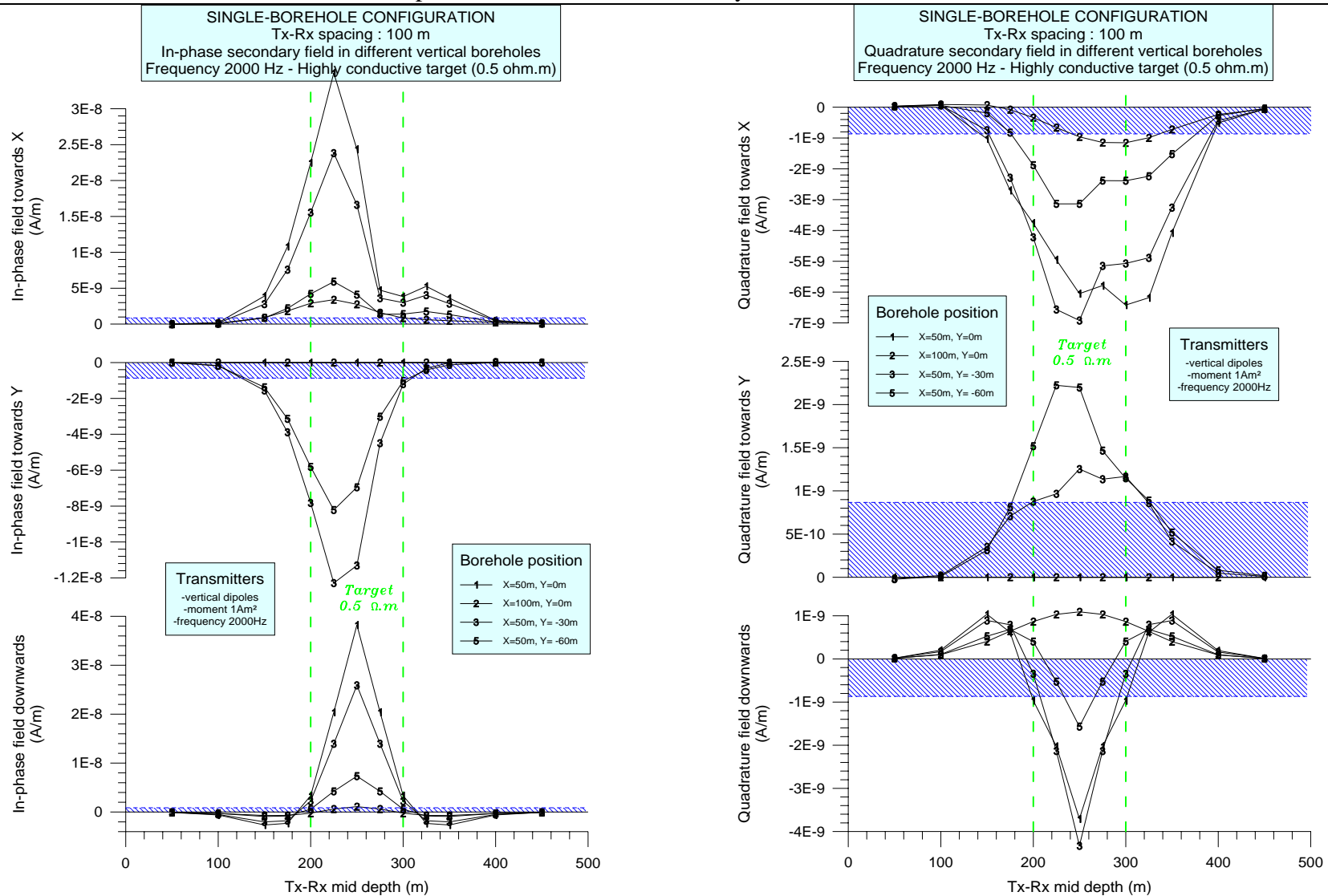


Fig. 2.3-18: Single-borehole configuration. Secondary field logs produced, with a 100 m spacing, in different vertical boreholes by the highly conductive target (0.5 $\Omega.m$), at 2 kHz. Labels 1 to 6 refer to Tx1 to Tx6 in Fig. 2.3-1. The indicated noise level is that given in Fig. 2.3-9 for a standard 1024 samples acquisition. Both noise and responses are normalized to 1 Am² in the transmitter. **Left:** In-phase field. **Right:** Quadrature field.

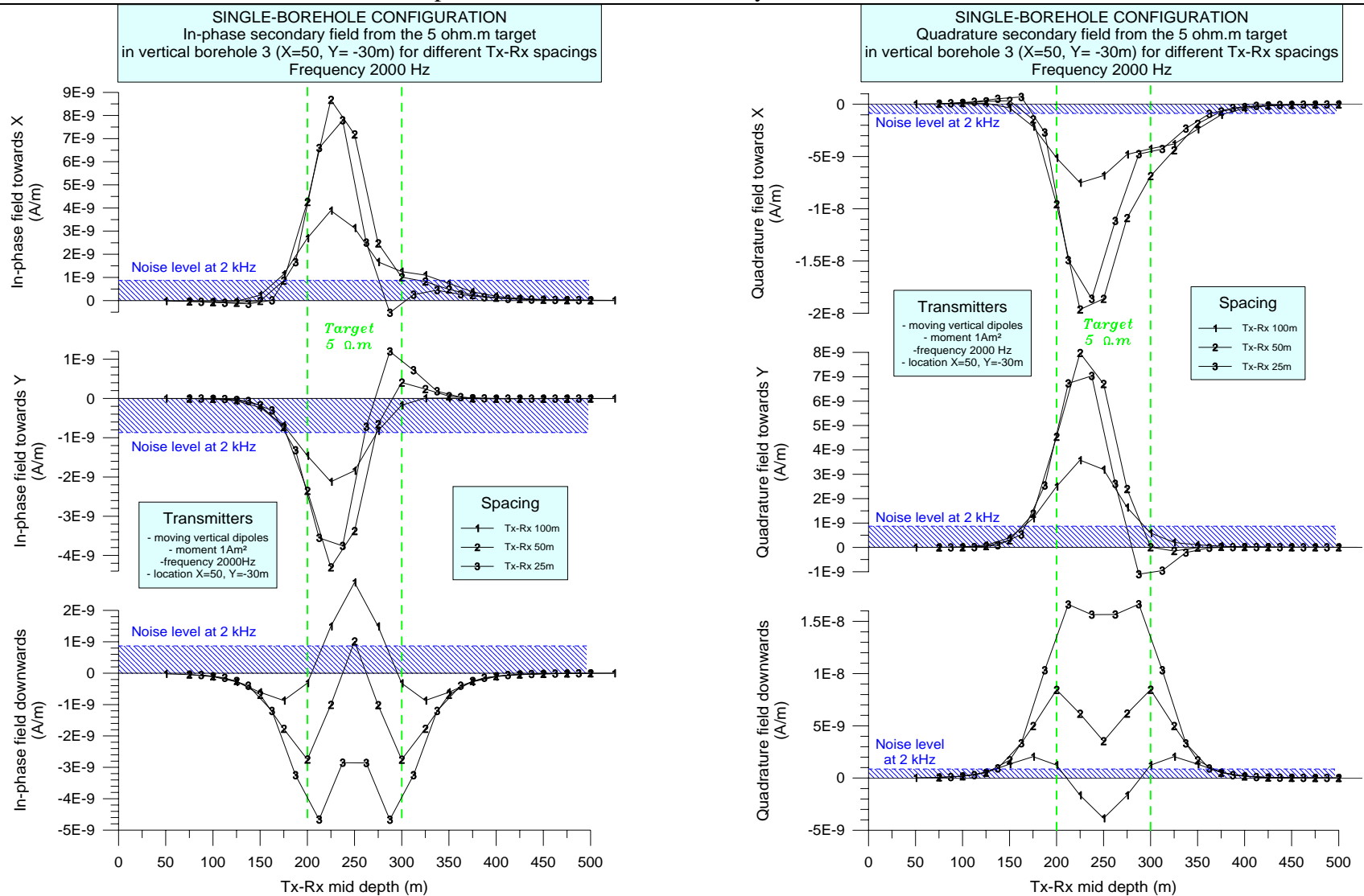


Fig. 2.3-19: Single-borehole configuration. Multi-spacing plots of the responses from the moderately conductive target ($5 \Omega.m$) at 2 kHz in borehole Tx3 ($X=50, Y=-30$ m). The indicated noise level is that given in Fig. 2.3-9 for a standard 1024 samples acquisition. Both noise and responses are normalized to 1 Am^2 in the transmitter. **Left:** In-phase field. **Right:** Quadrature field.

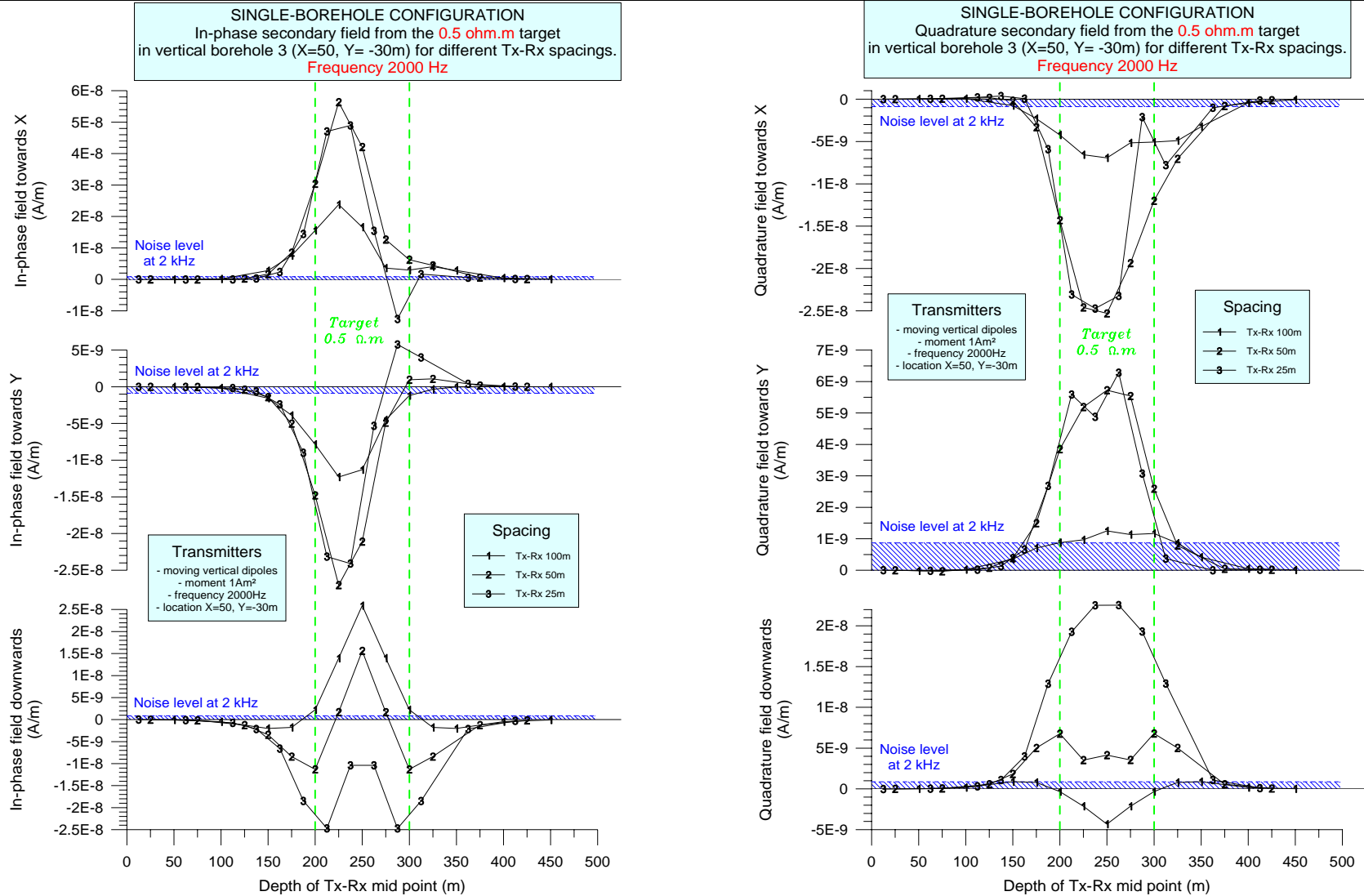


Fig. 2.3-20: Single-borehole configuration. Multi-spacing plots of the responses from the highly conductive target (0.5 Ω.m) at 2 kHz in borehole Tx3 (X=50, Y=-30 m). The indicated noise level is that given in Fig. 2.3-9 for a standard 1024 samples acquisition. Both noise and responses are normalized to 1 Am² in the transmitter. **Left:** In-phase field. **Right:** Quadrature field.

We further compare the responses for the three different spacings (Figs. 2.3-19 and 2.3-20) in borehole Tx3, about 60 m from target's center, at 2 kHz. This comparison first confirms that short spacings are the less critical with respect to noise. We will see later, however, that short spacings do present another problem, related to the secondary-to-primary field ratio, and thus that a best compromise has to be found in intermediate spacings (here around a 50 m spacing).

The synthetic presentations in Figures 2.3-19 and 2.3-20 show that borehole Slingram responses are extremely complex, with rapid variations from one spacing to another, especially for the axial component —the downward component here. For the 100 m spacing, the axial response is a single-pole anomaly with an extremum at depth of target's center, which apparently evolves, for the 50 m spacing, to a double-pole response, with peaks marking the upper and lower edges of the target. For the 25 m spacing, the axial response seems to be again a single-pole response, but with a polarity reversed from that of the 100 m spacing. This is better seen on the quadrature field. For the in-phase field, a shorter spacing (e.g. 10 m) would be useful to better establish this surprising behaviour, the reason of which is not yet well understood. In addition, we will see later that, at very short distance from the target, there is no longer evidence of the double-pole response —the lateral shoulders disappear into the main, central peak.

Further study would be necessary to better understand the behaviour of borehole Slingram responses as a function of both Tx-Rx spacing and target-to-borehole distance. If this behaviour was clarified, precious information concerning the target size in the direction parallel to the borehole could probably be inferred from the analysis of multi-spacing borehole Slingram data.

Note that the conductive host (500 Ω .m) taken in this model probably makes the responses more complex than in free-space, due to the presence of the galvanic effect, but it also makes the study more realistic than with a simple free-space model.

Table 2.3-3 gives the response extrema in borehole Slingram at various spacings for the reference target in borehole Tx1 (X=50, Y=0 m). The symmetrical position of this borehole results in only Hx (transverse) and Hz (axial) components (Hy is uniformly zero).

	Component	100 m spacing	50 m spacing	25 m spacing
Moderately conductive target Contrast 1/100	Hq_X	1.2 $\mu\text{A/m}$ (7.1 %)	3.0 $\mu\text{A/m}$ (2.4 %)	2.9 $\mu\text{A/m}$ (0.28 %)
	Hq_Z	0.65 $\mu\text{A/m}$ (4.1 %)	-1.2 $\mu\text{A/m}$ (-0.9 %)	-2.3 $\mu\text{A/m}$ (-0.23 %)
Highly conductive target (0.5 Ohm.m) Contrast 1/1000	Hp_X	3.5 $\mu\text{A/m}$ (22 %)	9.1 $\mu\text{A/m}$ (7.1 %)	8.8 $\mu\text{A/m}$ (0.87 %)
	Hp_Z	3.8 $\mu\text{A/m}$ (24 %)	2.9 $\mu\text{A/m}$ (2.4 %)	-3.7 $\mu\text{A/m}$ (-0.37 %)

Table 2.3-3: Extrema of the secondary field from the reference target in the single-borehole configuration at various spacings. These results are for borehole Tx1 (X=50, Y=0 m), located at 50 m from target's center, in a symmetrical position giving zero H_y component. Tx moment is 100 A.m², frequency is 2 kHz. Only the strongest components of the field are indicated, i.e. the quadrature components (Hq) for the 5 $\Omega\cdot\text{m}$ target, and the in-phase (Hp) for the 0.5 $\Omega\cdot\text{m}$ target. Responses have to be compared to a noise level of about 0.13 $\mu\text{A/m}$ (Table 2.3-2). Percentages are expressed with respect to the free-space primary field at Rx.

NB: The sign convention used for the quadrature field in this table is reversed from that used in the previous figures. This convention is more universal and has the advantage of giving in-phase and quadrature anomalies of the same sign in most cases.

2.5.3.3.2. Detectability of target responses over the primary field

The question of the detectability of a target's response over the Tx primary field (or secondary-to-primary field ratio) takes proper aspects for the cross-borehole (or surface-to-hole) and for the single-borehole configurations.

In cross-borehole, this question is essentially linked to the ability of visually separating, on the measured logs, a target response (i.e. anomalous field) from the Tx primary field. In single-borehole, it also refers to the numerical resolution and to the possible need for primary-field compensation before A/D conversion.

2.5.3.3.2.1 Cross-borehole configuration

The question of the detectability of a target's response over the primary field is very important in cross-borehole configuration where the dipolar primary field shows rapid variations along the receiver borehole. In this configuration, a target anomaly must be strong enough to be visually detected over the primary field variations, which must not be confused with a target response.

This visual detection is fundamental for cross-borehole (and also surface-to-hole) field data, because it is a requirement for continuing the data processing to subsequent steps, namely: a) reduction of the total field by the Tx primary field, and b) interpretation of the residual field, equated to the secondary field of a target, by adequate inverse models. If no anomaly is visible, no further processing is done, the data are abandoned.

To illustrate this problem, Figure 2.3-21 shows total-field curves (i.e. primary plus secondary field) modelled in cross-borehole for the moderately target ($5 \Omega.m$). These data are similar to experimental data, as obtained in the field, before any primary-field reduction. The geometrical configuration is that of Figs. 2.3-11, i.e. two boreholes distant of 117 m with the target at the center.

For each part of the field (either in-phase or quadrature), we present only the frequency giving the best response-to-noise ratio, as would be done for field data. Fig. 2.3-21a thus shows the in-phase field at 10 kHz, and Fig. 2.3-21b shows the quadrature field at 2 kHz. By a concurrence of circumstances, these frequencies also give the best secondary-to-primary field ratio.

In the cases presented, the detection of the anomalous secondary field over the dipolar primary field is clear and easy, i.e. the total-field curves are sufficiently distinct from the primary-field curves to signal the anomalous response without ambiguity.

For the highly conductive target (not shown), the anomalous field is clearly visible over the primary field from 600 Hz up to 10 kHz.

Note that the primary field considered here is the primary field of the Tx in the conductive host, not in free-space. In practice, determining the appropriate host resistivity for primary field reduction is the major difficulty in processing cross-borehole EM data (and also surface-to-hole), especially at high frequency where the host effect is important. The same problem, however, exists in time-domain EM methods.

In-phase total field at 10 kHz in the presence of the 5 ohm.m target. Tx and Rx boreholes are separated by 117m, with the target at the center; Tx dipole is at the depth of target's top (Z=200m).

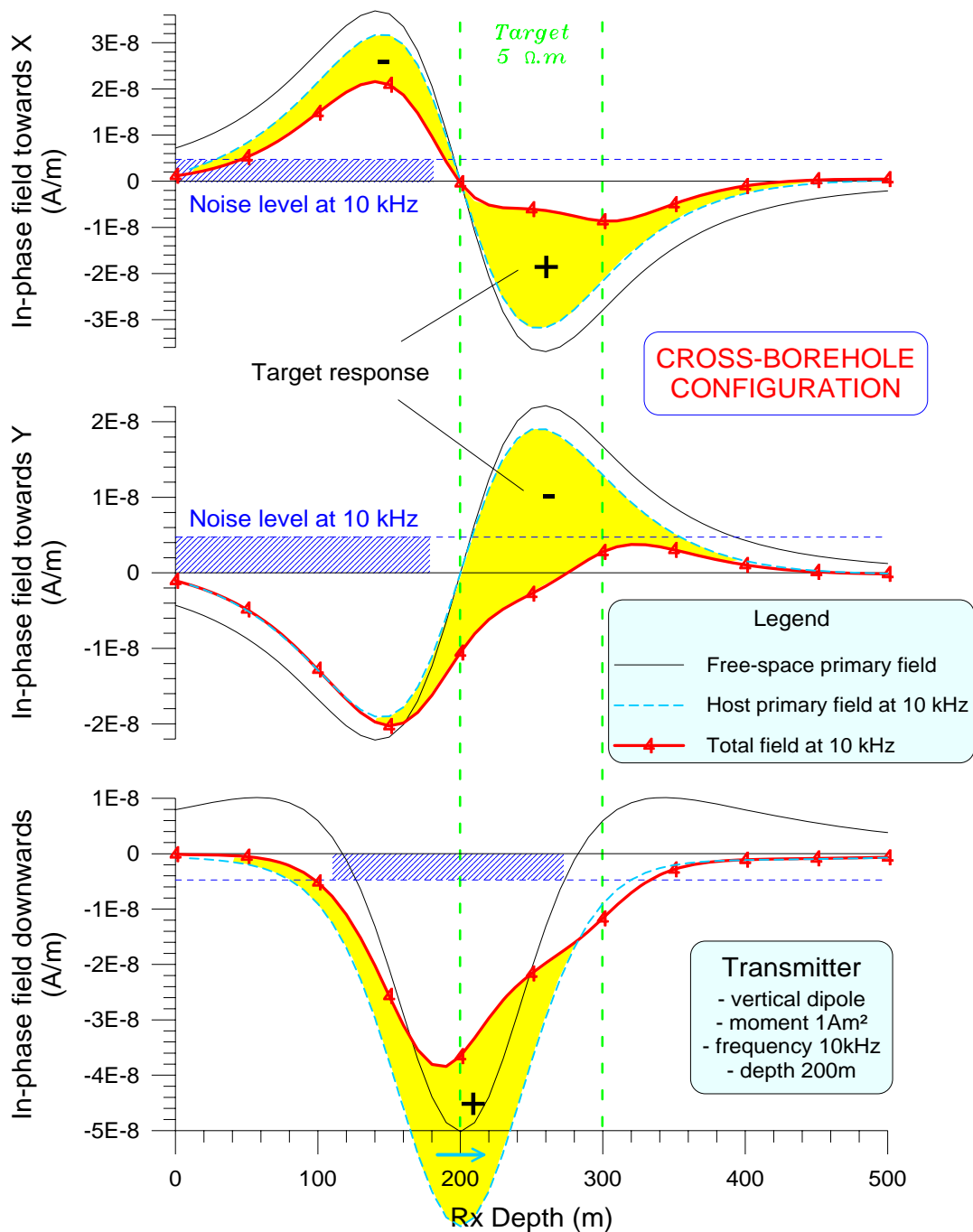


Fig. 2.3-21a: Cross-borehole configuration. In-phase total magnetic field at 10 kHz in the presence of the moderately conductive target (5 Ω.m), compared to the dipolar primary field in the conductive host (500 Ω.m) and to the normalized noise level. As in Fig. 2.3-11, the receiver borehole is F0 (X=-50, Y=30 m), and the VMD transmitter is at Z=200 m in Tx borehole 3 (X=50, Y=-30 m); the two boreholes are separated by 117 m, with the target at the center. The primary field in free-space is given as a reference, showing that, at such a high frequency, the host effect is significant. The difficulty with practical data will be to determine the appropriate host resistivity for reduction. Only at this frequency is the in-phase anomalous field clearly visible over the primary field—other frequencies are not shown.

Quadrature total field at 2 kHz in the presence of the 5 ohm.m target. Tx and Rx boreholes are separated by 117m, with the target at the center; Tx dipole is at the depth of target's top (Z=200m).

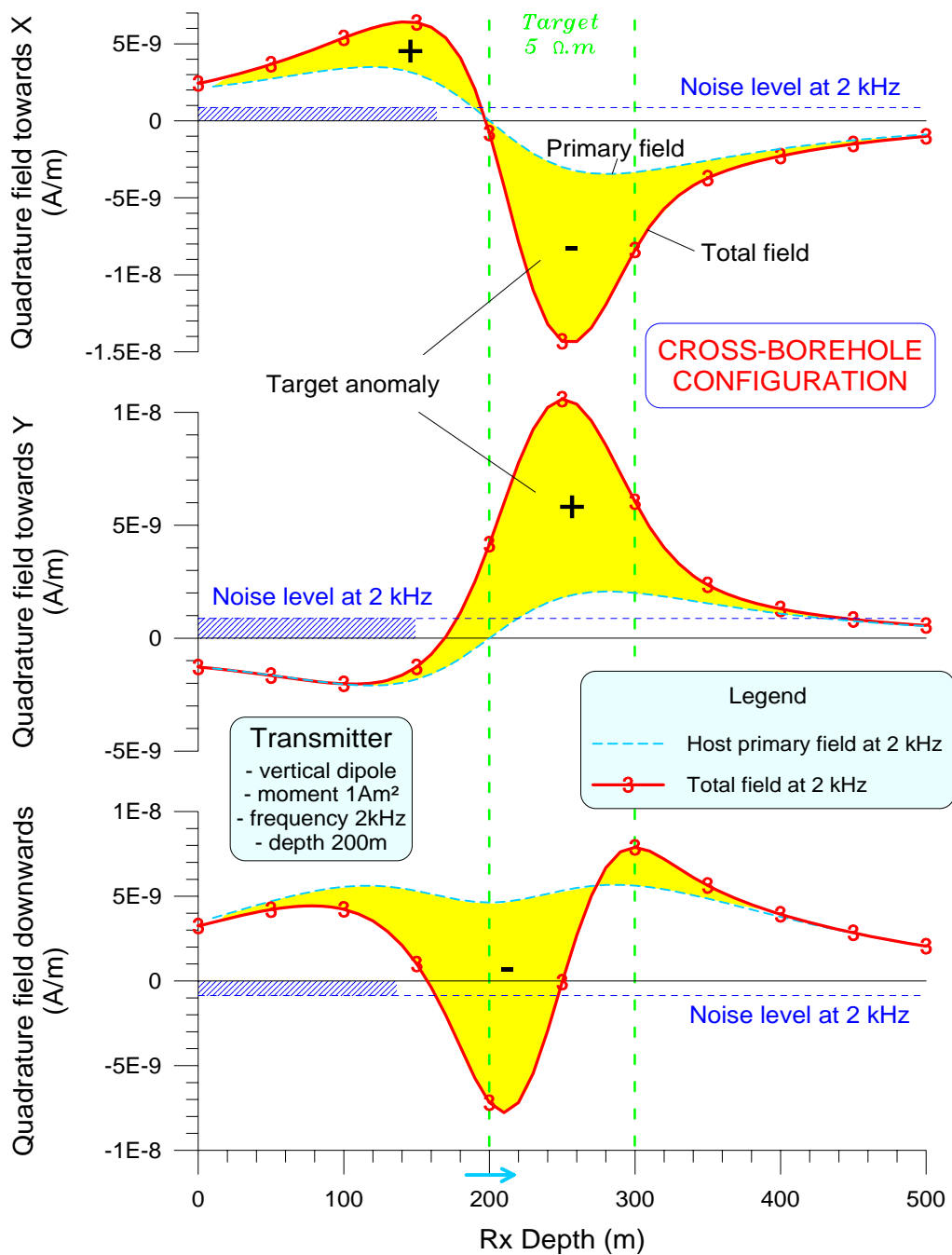


Fig. 2.3-21b: Cross-borehole configuration. Quadrature total magnetic field at 2 kHz in the presence of the moderately conductive target (5 Ω.m), compared to the primary field in the conductive host (500 Ω.m) and to the normalized noise level. The geometrical configuration is the same as in Fig. 2.3-21a. Note the variations of the quadrature primary field in the conductive host (500 Ω.m). The downward component of this field behaves very differently from its in-phase counterpart. Hence, it can be stated that the quadrature primary field is very different from the field of a dipole in free-space. The difficulty with practical data will be to determine the appropriate host resistivity for reduction. The quadrature anomalous field is clearly visible over the primary field at 2 kHz (resonance frequency), but also at 600 Hz and 10 kHz (not shown).

Another difficulty in cross-borehole is that the variations of the dipolar primary field are similar in shape and wavelength to those of the secondary field of the target, and appear in the same depth interval, due to the limited Tx power. These coincidences may be confusing, especially at high frequency in an unknown host, where the levels of the primary field curves are badly constrained.

We conclude from figure 2.3-21 that, assuming an adequate coupling of the primary field with the target, the detection of the response over the primary field should be easy in a radius of at least 50 m around the target (for both Tx and Rx boreholes), when the target is located **between the boreholes**, i.e. in a **transmission geometry**.

In a reflection geometry, where the two boreholes are located at the same side of the target (e.g. Tx3 and Tx1, both to the right of the target), the detection will be possible only within a much smaller radius. This can be shown by simple considerations. Let us take, for example, the usual transmitter located at $Z=200$ m in Tx3, and a moving receiver in borehole Tx1, distant of only 30 m from Tx3. Having in mind that the system of induced currents is the same as usual, and due to the almost symmetrical position of borehole Tx1 with respect to borehole F0 used up to now, we can assume that the secondary field in Tx1 is about the same as in F0 (or only slightly increased). But, on the other hand, the primary field at the receiver, varying as the third power of the Tx-Rx distance, is dramatically increased by a factor of $(117/30)^3$, i.e. about 60. As a consequence, the secondary-to-primary ratio is decreased by this same factor of about 60, making the visual detection evidently impossible—imagine the responses of Fig. 2.3-21 flattened by a factor of 60.

It is thus important to remind that, in cross-borehole (like in surface-to-borehole), the **transmission geometry**, where the receiver borehole stands in the shadow of the target as illuminated by the transmitter, is to be much preferred to the reflection geometry whenever it is possible, for a simple reason of secondary-to-primary field ratio.

Concerning the cross-borehole configuration, it may be concluded that an effective working radius of at least 50 m around the target (for both Tx and Rx boreholes) is confirmed for either the moderately or the highly conductive target in the **transmission geometry**. This means that both sufficient response-to-noise ratio and secondary-to-primary field ratio can be obtained in this radius and in this geometry.

2.5.3.3.2.2. Single-borehole numerical resolution and primary-field compensation

In the single-hole configuration, visual detection of the anomalies over the primary field should be direct, even when the response is small compared to the primary field, because in such a fixed-spacing method, the primary field at the receiver is constant, at least as a first-order approximation. Moreover, this primary field is only axial (transverse components are uniformly zero) and purely in-phase (no quadrature part).

Consequently, if we assume a perfect situation without geological noise, the problem in single-borehole is to determine whether the axial component of the secondary field will be strong enough to be properly sampled by the digital acquisition chain, in the presence of the primary field. If this is not the case, an appropriate compensation circuitry should be devised for analogic compensation of the axial primary field before A/D conversion. The worst case is of course for the shortest Tx-Rx separation, where the primary field at the receiver is the strongest.

With a compensation device, the number of bits available in the digital chain are entirely kept for the numerical resolution of the secondary field. Such devices were indispensable until recent times, when the number of bits proposed by standard A/D converters (ADC) and microprocessors was small (e.g. 8 or 12). Even with the present components, using 16 or more bits, such devices are still necessary when the dynamics of the problem, which is scaled by the primary-to-secondary field ratio, is greater than the numerical range of the microprocessor, e.g. for very short spacings.

Several problems, however, are inherent to these compensation devices, such as time and temperature drifts, as well as the difficulty to control the real value of the compensation applied and its suitability to the transmitted moment. This is particularly true in non-rigid systems, such as the borehole Slingram, for which the coaxial geometry ('coaxiality') of the Tx and Rx probes is not perfect. In addition, such devices significantly increase the cost of a system. For all these reasons, it is much preferable when they can be avoided.

This point was thoroughly discussed among WP2 partners during the first technical meetings, devoted to prototype specifications. In the equipment design, it has been checked that a 20-bit A/D converter with a gain-16 preamplification, and a 16-bit microprocessor offered sufficient numerical resolution to avoid compensation, even with a 25 m spacing.

The whole reasoning is better expanded in the final BRGM report. Only a few considerations are given here to justify the choice of not compensating the primary field. Table 2.3-4 synthesizes the study.

The digital stage of the acquisition chain is composed of:

- a) a 20-bit (sigma-delta) A/D converter, set on a full scale of [-24,+24] mA/m.
The least significant bit (LSB) of this ADC, i.e. the smallest measurement that it can give, is thus $LSB = \frac{2 \times A_{max}}{2^{20} - 1}$, where A_{max} is the full scale. Here, $A_{max}=24$ mA/m, so $LSB \approx 0.046 \mu A/m$.
- b) a gain-16 preamplification, which augments the ADC dynamics to 24 bits when the signal is weak, i.e. when $H_t < 24 / 16 = 1.5$ mA/m, with H_t the total field (primary plus secondary). With this preamplification, the LSB is divided by 16, so we have now $LSB \approx 0.003 \mu A/m$.
- c) a 16-bit microprocessor, giving a numerical resolution of $\frac{1}{2^{16} - 1} = \frac{1}{65535} \approx 15ppm$.

The greatest number handled by such a microprocessor is 65535. When a number is greater than this limit, the bits are shifted by one unit towards small exponents, resulting in a numerical resolution of 2 instead of 1. If a single shift is not sufficient to fit inside the 65535 limit, the operation is repeated iteratively as many times as necessary.

Concerning the accuracy of the A/D conversion, we have to check that the smallest secondary signal that the system should be able to measure (H_s) is digitized into a sufficient number (N) of LSB's. The condition to be satisfied is thus:

$$H_s \geq N \times \text{LSB} \quad (1)$$

For a good accuracy, we can take $N=10$, which gives a maximum round-off error of $\pm 5\%$ of H_s , quite acceptable indeed.

As for the signal H_s , in a controlled source EM method the smallest secondary signal that we may want to measure is equal to the natural MT noise. Taking H_s as the MT noise is really the most severe situation that can be envisioned because, in practice, a signal will be usable only if it is at least 3 to 5 times the noise (in Sec. 2.5.3.3.1., a clearance of 5 was used).

The primary field (H_p) at the receiver is calculated, for each frequency and spacing, using the magnetic moment emitted at this frequency (Fig. 2.3-49). The value is used to control whether the preamplification will be applied or not, and thus determine the exact value of the LSB. The secondary signal H_s , equated to the MT noise, is then digitized into this LSB value. The final results H_s/LSB for each frequency and spacing are reported in Table 2.3-4.

The fact that the microprocessor has a smaller number of bits than the ADC slightly complicates the problem, because we must consider what happens when the number of bits (H_s/LSB) overflows the capacity of the microprocessor. A second condition concerning the microprocessor has thus to be satisfied:

$$H_t \leq 65535 \times \text{LSB} \quad (2)$$

As explained before, when this condition is not satisfied, the numerical process explained before results in a degradation of the resolution, i.e. an increase of the LSB by as many powers of 2 as the numbers of shifts required. At the end of this iterative process, the term LSB in equations (1) and (2) and in Table 2.3-4 must be understood as the effective LSB, i.e. actual LSB multiplied by 2^k , $k=1,..4$.

This process has the same effect as degrading the actual gain to a smaller value (apparent gain) obtained by a 2^k division. These apparent gains (different from 1 or 16) are written in parentheses in Table 2.3-4. When the actual gain is 16, for 25 and 50 m spacings, this process is often observed because the primary field overflows the microprocessor capacity, resulting in apparent gains comprised between 2 and 8.

Frequency (Hz)	Hs(μ A/m) =MT noise	Tx Moment (A.m ²)	Gain 25m	Gain 50m	Gain 100m	Hs/LSB 25m	Hs/LSB 50m	Hs/LSB 100m
35	1.9	293	1	16 (4)	16	42	166	664
70	1.75	292	1	16 (4)	16	38	153	612
140	1.1	217	1	16 (8)	16	24	192	384
280	0.55	253	1	16 (8)	16	12	96	192
560	0.35	225	1	16 (8)	16	8	61	122
1120	0.19	160	1	16 (8)	16	4	33	66
2240	0.13	105	16 (2)	16	16	6	45	45
4480	0.15	63.7	16 (4)	16	16	13	52	52
8960	0.19	48.3	16 (4)	16	16	17	66	66

Table 2.3-4: Numerical resolution achieved with the SlimBoris system in the least favourable situation, for which the secondary signal Hs is assumed to be equal to the MT noise.

The LSB (least significant bit) values used in this table for digitizing the signal are effective LSB's, obtained by multiplying the actual LSB by an adequate power of 2 (between 2 and 8), when the microprocessor is overflowed by a strong primary field. Similarly, the gains in parentheses (which differ from 1 or 16) are apparent gains obtained by dividing the actual gain by the same power of 2 in the same situation.

This table shows that only frequencies between 560 and 2240 Hz at 25 m spacing give poor numerical resolution of the MT noise, with only 4 to 8 LSB's. In these conditions, however, an anomaly detectable over this MT noise will thus represent at least 10 to 20 LSB's. Consequently, the possible round-off errors due to the poor resolution in these cases are less than 5% of the secondary field, which is quite acceptable.

In the worst case of Table 2.3-4 (25 m spacing at 1120 Hz), a response of 3 times the MT noise (the smallest response detectable over noise) will give 12 LSB's, i.e. a maximum round-off¹⁰ error of $\pm 4\%$, which is definitely less than the errors produced by any electronic compensation device.

We conclude from Table 2.3-4 that, with state of the art digital components, the single-borehole system can be designed without any compensation circuitry, if the minimum spacing to be used is 25 m. For smaller spacings (e.g. 10 m) a compensation device would be necessary to give adequate resolution of the secondary signal.

Coming back to our modelling study, Fig. 2.3-22 gives the borehole Slingram responses from Fig. 2.3-19-right and Fig. 2.3-20-left (i.e. the strongest between the in-phase and quadrature fields in each situation) in percent of the free-space primary field, which is the standard presentation in surface Slingram. This figure graphically illustrates the fact that

¹⁰ The maximum relative round-off error is $\pm 1/2N$.

long spacings give the greatest secondary-to-primary field ratio and thus are the less critical regarding the question of numerical resolution.

Keeping in mind that long spacings are also the most critical with respect to noise, it is clear that a best compromise has to be sought in intermediate spacings. Here the 50 m spacing apparently correspond to this best compromise, with responses higher than 1% and very good clearance from noise.

It should be noted that this best compromise spacing is of the same order as the target-to-borehole distance. This rule of thumb is often known as the **limitation of the effective radius of investigation by the spacing**.

Conclusion to Section 2.5.3.3

Regarding the instrument design and practical limitations, it appears that the transmitting moments produced by the SlimBoris downhole transmitter should enable an investigation radius of at least 50 m in the single-hole configuration and a separation of about 100 m between boreholes in the cross-hole configuration.

In the single-hole configuration, a Tx-Rx spacing of about 50 m should be a best compromise in order to obtain, within the expected investigation radius of about 50 m, both sufficient response-to-noise ratio and secondary-to-primary field ratio. Nevertheless, it is recommended to make multi-spacing measurements in order to distinguish between near and distant targets, and to give an estimation of the size of the target in the direction parallel to the borehole.

In the cross-borehole configuration, it is fundamental to use the transmission geometry, in which the receiver borehole stands in the shadow of the target as illuminated by the transmitter, in order to reach the expected 100 m separation between boreholes, with both sufficient response-to-noise ratio and secondary-to-primary field ratio.

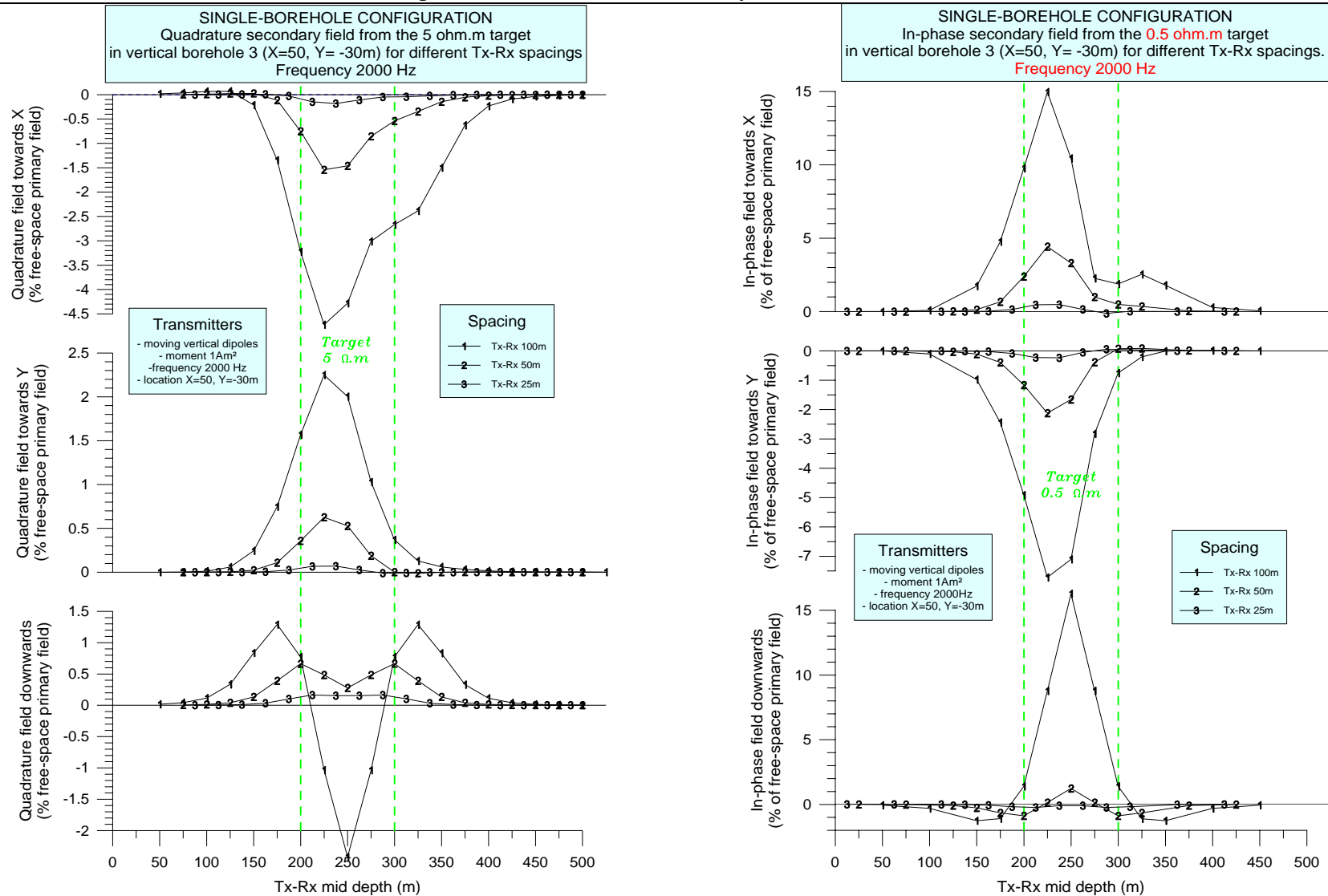


Fig. 2.3-22: Single-borehole responses from Figs. 2.3-19-right and 2.3-20-left expressed in percents of the free-space primary field at the receiver.

Left: Quadrature responses from the 5 Ω .m target at 2 kHz.

Right: In-phase responses from the 0.5 Ω .m target at 2 kHz.

2.5.3.4. Interpretation guidelines in single-borehole configuration

From the observation of modelled responses and from elementary reasoning, simple rules for localizing a target according to the signs of the anomalies on the transverse components have been derived for simple targets in the single-borehole configuration.

For our reference target, Figures 2.3-17 to 2.3-20 show that, whatever the Tx-Rx spacing and whatever the exact position of the borehole in a given quadrant around the target, the sign of the response for the X or Y component is a constant. For the in-phase field, the response is positive for the X channel and negative for the Y channel; for the quadrature field, with the convention used in the modelling¹¹, the signs are reversed.

If we adopt a more standard sign convention, the in-phase and quadrature responses then have identical signs. This more standard convention effectively has the advantage of giving in-phase and quadrature anomalies with the same sign at low frequencies (Fig. 2.3-14a). Nevertheless, Fig. 2.3-14a shows that a quadrature reversal may be expected at high frequency in a conductive host. In such a case, the in-phase and quadrature responses will have opposite signs with this standard convention.

In the rest of this section, we assume that this standard convention is used, as well as a relatively low frequency, so that in-phase and quadrature responses can be supposed to have the same sign.

If we identify the X direction with North and the Y direction with East, we see that boreholes Tx4 to Tx6, located in the Northwestern quadrant from the target center (Fig. 2.3-1), give positive responses for the Northward (X) component, and negative responses for the Eastward (Y) component. Similarly, boreholes Tx1 and Tx2, located exactly to the North of the target, give positive responses for the Northward component, and zero response for the Eastward component.

By simple symmetry considerations, these observations enable us to infer general rules for target localization in borehole Slingram (Table 2.3-5). In addition, Figure 2.3-23 shows the geometrical features of the vortex secondary magnetic field of a target of any orientation. This simple representation gives a direct understanding of the above rules, showing that, in single-borehole, the transverse (here horizontal) magnetic vectors roughly indicate the direction **from** the target.

However, Fig. 2.3-23 also shows that such elementary rules must be taken with some precaution because, strictly speaking, they are only valid for a massive target having two symmetry axis parallel to the coordinate axis, like in our reference model. For a plate-like conductor oblique to the coordinate axis, such rules can be slightly misleading.

¹¹ The convention used in the modelling study (except Table 3) defines the quadrature as the opposite of the imaginary part of the complex EM field, whereas the most widespread convention states the equality of the two values.

When no precision is given, it may be assumed that the convention used is that of the modelling study.

H_{North}	H_{East}	Direction of the target
+	-	Southeast
0	-	East
-	-	Northeast
-	0	North
-	+	Northwest
0	+	West
+	+	Southwest
+	0	South

Table 2.3-5: Rules of thumb for the borehole Slingram configuration, giving the direction of a massive target according to the signs of the transverse components of the response. When the target center is in a cardinal direction from the borehole, a zero response is obtained for the component which is perpendicular to this direction. For a thin plate target oblique to the coordinate axis, the behaviour is slightly different and the above rules may be somewhat misleading. In particular, the zero response for a given component will be obtained with the target in a direction slightly rotated from the direction given in the table. NB: This table primarily applies to the in phase field. However, with the standard quadrature convention used in Table 2.3-3, it also applies to the quadrature field.

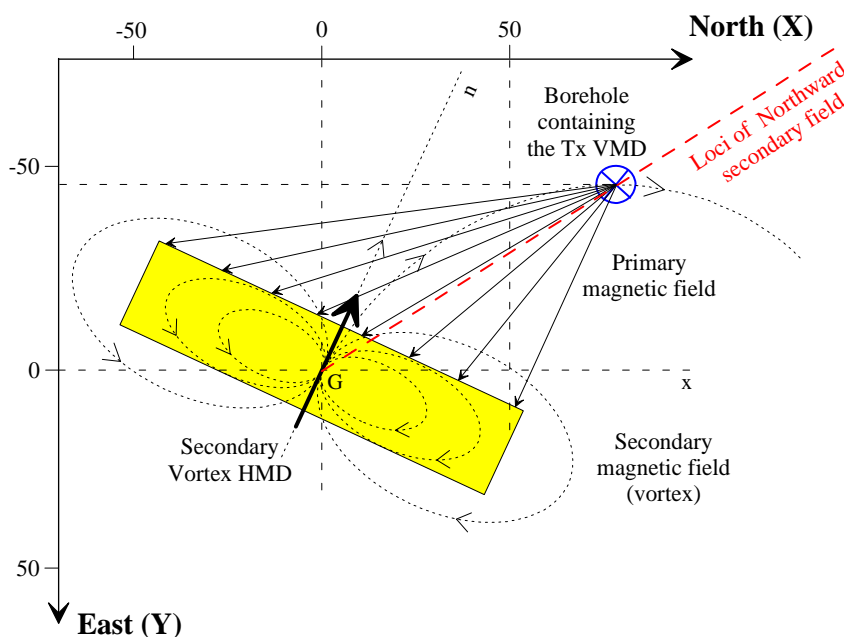


Fig. 28: Schematic representation of the vortex response of a target of any orientation, showing that the secondary magnetic field is opposed to the primary field. Consequently, in single-borehole, the horizontal magnetic vectors indicate the direction from the target. The figure also shows that, when the target is oblique to the coordinate axis, the loci where the Y component of the secondary field is zero (thick dashed line) do not coincide with the X axis passing by the target center (G_x), as was the case with the reference target, but are on a line intermediate between this G_x axis and the G_n axis perpendicular to the target.

In particular we see on Fig. 2.3-23 that, in the indicated borehole, a zero response is anticipated for the Eastward component, and a positive response for the Northward component. With such observation, the simple rules of Table 2.3-5 give the target exactly to the south of the borehole, while it is in fact to the southeast. Using these rules without precaution for siting a new borehole would result here in missing the target again, from a distance of about 20 m.

The problem is due to the fact that, for an oblique plate, the direction from the conductor stated before must be understood as the direction on a curved secondary field line (Fig. 2.3-23), not on a straight line.

We may thus conclude that, for the single-borehole configuration, the rules in Table 2.3-5 only give a very approximate localization of a target, with an uncertainty as high as $\pm 45^\circ$. If the strike angle of the expected target is known, simple reasoning like in Fig. 2.3-23 may help in reducing this uncertainty.

For the cross-borehole configuration, where the transmitter, target and receiver borehole can be in any positions (locations and orientations) relative to one another, we have not tried to infer any qualitative rule because the number of parameters to consider in order to be comprehensive is too important. However, in this configuration, models of EM dipoles or current filaments (see Sec. 2.5.6.3) are rapid and robust inversion tools which give the location and attitude of a target more rapidly and with greater reliability than any catalogue of responses or any approximate interpretation guidelines.

2.5.3.5. Response levels in single-borehole configuration

After the second field tests (in October 1998), during which the SlimBoris prototype provided for the first time consistent data in the borehole Slingram configuration, further modelling was performed to check whether the high responses obtained in this mode (several hundreds of percents of the primary field) were geophysically relevant or if some malfunctioning was still to be suspected on the equipment. The question was raised by the partners experienced in surface Slingram, who expected in boreholes a behaviour similar to what is assumed at the surface, i.e. a limit of about 100%.

The borehole Slingram method, however, presents major differences with its surface equivalent, the most important concerning the location of the measuring profile. Borehole profiles may obviously intersect the layering and can approach confined conductors very closely, whereas surface profiles stay almost parallel to layering and at significant distance from confined targets. In such conditions, it is not clear that the two methods should behave perfectly in the same way. On the contrary, it is intuitively possible to predict that borehole Slingram should produce much sharper and stronger anomalies than its surface equivalent, due to the proximity of the induced secondary currents. Verifying this intuition was the very aim of the new modelling.

This new modelling showed that confined conductive targets very close to a borehole can produce anomalies up to several hundreds of percents, when the spacing is equal to the extension of the target parallel to the borehole (i.e. the height of the target in our case). This result is opposed to what is believed for surface Slingram, where a theoretical limit of about 100% is assumed — may be wrongly however.

2.5.3.5.1. Borehole Slingram responses at short distance from a 3-D conductor

While the first set of 3-D modelling was mainly trying to determine up to which distance the response from a target could be measured over noise, and thus was considering boreholes at significant distance from the target, the second round of modelling for the single-borehole configuration was, on the contrary, dedicated to boreholes approaching the target very closely (down to 1 m from its face).

The results of this new modelling are presented in Figures 2.3-24 to 2.3-26, for the 100 m, 50 m and 25 m spacings. The responses were calculated for the reference model, with the highly conductive target (0.5 Ω .m), at 2 kHz. The vertical boreholes used are located on the main symmetry axis of the target ($Y=0$), at a distance from its right face ranging from 1 m to 17.5 m — note that the new boreholes are not shown in Fig. 2.3-1.

The highest percentages are obtained for the 100 m spacing (Fig. 2.3-24), which gives the greatest secondary-to-primary field ratio. For this spacing, secondary fields greater than 500% are observed at 1 m from the target for the axial (downward) component, either in-phase or in-quadrature¹². The transverse (X) component also shows a strong response, with a quadrature part higher than 400%. The anomalies are extremely narrow, especially at short distance from the target. The results are summarized in Table 2.3-6.

¹² It is worth noting that these very high relative responses are, at the same time, the weakest absolute responses (see Fig. 2.3-28), showing that the high secondary-to-primary ratios are essentially due to the weakness of the primary field at long spacings.

It should be noted in Fig. 2.3-24 that, whatever the distance to the target, the maximum of the axial response is achieved for a **centred position** of the Tx-Rx pair, i.e. for a mid point located at the level of the target's center¹³. In this symmetrical geometry, for the 100 m spacing and for our target, the Tx VMD is at the level of the target's top, a situation known to give the greatest primary magnetic flux through the main face of the conductor¹⁴. At the same time, the Rx is at the level of the target's bottom, thus in a position which is the closest to the eddy currents flowing at the base of the target.

The synchronism of these two good conditions explains the very high responses observed when the Tx-Rx spacing is equal to the target height (or extension parallel to the borehole), a configuration that we designate as the **'coincident' geometry**. When the borehole is very close to the target, a minor displacement in depth causes these good conditions to disappear very rapidly, explaining the narrowness of the anomalies for the 100 m spacing.

We do not expect that the 'coincident' geometry gives always the same percentages of response for any target size. We think that the very high relative responses observed in our case are partly due to the weakness of the primary, normalizing field, with a spacing as long as 100 m. In other words, we have the intuition that the 'coincident' geometry will yield the highest percentages for the longest spacings (and targets!).

We think for example that a 25 m-high target (of similar shape) surveyed with a 25 m spacing, should give smaller percentages than our 100 m target with a 100 m spacing. On the contrary, we expect that a 200 m-high target with a 200 m spacing should give much higher percentages than our target, probably higher than 2000%. This point has not been demonstrated; only a few partial results calculated with a 25 m-high body (5x20x25 m) tend to support this hypotheses.

Distance of borehole to target's edge	1 m	2.5 m	7.5 m	17.5 m	37.5 m
In-phase axial field (%)	+582	+469	+247	+102	+24
Quadrature axial field (%)	+525	+311	+71	+13	+2.3
In-phase transverse field (%)	+201 / -115	+174 / -100	+113 / -64	+58 / -15	+22
Quadrature transverse field (%)	+413 / -13	+224 / -7	+57 / -4	+7.6 / -3.5	+4

Table 2.3-6: Borehole Slingram responses for the highly conductive target (0.5 Ω.m) in vertical boreholes passing at variable distance from the target's face, for a 100 m Tx-Rx spacing, at 2 kHz. (Percentages are expressed with respect to the free-space primary field at Rx. Quadrature data use the standard convention of sign defined in Section 2.5.3.4).

For spacings smaller than the target height, the percentages of responses are not so high, but they are still important. Responses well above 100% are observed for the 50 m spacing (Fig. 2.3-25), and around 40% for the 25 m spacing (Fig. 2.3-26).

The most remarkable feature when the spacing is equal to half the size of the target (i.e. 50 m) is the very quick variations for the quadrature response (Fig. 2.3-25-right) in boreholes very close to the target (X=15 m and X=20 m). The response is characterized by two lateral peaks on each side

¹³ This is true in fact for any spacing (see Figs. 2.3-25 and 2.3-26).

¹⁴ We thus conclude by the way that the strong maximum obtained for the axial response is mainly of inductive origin.

of the central, main response, giving a noisy aspect to the modelled logs (curves labelled 3 and 4). These peaks are obtained when either the Tx or Rx is passing abeam the target center, while the other is passing abeam its top or bottom, a situation giving one of the two good conditions seen before for the 'coincident' geometry.

We can assert that these lateral peaks are purely of galvanic origin, because we know that a Tx VMD located at the level of the target's center gives zero inductive coupling across the main face of the target (see Fig. 2.3-4). The same conclusion is inferred conversely for the other peak using the reciprocity theorem. With such a deduction in mind, we better understand why these lateral peaks are only visible for the quadrature field, as we know that the galvanic-to-inductive ratio is always greater for the quadrature than for the in-phase field (see Fig. 2.3-3). Finally, a better examination of Fig. 2.3-25-left shows that the lateral peaks also exist for the in-phase field, but only in the nearest borehole (curve 4) and with a smaller magnitude.

We may conclude again that a significant part of the complexity in our modelling comes from the combination of the galvanic and inductive effects, in this conductive host.

Figures 2.3-27 and 2.3-28 show the comparison of the simulated logs for different spacings, in a particular borehole located very close to the target (at $X=15$ m, i.e. only 2.5 m from the target's face). The comparison is given in percentages of the primary field in Fig. 2.3-27, and in absolute amplitudes (A/m) in Fig. 2.3-28.

An observation worth to be done in this very close borehole is the fact that the transverse (X) in-phase response is a cross-over for certain spacings (100 and 50 m), instead of the maximum which was standard at greater distance (see Figs. 2.3-17 to 2.3-20) and which is observed here for the 25 m spacing. The case of the transverse quadrature response for the 50 m spacing is even worse because the response appears as a maximum instead of the standard minimum.

We conclude from these observations that applying the simple interpretation rules contained in Table 2.3-5 in a borehole very close to a target may be misleading if a single spacing has been used. However, if the three spacings have been recorded, then the comparison of the logs should enable a more reliable, and of course more complete, interpretation.

Concerning Fig. 2.3-28, another important point to observe is the fact that our greatest spacing (100 m), though it gives the highest percentages of responses due to its correspondence with the target size ('coincident' geometry), also gives the weakest absolute responses by virtue of the greatest target-to-Tx and target-to-Rx distances.

For spacings greater than the target size (e.g. 200 m), we have unfortunately not performed a complete study. However, several portions of logs have been calculated at certain depths and in certain boreholes to check some hypotheses. As opposed to the first intuition, in a borehole very close to the target, the percentages of responses are dramatically reduced for such a spacing (compared to the 100 m spacing), despite the 1:8 decrease of the primary, normalizing field. We get for example only about 10 to 15% for the maximum in-phase responses in the boreholes located between $X=15$ and $X=30$ m. This implies that the absolute responses must be decreased in an even more dramatic way.

All these observations demonstrate that the 'coincident' geometry is a very particular circumstance, which has some similarity with a resonance behaviour, although the origin of the

phenomenon is completely different (purely geometric in our case): when the spacing equals the extension of the target (parallel to the borehole), the response percentages are very high and they decrease rapidly when the spacing differs from the target size.

For each spacing, the response extrema (in absolute values) for the transverse and axial components, either in phase or in quadrature, have been plotted on a bilogarithmic scale, as a function of the distance of the borehole from the target center (Figs. 2.3-29 and 2.3-30 present two particular spacings). Note that these extrema are not always picked up at the same depth, and that responses may reverse at a certain distance from the target causing certain irregularities on the plots.

Figure 2.3-29 concerns the 'coincident' geometry. This plot seems to indicate that the responses are not bounded in the vicinity of the target center, because they increase as negative powers of the borehole-to-target distance (about $1/X^2$ for the in-phase and $1/X^5$ for the quadrature¹⁵). However, the target being of finite thickness, each response will be bounded de facto by the value reached on the target edge¹⁶. The limiting values seems to be about 700% for the axial component and a little bit less for the transverse component (about 230% for the in phase and 600% for the quadrature).

These exact values must be taken with caution, because several problems are known about 3-D modelling codes in EM, especially concerning the discretization¹⁷. The values obtained at GSF with various codes are somewhat smaller than those obtained at BRGM. However, they all agree to indicate that there is no theoretical limitation of the order of 100%.

Figure 2.3-30, for a spacing smaller than the target size, shows behaviours rather different from those observed in Fig. 2.3-29 for the 'coincident' spacing. In the vicinity of the target, the responses can no longer be fitted with power functions (represented as straight lines), but they have to be fitted with exponential functions, represented as curved lines with the concavity downwards. The same behaviour is obtained for spacings greater than the target size, e.g. 200 m (not shown).

This point has important connotation with the physics of the phenomenon: while the negative power functions are not bounded for X approaching zero, the exponential functions are; so, when the spacing is different from the target size, even in the limiting case of a zero-thickness target plate, finite limits can be found on the target edge (i.e. at $X=0$), which is not the case in the 'coincident' geometry.

Though it may appear a detail, this difference proves again that the 'coincident' geometry is a very singular case. The following analogy with a loaded filament (R-L circuit) helps understanding this peculiar behaviour, for the inductive part of the response.

¹⁵ The reason for these particular powers is not understood. The only thing that can be foreseen is a behaviour as $1/X^6$ at great distance from the target (square of a dipolar law in $1/X^3$), which seems to be verified asymptotically.

¹⁶ Beyond the edge, the responses decrease again towards the target center, due to the skin effect inside the conductive body.

¹⁷ During this modelling study, incoherent variations of the response magnitudes according to the shape of the grid cells were reported at both BRGM and GSF with different software, showing that we cannot warrant that our calculations are in the so-called convergence limit.

Let us take a square filament with the same geometry and position as our reference target (except for the thickness which is of course zero), and a nearby vertical borehole at a distance X.

The current intensity I induced in such an R-L circuit is given by: $I = \frac{-j\omega\phi}{R + jL\omega}$, where ϕ is the primary magnetic flux across the filament. The secondary field radiated by this filament is proportional to the current I, and thus to the flux ϕ .

In the 'coincident' geometry, i.e. for a 100 m spacing, and for the centred position of the Tx-Rx pair, which gives the greatest axial responses, the Tx VMD is located precisely at the level of the upper wire of the filament. In this situation, when the distance X is decreased to zero, the vector potential of the Tx magnetic dipole approaches infinity, and it happens the same for the magnetic flux ϕ .

For any other spacing, in the same centred Tx-Rx position, the Tx dipole is either above or below the fateful level of the upper wire. As a consequence, when the horizontal distance X is decreased to zero, the oblique distance of the dipole to the wire remains strictly positive, resulting in finite limits for either the magnetic vector potential or the magnetic flux ϕ through the filament.

This behaviour is exactly identical to what is observed in our 3-D modelling, with the only difference concerning the non-zero thickness of the 3-D model, which results in finite responses on the target edge even in the singular case of the 'coincident' spacing.

The limiting values obtained on the target edge are less important with the smaller spacings, as expected (Table 2.3-7). It is worth noting that the limiting values for the 25 m spacing are close to 100%, possibly because we approach the half-space model (with the resistivity of the target) in this case.

Spacing	100 m	50 m	25 m
In-phase axial field (%)	700	290	90
Quadrature axial field (%)	700	250	70
In-phase transverse field (%)	230	170	90
Quadrature transverse field (%)	600	20	90

Table 2.3-7: Limiting values of the borehole Slingram responses from the highly conductive target (0.5 Ω .m), at 2 kHz, for the three different spacings. These values are obtained by extrapolating on the target edge the responses obtained in boreholes very close to the target.

The new 3-D modelling study for the borehole Slingram method has thus reached its objective defined at the beginning of this section, showing that, at short distance from a confined conductor, very high responses must be expected when the spacing is equal to the target extension, a configuration that we have designated as the 'coincident' geometry. For long spacings, this

geometry yields responses of several hundreds of percents of the free-space primary field at the receiver.

Thus, as opposed to what is assumed for surface Slingram (and almost dogmatized by certain users), no theoretical limit around 100% can be advocated in borehole Slingram. Moreover, it appears more and more probable that such a limit in surface Slingram has no theoretical foundation, but is only based on the experience of the users, and on a misuse of the EM laws, through an attempt to extrapolate at the macroscopic level constitutive laws that are true only at the microscopic level. While it is effectively sound to state that **the secondary field within a conductive cell is bounded by about 100% of the primary field in this cell**, it is completely different, and definitely false, to state that the secondary field *at the receiver* (i.e. far outside the conductive cells) is bounded by the primary field *at the receiver*, i.e. again far outside the conductive cells.

Furthermore, although responses higher than 100% in surface Slingram have never been shown in the literature (to our knowledge), it must be noted on the other hand that nobody has ever proclaimed such a limitation in any scientific publication (to our knowledge). On the contrary, Frischknecht *et al.* (1991) open the door for high responses in surface Slingram. For the case of a shallow horizontal conductive slab with extension equal to the spacing, these authors declare that "the responses are large", whatever the configuration. For the horizontal coplanar configuration (HCP), the most frequent at the surface, they calculate a maximum response of about 40% at 10 m from a 100 m slab with the 'coincident' spacing. From the curves shown in the article, a response of about 300-400% can be extrapolated at 1 m from the slab, which is in the same order as our borehole results!

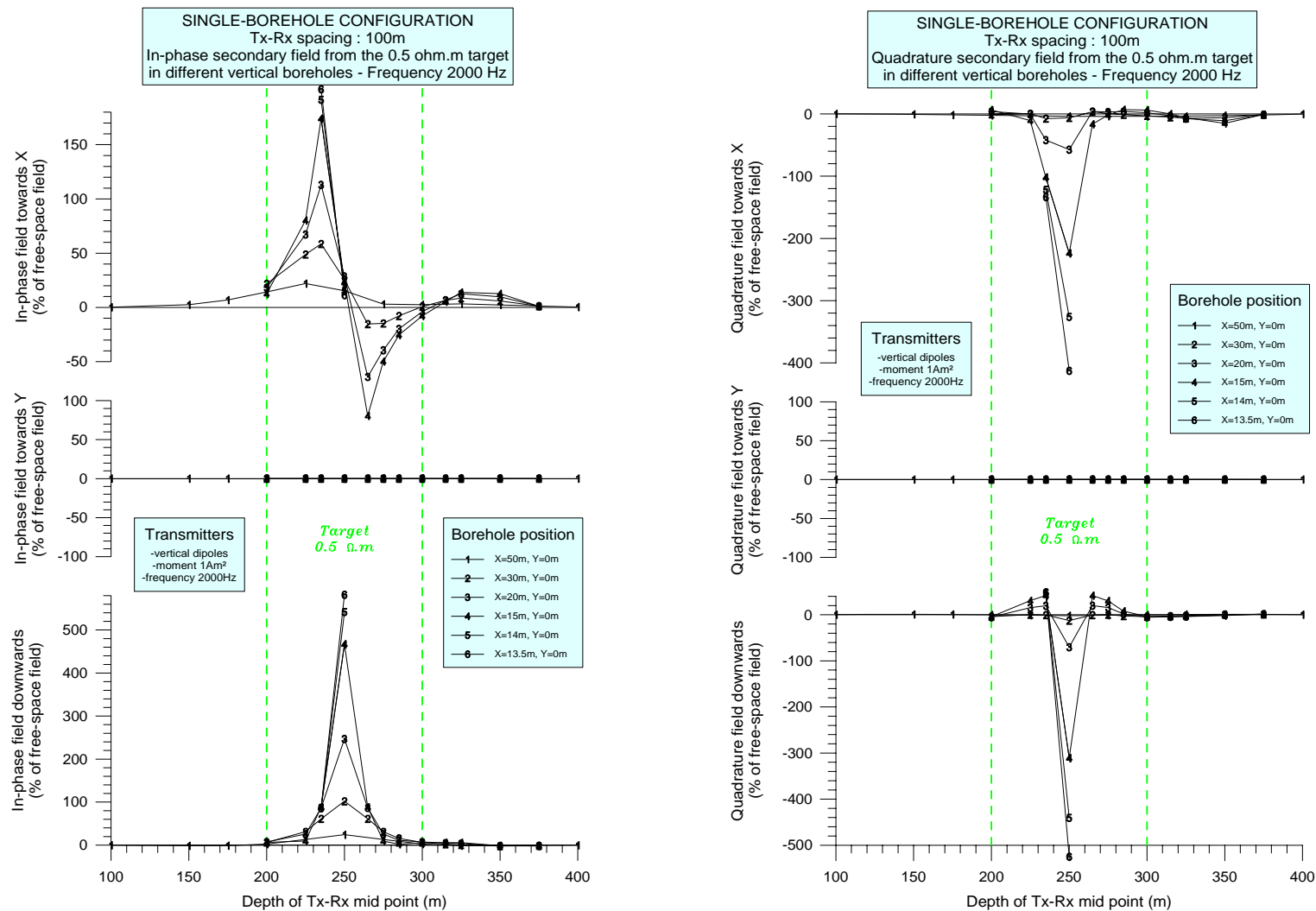


Fig. 2.3-24: Single-borehole configuration. Secondary field logs produced, with a 100 m spacing, in different vertical boreholes by the highly conductive target (0.5 Ω .m), at 2 kHz. All the boreholes are on the Y=0 main symmetry axis of the target, giving zero H_y component. Responses are expressed in percents of the free-space primary field at the receiver, as in surface Slingram. **Left:** In-phase field. **Right:** Quadrature field.

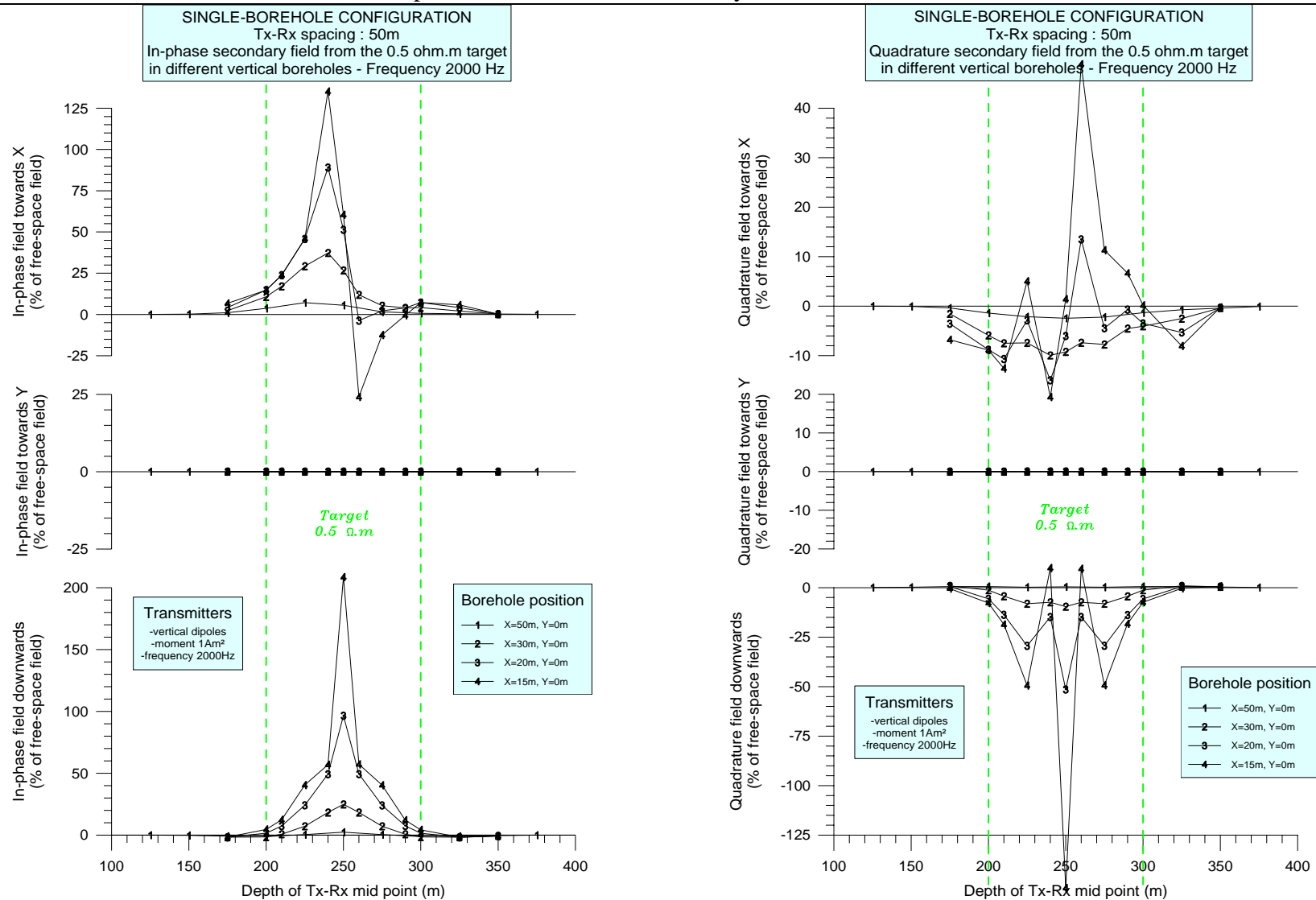


Fig. 2.3-25: Single-borehole configuration. Secondary field logs produced, with a 50 m spacing, in different vertical boreholes by the highly conductive target (0.5 Ω.m), at 2 kHz. All the boreholes are on the Y=0 main symmetry axis of the target, giving zero H_y component. Responses are expressed in percents of the free-space primary field at the receiver, as in surface Slingram. **Left:** In-phase field. **Right:** Quadrature field.

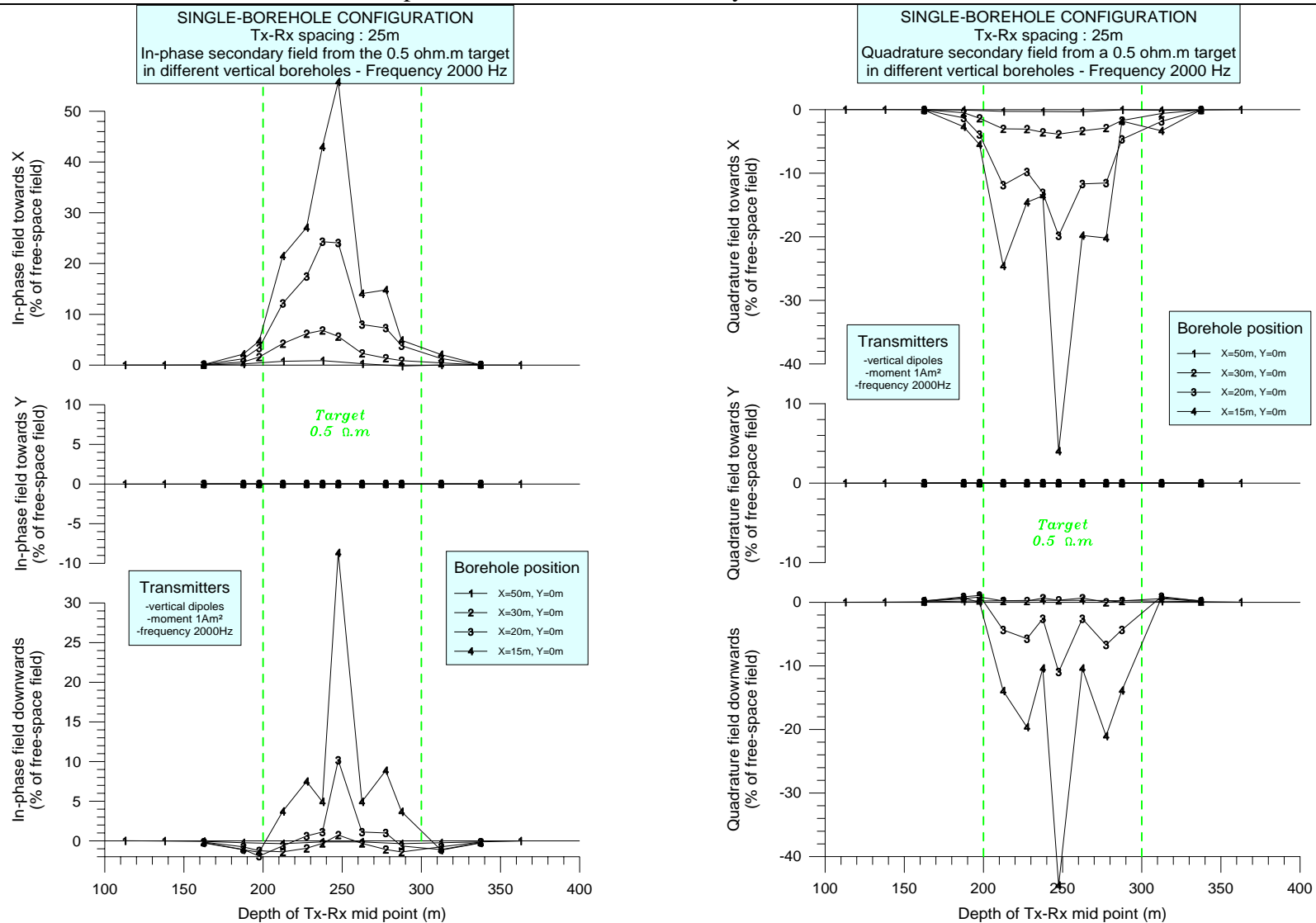


Fig. 2.3-26: Single-borehole configuration. Secondary field logs produced, with a 25 m spacing, in different vertical boreholes by the highly conductive target (0.5 Ω.m), at 2 kHz. All the boreholes are on the Y=0 main symmetry axis of the target, giving zero H_y component. Responses are expressed in percents of the free-space primary field at the receiver. **Left:** In-phase field. **Right:** Quadrature field.

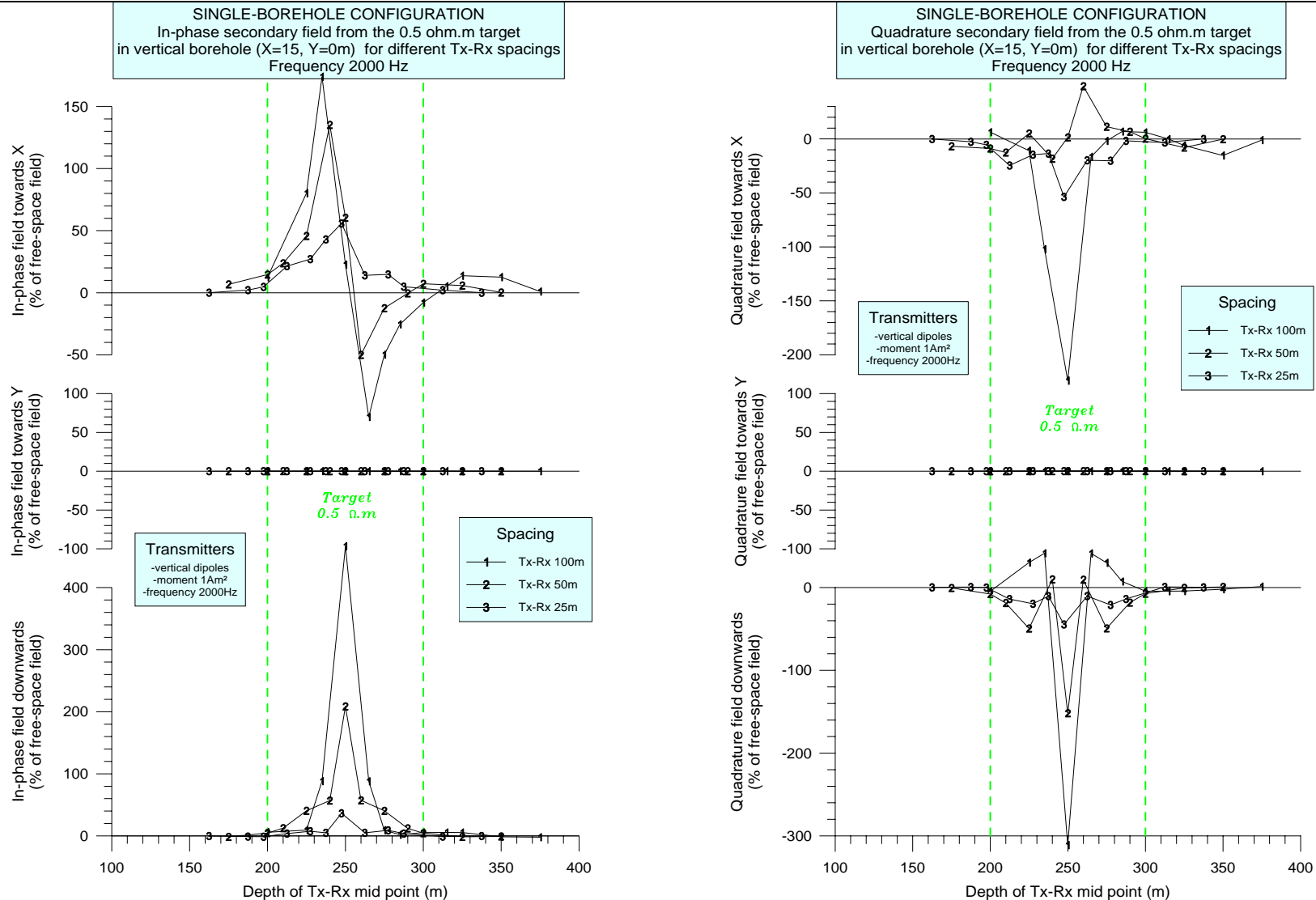


Fig. 2.3-27: Single-borehole configuration. Secondary field logs produced for different spacings, at 2 kHz, in a vertical borehole passing at 2.5 m from the right face of the highly conductive target (0.5 Ω .m). The borehole is on the Y=0 main symmetry axis of the target, which gives zero H_y component. Responses are expressed in percents of the free-space primary field at the receiver. **Left:** In-phase field. **Right:** Quadrature field.

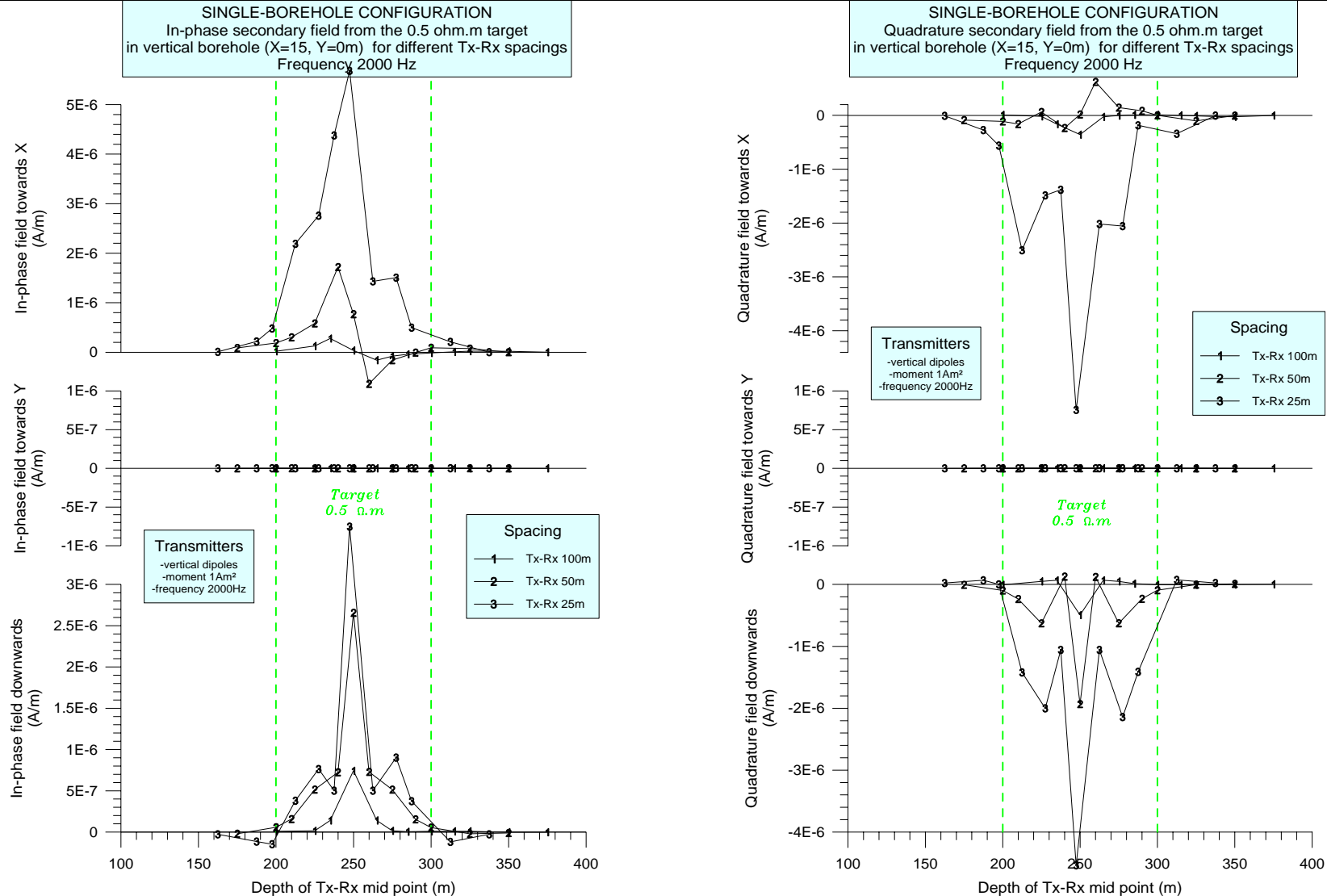


Fig. 2.3-28: Single-borehole configuration. Secondary field logs produced for different spacings, at 2 kHz, in a vertical borehole passing at 2.5 m from the right face of the highly conductive target (0.5 Ω.m). The borehole is on the Y=0 main symmetry axis of the target, which gives zero H_y component. Responses are in A/m. **Left:** In-phase field. **Right:** Quadrature field.

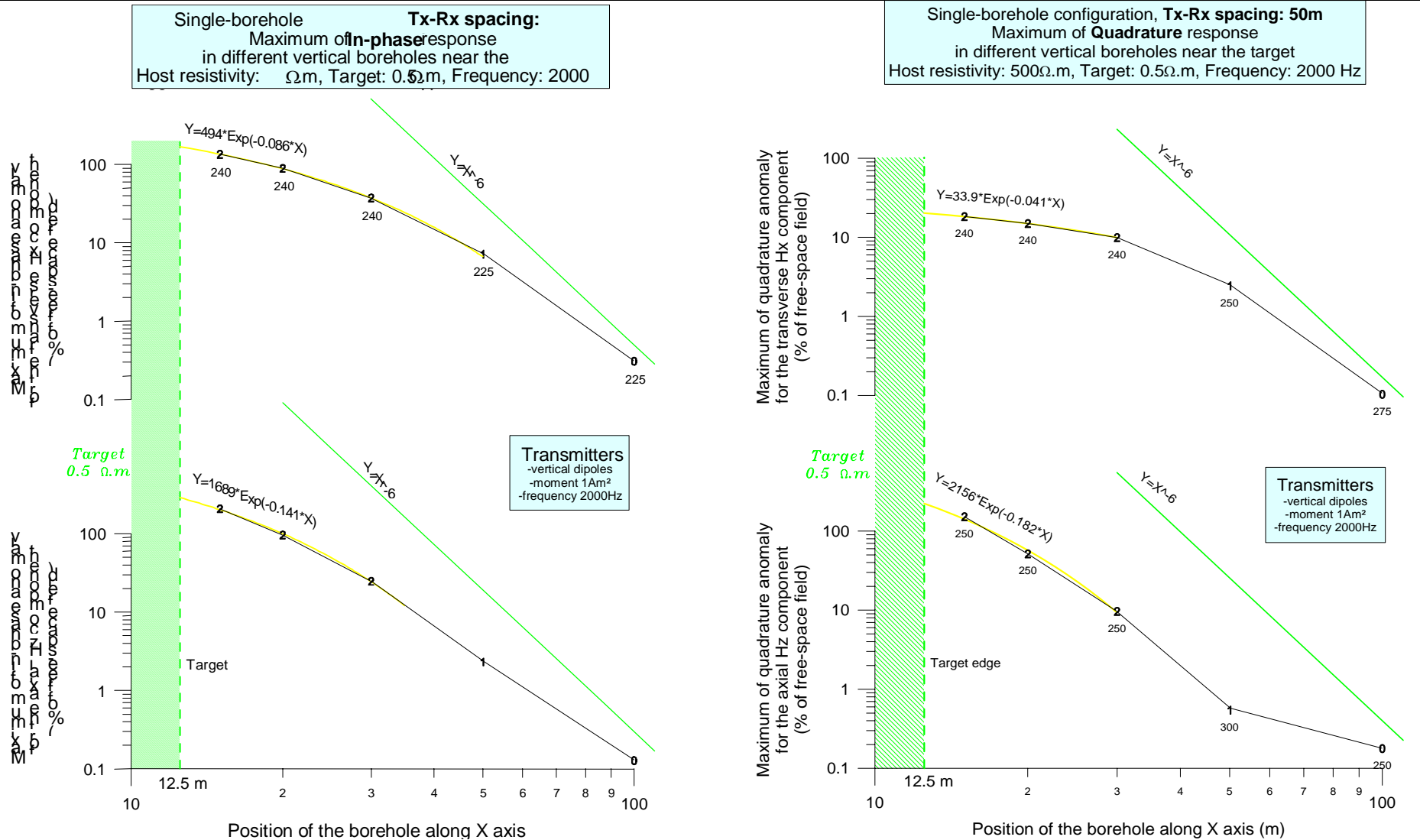


Fig. 2.3-30: Single-borehole configuration. Response extrema for the transverse and axial field components as a function of the distance of the borehole to the target center, for the highly conductive target ($0.5 \Omega \cdot m$), at 2 kHz, with a **50 m spacing**. The boreholes are on the $Y=0$ main symmetry axis of the target, which gives zero H_y component. Responses are in percents of the free-space primary field at the receiver. **Left:** In-phase field. **Right:** Quadrature field.

2.5.3.5.2. Borehole Slingram response of an horizontal conductive layer in a dipping borehole

The complexity and specificity of borehole Slingram responses for 3-D targets obliged us to revise many concepts. As a consequence, basic behavioural aspects such as response in a half-space or through a conductive layer had to be considered in detail.

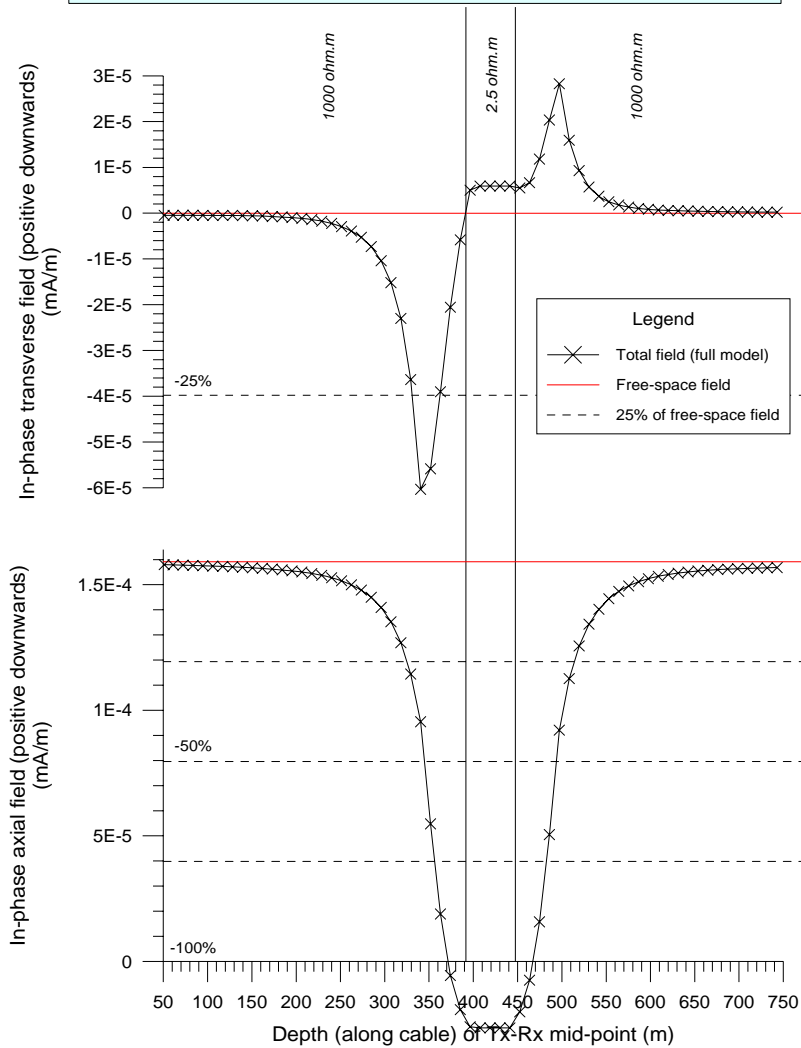
1D modelling was conducted in a borehole dipping 63° below the horizontal and passing through a 50 m-thick layer of variable resistivity embedded in a $1000 \Omega\cdot\text{m}$ half-space (Fig. 2.3-31). This modelling is summarized in Table 2.3-8. It shows a maximum in-phase response of -117% for a layer resistivity of $2.5 \Omega\cdot\text{m}$, corresponding to a kind of resonance slightly before saturation in the layer, instead of a maximum response of -104% for a half-space in surface Slingram (in HCP configuration).

Layer resistivity	50 $\Omega\cdot\text{m}$	10 $\Omega\cdot\text{m}$	2.5 $\Omega\cdot\text{m}$	0.5 $\Omega\cdot\text{m}$	0.1 $\Omega\cdot\text{m}$
In-phase axial field (%)	-14	-79	-117	-109	-104
Quadrature axial field (%)	-33	-56	-36	-20	-6
In-phase transverse field (%)	-5 / +1	-23 / +7	-41 / +18	-57 / +29	-67 / +34
Quadrature transverse field (%)	-7 / +5	-16 / +11	-16 / +20	-9 / +22	-3 / +5

Table 2.3-8: Borehole Slingram responses of a 50 m-thick horizontal conductive layer of variable resistivity, embedded in a $1000 \Omega\cdot\text{m}$ space, in a dipping borehole (63° from the horizontal), for a 100 m Tx-Rx spacing, at 2 kHz. (Percentages are expressed with respect to the free-space primary field at Rx. Quadrature data in this table follow the standard convention of sign defined in Section 1.4).

Comparing Tables 2.3-6 and 2.3-8 shows that, for a given conductivity, an off-hole confined target produces anomalies much greater than an intersected layer. This feature should enable to quickly discriminate between a nearby confined target and an intersected 1D layer. Only when a confined target is far enough is it possible to get response amplitudes similar to that from a 1D layer. Nevertheless, in this case, comparison of different spacings will certainly enable discrimination between the two types of conductors.

SINGLE-BOREHOLE CONFIGURATION - Tx-Rx Spacing: 100m
In-phase total field at 2kHz in a dipping borehole (63° below the horizontal)
passing through a 50m-thick horizontal conductive layer of 2.5 ohm.m.



SINGLE-BOREHOLE CONFIGURATION - Tx-Rx Spacing: 100m
Quadrature total field at 2kHz in a dipping borehole (63° below the horizontal)
passing through a 50m-thick horizontal conductive layer of 2.5 ohm.m.

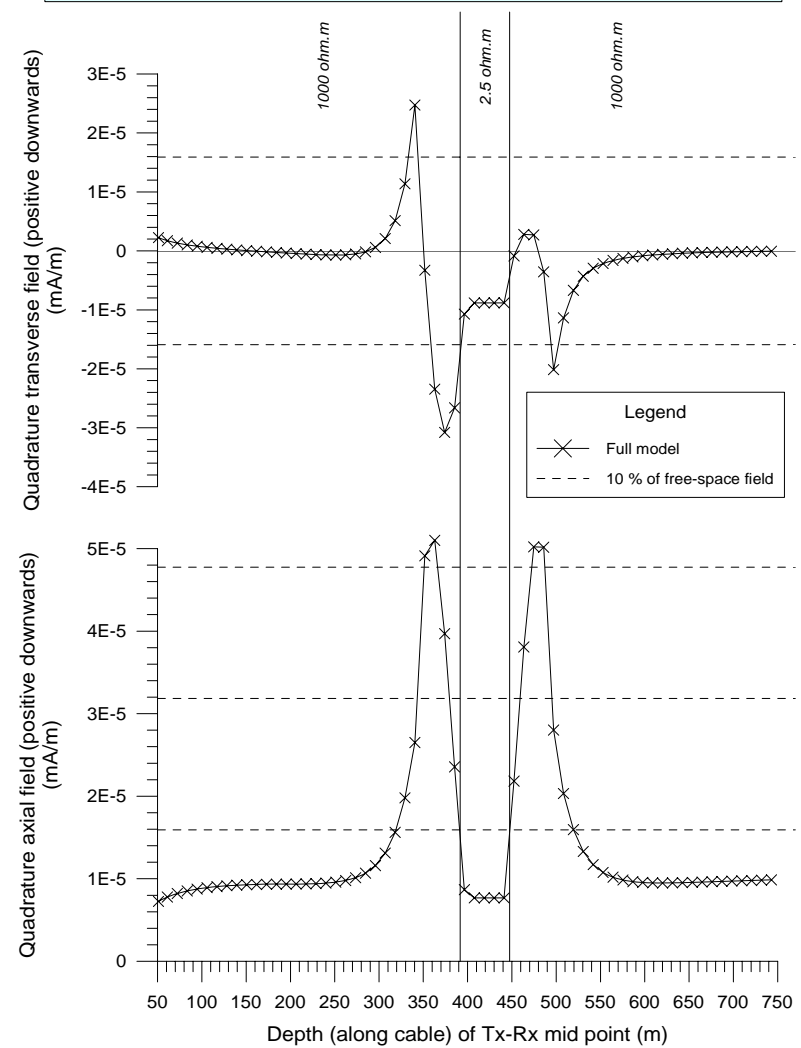


Fig. 2.3-31: Single-borehole configuration. Total field logs for a 100 m spacing in a dipping borehole (63° from the horizontal) passing through a 50 m-thick

2.5.4. Methodology study (GSF report): Behaviour of 3-component responses of a single borehole EM method

The numerical modelling has been carried out for a three component single borehole EM measurement system to find out the behaviour of the response for different geological situations. The objective was to develop rules for data interpretation. In single borehole system both the magnetic dipole transmitter and the three component receiver move in the same hole with a fixed coil spacing (Fig. 2.3-32). The separation can vary from 25 m to 120 m. The frequency range of the system is from 35 Hz to 8960 Hz.

Single Borehole EM System

- Transmitter and 3-component receiver in borehole
- Coil separation 20 m ... 120 m
- Frequency range 35 Hz ... 8960 Hz

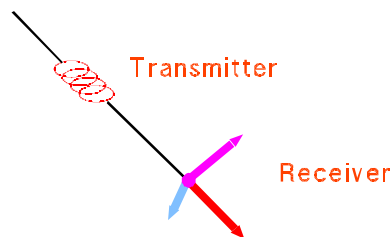


Fig. 2.3-32: A three component single borehole EM system.

2.5.4.1. Basic behavioural relations

In the interpretation of the borehole EM field data it is essential to understand the basic behavioural relations of the measured response. Let us first consider the response of a single borehole system in a homogeneous environment. For symmetry reasons only the axial component deviates from zero in the homogeneous case.

Fig. 2.3-34a shows the Argand diagrams for co-axial borehole (red curve) and co-axial ground (blue curve) systems. As a comparison a diagram for a normal ground Slingram system (horizontal loops) is also presented (orange curve). Calculations are made with MARCO software (Raiche, Sugeng and Xiong, 1998). The response parameter of the curves is $W = \mu_0 L^2 \sigma f$, where μ_0 is magnetic permeability of a vacuum $\mu_0 = 4\pi \times 10^{-7}$ H/m, L is

coil separation, σ is electric conductivity ($\sigma=1/\rho$, ρ is resistivity) and f is frequency. For example values of $L=100$ m, $\rho=89.6 \Omega\text{m}$ and $f=8960$ Hz give $W=1.26$ (marked in the figure). When W approaches infinity the in-phase component approaches -100 % for a borehole co-axial system whereas for a co-axial configuration on the ground the in-phase component approaches +100 % when W approaches infinity. In-phase component is defined here as the secondary in-phase component normalized by the primary field in a vacuum while quadrature component is a normalized component which is 90 degrees out of phase with the primary signal.

The Argand diagrams indicate that the co-axial borehole system has a wider dynamics of the response as a function of frequency than ground systems do. This means that the highest frequency of the borehole system (in the GeoNickel system $f_{\text{max}}=8960$ Hz) corresponds to higher frequency in comparable ground systems.

Maximum in-phase component is -117.9 % and it is reached at $W=3.14$, corresponding to e.g. $f=2500$ Hz, $L=100$ m and $\rho=10 \Omega\text{m}$. The maximum quadrature component is -67.4 % at $W=0.79$. Note that according to numerical modelling carried out much larger in-phase anomalies can be found for two or three dimensional structural models. Anomalies of several hundreds of percentages are obtained when the borehole passes near the target and the coil spacing is close to the dimension of the model. In Fig. 2.3-33 the in-phase anomaly is over 400 % for a conductive 100×100 m plate ($\sigma=400$ S, $f=8000$ Hz) situated in a free space. Distance of the vertical borehole to the vertical plate is 2 m. Coil spacing is 100 m. Calculation is carried out with Leroi_air software (Raiche et al., 1998). Important is to find out that the anomaly peak is very narrow. Half-width is only 6 m and the width of the part of the anomaly which exceeds 100 % is 10 m. This means that station interval in the measurement should be small enough in order that no anomalies are lost. As a comparison axial in-phase anomaly is calculated also for a plate which distance from the borehole is increased to 20 m. The anomaly amplitude has decreased to 87 % and the anomaly has become broader. Half-width is now 12.5 m.

Fig. 2.3-34 shows the responses for a contact model. The co-axial system is in vertical borehole situated 10 m from the contact of two media which have different resistivities such that $\rho_1=1 \Omega\text{m}$ and $10 \Omega\text{m}$ and $\rho_2=1000 \Omega\text{m}$. Red curves depict the case where the borehole is inside the more conductive medium and blue curves represent cases where the hole is in the medium which has higher resistivity ($\rho_2=1000 \Omega\text{m}$). Frequency range is from 35 to 8960 Hz.

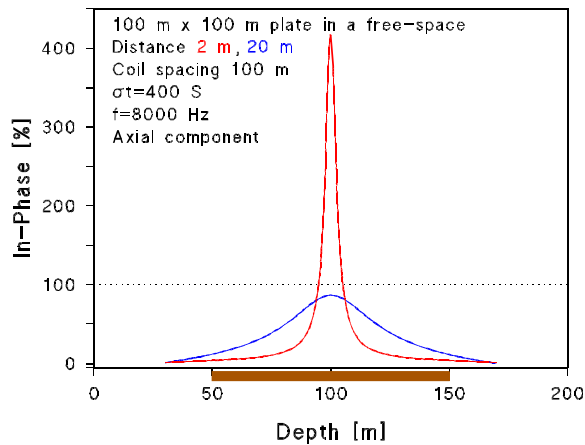


Fig. 2.3-33: Axial component anomaly (in-phase) for a plate model close to the borehole.

When the measuring system is inside the more conductive medium the in-phase component is negative and approaches -100 % as the frequency increases. When the measuring system is in resistive medium the in-phase component is positive except at the highest frequency. This behaviour explains why negative anomaly is obtained when the borehole intersects the conductive body whereas positive anomaly is obtained when the borehole runs outside the conductor.

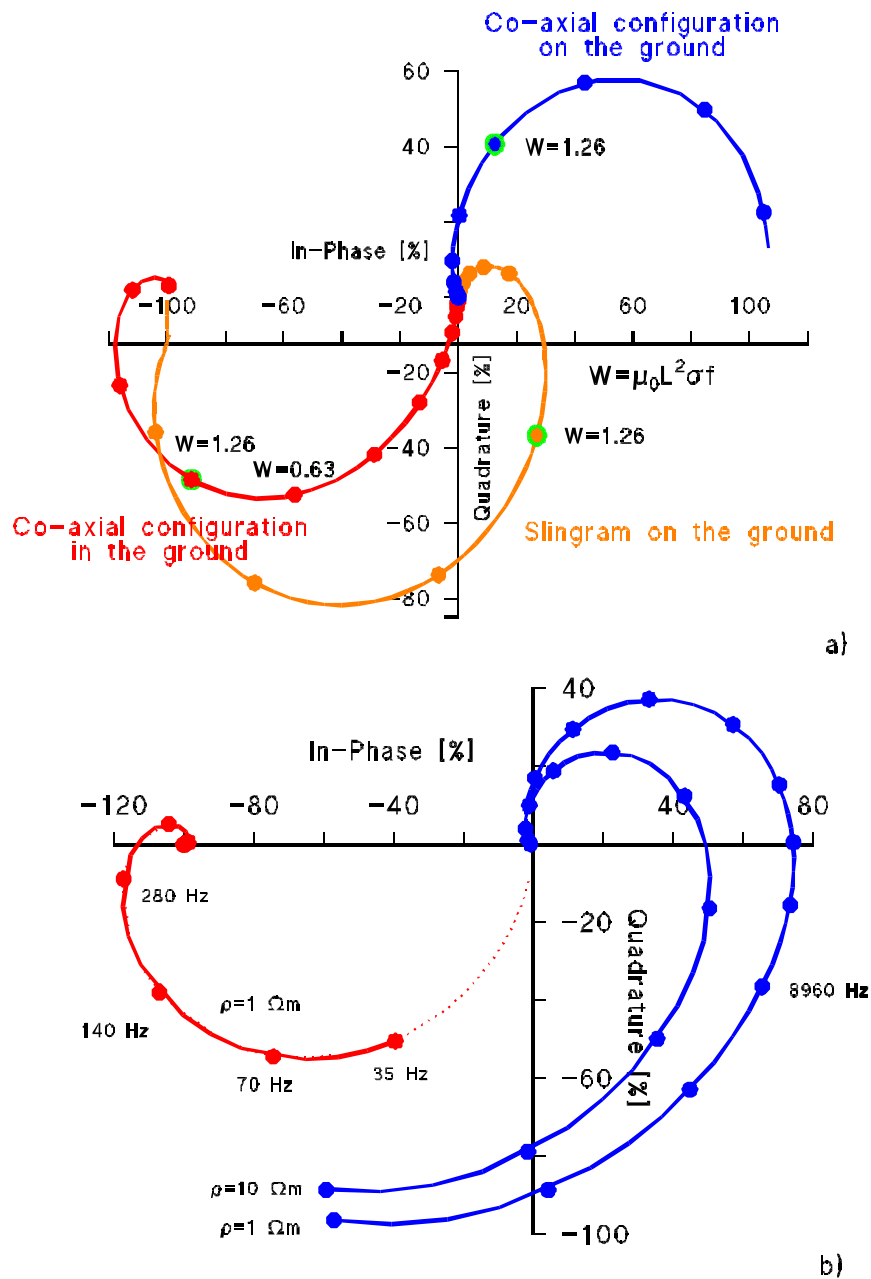


Fig. 2.3-34: a) Argand diagrams for co-axial borehole and ground configurations. Ground Slingram configuration is presented as a comparison. b) Argand diagrams for a contact model.

2.5.4.2. Responses of single borehole system for 3D models

In this section we consider a three dimensional case. Calculations were made by using MARCO software (Raiche et al., 1998). It is based on a volume integral equation formulation. A limitation of this formulation is that it works only with rather small (low) conductivity contrasts. In general the maximum contrast with MARCO program is about 1:300 (Raiche et al., 1998), but if the calculation point is outside of a conductor calculated results up to contrast 1:800 seem to be reliable according comparison with physical scale modelling made in VIRG-Rudgofizika (St. Petersburg, Russia).

In this work vertical and horizontal rectangular prismatic models were used as conductors. Boreholes were either vertical or inclined.

2.5.4.2.1. Calculated results compared with the scale modelling

In Figs. 2.3-35 to 2.3-38, calculated curves of vertical quadrature and in-phase component are compared with corresponding results of the scale modelling. For different contrasts aluminium, copper and lead were used as target and graphite as a host. The model was a 100 m x 100 m x 25 m prism. In figure 2.3-35 the hole is outside the conductor close to it (distance 7.5 m) and the conductivity contrast is 1:70 ($f=2100$ Hz, coil separation 60 m). Calculated and measured responses are close to each other. When contrast increases to 1:800 (Fig. 2.3-36, $F=2100$ Hz, coil separation 90 m) the similarity of the in-phase components is noteworthy, but in quadrature components the calculated curve shows an expected shape, while there seems to be some noise in scale modelling.

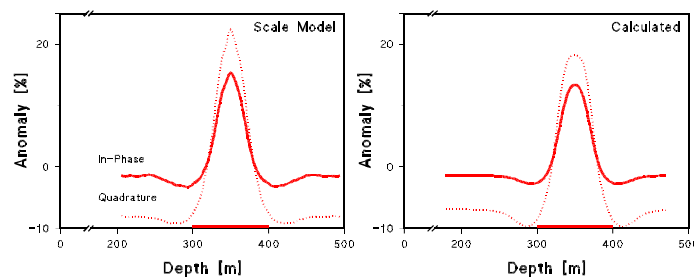


Fig. 2.3-35: Scale model and calculated results for a conductivity contrast 1:70. The borehole passes the body.

When the borehole intersects the target (Fig. 2.3-37) with a small conductivity contrast the curves has the same level and the shapes are considerably similar, but the size of the

anomalies is not equal. In an intersection with a large conductivity contrast shapes between calculated and physically modelled curves differ significantly. This is understandable because of the contrast limitations of the MARCO program. It is remarkable, that calculated curves were very similar to the curves of the scale modelling with the same contrast outside the conductor. It shows the expected result, that an intersection is more complicated situation to calculate. In examples showed the hole is rather close to the side of the conductor, which is difficult to both calculations and the scale modelling.

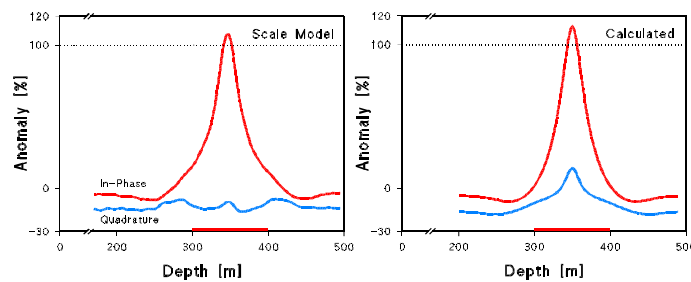


Fig. 2.3-36: Scale model and calculated results for a conductivity contrast 1:800. Borehole passes the body

In Fig. 2.3-37 there is remarkable a down pointing peak in the quadrature component of the scale model. The peak is upwards in the corresponding calculated curve. The same kind of peak is seen also in calculations with a low contrast and frequency 10000 Hz. It shows that the form is dependent on the frequency used.

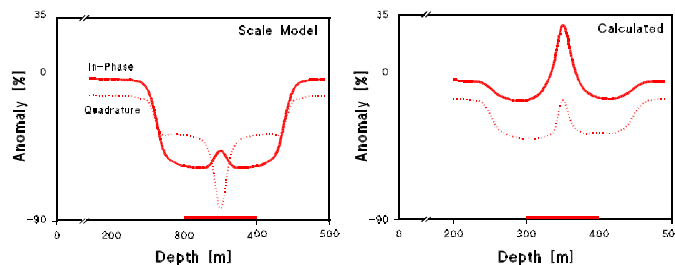


Fig. 2.3-37: Scale model and calculated results for a contrast 1:800. Intersection 4.5 m from the edge.

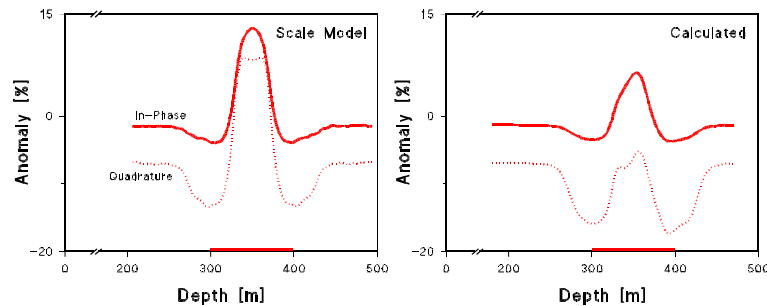


Fig. 2.3-38: Scale model and calculated results for a contrast 1:70, Intersection 4.5 m from the edge.

2.5.4.2.2. Distance from borehole

Measured three components give information about distance, size, position and shape of a conductor, and in which direction from the hole the conductor is located.

Information of the size of the body depends on the ratio between the size and the coil separation. The distance from the conductor to the borehole can be divided to classes “far”, “near” and “intersection”. In Fig. 2.3-39c, the class “far” has a coil separation of 60 m and the size of the conductor in a direction of the borehole is 100 m. The anomaly curves have smoothly arching shapes and are positive. An anomaly from the conductor can be got even from the distance of more than 50 m.

When the borehole is close to a conductor (class “near” in Fig. 2.3-39b), there are two peaks both in axial and radial components. This is characteristic to cases where coil separation is equal or larger than size of the body in axial direction.

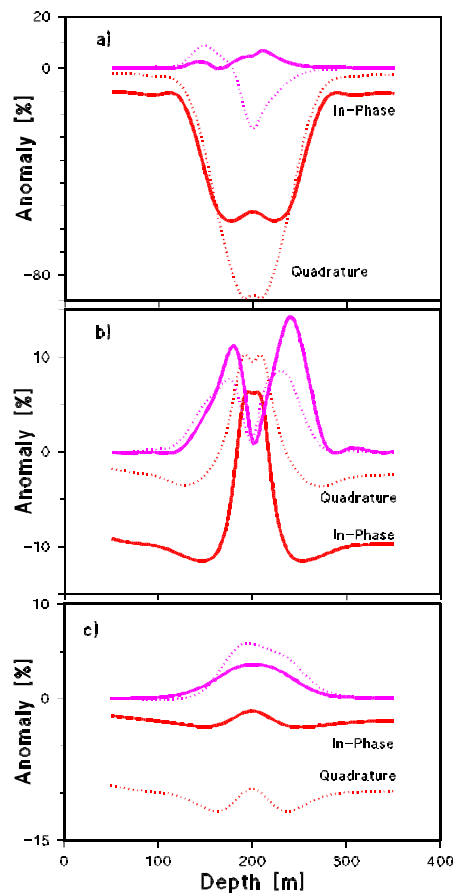


Fig. 2.3-39: Anomaly curves for a hole of different distance of a body.

Fig. 2.3-39a shows a case, in which the borehole intersects the conductor. The anomaly of the vertical component is negative. The same phenomenon can be seen as a negative level, when a measuring is carried out in a conductive surrounding without any anomalous body. Negative anomalies can be got also when a borehole is very close to the conductor. These cases can be separated from each other according to the signs of the anomalies of radial components (see next section).

2.5.4.2.3. Direction of the borehole to the conductor

The direction from the borehole to the conductor can be interpreted from the sign of the radial components. If the sign is positive, the borehole is in the positive direction of the component in question from the conductor (Fig. 2.3-40). More precise interpretation can be made using proper numerical modelling.

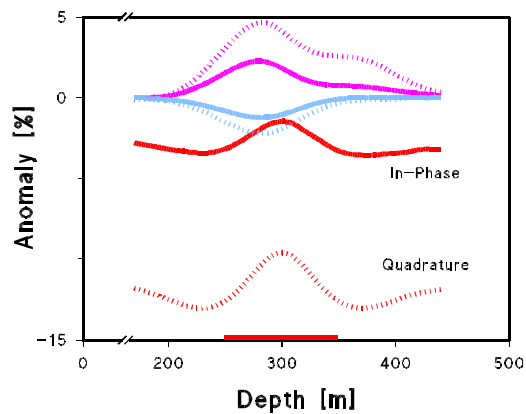


Fig. 2.3-40: Effect of direction. Borehole is in the negative x-direction (blue curves).

If the target is so large that the whole side towards the borehole can not be observed, the direction is to the centre of that side. In Section 2.5.4.2.6 it is discussed how the size of the body effects to anomalies. When the borehole intersects the conductor close to its edge (Fig. 2.3-41), in the quadrature component of the vertical component there is an effect of the small side as an asymmetric anomaly. This can be used to interpret the direction to an edge and at the same time to the centre of the conductor.

In Fig. 2.3-42, boreholes pass the dipping conductor close to it symmetric at the same distance. In the curves of the vertical component can be seen the same effect of a small side that was mentioned above. The curves of vertical component has the symmetric shape in relation to the centre of the conductor according to the symmetric position of that component. The radial components have not the same symmetry.

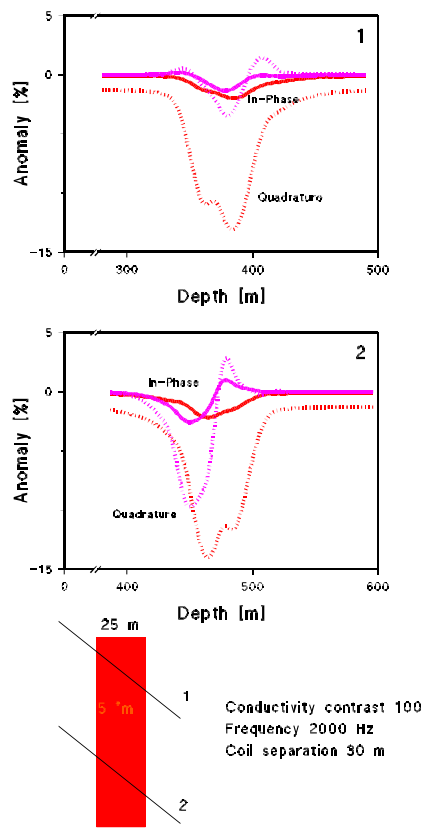


Fig. 2.3-41: Symmetry in an intersecting hole.

2.5.4.2.4. *Depth of the conductor*

The depth of the conductor in the direction of the borehole can be seen at the peak of the curves of vertical component. The peak can be either positive or negative. The peak is in the centre of the side that is towards the borehole (Fig. 2.3-40).

2.5.4.2.5. *Symmetry and position of the target*

When two holes are in a symmetric position to the conductor can the symmetry of the axial component be used to interpret the direction to the centre (or edges of the body).

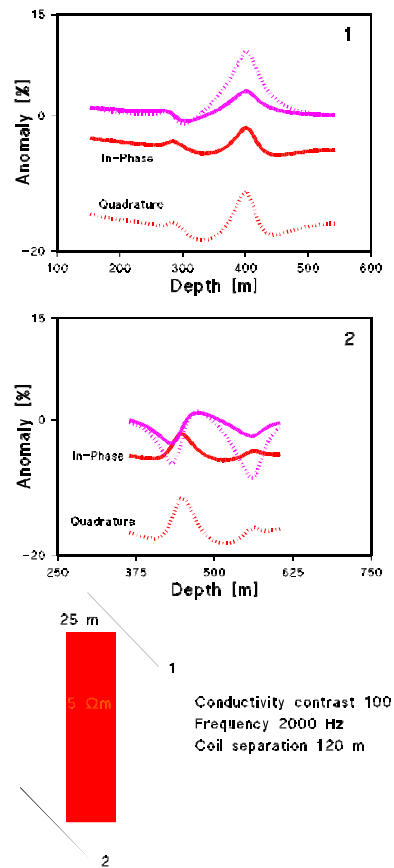


Fig. 2.3-42: Symmetry in passing holes.

In Fig. 2.3-42, two boreholes are passing the body. Small symmetric parts in red curves (vertical component) are effected by a small edge of the conductor, while the bigger peaks are from a great side of the conductor. According to the ratio between the peaks it is possible with a proper inclination to estimate the position of the conductor compared to the direction of the borehole.

In Fig. 2.3-41 and 2.3-42 in axial curves small symmetric parts show the order of the effect of a small side compared to a big side in the direction of the borehole.

2.5.4.2.6. Influence of the body size

The anomaly amplitude depends on the size of the conductor. Because the anomalies are mostly caused by the uppermost cover of the good conductor, due to the skin effect, it is the side towards the borehole that effects them. In the examples in Fig. 2.3-43, the faces towards the borehole are 100 m x 100 m and the thickness in figure is a) 100 m and b) 25 m. The anomalies are however equal in size. In figure c) a smaller side towards the hole gives also a smaller anomaly. When the side towards the borehole is so wide that the

measuring system can not see it entirely, the anomaly is equal from all equally conductive targets at the same distance.

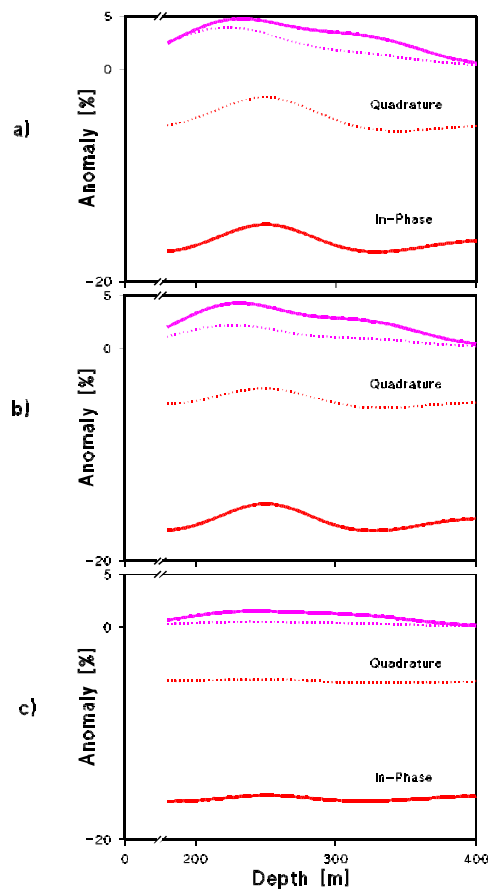


Fig 2.3-43: Effect of the body size.

2.5.4.2.7. Spatial resolution

The single borehole system has been criticised because of the disturbing effects of small conductors close to the hole (Dyck, 1991). However, according to the results of numerical modelling carried out this argument is unfounded. In calculations the cubes of 5 m and 10 m in size near the borehole between it and the larger conductor (100 m x 25 m x 100 m) did not cause any disturbing anomalies.

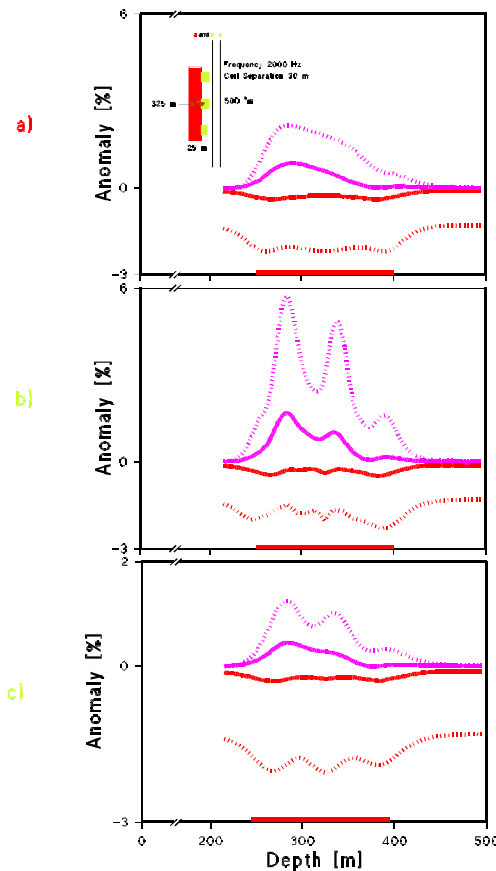


Fig. 2.3-44: Spatial resolution of a single-borehole system; a) with no overhangs; b) and c) with overhangs oriented towards the borehole.

Fig. 2.3.3.-10 shows another example of the discrimination of the system. Along the side towards the boreholes there are three horizontal 10 m and 15 m deep and 17,5 m and 20 m high overhangs. In figure a) there is the anomaly of the plain conductor and in figures b) and c) curves from the body with overhangs. The distances to the hole are 15 m and 20 m from the closest point of the target. Both in figure b) and c) the shape of the original conductor and the overhangs can be clearly seen.

2.5.4.3. Conclusion for Sec. 2.5.4.

The modelled Slingram-type borehole measurement system seems to be very promising equipment to seek conductive ore bodies in a conductive medium. It is not disturbed by conductive overburden and it can give very good information from a position of the sought conductor. At its best the system is to deduce the direction and the depth of the target.

2.5.5. Instrument development

A versatile prototype equipment for 3-component downhole EM measurements has been developed at IRIS Instruments. The 'SlimBoris' system covers the three configurations that can be envisioned in boreholes, i.e. the two configurations developed in this project using a downhole dipolar transmitter, plus the classical surface-to-hole configuration¹⁸ where the transmitter is a large loop at the surface.

The external diameter of the probes is 42.5 mm for use in slim exploration boreholes, most of which are drilled in 46 mm. The probe envelopes are pressure tested to 200 bars, corresponding to 2000 m in water. The frequency range is 35-8960 Hz, with nine frequencies in geometric progression of ratio 2. The transmitted magnetic moments are about 250 A.m² at low frequency, down to 50 A.m² at the highest frequency.

The system uses standard 4-conductor logging cables. Nevertheless, due to power losses in the cable, below 1000 m the transmitter should be operated with a 7-conductor cable. In the Slingram configuration, the two probes are separated by a fixed length of connecting cable. Three spacings are available: 25, 50 and 100 m, enabling pluri-decametric investigation around the borehole.

2.5.5.1. Specifications

The single multipurpose system which has been built advantageously replaces the two separate systems (one for each configuration) foreseen in the initial specifications of the work programme. The benefit for IRIS is of course a simplification of the manufacturing and maintenance, with a more attractive commercial offer. The benefit is also for the user who can perform complete borehole EM surveys with a single system.

Several other changes to the initial specifications of the work programme have been made. They are always in the positive sense, i.e. an improvement from the initial specifications.

2.5.5.1.1. Mechanical considerations

The most important change concerns the external diameter of the probes. A 45 mm diameter was indicated as an upper limit in the work programme, but it was decided during the first technical meetings that the clearance offered by this diameter was insufficient in 46 mm boreholes. A 42 mm diameter was thus targeted instead. It was finally increased to 42.5 mm because the envelopes imploded when pressure tested at 200 bars.

The challenge was to decrease the diameter of the probes while keeping adequate sensor sensitivities at Rx and sufficient transmitting moment at Tx. The final sensitivities are 30 mV/nT for the axial coil and 50 mV/nT for the radial coil, and final magnetic moments are about 250 A.m² at low frequency down to 50 A.m² at the highest frequency (see later).

¹⁸ Needing of course a surface transmitter in addition to the borehole system.

Testing in Finland has shown that the final 42.5 mm diameter is adequate, but is really an upper limit, because it was observed that the probe envelopes are severely scored after several measurements in 46 mm boreholes.

Maybe more problematic is the strong piston effect caused by the limited diameter clearance and the light weight of the probes, particularly the Rx. In slim holes, this effect can considerably slow down the descent of the probes or even stop it, introducing errors in the depth encoding if the cable skids on the winch. This effect can be even dangerous in the single-borehole configuration because the Tx probe, the heavier, pushes the Rx probe and its connecting cable, a situation which could result in tangling the cable or even jamming the system. IRIS is thus designing an additional weight to be mounted on the Rx probe, in order to produce a more rapid and safer descent of the probes in slim holes.

Another change in the specification is the operating depth. A 2000 m depth has been targeted by IRIS instead of the 1000 m initially planned. This has implication on the thickness of the probe's envelopes, on the communication schemes, and on the power supply of the transmitter.

The final thickness of the epoxy envelopes resulting from this choice is 3.25 mm, leaving an internal diameter of only 36 mm for hosting the Rx sensors, Tx dipole and electronics.

The requirement of using standard 4-conductor cable, though justified for the users, reinforces the difficulty related to a 2000 m operating depth, due to power losses in such a cable, especially for the transmitter. While receiver power supply and communication schemes have been achieved through 2000 m of 4-conductor cable, the transmitter power supply is limited to only 1000 m of such a cable. However, if required, the Tx probe can probably be operated down to 2000 m using a 7-conductor cable in which four wires instead of two would be used for the power supply of the Tx probe (not tested).

2.5.5.1.2. Primary-field compensation in single-borehole configuration

During the first technical meetings between partners involved in WP2, a point thoroughly discussed was to know whether a compensation circuitry was necessary or not, in order to cancel the primary field at the receiver and keep adequate numerical resolution for the secondary field.

This question is discussed in Section 2.5.3.3.2.2. It is concluded from Table 2.3-4 that a 20-bit A/D converter with a gain-16 preamplification, and a 16-bit microprocessor offers sufficient numerical resolution to avoid such compensation, even with a 25 m spacing.

This is much better because several problems are inherent to compensation devices, such as time and temperature drifts, as well as the difficulty to control the real value of the compensation applied and its suitability to the transmitted moment. This is particularly true in non-rigid systems, such as the borehole Slingram, for which the coaxial geometry ('coaxiality') of the Tx and Rx probes is not perfect. In addition, such devices significantly increase the cost of a system.

2.5.5.2. *Operating configurations*

The main elements of the equipment and their relationships in the single-borehole and cross-borehole configurations are shown on the simplified diagrams of Fig. 2.3-46.

In the single-hole configuration, the Tx probe is above the Rx probe. One advantage of this arrangement is that the wires supplying the power to the Tx probe do not cross the Rx probe, avoiding any disturbance. Another advantage is that the Rx probe sweeps a deeper portion of the hole, which is of course interesting for the EM measurements itself, but also for the orientation measurements and resulting calculation of the borehole trajectory which is thus recovered on a greater length.

As a result of this arrangement, and due to the versatility of the system, one difficulty appears concerning the design of the reference wiring in the Tx probe. For the single-borehole configuration, the reference signal must be available at the bottom connector of the probe, while it must be available at the top connector for the cross-borehole configuration. This problem has been solved by designing a specific switching cap to be plugged at the bottom of the probe when operated in the cross-borehole configuration. Besides its protection against water penetration, this cap has the function of switching the reference signal to the upper connector.

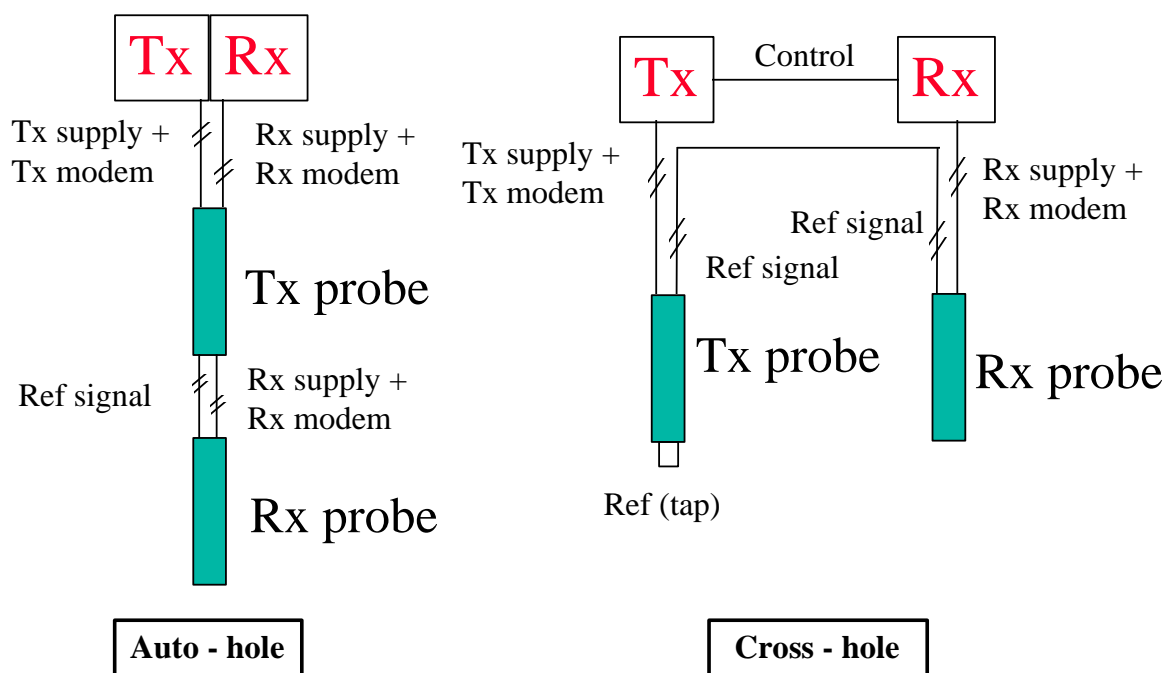


Fig. 2.3-46: SlimBoris operating diagram in the cross-hole and single-hole configurations.

2.5.5.3. *Technical description of the SlimBoris system*

As showed in Fig. 2.3-46, the probes are connected to two surface boxes performing the power supply and communication. The depths of the probes in the transmitter and receiver boreholes are given by two depth encoders connected to each surface box. The Rx surface box is powered by a battery, whereas the Tx box is powered by a light-weight motor generator.

The Rx probe contains, in addition to the three EM (magnetic) sensors, a temperature sensor and a full orientation module composed of three piezoelectric accelerometers and three fluxgate magnetometers, to derive the gravity and earth magnetic vectors. This enables projecting the measured EM components onto either a fixed reference system, such as North, East, Down, or onto the standard reference system used in gimbal-mounted probes —without the drawback of these probes of not being usable in vertical boreholes.

This kind of orientation module also enables to retrieve the borehole trajectory. The procedure has been validated even in environments presenting short wavelength magnetic anomalies producing local rotations of the magnetic North (Bourgeois *et al.*, 1999).

The Rx probe CPU performs 4-channel A/D conversion and FFT for the EM channels (three EM sensors plus reference signal), retrieves the temperature and orientation readings, and transfers the digital information to the surface Rx box.

Figures 2.3-47 and 2.3-48 give detailed description of the Tx and Rx probes.

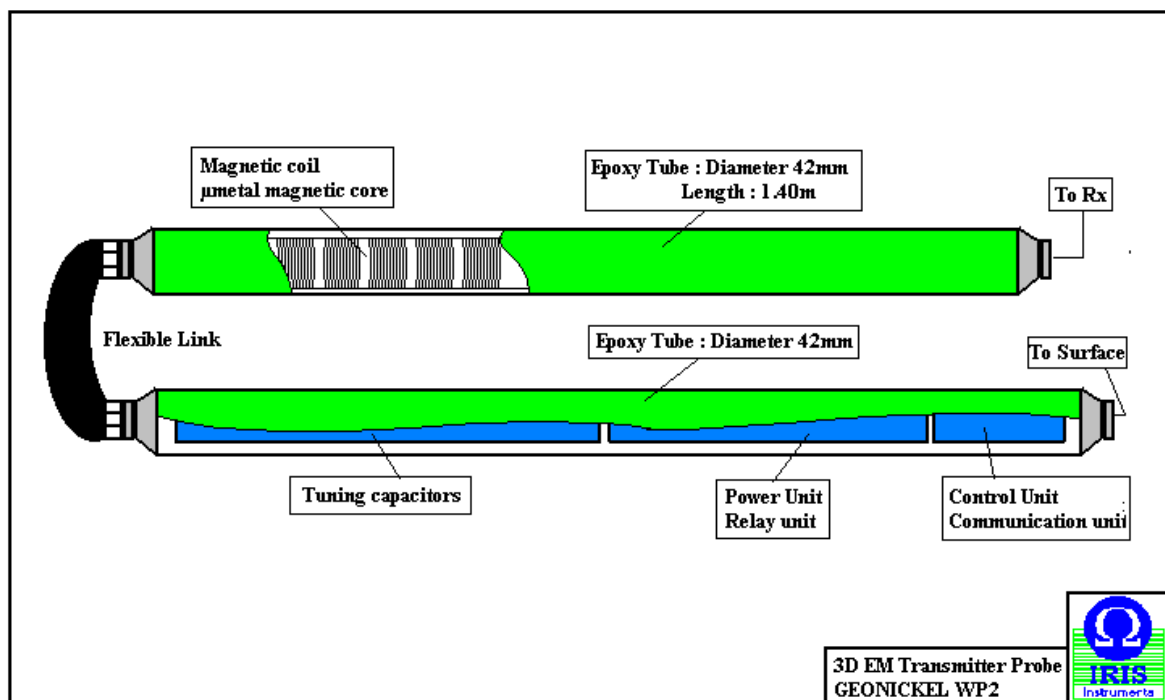


Fig. 2.3-47: Cutaway diagram of the Tx probe.

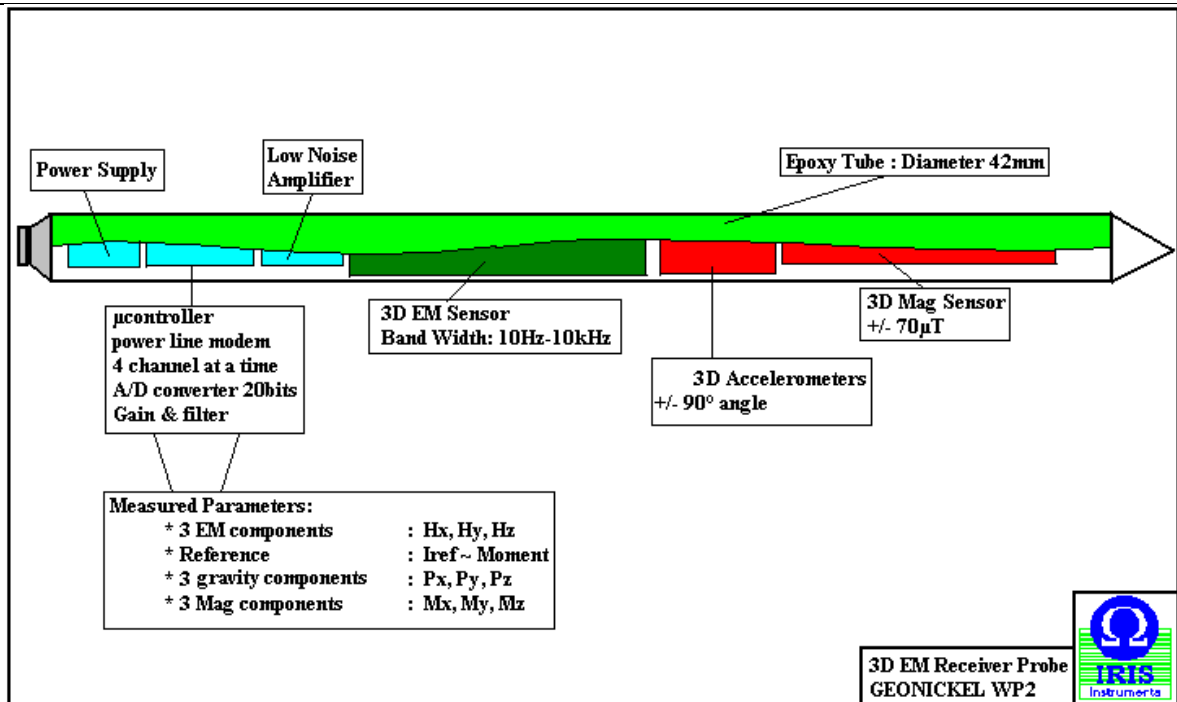


Fig. 2.3.48: Cutaway diagram of the Rx probe.

2.5.5.4. Performances of the SlimBoris system

2.5.5.4.1. Transmitter probe

The magnetic moments produced by the transmitter probe on a 500 m-long 4-conductor cable are shown in Fig. 2.3-49.

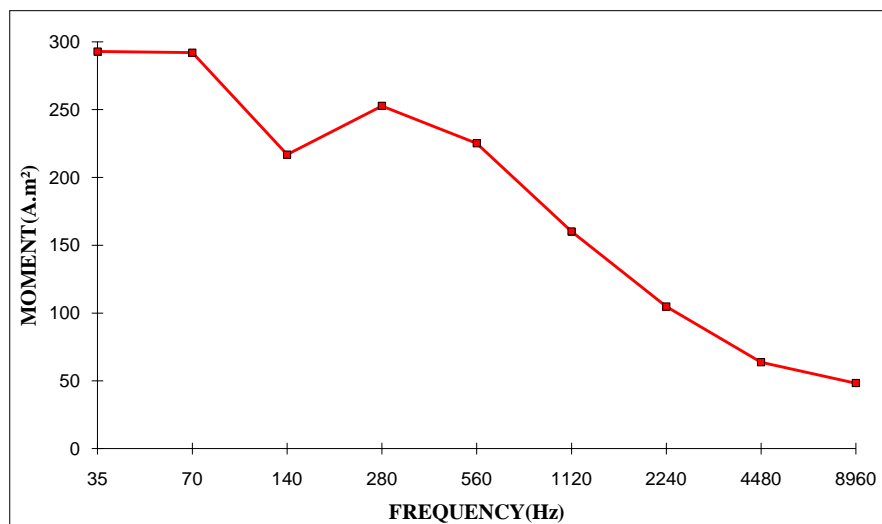


Fig. 2.3-49: Magnetic moments given by the final prototype transmitter probe on a 500 m cable.

2.5.5.4.2. Receiver probe

The main challenge of the receiver design was to obtain adequate sensitivities and acceptable noise levels for the EM sensors in the small internal diameter of the probe (36 mm).

The specifications which have been reached are an axial sensitivity of about 30 mV/nT and a radial sensitivity of about 50 mV/nT (Fig. 2.3-50).

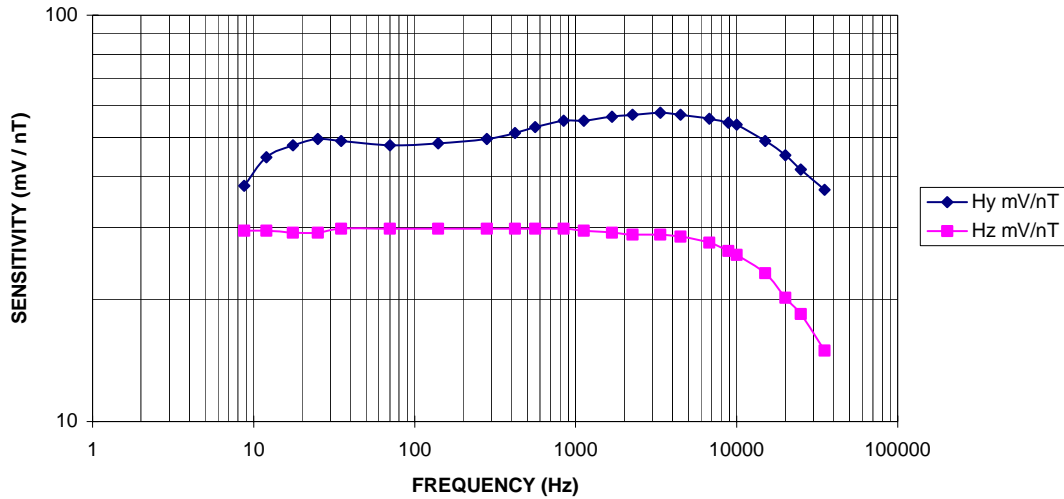


Fig. 2.3-50: Rx probe sensor coil sensitivity

In controlled source EM methods, sensors should be devised in such a way that their internal noise is (slightly) lower than the natural magnetotelluric noise. Fig. 2.3-51 shows that this condition is well achieved on the actual spectrum of the system (35 - 9000 Hz). We note on this figure that the transverse sensors are more noisy than the axial sensor. Cross talk is less than 60 dB (0.1%).

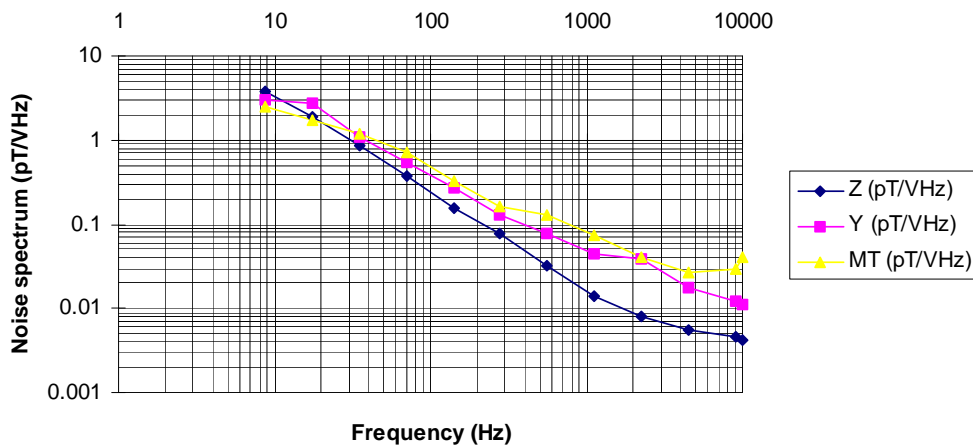


Fig. 2.3-51: Internal-noise spectral density for the axial and transverse sensors of the prototype receiver probe (IRIS data), compared to typical MT spectrum in low-activity periods (CNRS data).

2.5.6. Software development

Three PC software have been developed at BRGM for processing and interpreting the data. These software are research prototypes written in Fortran or Basic, and working in a DOS Window.

A fourth software (BORISLOG) was developed by IRIS for driving the SlimBoris equipment from a notebook PC. Developed in Visual Basics / Windows, it has a more professional look.

The input and output files for all these software are ASCII files with a comma as delimiter. The data are preceded by a heading line containing the label and unit of each data column. A few comment lines can be added, generally after the data. The only exception is the raw data file output by BORISLOG, which has the comment lines at the top of the file.

These software are described in the order of their utilization, i.e. a) BORISLOG, b) BOREM, c) REDSTRAT and d) OPTEM.

2.5.6.0. Acquisition software (BORISLOG)

The BORISLOG acquisition software pilots the SlimBoris equipment from a portable PC. It proposes real-time graphic visualization of the log being recorded. This feature enables in certain cases to use a loose sampling interval at the descent (e.g. 40 m) and to reduce this interval during the climb (e.g. 10 m or less) in order to confirm and better define sudden variations observed on certain components.

The measurement process consists in discrete measurements at several depths along the borehole, and at several frequencies. If six frequencies are used (e.g. 70, 280, 560, 1120, 2240, 4480, 8960 Hz), an average of 10 minutes is needed for a complete measurement at each depth (including the time of displacement between two depths).

The format of data used does not oblige the depth x frequency grid to be regular. For example, intermediate depths can be recorded for certain particular frequencies, without recording the entire frequency cycle at these depths. Similarly, a frequency can be repeated at a given depth without the obligation of repeating the whole frequency cycle at this depth.

2.5.6.1. Processing software (BOREM)

Borem is a PC software for processing the data recorded by the SlimBoris equipment. Note that this software covers all the three configurations proposed by the SlimBoris system (surface-to-hole, cross-hole or single-hole), as well as older surface-to-hole formats produced by the ARLETT and BORIS systems.

The basic processing tools proposed by Borem are a) borehole trajectory (for transmitter and receiver boreholes), b) projection of the measured components onto a fixed coordinate system ('derotation'), and c) primary field reduction, either in free-space, in homogeneous

conductive space or by the low-frequency field. The projection system can be either the current geographic system (e.g. North, East, Down) or the standard reference system used in gimbal-mounted probes.

The first function of the software is to project the measured field components onto a fixed coordinate system and to compute the borehole trajectory

The gravity and magnetic components given by the orientation module enable projecting the measured EM components onto either a fixed reference system, such as North, East, Down, or onto the standard reference system used in gimbal-mounted probes —without the drawback of these probes of not being usable in vertical boreholes.

The orientation module also enables to retrieve the borehole trajectory. The successive attitudes of the probe are integrated along the depth to recover the X, Y, Z coordinates of each measuring station, necessary for further EM reduction in cross-hole and surface-to-hole. The procedure has been validated even in environments presenting short wavelength magnetic anomalies producing local rotations of the magnetic North (Bourgeois *et al.*, 1999).

Primary field reduction is then performed using the trajectory information and the position of the loop or dipole transmitter. Primary field is calculated either in free space, in full conductive space, or by the field measured at a low frequency.

2.5.6.2. *Reduction software (REDSTRAT)*

REDSTRAT is a PC software to calculate the primary field created in a layered (1-D) half-space by an arbitrarily oriented magnetic dipole in the ground, or by a large horizontal loop at the surface.

Additionally, when the input file contains a measured (total) magnetic field, i.e. six columns describing the 3-D complex magnetic vector, the software performs the reduction of the measured field by the calculated transmitter's primary field (i.e. subtracts the latter to the former), so as to retain only the secondary field, or target response.

This tool is particularly useful in the cross-borehole and surface-to-borehole configurations where the primary field shows rapid variations along the borehole.

2.5.6.3. *Inversion software (OPTTEM) and methodology*

Both the classical surface-to-borehole configuration and the new cross-borehole and single-borehole configurations need simple and rapid inversion procedures to face the complexity and multi-dimensionality of the EM responses (3-component complex vector field observed in a 3-D measuring profile).

Exact 3-D models (by integral equations or finite-elements) are not practical in the field due to their demand in computer capacity and time, which definitely forbids their use in iterative inversion processes needing tens of iterations. By contrast, very simplified forward models such as EM dipoles or current filaments (argued in next section) are well suited to inversion because their calculation takes only a fraction of a second on a 486 PC.

These models however give with good accuracy the 3-D location and attitude of a target, as well as an estimate of its size.

Based on such simple models, an inversion software (Optem) using Marquardt-Levenberg algorithm (non-linear least-square fitting) has been developed at BRGM for rapid interpretation of 3-component borehole EM data in any configuration. Thanks to the speed of the forward calculation, the whole inversion process takes only a few seconds.

Note that current filaments have already been used for the inversion of surface-to-borehole (or surface-to-surface) single-component EM data in time domain (Boyd and Wiles, 1984; Barnett, 1984; Fullagar, 1987). In spite of good results (Taylor, 1985), the interest of such models was limited due to the absence of transverse components in the systems used at this time (the XY position of the target and its attitude were not accessible). These problems are overcome nowadays with the advent of fully oriented 3-component EM probes, such as the SlimBoris receiver probe.

Furthermore, contrary to a widespread belief, these models are theoretically more suited to frequency-domain than to time-domain EM methods. Effectively, in frequency domain, the measurement actually gives the magnetic field H , whereas only its time-derivative dH/dt is accessed in time-domain (with standard sensors). Time-domain filament-software thus equate dH/dt to H , but this can lead to substantial errors when several targets, with different time constants, are present¹⁹. The same errors are induced when a single parallelepiped target is observed on different faces having different sizes and thus different time-constants —which is the case for example with our reference model in a dipping borehole passing below the target, like in Sec. 2.5.4.2.5.

2.5.6.3.1. Dipole and filament models

We have seen that the response of a finite-size conductive target to the primary excitation of a transmitter located in a borehole (or at the surface) can be decomposed into inductive and galvanic responses.

The inductive effect is characterized by electrical currents circulating in closed loops within the conductor (eddy or vortex currents). Outside the body, the magnetic field created by these currents is equivalent to the field of a closed current filament. At a certain distance, this field is itself equivalent to the field of a magnetic dipole.

By contrast, the galvanic effect is characterized by currents flowing in open paths between two extremities of the body. Outside the body, the magnetic field created by these currents is equivalent to the field of an opened current filament (segment of current) having approximately the extension of the target along the primary current density, and with an intensity equal to the additional current flow across the target. At a certain distance, this field is itself equivalent to the field of an electrical dipole.

¹⁹ H and dH/dt are proportional over a portion of the space, e.g. a borehole, only if all the responses received in this borehole have the same time constant.

In the general case of combined inductive and galvanic effects, an off-hole target is thus equivalent to a pair of closed and opened current filaments. At greater distance, it is equivalent to a pair of magnetic and electrical dipoles.

The Optem software utilizes such simple schematizations as forward models.

In the terminology of inverse problems, this approach is termed 'inverse sources' problem (Perruson *et al.*, 1999). This approach is very rapid because the equivalent 'sources' are only conceptual objects, of which only geometrical features are sought. It can be said that they are 'passive' because their coupling with the transmitter is not even considered in the inversion. This gives of course great rapidity, but also great robustness (see next section) because the inverted parameters are few.

The major drawback of this approach is the fact that the Tx must be at a constant position for all the inverted dataset, which forbids their application to moving transmitter methods, such as borehole Slingram. Moreover, this approach can only consider one frequency at a time, and thus cannot bring any electrical parameter of the target.

By opposition, the 'inverse scattering problem' consists in directly seeking a more or less realistic 'reactive' object (e.g. sphere, plate, R-L filament), for which the coupling with the transmitter is considered, and whose electrical parameters are sought, in addition to the geometrical ones. In this approach, multi-frequency and moving transmitter data can be inverted, at the expense of a much reduced robustness and an increased computation time.

2.5.6.3.2. Validation of the dipole and filament models in cross-borehole configuration

The validity of these simple models in the cross-borehole configuration has been studied on synthetic data generated by 'exact' 3-D modelling software. The secondary fields calculated in certain boreholes for the methodology study (see Sec. 2.5.3) have been inverted with Optem, using several conceptual models.

Of particular interest are the two canonical situations discussed in Sec. 2.5.3.2, i.e. the purely vortex and the purely galvanic situations. These are presented in Figures 2.3-37 and 2.3-38.

The results are very satisfying: the 3-D attitude of the target is always very well retrieved and its 3-D location (i.e. location of its gravity center) is as accurate as a few percents of the target-to-borehole distance.

The dipolar models are very robust, i.e. they converge to the target center and attitude whatever the initial guess of the inversion. The filament models are much less robust. When the initial guess is too far from the solution, the algorithm diverges to an inconsistent solution (e.g. an infinite rectangular filament with very small intensity), or keeps the initial guess unchanged.

Consequently, the dipolar models should be employed first, in order to get, at the first inversion run, an estimate of the target center and attitude. The filaments model have to be employed in second, using previous dipolar estimate as initial guess.

Filament models also give an estimation of the target size. This parameter is not so well retrieved as the location and attitude of the target. The positive aspect is that the size is always underestimated, which is better than the opposite, because it cannot result in missing the target again, if the inversion is used for siting a new borehole.

For the purely vortex situation (Fig. 2.3-38) however, the extension of the target parallel to the borehole (i.e. its height in our case) is rather well retrieved. For the along-strike dimension, we have observed that a very bad estimation is obtained if the borehole is completely vertical, as here; if the borehole is slightly inclined in the strike direction, a much better estimate of this parameter is obtained.

The case of combined effects (e.g. case 3 in Fig. 2.3-3) has been addressed with models consisting of a pair of centred dipoles (one magnetic plus one electric dipole) or filaments (one closed plus one opened filament) at the same location. Poor results have been obtained because their orientations respective to one another have been left unconstrained in the inversion. A very good fit was always obtained, but with a meaningless inverse solution made of the two parallel dipoles of very strong moment compensating one another. It is inferred from Perruson *et al.* (1999) that the magnetic and electric dipoles should be constrained to stay perpendicular.

2.5.6.3.3. Extension to the single-borehole configuration

Based on similar concepts, an R-L filament model has been recently implemented for inverting single-borehole data (inverse scattering problem) —but for the sole vortex part of the response. The tests on synthetic data are promising, but the initial guess must be very close to the solution (less than 10 m offset) to converge. By lack of time, a dipolar model of this type has not yet been implemented, but we are confident that it will be more robust, and that it will be very useful as the initial step of the inversion.

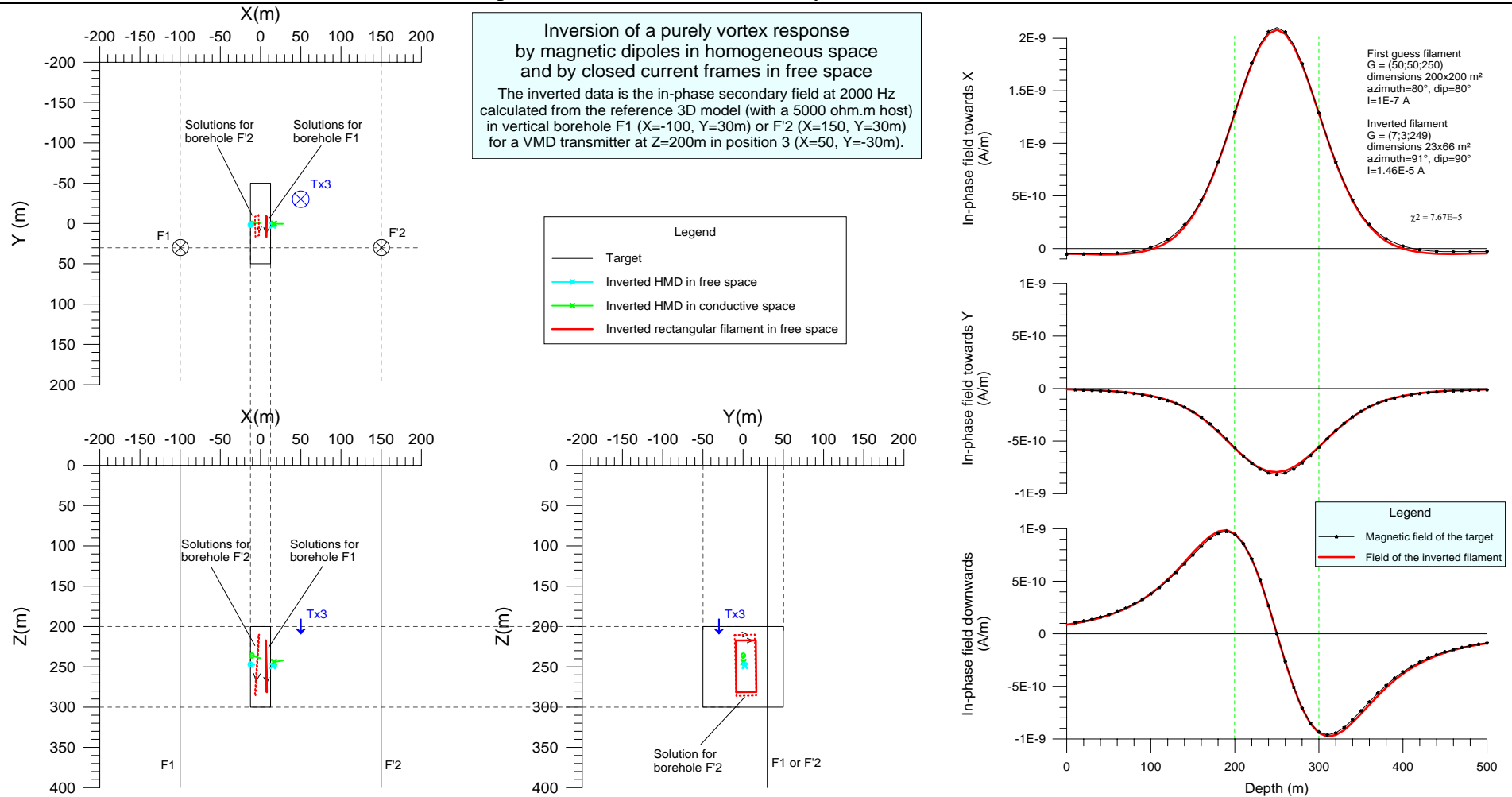


Fig. 2.3-52: Inversion of a purely vortex response (in cross-borehole configuration) by models of magnetic dipoles in infinite conductive space and closed current filaments (rectangular frames) in free-space. As explained in Sec. 2.5.3.2, the purely vortex response is obtained by putting the reference target (here at 5 Ω.m) within a resistive host (5000 Ω.m). **Left:** 3-D location of the best-fit models compared to the target, with indication of the transmitter dipole and of the receiver boreholes. **Right:** Graphic control of the best fit obtained with a rectangular filament.

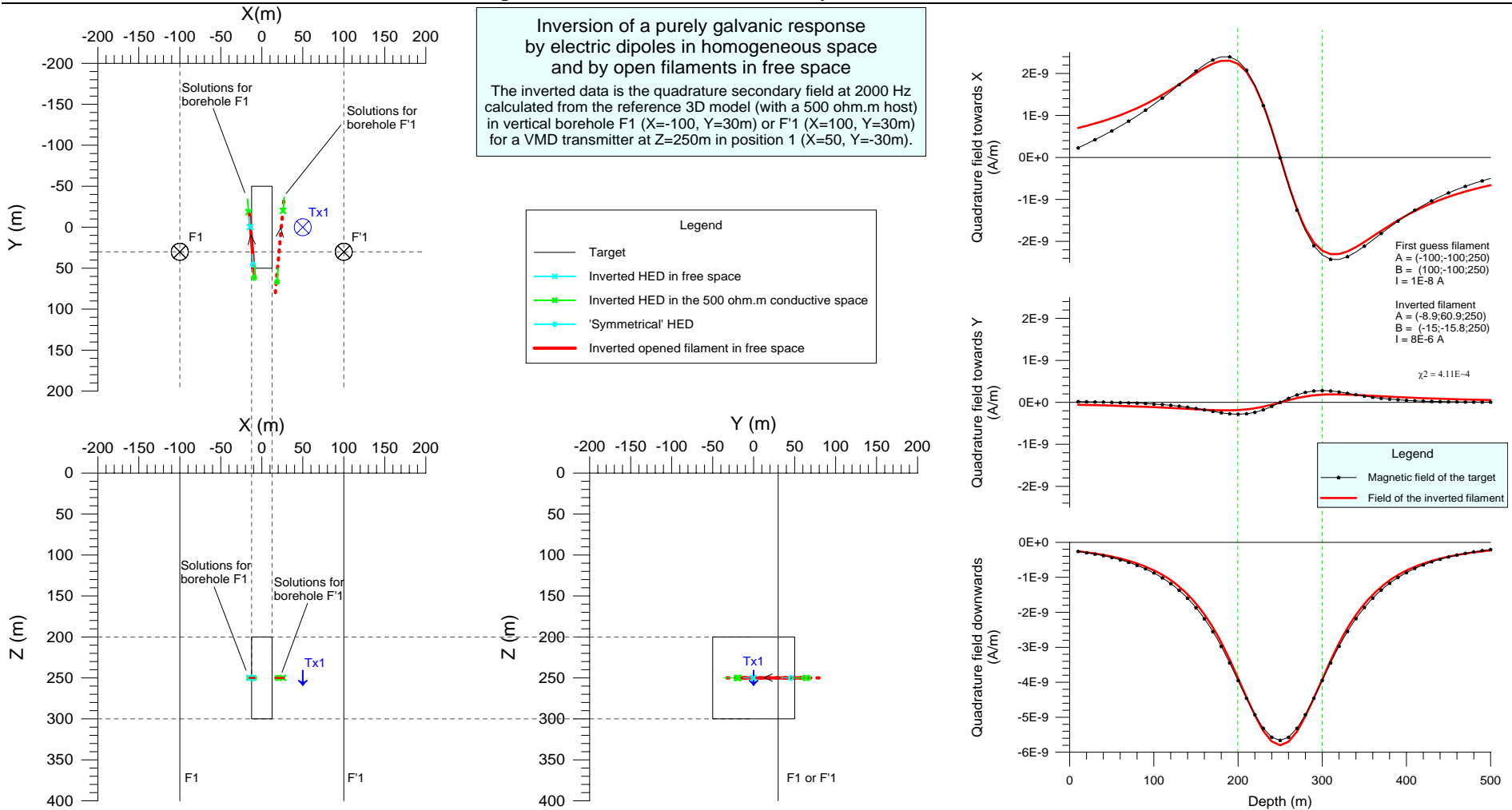


Fig. 2.3-53: Inversion of a purely galvanic response (in cross-borehole configuration) by models of electric dipoles in infinite conductive space and open filaments (segments of current) in free-space. As explained in Sec. 2.5.3.2, the purely galvanic response is obtained by putting the reference target (here at 5 Ω .m) within a conductive host (500 Ω.m). **Left:** 3-D location of the best-fit models compared to the target, with indication of the transmitter dipole and of the receiver boreholes. **Right:** Graphic control of the best fit obtained with an electric bipole (open segment of current).

2.5.7. Field tests at the Jakonmutka site

Field tests with the SlimBoris prototype took place in Finland on three exploration sites of Outokumpu. These tests are described in detail in the final BRGM report. We only present here the test performed on the Jakonmutka site, near Nivala, central Finland. This site can be considered as a true calibrating bench because a conductive target is known (or at least strongly suspected) from other geophysical data.

The Jakonmutka serpentinite intrusion is located in the Nivala area where Outokumpu Mining Oy is currently running the Hitura nickel mine. It was discovered in 1991, based on the interpretation of airborne and ground magnetic data. Outokumpu Mining Oy commenced a drilling program in 1992, which ended up with a small nickel mineralization close to the surface. Downhole geophysics in deeper holes discovered an interesting off-hole anomaly adjacent to the NW contact of the intrusion.

Due to higher priorities in other exploration targets, these deeper anomalies at Jakonmutka were not further drill tested. When the GeoNickel project needed relevant targets for testing the downhole frequency EM (FEM) prototype for nickel exploration, the Jakonmutka intrusion was brought out as one of the test sites because of the existing drilling information and the anomalous downhole data obtained by TEM.

2.5.7.1. Geological setting and previous Geophysics

The Jakonmutka serpentinite body is embedded in intensively migmatized metasedimentary environment which usually contains interlayered graphitic- and sulphide-bearing gneiss and amphibolite (Fig. 2.3-54). The major part of the intrusion is overlain by the glacial overburden and mica gneiss cap. Only minor part is exposed under the till cover. The size has been estimated at 500x350 m in plan view and is open at depth. The nickel mineralization (2.2 m, 0.65% Ni) intersected in borehole JM2 is very small in size and seems to be restricted to the upper part of the serpentinite intrusion.

Various geophysical methods were applied at Jakonmutka during the exploration, in particular 3-component downhole transient electromagnetics (DHTEM) used to discover off-hole mineralization. DHTEM was carried out with the Protem 3-component instrument (BH43-3D Rx) of Geonics. The rectangular transmitter loop (500x700 m) was positioned to the southern side of the intrusion (Fig. 2.3-54). It resulted in schoolbook anomalies both in hole JM9 and JM15 at the depth of 300m and 285 m respectively.

Based on filament inversion performed on these anomalies, it appears that the center of the current pattern is located to the west from the hole JM9 and in the very vicinity of JM15. The origin for these anomalies is not known. It could be either Nickel mineralization or a very conductive part of the serpentinite inclusion. According to the in-situ resistivity logging of hole JM17, the serpentinite resistivity is as low as 4 Ω .m in the contact area. Nevertheless, the main DHTEM anomaly at JM17 is found below the contact, not exactly in the intersected low resistivity spot.

According to decay analysis, the value of the time constant for the anomaly at JM15 (285 m depth) is of the order of 0.45 ms. The conductance value for the body which equals in size with the model resulted by filament inversion is 36 S correspondingly.

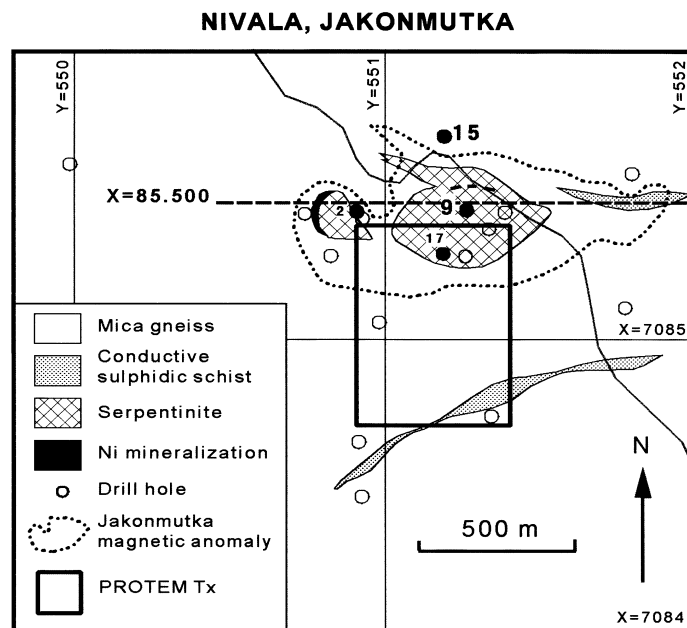


Fig. 2.3-54: Location map and geological setting at the Jakonmutka test site.

2.5.7.2. Surface-to-borehole measurements with the SlimBoris prototype

The tests with the SlimBoris prototype started with surface-to-hole measurements. This is explained because this configuration was the best known, and it was thus easy to assess the good functioning of the system. Moreover, a comparative test with previous equipment was possible only in this configuration. In addition, it was very interesting to have a comparison between the FEM data given by this system and the TEM data held by Outokumpu.

The surface-to-hole data were recorded in borehole JM15, for which TEM data were available. The 250×450 m Tx loop was located North of the intrusion (Fig. 2.3-56-right). The phase of the magnetic field measured with SlimBoris is shown in Fig. 2.3-55. A strong anomalous response is clearly visible over the regular phase decrease of the primary-field. The anomaly is well defined between 230 and 350 m, in good agreement with the TEM data (not shown), despite the very different transmitting loops used in the two experiments. Note that the overall resistivity of the country-rock has been estimated to about 1000 ohm.m considering the phase decay along the borehole, which is consistent with the geology.

The measured field at each frequency was subsequently reduced by the low-frequency data measured at 140 Hz. This process is often more efficient than reduction by the calculated primary field. Note that the quadrature components were reduced using the following formula: $H_r(f) = [f_0 \times H(f) - f \times H(f_0)] / (f_0 - f)$, which assumes low induction in the host and intermediate or high induction in the target(s). Further conditioning of the data consists in removing the “regional” trends remaining on the reduced curves, so that the final data tend to zero on both side of the anomalies.

The final in-phase curves obtained in this way at frequency 1120 Hz are presented on Figure 2.3-56-left, labelled with ‘6’. Note that this frequency has been selected because it

gives the best quadrature response, being probably close to the resonance frequency of the detected target. On this plot, the horizontal components show a maximum at 285 m coinciding exactly with the anomaly found by TEM measurements.

These data have been inverted by equivalent dipoles and filaments (Fig. 2.3-55-left). Closed rectangular filaments and magnetic dipoles were used to represent a vortex effect, whereas open segments of current and electric dipoles were used to represent a possible galvanic effect. Here, despite a resistive country-rock, a galvanic effect could be produced by currents induced in the serpentinite body, then channelled into a more conductive zone in electrical contact with the main serpentinite body. Such a zone could be either a more conductive part of the serpentinite or ore ?.

All the inversions place the model between the two barren drill holes JM9 and JM15 without any constraint. For the in-phase components, the best fit is obtained with a closed rectangular filament (0.05 % RMS). On the contrary, when inverting the quadrature field (not shown), it was impossible to find a relevant closed filament. A very good fit (0.016 % RMS) could only be obtained with a galvanic (electric) dipole. This feature is strong diagnostic of a dominant galvanic effect for the quadrature field. As a matter of fact, it is known from the methodology study (see Sec. 2.5.3.2) that, when vortex and galvanic responses are combined, the galvanic-to-vortex ratio is always more important in quadrature than in phase.

The locations of the inverted filaments and dipoles are consistent with the upper eastern part of the circular filaments found with TEM data. If we assume that the size of the target given by the different inversions (about 100 m) is correct, and that 1120 Hz is effectively the resonance frequency of the target, then we can derive a resistivity of about 4 ohm.m for the target, which could well correspond in this respect to a more conductive zone of the serpentinite. There is thus a doubt about the nature of the detected conductor.

The very good results of this test bring multiple conclusions:

- a) The very good agreement between downhole FEM and TEM, despite different Tx loops, is very important to us because, to our knowledge, no other comparison of surface-to-hole FEM with respect to TEM was previously done. TEM is often preferred to FEM advocating the presence of the primary field superimposed on the target responses. In practice, extraction of the FEM primary field is not more difficult than removing overburden or host effects in TEM methods, and once this extraction is performed, it is demonstrated by this example that the two methods give equivalent information.
- b) Still more important for the GeoNickel project is the demonstration of the capabilities of the SlimBoris system and of the inversion procedures developed in the project.

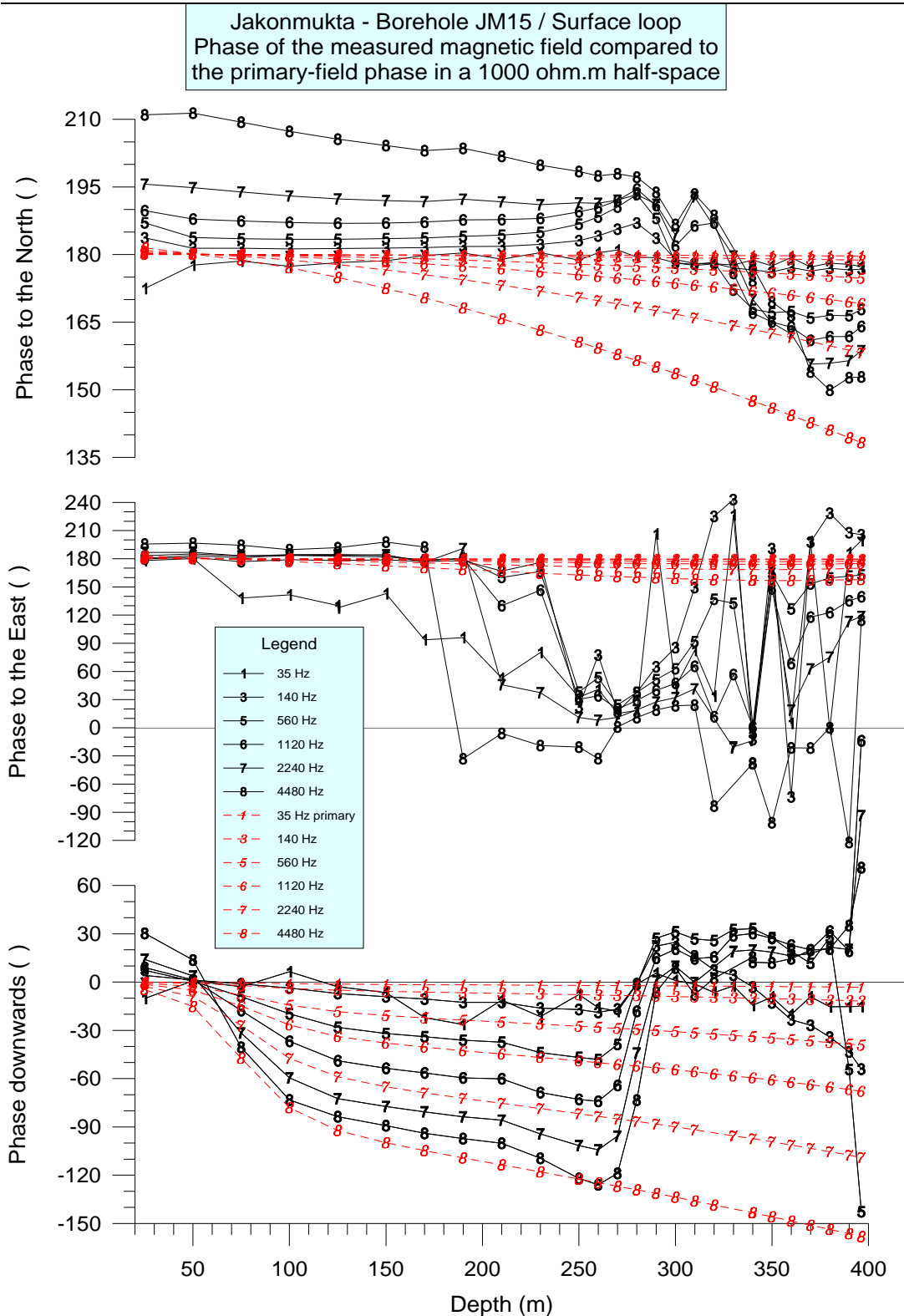


Fig. 2.3-55: Surface-to-hole configuration. 3-component phase log of the (total) magnetic field measured at different frequencies in borehole JM15, compared to the primary-field phases calculated for the Tx loop in a 1000 Ω.m conductive host. At the highest frequencies, the host effect is significant. The anomalous response is clearly visible over the primary field between 230 and 350 m.

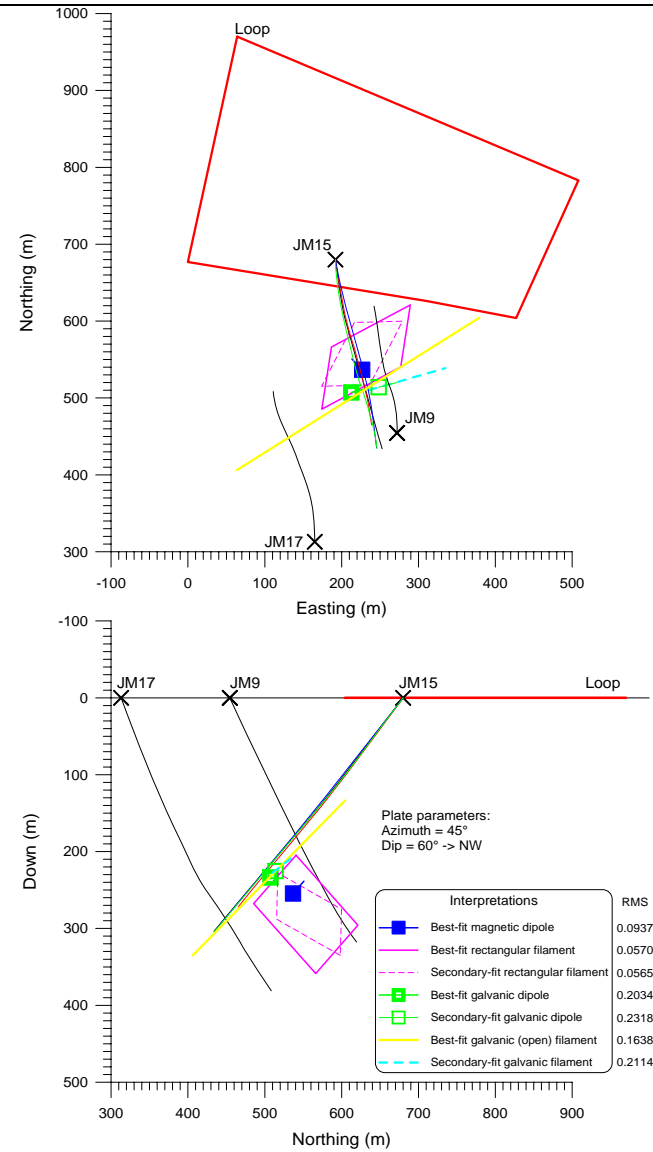
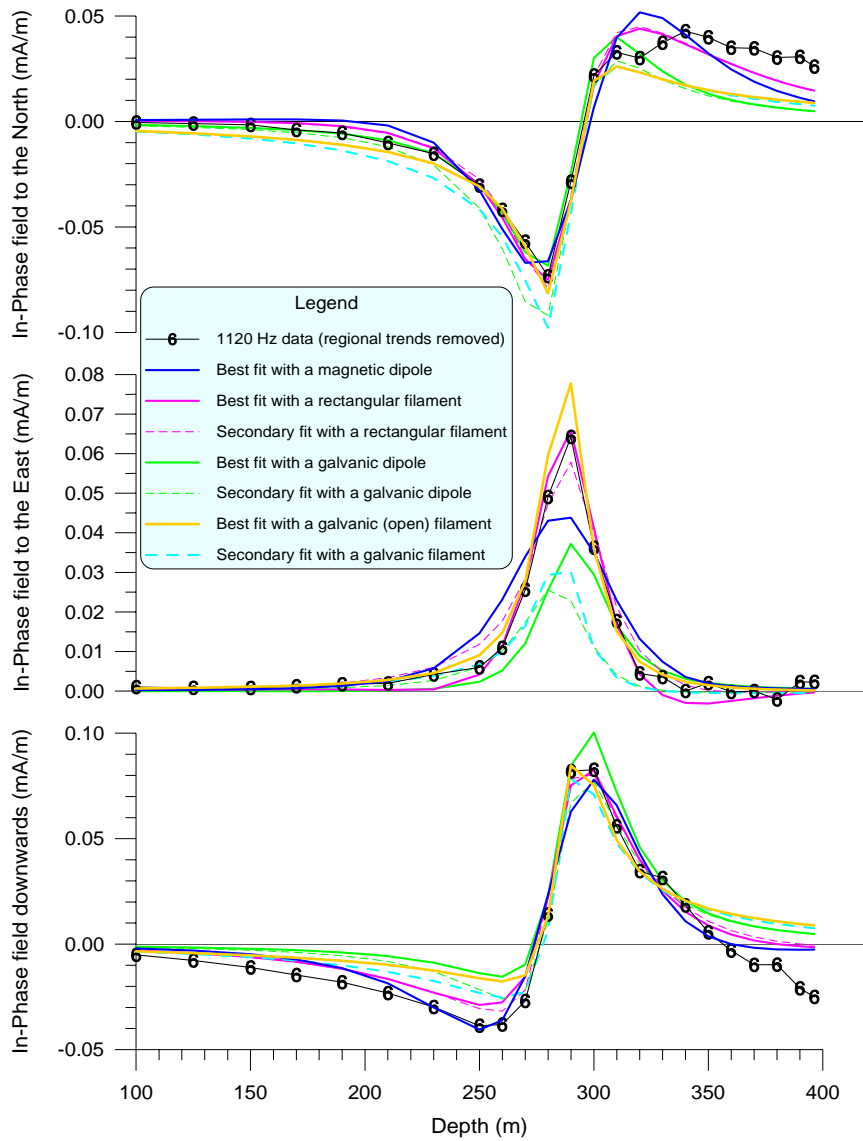


Fig. 2.3-56 Left: Fits obtained by equivalent dipoles and filaments for the In-phase field at 1120 Hz. **Right:** Location of the corresponding best-fit models.

2.5.7.3. Single-hole measurements with the SlimBoris prototype

The single-borehole data which are presented here were recorded during the second field test, i.e. after IRIS fixed the problems found in this configuration. Unfortunately, at this moment, the previous borehole JM15 revealed to be blocked at a shallow depth. As a consequence, borehole JM9 was logged instead. The test was performed at the three different spacings and for a large frequency span.

The data are presented in Fig. 2.3-57. The left part of the figure shows the 3-component plot for the 100 m spacing at three frequencies. The right part shows compares the axial component for the three different spacings. Two anomalies are visible. On these anomalies, the different curves show good consistency between different frequencies and between different spacings, indicating that the system works properly. In particular the respective evolutions of the in-phase and quadrature parts at high frequency is in perfect agreement with the schematization in Fig. 2.3-8, with a resonance frequency which can be estimated around 2000 Hz.

The main anomaly is characterized by responses well above 100%. We know from the methodology study that this feature is characteristic of confined 3-D conductors. Being centred at around 150 m, it seems that this anomaly can be related to the upper part of the serpentinite body, intersected in this borehole between 145 and 185 m, at its northern edge. The 3D nature of this body and its relatively high conductivity ($\approx 5 \Omega \cdot \text{m}$) explain that the response is more similar to that of a confined target rather than that of a 1-D layer.

A second interesting anomaly, centred at around 250-260 m, appears more clearly on short spacings (at 100 m spacing, it seems that the axial anomaly has not been closed at depth). This anomaly is related to the lower intersection with the serpentinite body, between 230 and 270 m. The unsymmetrical figure could be diagnostic of an oblique intersection.

The second anomaly is not far in depth from the response observed by surface-to-hole TEM around 300 m in this hole. However, we cannot affirm that it is linked to the same conductor.

If we apply, for the main anomaly, the simple interpretation rules given in Table 2.3-5, we find that the target is NW of borehole JM9, in good agreement with the surface-to-hole interpretation given in Fig. 2.3-56-right.

From this test, it appears that the borehole Slingram equipment has been validated. The responses obtained in borehole JM9 are consistent in magnitude with the modelling results, and consistent in depth with the known geology. The benefit of the modelling study is also demonstrated, considering for example the simple interpretation rules or the question of high response percentages.

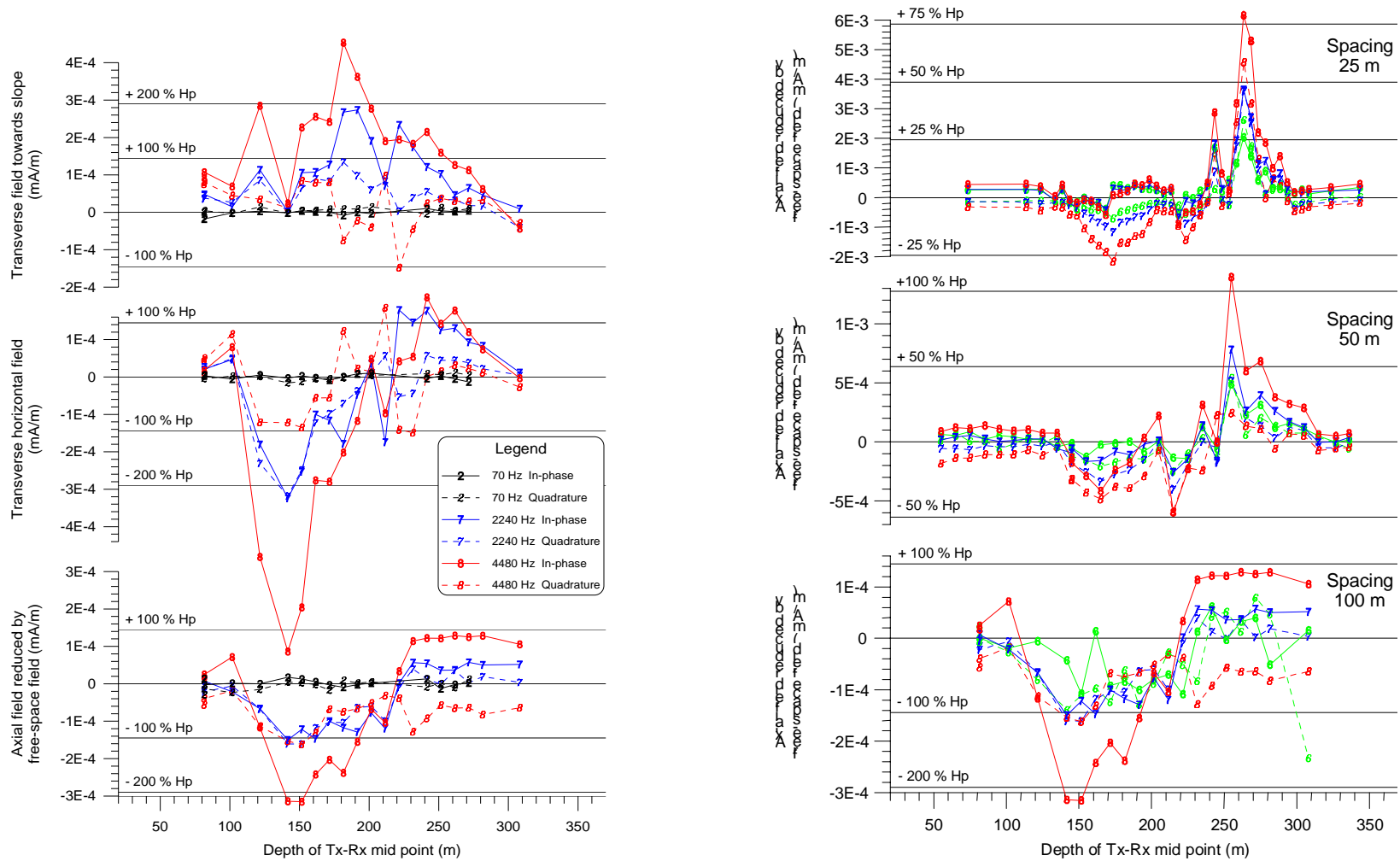


Fig. 2.3-57: In-phase and quadrature components of the borehole Slingram data recorded in borehole JM9, Jakonmutka. H fields are projected onto a gimbal-like right-handed system (transverse towards slope, horizontal, axial downwards). The axial component is reduced by the free-space primary field (H_p). Quadrature convention is standard. **Left:** Three H components for 100 m spacing at 70, 2240 and 4480 Hz. **Right:** Axial H component for three different spacings at 1120, 2240 and 4480 Hz.

2.5.8. Conclusion

A prototype equipment for 3-component downhole EM measurements in frequency-domain has been developed and validated during field tests in Finland. Comparison with an older equipment in surface-to-hole configuration is excellent. Several problems found during the tests have been fixed. The last experiment in single-borehole configuration proves that the system is operational. A further test in April 1999 will take place in Finland to check that the problem found in salty water has effectively disappeared.

The methodology concerning the new cross- and single-borehole methods is comprehensive. Only a few points remain to be studied in the innovative borehole Slingram configuration.

The necessary processing and interpretation software are also operational. The study concerning dipole and filament inversion has shown the interest of such models and the best way to use them successively for quick and reliable localization of targets.

2.5.9. References

Barnett, C., T., 1984, Simple inversion of time-domain electromagnetic data: *Geophysics*, 49, 925-933.

Bourgeois, B., Alayrac, C., and Soininen, H., 1998, Requirements for a 3-component downhole frequency EM system for mineral exploration, 60th EAGE meeting, Leipzig, June 1998.

Bourgeois, B., and Alayrac, C., 1999, The borehole Slingram method in mineral exploration using the SlimBoris system, submitted to the 61st EAGE meeting, Helsinki, June 1999.

Bourgeois, B., Legendre, D., Lambert, M., and Hendrickson, G., 1999, ARLETT: a prototype 3-component borehole EM system, in Oristaglio, M., and Spies, B., Eds., *Three-Dimensional Electromagnetics* (SEG series 'Investigations in Geophysics').

Boyd, G. W., and Wiles, C. J., 1984, The Newmont drill-hole EMP system — Examples from eastern Australia: *Geophysics*, 49, 949-956.

Dyck, A. V., 1991, Drill-hole Electromagnetic Methods, in Nabighian, M. N., Ed., *Electromagnetic methods in applied geophysics*, Vol. II, Part B, 881-930.

Frischknecht, F., C., Labson, V., F., Spies, B., R., and Anderson, W., L., 1991, Profiling methods using small sources, in Nabighian, M. N., Ed., *Electromagnetic Methods in Applied Geophysics*, Vol. II, Part A, 105-252.

Fullagar, P. K., 1987, Inversion of down-hole TEM data using circular current filaments: *Exploration Geophysics*, 18, 341-344.

Lajoie, J., J., and West, G., F., 1976, The electromagnetic response of a conductive inhomogeneity in a layered earth, *Geophysics*, 41, 1133-1156.

Mononen, R., Oksama, M., and Soininen, H., 1998, Modelling of 3-component EM borehole measurements to 3D targets, 60th EAGE meeting, Leipzig, June 1998.

Nabighian, M., N., and Macnae, J. C., 1991, Time Domain Electromagnetic Prospecting Methods, in Nabighian, M. N., Ed., *Electromagnetic Methods in Applied Geophysics*, Vol. II, Part A, 427-520.

Newman, G., A., and Hohmann, G., W., 1988, Transient electromagnetic responses of high contrast prisms in a layered earth, *Geophysics*, 53, 691-706.

Perruson, G., Bourgeois, B., Lesselier, D., Lambert, M. and Duchene, B., 1999, Probing conductive masses in the diffusive regime: equivalent sources and bodies, submitted to the 61st EAGE meeting, Helsinki, June 1999.

Pietila, R., and Bourgeois, B., 1999, Surface-to-hole FEM measurements compared with time-domain EM data in Central Finland, submitted to 61st EAGE meeting, Helsinki, June 1999.

Raiche, A., Sugeng, F. and Xiong, Z., 1998: Final report for AMIRA project P223C full-domain EM modelling. CRC AMET - CSIRO Exploration & Mining, Mathematical Geophysics Group.

Taylor, S., I., 1985, A simple inversion method to aid in the interpretation of borehole TDEM data: M. Sc. Thesis, Queen's Univ.

West, G., F., and Edwards, R., N., 1985, A simple parametric model for the electromagnetic response of an anomalous body in a host medium, *Geophysics*, 50, 2542-2557.

West, G., F., and Macnae, J., C., 1991, Physics of the Electromagnetic Induction Exploration Method, in Nabighian, M. N., Ed., *Electromagnetic Methods in Applied Geophysics*, Vol. II, Part A, 1-70.

2.5.10. Annexes

Reports

BRGM report for task 2.3: Bourgeois, B., 1999, Three components borehole EM methods: Methodology, Instrumentation, Software, and Field Tests. Rapport BRGM R39968, 105p.

Publications / presentations

Bourgeois, B., Alayrac, C., and Soininen, H., 1998, Requirements for a 3-component downhole frequency EM system for mineral exploration, presented to the 60th EAGE conference, Leipzig, June 1998.

Bourgeois, B., and Alayrac, C., 1999, The borehole Slingram method in mineral exploration using the SlimBoris system, submitted to the 61st EAGE conference, Helsinki, June 1999.

Pietila, R., and Bourgeois, B., 1999, Surface-to-hole FEM measurements compared with time-domain EM data in Central Finland, submitted to the 61st EAGE conference, Helsinki, June 1999.

Deliverables

- Prototype system (SlimBoris) for 3-component downhole EM measurements in slim boreholes (probes diameter 42.5 mm), covering the surface-to-hole, cross-hole and single-hole (or borehole Slingram) configurations;
- PC software (BORISLOG) for piloting the equipment
- PC software (BOREM) for processing the data (field rotation, trajectory computation, primary field reduction)
- PC software (REDSTRAT) for layered half-space data reduction
- PC software (OPTTEM) for inverting the data with models of current filaments or other equivalent sources such as magnetic or electric dipoles

2.6. Task 2.4: Compilation of a petrophysical database

2.6.1 Introduction

The main aims of the task were to measure magnetic susceptibility, magnetic remanence, and density of rock samples from nickel deposits in Finland and Norway and build a digital database of the measurements, retrieve an old database, and perform an extensive statistical analysis on the data. All deposits were tested against the database results using basic statistical and Factor Analysis techniques. The measurements also included tests for the anisotropy of magnetic susceptibility.

Results from various petrophysical measurements were entered into Microsoft Excel spreadsheets. Chemical analysis and rock types were also entered for the deposits of Bruvann (Norway), and Laukunkangas, Stormi, Ekojoki, Rausenkulma, Uusiniitty and Posionlahti (Finland). Results from an old petrophysical database that covered the Stormi, Ekojoki, Laukunkangas, Hyvelä, Oravainen and Sahakoski deposits were also incorporated into the spreadsheets (see Plate 2.4-1).

Statistical analysis of the data enables correlations to be made between rock types and geophysical measurements. Integrated geophysical surveys and measurements can enable country rocks, host rocks and ore rocks to be distinguished using statistical tables, histograms, box and whisker plots, and density versus magnetic susceptibility scatterplots as produced in this report.

Factor analysis offers a useful tool to analyse the internal variance of nickel ores. In this report, 5 factors are presented that explain 63.1% of the total variability. By using factor analysis, independent variables were analysed using 3 factors in a 3D- space. This way the behaviour of variables was visualized and a new “densus” variable was developed. This densus variable has a correlation coefficient of 0.8 with nickel content. The densus variable works fairly well in tests where drill-hole measurement data from different deposits were used.

Petrophysical measurements and subsequent statistical analyses were also made to 33 laterite samples from Greece. Based on the analysis, high nickel contents (over 0.5% in weight) are associated with high La, MnO, CaO, CO₂, K₂O, P₂O₅, Zn and SrO contents and have negative correlation with density, magnetic susceptibility and FeO, Cu and Cr₂O₃. The sample population was however small. Further analysis using a greater sample population, preferably from different laterite deposits, is recommended. Furthermore, addition of data on electrical conductivity and induced polarization (IP) to the database which has now been built would increase its value as a useful tool in nickel exploration.

2.6.2. Implementation

The GeoNickel WorkPackage 2.4. was started on behalf of the Helsinki University of Technology on February 1st 1996 by Petri Jääskeläinen who was hired to perform petrophysical measurements (magnetic susceptibility, remanence and density) on drill-core

samples from deposits selected for the GeoNickel WorkPackage 1.1. Retrieving previous petrophysical database was also included in his work program.

The plan also was to retrieve the old database. The “old database” consists of petrophysical and chemical analysis data from 13 deposits. Three deposits from the old database were selected to the GeoNickel - project: Enonkoski, Ekojoki and Stormi. The total number of measurements are: Ekojoki 4745, Enonkoski 10217 and Stormi 10360 lines of data. The actual amount of valid data after filtering was less. Data consisted of magnetic susceptibility, density, resistivity and grounding resistance values, iron, sulphur and nickel contents. Iron and nickel contents have been analysed using bromine-methanol dissolution. Sulphur content has been analysed with S-leco analysis. Analysis results were rather randomly distributed between samples.

The new deposits from which drill-core samples were measured during 1996 were: Stormi, Posionlahti, Ekojoki, Uusiniitty, Rausenkulma and Enonkoski from Finland, and Brevann/Råna from Norway. The total number of samples was 442 included in the analysis. The samples were mainly split halves of drill-cores with a diameter of 3.2 centimetres. The first set of samples were measured in the Petrophysical Laboratory of the GSF with modern equipment that produces reliable results and has good error control. The weighing accuracy for density is 0.1 grams. The standard error of repeated density determinations was below 5 kg/m³ or about 0.1%. The measuring error is lower than 2% for magnetic susceptibility. The anisotropy of magnetic susceptibility varies in intensity depending on direction. This intensity variation can be up to 20%. The standard error of repeated remanence measurements is about 10 mA/m. However, for inhomogenous, strongly magnetized block samples the remanence estimates can vary more than 10%. All samples were measured for density, magnetic susceptibility and remanence. Nine samples were selected for determination of the anisotropy of magnetic susceptibility.

Chemical analyses and petrophysical measurement results of the GeoNickel samples were integrated into a single database. Chemical analyses have been made with a XRF-analyser. Sulphur content and LOI have been analysed with a S-leco analyser. Rock types and chemical composition have been defined by Pertti Lamberg, Outokumpu Research, Geoanalytical Laboratory.

2.6.3. Main Results

The samples were grouped geologically into five major groups as follows: country rocks, host rocks, sheared rocks, ore and others. Other subgroups were created within these 5 groups. In addition to the basic descriptive statistical parameters the statistics for the selected three deposits contains also histograms, correlation charts and boxplots.

Statistical analysis enables the correlation of the petrophysical properties of rock types and geophysical measurements. The integration of geophysical surveys and petrophysical measurements helps us to distinguish the physical contrasts of the lithology in question. Major tools are statistical tables, histograms, boxplots, and scatterplots (density versus magnetic susceptibility). Similar procedure of statistical analysis was applied also for electrical resistivity and induced polarization data. Plates 2.4-2 and 2.4-3 show the typical scatterplots for magnetic susceptibility, density and conductivity data.

After studying the independent variables, factor analysis was applied to go over the internal variance of nickel ores and to find correlations between multiple independent variables. Independent variables derived from magnetic and density data were analysed by using 3 factors in a 3-dimensional space. The first two factors explained 44.5 % of the total variance of the phenomenon. The first factor was the ore factor which seems to increase all analysed petrophysical parameters. The second factor was norite-plagioclase factor which decreased magnetic susceptibility only. The third factor was acidic country rock factor and it didn't influence on the petrophysics at all. The fourth factor was country rock factor and it didn't influence petrophysics either. The fifth factor was an interesting one. It was named as serpentinized rock factor and it increased magnetic susceptibility and magnetic remanence while decreasing density.

The behaviour of variables was visualized and a new "DENSUS" variable (density multiplied by magnetic susceptibility) was developed (Fig. 2.4-1). This DENSUS variable has a high correlation coefficient of 0.8 with nickel content. The other ore factor elements (S, FeO_{tot}, Cu and Co) have also high correlation coefficients with the DENSUS variable (see Fig. 2.4-1). Based on these results, scatterplots of densus variable versus nickel content were plotted. The nickel deposits of Bruvann, Norway (Fig. 2.4-2) and Laukunkangas, Finland have strong positive correlation between the variables. For the Stormi deposit the correlation is not so clear. The nickel content of subeconomic deposits does not correlate so well with the DENSUS variable.

Both massive and disseminated ore samples are dense and magnetic. Therefore when density is multiplied by magnetic susceptibility, rocks rich in nickel stand out from the high density dunites, peridotites and pyroxenites. Similarly, nickel rich rocks stand out from highly magnetised serpentines, serpentinites and pyroxenites. The DENSUS variable worked fairly well in tests where drill-hole measurement from different non-lateritic deposits were used. Hence, it may provide a useful and powerful tool in Ni exploration, and its further testing is recommended.

Petrophysical measurements and subsequent statistical analyses were also made to 33 laterite samples from Greece. Based on that, high nickel contents (over 0.5% in weight) are associated with high La, MnO, CaO, CO₂, K₂O, P₂O₅, Zn and SrO values and have negative correlation with density, magnetic susceptibility and FeO, Cu and Cr₂O₃. The sample population was however small, and hence, a further analysis using a greater sample population, preferably from several laterite deposits is recommended.

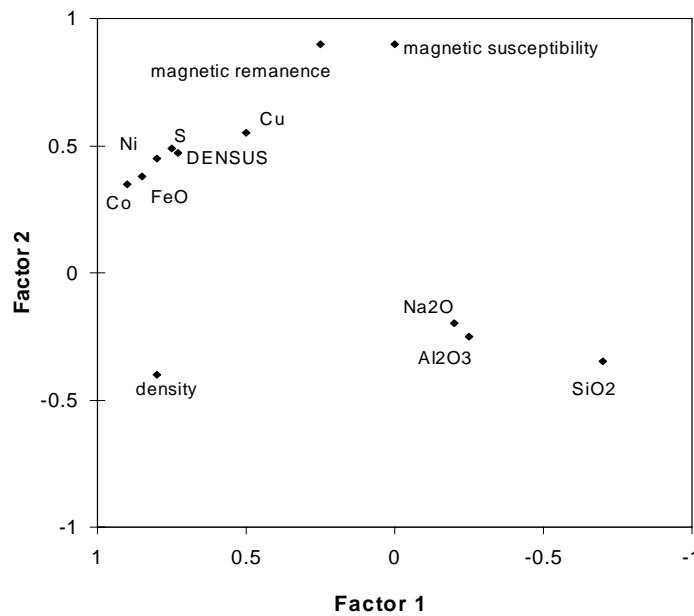


Figure 2.4-1. Rotated factor space with DENSUS variable.

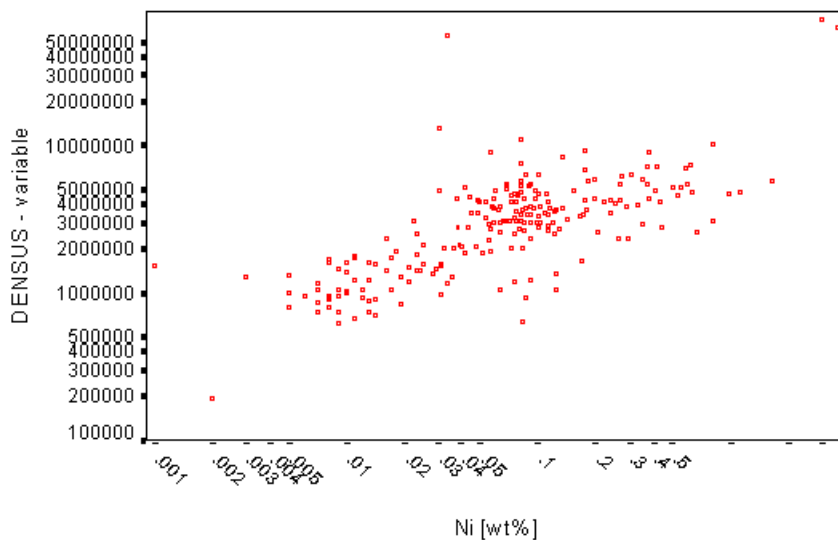


Figure 2.4-2. Scatterplot of DENSUS variable versus nickel, Bruvann, Norway.

Based on the factor analysis of down-hole logging data from the Pulju komatiite, the first factor shows that the elements Co, Ni, Fe, S, Cu and Zn correlate positively with induced polarization response and electrical conductivity. In the second factor, the elements Mg, Mn and Cr show a fair positive, and Al, Cu and Li a negative correlation with magnetic susceptibility. Factor analysis of the disseminated samples from Hitura indicate that a new IPSUSC-variable (IP-effect multiplied by magnetic susceptibility) correlates fairly well with nickel and copper. Density and IP correlate with sulphide content. In discriminating massive

nickel ore and black schists from each other at Laukunkangas, density was found to be the most useful single petrophysical parameter.

The measurements of resistivity and the corresponding data in literature show a wide range of resistivity values for black schists. Resistivity values of massive Ni-ore and black schist are overlapping in the low resistivity range. The laboratory measurement results, when keeping the restrictions of mutual coupling of magnetic susceptibility and conductivity in mind, indicate that indeed the massive sulphidic ores produce the most conductive responses in measurements. However, the resistivity ranges for these groups are so broad that statistically it is very difficult to reliably divide them into groups that would have characteristic resistivities. Because every deposit has its own unique characteristics one should pay special attention in separating responses from these two groups during practical exploration work.

2.6.4 Conclusion

By using factor analysis to the multivariable problem described above it is easy to create new variables and include them in further processing. Preferably several petrophysical parameters should be determined and some samples assayed by XRF in order to create combination of new variables which illustrate the relation between mineralogy and physical parameters. This can enhance practical exploration work by giving new perspective for geophysical interpretations. The procedure discussed here is not only relevant for petrophysical or geophysical applications, but for any measurement data obtained in laboratory or from the field.

2.6.5 References

Jääskeläinen, P., 1996, Petrophysical measurements, database and statistical analysis of Nickel deposits. M.Sc. thesis, Helsinki University of Technology, Espoo, Finland. 133 pp

Niemi, A., 1989, Petrophysical properties of Finnish nickel ores. Vuorimiesyhdistys–Bergsmannaföreningen, Research Report A 88, Outokumpu, Finland (in Finnish, with Abstract in English). 177 pp

Papunen, H. & Vormaa, A., 1985, Nickel deposits in Finland, a review. Geological Survey of Finland, Bulletin Vol. 333, pp 123-143, Espoo, Finland

Puustinen, K., Saltikoff, B. & Tontti, M., 1995, Distribution and metallogenic types of nickel deposits in Finland. Geological Survey of Finland, Report of Investigation Vol. 132, Espoo, Finland. 38 pp

2.6.6 Annexes

Reports

Final report on Task 2.4: Petrophysical database and statistical analysis of Nickel deposits. Petri Jääskeläinen, Outokumpu Mining Oy, 1997, 238 pages.

Thesis

Jääskeläinen, P., 1996, Petrophysical measurements, database and statistical analysis of Nickel deposits. M.Sc. thesis, Helsinki University of Technology, Espoo, Finland. 133 pp

Publications / presentations

P.K. Jääskeläinen, R. Pietilä, A. Hattula and M. Peltoniemi, 1999: Multivariate analysis of petrophysics and lithochemistry of nickel deposits, to be held at EAGE Helsinki'99 conference.

COMPARISON OF INITIALLY PLANNED ACTIVITIES AND WORK ACTUALLY ACCOMPLISHED

Task 2.2.2 Development of interpretation software for ground EM methods

The work were executed according to the original work programme. The development of the user interface for Windows NT/95 has been the most time consuming task. There, testing and the study on the magnetic effects were given less time than planned.

Task 2.2.3-2.2.6

All sub-tasks are conformable to the time chart for both areas . Minor modifications facilitated the project implementation . Equipment necessary for quick IP measurements was purchased for this purpose (Time domain multichannel IP Receiver, IGME and SISCAL R6 LARKO) . Software for seismic processing was bought from KANSAS GEOLOGICAL SURVEY and for IP/Resistivity inversion from NEW JERSEY GEOLOGICAL SURVEY.

Task 2.3

No deviation is observed at the end of the project.

Task 2.4 Compilation of the petrophysical database;

Task 2.4. was executed fairly well according to the initially planned schedule.

ACKNOWLEDGEMENTS

Task 2.2.2

This work was part of the GeoNickel research project funded by the European Union under contract BRP-CT95-0052. The authors wish to thank both European Union and Outokumpu Mining Oy for the backing and financial support.

Task 2.4

This work was part of the GeoNickel research project funded by the European Union under contract BRP-CT95-0052. The authors wish to thank both European Union and Outokumpu Mining Oy for the backing and financial support.

PLATES

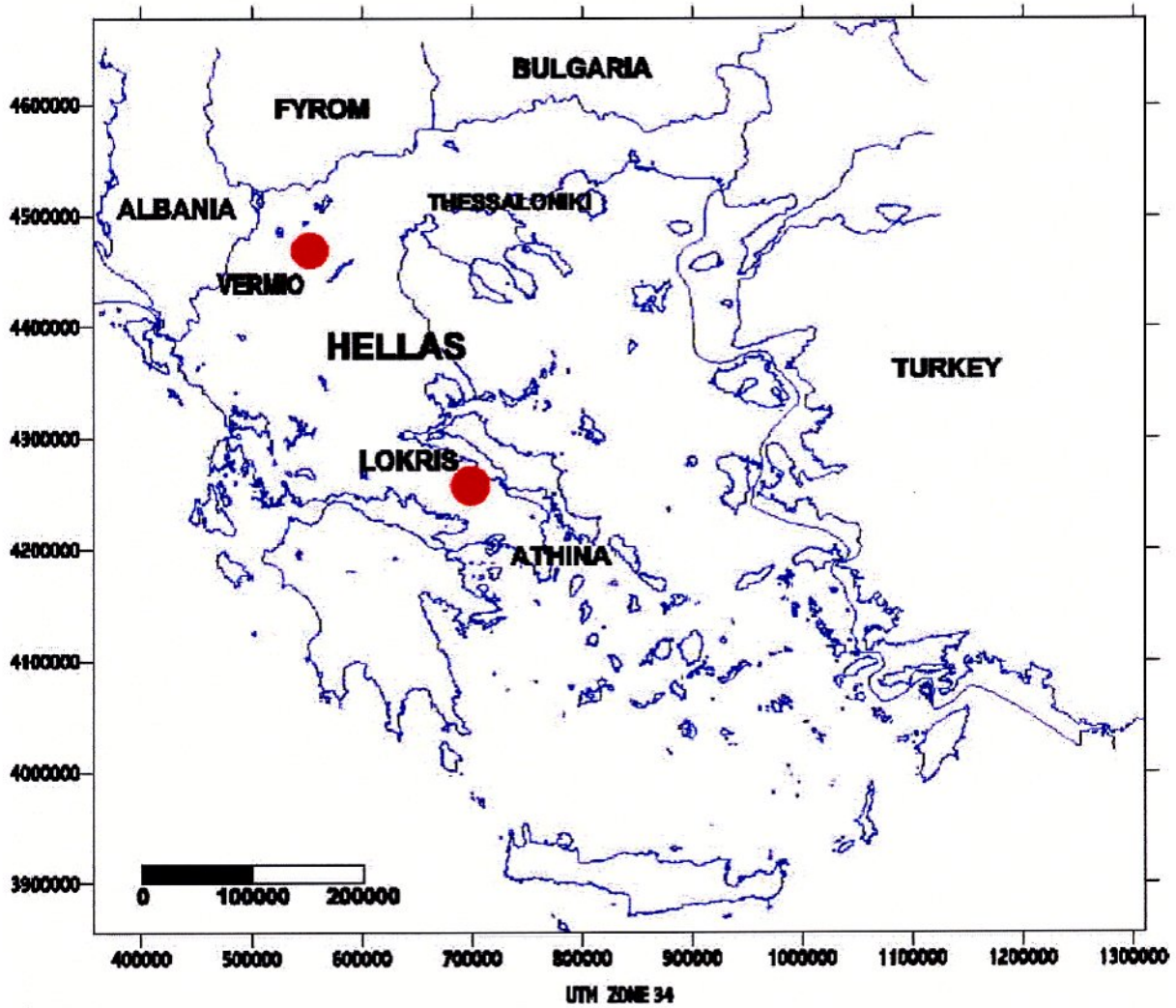


Plate 2.2.3.1 Geonickel WorkPackage 2, Sub tasks 2.2.3- 2.2.6
Location map of the investigated areas in Greece
Referred to WP2.

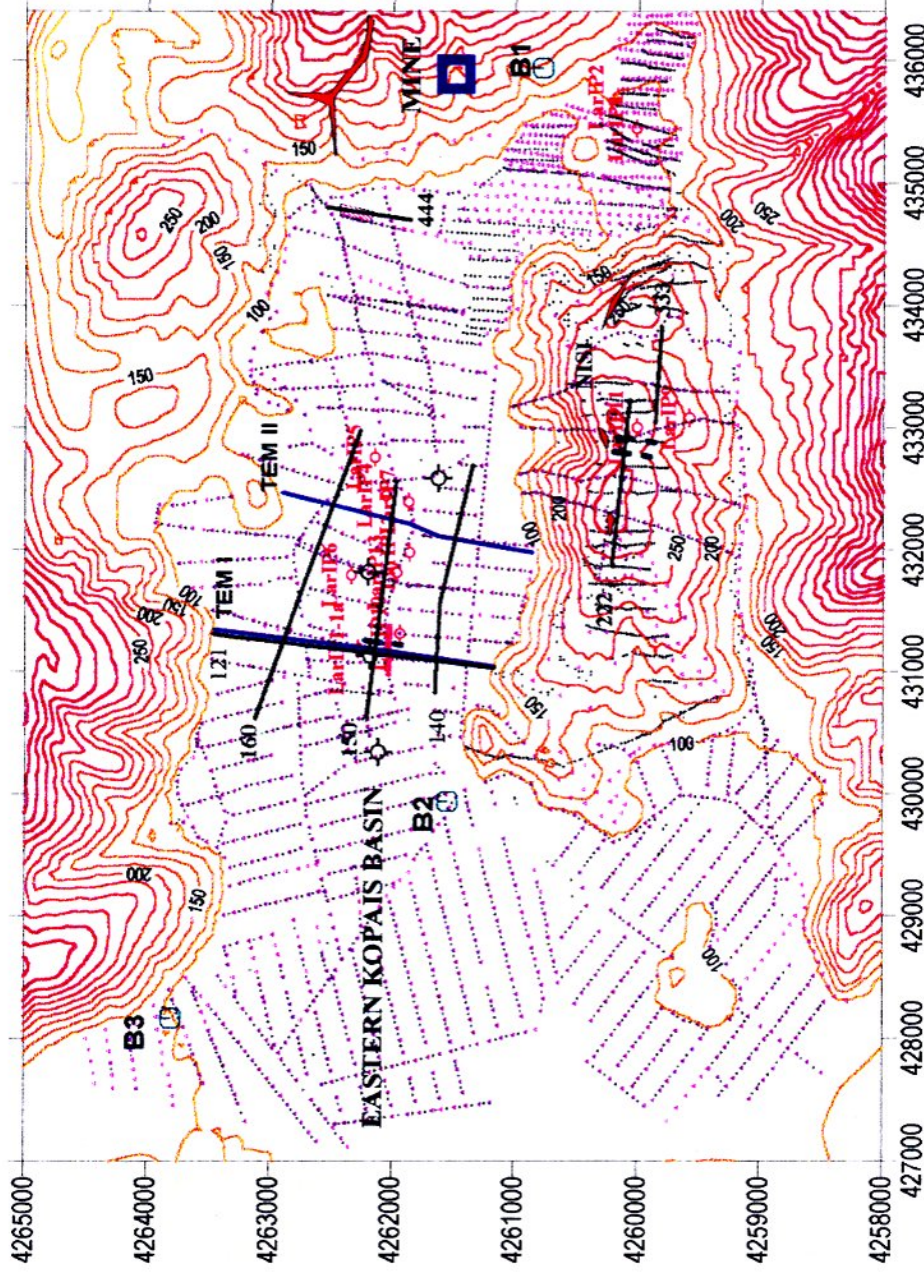


Plate 2.2.3.2 Geonickel Work Package 2, sub tasks 2.2.3-2.2.6
Location map of Ag.Ioannis mine area

- ▲ + Grav-Mag stations
- Grav base stations
- IP pole-dipole lines
- FeNi ore
- Seismic line Makrini
- Area of preliminary tests & seismic lines (T0 ,T2,T4)
- VES IP
- TEST HOLES
- mise alla mase IP

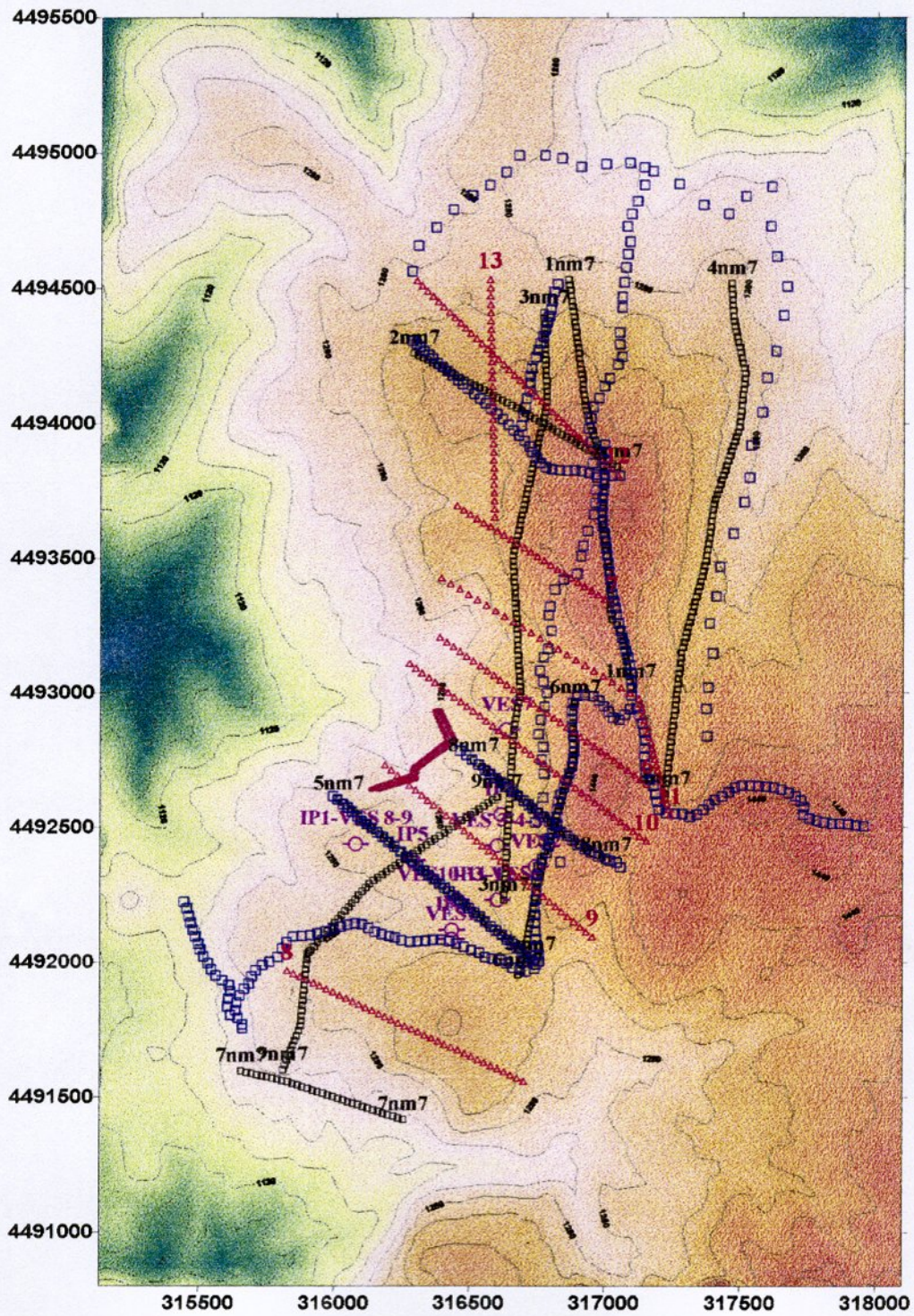


Plate 2.2.3.3 . Geonickel WorkPackage 2, sub tasks 2.2.3- 2.2.6
 Vermion location map with topographic contours.
 IP dipole-dipole (black), Magnetic and SP (red),
 Gravity-Magnetic (blue). VES IP -  .
 FeNi outcrop.

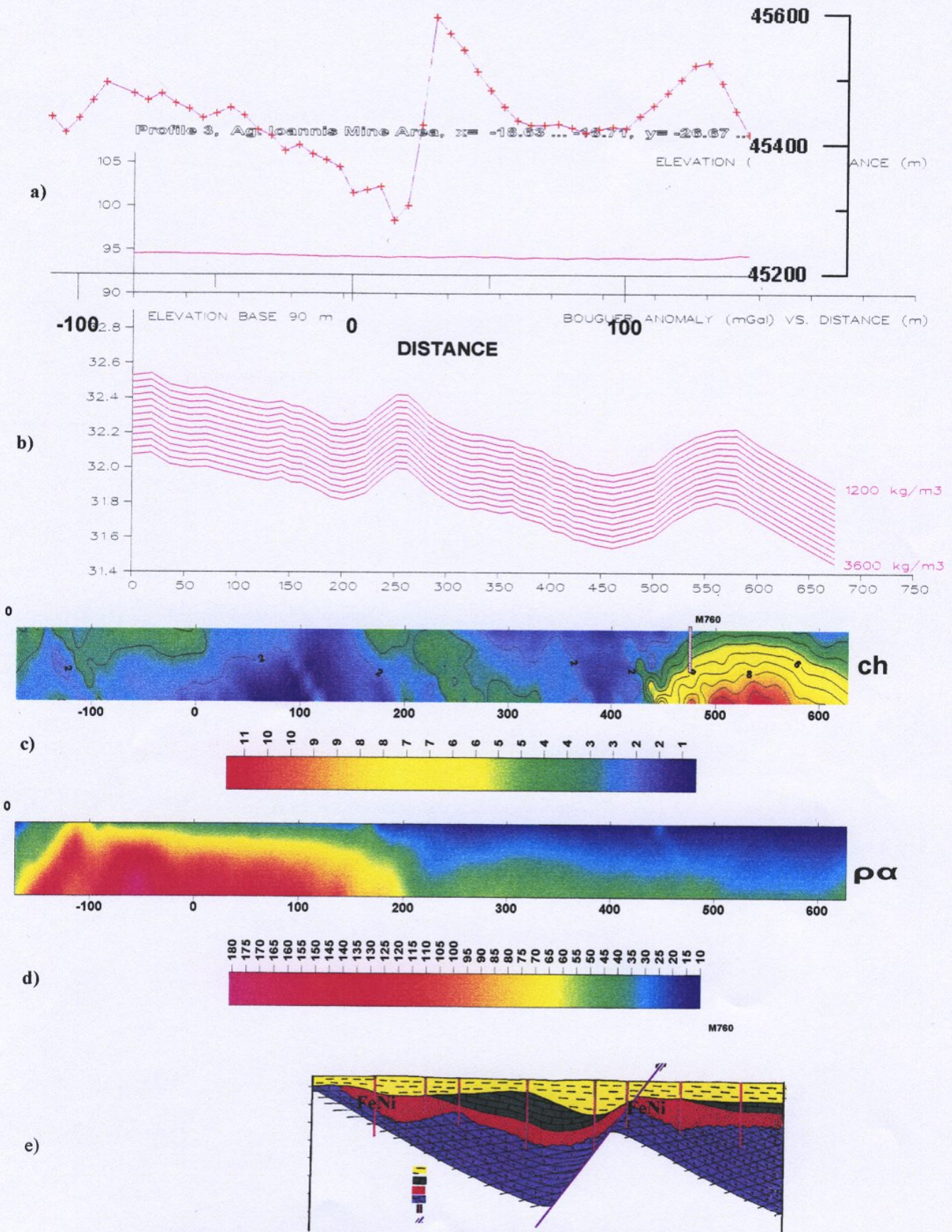


Plate 2.2.3.4 Geonickel WorkPackage 2, Sub tasks 2.2.3- 2.2.6
a) Magnetics, b) Gravity, c) IP CH, d) IP resistivity,
e) T2 Geologic section, Agt Ioannnis mine area.

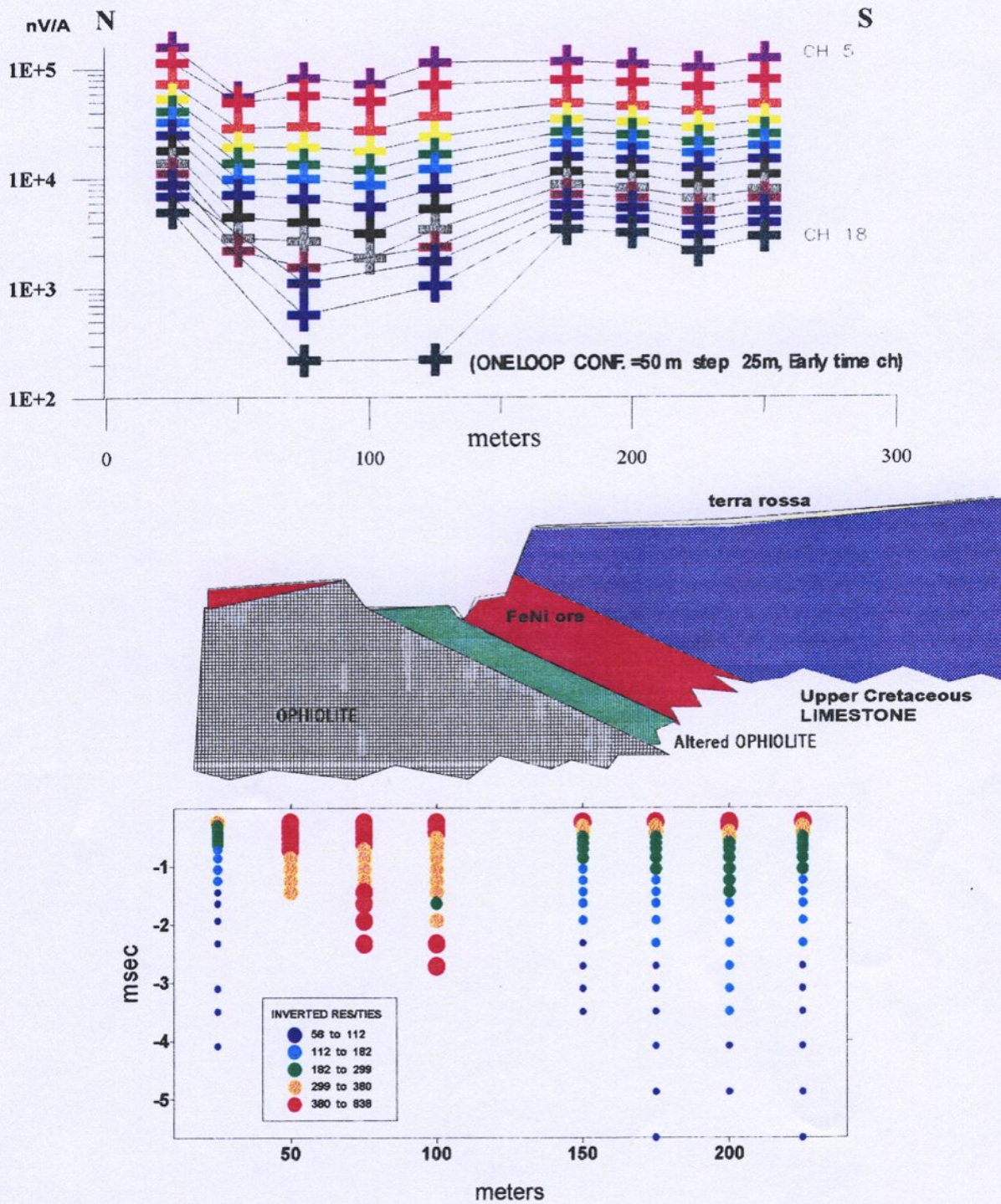


Plate 2.2.3.5

Geonickel Work Package 2, Sub tasks 2.2.3-2.2.6
Sirotem test line 1, schematic geologic section
and inverted TEM data.

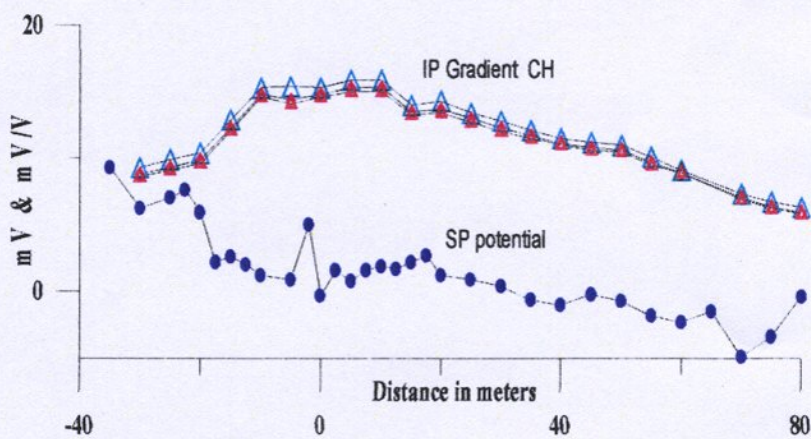
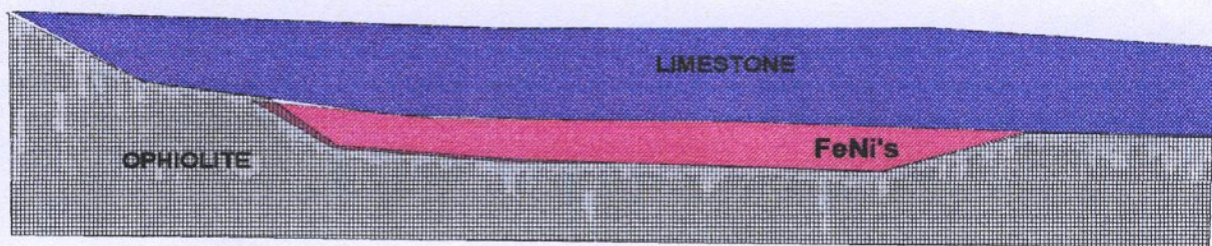
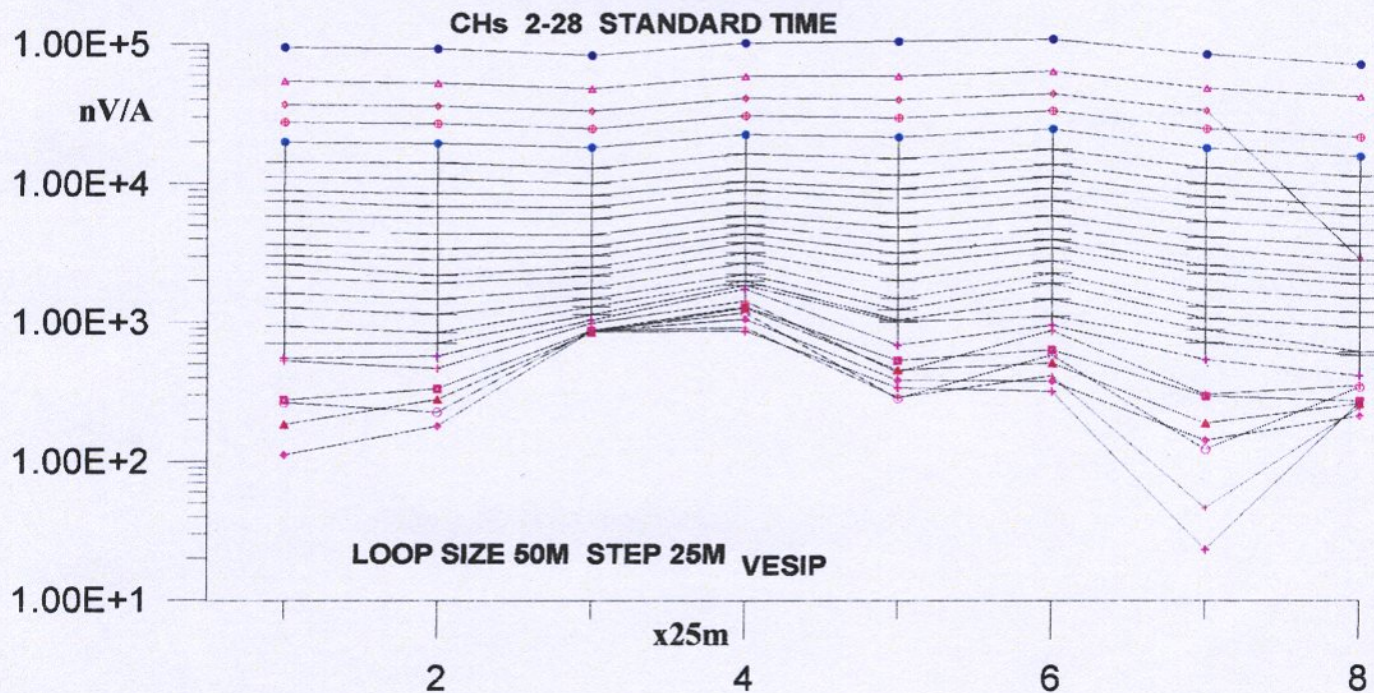


Plate 2.2.3.6 Geonickel Work Package 2, Sub tasks 2.2.3-2.2.6
Tsouka test line ,Lokris :Sirotem TEM ,schematic
geologic section ,Gradient IP &SP data.
(IP &SP are aquired above the ore and 60 m away
from TEM line).

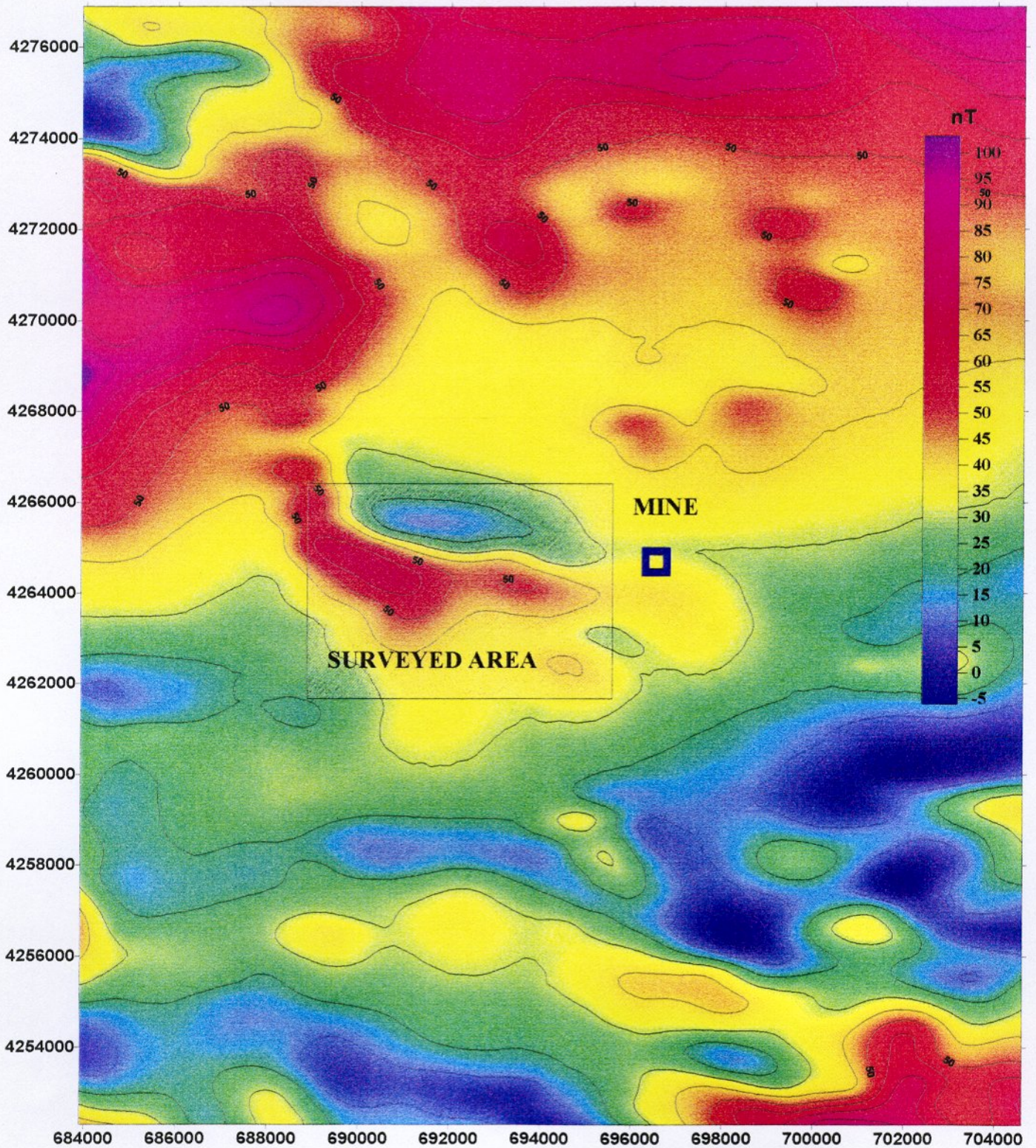


Plate 2.2.3.7 . Geonickel WorkPackage 2, sub tasks 2.2.3- 2.2.6
Aeromagnetic map, Ag.Ioannis mine area, lokris.
Surveyed area (shaded).

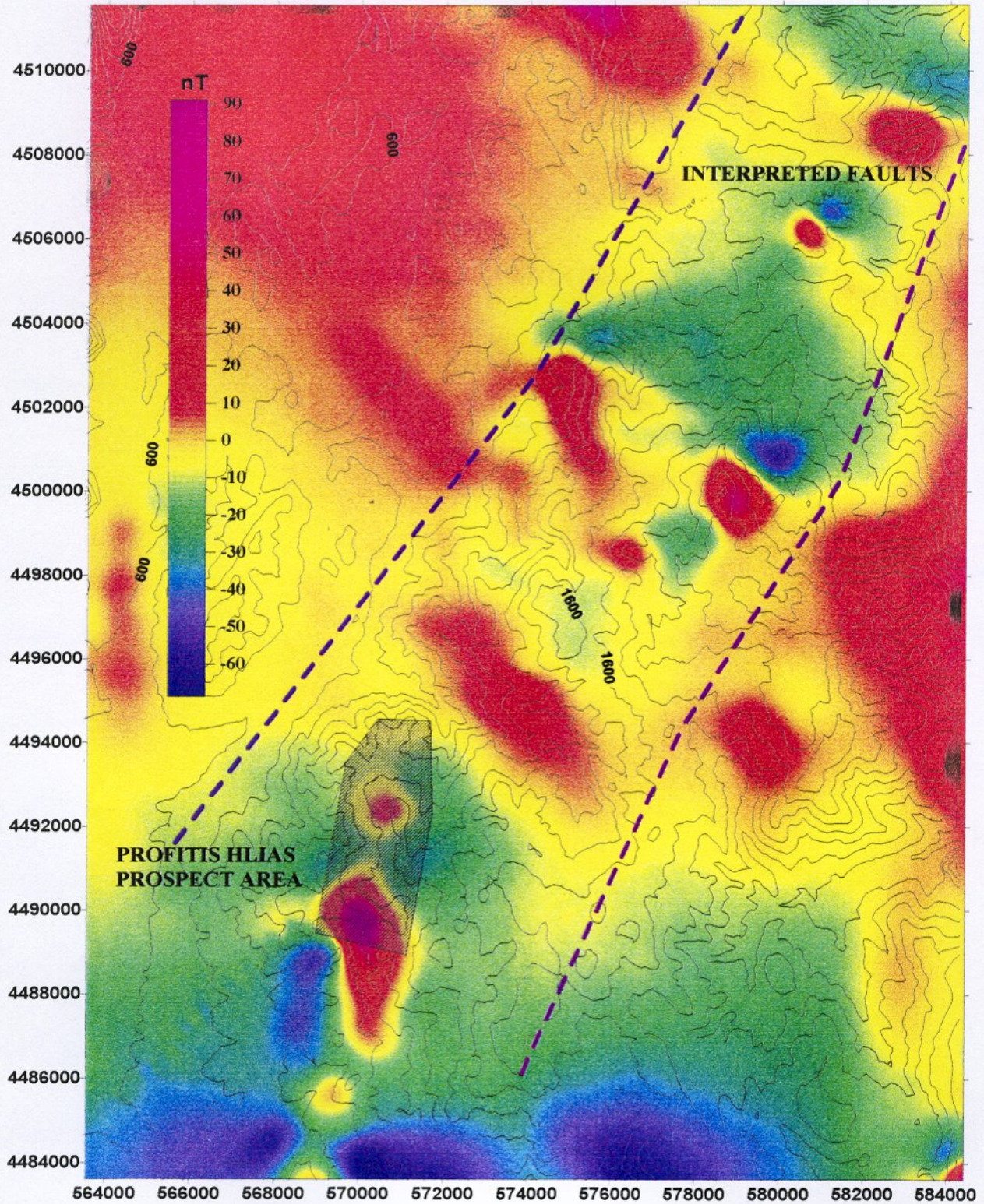


Plate 2.2.3.8 Geonickel WorkPackage 2, Sub tasks 2.2.3 - 2.2.6
Aeromagnetic map of Vermion area with topographic countours.
Interpreted tectonic lines / Profitis Hlias surveyed area (shaded)

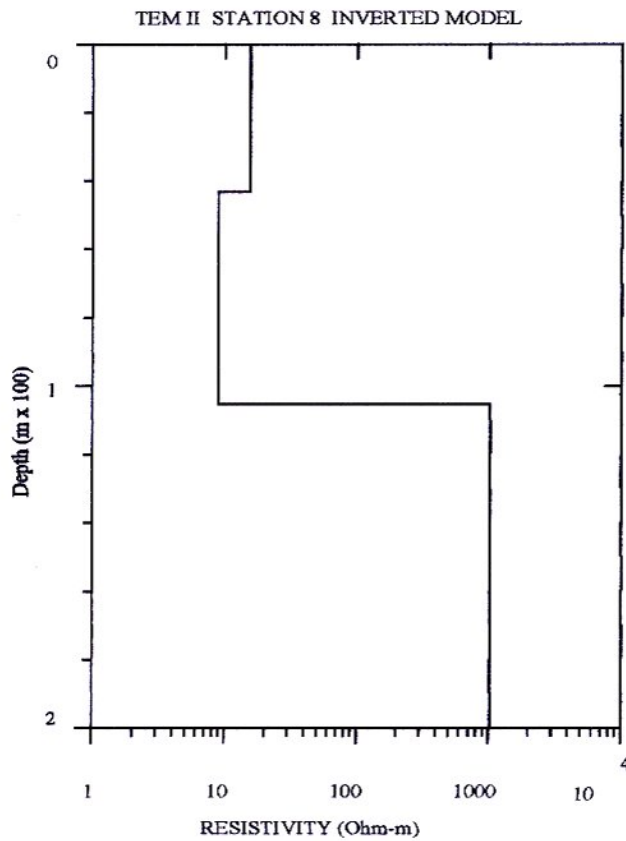
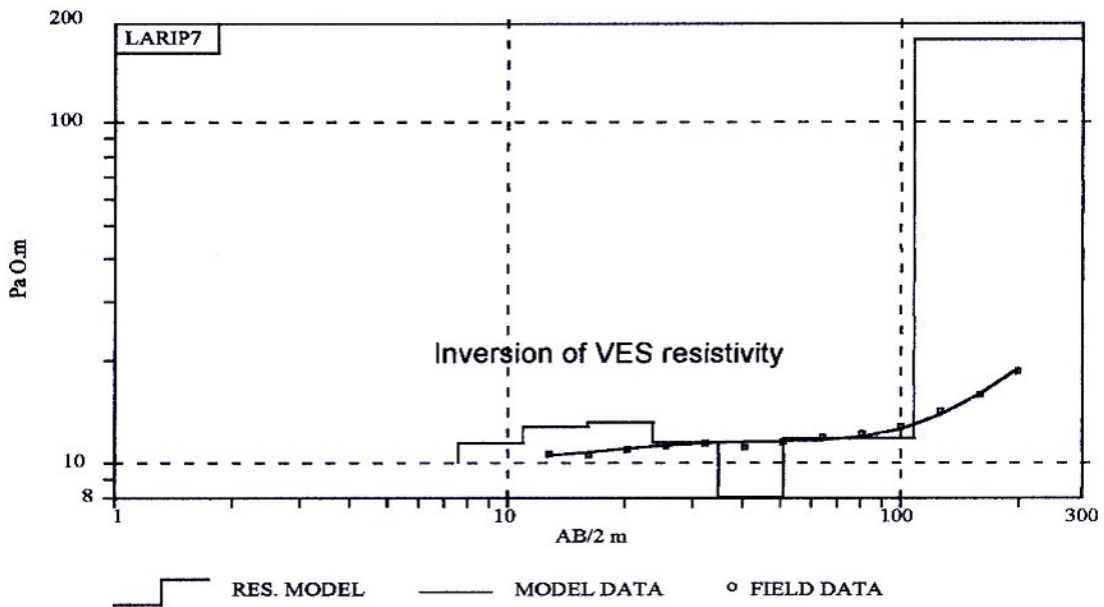


Plate 2.2.4.1 . Geonickel WorkPackage 2, Sub tasks 2.2.3- 2.2.6
Inversion of VES Resistivity data of LARIP 7
and TEM II station 8 at Kopais Basin ,Lokris.

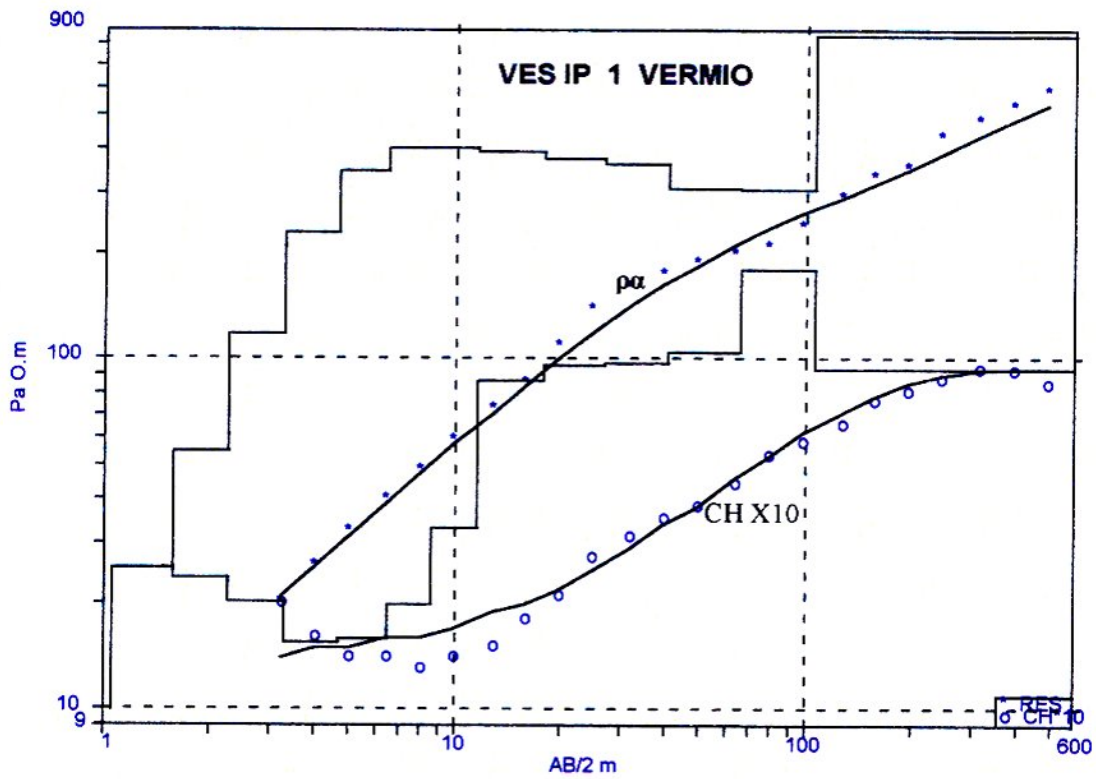
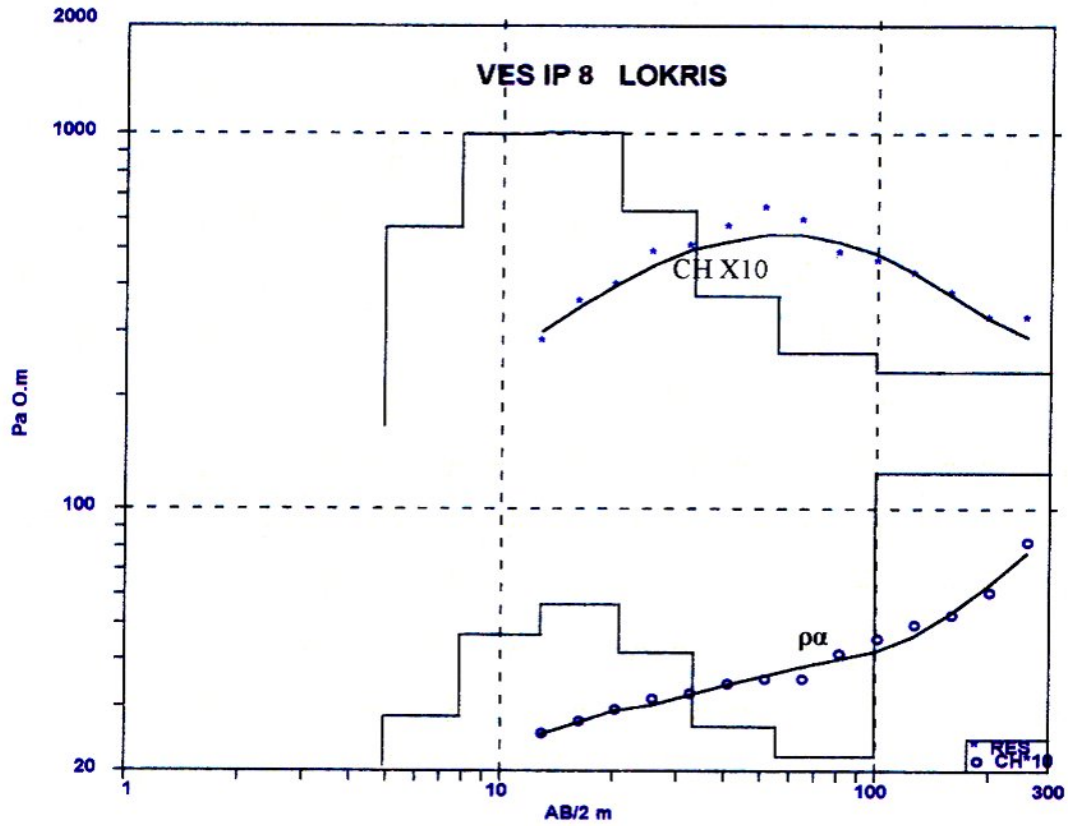


Plate 2.2.5.1 . Geonickel WorkPackage 2, Sub tasks 2.2.3-2.2.6
VES IP/Resistivity measured and inverted results
for Lokris and Vermio.

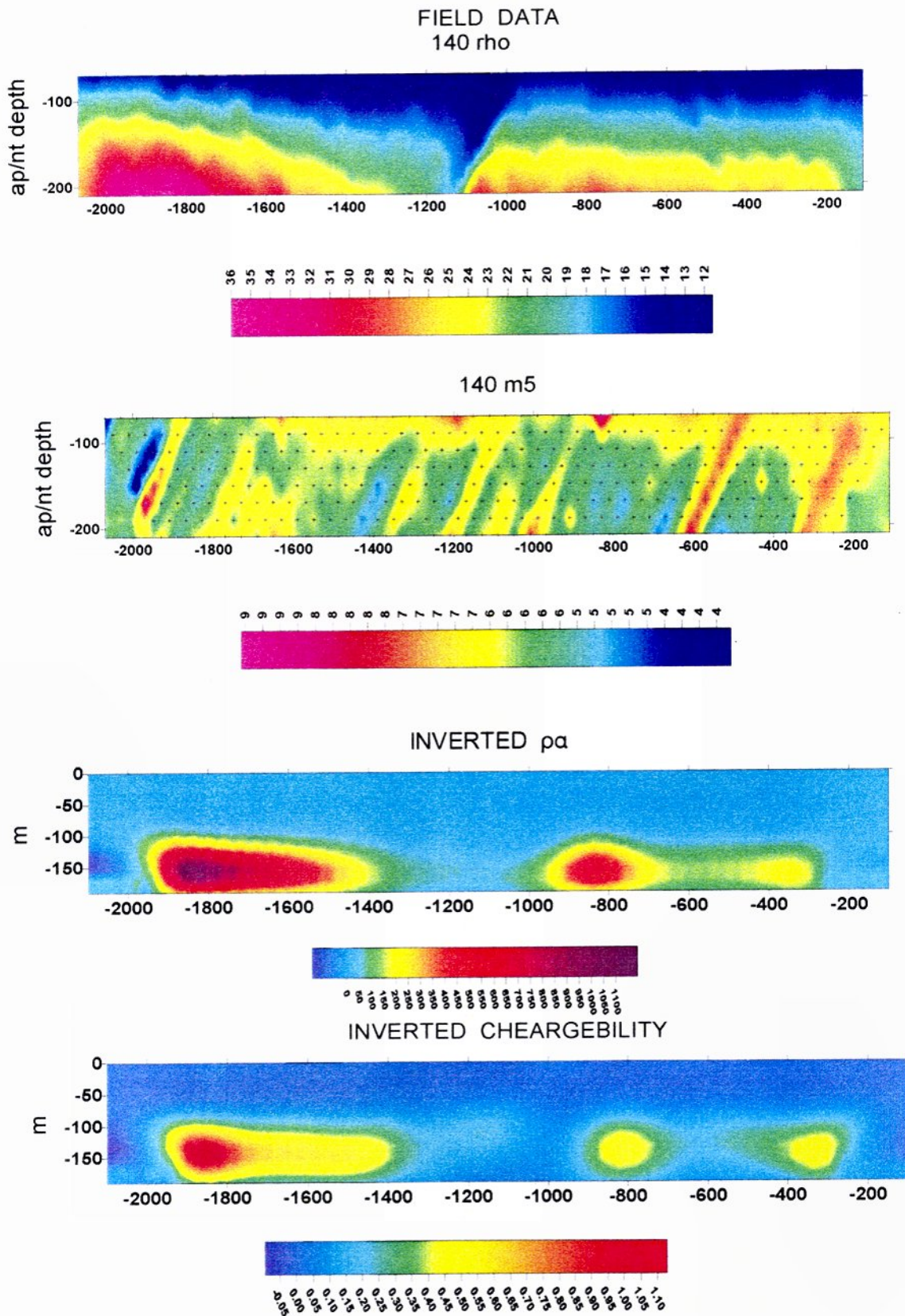


Plate 2.2.5.2 Geonickel WorkPackage 2, Sub tasks 2.2.3 - 2.2.6
140 pole-dipole line and inverted results.
Ag. Ioannis mine area Lokris.

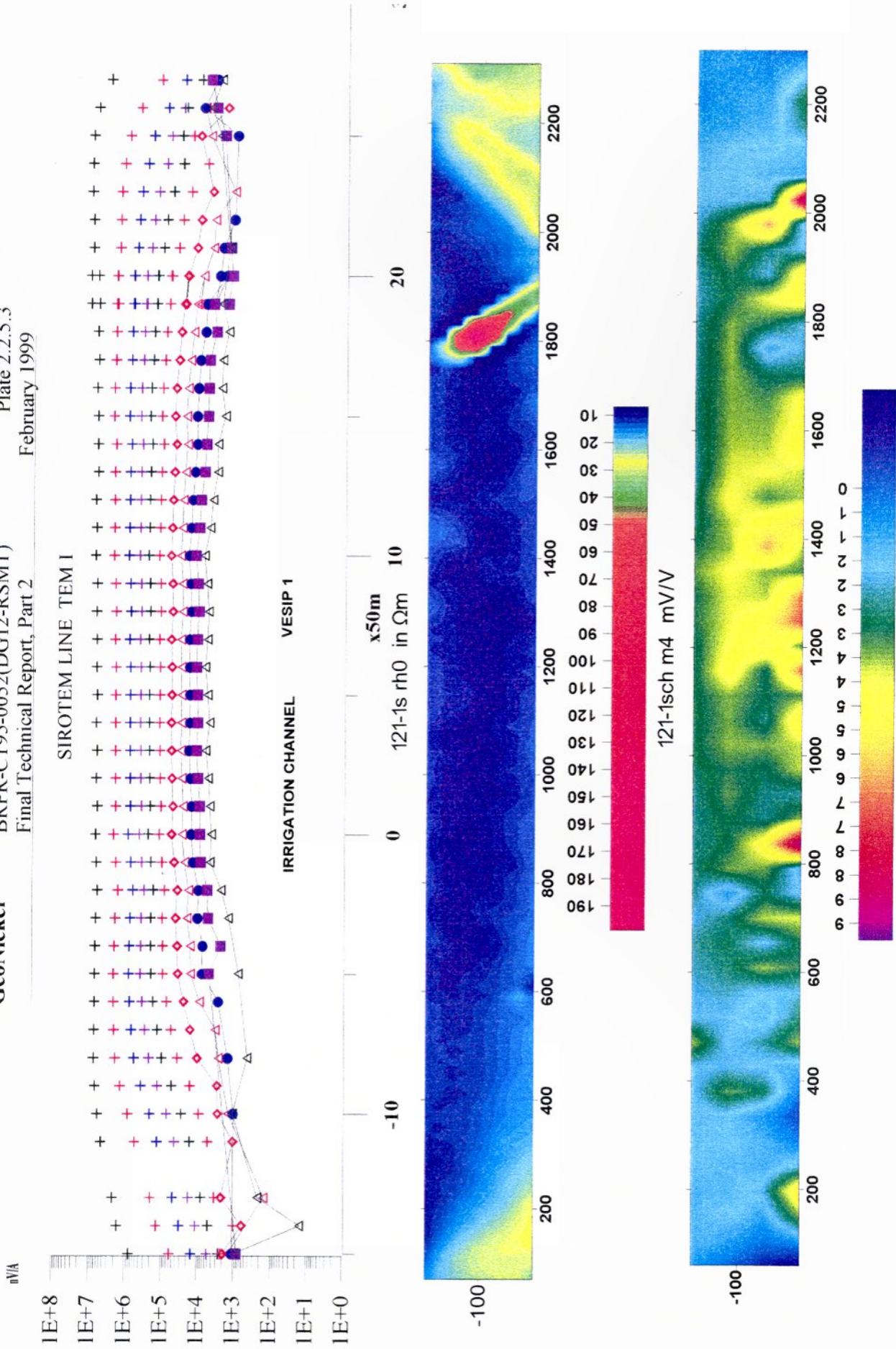


Plate 2.2.5.3 Geonickel WorkPackage 2, Sub tasks 2.2.2-2.2.6
121 dipole -dipole line and TEM I. Ag.Ioannis mine area.

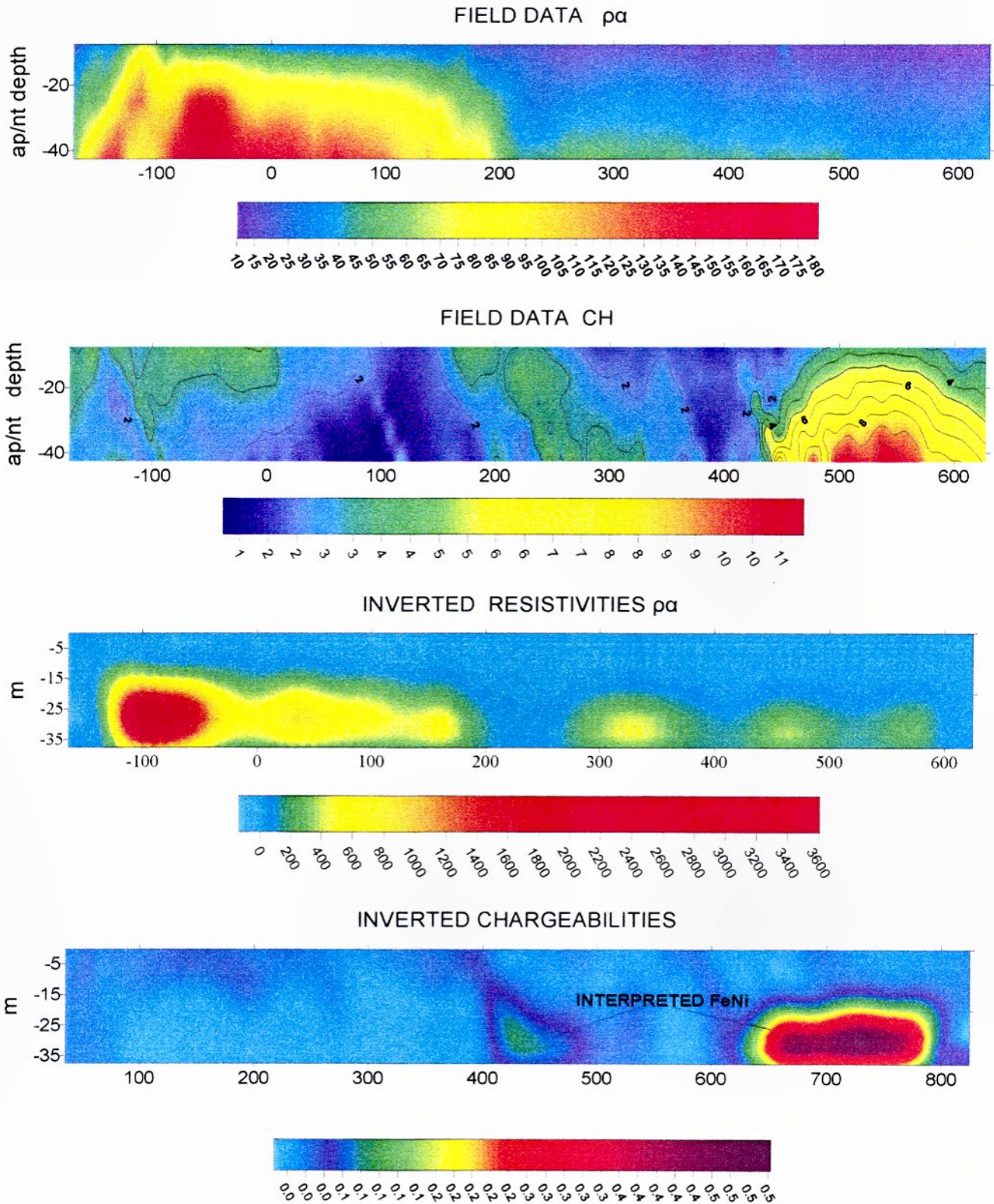


Plate 2.2.5.4 Geonickel WorkPackage 2, Task 2.2, 2.2.5.2
444 pole-dipole IP/Resistivity line and inverted results,
Ag.Ioannis mine area Lokris (same as seismic line T2
Plate 2.2.6.9).

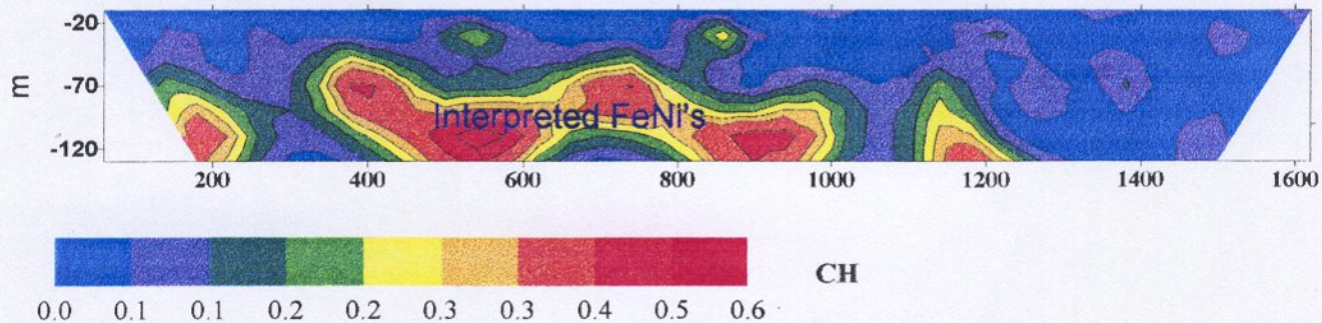
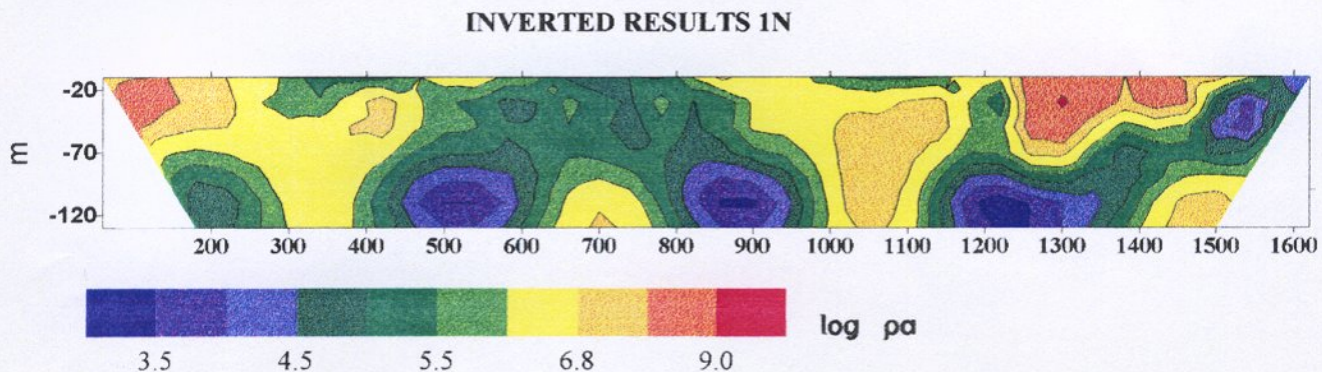
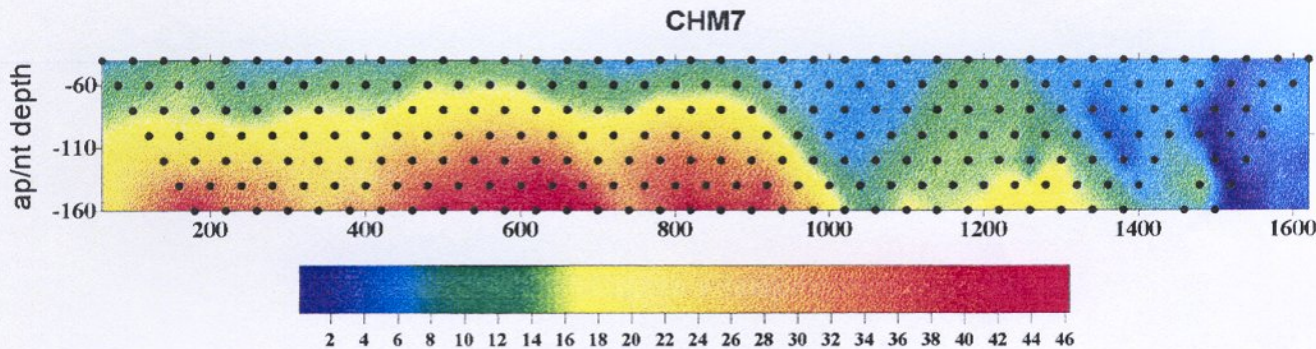
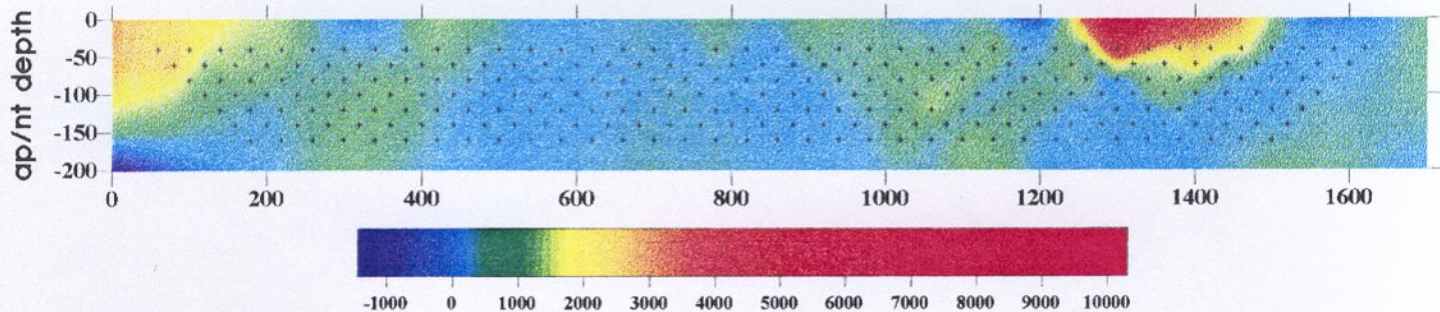
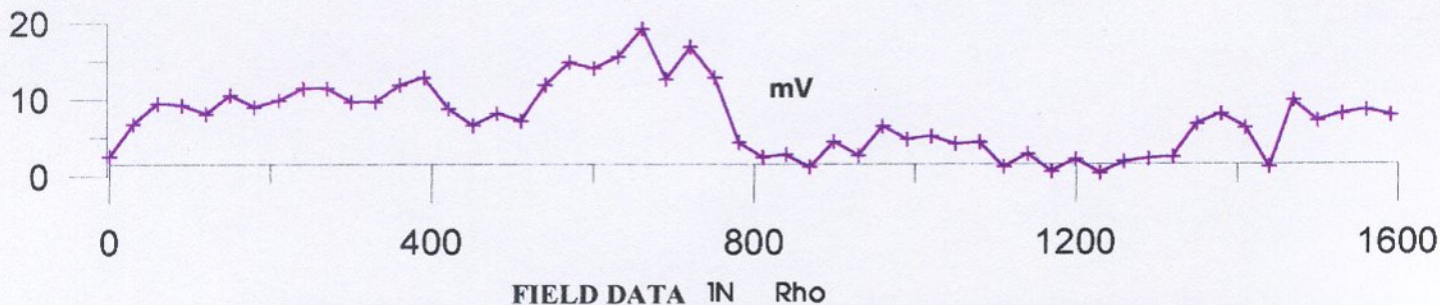
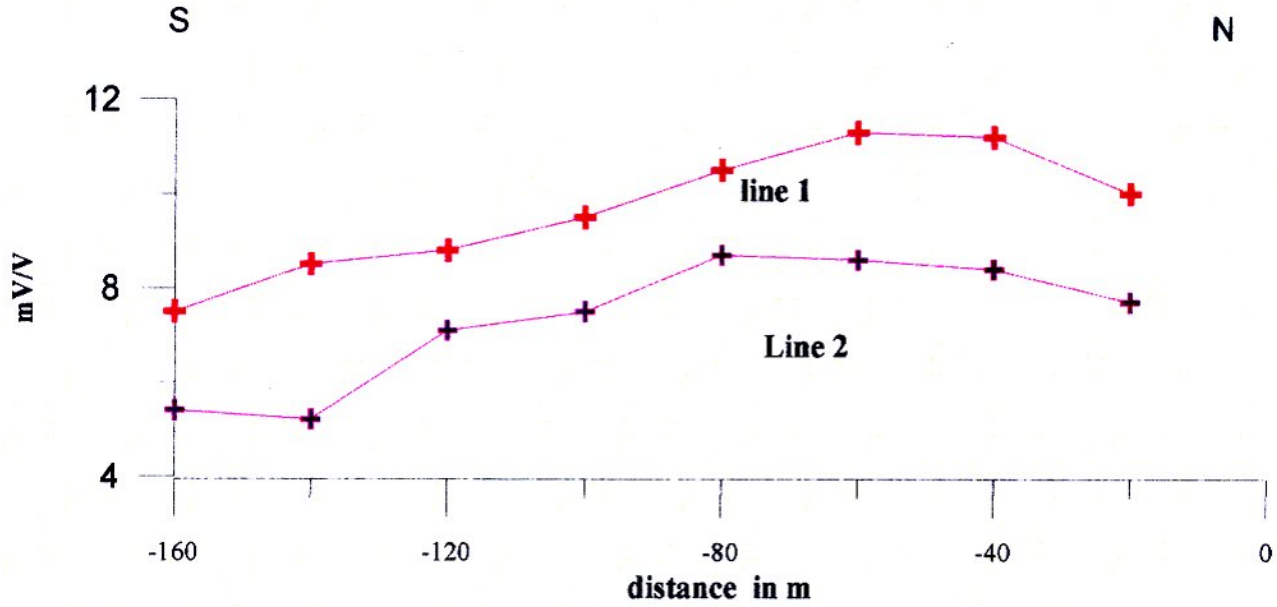


Plate 2.2.5.5 Geonickel WorkPackage 2, Sub tasks 2.2.3- 2.2.6
N1 IP/Resistivity dipole-dipole line in Vermion
and inverted results. The SP profile is also shown.



MISE ALLA MASE IP NISI ,LOKRIS

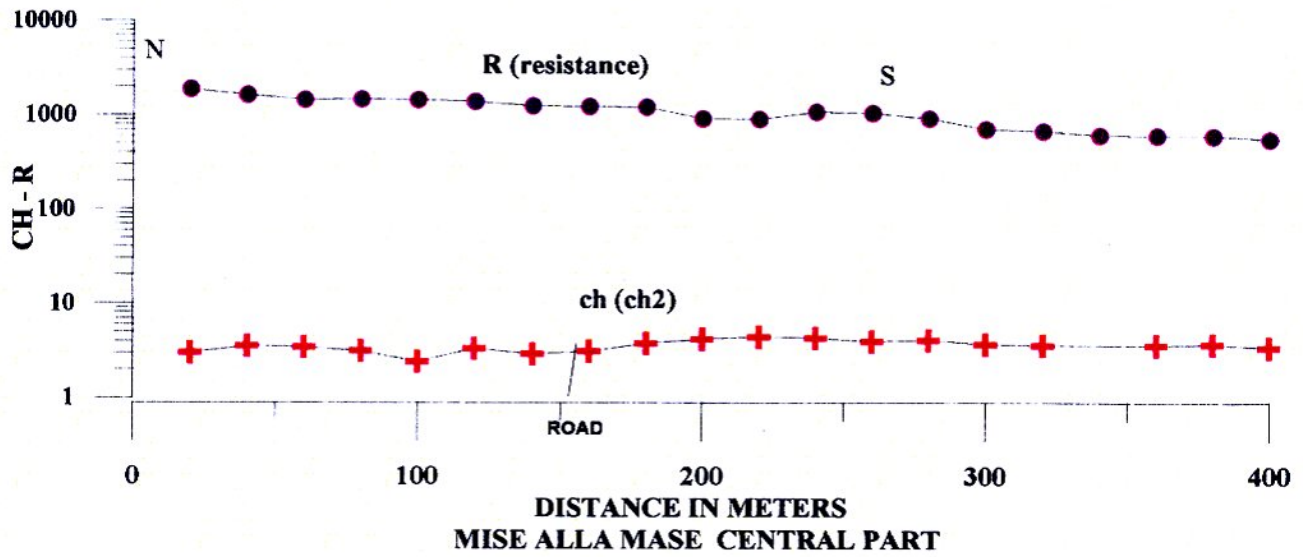


Plate 2.2.5.6 Geonickel Work Package 2,Sub tasks 2.2.3-2.2.6
Mise alla masse IP Gradient profiles at Nisi and Central part
of basin.

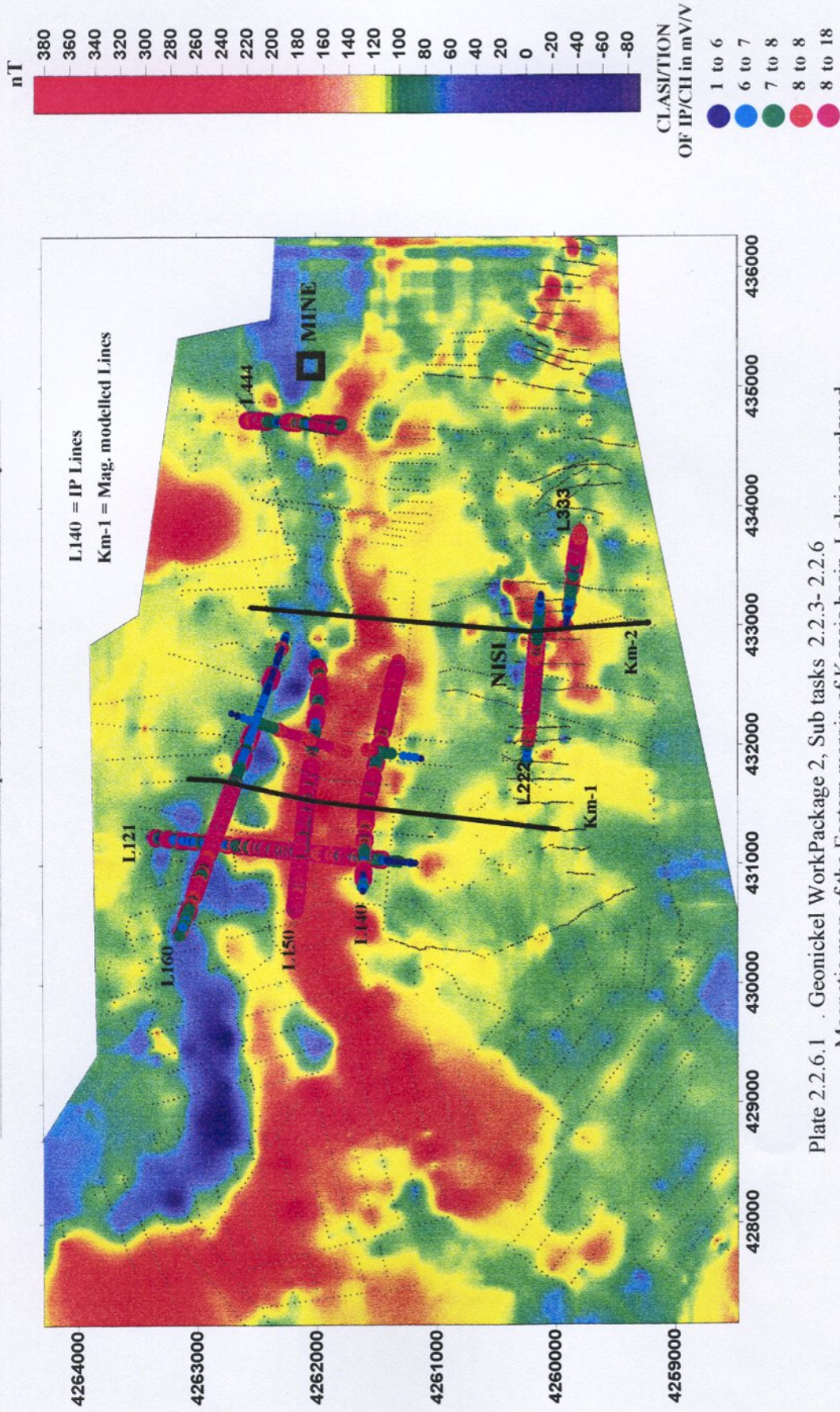


Plate 2.2.6.1 . Geonickel WorkPackage 2, Sub tasks 2.2.3- 2.2.6
Magnetic map of the Eastern margin of Kopais basin Lokris overlaid
IP CH 5 projected on surface plane, modelled lines are also shown.

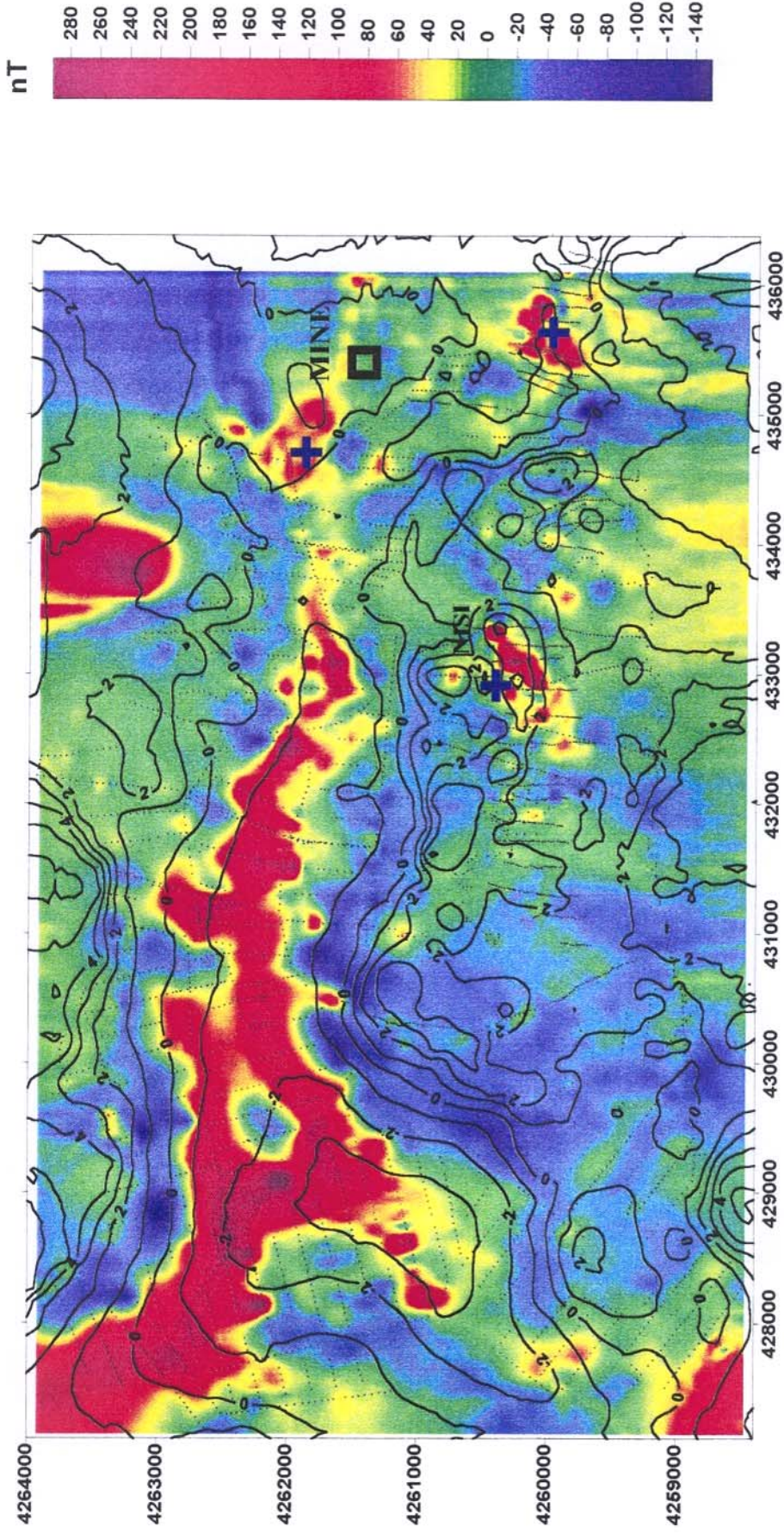


Plate 2.2.6.2 Geonickel WorkPackage 2, Sub tsaks 2.2.3 - 2.2.6
Magnetic(pole to pole) map with residual gravity contours ,LOKRIS.
+ Areas of positive Mag and Grav correlation

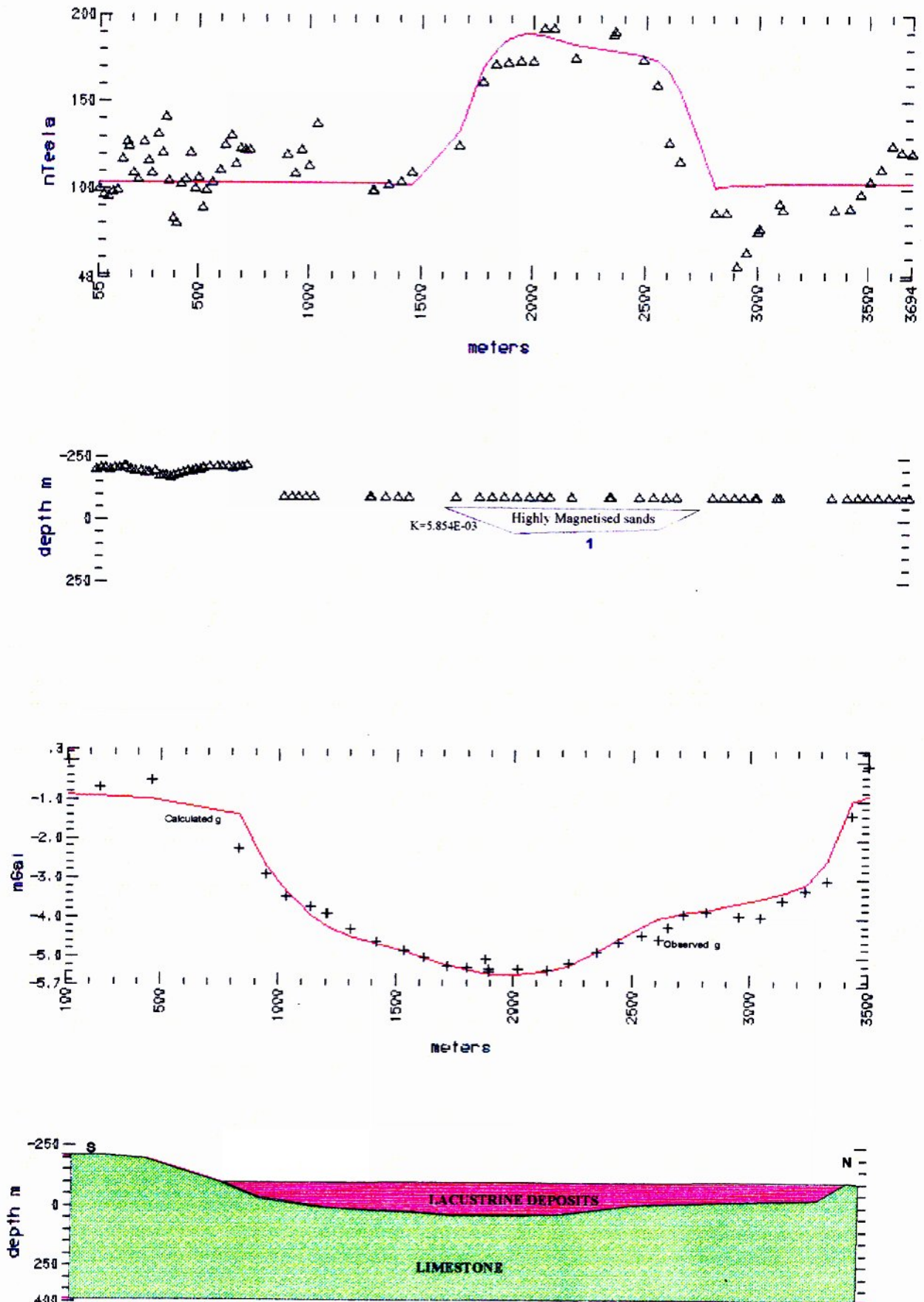


Plate 2.2.6.3 Geonickel WorkPackage 2, Sub tasks 2.2.3 - 2.2.6
Inverted Magnetic and Gravity profile across the Eastern Kopais basin

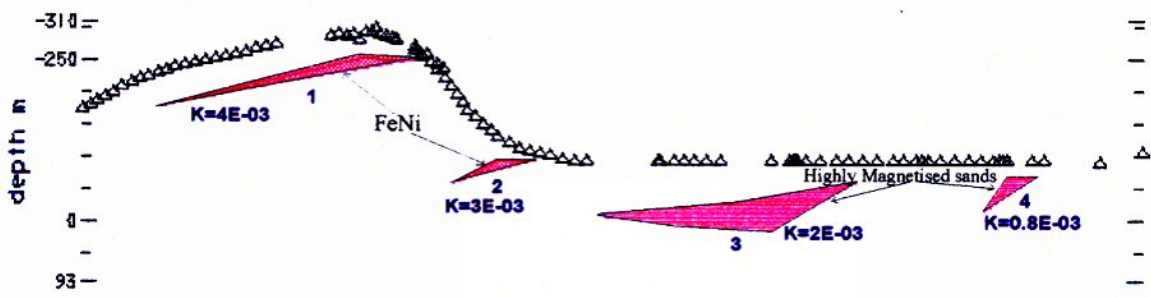
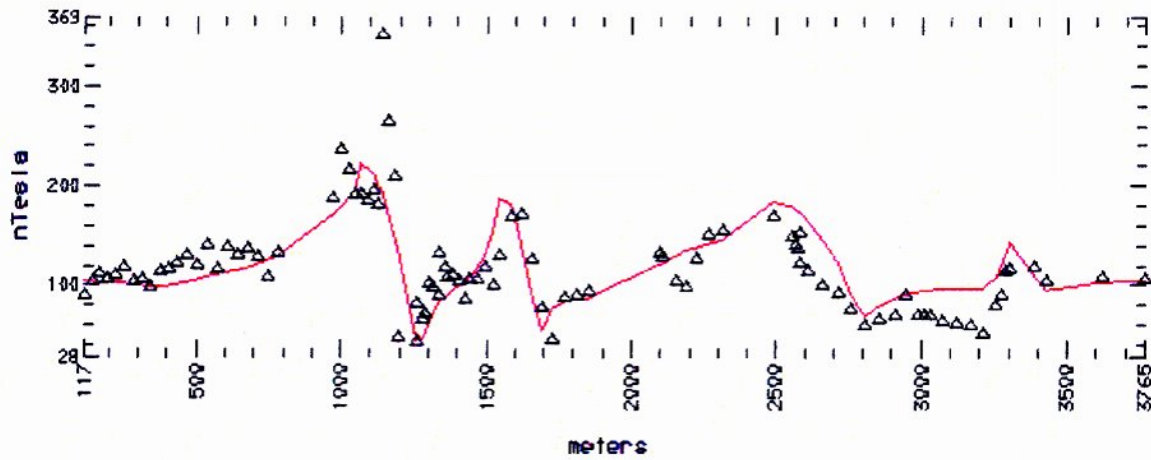


Plate 2.2.6.4 Geonickel WorkPackage 2, Sub tasks 2.2.3- 2.2.6
Inverted Magnetic profile across the Eastern Kopais basin
Line Km-2

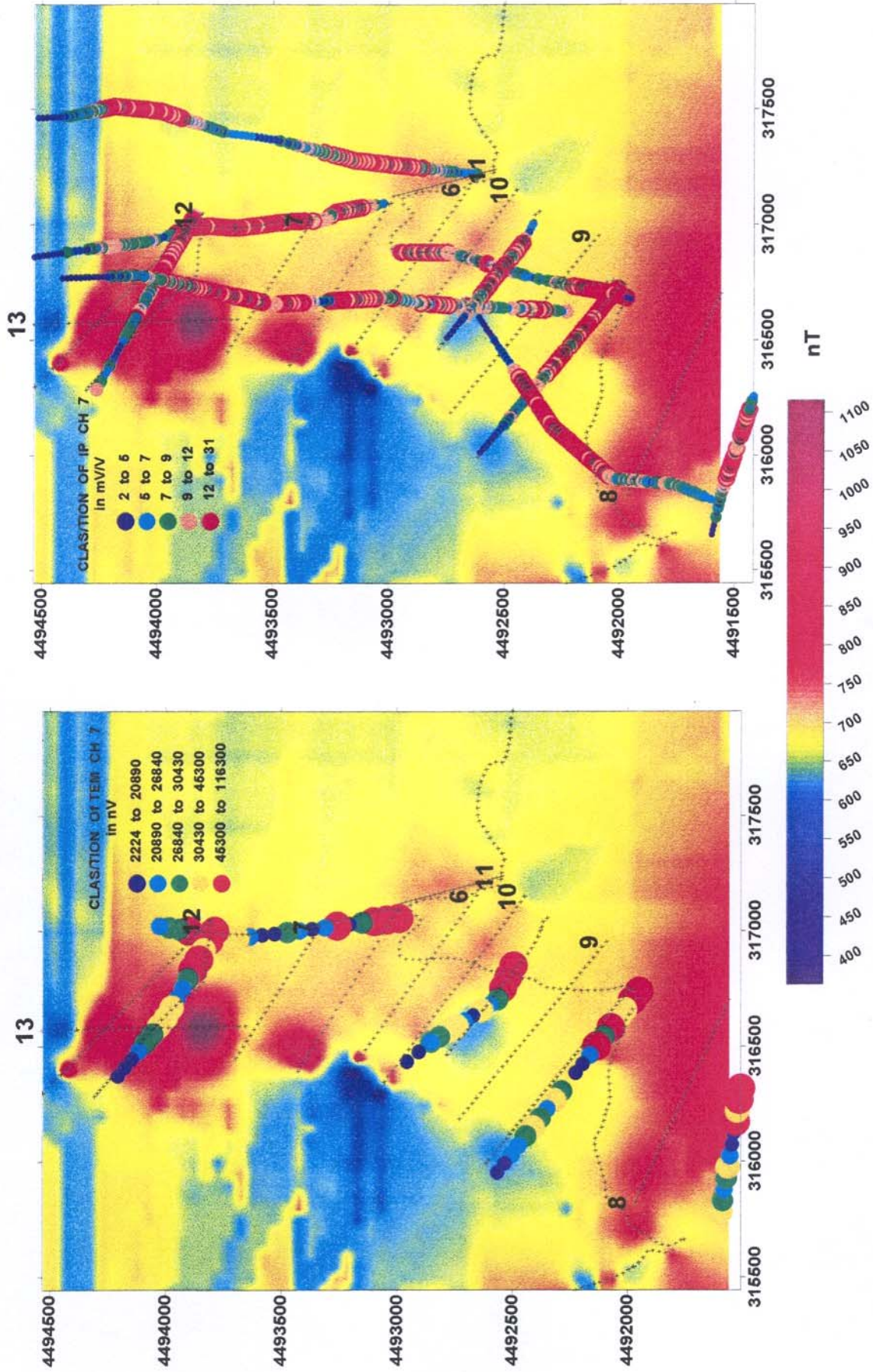


Plate 2.2.6.5 Geonickel WorkPackage 2, Sub tasks 2.2.3 - 2.2.6
Magnetic map of Prof. Elias area VERMION and
overlayed classified TEM and IP CH results.

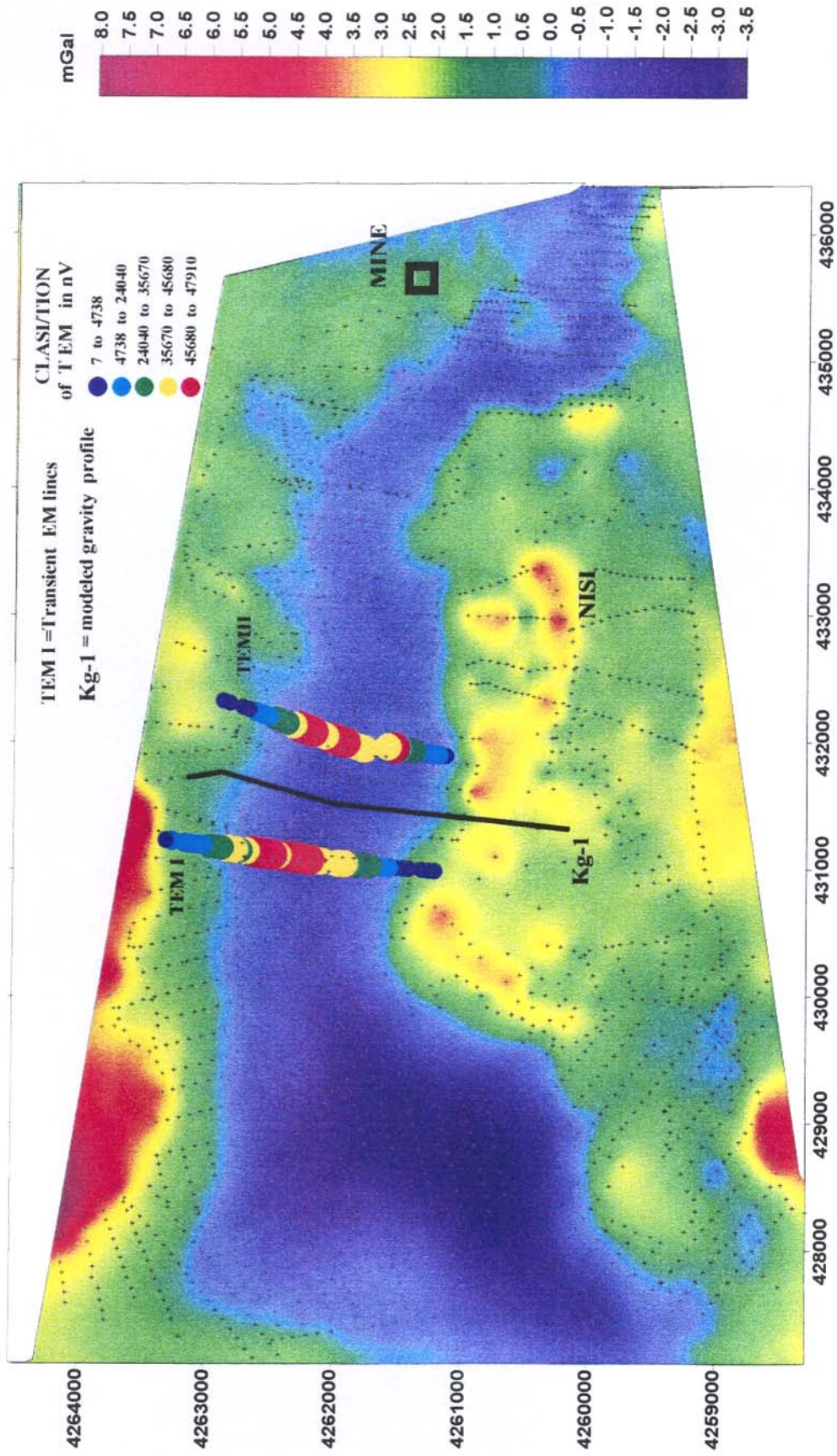


Plate 2.2.6.6 . Geonickel WorkPackage 2, Sub tasks 2.2.3- 2.2.6
Residual Bouguer gravity map, with TEM Channel 7 in nV
& modelled gravity profile, Lokris.

E

W

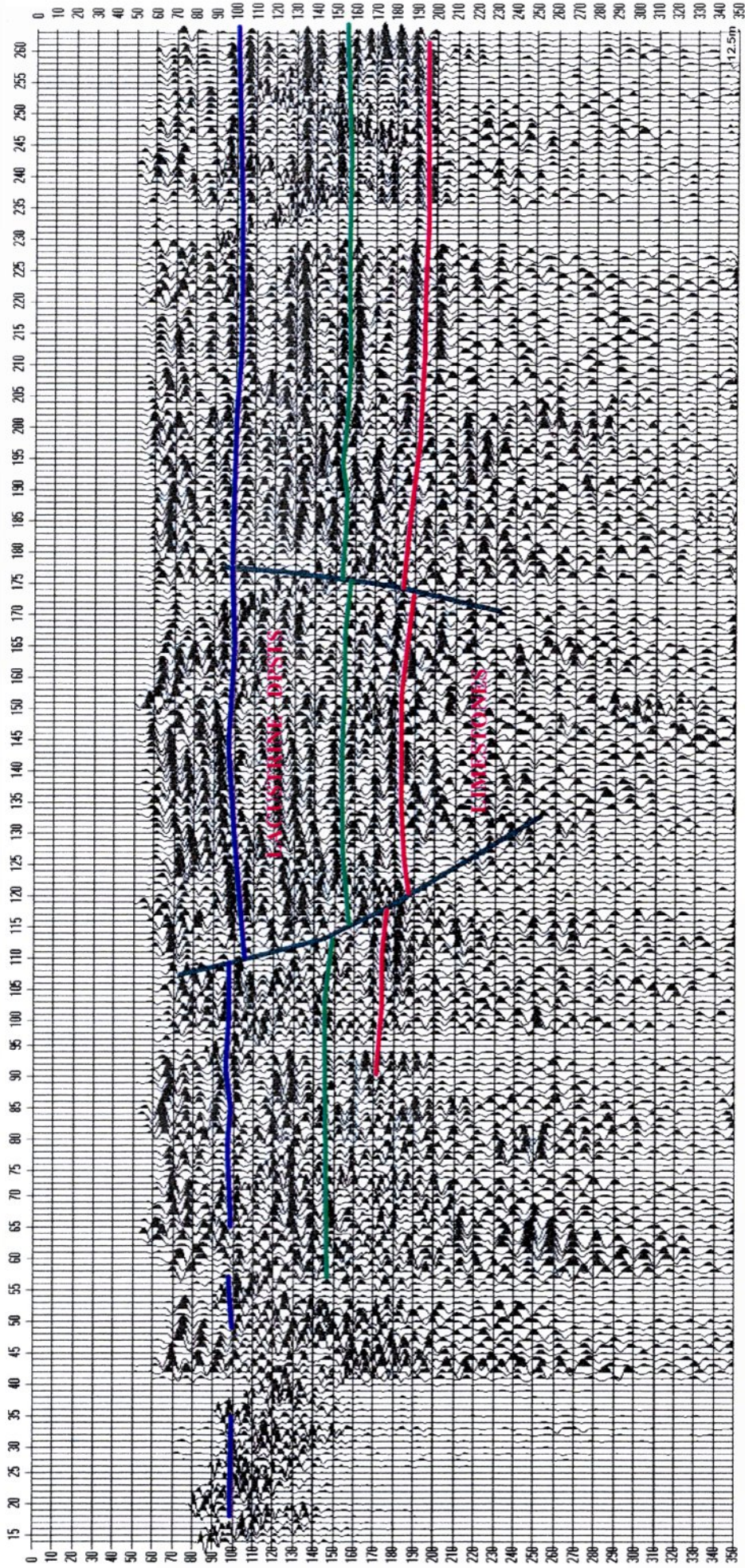


Plate 2.2.6.7 Geonickel WorkPackage 2, Sub taks 2.2.3- 2.2.6
Makryni seismic section in centre of the basin.
Ag.Ioannis mine area, Lokris .

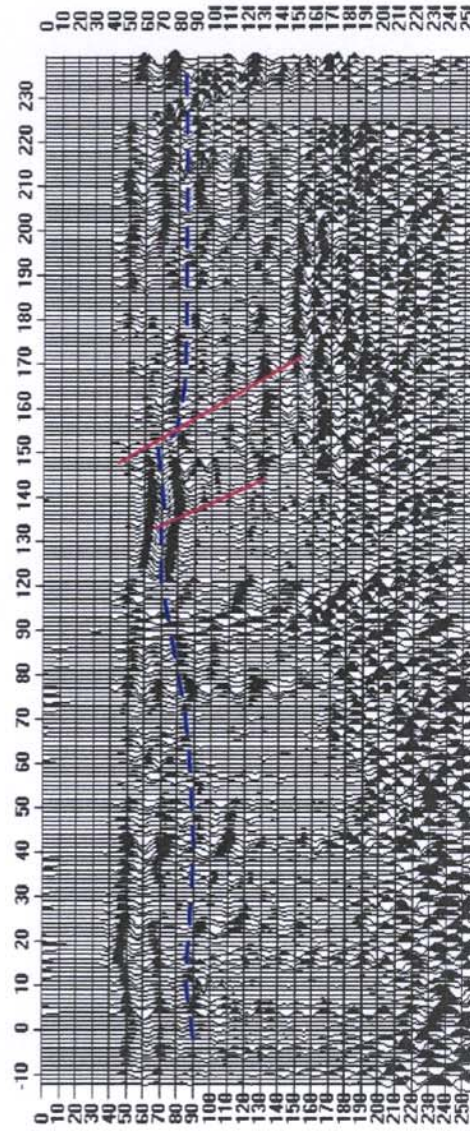
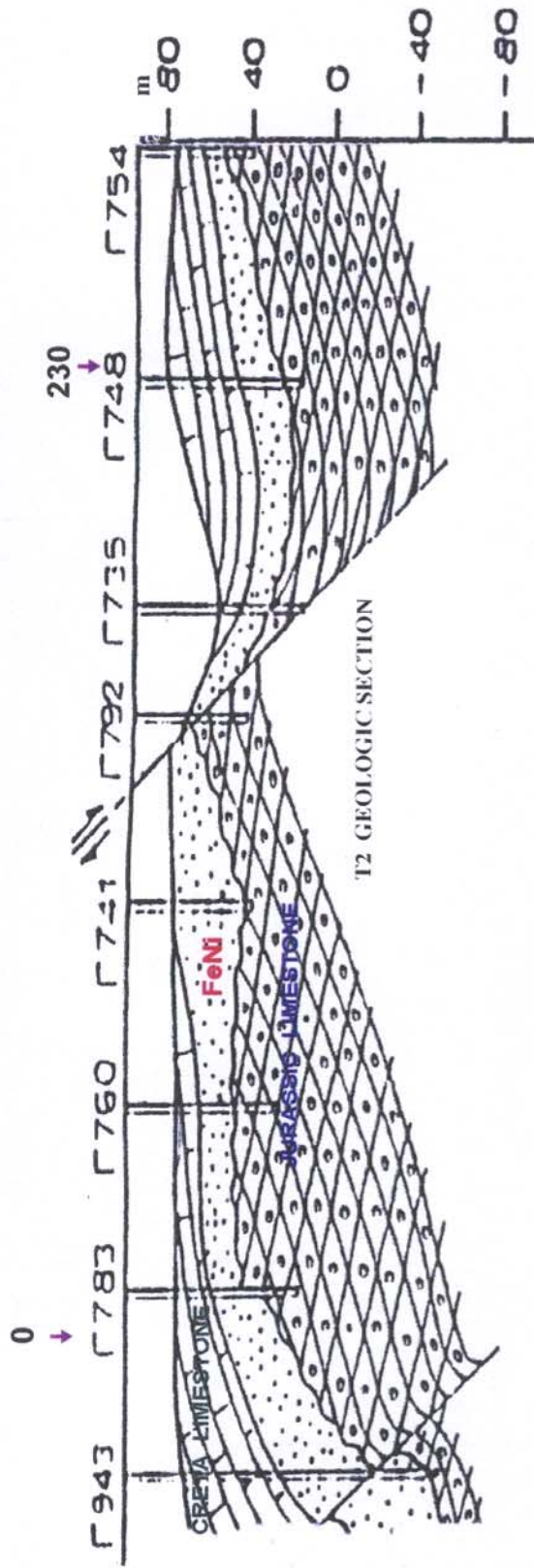
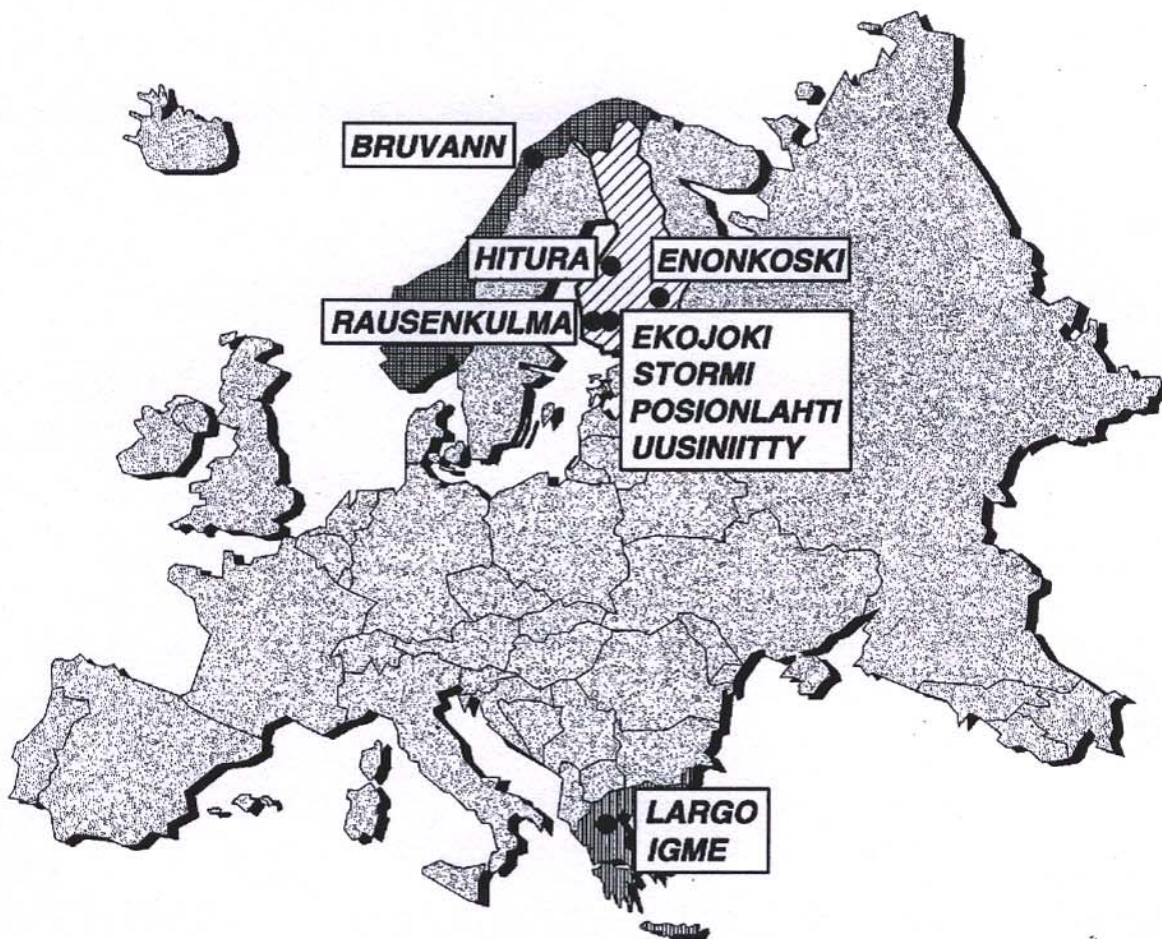


Plate 2.2.6.8 . Geonickel WorkPackage 2, Sub tasks 2.2.3- 2.2.6
T2 Geologic section and corresponding seismic section
Ag. Ioannis mine area.

GEONICKEL
Task 2.4 Compilation of petrophysical database



NI DEPOSITS USED IN THE STUDY

- 442 SAMPLES SUSC. + DENSITY

- 133 —||— CONDUCTIVITY

Plate 2.4-1. The location map for the Ni-deposits .

PETROPHYSICAL DATABASE AND STATISTICAL ANALYSIS OF Ni DEPOSITS

- MAGNETIC PROPERTIES
- DENSITY

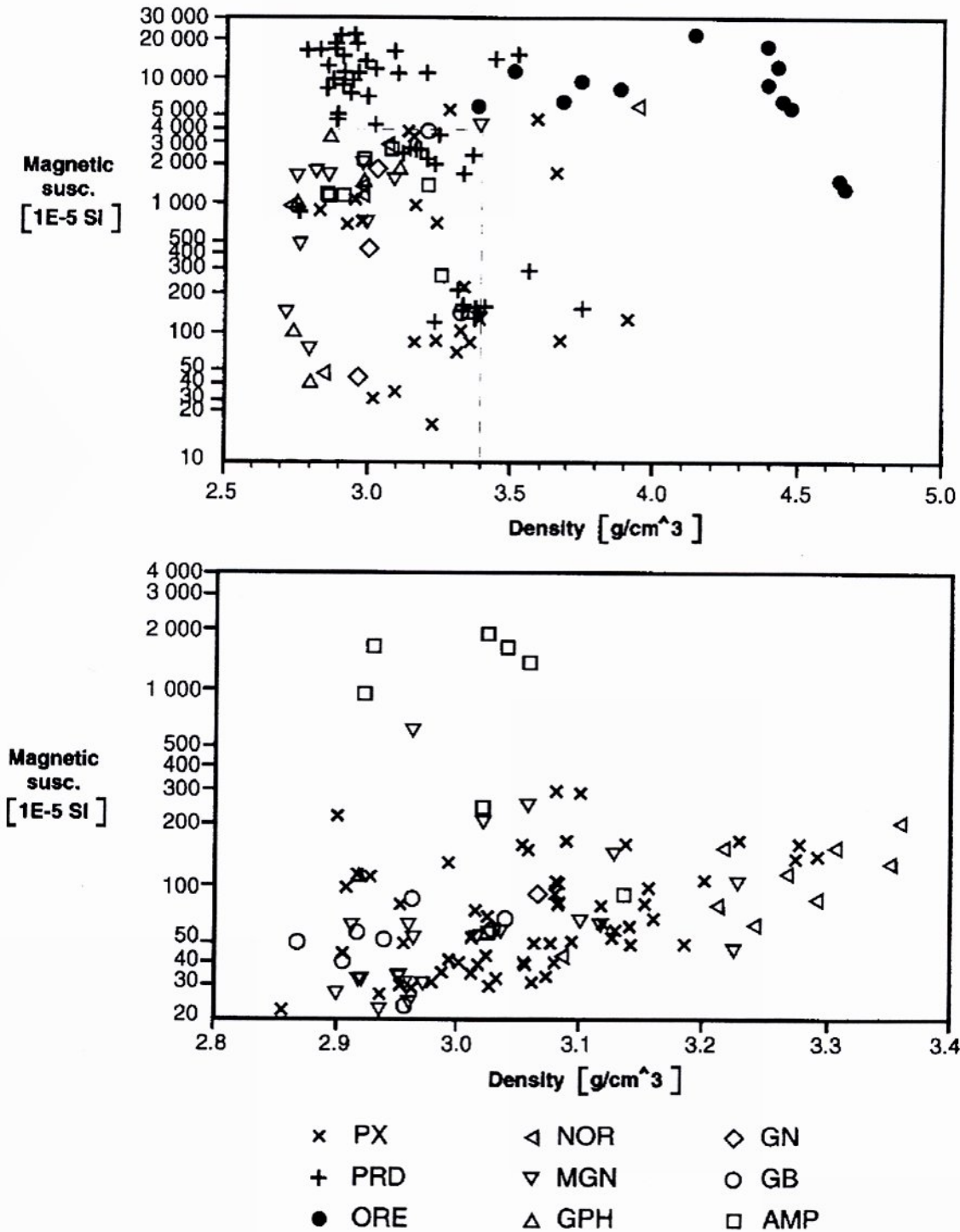
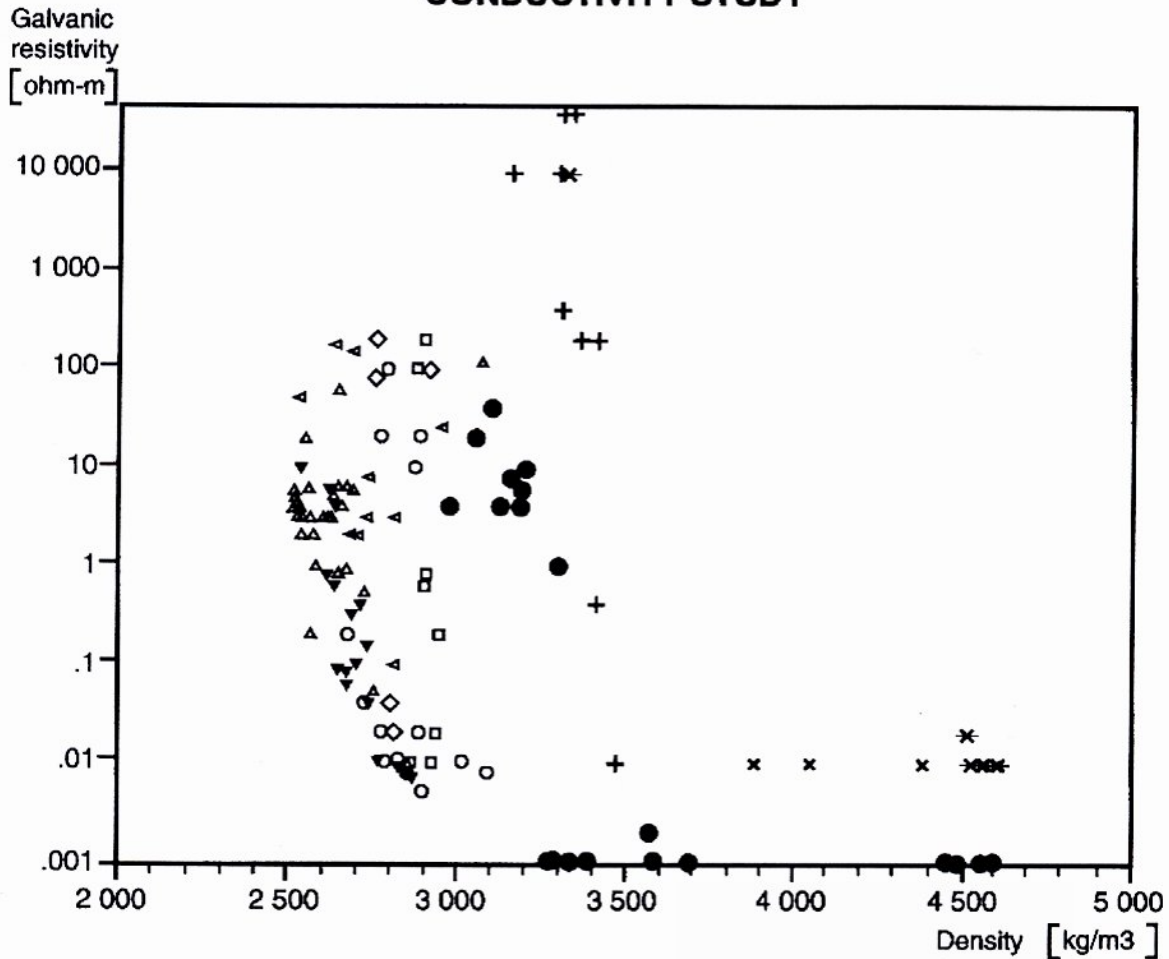


Plate 2.4-2. Scatterplot of magnetic susceptibility versus density for host rocks.

PETROPHYSICAL DATABASE AND STATISTICAL ANALYSIS OF NI DEPOSITS

CONDUCTIVITY STUDY



- ▲ serpentinite, host rock Hitura
- ore Laukunkangas
- mica gneiss Hitura
- ◇ graphite gneiss Laukunkangas
- ▲ disseminated ore central Hitura
- ▼ disseminated fine grained ore Hitura
- ◄ disseminated coarse grained ore Hitura
- black schist Laukunkangas
- × fine grained ore Bruvann
- + disseminated ore Bruvann
- * coarse grained ore Bruvann

Plate 2.4-3. Scatterplot of galvanic resistivity versus density for Ni-deposits included in the conductivity study.